



UNIVERSITAT<sup>DE</sup>  
BARCELONA

# Root traits and stable isotopes as phenotyping approaches to enhance wheat adaptation to Mediterranean conditions


Fatima Zahra Rezzouk



Aquesta tesi doctoral està subjecta a la llicència **Reconeixement 4.0. Espanya de Creative Commons.**

Esta tesis doctoral está sujeta a la licencia **Reconocimiento 4.0. España de Creative Commons.**

This doctoral thesis is licensed under the **Creative Commons Attribution 4.0. Spain License.**

The background of the entire page is a photograph of a vast wheat field during a golden sunset. The sun is low on the horizon, casting a warm, orange glow over the scene. In the foreground, several wheat stalks are in sharp focus, showing the texture of the grain heads. The background is softly blurred, showing rows of wheat stretching towards a range of low mountains under the bright sky.

Root traits and stable isotopes as phenotyping  
approaches to enhance wheat adaptation to  
Mediterranean conditions

**Fatima Zahra Rezzouk**

Doctoral thesis  
Barcelona 2023





UNIVERSITAT DE  
BARCELONA

**Root traits and stable isotopes as phenotyping approaches to enhance wheat adaptation to Mediterranean conditions**

Dissertation presented by Fatima Zahra Rezzouk to obtain the degree of Doctor from the University of Barcelona.

This work is part of the doctoral program in Ecology, Environmental Sciences, and Plant Physiology of the Department of Evolutionary Biology, Ecology and Environmental Sciences (BEECA) of the Faculty of Biology of the University of Barcelona.

This work has been carried out in the Integrative Crop Ecophysiology Group research group, under the direction of Dr. Jose Luis Araus Ortega and Dr. Maria Dolors Serret Molins.

Doctorant

Director and tutor

Director

Fatima Zahra Rezzouk

Dr. José Luis Araus

Dr. Maria Dolors Serret

BARCELONA, JUNE 2023





*TO ALLAH, TOUT PUISSANT*

*A YOUSRA, MI CONFIDENTE*

*ALS MEUS PARES I GHITA, WHO GAVE ME EVERY REASON*

*TO REACH THE VERSION OF ME TODAY*



## ABSTRACT

Wheat is a major staple food worldwide. Its cultural and economic importance is mainly highlighted in the Mediterranean region, among other regions of the world. However, wheat production is frequently challenged by environmental factors such as interannual variability in precipitation and temperatures, which translates in further shortage in water and nutrients availability. These environmental events are expected to worsen even more in the near future. Therefore, tailoring wheat cultivars that are simultaneously climate-resilient and high yielding under Mediterranean growing conditions is becoming a main focus of breeders and researchers. To this end, the main objective of the present dissertation was to identify ideotypic characteristics of wheat cultivars grown under different Mediterranean conditions through the implementation of diverse phenotyping approaches, targeting the aboveground biomass using remote and proximate sensing techniques, and the belowground biomass using shovelomics and soil coring techniques. These phenotypical platforms were further combined with stable isotopes as physiological traits assessing water and nitrogen status in different plant tissues and soil profile, as well as crop growth traits, mainly phenology, biomass and plant height, and yield components to assess potential traits to breed for in the selected ideotypic traits. Overall, phenology had a clear role in drought adaptation under the Mediterranean conditions, under wet seasons phenological durations were longer in high yielding genotypes, whereas under dry seasons, shorter days to anthesis followed by longer grain filling period were the characteristics shown by high yielding genotypes. Furthermore, predictive models integrated water status indicators (carbon isotope composition ( $\delta^{13}\text{C}$ ) and canopy temperature depression (CTD)) as main explicative variables to grain yield, followed by root traits and nitrogen status. The best yielding genotypes were associated with shorter days to heading, better water status mainly through lower  $\delta^{13}\text{C}$  and higher CTD, and higher nitrogen status as demonstrated through higher growth traits (plant height and biomass), delayed senescence (higher stay green status), but also to deeper root development as shown by lower  $\delta^{18}\text{O}$  and  $\delta^2\text{H}$ , thinner roots and root biomass distribution across soil profile. These traits altogether provided the needs in water and nutrient sources for plant growth, and translated to higher growth, longer grain filling, better photosynthesis activities and therefore

higher productivity. Furthermore, depending on water availability (irrigation vs rainfed), roots traits in the upper soil demonstrated a plastic response to their targeted environment. When support irrigation is supplied, the best yielding genotypes exhibited a dual root development with a shallower root angle and thin roots that explore the superficially and in deeper soil sections for water and nutrients capturing. In contrast, under rainfed conditions, a deep rooting is observed with steeper root angle, and thinner roots with are thinner with tendencies to extract water from deeper soil levels. Moreover, oxygen ( $\delta^{18}\text{O}$ ) and hydrogen ( $\delta^2\text{H}$ ) isotope analyses of different plant tissues demonstrated similar fractionation pattern associated with evaporative processes in water tissues, whereas in the organic matter of the plant tissues, variations in  $\delta^{18}\text{O}$  were driven by evaporation, and variations in  $\delta^2\text{H}$  values in tissues were associated with plant trophism. Chapters along this work highlighted the advantages and the limitations of shoot and root phenotyping techniques and proposed the stable isotopes as potential phenotyping traits to consider in breeding programs under Mediterranean conditions.



## ACKNOWLEDGMENTS

I dedicate my most sincere gratitude to my supervisors and directors **José Luis** and **Dolors**, from whom I've learnt a lot on professional and personal levels. Their support to me in my hard times as an international student and their continuous guidance throughout my stay in Barcelona cannot be described in words only. Thank you.

I extend my gratitude to the former and new members of my research group "Integrative crop Ecophysiology Group": **Adrian, Luisa, Melissa, Thomas, Omar, Fadia, José Armando, Ludo, Joel, Rut, Shawn, Cristina, Jordi, Yassine** and **Jara**. With whom we shared many great times and without whom this dissertation wouldn't have reached its final stages. **Adrian**, he was my very first friend in Barcelona and my forever respected coworker, I'm grateful for the moments we shared in the office and field trips, conferences and discussions, I'm grateful for his guidance during my first months within the group, and his continuous support throughout my PhD journey. **Luisa** and **Melissa**, my food squad and beautiful souls that I am grateful for crossing paths and becoming best friends with, we were each other's support in our greatest and toughest times.

To **Houda, Bety, Amine** and **Abdesamad**, my long-lasting best friends, for their immense and continuous support.

To **Keaton**, my significant other who supported me unconditionally towards the end of PhD journey.

To **Yousra**, who kept me going whenever I lost my way, who stayed by my side in my brightest and darkest moments. There are simply no words that can describe my gratitude to her.

Lastly, I'd like to thank **Pili** and **Ana** from the Scientific facilities of the UB; **Nieves, Menchu, Ismael, Soraya** and **Chema** from Agro-technological Institute of Castilla y León (ITACyL), Valladolid; **Mariate** from Instituto Nacional de Investigación y Tecnología Agraria y Alimentaria (INIA), Madrid; **Alvaro, Ian, Keaton** and **Joan** from Auburn University; and every person that contributed in a way or another in the elaboration of this PhD dissertation. I am truly grateful.



## TABLE OF CONTENTS

<b>ABBREVIATIONS .....</b>	<b>1</b>
<b>GENERAL INTRODUCTION .....</b>	<b>3</b>
<b>OBJECTIVES .....</b>	<b>17</b>
<b>REPORT OF THE THESIS DIRECTORS.....</b>	<b>21</b>
<b>CHAPTER 1. Assessing performance of European elite bread wheat cultivars under Mediterranean conditions: ideotypic implications. ....</b>	<b>31</b>
<b>CHAPTER 2. Remote sensing techniques and stable isotopes as phenotyping tools to assess wheat yield performance: effects of growing temperature and vernalization.....</b>	<b>79</b>
<b>CHAPTER 3. Durum wheat ideotypes in Mediterranean environments differing in water and temperature conditions.....</b>	<b>97</b>
<b>CHAPTER 4. Root traits determining durum wheat performance under Mediterranean conditions.....</b>	<b>115</b>
<b>CHAPTER 5. <math>\delta^2\text{H}</math> and <math>\delta^{18}\text{O}</math> assessment of transpirative and photosynthetic performance in wheat under different humidity conditions. ....</b>	<b>191</b>
<b>GENERAL DISCUSSION .....</b>	<b>235</b>
<b>GENERAL CONCLUSIONS.....</b>	<b>253</b>
<b>RESUMEN GENERAL DE LA TESIS.....</b>	<b>259</b>
<b>REFERENCES .....</b>	<b>263</b>

## LIST OF ABBREVIATIONS

$\delta^{13}\text{C}$ : carbon isotope composition	Fv'/Fm': intrinsic efficiency of photosystem II
$\delta^2\text{H}$ : hydrogen isotope composition	GN: grain number
$\delta^{15}\text{N}$ : nitrogen isotope composition	GNy: grain nitrogen yield
$\delta^{18}\text{O}$ : oxygen isotope composition	GY: grain yield
Amax: photosynthetic rate	GA: green area
Bush: root network bushiness	GGA: greener area
CCI: chlorophyll/carotenoid index	gs: stomatal conductance
CCiTUB: centres científics i tecnològics de la universitat de barcelona	HI: harvest index
Ci: sub-stomatal CO <sub>2</sub>	HSI: hue-saturation-intensity
CIELab: international commission on illumination lightness a* b*	HTPPs: high throughput phenotyping platforms
CIELuv: international commission on illumination lightness u* v*	LASSO: least absolute shrinkage and selection operator
ConvA: convex area:	Ldist: network length distribution:
CT: canopy temperature	ILP: irrigated normal planting
CTD: canopy temperature depression	INIA: Instituto Nacional de Investigación y Tecnología Agraria y Alimentaria
DM: dry matter	INP: irrigated late planting
DTA: days to anthesis	IR: infrared
DTB: days to booting	IRMS: infrared mass spectrometer
DTE: days to elongation	ITACyL: instituto técnico y agrario de castilla y león
DTH: days to heading	MaxR: maximum number of roots:
DTT: days to tillering	MedR: median number of roots:
ED: ear density	N1: 50% of the recommended N fertilization dose
ETR: photosynthetic electron transport rate	N2: the recommended N fertilization dose
EVI: enhanced vegetation index	
FIIJ: fiji is just imageJ	

N3: 30% above the recommended N fertilization dose

NBI: nitrogen balance index

Ndepth: network depth

NDVI: normalized difference vegetation index

NIRS: near infrared spectrometers

NP: normal planting

Nleaf: nitrogen concentration in the flag leaf

Nlen: network length

Ngrain: nitrogen concentration in grains

Nsurf: network surface area

Nvol: network volume

NwA: network area

NWDR: network width to depth ratio

Nwidth: network width

PCA: principal component analysis

PH: plant height

PhiPS2: quantum efficiencies of photosynthetic electron transport through photosystem II

PRIm: modified photochemical reflectance index

RA: root angle

Rccomp: number of connected components

RDW: root dry weight

RGB: red-green-blue

RF: random forest

RH: air relative humidity

RLN: rainfed normal planting and low nitrogen fertilization

RNP: rainfed normal planting and recommended nitrogen fertilization

Rwidth: average root width

SRL: specific root length

TCARI/OSAVI: transformed chlorophyll absorption reflectance index/optimized soil adjusted vegetation index

TGW: thousand grain weight

TKW: thousand kernel weight

Tr: transpiration

UAV: unmanned aerial vehicle

Vis: vegetation indices

VIF: variance inflation factor

VPD: vapor pressure deficit

WBI: water balance index





# **GENERAL INTRODUCTION**



## GENERAL INTRODUCTION

In the course of the 21<sup>st</sup> century, it is common knowledge that the Mediterranean region is prone to climate change events and its impacts on crop production. Ensuring a wheat-based food balance depends highly on wheat production and its interannual variability (Zampieri et al., 2020), particularly in the Mediterranean basin, where high seasonal variations, reduced precipitation and increased temperatures are common climatic events (IPCC, 2014). Global warming incrementation is expected to widen the gap in regional changes in mean climate, mainly in temperature, soil moisture and precipitation (Figure 1), and subsequently, these environmental factors not only would increase water demand for plants but can also decrease yield performance in grains (Bindi and Olesen, 2011). Recent studies have reported that between 5% to 20% of yield losses in wheat crop were observed for every 1 °C rise in temperature (Innes et al., 2015; Lobell et al., 2008; Mondal et al., 2013; Telfer et al., 2018; Ullah et al., 2019). Therewith, adopting an integrative approach that takes into consideration the choice of climate-resilient wheat cultivars under the influence of diverse abiotic stresses, crop management practices, and the implementation of phenotyping platforms for early assessment of events affecting crop growth, can not only mitigate the impact of climate events on productivity and yield losses, but also secure and maintain higher grain yield productions in wheat cultivars.

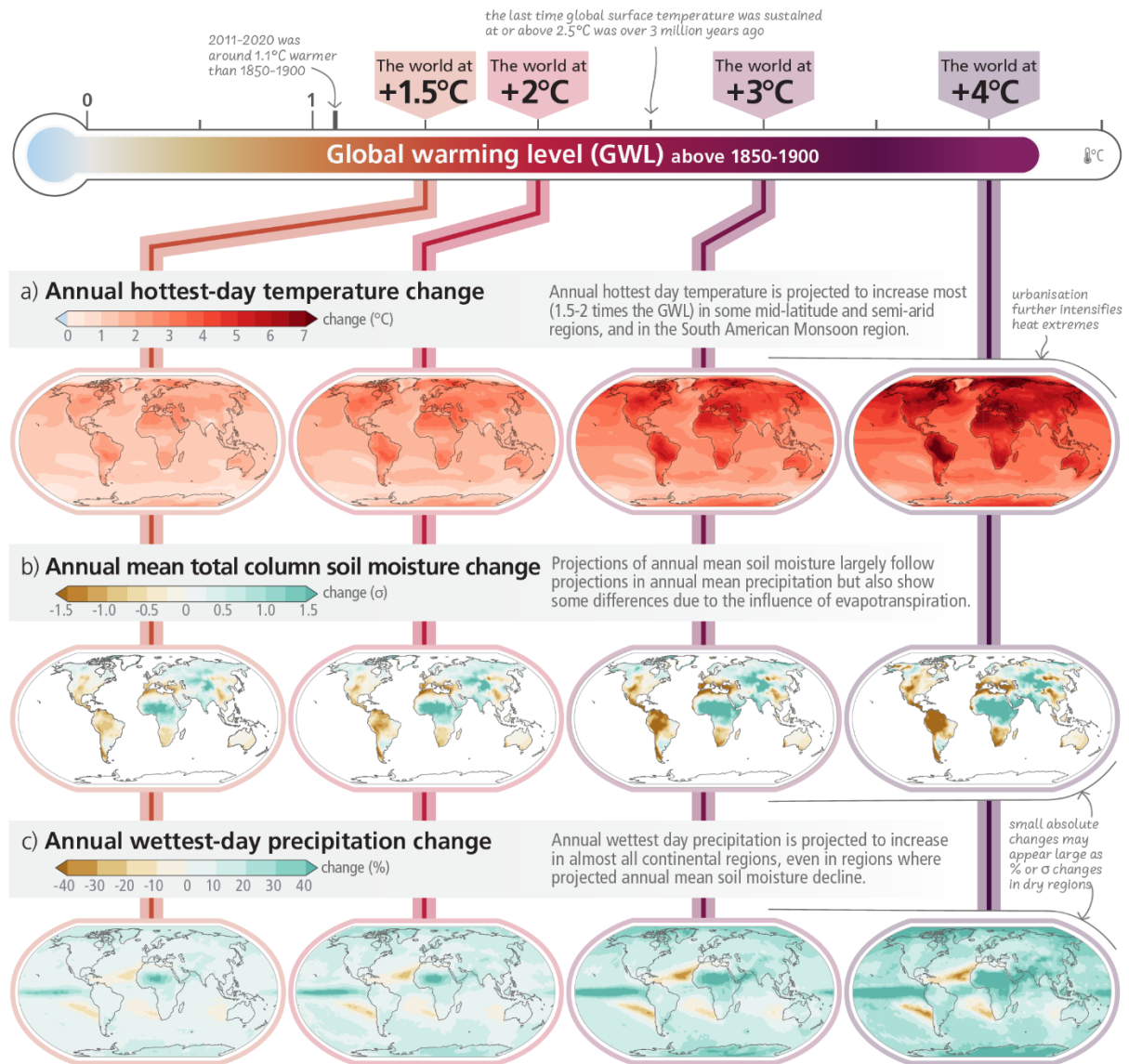


**Figure 1.** Projected changes of annual maximum daily maximum temperature, annual mean total column soil moisture and annual maximum 1-day precipitation at global warming levels of 1.5°C, 2°C, 3°C, and 4°C relative to 1850–1900. Map taken from the AR6 Synthesis Report (IPCC 2023).

Indeed, several breeding programs were launched in the late 19<sup>th</sup> century in Italy focusing mainly on bread wheat cultivars improvement. These programs targeted dwarfing, day length insensitivity and high yield potential, among other traits, and succeeded in releasing multiple varieties that were popular across and beyond the Mediterranean region. Years later, further breeding programs initiatives were dedicated to durum wheat cultivars improvement due to the high demand for pasta that the world has shown (Martínez-Moreno et al., 2020), but also because of the high adaptation of durum wheat to heat and drought conditions even under poor soils (Royo, 2005). Currently, wheat is cultivated in most parts of the world due to its

cultural and economic importance (Figure 2), with Europe holding the second position in wheat production worldwide, with a share that amounts to 33.3%, with Spain among other countries, being a main producer to wheat crop (FAOSTAT, 2021).

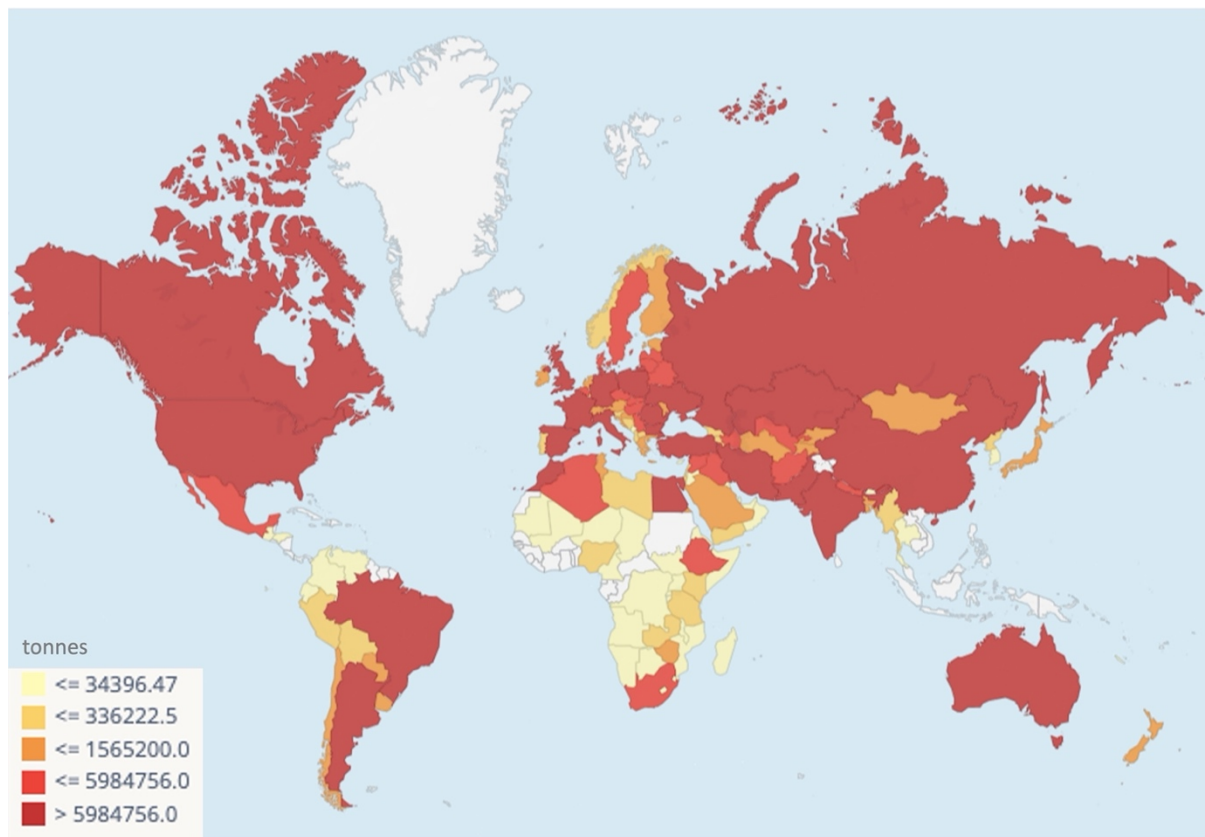


**Figure 2.** Average production quantities of wheat worldwide during 2021. Map taken from (FAOSTAT, 2021)

In addition to the choice of cultivar, crop management practices are essential to achieve the yield potential of the cultivar in question. For many decades, versatile choices of field practices were recommended especially under the Mediterranean region, those practices include among others, irrigation, sowing time, rotation, tillage, nitrogen fertilization (Incerti and O’Leary, 1990; Kirkegaard and Lilley, 2007). Unfortunately, the environmental effects driven by climate change consequences restrict the availability of mainly water and nutrients (e.g. nitrogen), which stresses the need to address water and nitrogen shortages through recurring to alternatives that are amenable to still ensure high yielding potential in wheat instead of increasing water and N fertilization supplying. To this end, observing and understanding the cultivars responsiveness to their growth conditions, may provide new insights towards tailoring climate-resilient genotypes capable of achieving higher grain yield potential with the



least possible resources, using aboveground and belowground phenotyping platforms for crop monitoring and yield prediction purposes.

### **Aboveground (canopy) phenotyping**

High throughput phenotyping platforms (HTPPs) have been widely used in the recent decades to assess different crop traits using sensors which nature ranges from conventional red-green-blue (RGB) imaging, to thermal and spectroradiometer sensors (Gracia-Romero et al., 2019; Kefauver et al., 2015, 2017; Rezzouk et al., 2020). The techniques lying behind HTPPs are known for their rapid, cost-effective and a non-invasive nature during measurement, and can be implemented from ground platforms (proximate sensing) to aerial and satellite platforms (remote sensing) (Araus et al., 2022; Araus and Cairns, 2014). The first category (i.e proximate sensing) consists of hand-held devices equipped with sensors that determine the reflectance specific to the assessed trait in wheat genotypes grown under Mediterranean conditions (Figure 3). For instance, the Greenseeker (Trimble, Sunnyvale, CA, USA) is a device usually deployed to determine the Normalized Difference Vegetation Index (NDVI) using VIS (660 nm) and NIR (780 nm) wavelengths on targeted canopy. NDVI has been often used as an indicator to green canopy biomass (Christopher et al., 2014; Fischer et al., 1998; Kipp et al., 2014; Lopes and Reynolds, 2012); Dualex (Dualex, Force-A, Orsay, France) or SPAD (Minolta SPAD-502, Spectrum Technologies Inc., Plainfield, IL, USA) are portable leaf-clip devices which operate on the leaf level to assess chlorophyll (SPAD and Dualex) and other pigment contents indices such as anthocyanin, flavonoids and NBI (Dualex) (Cerovic et al., 2012; Goulas et al., 2004; Lin et al., 2015); the infrared thermometer (PhotoTemp™ MXSTM TD Raytek®, California; USA) is another frequently used device to estimate instantly canopy temperature and infer crop water status (Amani et al., 1996; Blum et al., 1982; Gracia-Romero et al., 2019; Nielsen and Halvorson, 1991; Rezzouk et al., 2020; Yousfi et al., 2016).

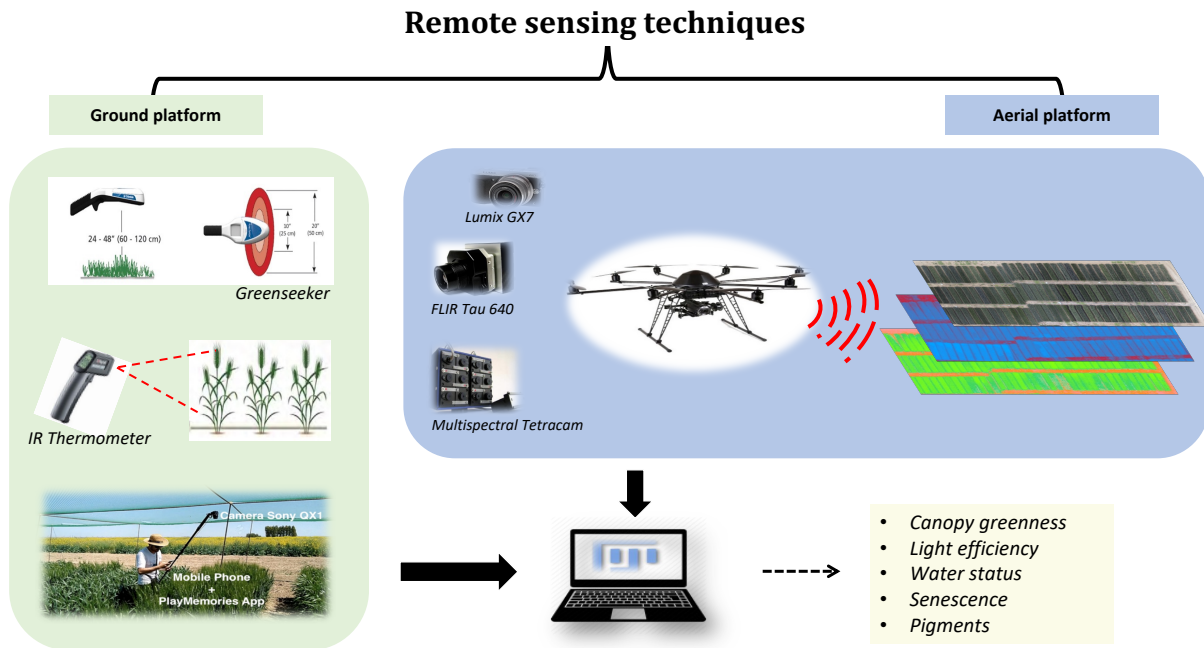


**Figure 3.** Examples of proximate and remote sensing tools to plant phenotyping.

On a larger scale, the second category (remote sensing) relies on the implementation of HTPPs from aerial platforms via the use of unmanned aerial vehicles (UAV), usually mounted with cameras equipped with near-infrared spectroscopy and spectral reflectance sensors (RGB, thermal, multispectral or hyperspectral sensors) for plant canopies (Gracia-Romero et al., 2019; Kefauver et al., 2017; Skendži et al., 2023). These HTPPs are often used for fast screening of larger populations in an affordable and non-invasive manner, and therefore suitable not only for medium size field trials, but also larger field crops dedicated to breeding purposes (Figure 3). Besides UAVs, implementation of satellites-based sensors for special screening and crop monitoring has been well documented in the recent decades (Belgiu et al., 2023; Segarra et al., 2020).

### Belowground (Root) phenotyping

Differently from remote sensing high throughput phenotyping platforms (HTPPs). Root phenotyping techniques are viewed as average to low throughput because of the high cost and the low effectiveness of the platforms implemented, the laborious nature of root excavation and the low accuracy of the derived traits. Nevertheless, root phenotyping is becoming more necessary than before to understand roots responsiveness to a target environment, with the aim to identify root traits that can potentially enable plants to have

better access to soil water and nutrients and provide higher yielding under the Mediterranean growth conditions (Araus et al., 2022; Atkinson et al., 2019). To this end, Shovelomics and soil coring are common root phenotyping techniques, among others, that are used together to study directly roots root crown architecture characteristics (shovelomics) and distribution (soil coring) in wheat genotypes when grown under Mediterranean field conditions (Atkinson et al., 2019; Bucksch et al., 2014; Ober et al., 2021; York et al., 2018a, 2018b).

The study of root system characteristics in the upper layer of soil (ca. 0-20 cm) is referred to as “shovelomics” (Figure 4). This technique targets the study of the architecture, distribution and morphology of root systems and their contribution to plants productivity (Lynch, 1995). To this end, the “shovelomics” approach relies on the use of a “shovel” to excavate root system from the first 20 cm of the upper soil layer, clean the roots from soil carefully using buckets filled with water, then digitalize them in situ for later imagery use (Bucksch et al., 2014; Fradgley et al., 2020; Rezzouk et al., 2022; Wasson et al., 2016). Shovelomics derived traits reveal pertinent information on root morphology such as root diameter (Price et al., 2002) root specific length (Eissenstat, 1991), root angle and the number of crown roots (Rezzouk et al., 2022; York et al., 2018a, 2018b). Understanding how these morphological traits integrate in an overall root system to respond to given conditions (Wasaya et al., 2018), and which root traits are involved in determining the level of root plasticity (Malamy, 2005), facilitate targeting specific root traits that may be amenable to consider in breeding programs with the aim to achieve higher productivity (Lynch, 1995).

Besides root characteristics in the topsoil layer, root distribution and intensity are often assessed using soil coring, as this technique provides an accurate measurement to not only root length and mass and their relationship with water and nutrient uptake, but also moisture content and the subsequent root water uptake (Pask et al., 2012; Reynolds et al., 2012). Soil coring is usually carried out either by using a hand corer, or by a tractor-mounted hydraulic soil corer. In both cases, the inserted corer cylinders are pushed downwards the soil to reach the desired depth then laid out for observation and soil moisture and root samplings. The sampling can be tedious in the sense that in the extracted cores, soil is manually washed away to isolate roots. Afterwards, roots are dyed and scanned for further traits extraction, and their subsequent root dry weight is assessed (Figure 4). Rooting depth can be influenced by several environmental factors such as soil type and limitations (Tennant and Hall, 2001), reduced

rainfall season and the subsequent incomplete wetting of the soil profile (Henderson, 1991; Tennant, 1976), or agronomic crop management techniques such as delayed sowing (Barraclough and Leigh, 1984; Incerti and O’Leary, 1990) and nitrogen fertilization (Incerti and O’Leary, 1990). Identifying roots distribution along the soil profile provides a better understanding to the potential soil zone from which roots uptake soil and nutrients, and the implications of roots functionality for crop productivity (Kirkegaard and Lilley, 2007).

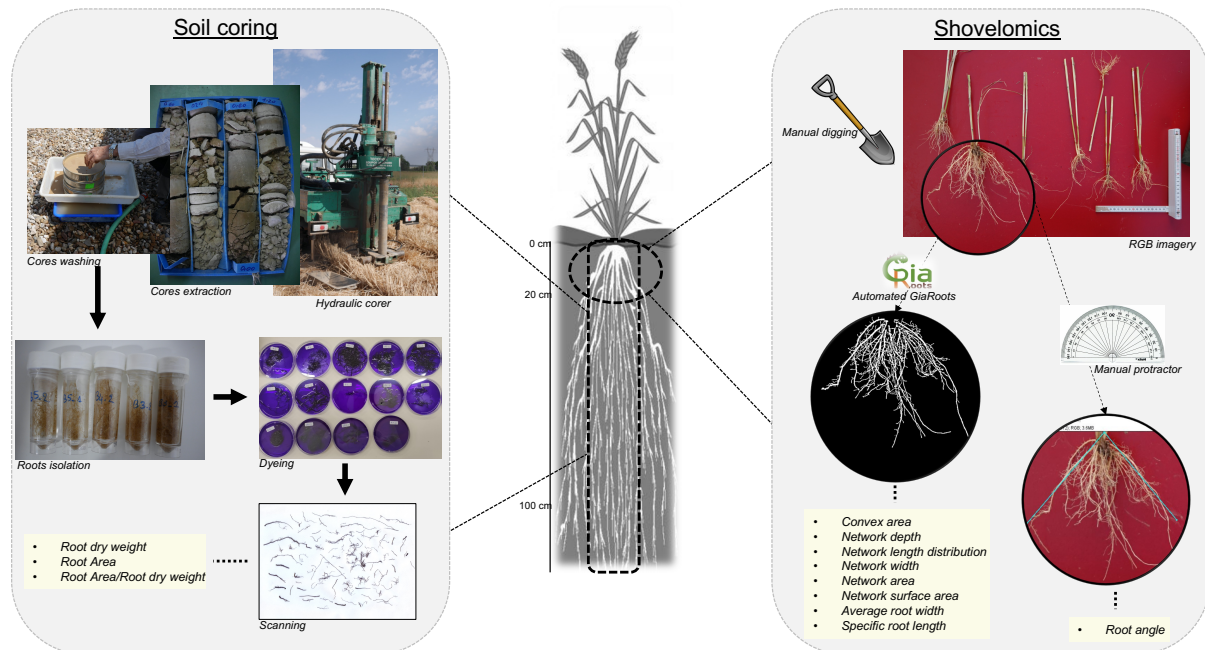


**Figure 4.** Shovelomics and soil coring approaches to root phenotyping

Given the laborious and time ineffectiveness of the above-mentioned techniques, imagery processing has been a frequent complementing phenotyping technique to root phenotyping for a quicker assessment of the desired root traits (Araus et al., 2022; Chen et al., 2017). A broad spectrum of root phenotyping softwares has been developed to assess roots traits from both 2D and 3D representations, ranging from manual to semi-automated and automated programs (Araus et al., 2022; Clark et al., 2011; Iyer-Pascuzzi et al., 2010).

### Stable isotope Compositions

Stable isotopes have been often used as physiological traits to study plants response to their environment. The assessment of carbon and nitrogen isotope compositions in plant tissues, mainly the flag leaf and mature grains in wheat crop, provides an estimation to nitrogen and water status in genotypes, while the assessment of oxygen and hydrogen isotope

compositions facilitates information on the water source extracted by plants when measured in the stem basis, and roots functionality across the soil profile when measured in different soil sections/depths.

### *Carbon isotope composition*

Craig in 1954 was the first to suggest the presence of a  $\delta^{13}\text{C}$  depleted process in leaves as a response to environmental effects (Craig, 1954). Park and coworker in 1960 later introduced a  $\delta^{13}\text{C}$  fractionating model attributed to carbon isotope composition and relying on three fundamentals:  $\text{CO}_2$  diffusion, photosynthesis and secondary metabolism (Park and Epstein, 1960). And only two decades later, O' Leary (1981) and Farquhar and coworkers (1982) proposed a more detailed  $\delta^{13}\text{C}$  model that can be used in crop ecophysiology. Naturally, plants prioritize the assimilation of lighter carbon isotope  $^{12}\text{C}$  over the heavy isotope  $^{13}\text{C}$ , which is more abundant in the air (Farquhar et al., 1982; O'Leary, 1981). Thus, the depletion in  $\delta^{13}\text{C}$  observed plant tissue is the consequence of different fractionation processes occurring during transpiration ( $\text{CO}_2$  diffusion) and photosynthesis ( $\text{CO}_2$  fixation), especially in  $\text{C}_3$  plants studies where  $\text{CO}_2$  concentrations limit photosynthesis (Beerling and Woodward, 1995; Park and Epstein, 1960; Polley et al., 1993). Depending on the environmental and genotypic effects, important differences in  $\delta^{13}\text{C}$  can be found in distinct plant tissues informing on the integrated  $\delta^{13}\text{C}$  isotopic signal during the assessed development stage (Araus et al., 1992; Condon et al., 1992). Under drought conditions,  $\delta^{13}\text{C}$  are considered as an excellent indicator to plant water status and the effective use of water in crops (Blum, 2009). Its time-integrative character throughout the crop growth cycle offers an overall estimation to the water status the plant has undergone, especially when measured during the last stage of development, such as mature grains in wheat. Furthermore, the nature of  $\delta^{13}\text{C}$  fractionation processes which integrates transpiration and photosynthesis not only reflects plants evapotranspiration processes, but also allows a better understanding to grain yield performance in wheat genotypes. Several studies reported the strong correlations between  $\delta^{13}\text{C}$  and stomatal conductance (Barbour, 2007; Farquhar et al., 1982) and grain yield (Araus et al., 2013; Chairi et al., 2018; Rezzouk et al., 2020).

*Nitrogen isotope composition*

For decades,  $\delta^{15}\text{N}$  was used as a nitrogen tracer in applied fertilization (Bremner, 1965; Hoering, 1955). And years later, more studies were introduced on the utility of  $\delta^{15}\text{N}$  to determine nitrogen source in plants (fixation, organic or chemical) (Kohl et al., 1973; Shearer and Kohl, 1978).  $\delta^{15}\text{N}$  Fractionation processes involved in plant tissues are associated mainly with  $\text{NO}_3^-$  and  $\text{NH}_4^+$  assimilation, nitrogen transportation upwards plant tissues, and nitrogen metabolism occurring in the cytoplasm. Interpretations of  $\delta^{15}\text{N}$  values can be sometimes confusing given that (i) the atmospheric  $\text{N}_2$  which is used as a reference to calculate nitrogen isotope composition reflects a  $\delta^{15}\text{N}_{\text{Air}} = 0\text{‰}$ , therefore isotopic analysis must be carried out with caution to avoid possible contamination source; and (ii), several factors can present low  $\delta^{15}\text{N}$  values that are close to the atmospheric reference  $\text{N}_2$ , for instance  $\delta^{15}\text{N}$  associated with  $\text{NO}_3^-$  ranges from 0.3‰ to 3‰,  $\delta^{15}\text{N}$  of chemical fertilizers are around 0‰, and  $\delta^{15}\text{N}$  in crops with  $\text{N}_2$  fixation fractionation process oscillate between -0.4‰ and 4.1‰ (Kohl and Shearer, 1980; Mateo et al., 2004; Wada and Hattori, 1978). Regardless,  $\delta^{15}\text{N}$  is still a relevant indicator to nitrogen source when plants are fertilized with organic matter, which is known for its high  $\delta^{15}\text{N}$  values (up to 15‰). Or as reliable nitrogen status indicator when plants are supplied with chemical fertilizers and grown under well-watered conditions. In fact,  $\delta^{15}\text{N}$  increases were associated with higher production in wheat genotypes under optimal growth conditions with supplied N fertilization and irrigation (Rezzouk et al., 2022; Sanchez-Bragado et al., 2017; Yousfi et al., 2009).

*Oxygen and hydrogen isotope compositions*

Oxygen ( $\delta^{18}\text{O}$ ) and hydrogen ( $\delta^2\text{H}$ ) isotope composition studies started with the analysis of those elements in continental and marine waters (Dansgaard, 1964), before oxygen and hydrogen were introduced in plant ecophysiology. Gonfiantini and coworkers were pioneers to demonstrate that leaf water was enriched in heavy isotopes during transpiration (Gonfiantini et al., 1965). And since then, several studies were carried out highlighting the importance of  $\delta^{18}\text{O}$  and  $\delta^2\text{H}$  in different disciplines, paleoclimatic reconstruction from tree rings, ecophysiology of plant water loss, plant breeding for an improved water status, and the identification of the origin of plant tissue (Barbour, 2007; Epstein et al., 1977).

Soil and metabolic water evaporative processes are the main factors affecting  $\delta^{18}\text{O}$ , whereas evaporative but especially photosynthesis processes, are the major factors determining  $\delta^2\text{H}$ . Previous studies reported that most oxygen that was incorporated by plant during photosynthesis originated from the water source, likewise, water source is the only source of organic hydrogen in plants (DeNiro and Epstein, 1979; Mateo et al., 2004); albeit the isotopic signature of water source can vary considerably depending on precipitation and/or irrigation, or in a minimal importance through the temporal evaporation that occurs from the soil surface before root water uptake. Besides the water source, the water isotopic signatures of different plant tissues (e.g. leaves, ears or grains) vary from the stem isotopic signature as a consequence of post-photosynthetic processes such as stomatal diffusion, the Peclet number and its influence on transpiration, the leaf blade layer which comprises both stomatal diffusion and stomatal pores effects, and the proportional depression of water vapor by the heavier  $\text{H}_2^{18}\text{O}$  molecules (Barbour et al., 2004; Farquhar and Lloyd, 1993; Ogée et al., 2007). In the organic matter of plant tissues,  $\delta^{18}\text{O}$  and  $\delta^2\text{H}$  signatures are rather different.  $\delta^{18}\text{O}$  isotopic signature is enriched in leaves, ears and grains above the stem water signature as a result of a complete exchange with water before fixation in organic compounds (Helliker and Ehleringer, 2002). In the case of hydrogen, the resulted isotopic signature is the mixture of the remarkably depleted  $\delta^2\text{H}$  values as a result of photosynthesis processes, and the enriched  $\delta^2\text{H}$  originating from the transported water. Depends on plant trophism, autotrophic organs (such as leaves and ears) can show highly depleted  $\delta^2\text{H}$  signature, whereas in heterotrophic organs (e.g. grains),  $\delta^2\text{H}$  signatures are rather enriched (Estep and Hoering, 1981; Yakir and DeNiro, 1990).

In summary, this present dissertation focused on the implementation of integrative approaches to evaluate the performance of wheat genotypes grown under different Mediterranean conditions (Figure 5). These approaches consisted in a first step in the assessment of aboveground traits using vegetative indices (HTPPs) to predict grain yield (Rezzouk et al., 2020) and define ideotypes from European elite bread wheat cultivars under Mediterranean conditions (Rezzouk et al., 2023; submitted), and in a second step in the assessment of combined above and belowground traits together with physiological traits, mainly phenology, stable isotope compositions and photosynthesis, for further ideotypic implications in durum wheat cultivars grown under different Mediterranean conditions (Rezzouk et al., 2022; Rezzouk et al., 2023 “submitted”).

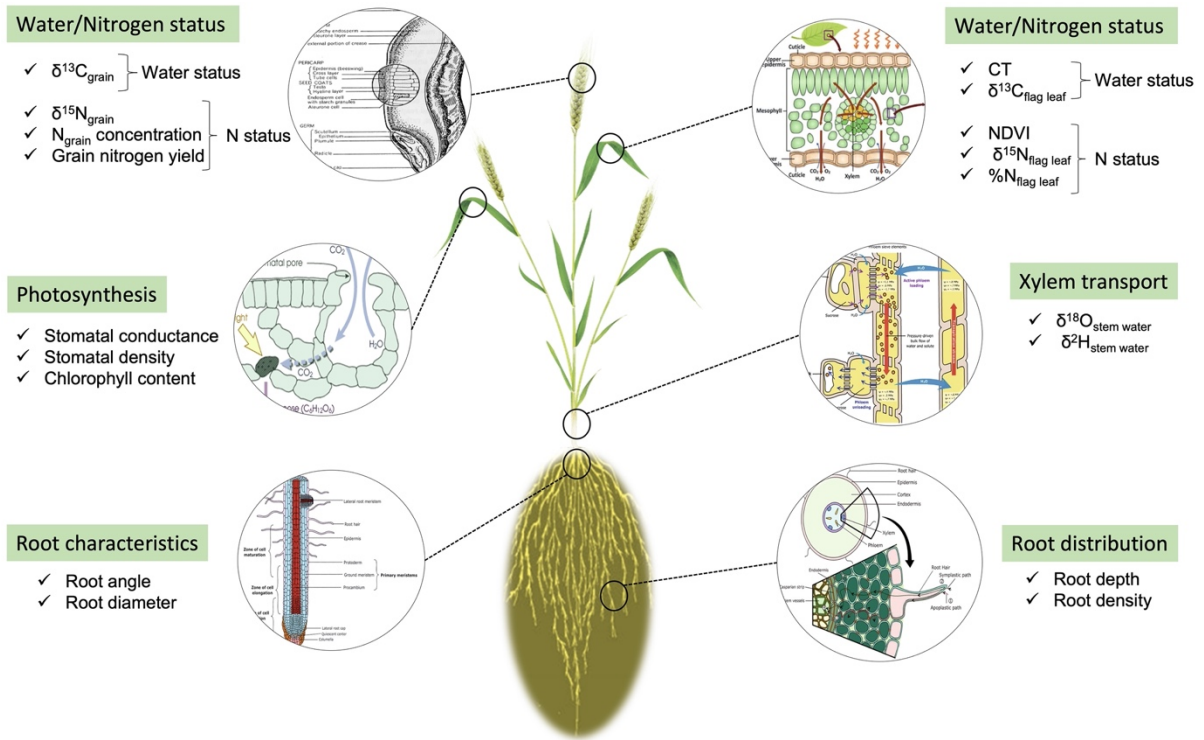


**Figure 5.** Physiological and morphological traits that can potentially explain crop responsiveness to its target environment and contribute to yield prediction in wheat genotypes grown under Mediterranean conditions.







## **OBJECTIVES**



## OBJECTIVES

The main objective of the present dissertation aims to identify ideotypic characteristics of Wheat genotypes with better climate-resilience and higher yielding when grown under different Mediterranean climate and growth conditions. To this end, an integrative phenotyping approach was implemented targeting canopy growth using remote sensing techniques, root architecture and distribution through root phenotyping techniques, and yield components together with the assessment of water and nitrogen status in different plant tissues, using mainly carbon and nitrogen isotope compositions in flag leaves and grains, and oxygen and hydrogen isotope compositions in stem water and soil profile. A further mechanistic objective was to assess the performance of hydrogen and oxygen isotope compositions ( $\delta^2\text{H}$  and  $\delta^{18}\text{O}$ ) in different plant tissues and under different relative humidity conditions, and to track the loading and unloading of water and sugar compounds from source to sink tissues.

### Specific aims

- The first chapter aimed to identify ideotypic traits conferring the adaption of high-yielding European bread wheat cultivars (*Triticum aestivum* L.) to the Mediterranean conditions. To this end, phenology, water and nitrogen status were assessed to identify traits contributing to high yielding performance in European wheat cultivars under Mediterranean conditions. This study has been submitted to Field Crop Research.
- The focus of the second chapter was to compare the performance of spring and facultative bread wheat genotypes (*Triticum aestivum* L.) under different growing temperatures and vernalization needs. Different physiological traits were assessed using vegetation indices and stable isotopes, and further combined with phenology, crop growth and yield components. Lastly, grain yield was predicted using all the assessed traits. This study has been published in Plant Science.
- The third chapter proposed ideotypic characteristics of durum wheat (*Triticum turgidum* L. *subsp. durum* (Desf) Husn.) associated with higher yield under different water and temperature regimes were studied under Mediterranean conditions. Different phenotyping approaches were combined from plants aboveground and belowground traits to identify ideotypic characteristics associated with a better genotypic performance

in durum wheat grown in Spain. This work has been published in *Agricultural Water Management*.

- The fourth chapter focused on identifying root traits determining durum wheat performance under Mediterranean conditions. Root phenotyping assessment was carried out together with the use of stable isotopes to assess nitrogen status, water status and water of the stem, precipitation and irrigation, and water of different soil depths). Those traits were combined with growth traits, yield components and grain yield. This work has been submitted to *Science of The Total Environment*.
- The fifth chapter focused on the performance of hydrogen and oxygen isotope compositions ( $\delta^2\text{H}$  and  $\delta^{18}\text{O}$ ) across the water and the organic matter of different plant tissues and under different vapor pressure deficit levels (high vs low VPDs). The main objective was to trace the loading and unloading of water and sugar compounds from source to sink tissues. This work has not been yet submitted.



# **REPORT OF THE THESIS DIRECTORS**



## REPORT OF THE THESIS DIRECTORS

Integrative Crop Ecophysiology Group

<https://integrativecropecophysiology.com>

Plant Physiology Section, Department of Evolutionary Biology, Ecology and  
Environmental Sciences, Faculty of Biology, University of Barcelona, Diagonal 643,  
08028, Barcelona, Spain.

Dr. José Luis Araus Ortega and Dra. Maria Dolors Serret Molins, as supervisors of the thesis entitled: “**Root traits and stable isotopes as phenotyping approaches to enhance wheat adaptation to Mediterranean conditions**”, that has developed the doctoral student Fatima Zahra Rezzouk,

INFORM about the impact and participation of the doctoral student in each of the papers included in the memory of the Doctoral Thesis.

**Chapter 1.** The article entitled “Assessing performance of European elite bread wheat cultivars under Mediterranean conditions: ideotypic implications” has been submitted to **Field crop Research in 2022** with an impact factor of 6.145, which corresponds to the first decile within the Science Area: Agricultural and Biological Sciences: Agronomy and Crop Science. In this study, Phenology and stable isotopes were used as phenotyping traits to identify ideotypic traits of high-yielding European wheat cultivars conferring adaption to actual Mediterranean conditions. The main findings are the need to rationalize N fertilization supply within the region, the interactive effect of season (wet vs dry) on phenological adjustment in selected high yielding European bread wheat genotypes, including genotypes bred for northern and central Europe conditions, as potential material for genetic increase under the Mediterranean conditions. Fatima Zahra Rezzouk conducted the stable isotope analyses, processed the collected data and she was responsible for the draft writing.

**Chapter 2.** The article entitled “Remote sensing techniques and stable isotopes as phenotyping tools to assess wheat yield performance: effects of growing temperature and



vernalization” published in **Plant Science in 2020** with an impact factor of 4.729 in 2020, is a journal placed within the first decile of the Science Area: Agricultural and Biological Sciences: Plant Science. To date, this work has accumulated 20 citations (Google Scholar, revised in June 2023). This study compared grain yield performance under optimum conditions and high temperature conditions, using an integrated phenotyping approach of high throughput phenotyping platforms (HTPPs), including remote sensing together with stable isotopes and nitrogen concentration as physiological phenotyping techniques. Overall, each phenotyping approach proved its efficiency at detecting genotypic differences in a set of 38 wheat bread wheat cultivars, with the best GY prediction achieved by the combination of remote sensing and stable isotopes. The study proposes also, the facultative genotypes as potential plant material with key traits that are best adapted to drought conditions. Herein, Fatima Zahra Rezzouk processed and analysed the remote sensing data collected from the field, analysed the stable isotopes, gathered and processed all data and she was responsible for writing the draft.

**Chapter 3.** The article entitled “Durum wheat ideotypes in Mediterranean environments differing in water and temperature conditions” published in **Agricultural Water Management in 2022** with an impact factor of 6.611 in 2022, is a journal placed within the first decile of the Science Area: Agricultural and Biological Sciences: Agronomy and Crop Science. To date, this work has accumulated 11 citations (Google Scholar, revised in June 2023). This work suggested specific ideotypes to different scenarios of the Mediterranean environment. Therefore, phenology, growth traits, water status, photosynthetic capacity and root characteristics in the topsoil were assessed to evaluate the performance of grain yield in durum wheat cultivars. Fatima Zahra Rezzouk had an active role in field measurements, processed image data collected from shovelomics, analysed the stable isotopes, processed all data and she was responsible for writing the draft.

**Chapter 4.** The article entitled “Root traits determining durum wheat performance under Mediterranean conditions” has been submitted to **Science of The Total Environment in 2023** with an impact factor of 10.754, which is a journal placed within the first decile of the Science Area: Environmental Science: Environmental Engineering. This work focused on evaluating yield performance in durum wheat cultivars through the assessment of aerial and root traits. Aerial assessment provided information on water and nitrogen status together with crop

growth traits, whereas root phenotyping covered the morphological characteristics of roots in the topsoil, roots distribution across soil sections to up to one meter, as well as root functioning through the assessment of oxygen and hydrogen isotope compositions in the stem water, water sources (irrigation and precipitation) and soil water. Fatima Zahra Rezzouk had an active role in field measurements, analysed root traits and processed the corresponding image data, conducted stables isotope analyses and she was responsible for writing the draft.

**Chapter 5.** The article entitled “ $\delta^2\text{H}$  and  $\delta^{18}\text{O}$  assessment of transpirative and photosynthetic performance in wheat under different humidity conditions” is a draft in preparation. The main objectives of this work were to study the factors responsible for hydrogen and oxygen isotope compositions ( $\delta^2\text{H}$  and  $\delta^{18}\text{O}$ ) fractionation patterns in the water as well as organic matter of plant tissues, and which affect the load and unload of nutrients from source to sink organs. To respond to these objectives, a drought tolerant and high yielding durum wheat cultivar “*Sula*” was evaluated under contrasting and controlled VPD conditions, and a dual isotope labelling method was applied to trace oxygen and hydrogen isotope compositions ( $\delta^2\text{H}$  and  $\delta^{18}\text{O}$ ) across plant tissues. Fatima Zahra Rezzouk participated in stables isotope analyses, curated and processed all data and she was responsible for writing the draft.

It should be noted that Engineer Fatima Zahra Rezzouk, since she arrived in Barcelona, has integrated perfectly into our team. She has collaborated autonomously in the realization of all the experiments of her doctoral thesis participating in their design, data collection, chemical analysis, statistical treatment, preparation of tables and figures, discussion of results and writing of publications. The doctoral student has shown a great capacity for work, both in the laboratory and field. As a result of these years of work, she has reached a high level of maturity and knowledge on the subject, in addition to having demonstrated an initiative and capacity for work. As a result, she published and co-authored the following publications:

**Publications:**

- **Rezzouk, F.Z.,** Shahid, M.A., Elouafi, I.A., Zhou, B., Araus, J.L., Serret, M.D., 2020. Agronomic performance of irrigated quinoa in desert areas: Comparing different approaches for early assessment of salinity stress. *Agric. Water Manag.* 240, 1–15. <https://doi.org/10.1016/j.agwat.2020.106205>

- **Rezzouk, F.Z.**, Shahid, M.A., Elouafi, I.A., Zhou, B., Araus, J.L., Serret, M.D., 2020. Agronomical and analytical trait data assessed in a set of quinoa genotypes growing in the UAE under different irrigation salinity conditions. *Data Br.* 31, 1–11. <https://doi.org/10.1016/j.dib.2020.105758>
- **Rezzouk, F.Z.**, Gracia-Romero, A., Kefauver, S.C., Nieto-Taladriz, M.T., Dolores, M., Araus, J.L., 2022. Dataset of above and below ground traits assessed in Durum wheat cultivars grown under Mediterranean environments differing in water and temperature conditions. *Data Br.* 40, 1–6. <https://doi.org/10.1016/j.dib.2021.107754>
- de Lima, V.J., Gracia-romero, A., **Rezzouk, F.Z.**, Díez-fraile, M.C., Araus-Gonzalez, I., Henrique Kamphorst, S., Teixeira do Amaral Júnior, A., Kefauver, S.C., Aparicio, N., Araus, J.L., 2021. Comparative performance of high-yielding european wheat cultivars under contrasting mediterranean conditions. *Front. Plant Sci.* 12, 1–19. <https://doi.org/10.3389/fpls.2021.687622>
- Araus, J.L., **Rezzouk, F.Z.**, Thushar, S., Shahid, M., Elouafi, I.A., Bort, J., Serret, M.D., 2021. Effect of irrigation salinity and ecotype on the growth, physiological indicators and seed yield and quality of *Salicornia europaea*. *Plant Sci.* 304, 1–13. <https://doi.org/10.1016/j.plantsci.2021.110819>
- Araus, J.L., Kefauver, S.C., Vergara-Díaz, O., Gracia-Romero, A., **Rezzouk, F.Z.**, Segarra, J., Buchailot, M.L., Chang-Espino, M., Vatter, T., Sanchez-Bragado, R., Fernandez-Gallego, J.A., Serret, M.D., Bort, J., 2022. Crop phenotyping in a context of global change: What to measure and how to do it. *J. Integr. Plant Biol.* 64, 592–618. <https://doi.org/10.1111/jipb.13191>
- Kamphorst, S.H., Amaral Júnior, A.T. do, Vergara-díaz, O., Gracia-romero, A., Fernandez-gallego, J.A., Chang-espino, M.C., Buchailot, M.L., **Rezzouk, F.Z.**, de Lima, V.J., Serret, M.D., Araus, J.L., 2022. Heterosis and reciprocal effects for physiological and morphological traits of popcorn plants under different water conditions. *Agric. WATER Manag.* 261, 1–14. <https://doi.org/10.1016/j.agwat.2021.107371>
- Caldelas, C., **Rezzouk, F.Z.**, Aparicio-Gutiérrez, N., Araus, J.L., 2023. Interaction of genotype, water availability, and nitrogen fertilization on the mineral content of wheat grain. *Food Chem.* 404, 1–9. <https://doi.org/10.1016/j.foodchem.2022.134565>
- Martínez-Peña, R., **Rezzouk, F. Z.**, Díez-Fraile, M. D. C., Nieto-Taladriz, M. T., Araus, J. L., Aparicio, N., Vicente, R., 2023. Genotype-by-Environment Interaction for Grain Yield

and Quality Traits in Durum Wheat: Identification of Ideotypes Adapted to the Spanish Region of Castile and León. Available at SSRN 4422030.

- Araus, J.L., **Rezzouk, F.Z.**, Sanchez-Bragado, R., Aparicio-Gutiérrez, N., Serret, M.D., 2023. Phenotyping genotypic performance under multistress conditions: Mediterranean wheat as a case study. *Field Crop Research* (Under review).
- Gracia-Romero, A., Vatter, T., Kefauver, S.C., **Rezzouk, F.Z.**, Segarra, J., Nieto-Taladriz, M.T., Aparicio, N., Araus, J.L., 2023. Defining durum wheat ideotypes adapted to Mediterranean environments through remote sensing traits. *Plant Phenomics* (Submitted).
- Hamdane, Y., Segarra, J., Buchailot, M.L., **Rezzouk, F.Z.**, Gracia-Romero, A., Vatter, T., Benfredj, N., Arslan, R.H., Aparicio Gutiérrez, N., Torró, I., Araus, J.L., Kefauver, S.C., 2023. Using ground and UAV vegetation indexes for the selection of fungal resistant bread wheat varieties. *Drones* (accepted).
- Baslam, M., Takamatsu, T., Aycañ, M., Fakhet, D., **Rezzouk, F.Z.**, Gakière, B., Araus, J.L., Aranjuelo, I., Mitsui, T., 2023. Functional traits of field-droughted contrasting rice genotypes reveal multiple independent genomic adaptations and metabolic responses. *Environmental and Experimental Botany* (Submitted).
- Araus, J.L., Gascón, M., Ros-Sabé, E., Piqué, R., **Rezzouk, F.Z.**, Aguilera, M., Voltas, J., Terradas, X., Palomo, A., Ferrio, J.P., Antolín, F., 2023. Isotope and morphometrical evidence reveal the technological package associated with agriculture adoption in Western Europe. *Nature Plants* (Submitted).

### **Internships:**

- 05/2023-07/2023. Recipient of the grant Marie Skłodowska-Curie Actions (MSCA)/Research and Innovation Staff Exchange (RISE) (H2020-MSCA-RISE-2019)- GA-872602, as an exchange researcher in the university of Barcelona to process data and write a draft article paper on a Peanuts experiment previously conducted under drought conditions in Auburn university (AU), Alabama, USA. In collaboration with the Integrative Crop Ecophysiology Group of the University of Barcelona (UB).
- 07/2022-09/2022. Recipient of the grant Marie Skłodowska-Curie Actions (MSCA)/Research and Innovation Staff Exchange (RISE) (H2020-MSCA-RISE-2019)- GA-872602, as an exchange researcher in the university of Barcelona to conduct an

experiment on Peanuts under drought conditions in Auburn university (AU), Alabama, USA. In collaboration with the Integrative Crop Ecophysiology Group of the University of Barcelona (UB).

- 11/2020-11/2023. Recipient of a Research FI-AGAUR fellowship to develop PhD thesis titled: “Shovelomics and stable isotopic composition as phenotyping approaches to enhance drought stress resistance in Wheat genotypes” within the Integrative Crop Ecophysiology Group.

### **Trainings, courses and workshops:**

- 10/2019. Course on the Spanish language certificate with level A2, under the title: “Cursos de de lengua catalana, Básic 1”. Organized by the University of Barcelona.
- 01/2020. Workshop on “Writing effective research manuscripts”, organized by the Department of Evolutive Biology, Ecology and Environmental Sciences of the University of Barcelona, Barcelona, Spain.
- 01/2020. Course “Statistical tools for plant phenomic data analysis”, organized by IAMZ-CIHEAM with the collaboration of the European Plant Phenotyping Network (EPPN2020), Zaragoza, Spain.
- 07/2021. Virtual course ““Diseño de experimentos y uso de modelos mixtos en R”, Organized by by the Department of Evolutive Biology, Ecology and Environmental Sciences of the University of Barcelona, Barcelona, Spain.
- 02/2021-02/2023. AESA certified Drone Pilot: “A1/A3 Open Sub-Category” & AESA certified Drone Pilot: “STS Standard Scenarios”, organized by AEROCAMARAS, Barcelona, Spain.

### **Communications in symposiums and conferences**

- IV Simposio Español De Fisiologia Y Mejora De Cereales 2021. “ $\delta^{18}\text{O}$  and  $\delta^2\text{H}$  isotope labelling as a tracking method to assess evaporative and photosynthetic wheat performance” (Oral presentation). December 16th and 17th, 2021 (Pamplona, Spain).
- III Simposio Español De Fisiologia Y Mejora De Cereales 2020. “Durum wheat ideotypes to Spanish environments differing in water and temperature conditions” (Virtual Oral presentation). September 1st, 2nd and 3rd, 2020 (Pamplona, Spain).

- II Simposio Español De Fisiología Y Mejora De Cereales 2019. “Remote sensing techniques and stable isotopes as phenotyping tools to assess wheat yield performance: effects of growing temperature and vernalization needs” (Oral presentation). September 6<sup>th</sup> and 7<sup>th</sup>, 2019 (Cordoba, Spain).
- Evolution Of Mediterranean Agriculture (AGYA). “Wheat phenotyping: combining phenotyping techniques (HTPPs) and isotopic signature for an enhanced yield prediction”. (Oral Presentation & Poster). November 22<sup>th</sup> and 23<sup>th</sup>, 2018 (Barcelona, Spain).
- III Jornada De Joves Investigadors De L’IdRA. “Phenotyping under drought stress” (Oral presentation). May 24<sup>th</sup>, 2018. <http://www.ub.edu/ubtv/video/phenotyping-under-drought-stress-fatima-zahra-rezzouk-i-adrian-graciaromero>.
- KAAB International Symposium 2018. “Remote sensing techniques and stable isotopes as phenotyping tools to assess wheat yield performance: effect of growing temperature and vernalization needs”. (Oral presentation). September 27<sup>th</sup>, 2018 (Niigata/Japan).

To certify this for corresponding purposes,



Dr. José Luis Araus Ortega



Dr. Maria Dolores Serret





## CHAPTER I

# **Assessing performance of European elite bread wheat cultivars under Mediterranean conditions: ideotypic implications**

Fatima Zahra Rezzouk, Valter Jario del Lima, Maria Carmen Diez-Fraile, Nieves Aparicio, Maria Dolors Serret, José Luis Araus

Submitted to:  
Field Crop Research





## **Assessing performance of European elite bread wheat cultivars under Mediterranean conditions: ideotypic implications**

Fatima Zahra Rezzouk<sup>1,2</sup>, Valter Jário del Lima<sup>3</sup>, Maria Carmen Diez-Fraile<sup>4</sup>, Nieves Aparicio<sup>4</sup>, Maria Dolores Serret<sup>1,2</sup>, José Luis Araus<sup>1,2\*</sup>

<sup>1</sup>*Integrative Crop Ecophysiology Group, Plant Physiology Section, Faculty of Biology, University of Barcelona, Spain*

<sup>2</sup>*AGROTECNIO (Center for Research in Agrotechnology), Lleida, Spain*

<sup>3</sup>*Laboratório de Melhoramento Genético Vegetal, Centro de Ciências e Tecnologias Agropecuárias (CCTA), Universidade Estadual do Norte Fluminense Darcy Ribeiro – UENF, Campos dos Goytacazes, Brazil*

<sup>4</sup>*Agro-technological Institute of Castilla y León (ITACyL), Valladolid, Spain*

### **Highlights**

- Recommended N topdressing levels place wheat fertilization in the saturation zone.
- Genotypic yield performance is associated with higher grain number rather than weight.
- Crop duration and phenology are key to adapting genotypes to Mediterranean conditions.
- Regardless of the season, the best genotypes exhibit better water status (lower  $\delta^{13}\text{C}$ ).
- Some northern European wheat cultivars are well adapted to Mediterranean conditions.

### **Abstract**

#### **1. CONTEXT OR PROBLEM**

Identifying traits conferring high yield in target environments has become a main concern of wheat breeders. This is particularly relevant for the current Mediterranean conditions as well as for the expected scenarios driven by climate change for central and northern Europe.

#### **2. OBJECTIVE OR RESEARCH QUESTION**

The objective of this study was to identify ideotypic traits conferring adaption of high-yielding European wheat cultivars to actual Mediterranean conditions.

### 3. METHODS

Twelve elite winter wheat cultivars from different European (northern, central and southern) regions were grown under Mediterranean continental conditions across three consecutive crop seasons and three different topdressing nitrogen fertilization levels. Phenology was assessed throughout the crop cycle. At maturity, grain yield (GY), grain number and thousand grain weight were determined. Further, carbon ( $\delta^{13}\text{C}$ ) and nitrogen ( $\delta^{15}\text{N}$ ) stable isotope compositions and nitrogen concentration were analyzed in mature grains as proxies for water and nitrogen status, respectively.

### 4. RESULTS

The nitrogen fertilization effect was minor for GY compared with the season and genotypic effects. Concerning genotypic performance, the effect of phenology varied across seasons, with longer crop durations being associated with higher GY under the wettest season (2017-2018), no effect under mildly wet conditions (2019-2020) and being negatively associated with GY under dry conditions (2018-2019). Furthermore, the relative duration of each phenological stage had an effect on genotypic performance, particularly during the dry season (2018-2019). Moreover, regardless of the season considered, the highest-yielding genotypes were associated with better water status (lower  $\delta^{13}\text{C}$ ). Under wet season conditions, northern European genotypes had 6% higher yields, whereas in the dry season, southern European genotypes had 2% higher yields.

### 5. CONCLUSIONS

The differences in GY among the top wheat cultivars originating from different European regions were fairly minor across the seasons and across the N fertilization levels recommended in the region.

### 6. IMPLICATIONS OR SIGNIFICANCE

The study suggests that selection for the high-yielding conditions of central and northern Europe also delivers genetic increases under Mediterranean water stress conditions.

Keywords: drought, nitrogen fertilization, phenology, stable isotopes, wheat.

## 1. Introduction

While wheat remains the main staple crop globally, with Europe's 33.2% production share making it the second largest producer (FAOSTAT, 2022), wheat production must overcome the challenges imposed by climate change. In particular, wheat production in southern Europe has been conditioned with high temperatures and decreased rainfall, whereas in central and northern Europe, temperature and variability in water conditions are evolving to resemble current Mediterranean conditions (Bindi and Olesen, 2011).

The mechanisms that may contribute to higher yield and/or more stable wheat yields include matching crop development with environmental conditions, which is known as phenological adjustment (Hyles et al., 2020; Rezzouk et al., 2022). The second aspect to consider is that crop yield depends on the availability of resources (i.e. water and nutrients, in addition to the accumulated radiation) captured by the crop during its cycle (Araus et al., 2008). For instance, in the case of water, the amount captured is known as effective use of water (Blum 2009), and is key in determining yield (Araus et al., 2008; Blum, 2009). Thus, providing that resources are always available for the crop (i.e. optimal agronomic conditions), the longer the crop remains active, the more resources will be captured, and the greater the levels of crop photosynthesis, and so the resulting grain yield will be higher. This is the case of the wheats in the UK where genetic advance has correlated with constitutive stay green condition, which means the crop keeping active longer during grain filling (Carmo-Silva et al., 2017; Voss-Fels et al., 2019). By contrast, and even in the absence of water stress, yield potential under Mediterranean conditions is lower because of the higher temperatures, which reduces crop duration while increasing respiratory losses (Chowdhury and Wardlaw, 1978; Wardlaw et al., 1980). Moreover, a longer crop duration may be usually considered a negative trait under Mediterranean conditions because of the seasonally progressive increase in temperature and the decrease in precipitation, which may cause drought stress during the last part of the crop cycle (i.e. the reproductive period). This "terminal" drought may therefore compromise the setting and further filling of grains or, depending on the severity of the stress, it may even accelerate crop senescence and thus shorten grain filling (Senapati and Semenov, 2020). In this sense, adaptive stay green, which is understood as the crop's ability to withstand stress conditions, may be considered a positive trait under Mediterranean conditions (Christopher et al., 2016; Fischer, 2011; Padovan et al., 2020). Nevertheless, this trait must be viewed with caution and not confounded with a constitutively longer crop duration, which may account for the reports of a negative association of long phenology with grain yield in wheat under Mediterranean conditions (Chairi et al., 2020). In

fact, phenological adjustment has been regarded as a trait with prospects of achieving genetic adaptation and enhancing genetic yield potential in the wheat varieties grown in Europe (Senapati and Semenov, 2020), and securing adaptation to Mediterranean conditions in particular. However, while the duration of the crop cycle of cultivars grown under Mediterranean conditions has decreased throughout the past century as a result of breeding (Collins and Chenu, 2021; Long et al., 2022; Loss and Siddique, 1994), the duration of grain filling has remained unchanged (Araus et al., 2002) or has even increased (Foulkes et al., 2011; Miralles and Slafer, 2007; Reynolds et al., 2009, 2012). Thus, under Mediterranean conditions, an extended grain filling period provides plants with longer duration to intercept radiation, carry out photosynthetic activities and translocate assimilates from tissues into grains (Soriano et al., 2018). Because flowering is the most sensitive phenological stage in the wheat lifecycle, a suitable flowering time is vital to achieve an optimum biomass/grain set balance (Flohr et al., 2017; Kamran et al., 2014). In southern Europe, wheat cultivars usually undergo early anthesis to avoid drought conditions (Shavrukov et al., 2017), whereas in northern and central Europe, inducing flowering in winter engenders exposure to frost, damaging reproductive organs and reducing light interception, all of which constrain yield. Therefore, a late flowering behavior has been preferred with the aim of securing higher yields through maximizing biomass production during pre-anthesis (Senapati and Semenov, 2020). Nevertheless, while other traits may be also involved in wheat performance under Mediterranean conditions, particularly in terms of capture of resources (water and nitrogen) by the plant (Sadras and Lawson, 2011, 2013; Kitonyo et al., 2017), phenology is still a key component.

Under Mediterranean conditions, the role of phenological adjustment in crop yield is to ensure an adequate (well balanced) capture of resources - basically water and secondly nutrients - throughout the crop cycle. In terms of water availability, carbon isotope composition ( $\delta^{13}\text{C}$ ) in plant dry matter has been proven in wheat as a proxy indicator of water use efficiency (WUE), which is understood as the ratio of grain yield to transpiration (Farquhar et al., 1989). More relevant to this study,  $\delta^{13}\text{C}$  even informs about grain yield per unit of evapotranspiration (French and Schultz, 1984), with higher (less negative)  $\delta^{13}\text{C}$  indicating a higher water use efficiency (Farquhar et al., 1989). However, since water use efficiency and the effective (or efficient) use of water are not independent traits, but to a large extent inversely proportional to one another,  $\delta^{13}\text{C}$  has been associated negatively with the effective use of water (Araus et al., 2003, 2008; Blum, 2009) and therefore  $\delta^{13}\text{C}$  behaves as an indicator of water used by the plant and then of crop water status. Moreover, since genotypic and environmentally driven variability in grain yield depend more on the water available and its effective

use rather than on the water use efficiency (Blum, 2009), usually the  $\delta^{13}\text{C}$  of mature grains (or other plant parts developed during the last period of the crop cycle) correlates negatively with grain yield across environments and even (except for very harsh environments), also negatively across genotypes within a given environment. Negative genotypic relationships have been reported not only in wheat (Condon et al., 1987; Araus et al., 2003) but also in other C3 cereals (Voltas et al., 1999). In favor of the capacity of  $\delta^{13}\text{C}$  as indicator of water status and thus yield, a lower  $\delta^{13}\text{C}$  together with indicators of higher transpiration, such as higher stomatal conductance (Condon et al., 1987) or a lower canopy temperature (Lopes and Reynolds, 2010), have been correlated with a more efficient root system (Lopes and Reynolds, 2010).

Nitrogen is usually the main nutrient that limits yield, with nitrogen availability and further assimilation by the plants being the main factors to consider. Since the green revolution, application of nitrogen fertilizer in crop management practices has been a frequent method to optimize wheat green biomass and therefore achieve higher yields. In fact, post green revolution wheat cultivars have been bred to maximize yield potential under well-watered and nitrogen-fertilized growing conditions. However, little emphasis has been given to the interplay between water availability and nitrogen uptake under winter-rainfall environments such as the Mediterranean, where water frequently becomes a limiting factor for wheat growth and yield (Sadras et al., 2016). Moreover, this limitation is increasing due to climate change (Basso et al., 2012), which in turn impacts plant nitrogen uptake and a variety's specific response to nitrogen fertilization (Sadras et al., 2016). In terms of indicators of nitrogen metabolism, and alongside the nitrogen accumulated by the plant, nitrogen isotope composition ( $\delta^{15}\text{N}$ ) in plant tissues has also been proposed (Yousfi et al., 2012). The  $\delta^{15}\text{N}$  also works as a tracer of the characteristics of the nitrogen source used by plants. Indeed, while plants growing with chemical fertilizers exhibit lower  $\delta^{15}\text{N}$  than plants subjected to organic fertilizers or to soil mineral N (with exceptions, e.g. rotation or intercropping legumes) as the main source of nitrogen, the relative amount of chemical fertilizer applied may therefore affect the nitrogen isotope signature of the plant (Serret et al., 2008). Moreover, both the  $\delta^{15}\text{N}$  and N contents in tissues are tracers of the available sources of N fertilizer, and they are also affected by stresses such as salinity and drought (Yousfi et al., 2012, 2013). In summary, analyzing  $\delta^{13}\text{C}$  and  $\delta^{15}\text{N}$  alongside N content in plant tissues throughout the lifecycle has been widely documented in the literature as a proxy for crop water and nitrogen status and to inform about the integrative effect of the environmental conditions on resource availability and the plant's demands (Cossani and

Sadras, 2021; Ferrio et al., 2007; Yousfi et al., 2012). In the case of wheat, mature grains are the most suitable plant part to analyze (Araus et al., 2013).

Identifying elite European wheat cultivars that maintain relatively high grain yield under Mediterranean conditions may lead the way to a better understanding of the ideotypic characteristics of wheat cultivars that combine high yield potential together with resilience to the current Mediterranean conditions and the environmental scenarios expected in central and northern Europe over the coming decades. Moreover, tailoring management practices that consider the interplay between water conditions, nitrogen fertilization and variety is necessary to reduce the yield gap and achieve better yield responses to the current climatic challenges in the Mediterranean basin. The general objectives of this study were to assess which traits contribute towards European wheats with high performance under Mediterranean conditions. Specific objectives were to identify traits related to phenology, water status and nitrogen metabolism. To achieve this, the present study compared the performance of twelve high-yielding winter wheat cultivars of different European (south, central and north-western) provenances grown under different levels of nitrogen fertilizer topdressing (following the usual recommended doses for the region), and three consecutive crop seasons with fluctuating climatic conditions, under the Mediterranean continental conditions of the Castilla y León region (northern part of Spain). In addition to grain yield, the main agronomic yield components, and grain N accumulation, crop phenology and the  $\delta^{13}\text{C}$  and  $\delta^{15}\text{N}$  in mature grains were assessed. This study has been performed in the framework of the European research network ECOFE (European Consortium for Open Field Experimentation), which investigates wheat performance in a genotype x environment x management context, with the aim to narrow yield gaps in different European environments and provide more resilient cultivars alongside affordable management practices.

## **2. Materials and methods**

### **2.1. Plant material and field experiments**

Field trials were carried out during three consecutive crop seasons (2017-2018, 2018-2019 and 2019-2020) at the experimental station of Zamadueñas, Valladolid (41° 39' 8'' N and 4° 43' 24'' W, 690 m.a.s.l.) of the Agro-technological Institute of Castilla y León (ITACyL) in Valladolid (Spain). Twelve European winter bread wheat genotypes (*Triticum aestivum* L.) were selected from three main European regions (north, central and south), based on their high-yielding performance (Supplemental Table 1). Three different levels of nitrogen fertilization were tested during the three

seasons: 50% of the recommended topdressing nitrogen fertilization dose used in the region (N1), the recommended topdressing dose (N2) and 30% above the recommended topdressing dose (N3) (Fertiberia, 2022). N fertilization was applied as three dressings totaling around 64 kg ha<sup>-1</sup> in the N1 treatment, 104 kg ha<sup>-1</sup> in N2, and 129-130 kg ha<sup>-1</sup> in N3 (Supplemental Table 2). During the first and third crop seasons (2017-2018 and 2019-2020), wheat was preceded by annual fallow, and by lentils during the 2018-2019 season. Field soil had a silt-loam texture, and a constant pH of 8.5 during the three crop seasons, with total organic matter and nitrogen contents (down to 30 cm in depth) prior to sowing of 1.10% (2017-2018), 2.45% (2018-2019), and 1.17% (2019-2020) and 0.139% (2017-2018), 0.065% (2018-2019), and 0.067% (2019-2020), respectively. The initial mineral N (NO<sub>3</sub> plus NH<sub>4</sub>) content for the upper 30 cm of soil prior to planting in the 2018-2019 season was 65.1 kg ha<sup>-1</sup>. In addition, total nitrogen and mineral N contents for the upper 20 cm of soil from the fields used on (2018-2019) and (2019-2020) were analyzed on September 1<sup>st</sup> 2022. The (2017-2018) site was not analyzed due to the presence of a summer (maize) crop (Supplemental Table 2).

The experimental design was a split plot with the main plots (nitrogen levels and blocks) arranged as a randomized complete block design, and varieties as subplots. Within each block and nitrogen level, varieties were randomized with three replicates in elemental plots of 12 m long and 1.5 m wide. The sowing rate was 450 seeds m<sup>-2</sup>, planted in seven rows that were 21 cm apart. Phytosanitary treatments were applied all years for all trials following the recommended practices in the region. For the three seasons and trials, genotypes were grown under rainfed conditions. The soil water contents accumulated in the whole (1 m) profile by the end of September 2017 and 2018 were 121 mm and 119 mm, respectively. During the first season (2017-2018), sowing took place on November 2<sup>nd</sup> 2017, and the season was characterized by a moderate average temperature of 7.7 °C and a total accumulated precipitation of 454 mm during the crop cycle. For the second crop season (2018-2019), sowing was delayed until November 29<sup>th</sup> 2018 because of a rainfall shortage, with an average temperature of 8.5 °C and an accumulated precipitation of 188 mm. Moreover, the second crop season exhibited higher potential evapotranspiration than the other two crop seasons. During the third crop season (2019-2020), sowing took place on October 28<sup>th</sup> 2019, with an average temperature of 9.3 °C and a total accumulated precipitation of 533 mm. Patterns of daily precipitation and the average, minimum and maximum temperatures and potential evapotranspiration during the three crop seasons are displayed in Figure 1.



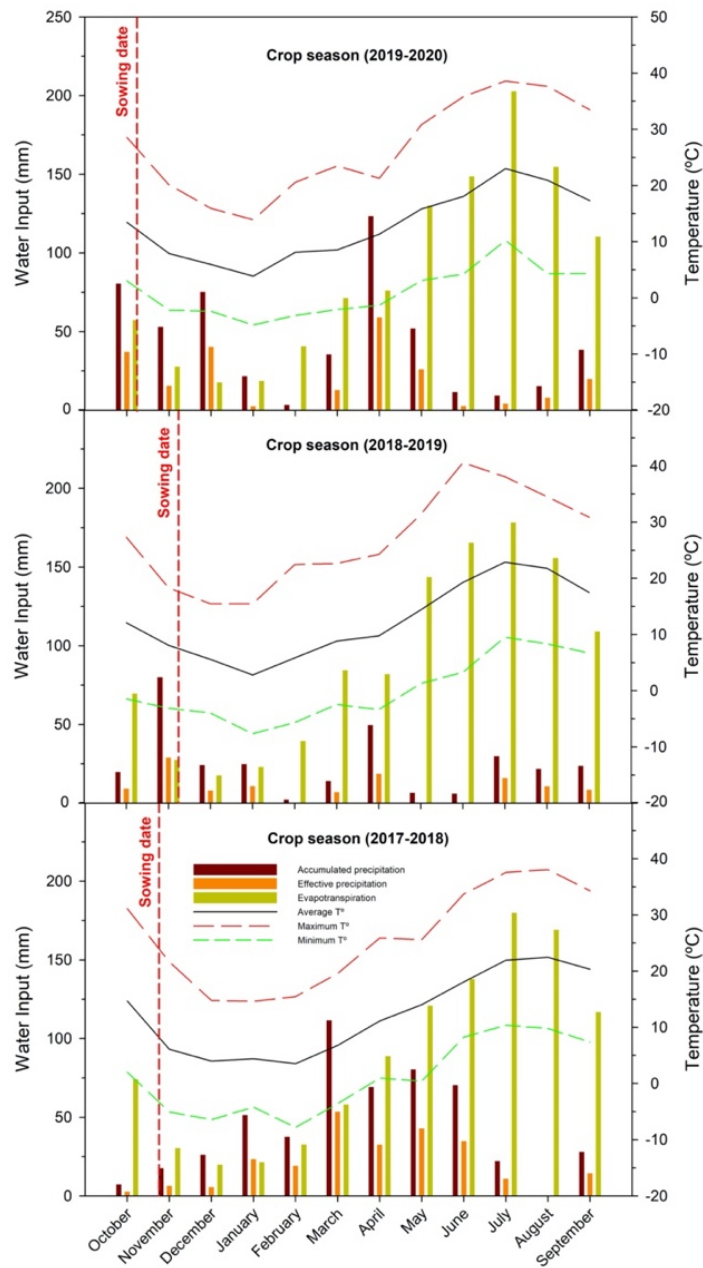


**Figure 1.** Distribution of monthly accumulated precipitation, mean temperature (average, minimum and maximum) and mean evapotranspiration during the growing period covering the crop seasons (2017-2018), (2018-2019) and (2019-2020). On the X axis, ticks indicate the middle of the month during each crop season.

## 2.2. Agronomic traits

Phenological stage dates were recorded in Zadoks units (Zadoks et al., 1974) for each plot when 50% of plants reached a given stage. The studied phenological stages were days from planting to tillering (DTT), Zadoks 20-29; days from planting to stem elongation (DTE), Zadoks 30; days from planting to booting (DTB), Zadoks 45; days from planting to heading (DTH), Zadoks 55; days from planting to anthesis (DTA), Zadoks 65; and days from planting to mid grain filling (MGF), Zadoks 75. In addition, duration in days from consecutive stages was also calculated. Then at maturity each plot was machine harvested and grain yield (GY) was determined after an adjustment to a 10% moisture level. Thousand kernel weight (TKW) was determined after harvest for each plot in a subsample of seeds. Grain number (GN), expressed as the number of grains per square meter, was inferred from GY and TKW values. In addition, grain nitrogen yield (GNY) was calculated as the product of GY by the grain N concentration (see next section).

## 2.3. Stable isotope composition and elemental analysis

During the three crop seasons, and for each individual plot, samples of mature grains obtained at harvest were oven dried at 60 °C for a minimum of 48 h and reduced to a fine powder. For each subsequent sample, approximately 1 mg was enclosed in tin capsules, and processed using an elemental analyzer (Flash 1112 EA; Thermo- Finnigan, Schwerte, Germany) coupled with a Delta V Advantage isotope ratio mass spectrometer (Delta V Advantage IRMS; ThermoFisher Scientific Inc., Waltham, Massachusetts, USA) at the Scientific and Technical facilities of the University of Barcelona. Different secondary standards were used for carbon (IAEA-CH7, UCGEMA K, UCGEMA CH and fructose) and nitrogen (IAEA-600, IAEA-N1, UCGEMA-K, UCGEMA-CH, and UCGEMA) isotope analyses. Nitrogen concentrations in grains were expressed in percentages (%), and carbon and nitrogen isotope compositions in parts per thousand (‰), with an analytical precision (standard deviation) of 0.2‰ for both  $\delta^{13}\text{C}$  and  $\delta^{15}\text{N}$ , and following Eq. (1):

$$\delta^{13}\text{C}/\delta^{15}\text{N} (\text{‰}) = [R_{\text{sample}}/R_{\text{standard}} - 1] \times 1000 \quad (1)$$

Where  $R_{\text{standard}}$  is the molar abundance ratio of the secondary standard calibrated against the primary standard Pee Dee Belemnite (PDB) for carbon isotope composition ( $\delta^{13}\text{C}$ ), and  $\text{N}_2$  from air for nitrogen isotope composition ( $\delta^{15}\text{N}$ ) (Farquhar et al., 1989).

## 2.4. Statistical analysis

The open-source software RStudio 1.2.5 (R Foundation for Statistical Computing, Vienna, Austria) was used to run analyses of variance (ANOVA) using mixed models to test the effects of nitrogen, genotype, and their interactions in each crop season and combined seasons, for all dependent variables (grain yield, phenology, agronomic yield components, N concentration, and stable isotopes), where model selection was based on the smallest standard Akaike's Information Criterion (AIC) (Akaike, 1974) (Supplemental Table 3). The same software (RStudio 1.2.5) was used to (i) reveal differences within seasons, nitrogen levels and genotypes following the post-hoc Tukey-b test; (ii) to determine Pearson correlations between grain yield and the rest of the parameters; and (iii) to analyze the studied traits in a reduced bi-dimensional platform using principal component (PCA) and genotype plus genotype by environment (GGE) biplot analyses. META-R 6.0 software (Alvarado et al., 2020) was deployed to assess genetic correlations between traits for the applied treatments and to analyze data in a bi-dimensional platform using genotypic correlations. SPSS software (IBM SPSS Statistics 25, Inc., Chicago, IL; USA) was used to predict grain yield by implementing stepwise multiple regression models, where a multicollinearity level was controlled by setting the maximum variance inflation factor (VIF) to 10. GY predictive models were developed by using the least absolute shrinkage and selection operator (LASSO) regression. Data were randomly separated into two sets: 80% as a training set 20% as a test set. Optimal lambda ( $\lambda$ ) obtained using a 10-fold cross validation repeated 10 times on the training set. To define the predictive ability of the predictive models, the coefficient of determination ( $R^2_{\text{Trainingset}}$ ) was determined as the optimum determination coefficient using the training set, together with root mean square error ( $\text{RMSE}_{\text{Train}}$ ) and the shrinkage penalty ( $\lambda$ ) of the training set to determine the models' accuracy. Graphs were created using Sigma-plot 10.0 (Systat Software Inc, California; USA).

## 3. Results

### 3.1. Effect of crop season, N fertilization and genotypes on grain yield, yield components and phenology

During the first crop season (2017-2018), N fertilization had a significant albeit minor effect (<10% differences) on grain yield (GY), grain number (GN), and days to tillering (DTT), and a somewhat higher effect (ca. 20% differences for grain nitrogen yield (GNY)) and no effect on thousand grain weight (TKW) or the rest of phenological stages except for days to tillering (DTT). The GY achieved under the recommended topdressing dose (N2) was the highest, and under the 50% recommended

topdressing dose (N1) was the lowest (Table 1). The genotypic effect was highly significant on GY, GNY, GN, TKW, and all phenological stages except for DTT. The interaction between N fertilization and genotypic effect was only significant for days to anthesis (DTA) (Table 1). KWS Siskin exhibited the highest GY, GNY and GN, with intermediate days to stem elongation (DTE), days to booting (DTB), days to anthesis (DTH), DTA and mid grain filling (MGF) (Supplemental Table 4), as well as intermediate durations from stem elongation to booting (DTE-DTB), to heading (DTE-DTH) and to anthesis (DTE-DTA), and from anthesis to mid grain filling (DTA-MGF), although there were shorter durations from booting to heading (DTB-DTH) and heading to anthesis (DTH-DTA), and a longer duration of stem elongation to mid grain filling (DTE-MGF) duration (Supplemental Table 5).

The second crop season (2018-2019) was characterized by reduced rainfall and higher temperatures and evapotranspiration compared with the other two seasons. N fertilization only slightly increased TKW, with no effect on GY, GNY, GN or dates of any of the phenological stages (Table 1). The genotypic effect was significant for GY, GNY, GN, TKW and dates of phenological stages. The interaction of N fertilization and genotype was only significant for DTE (Table 1). Soberbio exhibited the highest GY and GNY among the set of genotypes, together with high GN and intermediate TKW, slightly shorter DTE and DTB, and earlier reproductive stages (shorter DTH, DTA and MGF) including shorter DTE-DTB and DTH-DTA. KWS Siskin was the second genotype in terms of GY, GNY and GN, whereas it exhibited lower TKW, delayed DTT, longer DTE-DTB and DTH-DTA durations and earlier DTE, DTH, DTA and MGF dates across the set of genotypes (Supplemental Tables 4, 5).

During the third crop season (2019-2020), N fertilization affected GNY and GN only, with both GN and GNY being slightly (2% and 10%, respectively) higher under N3 compared with N1 (Table 1). The genotypic effect was highly significant for GY, GNY, GN, TKW and all phenological dates. There was no interaction effect of N fertilization by genotype (Table 1). Similar, to the previous crop season, KWS Siskin and Soberbio exhibited the highest GY and GNY but shared this ranking with Bennington and Henrik, while GN was the highest in KWS Siskin, followed by Bennington and Henrik, and lower in Soberbio. Dates for most of the phenological stages were intermediate to late, and the durations of phenological stages were longer to intermediate in Bennington, Henrik and KWS Siskin, and in general earlier/shorter for Soberbio compared with the whole set of genotypes (Supplemental Tables 4, 5).

When considering the three years together, the crop season (year) effect was significant on GY, GNY, GN, TKW, and all the assessed phenological stages (Table 1). The N fertilization effect was only

significant on GY, GNY and GN, but not on TKW or phenology, while the genotypic effect was highly significant on all assessed traits except DTT. In a similar manner, the year by N fertilization interaction effect was relevant for GY, GNY, GN and TKW alone, whereas the year by genotype interaction effect was highly significant on all traits except for DTT. The three-way interaction effect was significant for DTA only (Table 1). The (2017-2018) and (2019-2020) crop seasons had higher yields (8.4 Mg ha<sup>-1</sup> and 7.9 Mg ha<sup>-1</sup> on average, respectively) than the (2018-2019) crop season, where GY was reduced by more than three-fold (2.5 Mg ha<sup>-1</sup>). The (2018-2019) crop season also exhibited lower GNY and GN (less than a half) and TKW (slightly more than 20%) than the other two seasons. Regarding phenological stages, DTT and DTE were the longest during the first crop season (2017-2018), intermediate during the second (2018-2019) and shorter during last (2019-2020). However, DTB, DTH, DTA and MGF were the longest during the first season (2017-2018), intermediate during the third (2019-2020) and the shortest during the second (2018-2019) (Table 1). N fertilization slightly increased GY, GNY and GN from N1 to N2 (between 5-10% depending on the traits), with no further effect under N3 (Table 1). Among all tested genotypes, KWS Siskin exhibited the highest GY, GNY and GN, but a low TKW and intermediate phenological stages and durations (particularly DTB-DTH and DTH-DTA), followed by Henrik and Soberbio with high GY and TKW, and intermediate GNY and GN. In terms of phenology, Henrik has shown intermediate dates to phenological stages and DTB-DTH duration, although a shorter DTH-DTA duration, whereas Soberbio had shorter dates to phenological stages, but intermediate (DTB-DTH) to longer (DTH-DTA) phenology durations (Supplemental Tables 4, 5).

**Table 1.** Effect of crop season (year), N fertilization, genotype and their interaction on grain yield (GY), grain nitrogen yield (GNY), grain number (GN), thousand kernel weight (TKW), and days from planting to different phenological stages: tillering “DTT”, stem elongation “DTE”, booting “DTB”, heading “DTH”, anthesis “DTA”, mid grain filling “MGF”. Numbers in parentheses refer to the Zadoks scale (Zadoks et al., 1974).

		GY (Mg ha <sup>-1</sup> )	GNY (Mg ha <sup>-1</sup> )	GN (m <sup>2</sup> )	TKW (g)	DTT (20-29) (d)	DTE (30) (d)	DTB (45) (d)	DTH (55) (d)	DTA (65) (d)	MGF (75) (d)	
2017-2018	N1	7.41 <sup>a</sup> ±0.14	0.14 <sup>b</sup> ±0.00	21245.9 <sup>b</sup> ±562.3	35.21 <sup>a</sup> ±0.80	114.1 <sup>a</sup> ±0.8	137.4 <sup>a</sup> ±1.1	196.9 <sup>a</sup> ±1.0	203.0 <sup>a</sup> ±1.0	210.7 <sup>a</sup> ±0.7	227.3 <sup>a</sup> ±0.8	
	N2	8.35 <sup>a</sup> ±0.15	0.17 <sup>a</sup> ±0.00	24153.6 <sup>a</sup> ±424.6	34.78 <sup>a</sup> ±0.48	111.4 <sup>b</sup> ±0.5	139.0 <sup>a</sup> ±1.0	196.9 <sup>a</sup> ±0.9	203.3 <sup>a</sup> ±0.9	211.6 <sup>a</sup> ±0.9	227.4 <sup>a</sup> ±0.8	
	N3	8.09 <sup>b</sup> ±0.18	0.17 <sup>a</sup> ±0.01	23426.8 <sup>a</sup> ±598.1	34.89 <sup>a</sup> ±0.62	113.4 <sup>a</sup> ±0.6	137.7 <sup>a</sup> ±1.0	196.8 <sup>a</sup> ±0.9	203.3 <sup>a</sup> ±0.9	211.4 <sup>a</sup> ±0.6	227.6 <sup>a</sup> ±0.8	
	<b>ANOVA</b>											
	N fertilization	<0.001	<0.001	<0.001	ns	<0.050	ns	ns	ns	ns	ns	
	Genotype	<0.001	<0.010	<0.001	<0.001	ns	<0.001	<0.001	<0.001	<0.001	<0.001	
	N*G	ns	ns	ns	ns	ns	ns	ns	ns	<0.050	ns	
2018-2019	N1	2.39 <sup>a</sup> ±0.11	0.07 <sup>a</sup> ±0.00	9231.7 <sup>a</sup> ±519.7	27.0 <sup>b</sup> ±0.96	97.0 <sup>a</sup> ±1.0	126.2 <sup>a</sup> ±1.1	161.8 <sup>a</sup> ±0.7	168.8 <sup>a</sup> ±0.6	171.9 <sup>a</sup> ±0.5	192.4 <sup>a</sup> ±0.2	
	N2	2.46 <sup>a</sup> ±0.14	0.06 <sup>a</sup> ±0.00	8945.4 <sup>a</sup> ±506.9	28.3 <sup>ab</sup> ±0.94	98.3 <sup>a</sup> ±0.9	126.3 <sup>a</sup> ±1.1	161.9 <sup>a</sup> ±0.8	169.2 <sup>a</sup> ±0.7	172.3 <sup>a</sup> ±0.4	192.6 <sup>a</sup> ±0.3	
	N3	2.72 <sup>a</sup> ±0.12	0.07 <sup>a</sup> ±0.00	9506.3 <sup>a</sup> ±535.7	29.6 <sup>a</sup> ±0.95	98.8 <sup>a</sup> ±1.0	125.7 <sup>a</sup> ±1.2	161.6 <sup>a</sup> ±0.9	168.8 <sup>a</sup> ±0.7	172.0 <sup>a</sup> ±0.5	192.8 <sup>a</sup> ±0.2	
	<b>ANOVA</b>											
	N fertilization	ns	ns	ns	<0.010	ns	ns	ns	ns	ns	ns	
	Genotype	<0.001	<0.001	<0.001	<0.001	<0.010	<0.001	<0.001	<0.001	<0.001	<0.001	
	N*G	ns	ns	ns	ns	ns	<0.001	ns	ns	ns	ns	
2019-2020	N1	8.33 <sup>a</sup> ±0.25	0.14 <sup>b</sup> ±0.01	22687.4 <sup>b</sup> ±585.2	36.7 <sup>a</sup> ±0.96	-	116.4 <sup>a</sup> ±1.1	180.7 <sup>a</sup> ±1.3	189.3 <sup>a</sup> ±1.5	197.8 <sup>a</sup> ±0.9	-	
	N2	8.36 <sup>a</sup> ±0.21	0.15 <sup>b</sup> ±0.00	22717.7 <sup>b</sup> ±546.4	36.9 <sup>a</sup> ±0.87	-	115.9 <sup>a</sup> ±1.1	180.7 <sup>a</sup> ±1.3	189.1 <sup>a</sup> ±1.4	197.9 <sup>a</sup> ±1.0	-	
	N3	8.51 <sup>a</sup> ±0.20	0.16 <sup>a</sup> ±0.00	23774.7 <sup>a</sup> ±473.8	35.8 <sup>a</sup> ±1.27	-	115.6 <sup>a</sup> ±1.0	180.8 <sup>a</sup> ±1.4	189.4 <sup>a</sup> ±1.5	198.1 <sup>a</sup> ±1.0	-	
	<b>ANOVA</b>											
	N fertilization	ns	<0.050	<0.050	ns	-	ns	ns	ns	ns	-	
	Genotype	<0.001	<0.050	<0.001	<0.001	-	<0.001	<0.001	<0.001	<0.001	-	
	N*G	ns	ns	ns	ns	-	ns	ns	ns	ns	-	
Combined seasons	Year	2017-2018	7.94 <sup>b</sup> ±0.10	0.16 <sup>a</sup> ±0.00	22913.6 <sup>a</sup> ±347.3	34.96 <sup>b</sup> ±0.30	113.0 <sup>a</sup> ±0.4	137.7 <sup>a</sup> ±0.6	196.9 <sup>a</sup> ±0.5	203.0 <sup>a</sup> ±0.5	211.2 <sup>a</sup> ±0.4	227.4 <sup>a</sup> ±0.5
		2018-2019	2.52 <sup>c</sup> ±0.07	0.07 <sup>b</sup> ±0.00	9230.6 <sup>b</sup> ±306.4	28.28 <sup>c</sup> ±0.42	97.9 <sup>b</sup> ±0.6	126.0 <sup>b</sup> ±0.7	161.8 <sup>c</sup> ±0.4	168.9 <sup>c</sup> ±0.4	172.1 <sup>c</sup> ±0.3	192.6 <sup>b</sup> ±0.1
		2019-2020	8.40 <sup>a</sup> ±0.13	0.15 <sup>a</sup> ±0.00	23059.9 <sup>a</sup> ±318.6	36.48 <sup>a</sup> ±0.31	-	116.0 <sup>c</sup> ±0.6	180.7 <sup>b</sup> ±0.8	189.3 <sup>b</sup> ±0.8	197.9 <sup>b</sup> ±0.5	-
	Nitrogen	N1	6.04 <sup>b</sup> ±0.27	0.11 <sup>b</sup> ±0.00	17721.7 <sup>b</sup> ±665.9	32.97 <sup>a</sup> ±0.54	105.3 <sup>a</sup> ±1.2	126.7 <sup>a</sup> ±1.0	179.8 <sup>a</sup> ±1.5	186.8 <sup>a</sup> ±1.5	193.4 <sup>a</sup> ±1.6	212.3 <sup>a</sup> ±1.5
		N2	6.46 <sup>a</sup> ±0.28	0.13 <sup>a</sup> ±0.01	18787.9 <sup>a</sup> ±728.2	33.32 <sup>a</sup> ±0.49	104.9 <sup>a</sup> ±1.1	126.9 <sup>a</sup> ±1.1	179.8 <sup>a</sup> ±1.5	187.2 <sup>a</sup> ±1.5	193.9 <sup>a</sup> ±1.6	212.4 <sup>a</sup> ±1.5
		N3	6.38 <sup>a</sup> ±0.28	0.13 <sup>a</sup> ±0.01	18726.8 <sup>a</sup> ±735.6	33.44 <sup>a</sup> ±0.43	106.1 <sup>a</sup> ±1.0	126.3 <sup>a</sup> ±1.1	179.7 <sup>a</sup> ±1.5	187.2 <sup>a</sup> ±1.5	193.8 <sup>a</sup> ±1.6	212.5 <sup>a</sup> ±1.5
	<b>ANOVA</b>											
		Year (Y)	<0.010	<0.050	<0.010	<0.010	<0.010	<0.010	<0.010	<0.001	<0.001	<0.001
		N fertilization	<0.001	<0.050	<0.010	ns	ns	ns	ns	ns	ns	ns
		Genotype (G)	<0.001	ns	<0.001	<0.001	<0.001	ns	<0.001	<0.001	<0.001	<0.001
	Y*N	<0.001	<0.010	<0.001	<0.010	<0.010	ns	ns	ns	ns	ns	
	Y*G	<0.001	ns	<0.001	<0.001	<0.001	ns	<0.001	<0.001	<0.001	<0.001	
	N*G	ns	ns	ns	ns	ns	ns	ns	ns	ns	ns	
	Y*N*G	ns	ns	ns	ns	<0.010	<0.010	<0.010	<0.001	<0.001	<0.001	

Values are means ± standard error of 12 bread wheat genotypes with three replicates. Levels of significance for the ANOVA: P<0.050, P<0.010 and P<0.001. Within each year, means exhibiting different letters are significantly different (P<0.05) according the post-hoc test (Tukey-b) on independent samples.

### 3.2. Effect of crop season, N fertilization and genotype on stable isotope composition and the N concentration of grains

In the first crop season (2017-2018), the N concentration increased slightly (around 10%) under N3 relative to N1, as did the nitrogen ( $\delta^{15}\text{N}$ ) and carbon ( $\delta^{13}\text{C}$ ) isotope compositions of mature grains (Table 2). The genotypic effect was significant on N,  $\delta^{13}\text{C}$  and  $\delta^{15}\text{N}$ . The N fertilization and genotype interaction effect was only significant on  $\delta^{15}\text{N}$  (Table 2). Comparing all varieties, Soberbio had the lowest  $\delta^{13}\text{C}$  and the highest  $\delta^{15}\text{N}$ , whereas KWS Siskin had an intermediate  $\delta^{13}\text{C}$ , and slightly higher  $\delta^{15}\text{N}$  and lower N concentration compared with the other varieties (Supplemental Table 6).

During the second crop season (2018-2019), the N fertilization effect was significant on  $\delta^{15}\text{N}$  only. The interaction between N fertilization and genotype was significant for N concentration only (Table 2). Moreover, the genotypic effect was absent for most traits except for  $\delta^{13}\text{C}$  (Table 2), with KWS Siskin and Soberbio being among the genotypes that exhibited the lowest  $\delta^{13}\text{C}$  (Supplemental Table 6).

During the third crop season (2019-2020), the N fertilization effect was not significant on any analytical trait (Table 2). As for the genotypic effect, significant differences were found for N concentration and  $\delta^{13}\text{C}$ . No interaction effect was found between N fertilization and genotype (Table 2). Similarly to previous crop seasons, Soberbio exhibited the lowest  $\delta^{13}\text{C}$  and N concentration, followed by KWS Siskin (Supplemental Table 6).

Across all crop seasons, the effect of the year was significant on N concentration,  $\delta^{15}\text{N}$  and  $\delta^{13}\text{C}$ . An N fertilization effect was absent for all traits, and the genotypic effect was significant on N concentration and  $\delta^{13}\text{C}$  alone (Table 3). The grain N concentration was highest during the second season (2018-2019), intermediate during the first season (2017-2018), and lowest during the third season (2019-2020). The  $\delta^{15}\text{N}$  was higher during the first (2017-2018) and third (2019-2020) crop seasons than during the second crop season (2018-2019), while  $\delta^{13}\text{C}$  was highest during the second season (2018-2019), intermediate during the third season (2019-2020), and lowest during the first season (2017-2018). Nevertheless, values for the three traits were far more different during the second season than the other two seasons. Regarding the interactions effect, the year by N fertilization interaction was significant for all traits except for  $\delta^{13}\text{C}$ , while the year by genotype interaction was only significant for  $\delta^{13}\text{C}$ , and the N fertilization by genotype interaction was only significant for grain N concentration. Concerning the three-way interaction year by N fertilization and genotype, significance only existed for  $\delta^{15}\text{N}$  (Table 2). Furthermore, when combining the three seasons, Soberbio had the lowest  $\delta^{13}\text{C}$  with low grain N concentration, followed by KWS Siskin with low  $\delta^{13}\text{C}$  and N concentration, and Henrik with the lowest N concentration but an intermediate  $\delta^{13}\text{C}$  (Supplemental Table 6).

**Table 2.** Effect of crop season (year), N fertilization, genotype and their interaction on the total nitrogen concentration (N) and the stable nitrogen ( $\delta^{15}\text{N}$ ) and carbon ( $\delta^{13}\text{C}$ ) isotope compositions in mature kernels of twelve bread wheat cultivars.

		N (%)	$\delta^{15}\text{N}$ (‰)	$\delta^{13}\text{C}$ (‰)	
2017-2018	N1	1.9 <sup>b</sup> ±0.0	2.7 <sup>b</sup> ±0.1	-27.1 <sup>b</sup> ±0.1	
	N2	2.0 <sup>a</sup> ±0.1	2.6 <sup>b</sup> ±0.1	-27.0 <sup>ab</sup> ±0.1	
	N3	2.1 <sup>a</sup> ±0.1	3.0 <sup>a</sup> ±0.1	-26.9 <sup>a</sup> ±0.1	
	<b>ANOVA</b>				
	N fertilization	<0.001	<0.001	<0.010	
	Genotype	<0.001	<0.050	<0.001	
	N*G	ns	<0.010	ns	
2018-2019	N1	2.8 <sup>a</sup> ±0.1	1.7 <sup>a</sup> ±0.1	-21.9 <sup>a</sup> ±0.1	
	N2	2.7 <sup>a</sup> ±0.1	1.4 <sup>ab</sup> ±0.1	-22.0 <sup>a</sup> ±0.1	
	N3	2.6 <sup>a</sup> ±0.1	1.2 <sup>b</sup> ±0.1	-22.0 <sup>a</sup> ±0.1	
	<b>ANOVA</b>				
	N fertilization	ns	<0.001	ns	
	Genotype	ns	ns	<0.001	
	N*G	<0.050	ns	ns	
2019-2020	N1	1.7 <sup>b</sup> ±0.1	2.6 <sup>a</sup> ±0.1	-26.6 <sup>a</sup> ±0.1	
	N2	1.8 <sup>ab</sup> ±0.1	2.6 <sup>a</sup> ±0.1	-26.5 <sup>a</sup> ±0.1	
	N3	1.9 <sup>a</sup> ±0.1	2.6 <sup>a</sup> ±0.1	-26.5 <sup>a</sup> ±0.1	
	<b>ANOVA</b>				
	N fertilization	ns	ns	ns	
	Genotype	<0.010	ns	<0.001	
	N*G	ns	ns	ns	
Combined seasons	Year	2017-2018	2.0 <sup>b</sup> ±0.0	2.8 <sup>a</sup> ±0.0	-27.0 <sup>a</sup> ±0.0
		2018-2019	2.7 <sup>a</sup> ±0.1	1.5 <sup>b</sup> ±0.1	-21.9 <sup>a</sup> ±0.1
		2019-2020	1.8 <sup>a</sup> ±0.1	2.6 <sup>a</sup> ±0.0	-26.5 <sup>b</sup> ±0.0
	Nitrogen	N1	2.2 <sup>a</sup> ±0.1	2.3 <sup>a</sup> ±0.1	-25.0 <sup>a</sup> ±0.3
		N2	2.2 <sup>a</sup> ±0.1	2.2 <sup>a</sup> ±0.1	-25.2 <sup>a</sup> ±0.2
		N3	2.2 <sup>a</sup> ±0.0	2.3 <sup>a</sup> ±0.1	-25.1 <sup>a</sup> ±0.2
		<b>ANOVA</b>			
		Year (Y)	<0.050	<0.010	<0.001
		N fertilization	ns	ns	ns
		Genotype (G)	<0.001	ns	<0.001
	Y*N	<0.010	<0.001	ns	
	Y*G	ns	ns	<0.050	
	N*G	<0.050	ns	ns	
	Y*N*G	ns	<0.050	ns	

Values are means  $\pm$  standard error of 12 bread wheat genotypes with three replicates. Levels of significance for the ANOVA:  $P<0.050$ ,  $P<0.010$  and  $P<0.001$ . Within each year, means exhibiting different letters are significantly different ( $P<0.050$ ) according the post-hoc test (Tukey-b) on independent samples.

### 3.3. Relationships among agronomic and analytical traits

When combining the three seasons, high and positive phenotypic correlations were found for GY with GNY, GN and TKW, for GNY with GN and TKW, and for GN with TKW (Table 3). Moreover, correlations of all agronomic traits with the dates of most of the phenological stages and  $\delta^{15}\text{N}$  were positive, and with N concentration and  $\delta^{13}\text{C}$ , negative. Moreover, correlations of dates of phenological stages with GY were progressively stronger in the later phenological stages. In fact, the differences in DTE-MGF among genotypes (Supplemental Table 5) were smaller in the wetter years (8 days in 2017-2018; 8 days in 2019-2020) and the Pearson correlations between GY and phenology stages were not significant. In the dry year, genotypic differences in phenology were greater (16 days in 2018-2019), and the correlations between GY and phenological stages were negative, indicating that late-flowering genotypes were more affected by the drought (Table 3). Thus, the high positive correlations between



phenological stages and GY (and GNY, GN TGW) observed when the three seasons were combined are mainly driven by the differences in phenology among years, particularly the precocity observed in the second season (the dry year and with lowest GY). Similar results were observed for the genetic correlation coefficients (Supplemental Table 7).

**Table 3.** Pearson correlation coefficients of linear regressions between agronomic traits (grain yield (GY), grain nitrogen yield (GNY), grain number (GN) and thousand kernel weight (TKW), and days from planting to different phenological stages (tillering “DTT”, elongation “DTE”, booting “DTB”, heading “DTH”, anthesis “DTA”, mid grain filling “MGF”), grain nitrogen concentration (N) and grain carbon ( $\delta^{13}\text{C}$ ) and nitrogen ( $\delta^{15}\text{N}$ ) isotope compositions. Correlations were calculated using individual plot values and combining all three N fertilization treatments.

		Combined seasons				2017-2018				2018-2019				2019-2020			
		GY	GNY	GN	TKW	GY	GNY	GN	TKW	GY	GNY	GN	TKW	GY	GNY	GN	TKW
<i>Agronomic traits</i>	<b>GY</b>	1	-	-	-	1	-	-	-	1	-	-	-	1	-	-	-
	<b>GNY</b>	0.914**	1	-	-	0.568**	1	-	-	0.874**	1	-	-	0.664**	1	-	-
	<b>GN</b>	0.962**	0.913**	1	-	0.798**	0.529**	1	-	0.875**	0.809**	1	-	0.829**	0.716**	1	-
	<b>TKW</b>	0.686**	0.543**	0.477**	1	ns	ns	-0.572**	1	ns	-0.233*	-0.592**	1	0.454**	ns	ns	1
<i>Phenology</i>	<b>DTT</b>	0.221**	0.273**	0.223**	0.146*	-0.267**	-0.232*	ns	ns	ns	ns	ns	ns	-	-	ns	-
	<b>DTE</b>	ns	ns	ns	ns	ns	-0.199*	ns	ns	-0.339**	-0.336**	-0.500**	0.462**	ns	ns	ns	ns
	<b>DTB</b>	0.724**	0.691**	0.708**	0.549**	ns	ns	ns	ns	-0.341**	-0.361**	-0.503**	0.448**	ns	ns	ns	ns
	<b>DTH</b>	0.741**	0.707**	0.728**	0.552**	0.284**	ns	ns	ns	-0.398**	-0.422**	-0.582**	0.538**	ns	ns	ns	-0.250**
	<b>DTA</b>	0.830**	0.777**	0.806**	0.617**	0.356**	ns	ns	0.220*	-0.345**	-0.338**	-0.526**	0.484**	ns	ns	ns	ns
	<b>MGF</b>	0.908**	0.791**	0.824**	0.689**	ns	ns	ns	ns	-0.239*	-0.241*	-0.353**	0.332**	-	-	ns	-
<i>Isotopes</i>	<b>N</b>	-0.689**	-0.439**	-0.670**	-0.591**	ns	0.698**	ns	ns	-0.209*	0.307**	ns	ns	ns	ns	ns	-0.369**
	<b><math>\delta^{15}\text{N}</math></b>	0.686**	0.672**	0.681**	0.504**	ns	ns	ns	ns	ns	ns	ns	ns	ns	ns	ns	ns
	<b><math>\delta^{13}\text{C}</math></b>	-0.923**	-0.815**	-0.893**	-0.663**	-0.285**	ns	-0.317**	ns	-0.303**	ns	-0.325**	ns	-0.255*	-0.249*	ns	-0.245*

ns, not significant; \*,  $P < 0.05$ ; \*\*,  $P < 0.01$ .

Relationships were further analyzed within each season. During (2017-2018) GY was positively correlated with DTH and DTA, and negatively correlated with DTT and  $\delta^{13}\text{C}$ . During (2018-2019), GY correlated positively with GNY and GN, but not with TKW, while. In addition, GY, was negatively correlated with the dates of most of the phenological stages, N concentration and  $\delta^{13}\text{C}$  of grains (Supplemental Fig. 1). During (2019-2020), GY exhibited positive correlations against GNY, GN and TKW, a negative correlation with  $\delta^{13}\text{C}$ , and no correlation with phenology.

Genetic correlations of GY with the studied traits were assessed (Supplemental Table 7). GY correlated positively with GNY and GN within each season. Regarding phenology, negative correlations with GY were mainly found during (2018-2019). In grain analytical traits, N concentration and  $\delta^{13}\text{C}$  had negative relationships with GY across seasons, as well as under combined N fertilization treatments during (2017-2018) and (2019-2020).  $\delta^{15}\text{N}$  correlated negatively with GY only in (2017-2018) when the three N levels were combined.

In addition, correlations between the duration of the different phenological stages, calculated as the duration from one stage to the next (rather than as the number of days from planting), with GY, GNY, GN, TKW, and stable isotopes were assessed (Supplemental Table 8). When combining the three crop seasons and N fertilization levels, the duration of most of the phenological stages correlated positively with GY, GNY, GN, TKW, and  $\delta^{15}\text{N}$ , and negatively with N concentration and  $\delta^{13}\text{C}$ , with the strongest correlations usually achieved with the stem elongation to anthesis (DTE-DTA) duration. When considering each season separately, only the (2017-2018) and (2018-2019) crop seasons showed significant positive correlations of GY with the durations of DTE-DTA and anthesis to mid grain filling (DTA-MGF).

#### 3.4. Predictive regression models and principal component analyses

Multi-linear stepwise regression models were constructed to assess the main contributors to GY (Supplemental Table 9). Phenology and grain analytical traits were considered as independent variables, whereas the agronomic components were not included. The strongest regression models were achieved when combining the three crop seasons. The coefficient  $R^2_{\text{adjusted}}$ , which represents the part of variability explained by the predictors, accounted for 88.9%, with  $\delta^{13}\text{C}$ , DTE and DTA as the main explanatory traits of GY across the whole set of genotypes and replicates. Within each season the  $R^2_{\text{Adjusted}}$  was significant but much lower than with the three seasons combined. In this case, later anthesis (higher DTA) followed by an earlier tillering (smaller DTT) and a lower  $\delta^{13}\text{C}$  were the traits chosen for the wettest season (2017-2018), whereas an earlier heading (lower DTH) followed by a lower  $\delta^{13}\text{C}$  were chosen for the dry season (2018-2019). During the mildly wet season (2019-2020),

only a lower  $\delta^{13}\text{C}$  was chosen by the model. To delve further into genotypic specificity, the same regression model was fitted across the combined three crop seasons but for cultivars separated by their provenance (northern, central and southern Europe). In all scenarios, water status (with a lower  $\delta^{13}\text{C}$  as indicator) was the primary explanatory trait for yield performance, followed by phenology (specifically lower DTE in northern and central European genotypes and shorter DTH for southern European genotypes). To avoid overfitting problems in our database, a LASSO regression analysis was performed and is presented in (Supplemental Table 10); the  $R^2_{\text{adjusted}}$  obtained for each case and using all variables were similar to the Stepwise regression analysis. Further, to simplify the predictive LASSO models, we selected the most relevant variables based on the stepwise results. Indeed, using  $\delta^{13}\text{C}$  and DTH/DTA only as explicative variables slightly improve the predictive ability of the LASSO models for GY. In fact, the shrinkage penalty ( $\lambda$ ) in each model was mostly null, which explains the similarities between LASSO and stepwise regression models, despite the presence of high correlations between the explicative variables.

For each crop season and combined N fertilization treatments, a phenotypic analysis of principal components (PCA) was performed. The first two components explained 52.6%, 62.1% and 58.9% of the variability during the (2017-2018), (2018-2019) and (2019-2020) seasons, respectively (Figure 2A, B, C). Further, a genotypic PCA, which removes the spatial variability, was also performed. In this case, the first two components accounted for 89.9%, 97.8% and 96.4% of the three consecutive seasons, respectively (Figure 2D, E, F). In the phenotypic PCA and during the wet seasons (2017-2018 and 2019-2020), vectors indicating phenology (the duration from planting of different phenological stages) were placed perpendicularly to GY, indicating an absent relationship between phenology and GY during these seasons, as opposed to the dry season (2018-2019), where phenology vectors were placed on the opposite side of GY, which indicated their negative relationship. However, in the genotypic PCA, phenological stages were placed in the same direction as GY during (2017-2018), and particularly in the case of DTH and DTA, in the opposite direction to GY during (2018-2019), and perpendicular to GY during (2019-2020). These results suggest that in a wet season (as typified by 2017-2018), longer crop seasons were associated with better yield performance, whereas in the case of the dry season (2018-2019), a shorter cycle was related to higher yield. Finally, for the (2019-2020) season, which is characterized by somewhat less wet conditions during the reproductive stage than the first season, the situation was in between (i.e. no clear relationship between phenology and GY). Regarding grain analytical traits, and in both the phenotypic and genotypic PCAs,  $\delta^{13}\text{C}$  was placed opposite to GY in all crop seasons, whereas N concentration was positioned opposite to GY during the wet crop seasons (2017-2018 and 2019-2020), and in the same direction as GY during the dry season (2018-2019).

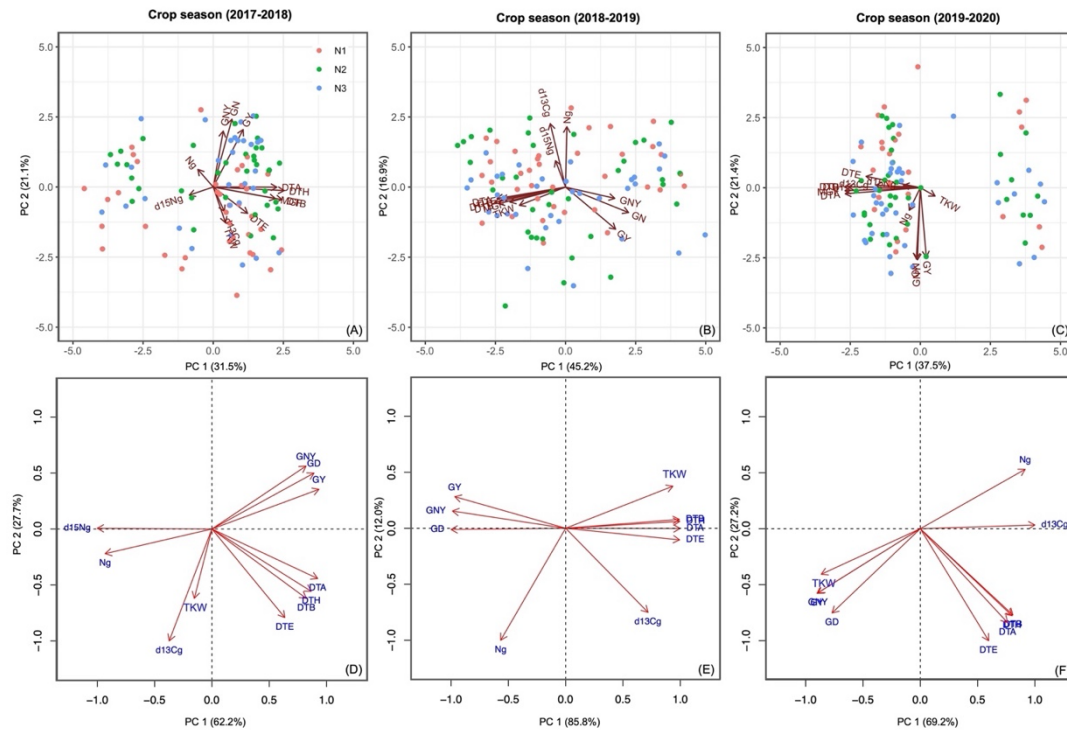


**Figure 2.** Principal component analysis (PCA) of 12 high-yielding European cultivars of winter wheat grown under Mediterranean continental conditions during each of the three consecutive crop seasons (2017-2018; 2018-2019 and 2019-2020), and under three different topdressing nitrogen fertilizer applications (50% of the recommended N fertilization dose “N1”, the recommended N fertilization dose “N2”, and 30% above the recommended N fertilization dose “N3”). The upper three PCAs were generated on the basis of phenotypic correlations, whereas the lower three PCAs were generated using genotypic correlations. The variables included in the analysis are grain yield (GY), grain nitrogen yield (GNY), grain number (GN), thousand kernel weight (TKW), days from planting to elongation (DTE), days from planting to booting (DTB), days from planting to heading (DTH), and days from planting to anthesis (DTA), and the stable carbon ( $\delta^{13}\text{C}$ ) and nitrogen ( $\delta^{15}\text{N}$ ) compositions and nitrogen concentration (N) of mature grains.

Finally, genotypes were categorized based on their provenance (northern, central and southern Europe) to evaluate their performance under nine different environments, understood as the combination of three crop seasons by three N fertilization levels. Northern European genotypes had a 6% higher yield than central and southern genotypes under wet conditions (2017-2018 and 2019-2020), whereas under dry conditions (2018-2019) southern European cultivars yielded the highest, with a 2% increase in GY (Supplemental Table 11).

Phenotypic yield performance (Figure 3A) was the lowest during the second season (2018-2019), disregarding provenance, with higher  $\delta^{13}\text{C}$ , higher grain N concentration and lower TKW, and shorter phenology (except for DTE). Southern varieties, namely Soberbio and Chambo, performed better under drier conditions (2018-2019) compared to the rest of the genotypes. However, under wet

conditions (2017-2018 and 2019-2020), northern genotypes (KWS Siskin and Bennington) had better GY than the other genotypes (Figure 3B). In addition, we applied a Finlay Wilkinson approach (Supplemental Fig. 2), which assembles genotype behaviour into three categories based on their adaptability to the studied environments and these were presented as the combination of crop seasons and N fertilization levels. These categories were: (I), least stable genotypes, (II) moderately stable genotypes and (III) resilient high-yielding genotypes.

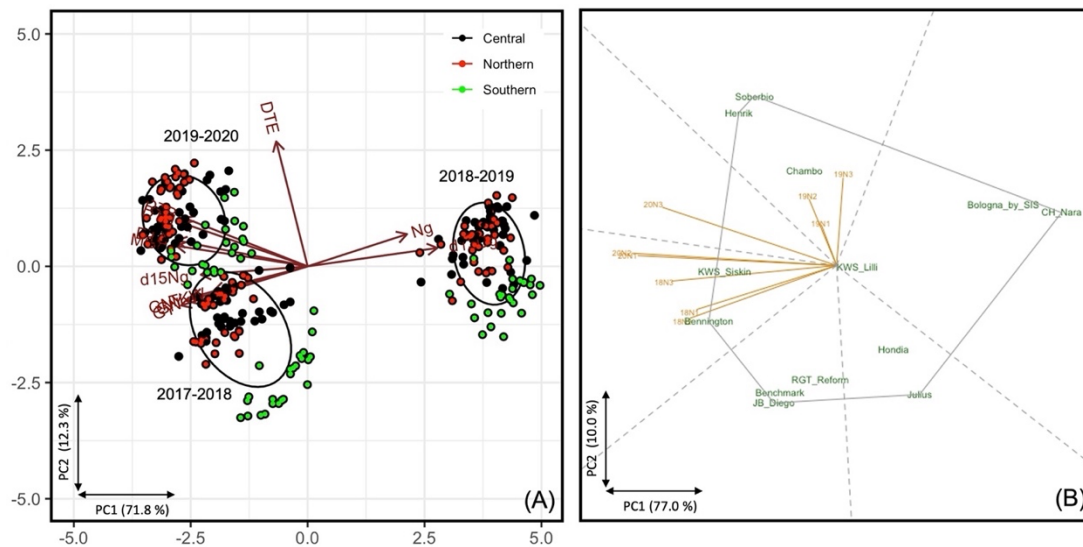


**Figure 3.** (A) Principal component analysis of 12 high-yielding cultivars of winter wheat originating from different European regions (central, northern, southern), grown under Mediterranean continental conditions and nine different environments. The variables included in the analysis are grain yield (GY), grain nitrogen yield (GNY), grain number (GN), thousand kernel weight (TKW), days from planting to elongation (DTE), days from planting to booting (DTB), days from planting to heading (DTH), and days from planting to anthesis (DTA), stable carbon ( $\delta^{13}\text{C}$ ) and nitrogen ( $\delta^{15}\text{N}$ ) compositions and nitrogen concentration (N) of mature grains. (B) The spatial distribution of genotypes with regards to nine environments is displayed in a GGE biplot. For both graphs, each of the nine environment is the specific combination of three consecutive crop seasons (2017-2018; 2018-2019 and 2019-2020) and three different topdressing nitrogen fertilization levels (N1, N2 and N2),

## 4. Discussion

### 4.1. Environmental, N management and genotypic effects on yield performance

The use of N fertilization as a basic dressing before sowing, and particularly after sowing as split applications in the form of top dressing, has been a common strategy to ensure vigorous plants with optimal yields, including under rainfed systems (López-Bellido et al., 2005). In our study, doubling the total amount of N applied via the top dressing (from N1 to N3) only had a significant, albeit minor, positive effect (8%) on GY during the (2017-2018) crop season, which was not only a wet season with abundant rainfall, but also exhibited moderate temperatures throughout the crop cycle, which

together with an earlier planting, resulted in a longer crop cycle than during the two following seasons. This small increase in GY was associated with concomitant increases in GN, since no differences in TKW occurred in response to N fertilization. By contrast, GNY increased 22% from N1 to N3, as a combined result of small increases in GY and grain N concentration. The increase in the grain N concentration was a consequence of an excess concentration of N fertilizer because TKW did not change in response to N fertilization (Supplemental Table 2). The effect of N top dressing on GY during the dry (2018-2019) and mildly wet (2019-2020) seasons did not reach significance. Besides that, under the mildly wet conditions of the last season, GNY increased by 17% following N fertilization. In accordance with the above results, the interaction of N fertilization with crop season was highly significant for GY and the other yield components (GNY, GN, TKW). Our study supports the fact that the recommended level of N fertilization (N2) for the Mediterranean continental region of the rainfed wheat regions of central/northern Spain (Fertiberia, 2022; Sativum, 2022) fully covers crop needs, not only in dry seasons but also under wet conditions, and places the crop in the saturation response zone for this nutrient, whereas N1 was probably the best N fertilization option in terms of economic and environmental benefits. In accordance with this saturation pattern, the increase in N top dressing had some effect on increasing the grain N concentration under the wet conditions of the first and third seasons. Increasing N top dressing as a way to improve grain protein concentration in the grains is a well-known practice in spite of the fact that it is not usually economically sound (i.e. grain-quality premium), and it has a negative environmental effect (Medio Ambiente, 2020). Moreover, during the dry season of (2018-2019) the effect of N top dressing fertilization was even null in terms of grain protein content which indicates a rapid N-uptake saturation (Lassaletta et al., 2021; Zhang et al., 2021). In fact, the lower  $\delta^{15}\text{N}$  of the grains from the dry (2018-2019) crop season compared with the other two seasons agrees with a saturation pattern due to an excess of chemical nitrogen fertilizer (Choi et al., 2003; Serret et al. 2008; Yousfi et al., 2012, 2013).

Environmental variability in Western Europe (Spain among other countries) has been reported to explain around 31-51% of yield variability in wheat (Ray et al., 2015). In rainfed Mediterranean systems, temperature and particularly seasonal precipitation patterns are the main factors explaining the environmental variability in GY (Páscoa et al., 2017; Ray et al., 2015) which will increase as a consequence of climate change (Yang et al., 2019). Under the rainfed conditions of our study, the season effect was the most dominant with GY decreasing three-fold during the dry season (2018-2019) and average GNY being halved during the same season, compared with the two wet seasons (2017-2018 and 2019-2020). The poor water status recorded during (2018-2019) was also indicated by the seasonal average  $\delta^{13}\text{C}$  being the highest among the three seasons (Table 2), and in accordance with values reported for severe drought stress in wheat under Mediterranean conditions (Araus et al.,

2003, 2013; del Pozo et al., 2016; Rezzouk et al., 2022). Moreover, the grain N concentration was around 40% higher during the dry season (2018-2019) compared with the other two seasons due to a concentration effect caused, at least in part, by the lower TKW (Li et al., 2011; Triboi et al., 2006).

The genotypic effect was the second most prevalent factor after crop season. Moreover, interactions of genotype by season on the three traits were also significant, meaning a different genotypic performance depending on the season. Previous reports have stated that when grown in their natural agrosystems, the highest yield potential was attained by north-western European cultivars, followed by central European and finally south-western cultivars (Senapati and Semenov, 2020). The GY of slightly above 8 Mg ha<sup>-1</sup> that was achieved in our study during the two wet seasons is in line with potential yields reported in the continental Mediterranean conditions of Spain (Rezzouk et al., 2020). However, our study shows that when grown under Mediterranean conditions, the impact of genotypic provenance was evident on GY in each season but strongly affected by seasonal conditions. Thus, during the two wet seasons northern European cultivars (in particular KWS Siskin and Bennington) exhibited the highest GY, whereas cultivars from central (RGT Reform and Henrik) and southern (Chambo and Soberbio) Europe exhibited yields around 5-10 % lower. An opposite trend was observed during the dry season (2018-2019), where the southern cultivar Soberbio yielded the highest, followed by the northern cultivar KWS Siskin and the central cultivar Henrik, both exhibiting yields around 5% lower. Therefore, even if agronomic adaptation was evidenced in our results, differences across the top yielders of each region were rather modest, no matter the growing conditions. Moreover, although all tested genotypes were selected based on their high yield potentials within a given country, the range of variability within genotypic categories of the same provenance was larger (even among genotypes bred for Mediterranean conditions) than the differences in GY across the highest yielding cultivars of each region. Therefore, the study shows that there exists winter wheat germplasm from northern and even central Europe that is quite well adapted to Mediterranean continental conditions, even for the severe dry seasons. Our results stress the need to emphasize the role of phenological adjustment (Hyles et al., 2020) and water status (Rezzouk et al., 2022) as crucial genotypic traits to optimize adaptation to current Mediterranean conditions and eventually cope with changing conditions in western Europe as a result of climate change. In fact, Senapati and Semenov (2020) concluded that a large genetic yield gap still exists in European wheat, with heat and drought tolerance around flowering, optimal canopy structure and phenology, improved root water uptake and reduced leaf senescence being identified as key traits for improvement. This perception by breeders is probably the basis for the existence of high-yielding cultivars from northern and central Europe that already have a high performance under Mediterranean conditions.



#### 4.2. Defining genotypic ideotypes for Mediterranean conditions: phenology and water status

In wheat, three major crop phases are emphasized as contributors to the final grain yield to varying degrees: (i) vegetative phase, considered from emergence to floral initiation; (ii) reproductive phase, extending from floral initiation to anthesis; and (iii) grain filling stage (Fischer, 2016). Whereas the two first phases mostly determine GN (grains m<sup>-2</sup>), grain filling affects TKW. Nevertheless, regardless of the seasonal conditions, the highest yielding genotypes were characterized by higher GN, while the effect of TKW was minor, and depending on the environmental conditions of the season, not necessarily in a positive sense, which has been widely reported (Slafer et al., 2013). GN is the result of two subordinated agronomic components (ear number and grains per ear) that are determined by phenological stages encompassing planting to anthesis (Sadras and Slafer, 2012; Slafer et al., 2014).

In our study, delayed DTH and DTA during the wettest season (2017-2018) were related to higher GY, and GNY (Table 3; Fig. 2A, D). A positive relationship to GY was also observed for the duration of different phenological stages, particularly from the beginning of stem elongation to heading (DTE-DTH) and anthesis (DTE-DTA) (Supplemental Table 7). Moreover, GY correlated with GN but not with TKW (Table 3). In fact, an extended period prior to anthesis supports higher biomass production, including higher numbers of grains per square meter, and subsequently higher yield production (González et al., 2011; Miralles and Slafer, 2007). In the case of northern genotypes from the UK, higher yields have also been associated with a constitutive stay green condition, which means extended grain filling (Carmo-Silva et al., 2017).

In the case of the mildly wet season (2019-2020), the rainfall that occurred during April and May, which is a key time period covering heading to the middle of grain filling, was lower than for the (2017-2018) crop season, whereas evapotranspiration was higher. Together these caused a certain degree of terminal stress, which in turn was supported by the fact that the  $\delta^{13}\text{C}$  of mature grains was higher (less negative) in (2018-2019) than in (2017-2018). This would explain the lack of correlations between GY and phenological stages, calculated either as days from planting (Table 3; Fig. 2C, F) or as intervals between two consecutive phases (Supplemental Table 7). Nonetheless, the GY achieved in (2019-2020) was higher than the other two seasons. In fact, GY was positively correlated with both GN and TKW, which means a balance between the different phenological phases may also have been involved.

The dry season (2018-2019) negatively impacted crop duration and subsequently the final GY. Unlike the (2017-2018) season, phenology assessed as the crop duration from planting to the different phenological stages was negatively correlated with GY (Table 3, Fig. B, E), which agrees with the fact that phenological escape from increasing crop temperature conditions is a key strategy to deal with severe water stress under Mediterranean conditions (Loss and Siddique, 1994; Araus et al., 2002).

During (2018-2019), crop phenology was the shortest for all genotypes, but a positive phenotypic relationship between specific durations of the reproductive phases with GY, as well as with GN and TKW was found across genotypes (Supplemental Table 7). In fact, increased duration of the stem elongation to heading and/or anthesis period in wheat has been reported to increase assimilate partitioning to the ears and secure greater numbers of fertile florets per ear (González et al., 2011; Miralles et al., 2000), while extending photosynthesis activities for later reallocation of the pre-stored assimilates from source to sink tissues (Senapati and Semenov, 2020; Soriano et al., 2018). Moreover, the positive relationships of a longer grain filling duration with GY suggests the presence of the stay green condition as a positive trait (Christopher et al., 2008).

Overall, genotypic performance under dry conditions implies a rebalanced duration of phenological stages, with a long duration of grain filling relative to the total crop duration being associated with better performance (Araus et al., 2002). In support of that, the duration from planting to the beginning of stem elongation was negatively correlated with GY, whereas the duration of the late phenological stages correlated positively with GY when the three seasons were combined was mainly driven by the differences in phenology among years, particularly the precocity observed in the second season (the dry year and with lowest GY). Furthermore, while genotypes from northern and central Europe exhibited longer crop durations compared to southern European genotypes for the three seasons, the durations of the late phenological stages were longer in southern genotypes, particularly Soberbio and Chambo (Supplemental Table 5). Therefore, earlier anthesis is one common strategy to escape drought during flowering and secure high grain yield under Mediterranean conditions (Senapati and Semenov, 2020), but increasing the relative importance of reproductive stages with regards to the total crop duration (and eventually presenting the stay green condition) may also explain the better performance of southern genotypes relative to the northern and central genotypes during the dry season (Supplemental Table 11). In contrast, during the two wet seasons the somewhat higher yield of northern and central European genotypes (Supplemental Table 11) seemed to be related to their longer duration, particularly of the tillering phase, which may contribute towards a higher spike density and then higher grain yield (Elhani et al., 2007; Moragues et al., 2006).

Water availability is the main constraint to crop growth and production in the Mediterranean region, but also a key limiting factor across Europe where it may account for a genetic yield gap of at least 30-50% under rainfed conditions (Senapati and Semenov, 2020). The  $\delta^{13}\text{C}$  of grains was negatively correlated with GY across the three seasons combined and within each season (Table 3, Fig. 2), indicating that genotypes that kept their stomata more open (Condon et al., 1987) and eventually used more water (Araus et al., 2003), were the most productive (Araus et al., 2008). This agrees with the fact that effective use of water rather than water use efficiency is the trait to consider (Blum 2009).

Indeed, the genotypic effect was significant within each of the three seasons, both for GY and  $\delta^{13}\text{C}$  (Table 2). Overall, despite climate variability across the three studied seasons, some of the northern and southern European cultivars with their higher yields have demonstrated more favorable water status across their lifecycle (lower  $\delta^{13}\text{C}$  in grains) than the central European genotypes. Thus, the southern cultivar Soberbio exhibited the lowest  $\delta^{13}\text{C}$  during the two wet seasons followed by Chambo during (2019-2020), while the northern European cultivar KWS Siskin ranked first during the dry season (2018-2019) (Supplemental Table 6). As an indicator of water status, the  $\delta^{13}\text{C}$  in grains has contributed frequently to prediction models as an explanatory trait for grain yield performance in wheat grown under water-limited environments (Cossani and Sadras, 2021; Ferrio et al., 2007; Rezzouk et al., 2020). Following the same trend in the current study, GY stepwise and LASSO models have determined that the  $\delta^{13}\text{C}$  in grains is a primary explanatory (and negative) variable that contributes to GY (Supplemental Table 9; Supplemental Table 10). These results suggest that water availability remains among the main environmental factors that determine interannual variability in yield performance under Mediterranean conditions.

#### 4.3 Conclusion

There is a clear interplay between environmental factors (basically water status), phenology and yield performance when dealing with winter wheat grown in the Mediterranean. However, N fertilization needs to be finely tuned; while it remains a key management practice to maximize grain yield, and eventually grain quality, its application must be rationalized in the context of the environmental conditions and most importantly water availability. Northern and southern European genotypes may possess candidate traits that give further insights into the strategies that crop breeders use to adapt wheat to drought, whether it is by manipulating the relative duration of the different phenological stages or considering the expected prevalence of wet or dry seasons. Thus, for wet scenarios, a longer stem elongation to anthesis phase may be an approach, while under dry seasons, drought escape (early anthesis) together with a longer reproductive phase, as in the case of southern genotypes, may be the alternative phenological characteristic.

In terms of specific genotypes, Soberbio and Chambo from southern Europe, along with KWS Siskin from northern Europe and Henrik from central Europe were the cultivars best adapted to dry conditions, being the most resilient and high-yielding genotypes of the set. In the case of southern genotypes, the shortening in crop duration was balanced by a more extended duration of the reproductive stage; particularly from heading to grain filling, to secure an optimized final yield. Under wetter conditions however, northern European genotypes, mainly Bennington and KWS Siskin, were the best adapted. Nevertheless, the differences in grain yield among the top winter wheat cultivars

originating from different regions were rather minor, regardless of the season, which supports the fact that breeding for the high-yielding conditions of central and northern Europe delivers good genotypic performance under Mediterranean conditions.

#### **Credit authorship contribution statement**

FZR wrote the first draft, conducted the stable isotope and statistical analyses, drew the tables and figures and implemented the edits; JLA participated in the field evaluation, conceived the study and implemented the edits in the consecutive drafts; MDS collaborated on the stable isotope analyses and revised the drafts; VL conducted a part of the stable isotope analyses; NA conducted the field trials, coordinated the agronomic and phenological data collection, and contributed to writing the Materials and Methods and revising the manuscript draft. MCD-F collected the grain yield, the agronomic yield components and the phenological data.

#### **Declaration of Competing Interest**

The authors declare that they have no known competing financial interests or personal relationships that could have appeared to influence the work reported in this paper.

#### **Acknowledgments**

This study was supported by the Spanish Project PID2019-106650RB-C2 from the Ministerio de Ciencia e Innovación. We thank the partners of the European network ECOFE for providing cultivars from different European countries. JLA acknowledges support from the Catalan Institution for Research and Advanced Studies, Generalitat de Catalunya, Spain, through its program ICREA Academia. FZR is a recipient of a research grant (FI-AGAUR) sponsored by the Agency for Management of University and Research Grants (AGAUR), in collaboration with the University of Barcelona. VL also acknowledges support from a scholarship awarded by the Rio de Janeiro Research Foundation (Fundação de Amparo à Pesquisa do Estado do Rio de Janeiro – FAPERJ) and institutional support from the Graduate Program in Genetics and Plant Breeding and the Universidade Estadual do Norte Fluminense Darcy Ribeiro (UENF). We thank the personnel from the experimental station of ITACYL at Zamadueñas (Valladolid) for their continued support of our research. We extend our thanks to The Water Research Institute (IdRA) for their financial support to cover laboratory analyses.

#### **References**

Akaike, H., 1974. A new look at the statistical model identification. *IEEE Trans. Automat. Contr.* 19, 716–723. <https://doi.org/10.1109/TAC.1974.1100705>

- Alvarado, G., Rodríguez, F.M., Pacheco, A., Burgueño, J., Crossa, J., Vargas, M., Pérez-Rodríguez, P., Lopez-Cruz, M.A., 2020. META-R: a software to analyze data from multi-environment plant breeding trials. *Crop J.* 8, 745–756. <https://doi.org/10.1016/j.cj.2020.03.010>
- Araus, J.L., Slafer, G.A., Reynolds, M.P., Royo, C., 2002. Plant breeding and drought in C3 cereals: what should we breed for? *Ann. Bot.* 89, 925–940. <https://doi.org/10.1093/aob/mcf049>
- Araus, J.L., Slafer, G.A., Royo, C., Serret, M.D., 2008. Breeding for yield potential and stress adaptation in cereals. *CRC Crit. Rev. Plant Sci.* 27, 377–412. <https://doi.org/10.1080/07352680802467736>
- Araus, J.L., Cabrera-Bosquet, L., Serret, M.D., Bort, J., Nieto-Taladriz, M.T., 2013. Combined use of  $\delta^{13}\text{C}$ ,  $\delta^{18}\text{O}$  and  $\delta^{15}\text{N}$  tracks nitrogen metabolism and genotypic adaptation of durum wheat to salinity and water deficit. *Funct. Plant Physiol.* 40, 595–608. <https://doi.org/10.1071/FP12254>
- Araus, J.L., Villegas, D., Aparicio, N., García del Moral, L.F., El-Hani, S., Rharrabti, Y., Ferrio, J.P., Royo, C., 2003. Environmental factors determining carbon isotope discrimination and yield in durum wheat under Mediterranean conditions. *Crop Sci.* 43, 170–180. <https://doi.org/10.2135/cropsci2003.0170>
- Basso, B., Fiorentino, C., Cammarano, D., Cafiero, G., Dardanelli, J., 2012. Analysis of rainfall distribution on spatial and temporal patterns of wheat yield in Mediterranean environment. *Eur. J. Agron.* 41, 52–65. <https://doi.org/10.1016/j.eja.2012.03.007>
- Blum, A., 2009. Effective use of water (EUW) and not water-use efficiency (WUE) is the target of crop yield improvement under drought stress. *F. Crop. Res.* 112, 119–123. <https://doi.org/10.1016/j.fcr.2009.03.009>
- Cabrera-Bosquet, L., Molero, G., Bort, J., Nogués, S., Araus, J.L., 2007. The combined effect of constant water deficit and nitrogen supply on WUE, NUE and  $\Delta^{13}\text{C}$  in durum wheat potted plants. *Ann. Appl. Biol.* 151, 277–289. <https://doi.org/10.1111/j.1744-7348.2007.00195.x>
- Carmo-Silva, E., Andralojc, P.J., Scales, J.C., Driever, S.M., Mead, A., Lawson, T., Raines, C.A., Parry, M.A.J., 2017. Phenotyping of field-grown wheat in the UK highlights contribution of light response of photosynthesis and flag leaf longevity to grain yield. *J. Exp. Bot.* 68, 3473–3486. <https://doi.org/10.1093/jxb/erx169>
- Chairi, F., Sanchez-Bragado, R., Serret, M.D., Aparicio, N., Nieto-Taladriz, M.T., Luis Araus, J., 2020. Agronomic and physiological traits related to the genetic advance of semi-dwarf durum wheat: the case of Spain. *Plant Sci.* 295, 1–14. <https://doi.org/10.1016/j.plantsci.2019.110210>

Choi, W., Ro, H., Lee, S., 2003. Natural <sup>15</sup>N abundances of inorganic nitrogen in soil treated with fertilizer and compost under changing soil moisture regimes. *Soil Biol. Chem.* 35, 1289–1298. [https://doi.org/10.1016/S0038-0717\(03\)00199-8](https://doi.org/10.1016/S0038-0717(03)00199-8)

Chowdhury, S.I., Wardlaw, I.F., 1978. The effect of temperature on kernel development in cereals. *Aust. J. Agric. Res.* 29, 205–223. <https://doi.org/10.1071/AR9780205>

Christopher, J.T., Christopher, M.J., Borrell, A.K., Fletcher, S., Chenu, K., 2016. Stay-green traits to improve wheat adaptation in well-watered and water-limited environments. *J. Exp. Bot.* 67, 5159–5172. <https://doi.org/10.1093/jxb/erw276>

Christopher, J.T., Manschadi, A.M., Hammer, G.L., Borrell, A.K., 2008. Developmental and physiological traits associated with high yield and stay-green phenotype in wheat. *Aust. J. Agric. Res.* 59, 354–364. <https://doi.org/10.1071/AR07193>

Collins, B., Chenu, K., 2021. Improving productivity of Australian wheat by adapting sowing date and genotype phenology to future climate. *Clim. Risk Manag.* 32, 100300. <https://doi.org/10.1016/j.crm.2021.100300>

Condon, A.G., Richards, R.A., Farquhar, G.D. 1987. Carbon isotope discrimination is positively correlated with grain yield and dry matter production in field-grown wheat 1. *Crop Sci.*, 27, 99-1001. <https://doi.org/10.2135/cropsci1987.0011183X002700050035x>

Cossani, M., Sadras, V.O., 2021. Carbon isotope composition for agronomic diagnostic: predicting yield and yield response to nitrogen in wheat. *Carbon isotope composition for agronomic diagnostic: predicting yield and yield response to nitrogen in wheat.* *F. Crops Res.* 279, 108451.

Del Pozo, A., Yáñez, A., Matus, I.A., Tapia, G., Castillo, D., Sanchez-Jardón, L., Araus, J.L., 2016. Physiological traits associated with wheat yield potential and performance under water-stress in a mediterranean environment. *Front. Plant Sci.* 7, 1–13. <https://doi.org/10.3389/fpls.2016.00987>

Elhani, S., Martos, V., Rharrabti, Y., Royo, C., García del Moral, L.F., 2007. Contribution of main stem and tillers to durum wheat (*Triticum turgidum* L. var. durum) grain yield and its components grown in Mediterranean environments. *F. Crop. Res.* 103, 25–35. <https://doi.org/10.1016/j.fcr.2007.05.008>

Evans, R.D., 2001. Physiological mechanisms influencing plant nitrogen isotope composition. *Trends Plant Sci.* 6, 121–126. [https://doi.org/10.1016/S1360-1385\(01\)01889-1](https://doi.org/10.1016/S1360-1385(01)01889-1)

Farquhar, G.D., Ehleringer, J.R., Hubick, K.T., 1989. Carbon isotope discrimination and photosynthesis. *Annu. Rev. Plant Physiol.* 40, 503–537. <https://doi.org/10.1146/annurev.pp.40.060189.002443>

Ferrio, J.P., Mateo, M.A., Bort, J., Abdalla, O., Voltas, J., Araus, J.L., 2007. Relationships of grain  $\delta^{13}\text{C}$  and  $\delta^{18}\text{O}$  with wheat phenology and yield under water-limited conditions. *Ann. Appl. Biol.* 150, 207–215. <https://doi.org/10.1111/j.1744-7348.2007.00115.x>

Fertiberia, 2022. <https://www.fertiberia.com/es/agricultura/servicios-al-agricultor/guia-del-abonado/trigo> (Accessed on April 12<sup>th</sup>, 2022)

Fischer, R.A., 2016. The effect of duration of the vegetative phase in irrigated semi-dwarf spring wheat on phenology, growth and potential yield across sowing dates at low latitude. *F. Crop. Res.* 198, 188–199. <https://doi.org/10.1016/j.fcr.2016.06.019>

Fischer, R.A., 2011. Wheat physiology: a review of recent developments. *Crop Pasture Sci.* 62, 95–114. <https://doi.org/10.1071/CP10344>

Flohr, B.M., Hunt, J.R., Kirkegaard, J.A., Evans, J.R., 2017. Water and temperature stress define the optimal flowering period for wheat in south-eastern Australia. *F. Crop. Res.* 209, 108–119. <https://doi.org/10.1016/j.fcr.2017.04.012>

Foulkes, M.J., Slafer, G.A., Davies, W.J., Berry, P.M., Sylvester-Bradley, R., Martre, P., Calderini, D.F., Griffiths, S., Reynolds, M.P., 2011. Raising yield potential of wheat. III. Optimizing partitioning to grain while maintaining lodging resistance. *J. Exp. Bot.* 62, 469–486. <https://doi.org/10.1093/jxb/erq300>

French, R.J., Schultz, J.E., 1984. Water use efficiency of wheat in a Mediterranean-type environment. I the relation between yield, water use and climate. *Aust. J. Agric. Res.* 35, 765–775. <https://doi.org/10.1071/AR9840765>

González, F.G., Terrile, I.I., Falcón, M.O., 2011. Spike fertility and duration of stem elongation as promising traits to improve potential grain number (and yield): variation in modern Argentinean wheats. *Crop Sci.* 51, 1693–1702. <https://doi.org/10.2135/cropsci2010.08.0447>

Hyles, J., Bloom, M.T., Hunt, J.R., Trethowan, R.M., Trevaskis, B., 2020. Phenology and related traits for wheat adaptation. *Heredity (Edinb)*. 125, 417–430. <https://doi.org/10.1038/s41437-020-0320-1>

Kamran, A., Iqbal, M., Spaner, D., 2014. Flowering time in wheat (*Triticum aestivum* L.): a key factor for global adaptability. *Euphytica* 197, 1–26. <https://doi.org/10.1007/s10681-014-1075-7>

Kitonyo, O.M., Sadras, V.O., Zhou, Y., Denton, M.D., 2017. Evaluation of historic Australian wheat varieties reveals increased grain yield and changes in senescence patterns but limited adaptation to tillage systems. *Field Crops Res.* 206, 65–73. <https://doi.org/10.1016/j.fcr.2017.02.017>

Lassaletta, L., Sanz-Cobena, A., Aguilera, E., Quemada, M., Billen, G., Bondeau, A., Cayuela, M.L., Cramer, W., Eekhout, J.P.C., Garnier, J., Grizzetti, B., Intrigliolo, D.S., Ramos, M.R., Romero, E., Vallejo, A., Gimeno, B.S., 2021. Nitrogen dynamics in cropping systems under Mediterranean climate: a systemic analysis. *Environ. Res. Lett.* 16, 2–24. <https://doi.org/10.1088/1748-9326/ac002c>

Li, P., Chen, J., Wu, P., 2011. Agronomic characteristics and grain yield of 30 spring wheat genotypes under drought stress and nonstress conditions. *Agron. J.* 103, 1619–1628. <https://doi.org/10.2134/agronj2011.0013>

Lobos, G.A., Matus, I., Rodriguez, A., Romero-Bravo, S., Araus, J.L., Del Pozo, A., 2014. Wheat genotypic variability in grain yield and carbon isotope discrimination under Mediterranean conditions assessed by spectral reflectance. *J. Integr. Plant Biol.* 56, 470–479. <https://doi.org/10.1111/jipb.12114>

Long, X.X., Ju, H., Wang, J.D., Gong, S.H., Li, G.Y., 2022. Impact of climate change on wheat yield and quality in the Yellow River Basin under RCP8.5 during 2020–2050. *Adv. Clim. Chang. Res.* 13, 397–407. <https://doi.org/10.1016/j.accre.2022.02.006>

Lopes, M.S., Reynolds, M.P., 2010. Partitioning of assimilates to deeper roots is associated with cooler canopies and increased yield under drought in wheat. *Funct. Plant Biol.* 37, 147–156. <https://doi.org/https://doi.org/10.1071/FP09121>

López-Bellido, L., López-Bellido, R.J., Redondo, R., 2005. Nitrogen efficiency in wheat under rainfed Mediterranean conditions as affected by split nitrogen application. *Field Crop. Res.* 94, 86–97. <https://doi.org/10.1016/j.fcr.2004.11.004>

Loss, S.P., Siddique, K.H.M., 1994. Morphological and physiological traits associated with wheat yield increases in Mediterranean environments. *Adv. Agron.* 52, 229–276. [https://doi.org/10.1016/S0065-2113\(08\)60625-2](https://doi.org/10.1016/S0065-2113(08)60625-2)

Medio ambiente. Junta de Castilla y León, 2020. <https://medioambiente.jcyl.es/web/jcyl/MedioAmbiente/es/Plantilla100Detalle/1246988359553/Noticia/1284966161459/Comunicacion> (Accessed on April 12<sup>th</sup>, 2022)

Miralles, D.J., Richards, R.A., Slafer, G.A., 2000. Duration of the stem elongation period influences the number of fertile florets in wheat and barley. p 27, 931–940. <https://doi.org/10.1071/pp00021>

Miralles, D.J., Slafer, G.A., 2007. Sink limitations to yield in wheat: how could it be reduced? *J. Agric. Sci.* 145, 139–149. <https://doi.org/10.1017/S0021859607006752>



Moragues, M., García Del Moral, L.F., Moralejo, M., Royo, C., 2006. Yield formation strategies of durum wheat landraces with distinct pattern of dispersal within the Mediterranean basin: II. Biomass production and allocation. *F. Crop. Res.* 95, 182–193. <https://doi.org/10.1016/j.fcr.2005.02.008>

Nielsen, D.C., Halvorson, A.D., 1991. Nitrogen fertility influence on water stress and yield of winter wheat. *Agron. J.* 83, 1065–1070. <https://doi.org/10.2134/agronj1991.00021962008300060025x>

Padovan, G., Martre, P., Semenov, M.A., Masoni, A., Bregaglio, S., Ventrella, D., Lorite, I.J., Santos, C., Bindi, M., Ferrise, R., Dibari, C., 2020. Understanding effects of genotype × environment × sowing window interactions for durum wheat in the Mediterranean basin. *F. Crop. Res.* 259, 1–15. <https://doi.org/10.1016/j.fcr.2020.107969>

Páscoa, P., Gouveia, C.M., Russo, A., Trigo, R.M., 2017. The role of drought on wheat yield interannual variability in the Iberian Peninsula from 1929 to 2012. *Int. J. Biometeorol.* 61, 439–451. <https://doi.org/10.1007/s00484-016-1224-x>

Ray, D.K., Gerber, J.S., Macdonald, G.K., West, P.C., 2015. Climate variation explains a third of global crop yield variability. *Nat. Commun.* 6, 1–9. <https://doi.org/10.1038/ncomms6989>

Reynolds, M., Foulkes, J., Furbank, R., Griffiths, S., King, J., Murchie, E., Parry, M., Slafer, G., 2012. Achieving yield gains in wheat. *Plant, Cell Environ.* 35, 1799–1823. <https://doi.org/10.1111/j.1365-3040.2012.02588.x>

Reynolds, M., Foulkes, M.J., Slafer, G.A., Berry, P., Parry, M.A.J., Snape, J.W., Angus, W.J., 2009. Raising yield potential in wheat. *J. Exp. Bot.* 60, 1899–1918. <https://doi.org/10.1093/jxb/erp016>

Rezzouk, F.Z., Gracia-Romero, A., Kefauver, S.C., Gutiérrez, N.A., Aranjuelo, I., Serret, M.D., Araus, J.L., 2020. Remote sensing techniques and stable isotopes as phenotyping tools to assess wheat yield performance: effects of growing temperature and vernalization. *Plant Sci.* 295, 1–16. <https://doi.org/10.1016/j.plantsci.2019.110281>

Rezzouk, F.Z., Gracia-Romero, A., Kefauver, S.C., Nieto-Taladriz, M.T., Serret, M.D., Araus, J.L., 2022. Durum wheat ideotypes in Mediterranean environments differing in water and temperature conditions. *Agric. Water Manag.* 259, 1–15. <https://doi.org/10.1016/j.agwat.2021.107257>

Sativum, 2022. <https://www.sativum.es/web/sativum/home#queEsSativum> (Accessed on April 12<sup>th</sup>, 2022)

Sadras, V.O., Lawson, C., 2011. Genetic gain in yield and associated changes in phenotype, trait plasticity and competitive ability of South Australian wheat varieties released between 1958 and 2007. *Crop Pasture Sci.* 62, 533-549. <https://doi.org/10.1071/CP11060>

- Sadras, V.O., Slafer, G.A., 2012. Environmental modulation of yield components in cereals: Heritabilities reveal a hierarchy of phenotypic plasticities. *F. Crop. Res.* 127, 215-224. <https://doi.org/10.1016/j.fcr.2011.11.014>
- Sadras, V.O., Lawson, C., 2013. Nitrogen and water-use efficiency of Australian wheat varieties released between 1958 and 2007. *Eur. J. Agron.* 46, 34-41. <https://doi.org/10.1016/j.eja.2012.11.008>
- Sadras, V.O., Hayman, P.T., Rodriguez, D., Monjardino, M., Bielich, M., Unkovich, M., Mudge, B., Wang, E., 2016. Interactions between water and nitrogen in Australian cropping systems: Physiological, agronomic, economic, breeding and modelling perspectives. *Crop Pasture Sci.* 67, 1019–1053. <https://doi.org/10.1071/CP16027>
- Senapati, N., Semenov, M.A., 2020. Large genetic yield potential and genetic yield gap estimated for wheat in Europe. *Glob. Food Sec.* 24, 1–9. <https://doi.org/10.1016/j.gfs.2019.100340>
- Serret, M.D., Ortiz-Monasterio, I., Pardo, A., Araus, J.L., 2008. The effects of urea fertilisation and genotype on yield, nitrogen use efficiency,  $\delta^{15}\text{N}$  and  $\delta^{13}\text{C}$  in wheat. *Ann. Appl. Biol.* 153, 243–257. <https://doi.org/10.1111/j.1744-7348.2008.00259.x>
- Shavrukov, Y., Kurishbayev, A., Jatayev, S., Shvidchenko, V., Zotova, L., Koekemoer, F., de Groot, S., Soole, K., Langridge, P., 2017. Early flowering as a drought escape mechanism in plants: how can it aid wheat production? *Front. Plant Sci.* 8, 1–8. <https://doi.org/10.3389/fpls.2017.01950>
- Slafer, G.A., Savin, R., 1994. Source-sink relationships and grain mass at different positions within the spike in wheat. *Field Crop. Res.* 37, 39–49. [https://doi.org/10.1016/0378-4290\(94\)90080-9](https://doi.org/10.1016/0378-4290(94)90080-9)
- Slafer, G.A., Savin, R., Sadras, V.O., 2014. Coarse and fine regulation of wheat yield components in response to genotype and environment. *F. Crop. Res.* 157, 71-83. <https://doi.org/10.1016/j.fcr.2013.12.004>
- Soriano, J.M., Villegas, D., Sorrells, M.E., Royo, C., 2018. Durum wheat landraces from east and west regions of the Mediterranean basin are genetically distinct for yield components and phenology. *Front. Plant Sci.* 9, 1–9. <https://doi.org/10.3389/fpls.2018.00080>
- Triboi, E., Martre, P., Girousse, C., Ravel, C., Triboi-Blondel, A.M., 2006. Unravelling environmental and genetic relationships between grain yield and nitrogen concentration for wheat. *Eur. J. Agron.* 25, 108–118. <https://doi.org/10.1016/j.eja.2006.04.004>
- Vergara-Díaz, O., Zaman-Allah, M.A., Masuka, B., Hornero, A., Zarco-Tejada, P., Prasanna, B.M., Cairns, J.E., Araus, J.L., 2016. A Novel remote sensing approach for prediction of maize yield under different conditions of nitrogen fertilization. *Front. Plant Sci.* 7, 1–13. <https://doi.org/10.3389/fpls.2016.00666>

- Voltas, J., Romagosa, I., Lafarga, A., Armesto, A.P., Sombrero, A., Araus, J.L. 1999. Genotype by environment interaction for grain yield and carbon isotope discrimination of barley in Mediterranean Spain. *Aust. J. Agric. Res.* 50, 1263-1271. <https://doi.org/10.1071/AR98137>
- Voss-Fels, K.P., Stahl, A., Wittkop, B., Lichthardt, C., Nagler, S., Rose, T., Chen, T.W., Zetzsche, H., Seddig, S., Majid Baig, M., Ballvora, A., Frisch, M., Ross, E., Hayes, B.J., Hayden, M.J., Ordon, F., Leon, J., Kage, H., Friedt, W., Stützel, H., Snowdon, R.J., 2019. Breeding improves wheat productivity under contrasting agrochemical input levels. *Nat. Plants* 5, 706–714. <https://doi.org/10.1038/s41477-019-0445-5>
- Wardlaw, I., Sofield, I., Cartwright, P., 1980. Factors limiting the rate of dry matter accumulation in the grain of wheat grown at high temperature. *Funct. Plant Biol.* 7, 1–14. <https://doi.org/10.1071/pp9800387>
- Xu, C., Tao, H., Tian, B., Gao, Y., Ren, J., Wang, P., 2016. Limited-irrigation improves water use efficiency and soil reservoir capacity through regulating root and canopy growth of winter wheat. *F. Crop. Res.* 196, 268–275. <https://doi.org/10.1016/j.fcr.2016.07.009>
- Yang, C., Fraga, H., van Ieperen, W., Trindade, H., Santos, J.A., 2019. Effects of climate change and adaptation options on winter wheat yield under rainfed Mediterranean conditions in southern Portugal. *Clim. Change* 154, 159–178. <https://doi.org/10.1007/s10584-019-02419-4>
- Yousfi, S., Serret, M.D., Araus, J.L., 2013. Comparative response of  $\delta^{13}\text{C}$ ,  $\delta^{18}\text{O}$  and  $\delta^{15}\text{N}$  in durum wheat exposed to salinity at the vegetative and reproductive stages. *Plant, Cell Environ.* 36, 1214–1227. <https://doi.org/10.1111/pce.12055>
- Yousfi, S., Serret, M.D., Márquez, A.J., Voltas, J., Araus, J.L., 2012. Combined use of  $\delta^{13}\text{C}$ ,  $\delta^{18}\text{O}$  and  $\delta^{15}\text{N}$  tracks nitrogen metabolism and genotypic adaptation of durum wheat to salinity and water deficit. *New Phytol.* 194, 230–244. <https://doi.org/10.1111/j.1469-8137.2011.04036.x>
- Zadoks, J.C., Chang, T.T., Konzak, C.F., 1974. Data sheet highlights close coupled pumps. *WEED Res.* 14, 415–421. [https://doi.org/10.1016/s0262-1762\(99\)80614-2](https://doi.org/10.1016/s0262-1762(99)80614-2)
- Zhang, P., Qi, Y.K., Wang, H.G., He, J.N., Li, R.Q., Liang, W.L., 2021. Optimizing nitrogen fertilizer amount for best performance and highest economic return of winter wheat under limited irrigation conditions. *PLoS One* 16, 1–17. <https://doi.org/10.1371/journal.pone.0260379>

## Supplemental tables

**Supplemental Table 1.** List of the elite European winter wheat genotypes (*Triticum aestivum* L.) used in the study, selected for their high yield and grain performance.

Genotype	Region	Country	Recommended by
<i>Bennington</i> *	Northern	United Kingdom	Elsoms Seeds
<i>JB Diego</i>	Northern	Ireland	National University of Ireland, Galway
<i>Julius</i>	Northern	Sweden	Swedish University of Agricultural Sciences
<i>KWS Lili</i> *	Northern	Ireland	Teagasc-Agriculture and Food Development Authority
<i>KWS Siskin</i>	Northern	United Kingdom	Rothamsted Research
<i>Benchmark</i>	Central	Germany	Hannover University
<i>CH-Nara</i>	Central	Switzerland	Agroscope
<i>Henrik</i>	Central	Belgium	Ghent University-Flanders Research Institute for Agriculture, Fisheries and Food-ILVO
<i>Hondia</i>	Central	Poland	Institute of Soil Science and Plant Cultivation-State Research Institute
<i>RGT reform</i>	Central	Germany	Hohenheim University
<i>Bologna</i>	Southern	Italy	University of Bologna
<i>Chambo</i>	Southern	Spain	Institute of Agrifood Research and Technology-IRTA
<i>Soberbio</i>	Southern	Spain	Instituto Técnico y Agrario de Castilla y León -ITACyL

\*KWS Lili was replaced by Bennington during the last two crop seasons (2018-2019 and 2019-2020).

**Supplemental Table 2.** Nitrogen fertilization supply in different treatments (N1, N2 and N3), as basic dressing using N-P-K, and top dressing supplied using calcium ammonium nitrate (CAN) as a first amendment, and nitrosyl sulfuric acid (NSA) as a second amendment, as used throughout the three crop seasons (2017-2018; 2018-2019; 2019-2020). Information on soil texture, previous crops, organic matter, total nitrogen content and available mineral N in soil before sowing and soil water content are also displayed.

		2017-2018			2018-2019			2019-2020			
		Date	kg ha <sup>-1</sup>	UN	Date	kg ha <sup>-1</sup>	UN	Date	kg ha <sup>-1</sup>	UN	
Basic dressing	N1	8-15-15	30/10/:	300	24.0	16/11/18	300	24.0	22/10/19	300	24.0
	N2	8-15-15	30/10/:	300	24.0	16/11/18	300	24.0	22/10/19	300	24.0
	N3	8-15-15	30/10/:	300	24.0	16/11/18	300	24.0	22/10/19	300	24.0
1 <sup>st</sup> Top dressing	N1	CAN 27%	8/2/18	150	40.5	28/2/19	75	20.3	14/1/20	75	20.3
	N2	CAN 27%	8/2/18	150	40.5	28/2/19	150	40.5	14/1/20	150	40.5
	N3	CAN 27%	8/2/18	150	40.5	28/2/19	200	54.0	14/1/20	200	54.0
2 <sup>nd</sup> Top dressing	N1	NSA 26%	-	-	-	12/4/19	75	19.5	12/3/20	75	19.5
	N2	NSA 26%	26/3/18	150	39.0	12/4/19	150	39.0	12/3/20	150	39.0
	N3	NSA 26%	26/3/18	240	62.4	12/4/19	200	52.0	12/3/20	200	52.0
Total N	N1			64.5			63.8			63.8	
	N2	UN (kg ha <sup>-1</sup> )		103.5			103.5			103.5	
	N3			126.9			130.0			130.0	
<b>Soil texture</b>											
				Silk-loam			Silk-loam			Silk-loam	
<b>Previous year's crop</b>											
				Fallow			Rainfed lentils			Fallow	
<b>Organic matter<sup>a</sup></b>											
	%			1.10			2.45			1.17	
<b>Mineral N (NO<sub>3</sub><sup>-</sup> + NH<sub>4</sub><sup>+</sup>) before sowing<sup>a</sup></b>											
	Kg ha <sup>-1</sup>			-			65.1			-	
<b>Total N before sowing<sup>a</sup></b>											
	%			0.139			0.065			0.067	
<b>Soil water content (end of September)<sup>b</sup></b>											
	mm			121			119			-	
<b>Current situation (September 1<sup>st</sup>, 2022)</b>											
<b>Mineral N (NO<sub>3</sub><sup>-</sup> + NH<sub>4</sub><sup>+</sup>) content<sup>c</sup></b>											
	Kg ha <sup>-1</sup>			-			157.6			98.8	
<b>Total N<sup>c</sup></b>											
	%			-			0.123			0.112	

UN = Kg N ha<sup>-1</sup>; <sup>a</sup> measured for the upper 30 cm of soil depth; NH<sub>4</sub><sup>+</sup> represented only about 2% of total mineral N content; <sup>b</sup> measured for the whole (ca. 100 cm) profile; <sup>c</sup> availability measured for the upper 20 cm of soil depth; analyses were carried out in soil samples on September 1<sup>st</sup> 2022, from the experimental fields that were used for the study during 2018-2019 and 2019-2020 crop seasons; NH<sub>4</sub><sup>+</sup> represented about 5% of total mineral N content. For both fields, the previous year's crop was rainfed wheat. The (2017-2018) site was not analyzed due to the presence of a summer (maize) crop.

**Supplemental Table 3.** Comparison of mixed models tested for each dependent variable during the combined and separate crop seasons. Model selection was based on the smallest value of the standard Akaike Information Criterion (AIC) (Akaike, 1974).

Crop season	Models	df	AIC	Selection
2017-2018	GY ~ N fertilization*Genotype + (1 Block)	38	185.50	Yes
	GY ~ N fertilization*Genotype + (N fertilization Block)	43	190.70	No
	GY ~ N fertilization*Genotype + (1 Block) + (N fertilization Block)	44	192.70	No
2018-2019	GY ~ N fertilization*Genotype + (1 Block)	38	258.25	No
	GY ~ N fertilization*Genotype + (N fertilization Block)	43	251.23	Yes
	GY ~ N fertilization*Genotype + (1 Block) + (N fertilization Block)	44	253.23	No
2019-2020	GY ~ N fertilization*Genotype + (1 Block)	38	281.73	No
	GY ~ N fertilization*Genotype + (N fertilization Block)	43	280.56	Yes
	GY ~ N fertilization*Genotype + (1 Block) + (N fertilization Block)	44	282.56	No
Combined seasons	GY ~ Year*N fertilization*Genotype + (1 Block)	110	784.25	No
	GY ~ Year*N fertilization*Genotype + (Year Block)	115	742.31	Yes
	GY ~ Year*N fertilization*Genotype + (N fertilization Block)	115	784.22	No
	GY ~ Year*N fertilization*Genotype + (1 Block) + (Year Block)	116	744.31	No
	GY ~ Year*N fertilization*Genotype + (1 Block) + (N fertilization Block)	116	786.22	No
	GY ~ Year*N fertilization*Genotype + (1 Block) + (Year Block) + (N fertilization Block)	122	745.45	No

*For each crop season and the combined seasons, the selected model was applied to the rest of dependent variables.*

**Supplemental Table 4.** Average grain yield (GY), grain nitrogen yield (GNY), grain number (GN), thousand kernel weight (TKW), and number of days from planting to different phenological stages (tillering “DTT”, elongation “DTE”, booting “DTB”, heading “DTH”, anthesis “DTA”, mid grain filling “MGF”), where the numbers in parentheses refer to the Zadoks et al. (1974) scale, of the twelve European bread wheat varieties grown under different N treatments (N1, N2, N3) and during different crop seasons (2017-2018; 2018-2019; 2019-2020). For each crop season, the upper, middle and lower subsets of genotypes refer to cultivars released in northern, central and southern Europe. Within each subset and season, varieties were ranked based on their grain yield performance (GY).

Crop season	Variety	GY (Mg ha <sup>-1</sup> )	GNY (Mg ha <sup>-1</sup> )	GN (m <sup>-2</sup> )	TKW (g)	DTT (20-29) (d)	DTE (30) (d)	DTB (45) (d)	DTH (55) (d)	DTA (65) (d)	MGF (75) (d)
2017-2018	<i>KWS Siskin</i>	9.09a±0.21	0.17a±0.01	28351.5a±1030.2	32.25ef±0.79	111.7a±0.9	138.8abc±2.1	198.7cd±0.3	203.6bc±0.4	211.3bc±0.7	228.3ab±0.9
	<i>JB Diego</i>	8.64ab±0.18	0.16abc±0.01	25564.1b±532.7	33.88de±0.73	111.6a±1.2	139.3abc±1.8	199.8bc±0.3	206.6a±0.5	213.8ab±1.0	229.6ab±1.0
	<i>KWS Lilli</i>	7.81cde±0.20	0.14bc±0.01	25132.0b±983.9	31.25f±0.49	113.8a±1.9	142.7a±2.1	200.3abc±0.4	207.6a±0.3	214.3ab±0.8	231.6a±0.4
	<i>Julius</i>	7.66de±0.21	0.15abc±0.01	20961.0de±800.5	36.73bc±0.77	112.8a±1.3	142.2ab±1.9	201.8a±0.7	208.0a±0.4	215.1a±0.8	232.7a±0.7
	<i>RGT Reform</i>	8.67ab±0.21	0.17ab±0.01	24058.4bc±2745.3	36.38bcd±0.54	113.2a±1.2	135.4abc±1.7	201.0ab±0.5	207.3a±0.4	214.0ab±0.8	229.4ab±1.4
	<i>Benchmark</i>	8.42b±0.14	0.14abc±0.01	24354.9bc±2760.3	34.22cde±0.64	115.3a±1.1	137.7abc±1.8	200.0bc±0.3	206.2ab±0.7	213.0ab±1.0	229.1ab±1.2
	<i>Henrik</i>	8.34bc±0.19	0.14c±0.01	21944.0cd±2484.6	37.93ab±0.43	112.7a±0.4	138.8abc±1.8	200.0bc±0.5	206.0ab±0.7	214.1ab±0.8	228.9ab±0.7
	<i>Hondia</i>	7.47e±0.23	0.15abc±0.01	19018.2ef±672.6	39.36a±0.43	114.3a±1.5	138.3abc±2.1	199.8bc±0.3	205.6ab±0.5	213.4ab±0.7	230.0ab±1.6
	<i>CH-Nara</i>	6.41f±0.17	0.15abc±0.01	18087.4f±2063.8	35.43bcd±0.34	112.8a±1.4	139.9abc±2.2	197.8d±0.3	201.9c±0.2	207.0de±0.0	225.7bc±0.8
	<i>Chambo</i>	8.13bcd±0.34	0.15abc±0.01	22228.7cd±2671.7	36.68bc±0.59	112.1a±1.7	132.1c±0.7	185.6f±0.5	191.6ab±0.7	205.1e±1.0	220.4d±0.5
	<i>Soberbio</i>	8.09bcd±0.22	0.16abc±0.01	22913.0bcd±2618.1	35.24cd±0.37	112.8a±1.6	134.9abc±1.8	189.2e±0.3	198.2d±1.6	209.0cd±1.4	220.9d±0.7
	<i>Bologna by SIS</i>	6.61f±0.13	0.15abc±0.01	21917.0d±460.6	30.18f±0.39	112.7a±1.4	134.3bc±1.6	188.7e±0.4	194.0e±0.0	204.6e±1.0	222.6cd±0.9
2018-2019	<i>KWS Siskin</i>	2.94ab±0.21	0.07abc±0.01	11372.5ab±1585.9	26.40c±0.93	100.3a±1.9	124.1c±2.2	162.7ab±0.8	168.3c±0.5	173.0ab±0.4	193.3ab±0.4
	<i>Bennington</i>	2.35abcd±0.22	0.06abc±0.01	7720.9bcde±681.3	30.63abc±1.54	99.3a±1.9	127.8bc±1.2	163.4a±0.8	170.1bc±0.8	172.6ab±0.4	193.2ab±0.3
	<i>Julius</i>	2.18bcd±0.23	0.06abc±0.01	7423.7cde±1072.2	29.60abc±0.95	96.0ab±2.0	130.0ab±1.0	165.2a±0.3	172.4ab±0.6	174.8a±0.4	193.6ab±0.4
	<i>JB Diego</i>	2.17bcd±0.15	0.06abc±0.01	7342.6de±635.3	30.06abc±0.87	100.0a±1.5	132.3a±0.4	165.0a±0.4	171.5ab±0.6	173.6ab±0.6	194.0a±0.0
	<i>Henrik</i>	2.92ab±0.27	0.07abc±0.01	9025.8bcde±839.7	32.54a±0.78	95.3ab±2.2	127.3bc±0.7	164.7a±0.5	171.6ab±0.4	173.3ab±0.5	193.1ab±0.3
	<i>CH-Nara</i>	2.55abcd±0.26	0.07abc±0.01	9876.5abcde±1008.4	26.20c±0.97	98.3ab±1.8	124.6c±2.1	159.4bc±1.0	165.8d±0.3	171.8b±0.5	192.0bc±0.6
	<i>RGT Reform</i>	2.33abcd±0.26	0.06abc±0.01	8457.1bcde±1209.6	28.52abc±1.24	99.0a±1.5	133.0a±0.0	165.2a±0.5	173.7a±0.5	174.3a±0.4	193.2ab±0.4
	<i>Benchmark</i>	2.00cd±0.16	0.05bc±0.01	7896.9bcde±952.1	26.80c±1.66	98.3ab±1.8	131.0ab±0.0	164.4a±0.5	171.6ab±0.6	173.1ab±0.5	193.1ab±0.3
	<i>Hondia</i>	1.92d±0.17	0.04c±0.01	6393.5e±1075.4	31.95ab±1.40	98.7ab±1.7	130.4ab±1.4	164.0a±1.3	172.7ab±1.0	174.3a±0.7	193.1ab±0.3
	<i>Soberbio</i>	3.15a±0.19	0.08a±0.01	11254.6abc±600.9	28.01abc±0.71	97.3ab±2.1	118.6d±1.0	156.5cd±1.6	164.7de±0.7	168.4c±0.7	190.9c±0.4
	<i>Chambo</i>	2.88abc±0.19	0.07abc±0.01	10485.4abcd±700.3	27.57bc±0.84	101.0a±1.5	118.9d±1.7	155.2d±0.9	163.3ef±0.5	168.6c±0.6	190.7c±0.3
	<i>Bologna by SIS</i>	2.79abcd±0.14	0.07ab±0.01	13239.2a±454.5	21.07d±0.64	90.9b±0.9	114.6e±0.9	155.1d±1.1	161.8f±0.3	167.0c±0.4	190.8c±0.2
2019-2019	<i>Bennington</i>	9.58a±0.25	0.16ab±0.01	25727.1ab±799.1	37.33bc±0.63	-	117.9abc±1.5	185.3ab±0.7	194.6a±0.3	201.2a±0.2	-
	<i>KWS Siskin</i>	9.13a±0.29	0.16ab±0.01	26299.0a±817.1	34.85cd±1.00	-	113.0cde±0.8	181.8c±1.0	190.1ab±0.9	201.2a±0.2	-
	<i>JB Diego</i>	8.82ab±0.21	0.15ab±0.01	24046.0abc±788.1	36.84bc±0.61	-	122.2a±1.7	184.9ab±0.6	194.6a±0.3	201.2a±0.2	-
	<i>Julius</i>	7.40cd±0.24	0.14ab±0.01	19755.0de±752.1	37.59bc±0.62	-	122.7a±1.1	186.2ab±0.7	194.6a±0.5	201.2a±0.2	-
	<i>Henrik</i>	9.53a±0.33	0.17a±0.01	25254.3ab±910.4	37.81bc±0.70	-	119.9ab±1.6	186.2ab±0.7	194.3a±0.5	201.2a±0.2	-
	<i>Benchmark</i>	8.88ab±0.18	0.15ab±0.01	25378.5ab±844.5	35.18cd±0.86	-	118.0abc±1.5	184.9ab±0.6	193.0a±1.0	201.2a±0.2	-
	<i>RGT Reform</i>	8.12bc±0.31	0.15ab±0.01	22052.7cd±1034.1	37.03bc±0.72	-	122.7a±1.3	185.3ab±0.7	194.3a±0.5	201.2a±0.2	-
	<i>Hondia</i>	7.98bc±0.14	0.14ab±0.01	21469.9cde±511.0	37.30bc±0.74	-	115.2bcd±1.3	187.1a±0.6	194.8a±0.3	201.2a±0.2	-
	<i>CH-Nara</i>	6.31e±0.23	0.14ab±0.01	19146.0e±721.6	33.00de±0.48	-	112.8cde±1.4	184.0bc±0.6	189.7ab±0.7	200.6a±0.7	-
	<i>Soberbio</i>	9.46a±0.33	0.16ab±0.01	23023.5bc±766.1	41.09a±0.54	-	107.9e±1.1	168.4d±0.9	175.6c±1.2	188.4b±0.3	-
	<i>Chambo</i>	8.63ab±0.42	0.15ab±0.01	22268.6cd±1017.2	38.69ab±0.55	-	109.4de±0.9	164.7e±0.7	170.9c±0.9	188.0b±0.0	-

	<i>Bologna by SIS</i>	6.95 <sup>de</sup> ±0.29	0.14 <sup>ab</sup> ±0.01	22298.5 <sup>cd</sup> ±685.6	31.12 <sup>e</sup> ±0.63	-	110.3 <sup>de</sup> ±0.8	170.0 <sup>d</sup> ±0.0	184.7 <sup>b</sup> ±4.2	188.0 <sup>b</sup> ±0.0	-
Combined seasons	<i>KWS Siskin</i>	7.09 <sup>a</sup> ±0.58	0.14 <sup>a</sup> ±0.01	22416.7 <sup>a</sup> ±1555.0	31.30 <sup>d</sup> ±0.86	-	126.0 <sup>b</sup> ±2.3	181.7 <sup>c</sup> ±2.8	187.7 <sup>c</sup> ±2.8	195.8 <sup>bc</sup> ±3.1	-
	<i>JB Diego</i>	6.44 <sup>b</sup> ±0.60	0.12 <sup>ab</sup> ±0.01	18984.2 <sup>b</sup> ±1633.8	33.40 <sup>bc</sup> ±0.68	-	131.6 <sup>a</sup> ±1.6	183.2 <sup>bc</sup> ±2.7	190.7 <sup>ab</sup> ±2.8	196.0 <sup>bc</sup> ±3.2	-
	<i>Julius</i>	5.79 <sup>de</sup> ±0.50	0.12 <sup>ab</sup> ±0.01	16387.2 <sup>cd</sup> ±1255.0	34.58 <sup>ab</sup> ±0.83	-	131.9 <sup>a</sup> ±1.7	184.3 <sup>a</sup> ±2.9	192.3 <sup>a</sup> ±2.8	197.8 <sup>a</sup> ±3.2	-
	<i>Henrik</i>	6.73 <sup>ab</sup> ±0.59	0.13 <sup>ab</sup> ±0.01	18618.2 <sup>b</sup> ±1466.4	36.05 <sup>a</sup> ±0.61	-	128.6 <sup>ab</sup> ±1.7	182.8 <sup>bc</sup> ±2.8	189.8 <sup>bc</sup> ±2.7	195.3 <sup>c</sup> ±3.2	-
	<i>Benchmark</i>	6.23 <sup>bcd</sup> ±0.63	0.12 <sup>b</sup> ±0.01	19012.2 <sup>b</sup> ±1657.7	31.93 <sup>cd</sup> ±0.97	-	129.2 <sup>ab</sup> ±1.7	182.4 <sup>c</sup> ±2.8	189.4 <sup>bc</sup> ±2.7	195.0 <sup>c</sup> ±3.2	-
	<i>RGT Reform</i>	6.18 <sup>bcd</sup> ±0.59	0.13 <sup>ab</sup> ±0.01	17963.7 <sup>bc</sup> ±1486.8	33.62 <sup>bc</sup> ±0.90	-	130.4 <sup>a</sup> ±1.3	183.1 <sup>bc</sup> ±2.8	191.0 <sup>ab</sup> ±2.6	195.5 <sup>bc</sup> ±3.1	-
	<i>Hondia</i>	5.84 <sup>cde</sup> ±0.54	0.12 <sup>b</sup> ±0.010	15982.3 <sup>d</sup> ±1329.2	36.10 <sup>a</sup> ±0.81	-	128.3 <sup>ab</sup> ±2.1	184.2 <sup>ab</sup> ±2.8	191.6 <sup>ab</sup> ±2.6	197.0 <sup>ab</sup> ±3.1	-
	<i>CH-Nara</i>	4.99 <sup>f</sup> ±0.38	0.12 <sup>ab</sup> ±0.01	15611.6 <sup>d</sup> ±940.5	31.38 <sup>d</sup> ±0.84	-	125.5 <sup>b</sup> ±2.4	180.4 <sup>d</sup> ±3	185.0 <sup>d</sup> ±2.8	192.2 <sup>d</sup> ±2.9	-
	<i>Soberbio</i>	6.70 <sup>ab</sup> ±0.56	0.13 <sup>ab</sup> ±0.01	18915.7 <sup>b</sup> ±1161.2	34.51 <sup>ab</sup> ±1.08	-	120.4 <sup>c</sup> ±2.3	170.8 <sup>e</sup> ±2.6	179.1 <sup>e</sup> ±2.7	187.9 <sup>e</sup> ±3.2	-
	<i>Chambo</i>	6.39 <sup>bc</sup> ±0.55	0.12 <sup>ab</sup> ±0.01	18177.5 <sup>bc</sup> ±1224.0	33.95 <sup>bc</sup> ±1.01	-	120.0 <sup>c</sup> ±1.9	168.0 <sup>f</sup> ±2.4	174.8 <sup>f</sup> ±2.3	186.4 <sup>f</sup> ±2.8	-
	<i>Bologna by SIS</i>	5.39 <sup>ef</sup> ±0.38	0.12 <sup>ab</sup> ±0.01	19151.6 <sup>b</sup> ±864.3	27.39 <sup>e</sup> ±0.93	-	120.2 <sup>c</sup> ±2.1	171.3 <sup>e</sup> ±2.6	179.1 <sup>e</sup> ±2.9	186.5 <sup>f</sup> ±2.9	-

Each genotypic value is the mean ± standard error of the three replicates, and three N fertilization levels per season (seasonal values) and for the set of three consecutive seasons (overall genotypic values). Within each year, means exhibiting different letters are significantly different ( $P < 0.05$ ) according to the post-hoc test (Tukey-

**Supplemental Table 5.** Average days from planting to the beginning of stem elongation (DTE), phenological durations from stem elongation to booting (DTE-DTB), stem elongation to heading (DTE-DTH), stem elongation to anthesis (DTE-DTA), stem elongation to mid grain filling (DTE-MGF), and phenological durations from booting to heading (DTB-DTH), heading to anthesis (DTH-DTA) and anthesis to mid grain filling (DTA-MGF), of the twelve European bread wheat varieties grown under different N treatments (N1, N2, N3) and during different crop seasons (2017-2018; 2018-2019; 2019-2020). For each crop season, the upper, middle and lower subsets of genotypes refer to cultivars released in northern, central and southern Europe. Within each subset and season, varieties were ranked based on their grain yield performance (GY).

Crop season	Variety	DTE-DTB	DTE-DTH	DTE-DTA	DTE-MGF	DTB-DTH	DTH-DTA	DTA-MGF
2017-2018	KWS Siskin	59.9ab±2.2	64.8ab±2.2	72.5ab±2.3	89.6a±2.1	4.9bc±0.4	7.7bcd±0.8	17.2ab±1.1
	JB Diego	60.5ab±1.8	67.3ab±2.2	74.5ab±2.7	90.3a±1.9	6.8abc±0.4	7.3cd±0.7	15.8ab±1.3
	KWS Lilli	57.7ab±2.1	64.9ab±2.2	71.7ab±2.5	88.9a±2.1	7.3ab±0.3	6.8d±0.8	17.3ab±1.0
	Julius	59.7ab±2.1	65.9ab±1.9	73.0ab±2.0	90.6a±1.7	6.3abc±0.4	7.2cd±0.5	17.6ab±1.2
	RGT Reform	65.6a±1.7	71.9a±1.7	78.6a±1.8	94.0a±2.3	6.4abc±0.4	6.7d±0.8	15.5ab±1.6
	Benchmark	62.4ab±1.7	68.6ab±2.0	75.4ab±2.0	91.5a±1.5	6.3abc±0.6	6.8d±0.7	16.2ab±1.6
	Henrik	61.3ab±1.7	67.3ab±1.8	75.4ab±1.7	90.2a±2.2	6.0bc±0.5	8.2bcd±0.6	14.8ab±1.1
	Hondia	61.5ab±2.1	67.3ab±2.2	75.2ab±2.6	91.7a±2.0	5.8bc±0.5	7.9bcd±0.8	16.6ab±1.9
	CH-Nara	57.9ab±2.3	62.0b±2.2	67.2b±2.2	85.8a±2.7	4.2c±0.3	5.2d±0.2	18.7a±0.8
	Chambo	53.5b±0.7	59.5b±0.7	73.0ab±1.0	88.4a±0.9	6.0bc±0.4	13.6a±1.4	15.4ab±1.3
	Soberbio	54.4b±1.8	63.4ab±2.8	74.2ab±2.6	86.0a±2.0	9.0a±1.7	10.8ab±0.5	11.9b±1.2
	Bologna by SIS	54.4b±1.7	59.7b±1.6	70.3ab±1.4	88.3a±1.8	5.4bc±0.4	10.6abc±1.0	18.0ab±1.1
2018-2019	KWS Siskin	38.6ab±2.4	44.3abc±2.5	48.9abc±2.2	69.3bc±2.3	5.7a±0.9	4.7ab±0.6	20.4bcd±0.5
	Bennington	35.9abc±1.3	42.4abc±1.0	44.8bcde±1.1	65.5cde±1.1	6.5a±0.6	2.5cd±0.5	20.7bcd±0.3
	Julius	35.2abc±1.0	42.5abc±0.6	44.8bcde±0.9	63.6cde±1.1	7.4a±0.6	2.4cd±0.5	18.8d±0.5
	JB Diego	32.7 bc±0.6	39.2c±0.7	41.3e±0.7	61.7de±0.4	6.5a±0.7	2.2cd±0.2	20.5bcd±0.6
	Henrik	37.4abc±0.9	44.3abc±0.9	46.0bcde±1.0	65.8cde±0.8	6.9a±0.6	1.8d±0.5	19.8d±0.4
	CH-Nara	34.9abc±1.9	41.3bc±2.1	47.3abcd±2.1	67.5bcd±2.5	6.4a±0.9	6.0a±0.4	20.3bcd±0.7
	RGT Reform	32.3c±0.5	40.7bc±0.5	41.4e±0.4	60.3e±0.4	8.5a±0.5	0.7d±0.3	18.9d±0.5
	Benchmark	33.5bc±0.5	40.6bc±0.6	42.2de±0.5	62.2de±0.3	7.2a±0.6	1.6d±0.4	20.0cd±0.4
	Hondia	33.6bc±0.5	42.3abc±0.7	43.9cde±0.9	62.7de±1.3	8.7a±0.6	1.7d±0.5	18.8d±0.6
	Soberbio	37.9abc±1.6	46.2ab±1.2	49.9ab±1.0	72.4ab±1.1	8.3a±1.2	3.8bc±0.6	22.5ab±0.6
	Chambo	36.4abc±1.3	44.5abc±1.3	49.7ab±1.2	71.8ab±1.5	8.2a±0.7	5.3ab±0.4	22.2abc±0.5
	Bologna by SIS	40.6a±1.2	47.3a±0.7	52.5a±1.0	76.3a±1.0	6.7a±1.1	5.3ab±0.6	23.8a±0.5
2019-2020	Bennington	67.5ab±1.7	76.7ab±1.7	83.4abc±1.6	102.2abc±1.5	9.3ab±0.8	6.7bc±0.3	-
	KWS Siskin	68.8ab±1.2	77.2ab±1.2	88.3a±0.8	107.0a±0.8	8.4ab±1.4	11.1c±0.8	-
	JB Diego	62.7bcd±1.7	72.4ab±1.8	79.0c±1.7	97.8c±1.7	9.7ab±0.6	6.7bc±0.3	-
	Julius	63.6bcd±1.4	71.9ab±1.2	78.6c±1.1	97.4c±1.1	8.4ab±0.7	6.7bc±0.5	-
	Henrik	66.4abc±1.4	74.5ab±1.6	81.4bc±1.7	100.2bc±1.6	8.2ab±0.6	6.9bc±0.5	-
	Benchmark	66.9abc±1.8	75.0ab±2.0	83.3abc±1.6	102.0abc±1.5	8.2ab±1.0	8.3bc±1.0	-
	RGT Reform	62.7bcd±1.3	71.7ab±1.5	78.6c±1.3	97.4c±1.3	9.0ab±0.7	6.9bc±0.5	-
	Hondia	71.9a±1.4	79.6a±1.3	86.0ab±1.3	104.8ab±1.3	7.7b±0.7	6.5bc±0.3	-
	CH-Nara	71.3a±1.4	76.9ab±1.7	87.8a±2.0	107.3a±1.4	5.7b±0.7	10.9b±0.8	-
	Soberbio	60.6cde±1.4	67.7bc±1.6	80.6bc±1.3	101.2bc±1.1	7.2b±0.5	12.9ab±1.1	-
	Chambo	55.3e±1.1	61.5c±1.2	78.6c±0.9	99.6bc±0.9	6.3b±0.3	17.2a±0.9	-
	Bologna by SIS	59.7de±0.8	74.4ab±4.5	77.7c±0.8	98.7c±0.8	14.7a±4.2	3.4c±4.2	-
Combined seasons	KWS Siskin	55.8a±2.7	62.1a±2.9	69.9a±3.3	-	6.3ab±0.7	7.9bc±0.7	-
	JB Diego	52.0a±2.8	59.6a±3.0	64.9a±3.5	-	7.7ab±0.5	5.4c±0.6	-
	Julius	52.8a±2.6	60.1a±2.6	65.5a±3.0	-	7.3ab±0.4	5.4c±0.5	-
	Henrik	55.0a±2.6	62.0a±2.7	67.6a±3.1	-	7.0ab±0.4	5.6c±0.7	-
	Benchmark	54.3a±3.0	61.4a±3.1	66.9a±3.6	-	7.2ab±0.5	5.6c±0.7	-
	RGT Reform	53.5a±3.0	61.5a±3.0	66.2a±3.5	-	8.0ab±0.4	4.8c±0.7	-
	Hondia	55.7a±3.3	63.0a±3.2	68.4a±3.6	-	7.4ab±0.4	5.4c±0.6	-
	CH-Nara	54.7a±3.1	60.1a±3.1	67.4a±3.5	-	5.4b±0.5	7.4bc±0.6	-
	Soberbio	51.0a±2.1	59.1a±2.2	68.2a±2.8	-	8.2ab±0.8	9.2ab±0.9	-
	Chambo	48.4a±1.8	55.2a±1.6	67.1a±2.5	-	6.8ab±0.4	12.0a±1.2	-
	Bologna by SIS	51.6a±1.8	60.5a±2.7	66.8a±2.2	-	8.9a±1.7	6.4bc±1.6	-

Each genotypic value is the mean ± standard error of the three replicates, and three N fertilization levels per season (seasonal values) and for the set of three consecutive seasons (overall genotypic values). Within each year, means exhibiting different letters are significantly different ( $P < 0.05$ ) according to the post-hoc test (Tukey-b).



**Supplemental Table 6.** Average grain nitrogen concentration (N), and the stable nitrogen ( $\delta^{15}\text{N}$ ) and carbon ( $\delta^{13}\text{C}$ ) isotope compositions in mature grains of twelve European bread wheat varieties grown under different nitrogen treatments (N1, N2, N3) and during different crop seasons (2017-2018; 2018-2019; 2019-2020) considered separately and in combination. For each crop season, the upper, middle and lower subsets of genotypes refer to cultivars released in northern, central and southern Europe. Within each subset and season, varieties were ranked based on water status performance ( $\delta^{13}\text{C}$ ).

Crop season	Variety	$\delta^{13}\text{C}$ (‰)	$\delta^{15}\text{N}$ (‰)	N (%)
2017-2018	<i>JB Diego</i>	-27.3 <sup>cd</sup> ±0.1	2.6 <sup>ab</sup> ±0.2	2.0 <sup>cd</sup> ±0.1
	<i>KWS Siskin</i>	-27.1 <sup>cd</sup> ±0.1	2.5 <sup>b</sup> ±0.2	1.9 <sup>cd</sup> ±0.2
	<i>KWS Lilli</i>	-26.9 <sup>bc</sup> ±0.2	2.8 <sup>ab</sup> ±0.1	1.8 <sup>cd</sup> ±0.1
	<i>Julius</i>	-26.5 <sup>a</sup> ±0.1	2.8 <sup>ab</sup> ±0.2	2.0 <sup>bcd</sup> ±0.2
	<i>Benchmark</i>	-27.3 <sup>cd</sup> ±0.1	2.7 <sup>ab</sup> ±0.2	1.9 <sup>cd</sup> ±0.1
	<i>RGT Reform</i>	-27.2 <sup>cd</sup> ±0.1	2.8 <sup>ab</sup> ±0.2	2.0 <sup>bcd</sup> ±0.1
	<i>Henrik</i>	-27.1 <sup>c</sup> ±0.2	2.8 <sup>ab</sup> ±0.2	1.8 <sup>d</sup> ±0.1
	<i>Hondia</i>	-26.7 <sup>ab</sup> ±0.1	2.8 <sup>ab</sup> ±0.2	2.1 <sup>bcd</sup> ±0.1
	<i>CH-Nara</i>	-26.6 <sup>a</sup> ±0.1	2.8 <sup>ab</sup> ±0.2	2.4 <sup>a</sup> ±0.1
	<i>Soberbio</i>	-27.4 <sup>d</sup> ±0.2	3.0 <sup>a</sup> ±0.1	2.0 <sup>bcd</sup> ±0.1
	<i>Bologna by SIS</i>	-27.1 <sup>cd</sup> ±0.2	3.1 <sup>a</sup> ±0.2	2.2 <sup>ab</sup> ±0.1
	<i>Chambo</i>	-27.1 <sup>cd</sup> ±0.1	3.0 <sup>ab</sup> ±0.2	1.9 <sup>cd</sup> ±0.1
2018-2019	<i>KWS Siskin</i>	-22.4 <sup>b</sup> ±0.2	1.5 <sup>a</sup> ±0.2	2.5 <sup>a</sup> ±0.2
	<i>Bennington</i>	-22.2 <sup>b</sup> ±0.3	1.5 <sup>a</sup> ±0.2	2.6 <sup>a</sup> ±0.2
	<i>Julius</i>	-21.8 <sup>ab</sup> ±0.2	1.7 <sup>a</sup> ±0.2	2.8 <sup>a</sup> ±0.2
	<i>JB Diego</i>	-21.8 <sup>ab</sup> ±0.2	1.7 <sup>a</sup> ±0.2	2.7 <sup>a</sup> ±0.1
	<i>Henrik</i>	-22.1 <sup>b</sup> ±0.2	1.4 <sup>a</sup> ±0.3	2.5 <sup>a</sup> ±0.2
	<i>Benchmark</i>	-22.1 <sup>b</sup> ±0.3	1.5 <sup>a</sup> ±0.2	2.6 <sup>a</sup> ±0.2
	<i>RGT Reform</i>	-21.9 <sup>ab</sup> ±0.2	1.5 <sup>a</sup> ±0.2	2.8 <sup>a</sup> ±0.1
	<i>Hondia</i>	-21.7 <sup>ab</sup> ±0.3	1.4 <sup>a</sup> ±0.3	2.5 <sup>a</sup> ±0.2
	<i>CH-Nara</i>	-21.3 <sup>a</sup> ±0.2	1.7 <sup>a</sup> ±0.2	2.9 <sup>a</sup> ±0.1
	<i>Soberbio</i>	-22.2 <sup>b</sup> ±0.2	1.5 <sup>a</sup> ±0.2	2.7 <sup>a</sup> ±0.2
	<i>Bologna by SIS</i>	-22.2 <sup>b</sup> ±0.2	1.2 <sup>a</sup> ±0.2	2.8 <sup>a</sup> ±0.2
	<i>Chambo</i>	-21.9 <sup>ab</sup> ±0.2	1.0 <sup>a</sup> ±0.2	2.6 <sup>a</sup> ±0.2
2019-2020	<i>Bennington</i>	-26.8 <sup>bcd</sup> ±0.1	2.5 <sup>a</sup> ±0.1	1.7 <sup>b</sup> ±0.1
	<i>JB Diego</i>	-26.8 <sup>bcd</sup> ±0.2	2.6 <sup>a</sup> ±0.2	1.7 <sup>b</sup> ±0.1
	<i>KWS Siskin</i>	-26.5 <sup>abcd</sup> ±0.1	2.6 <sup>a</sup> ±0.2	1.9 <sup>ab</sup> ±0.2
	<i>Julius</i>	-26.2 <sup>ab</sup> ±0.2	2.7 <sup>a</sup> ±0.2	1.9 <sup>ab</sup> ±0.2
	<i>Benchmark</i>	-26.4 <sup>abcd</sup> ±0.2	2.7 <sup>a</sup> ±0.2	1.7 <sup>b</sup> ±0.1
	<i>RGT Reform</i>	-26.4 <sup>abc</sup> ±0.1	2.7 <sup>a</sup> ±0.2	1.9 <sup>ab</sup> ±0.1
	<i>Hondia</i>	-26.3 <sup>abc</sup> ±0.2	2.5 <sup>a</sup> ±0.2	1.8 <sup>ab</sup> ±0.2
	<i>Henrik</i>	-26.3 <sup>abc</sup> ±0.2	2.6 <sup>a</sup> ±0.2	1.8 <sup>ab</sup> ±0.1
	<i>CH-Nara</i>	-26.0 <sup>a</sup> ±0.2	2.6 <sup>a</sup> ±0.2	2.2 <sup>a</sup> ±0.2
	<i>Soberbio</i>	-27.0 <sup>d</sup> ±0.1	2.6 <sup>a</sup> ±0.1	1.7 <sup>b</sup> ±0.1
	<i>Chambo</i>	-26.9 <sup>cd</sup> ±0.2	2.4 <sup>a</sup> ±0.1	1.7 <sup>b</sup> ±0.1
	<i>Bologna by SIS</i>	-26.7 <sup>bcd</sup> ±0.2	2.6 <sup>a</sup> ±0.1	2.0 <sup>ab</sup> ±0.2
Combined seasons	<i>KWS Siskin</i>	-25.2 <sup>d</sup> ±0.4	2.2 <sup>a</sup> ±0.1	2.1 <sup>bcd</sup> ±0.0
	<i>JB Diego</i>	-25.2 <sup>cde</sup> ±0.5	2.3 <sup>a</sup> ±0.1	2.2 <sup>bcd</sup> ±0.0
	<i>Julius</i>	-24.8 <sup>ab</sup> ±0.4	2.3 <sup>a</sup> ±0.1	2.2 <sup>bcd</sup> ±0.1
	<i>Benchmark</i>	-25.2 <sup>cde</sup> ±0.4	2.3 <sup>a</sup> ±0.1	2.0 <sup>bcd</sup> ±0.0
	<i>RGT Reform</i>	-25.1 <sup>bcd</sup> ±0.4	2.3 <sup>a</sup> ±0.1	2.3 <sup>ab</sup> ±0.0
	<i>Henrik</i>	-25.1 <sup>bcd</sup> ±0.4	2.3 <sup>a</sup> ±0.1	2.0 <sup>d</sup> ±0.0
	<i>Hondia</i>	-24.9 <sup>abc</sup> ±0.4	2.1 <sup>a</sup> ±0.1	2.1 <sup>bcd</sup> ±0.0
	<i>CH-Nara</i>	-24.5 <sup>a</sup> ±0.4	2.3 <sup>a</sup> ±0.1	2.5 <sup>a</sup> ±0.0
	<i>Soberbio</i>	-25.5 <sup>e</sup> ±0.4	2.3 <sup>a</sup> ±0.1	2.2 <sup>bcd</sup> ±0.0
	<i>Bologna by SIS</i>	-25.3 <sup>d</sup> ±0.4	2.3 <sup>a</sup> ±0.1	2.3 <sup>abc</sup> ±0.0
	<i>Chambo</i>	-25.2 <sup>cde</sup> ±0.4	2.1 <sup>a</sup> ±0.1	2.0 <sup>cd</sup> ±0.0
	<i>KWS Siskin</i>	-25.2 <sup>d</sup> ±0.4	2.2 <sup>a</sup> ±0.1	2.1 <sup>bcd</sup> ±0.0

Each genotypic value is the mean  $\pm$  standard error of the three replications, and three N fertilization levels per season (seasonal values) and for the set of three consecutive seasons (overall genotypic values). Within each year, means exhibiting different letters are significantly different ( $P < 0.05$ ) according the post-hoc test (Tukey-b).

**Supplemental Table 7.** Genetic correlation coefficients of grain yield (GY) between grain nitrogen yield (GNY), grain number (GN), thousand kernel weight (TKW), days from planting and different phenological stages (tillering “DTT”, elongation “DTE”, booting “DTB”, heading “DTH”, anthesis “DTA”, mid grain filling “MGF”), grain nitrogen concentration (N), and carbon ( $\delta^{13}\text{C}$ ) and nitrogen ( $\delta^{15}\text{N}$ ) isotope compositions measured in mature grains.

		<i>Combined seasons</i>	2017-2018	2018-2019	2019-2020	2017-2018			2018-2019			2019-2020		
		<i>N1+N2+N3</i>	<i>N1+N2+N3</i>			<i>N1</i>	<i>N2</i>	<i>N3</i>	<i>N1</i>	<i>N2</i>	<i>N3</i>	<i>N1</i>	<i>N2</i>	<i>N3</i>
<i>Yield components</i>	GNY	0.999***	0.696*	0.991***	0.999***	ns	ns	-	-	0.837***	0.923***	0.999***	0.999***	0.977***
	GN	-	0.783**	0.817***	0.842***	0.847***	0.766**	0.751**	0.698*	0.902***	0.620*	0.854***	0.890***	0.838***
	TKW	ns	ns	ns	ns	0.663*	ns	ns	ns	-0.627*	ns	ns	0.740**	ns
<i>Phenology</i>	DTT	0.580*	-	ns	-	-	ns	-	-	-0.999***	-0.670*	-	-	-
	DTE	ns	ns	-0.921***	ns	ns	ns	ns	-0.758**	-0.999***	-0.999***	ns	ns	ns
	DTB	ns	ns	-0.775**	ns	ns	ns	ns	-0.999***	ns	-0.927***	ns	ns	ns
	DTH	0.591*	ns	-0.808***	ns	ns	ns	ns	-0.999***	-0.590*	-0.945***	ns	ns	ns
	DTA	0.630*	ns	-0.802***	ns	ns	0.589*	ns	-0.999***	-0.680*	-0.855***	-	ns	-
	MGF	0.577*	ns	-0.791**	-	ns	ns	ns	-0.999***	ns	-0.999***	-	-	-
<i>Isotopes</i>	N	-0.981***	-0.912***	ns	-0.999***	-0.745**	-0.685*	-0.999***	-	ns	ns	-	-0.999***	-0.895***
	$\delta^{15}\text{N}$	-	-0.999***	-	-	-0.999***	ns	ns	-	-	ns	-	-	ns
	$\delta^{13}\text{C}$	-0.883***	-0.658*	ns	-0.645*	-0.825***	ns	-0.747**	-0.957***	-0.660*	-	-0.642*	-0.722**	-0.877***

The missing correlations were not calculated because of their low heritability. ns, not significant; \*,  $P < 0.05$ ; \*\*,  $P < 0.01$ ; \*\*\*,  $P < 0.001$ .

**Supplemental Table 8.** Pearson correlations between grain yield (GY), grain nitrogen yield (GNY), grain number (GN), thousand kernel weight (TKW), grain nitrogen concentration (N), and nitrogen ( $\delta^{15}\text{N}$ ) and carbon ( $\delta^{13}\text{C}$ ) isotope compositions of mature grains, and days from planting to the beginning of stem elongation (DTE), phenological durations from stem elongation to booting (DTE-DTB), to heading (DTE-DTH), to anthesis (DTE-DTA), to mid grain filling (DTE-MGF), and phenological durations from booting to heading (DTB-DTH), heading to anthesis (DTH-DTA) and anthesis to mid grain filling (DTA-MGF). Correlations were calculated using plot information and the three N fertilization treatments, during combined and separated crop seasons.

		DTE	DTE-DTB	DTE-DTH	DTE-DTA	DTE-MGF	DTB-DTH	DTH-DTA	DTA-MGF
All seasons	GY	ns	0.859**	0.838**	0.888**	0.860**	ns	0.553**	-
	GNY	ns	0.581**	0.550**	0.597**	0.573**	ns	0.414**	-
	GN	ns	0.829**	0.813**	0.854**	0.830**	ns	0.509**	-
	TKW	ns	0.604**	0.580**	0.622**	0.583**	ns	0.414**	-
2017-2018	GY	ns	0.273**	0.345**	0.343**	0.233*	0.280**	ns	-0.229*
	GNY	ns	ns	ns	ns	ns	ns	ns	ns
	GN	ns	ns	0.221*	0.203*	ns	0.253*	ns	ns
	TKW	ns	ns	ns	ns	ns	ns	ns	ns
2018-2019	GY	-0.339**	ns	ns	0.268**	0.320**	ns	0.324**	0.308**
	GNY	-0.310**	ns	ns	0.213*	0.276**	ns	0.364**	0.306**
	GN	-0.500**	0.239*	0.229*	0.385*	0.473**	ns	0.445**	0.478**
	TKW	0.462**	-0.242*	-0.209*	-0.355**	-0.435**	ns	-0.415**	-0.438**
2019-2020	GY	ns	ns	ns	ns	-	ns	ns	-
	GNY	ns	ns	ns	ns	-	ns	ns	-
	GN	ns	ns	ns	0.201*	ns	ns	ns	-
	TKW	ns	-0.243*	-0.366**	ns	-	-0.257**	0.316**	-

ns, not significant; \*,  $P < 0.05$ ; \*\*,  $P < 0.01$ ; \*\*\*,  $P < 0.001$ .

**Supplemental Table 9.** Multi-linear regression (stepwise) of grain yield (GY) as the dependent variable, and days from planting of different phenological stages (DTT, DTE, DTH, DTA, MGF), together with the stable carbon and nitrogen isotope compositions ( $\delta^{13}\text{C}$  and  $\delta^{15}\text{N}$ ), and nitrogen concentration (N) of mature grains as independent variables. For each equation, the fitted model was significant ( $P < 0.001$ ) with ( $1.2 < \text{Durbin-Watson} < 2$ ) and collinearity was within the acceptable range ( $\text{VIF} < 10$ ).  $R^2_{\text{adjusted}}$  displays the reliability of the fitted regression line to the data in use.

Crop season	Region	Equation	$R^2_{\text{Adjusted}}$
Combined seasons	All	$\text{GY} = -15.955 - 0.632 * \delta^{13}\text{C} - 0.258 * \text{DTE} + 0.353 * \text{DTA}$	0.889
	Northern Europe	$\text{GY} = 21.381 - 1.064 * \delta^{13}\text{C} - 0.199 * \text{DTE} + 0.110 * \text{N}$	0.943
	Central Europe	$\text{GY} = -15.672 - 0.927 * \delta^{13}\text{C} - 0.168 * \text{DTE}$	0.867
	Southern Europe	$\text{GY} = -12.712 - 1.149 * \delta^{13}\text{C} - 0.265 * \text{DTH} - 0.143 * \text{DTE}$	0.886
2017-2018	All	$\text{GY} = -20.751 + 0.380 * \text{DTA} - 0.297 * \text{DTT} - 0.287 * \delta^{13}\text{C}$	0.275
2018-2019	All	$\text{GY} = 6.438 - 0.381 * \text{DTH} - 0.280 * \delta^{13}\text{C}$	0.221
2019-2020	All	$\text{GY} = -10.763 - 0.255 * \delta^{13}\text{C}$	0.055

Regressions were generated using individual plot values of the 12 tested genotypes.

**Supplemental Table 10.** Grain yield prediction using the LASSO regression model using in a first step phenological stages (DTE, DTH, DTA), grain carbon and nitrogen stable isotopes ( $\delta^{13}\text{C}$  and  $\delta^{15}\text{N}$ ), and grain nitrogen concentration (N) as the explicative variables, and in a second step combinations of the most relevant variables as explicative variables.

Crop season	Region	LASSO Parameters	All variables	Selected variables				
				DTE+ $\delta^{13}\text{C}$	DTH+ $\delta^{13}\text{C}$	DTA+ $\delta^{13}\text{C}$	DTE+DTH+ $\delta^{13}\text{C}$	DTE+DTA+ $\delta^{13}\text{C}$
Combines seasons	All	$R^2_{\text{Adjusted}}$	0.868	0.861	0.851	0.85	0.862	0.871
		RMSE	1.022	1.047	1.196	1.091	1.04	1.049
		$\lambda$	0.0020	0.011	0.051	0.011	0.0273	0.051
	North	$R^2_{\text{Adjusted}}$	0.943	0.943	0.941	0.939	0.943	0.936
		RMSE	0.760	0.733	0.772	0.779	0.734	0.819
		$\lambda$	0.0009	0.026	0.012	0.012	0.026	0.026
	Central	$R^2_{\text{Adjusted}}$	0.881	0.862	0.851	0.85	0.873	0.874
		RMSE	0.996	1.056	1.099	1.103	1.024	1.010
		$\lambda$	0.0009	0.011	0.051	0.011	0.109	0.109
	South	$R^2_{\text{Adjusted}}$	0.873	0.870	0.866	0.858	0.859	0.877
		RMSE	1.001	0.993	1.014	1.038	1.055	0.971
		$\lambda$	0.0002	0.010	0.010	0.104	0.022	0.104
2017-2018	All	$R^2_{\text{Adjusted}}$	0.299	0.161	0.323	0.316	0.33	0.308
		RMSE	0.871	0.953	0.855	0.858	0.847	0.860
		$\lambda$	0.0006	0.108	0.016	0.038	0.016	0.081
2018-2019	All	$R^2_{\text{Adjusted}}$	0.273	0.315	0.341	0.315	0.321	0.302
		RMSE	0.673	0.659	0.641	0.663	0.651	0.662
		$\lambda$	0.0004	0.023	0.027	0.050	0.012	0.109
2019-2020	All	$R^2_{\text{Adjusted}}$	0.244	0.295	0.272	0.297	0.275	0.297
		RMSE	1.316	1.182	1.193	1.187	1.196	1.187
		$\lambda$	0.0006	0.092	0.427	0.198	0.198	0.198

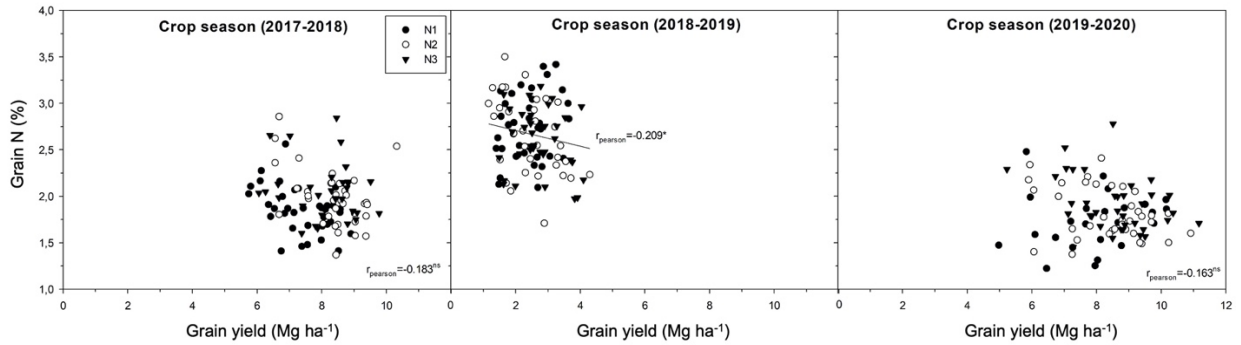
$R^2_{\text{Adjusted}}$ , coefficient of determination; RMSE, root mean square error;  $\lambda$ , amount of shrinkage.

**Supplemental Table 11.** Average grain yield of twelve European bread wheat varieties, separated by provenance (Northern, Central and Southern Europe), under combined nitrogen treatments (N1, N2, N3) and during different crop seasons (2017-2018; 2018-2019; 2019-2020) considered separately and in combination.

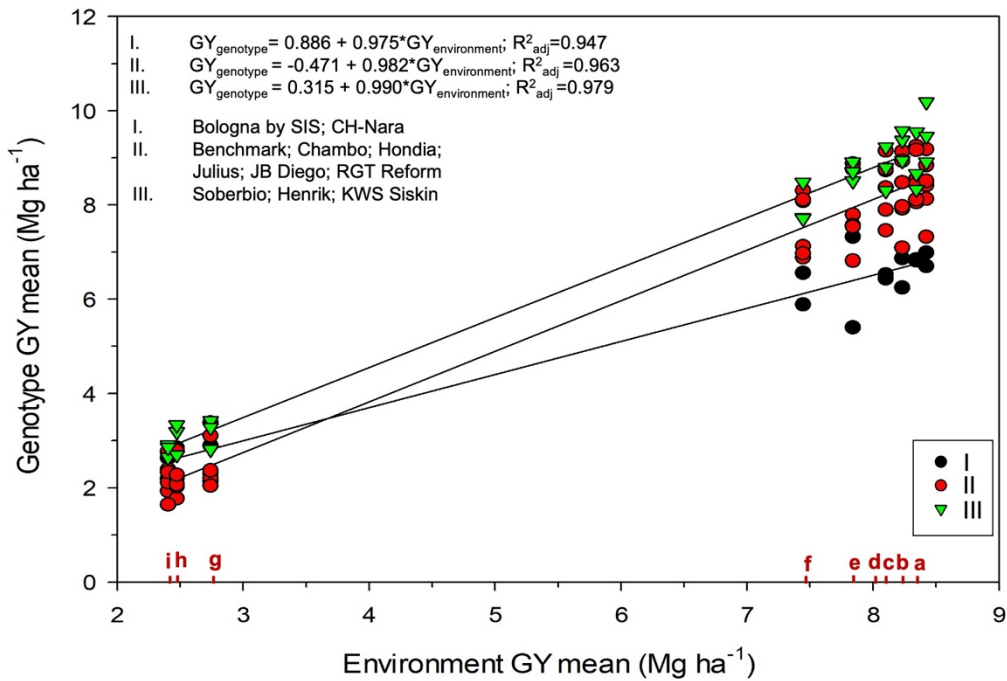
Crop season	Mean GY (Mg ha <sup>-1</sup> )			
	Northern European	Central European	Southern European	
Wet seasons	2017-2018	8.30a±0.12	7.85ab±0.15	7.57b±0.20
	2019-2020	8.73a±0.18	8.16a±0.20	8.35a±0.29
	2017-2018 and 2019-2020	8.52a±0.12	8.02b±0.13	7.97b±0.18
Dry season	2018-2019	2.40b±0.12	2.35b±0.12	2.94a±0.11
Combined seasons	2017-2018; 2018-2019; 2019-2020	6.57a±0.29	6.10b±0.25	6.25ab±0.30

Each genotypic value is the mean  $\pm$  standard error of the three replications, and three N fertilization levels per season (seasonal values) and for the set of three consecutive seasons (overall genotypic values). Within each year, means exhibiting different letters are significantly different ( $P < 0.05$ ) according to the post-hoc test (Tukey-b).

## Supplemental figures:



**Supplemental Figure 1.** Relationships between grain yield (GY) and grain nitrogen content (Grain N) of the twelve European bread wheat genotypes during each crop season (2017-2018; 2018-2019; 2019-2020) and sorted by N fertilization (N1, N2, N3). Each point represents a replicate (i.e. plot value) for a given cultivar and growing condition.



**Supplemental Figure 2.** Linear regressions of the relationship between the genotypic mean of grain yield (GY) of eleven bread wheat genotypes in nine environments (each one being a specific combination of crop season and growing conditions), and the mean grain yield across the whole set of genotypes tested in each environment. Letters on the horizontal axis of the figure refer to the descending values of the environmental means of the 11 bread wheat genotypes: a, 30% above the recommended topdressing nitrogen dose (N3) during 2019–2020; b, the recommended topdressing nitrogen dose (N2) during 2017–2018; c, N2 fertilization during the crop season (2019-2020); d, N3 fertilization during 2017-2018; e, 50% of the recommended topdressing nitrogen dose (N1) during 2019-2020; f, N1 fertilization during 2017-2018; g, N3 fertilization during 2018-2019; h, N2 fertilization during 2018-2019; i, N1 fertilization during 2018-2019.





## CHAPTER II

# **Remote sensing techniques and stable isotopes as phenotyping tools to assess wheat yield performance: Effects of growing temperature and vernalization**

Fatima Zahra Rezzouk, Adrian Gracia-Romero, Shawn C. Kefauver, Nieves Aparicio Gutiérrez, Iker Aranjuelo, Maria Dolors Serret, José Luis Araus

Published in:  
Plant Science 295 (2020): 110281







# Remote sensing techniques and stable isotopes as phenotyping tools to assess wheat yield performance: Effects of growing temperature and vernalization

Fatima Zahra Rezzouk<sup>a</sup>, Adrian Gracia-Romero<sup>a</sup>, Shawn C. Kefauver<sup>a</sup>, Nieves Aparicio Gutiérrez<sup>b</sup>, Iker Aranuelo<sup>c</sup>, Maria Dolors Serret<sup>a</sup>, José Luis Araus<sup>a,\*</sup>

<sup>a</sup> Section of Plant Physiology, University of Barcelona, Barcelona and AGROTECNIO (Center of Research in Agrotechnology), Lleida, Spain

<sup>b</sup> Agro-technological Institute of Castilla y León (ITACyL), Valladolid, Spain

<sup>c</sup> Instituto de Agrobiología (IdAB), Universidad Pública de Navarra-CSIC-, Multiva Baja, Navarra, Spain

## ARTICLE INFO

### Keywords:

Wheat  
High temperature  
Vernalization  
Remote sensing  
Stable isotopes  
Yield prediction

## ABSTRACT

This study compares distinct phenotypic approaches to assess wheat performance under different growing temperatures and vernalization needs. A set of 38 (winter and facultative) wheat cultivars were planted in Valladolid (Spain) under irrigation and two contrasting planting dates: normal (late autumn), and late (late winter). The late planting trial exhibited a 1.5 °C increase in average crop temperature. Measurements with different remote sensing techniques were performed at heading and grain filling, as well as carbon isotope composition ( $\delta^{13}\text{C}$ ) and nitrogen content analysis. Multispectral and RGB vegetation indices and canopy temperature related better to grain yield (GY) across the whole set of genotypes in the normal compared with the late planting, with indices (such as the RGB indices Hue,  $a^*$  and the spectral indices NDVI, EVI and CCI) measured at grain filling performing the best. Aerially assessed remote sensing indices only performed better than ground-acquired ones at heading. Nitrogen content and  $\delta^{13}\text{C}$  correlated with GY at both planting dates. Correlations within winter and facultative genotypes were much weaker, particularly in the facultative subset. For both planting dates, the best GY prediction models were achieved when combining remote sensing indices with  $\delta^{13}\text{C}$  and nitrogen of mature grains. Implications for phenotyping in the context of increasing temperatures are further discussed.

## 1. Introduction

Climate change is a prevalent concern that is already threatening food production and will even more so in the future, especially when addressing Mediterranean semi-arid climate regions [1–3]. Providing breeding and management practices are unchanged, annual rates of crop increase are more likely to decline as a response to drought periods and, even more importantly, to increases in temperature, including the frequency and strength of heat waves [4,5]. Therefore, efforts have to be harnessed into developing improved varieties that can be adapted to these rising challenges.

Wheat varieties have proven great adaptability to different agro-climatic regions [6]. Vernalization and photoperiod needs divide wheat genotypes into winter cultivars and spring (facultative) cultivars. The first category is usually sown in autumn or early winter [7,8], during which an exposure to low temperature (i.e. vernalization) is required in order to promote flowering. On the other hand, spring or facultative varieties do not require vernalization for flowering and thus, they can be more adapted to higher temperatures [8] and therefore they are more amenable for spring cultivation [7]. Besides the effect on floral induction, temperature also affects crop growth. High temperature accelerates the crop cycle and decreases the amount of accumulated

**Abbreviations:** CCI, chlorophyll/carotenoid index; CCiTUB, centres científics i tecnològics de la universitat de barcelona; CIELab, international commission on illumination lightness  $a^*$   $b^*$ ; CIELuv, international commission on illumination lightness  $u^*$   $v^*$ ; CT, canopy temperature; EVI, enhanced vegetation index; FLJI, fiji is just imageJ; GY, grain yield; GA, green area; GGA, greener area; HSI, hue-saturation-intensity; HTPPs, high throughput phenotyping platforms; IR, infrared; IRMS, infrared mass spectrometer; ITACyL, instituto técnico y agrario de castilla y león; NDVI, normalized difference vegetation index; NIRS, near infrared spectrometers; NP, normal planting; VIs, vegetation indices; PRIm, modified photochemical reflectance index; RGB, red-green-blue; TCARI/OSAVI, transformed chlorophyll absorption reflectance index/optimized soil adjusted vegetation index; TGW, thousand grain weight; UAV, unmanned aerial vehicle; VIF, variance inflation factor

\* Corresponding author. Permanent address: Faculty of Biology, Avinguda Diagonal 643, 08028, Barcelona, Spain.

E-mail address: [jaraus@ub.edu](mailto:jaraus@ub.edu) (J.L. Araus).

<https://doi.org/10.1016/j.plantsci.2019.110281>

Received 7 May 2019; Received in revised form 16 September 2019; Accepted 20 September 2019

Available online 21 September 2019

0168-9452/ © 2019 Elsevier B.V. All rights reserved.

photosynthesis, and the sinks (ear density and size in case of wheat), which subsequently reduces the final yield [9–11].

In recent years, the perception that crop phenotyping is a bottleneck that hinders breeding advances, has been widely recognized [12]. Presently, high throughput phenotyping platforms (HTPPs), placed at ground level or from the air (usually using unmanned aerial vehicles) have been developed to collect and handle accurately and in a non-invasive and fast way the large magnitude of information usually needed to properly phenotype crops in field conditions [13,14]. The main category of phenotyping techniques that may include HTPPs are categorized into remote (proximal) sensing and imaging. The most commonly deployed techniques deal with the use of spectroradiometrical and thermal sensors or imagers, together with an increasing use of conventional Red-Green-Blue (RGB) cameras [12,15,16]. The spectroradiometers measure different wavelength bands, within visible and near infrared regions of the spectrum, which allow the formulation of a wide range of vegetation indices informing on biomass [17,18], leaf area index [19,20], pigment content [21–23], nitrogen content [24,25], photosynthetic efficiency [26] and water status [26,27]. The thermal sensors and imagers measure the far infrared region of the spectrum informs on the plant canopy temperature and therefore of its water status [28,29]. Another category of remote sensing approaches is that derived from RGB images [12,30], with a wide range of vegetation indices being derived from different space colors which characterize the conventional images. It has been reported that frequently RGB indices work better than spectral indices in assessing differences in leaf color or green canopy area associated with genotypic performance, in optimal agronomical conditions as well as under different abiotic and biotic stress conditions [18,31]. Laboratory-category traits (i.e. analytical traits), may be also deployed for HTPPs [12]. When Mediterranean conditions are targeted, carbon and, to a lesser extent, nitrogen stable isotope compositions (or alternatively expressed as discrimination from the substrate) may be used as phenotyping tools, informing on the water regime and nitrogen metabolism conditions, respectively [32–34]. Several studies have highlighted the synergistic effect, in terms of quality of plant characterization, when combining spectroscopy performance with the biophysical information provided through stable isotope composition [35,36].

The efficient use of the HTPPs, including the most adequate traits to measure, may be affected by the growing conditions. In that sense, as indicated above, one of the main environmental variables associated with climate change is temperature. The present study compares the performance of different phenotyping approaches under “current” temperature conditions (provided by a normal planting date) and high temperature conditions (provided by a late planting). Therefore, the heat stress conditions tested implies a constant higher temperature, besides a higher probability of experiencing a heat wave during the last part of the crop cycle. Another aspect related with increase in temperature is the potential altering effects on the pattern of flowering, associated with the lack of vernalization induction. To that end, we have concluded in the wheat panel winter (i.e. requiring vernalization) and facultative (less dependent on vernalization) semi-dwarf wheat cultivars. Different remote sensing techniques were implemented from ground and aerial levels, combined with the analyses of the stable carbon and nitrogen isotope composition of the flag leaves and mature grains.

## 2. Materials & methods

A set of 36 post green revolution (i.e. semidwarf) bread wheat commercial cultivars (*Triticum aestivum* L.) were evaluated altogether with other 2 durum wheat cultivars (*Triticum turgidum* L. ssp. *durum* (Desf.) Husn.) (Table 1). In order to assess vernalization effects on final production and yield components, cultivars were separated into winter (27) and facultative genotypes (11). Field trials were carried out in the Experimental Station of Zamadueñas (41° 39′ 8″ N and 4° 43′ 24″ W,

**Table 1**

List of the 38 wheat varieties used in the study, with their provenance, register number and sorted by their attitude (winter and facultative): 36 were bread wheats (*Triticum aestivum* L), while the other two were durum wheats (*Triticum turgidum* L. ssp. *durum* (Desf.) Husn.). For each cultivar the register number is specific to the country where the cultivar was registered. Information can be accessed through the variety finder web of the Community Plant Variety Office (CPVO): <https://cpvo.europa.eu/en/cpvo-variety-finder>.

Genotype	Nature	Attitude	Provenance (seed company)	Spanish register number
ATOMO	bread	Facultative	LG SEEDS	20090316
BISANZIO	bread	Facultative	AGRAR	20151856
CREDIT	durum	Facultative	PRO.SE.ME	20101512
GALERA	bread	Facultative	LG SEEDS	20001714
TOGANO	bread	Facultative	ROLLY	20042601
VALBONA	bread	Facultative	PRO.SE.ME	20061701
MIMMO	durum	Facultative	PRO.SE.ME	20101513
ENEAS	bread	Facultative	DAFISA	20090257
08THES1262	bread	Facultative	BATLLE	20114988
ARTHUNICK	bread	Facultative	LG SEEDS	20021627
ALHAMBRA	bread	Facultative	LG SEEDS	20122397
ALBERTUS	bread	Winter	PRO.SE.ME	20130238
ALGORITMO	bread	Winter	RGT	20160437
BOLOGNA	bread	Winter	BATLLE	20152157
DOLLY	bread	Winter	ROLLY	20101741
FORCALLI	bread	Winter	KWS	1006401
INGENIO	bread	Winter	AGRUSA	20062285
GHAYTA	bread	Winter	AGRUSA	20122320
MECANO	bread	Winter	AGRUSA	20100121
REBELDE	bread	Winter	BATLLE	20132043
RIMBAUD	bread	Winter	BATLLE	1023863-
TRIBAT	bread	Winter	BATLLE	20120245
CHAMBO	bread	Winter	LG SEEDS	20110170
COMPLICE	bread	Winter	MARISA	20160212
COSMIC	bread	Winter	AGRUSA	4048820
IPPON	bread	Winter	FLORIMON	20151563
			DESPREZ	
NEMO	bread	Winter	AGRUSA	20143383
OREGRAIN	bread	Winter	FLORIMON	20120181
			DESPREZ	
PR22R58	bread	Winter	PROVASE	20041719
SOBERBIO	bread	Winter	CAUSSADE	20151744
SOISSON	bread	Winter	AGRUSA	199850256
MH1307	bread	Winter	KWS	Advanced breeding line
MH1341	bread	Winter	KWS	Advanced breeding line
MH1411	bread	Winter	KWS	Advanced breeding line
MH1444	bread	Winter	KWS	Advanced breeding line
CRACKLIN	bread	Winter	LG SEEDS	19990012
MARCOPOLO	bread	Winter	RGT	20132034
SEPTIMA	bread	Winter	AGRAR	20093-

690 m.a.s.l.); of the Instituto Técnico y Agrario de Castilla y León (ITACyL) in Valladolid (Spain) (Fig. 1). Temperature effects were investigated through implementing trials under contrasting planting dates: a normal planting (December 2nd, 2016), followed by a late planting (February 10th, 2017). The late planting trial (and specifically the facultative cultivars) caught up with the development of the facultative and winter genotypes of the normal planted trial around 90 days after sowing, corresponding to the heading-anthesis stages. Patterns of precipitation, temperature (average, minimum and maximum) and photoperiod throughout the crop season are displayed in Fig. 2. Accumulated precipitation from planting to maturity during the crop cycle were 129 mm and 89 mm, for the normal and late planting respectively. In order to restrict environmental stress factors to temperature, both trials were grown under support irrigation, supplied with periodical sprinkler irrigation totaling 60 mm during normal planting, and 140 mm during late planting. Fertilizers were applied as recommended; it consisted for both trials in 300 kg ha<sup>-1</sup> of basic dressing

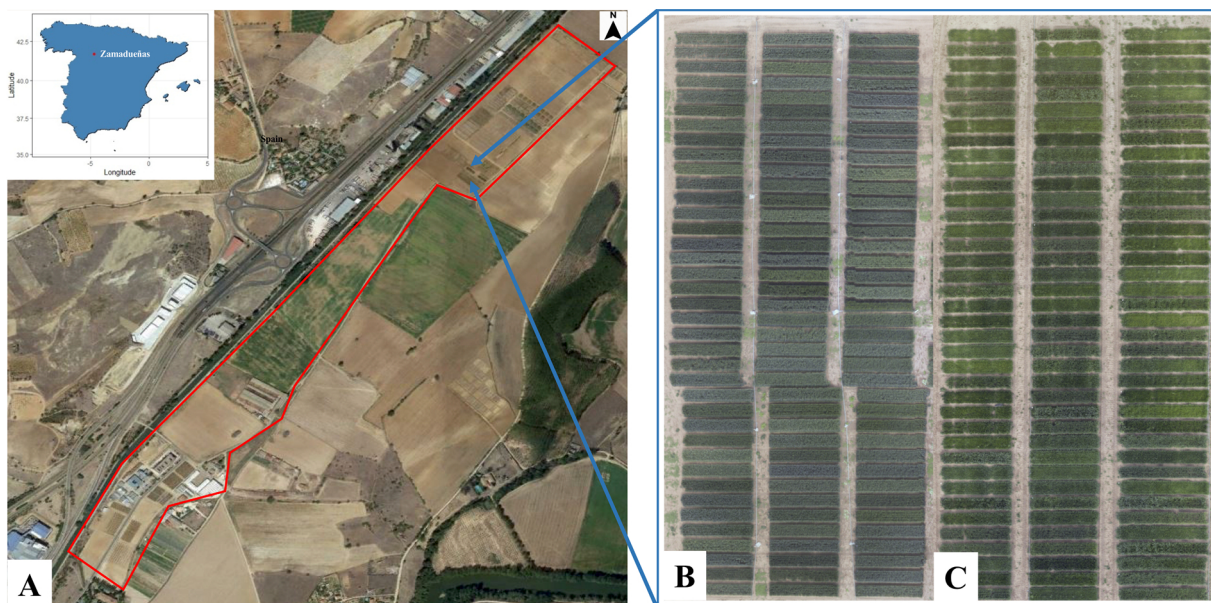


**Fig. 1.** Map of the location (red point) and the satellite image of the experimental station of Zamadueñas (ITACyL), Valladolid, Spain (A). RGB ortho-mosaics of the normal planting (B) and the late planting (C) trials during late heading. The shift in plot placement of normal planting was due to a problem during planting (for interpretation of the references to colour in this figure legend, the reader is referred to the web version of this article).

in the form of 8-15-15 (N-P-K) before seeding, ensued with a twofold partitioning of 300 kg ha<sup>-1</sup> of Nitrosylsulphuric acid (NSA, 27%) as top dressing during stem elongation and booting stages. Phytosanitary control included the spraying of herbicides (*Axial* and *Amadeus*, *Syngenta*), fungicide (*Karate Zeon*, *Syngenta*) and pesticide (*Prosaro*, *Bayer*) at the recommended rates during booting (late planting) and heading (normal planting) stages. For both trials, the experimental design was fully randomized with three replications (individual plots) per genotype, totaling for each trial 114 plots (81 and 33 plots per winter and facultative genotypes, respectively). Plots were 6 m long and 1.5 m wide, with 7 rows sown 20 cm apart (totaling 9 m<sup>2</sup> per plot). During early grain filling flag leaves were sampled, and by physiological maturity number of spikes per square meter was evaluated together with grain number per spike and thousand grain weight, for genotypes in normal planting, and only number of spikes per square meter in late

planting. For both trials, maturity was reached the second half of June. Then, plots were harvested mechanically on July 20th, 2017 for both trials and yield assessed.

### 2.1. Ground and aerial remote sensing

Plots were evaluated at ground level using a Red-Green-Blue (RGB) camera, an infrared thermometer and a spectro-radiometer. Aerial images were obtained during the same visits as ground data using an Unmanned Aerial Vehicle (UAV) (Drone Mikrokoopter OktoXL 6S12, Moormerland, Germany), controlled manually and flying at an altitude of 50 m, carrying a digital RGB camera just before solar noon in the first flight, and thermal and multispectral cameras within one hour of solar noon in the second flight. For normal planting, the range of heading dates for the whole set of genotypes was about 10 days, while in the late

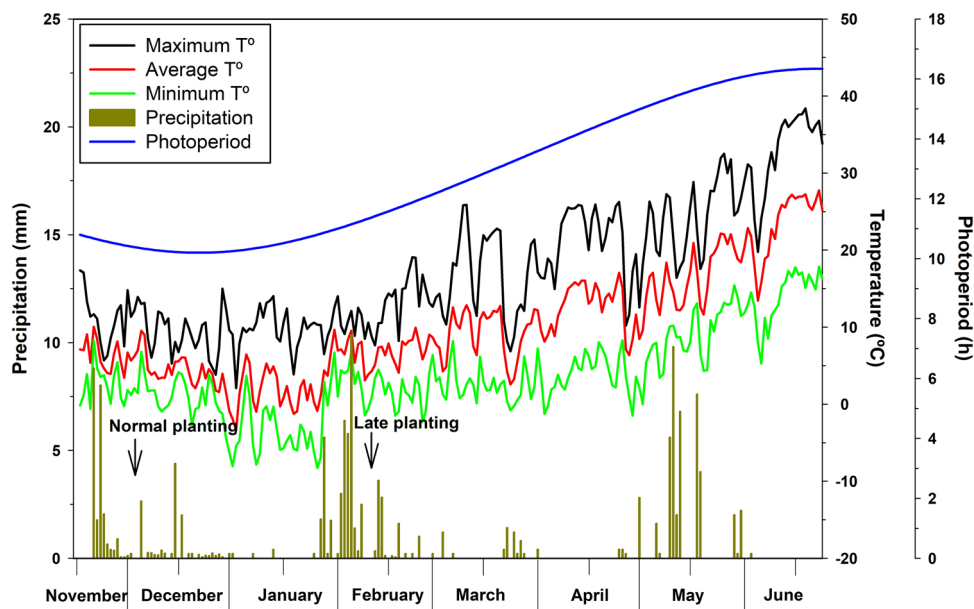


**Fig. 2.** Weekly precipitation, temperature (average, minimum and maximum) and photoperiod during the growing period covering both planting trials.



planting the range was larger (around 30 days) due to the delay in the reproductive stage experienced by the winter genotypes. During the first date of measurements (middle-May), the whole set of genotypes for the normal planting and the subset of facultative genotypes for the late planting were at late heading. During the second visit (second week June), the whole set of genotypes for the normal planting and the subset of facultative genotypes for the late planting were in the second half of grain filling.

### 2.1.1. Canopy temperature

Measurements of canopy temperature (CT) at ground level were carried out during both visits using an infrared (IR) thermometer (PhotoTemp™ MXS™TD Raytek®, California; USA), pointed towards plants leaves at a distance of 80 cm approximately, while having the sun towards the rear. For aerial thermal images, a FLIR Tau2 640 was used (FLIR Systems, Nashua, NH, USA) with a VOx uncooled microbolometer, equipped with a TEAX Thermal Capture model (TeAx Technology, Wilnsdorf; Germany) for recording thermal frames of full resolution (640 × 520 pixels at 20 frames per second).

### 2.1.2. RGB images

RGB images (one per plot) were taken from ground holding a Sony ILCE-QX1 (Sony Europe Limited, Brooklands; United Kingdom), digital camera of 20.1 megapixel resolution, equipped with 23.2 mm × 15.4 mm sensor size (type CMOS Exmor HD) and using 16 mm focal lens and an exposure time of 1/60 s. Images were captured zenithally at 80 cm above the plant canopy, focusing near the center of each plot, and then saved in JPEG format for later analysis. The ground sample distance (GSD) of the images captured was 0.021 cm/pixel, and the area captured in the image corresponded to 0.89 m<sup>2</sup>. For aerial data assessment, the RGB used camera was a Lumix GX7 (Panasonic, Osaka; Japan), a digital mirrorless camera of 16.0 megapixel resolution with an image sensor size of 17.3 × 13.0 mm (type Live MOS), using a 20 mm focal lens with an exposure time of 1/8000 s. The GSD of the aerial images for a flight at 50 m altitude was 0.941 cm/pixel, and the area captured in the image corresponded to 1404.55 m<sup>2</sup>. In practical consideration, mirrorless cameras provide equal imaging capacities for agricultural applications than traditional cameras in a more compact and lightweight body, which promote their flexible application in the field or mounted on a UAV.

### 2.1.3. Multispectral information

The normalized difference vegetation index (NDVI) was measured at ground (NDVI.g) on individual plots using a GreenSeeker (Trimble, Sunnyvale, CA, USA), a hand held spectroradiometer with active self-illuminated sensor in red (660 ± 10 nm) and near infrared (780 ± 15 nm) wavelengths [37]. The NDVI was measured by skimming the sensor across each plot, at a constant height of 60 cm while maintaining a perpendicular position from above the canopy [38]. At this distance the active sensor emits a radiation strip of 61 cm long and 1.5 cm thick.

Multispectral aerial images were acquired using a Tetracam micro-MCA (Tetracam Inc., Chatsworth, CA; USA). The Tetracam camera consists of eleven independent image sensors and optics each, using configurable filters of center wavelengths and full-width half-maximum bands with: 450 ± 40, 550 ± 10, 570 ± 10, 670 ± 10, 700 ± 10, 720 ± 10, 780 ± 10, 840 ± 10, 860 ± 10, 900 ± 20 and 950 ± 40 nm. In addition, the camera possesses one sensor dedicated to calibration (Incident Light Sensor, ILS), which provides band-by-band reflectance calibration in real-time, correcting the 11 bands to reduce atmospheric effects to at-sensor reflectance. The multispectral camera is equipped with rolling shutter sensors system, and captures 15.6 megapixels of image data that are transferred to twelve separate flash memory cards [17]. Every UAV flight included between 20–30 image capture moments, each consisting of the 12 images representing the 11 spectral bands and ILS of the sensor, which recorded data every 5 s.

### 2.1.4. Image processing

Pre-processing was required for multispectral and thermal images. Multispectral images were spatially aligned and radiometrically calibrated using PixelWrench 0.2 version 1.2.2.2 (Tetracam, Chatsworth, CA, USA) and exported as TIFF files. Whereas thermal frames were stacked to raw 16-bit TIFF format (temperature values expressed in Kelvin × 10000) using the ThermoViewer software (v1.3.13) by TEAX (TeAx Technology, Wilnsdorf, Germany). Therewith, RGB, thermal and multispectral images were 3D-reconstructed using Agisoft Photoscan Pro (Agisoft LLC, St. Petersburg, Russia, [www.agisoft.com](http://www.agisoft.com)) [39]. This later overlaps up to 30 images (with at least 80% overlap) and removes UAV flight effects to produce accurate ortho-mosaics. Afterwards, regions of interest (plots) were cropped and processed using the MosaicTool software (Prof. Shawn C. Kefauver, <https://integrativecropecophysiology.com/software-development/mosaicool/>, <https://gitlab.com/sckefauver/MosaicTool/>, University of Barcelona, Barcelona, Spain) integrated as a plugin for the open source image analysis platform FIJI (Fiji is Just ImageJ; <http://fiji.sc/Fiji>) [40].

Extracted RGB vegetation indices collected from both ground and aerial platforms were obtained using an updated version of the original Breedpix 2.0 software [41], which is a tool for fast calculation of pictures-based vegetation indices (Pic-VIs), adapted to JAVA8 and integrated as MosaicTool plugin within FIJI [40]. RGB indices are related to different color properties and based either on the average color of the entire image on the proportion of green pixels over the total number of pixels in the full image. CIELab and CIELuv color space models were defined by the CIE (Commission Internationale de l'Eclairage; the International Commission on Illumination) as the simultaneous contrast of green with red colors (CIELab), and yellow with blue colors (CIELuv) [42]. Both models operate similarly albeit on separate spectrums, and include lightness component (L\*), a\* and b\* dimensions for CIELab, and u\* and v\* coordinates for CIELuv. The indices a\* and u\* represent the green to red spectrum, where red is linked to positive values and green to negative ones; whereas b\* and v\* express the blue to yellow spectrum, where yellowish pixels are related to positive values and conversely, bluish pixels to negative ones. HSI color space, referring to the components Hue, Saturation and Intensity. This color space model describes saturation as the pure (chroma) concentration when diluted with white color, and intensity as the achromatic measurement of the reflected light. Regarding Hue, it is described as the chroma traversing the visible spectrum in the form of an angle between 0° and 360°, where 0° and 360° are decrypted into red, 60° into yellow, 120° into green and 180° into cyan. Derived from the Hue, the indices Green Area (GA) and Greener Area (GGA) were described as the fraction area presented by green pixels in the image, and which Hue ranges from 60° to 180° (GA) and from 80° to 180° (GGA). While GA gives a broader perception to canopy greenness, GGA excludes yellowish green pixels [31,41]. The current study was limited to the parameters (Hue, a\*, b\*, GA and GGA), as the best performed RGB indices.

Multispectral indices were formulated using a custom FIJI macro code built into the MosaicTool software (University of Barcelona, Spain). The macro operates through measuring the mean value of the plot image of each band to calculate the following indices: Normalized Difference Vegetation Index (NDVI), Enhanced Vegetation Index (EVI), Photochemical Reflectance Index (PRI<sub>m</sub>), Chlorophyll/Carotenoid Index (CCI), Transformed Chlorophyll Absorption Index (TCARI), and the TCARI/OSAVI index ratio. Likewise, aerial CT was acquired using a custom batch processing macro function in FIJI that converts 16-bit images (in Kelvin × 10000) to 32-bit images (in Celsius) [40]. Further information regarding the selected RGB and multispectral indices is summarized in Table 2. These indices represent a selection of the classic reference indices, the most relevant, enhanced, optimized, and transformed index variations and the best capacity of our Tetracam multispectral sensor to measure different traits separately.

**Table 2**  
Indices derived from RGB and multispectral visible and near infrared bands.

Function	Index	Equation	Reference
Greenness	Green Area (GA)	$60^\circ < \text{Hue} < 180^\circ$	[41]
	Greener Area (GGA)	$80^\circ < \text{Hue} < 180^\circ$	[41]
	Enhanced Vegetation Index (EVI)	$2.5 \times ((R_{\text{NIR}} - R_{\text{Red}}) / (R_{\text{NIR}} + 6 \times R_{\text{Red}} - 7.5 \times R_{\text{B}} + 1))$	[71]
	Normalized Difference Vegetation Index (NDVI)	$(R_{\text{NIR}} - R_{\text{Red}}) / (R_{\text{NIR}} + R_{\text{Red}})$	[58]
	Optimized Soil-Adjusted Vegetation Index (OSAVI)	$(R_{780} - R_{670}) / (R_{780} + R_{670} + 0.16)$	[72]
Photosynthetic Activity	Photochemical Reflectance Index (PRI)*	$(R_{550} - R_{570}) / (R_{550} + R_{570})$	[73]
	Chlorophyll/Carotenoid index (CCI)	$(R_{550} - R_{670}) / (R_{550} + R_{670})$	[21]
Leaf pigments	Transformed Chlorophyll Absorption Index (TCARI)	$3 \times (R_{700} - R_{670}) - 0.2 \times (R_{700} - R_{550}) \times (R_{700} / R_{670})$	[74]
	Index Ratio (TCARIOSAVI)	$\text{TCARI} / \text{OSAVI}$	[74]

\* For the PRI index,  $R_{550}$  is used instead of the  $R_{531}$  proposed by Gamon et al. [73], given the limitation in specific wavelengths of the multispectral camera used [75,76].

## 2.2. Carbon and nitrogen stable isotope composition

Flag leaves, sampled during grain filling (coinciding with the second measuring data), and mature grains, collected at harvest, were dried at 60 °C for a minimum of 48 h finely ground using a grinder machine (Mixer Mill MM 400; Retsch GmbH, Haan; Germany), and then weighed in tin capsules (approximately 1 mg) for further analysis of the carbon and nitrogen stable isotope signatures and the total nitrogen and carbon contents. Stable isotope values were expressed in composition ( $\delta$ ) units, as the deviation of the isotopic composition of the material from the standard. Thus, the carbon and nitrogen isotopic compositions ( $\delta^{13}\text{C}$  and  $\delta^{15}\text{N}$ ) were expressed as:

$$\delta^{13}\text{C} \text{ or } \delta^{15}\text{N} (\text{‰}) = [(R_{\text{sample}}/R_{\text{standard}}) - 1] \times 1000$$

Where the  $^{13}\text{C}/^{12}\text{C}$  and  $^{15}\text{N}/^{14}\text{N}$  ratios of the sample are notated as  $\delta^{13}\text{C}$  and  $\delta^{15}\text{N}$  and expressed in ‰, whereas  $R_{\text{standard}}$  is the molar abundance ratio of the secondary standard calibrated against the primary standard Pee Dee Belemnite ( $\delta^{13}\text{C}$ ) and  $\text{N}_2$  from air ( $\delta^{15}\text{N}$ ) [43]. Different secondary standards were used for carbon (IAEA-CH<sub>7</sub>, IAEA-CH<sub>6</sub> and IAEA-600, and USGS 40) and nitrogen (IAEA-600, N<sub>1</sub>, N<sub>2</sub>, NO<sub>3</sub>, UREA and Acetanilide) isotope analyses. Analytical precision of the  $\delta^{13}\text{C}$  and  $\delta^{15}\text{N}$  analyses were 0.1‰ and 0.3‰, respectively. Total carbon and nitrogen contents in flag leaves and grains were expressed as the percentage (%) of total carbon and nitrogen on dry matter basis. Isotopes and elemental analyses were performed employing an elemental analyzer operating in a continuous flow mode with a mass spectrometer (Delta C IRMS; ThermoFinnigan, Bremen; Germany), at the Scientific and Technical facilities of the University of Barcelona (Centres Científics i Tecnològics de la Universitat de Barcelona (CCiTUB)).

## 2.3. Statistical analysis

Analysis of variance (ANOVA) was performed using SPSS 20 (IBM SPSS Statistics 20, Inc., Chicago, IL; USA), to test the effects of planting date (normal vs late planting), genotypes attitude (winter vs facultative) and genotypic differences per subset (winter or facultative) and within each subset, for all parameters evaluated. The same analysis of variance was run also using days to heading (DTH) as a covariable to remove the effect of phenology. A bivariate Pearson correlation was used operating with the same statistical package SPSS 20 to evaluate relationships between all analytical traits and GY. Yield prediction was assessed by implementing stepwise multiple regression models within each treatment, where a multicollinearity level was controlled by setting a maximum variance inflation factor (VIF) at 10. Graphs were created using the softwares SigmaPlot 10.0 (Systat Software Inc, California; USA) and the open source software R and RStudio 1.0.44 (R Foundation for Statistical Computing, Vienna, Austria).

## 3. Results

### 3.1. Effect of planting date and genotype attitude on yield and agronomical components

Effects of planting date ( $P < 0.001$ ) and genotype attitude ( $P < 0.05$ ) on grain yield (GY) were significant (Table 3). Means of GY and the number of spikes per square meter (spikes  $\text{m}^{-2}$ ), as well as days to heading were greater in the normal planting compared to late planting regardless of the genotypic attitude (winter or facultative). Winter cultivars exhibited higher GY, spikes  $\text{m}^{-2}$ , grains spike<sup>-1</sup> and days to heading and lower thousand grain weight (TGW) and grain weight spike<sup>-1</sup> than the facultative genotypes in the normal planting. However, in late planting, days to heading was the only trait where genotypic attitude had a significant effect, with facultative cultivars reaching heading in average three weeks earlier than winter cultivars. Moreover, heading in the winter cultivars was not synchronized. For a given cultivar, the culms did not extrude the ears simultaneously but rather extended in time. Interaction between planting date and genotypic attitude was significant for GY and days to heading. In normal planting genotypic differences were also significant for GY and TGW within each subset of cultivars (winter and facultative), and with grain weight spike<sup>-1</sup> and spikes  $\text{m}^{-2}$  in winter cultivars. In late planting, genotypic differences were found for GY in winter cultivars, and for spikes  $\text{m}^{-2}$  within facultative ones (Supplemental Table 1).

### 3.2. Effect of planting date and genotypes attitude on RGB and multispectral indices

Remote sensing techniques were implemented during two consecutive visits (coinciding roughly with late heading and the second half of the grain filling). During heading, all the aerial RGB indices along with the multispectral NDVI.g were affected by planting date (Table 4). RGB vegetation indices were significantly lower in normal planting compared to late planting except for the Hue.a and GGA.a, while NDVI.g exhibited an opposite behavior. Among these indices solely the Hue.a, GA.a and NDVI.g were affected by genotypic attitude and its interaction with planting date. Furthermore, and within normal planting, b\*.a, GA.a and GGA.a and the multispectral index TCARIOSAVI.a were higher across facultative genotypes than within winter ones. However, the RGB and multispectral indices assessed at ground level failed to separate between genotypic attitudes (Table 4). In late planting, no significant effect was revealed between winter and facultative genotypes except for the RGB index a\*.a and NDVI.g (Table 4), while ground RGB indices and aerial multispectral indices were not assessed. In normal planting, genotypic differences within both subsets (winter and facultative) were shown for the RGB index Hue.g, and for most aerially assessed RGB indices (except a\*.a), while genotypic

**Table 3**

Effect of planting date and genotype attitude on wheat grain yield ( $\text{kg ha}^{-1}$ ), days to heading, grain dry weight per spike, number of grains per spike, thousand grain weight (TGW), and number of spikes per area. Range of genotypic values for yield within each category (winter versus facultative) of cultivars are shown in parenthesis.

	Yield ( $\text{kg ha}^{-1}$ )	Genotypic Yield ( $\text{kg ha}^{-1}$ )	Days to heading	Grain weight spike <sup>-1</sup> (g)	Grains spike <sup>-1</sup>	TGW (g)	N <sup>o</sup> spikes m <sup>-2</sup>
<i>Normal planting</i>							
All	8161 ± 115	(5694–9893)	149 ± 1	1.75 ± 0.03	43.11 ± 0.62	40.90 ± 0.58	607 ± 10
Winter	8498 <sup>a</sup> ± 104	(7344–9893)	152 <sup>a</sup> ± 1	1.71 <sup>b</sup> ± 0.03	43.96 <sup>a</sup> ± 0.69	39.01 <sup>b</sup> ± 0.55	622 <sup>a</sup> ± 11
Facultative	7296 <sup>b</sup> ± 251	(5694–9212)	143 <sup>b</sup> ± 1	1.90 <sup>a</sup> ± 0.1	40.94 <sup>b</sup> ± 1.22	45.76 <sup>a</sup> ± 1.06	568 <sup>b</sup> ± 22
<i>Late planting</i>							
All	4894 ± 110	(2770–5961)	104 ± 2	–	–	–	476 ± 10
Winter	4806 <sup>a</sup> ± 142	(2770–5961)	109 <sup>a</sup> ± 1	–	–	–	482 <sup>a</sup> ± 12
Facultative	5095 <sup>a</sup> ± 156	(4330–5907)	90 <sup>b</sup> ± 1	–	–	–	461 <sup>a</sup> ± 18
<b>ANOVA</b>							
PD	< 0.001	–	< 0.001	–	–	–	< 0.001
A	< 0.05	–	< 0.001	–	–	–	< 0.05
PD x A	< 0.001	–	< 0.001	–	–	–	0.617

Values are means ± standard error of the whole set (38) of genotypes and the winter (27) and facultative (11) subsets of genotypes. Levels of signification for the ANOVA: P < 0.01 and P < 0.001. PD, Planting date; A, Attitude. Within each planting date, means exhibiting different letters are significantly different (P < 0.05) by t-student on independent samples.

differences within the winter set of genotypes also existed for NDVI.g, the RGB indices a\*.g, b\*.g, GGA.g and a\*.a. In late planting, solely NDVI.g within facultative cultivars exhibited genotypic differences, while no genotypic effects were found for other indices within the subsets of winter and facultative genotypes (Supplemental Table 2).

The grain filling stage (assessed during the second visit) revealed significant planting date and genotypic attitude effects for almost all RGB and multispectral indices derived from both ground and aerial platforms, whereas the interaction effect between these factors was only significant for some RGB indices (Hue.g, a\*.g, GGA.g and GA.a). Regardless of being acquired at ground or from the aerial platform, multispectral indices PRIm and NDVI and RGB indices GA and GGA increased significantly in late planting compared to normal planting. Moreover, and in both planting dates, RGB and multispectral vegetation indices recorded significantly higher values in winter genotypes compared to facultative ones (Table 4). At the normal planting and within both subsets of cultivars, genotypic differences existed for the multispectral index (EVI.a), while genotypic differences for the RGB indices b\*.g and the GGA.a were found only across the winter subset. In late planting, genotypic differences were significant within both winter and facultative genotypes regarding RGB and multispectral indices (Hue.g, a\*.g, b\*.g and NDVI.g), while GA.g and GGA.g were only significant within facultative genotypes (Supplemental Table 2).

### 3.3. Effect of planting date and genotypes attitude on water regime and nitrogen status parameters

In both heading and grain filling canopy temperature (CT) assessed from ground (i.e. at single plot level) was affected significantly by planting date and genotypic attitude, while interaction for these factors occurred during grain filling only. Significant differences between genotypic attitudes were well evident in normal planting during heading and in the late planting during grain filling, where facultative genotypes exhibited higher CT.g than winter ones. Likewise, CT.a was significantly higher in facultative genotypes than winter ones in both phenological stages when measured in normal planting date (Table 5). Moreover, significant genotypic differences were shown within facultative genotypes at heading in both planting dates, but were not evidenced during grain filling (Supplemental Table 3).

Nitrogen content (N) and carbon isotope composition ( $\delta^{13}\text{C}$ ) of flag leaves and grains, together with nitrogen isotopic composition ( $\delta^{15}\text{N}$ ) of

flag leaves were significantly affected by planting date and genotypic attitude, while carbon content in grains was only affected by planting date. A significant interaction between planting date and genotypes attitude was found only for  $N_{\text{grain}}$  and  $\delta^{13}\text{C}_{\text{leaf}}$  (Table 5). In both flag leaves and grains, N and  $\delta^{13}\text{C}$  were higher in normal planting compared with late planting. Furthermore, winter genotypes exhibited higher  $N_{\text{leaf}}$  and lower  $\delta^{13}\text{C}_{\text{leaf}}$ ,  $N_{\text{grain}}$  and  $\delta^{13}\text{C}_{\text{grain}}$  than facultative genotypes in normal planting, and higher  $N_{\text{leaf}}$  and  $\delta^{13}\text{C}_{\text{leaf}}$  in late planting. In normal planting genotypic differences were shown for  $N_{\text{grain}}$  within both subsets (winter and facultative), and for  $\delta^{13}\text{C}_{\text{leaf}}$  and  $\delta^{15}\text{N}_{\text{leaf}}$  and  $\delta^{15}\text{N}_{\text{grain}}$  only within facultative cultivars. In late planting, genotypic differences were only found for  $\delta^{13}\text{C}_{\text{leaf}}$ ,  $\delta^{13}\text{C}_{\text{grain}}$  and  $N_{\text{grain}}$  within winter genotypes (Supplemental Table 3).

### 3.4. Effect of phenology on grain yield and phenotypical traits

For grain yield, agronomical components and all the phenotypical traits assayed, ANOVA was also run using days to heading as a covariate, to remove the effect of phenology. In this context, planting date did not have a significant effect on GY and number of spikes m<sup>-2</sup>. Moreover, phenology significantly affected GY, number of spikes m<sup>-2</sup>, the traits informing on water status (CT and heading and grain filling, and  $\delta^{13}\text{C}$  of the flag leaf and mature grains) and most of the remote sensing vegetation indices. Nevertheless, the effect of genotype attitude (winter versus facultative) was still significant for GY, number of spikes m<sup>-2</sup>,  $\delta^{13}\text{C}_{\text{leaf}}$  and  $\delta^{13}\text{C}_{\text{grain}}$  and N content of the grain, as well as most of the RGB vegetation indices measured during grain filling.

### 3.5. Performance of yield components assessing GY within planting dates and genotypic attitudes

Correlation coefficients of the linear regressions of GY against days to heading and agronomical yield components using genotypic means are presented (Table 6). In the case of normal planting, days to heading correlated positively and thousand grain weight negatively against GY only when combining both categories of genotypes. In the late planting, GY related negatively to days to heading and positively to spikes m<sup>-2</sup> (the only yield component measured) across both set of genotypes.

**Table 4**  
Effect of wheat planting dates (normal vs late), and placement of the sensors (aerial vs ground) on RGB and multispectral indices assessed in different phenological stages (Heading vs grain filling).

Heading	RGB Indices							a*.a
	Hue.g	a*.g	b*.g	GA.g	GGA.g	Hue.a		
<i>Normal planting</i>								
All	108 ± 1	-12.6 ± 0.3	15.2 ± 0.3	0.88 ± 0.01	0.75 ± 0.01	140 ± 3	-7.1 ± 0.1	
Winter	107 <sup>a</sup> ± 1	-12.5 <sup>a</sup> ± 0.3	15.2 <sup>a</sup> ± 0.4	0.88 <sup>a</sup> ± 0.01	0.75 <sup>a</sup> ± 0.01	145 <sup>a</sup> ± 3	-6.9 <sup>a</sup> ± 0.1	
Facultative	110 <sup>a</sup> ± 1	-13.1 <sup>a</sup> ± 0.5	15.1 <sup>a</sup> ± 0.4	0.88 <sup>a</sup> ± 0.01	0.75 <sup>a</sup> ± 0.02	127 <sup>b</sup> ± 4	-7.7 <sup>b</sup> ± 0.2	
<i>Late planting</i>								
All	-	-	-	-	-	93 ± 2	-10.1 ± 0.2	
Winter	-	-	-	-	-	93 <sup>a</sup> ± 2	-10.4 <sup>b</sup> ± 0.2	
Facultative	-	-	-	-	-	91.2 <sup>a</sup> ± 2	-9.4 <sup>a</sup> ± 0.2	
<b>ANOVA</b>								
PD	-	-	-	-	-	< 0.001	< 0.001	
A	-	-	-	-	-	< 0.05	0.238	
PD x A	-	-	-	-	-	< 0.05	< 0.001	
<i>Grain filling</i>								
<i>Normal planting</i>								
All	85.2 ± 1.8	-8.1 ± 0.1	14.9 ± 0.3	0.79 ± 0.02	0.51 ± 0.02	61.2 ± 1.6	-6.7 ± 0.5	
Winter	90.3 <sup>a</sup> ± 1.9	-8.4 <sup>b</sup> ± 0.1	14.3 <sup>b</sup> ± 0.4	0.84 <sup>a</sup> ± 0.01	0.57 <sup>a</sup> ± 0.02	65.4 <sup>a</sup> ± 1.8	-8.1 <sup>b</sup> ± 0.5	
Facultative	71.7 <sup>b</sup> ± 2.9	-7.4 <sup>a</sup> ± 0.3	16.7 <sup>a</sup> ± 0.6	0.68 <sup>b</sup> ± 0.05	0.33 <sup>b</sup> ± 0.05	50.1 <sup>b</sup> ± 2.4	-3.1 <sup>a</sup> ± 1.1	
<i>Late planting</i>								
All	92.7 ± 1.3	-9.8 ± 0.2	15.3 ± 0.4	0.94 ± 0.01	0.78 ± 0.02	84.5 ± 1.5	-14.8 ± 0.5	
Winter	95.4 <sup>a</sup> ± 1.2	-9.9 <sup>b</sup> ± 0.2	14.7 <sup>b</sup> ± 0.4	0.95 <sup>a</sup> ± 0.01	0.85 <sup>a</sup> ± 0.02	92.5 <sup>a</sup> ± 1.1	-17.2 <sup>b</sup> ± 0.3	
Facultative	86.5 <sup>b</sup> ± 2.7	-9.6 <sup>a</sup> ± 0.3	16.5 <sup>a</sup> ± 0.5	0.91 <sup>b</sup> ± 0.01	0.61 <sup>b</sup> ± 0.05	66.5 <sup>b</sup> ± 2.1	-9.4 <sup>a</sup> ± 0.7	
<b>ANOVA</b>								
PD	< 0.001	< 0.001	0.188	< 0.001	< 0.001	< 0.001	< 0.001	
A	< 0.001	< 0.01	< 0.01	< 0.001	< 0.001	< 0.001	< 0.001	
PD x A	< 0.01	< 0.01	0.051	0.978	< 0.001	0.055	0.285	

(continued on next page)



Table 4 (continued)

Heading	RGB Indices			Multispectral indices						
	b <sup>a</sup> .a	GA.a	GGA.a	NDVI.g	NDVI.a	EVI.a	PRIm.a	CCI.a	TCARIOSAVI.a	
<i>Normal planting</i>										
7.7 ± 0.3	0.76 ± 0.02	0.74 ± 0.02	0.74 ± 0.02	0.71 ± 0.01	0.82 ± 0.01	0.98 ± 0.01	0.20 ± 0.01	0.28 ± 0.01	0.21 ± 0.01	
7.1 <sup>b</sup> ± 0.3	0.73 <sup>b</sup> ± 0.02	0.71 <sup>b</sup> ± 0.02	0.71 <sup>b</sup> ± 0.02	0.71 <sup>a</sup> ± 0.01	0.82 <sup>a</sup> ± 0.01	0.98 <sup>a</sup> ± 0.01	0.21 <sup>a</sup> ± 0.01	0.28 <sup>a</sup> ± 0.01	0.21 <sup>b</sup> ± 0.01	
9.1 <sup>a</sup> ± 0.5	0.83 <sup>a</sup> ± 0.02	0.81 <sup>a</sup> ± 0.02	0.81 <sup>a</sup> ± 0.02	0.71 <sup>a</sup> ± 0.01	0.81 <sup>a</sup> ± 0.01	0.99 <sup>a</sup> ± 0.01	0.21 <sup>a</sup> ± 0.01	0.29 <sup>a</sup> ± 0.01	0.22 <sup>a</sup> ± 0.01	
<i>Late planting</i>										
16.4 ± 0.5	0.95 ± 0.01	0.72 ± 0.03	0.72 ± 0.03	0.76 ± 0.01	-	-	-	-	-	
16.9 <sup>a</sup> ± 0.7	0.95 <sup>a</sup> ± 0.01	0.73 <sup>a</sup> ± 0.03	0.73 <sup>a</sup> ± 0.03	0.77 <sup>a</sup> ± 0.01	-	-	-	-	-	
15.3 <sup>a</sup> ± 0.7	0.95 <sup>a</sup> ± 0.01	0.71 <sup>a</sup> ± 0.05	0.71 <sup>a</sup> ± 0.05	0.72 <sup>b</sup> ± 0.01	-	-	-	-	-	
<b>ANOVA</b>										
< 0.001	< 0.001	< 0.001	< 0.001	< 0.001	-	-	-	-	-	
0.702	< 0.05	0.392	< 0.001	< 0.001	-	-	-	-	-	
< 0.05	< 0.05	0.197	< 0.001	< 0.001	-	-	-	-	-	
<i>Grain filling</i>										
<i>Normal planting</i>										
25.3 ± 0.4	0.53 ± 0.03	0.27 ± 0.02	0.27 ± 0.02	0.56 ± 0.01	0.79 ± 0.01	0.88 ± 0.01	0.14 ± 0.01	0.28 ± 0.01	0.28 ± 0.01	
24.5 <sup>a</sup> ± 0.4	0.60 <sup>a</sup> ± 0.03	0.33 <sup>a</sup> ± 0.02	0.33 <sup>a</sup> ± 0.02	0.59 <sup>a</sup> ± 0.01	0.81 <sup>a</sup> ± 0.01	0.88 <sup>a</sup> ± 0.01	0.15 <sup>a</sup> ± 0.01	0.29 <sup>a</sup> ± 0.01	0.26 <sup>b</sup> ± 0.01	
27.4 <sup>b</sup> ± 0.5	0.33 <sup>b</sup> ± 0.05	0.13 <sup>b</sup> ± 0.03	0.13 <sup>b</sup> ± 0.03	0.47 <sup>b</sup> ± 0.02	0.74 <sup>b</sup> ± 0.02	0.82 <sup>b</sup> ± 0.02	0.13 <sup>b</sup> ± 0.01	0.24 <sup>b</sup> ± 0.02	0.35 <sup>a</sup> ± 0.02	
<i>Late planting</i>										
25.3 ± 0.3	0.84 ± 0.02	0.63 ± 0.02	0.63 ± 0.02	0.69 ± 0.01	0.81 ± 0.01	0.67 ± 0.01	0.17 ± 0.01	0.31 ± 0.01	0.28 ± 0.01	
25.1 <sup>b</sup> ± 0.4	0.91 <sup>a</sup> ± 0.01	0.76 <sup>a</sup> ± 0.02	0.76 <sup>a</sup> ± 0.02	0.73 <sup>a</sup> ± 0.01	0.82 <sup>a</sup> ± 0.01	0.68 <sup>a</sup> ± 0.01	0.17 <sup>a</sup> ± 0.01	0.31 <sup>a</sup> ± 0.01	0.26 <sup>b</sup> ± 0.01	
26 <sup>a</sup> ± 1	0.66 <sup>b</sup> ± 0.04	0.33 <sup>b</sup> ± 0.03	0.33 <sup>b</sup> ± 0.03	0.61 <sup>b</sup> ± 0.01	0.76 <sup>b</sup> ± 0.01	0.65 <sup>a</sup> ± 0.02	0.15 <sup>b</sup> ± 0.01	0.28 <sup>b</sup> ± 0.01	0.33 <sup>a</sup> ± 0.02	
<b>ANOVA</b>										
0.750	< 0.001	< 0.001	< 0.001	< 0.001	0.077	< 0.001	< 0.001	< 0.01	0.583	
< 0.001	< 0.001	< 0.001	< 0.001	< 0.001	< 0.001	< 0.001	< 0.001	< 0.001	< 0.001	
0.457	< 0.001	0.682	0.286	0.928	0.249	0.862	0.676	0.630	0.630	

Values are means ± standard error of the whole set (38) of genotypes and the winter (27) and facultative (11) subsets of genotypes. Levels of significance for the ANOVA: P < 0.05, P < 0.01 and P < 0.001. PD, Planting date; A, Attitude. Within each planting date, means exhibiting different letters are significantly different (P < 0.05) by t-student on independent samples. Sub-indices: g, ground; a, aerial.

**Table 5**  
Effect of planting date (normal vs late) and genotype attitude (winter vs facultative) on ground and aerial temperature in both visits (at heading and grain filling), flag leaf and grains dry matter's carbon and nitrogen contents (%C and %N) and carbon and nitrogen isotopic composition ( $\delta^{15}\text{N}$  and  $\delta^{13}\text{C}$ ).

	Canopy temperature				Isotopic composition							
	Heading				Grain filling			Maturity				
	CT.g (°C)	CT.a (°C)	CT.g (°C)	CT.a (°C)	$\delta^{13}\text{C}_{\text{leaf}}$ (‰)	$\delta^{15}\text{N}_{\text{leaf}}$ (‰)	C <sub>leaf</sub> (%)	N <sub>leaf</sub> (%)	$\delta^{13}\text{C}_{\text{grain}}$ (‰)	$\delta^{15}\text{N}_{\text{grain}}$ (‰)	C <sub>grain</sub> (%)	N <sub>grain</sub> (%)
<b>Normal planting</b>												
All	26.1 ± 0.1	26.9 ± 0.11	28.9 ± 0.9	27.7 ± 0.2	-26.43 ± 0.09	2.23 ± 0.07	40.58 ± 0.17	3.07 ± 0.04	-25.66 ± 0.06	3.82 ± 0.04	42.24 ± 0.09	2.36 ± 0.02
Winter	25.9 <sup>b</sup> ± 0.1	26.8 <sup>b</sup> ± 0.1	28.7 <sup>a</sup> ± 0.2	27.4 <sup>b</sup> ± 0.2	-26.51 <sup>b</sup> ± 0.11	2.36 <sup>a</sup> ± 0.07	40.53 <sup>a</sup> ± 0.19	3.21 <sup>a</sup> ± 0.04	-25.76 <sup>b</sup> ± 0.07	3.86 <sup>a</sup> ± 0.05	42.23 <sup>a</sup> ± 0.09	2.29 <sup>b</sup> ± 0.02
Facultative	26.4 <sup>a</sup> ± 0.2	27.4 <sup>a</sup> ± 0.2	29.3 <sup>a</sup> ± 0.3	28.6 <sup>a</sup> ± 0.5	-26.24 <sup>a</sup> ± 0.15	1.90 <sup>b</sup> ± 0.13	40.72 <sup>a</sup> ± 0.33	2.70 <sup>b</sup> ± 0.07	-25.42 <sup>a</sup> ± 0.13	3.72 <sup>a</sup> ± 0.08	42.3 <sup>a</sup> ± 0.2	2.53 <sup>a</sup> ± 0.04
<b>Late planting</b>												
All	25.6 ± 0.1	-	26.8 ± 0.1	-	-28.76 ± 0.07	2.94 ± 0.06	40.19 ± 0.24	2.76 ± 0.06	-26.76 ± 0.05	3.89 ± 0.04	42.47 ± 0.06	2.26 ± 0.03
Winter	25.5 <sup>a</sup> ± 0.2	-	26.4 <sup>b</sup> ± 0.1	-	-28.52 <sup>a</sup> ± 0.07	3.08 <sup>a</sup> ± 0.07	40.22 <sup>a</sup> ± 0.28	2.96 <sup>a</sup> ± 0.06	-26.76 <sup>a</sup> ± 0.06	3.87 <sup>a</sup> ± 0.05	42.36 <sup>b</sup> ± 0.07	2.26 <sup>a</sup> ± 0.03
Facultative	25.8 <sup>a</sup> ± 0.2	-	27.7 <sup>a</sup> ± 0.3	-	-29.33 <sup>b</sup> ± 0.09	2.62 <sup>b</sup> ± 0.09	40.13 <sup>a</sup> ± 0.45	2.27 <sup>b</sup> ± 0.11	-26.77 <sup>a</sup> ± 0.08	3.93 <sup>a</sup> ± 0.07	42.73 <sup>a</sup> ± 0.09	2.26 <sup>a</sup> ± 0.05
<b>ANOVA</b>												
PD	< 0.01	-	< 0.001	-	< 0.001	< 0.001	0.194	< 0.001	< 0.001	0.063	< 0.01	< 0.001
A	< 0.05	-	< 0.001	-	< 0.05	< 0.001	0.987	< 0.001	< 0.05	0.605	0.053	< 0.001
PD x A	0.941	-	< 0.05	-	< 0.001	0.982	0.640	0.165	0.088	0.136	0.162	< 0.01

Values are means ± standard error of the whole set (38) of genotypes and the winter (27) and facultative (11) subsets of genotypes. Levels of signification for the ANOVA: P < 0.05, P < 0.01 and P < 0.001. PD, Planting date; A, Attitude. Within each planting date, means exhibiting different letters are significantly different (P < 0.05) by t-student on independent samples. Sub-indices: g, ground; a, aerial.

**Table 6**

Correlation coefficients of the linear regressions of wheat grain yield (GY) against days to heading, grain dry weight per spike (Grain weight spike<sup>-1</sup>), number of grains per spike (grains spike<sup>-1</sup>), thousand grains weight (TGW), number of spikes per grown area (spikes m<sup>-2</sup>), per planting date.

	Days to heading	Grain weight spike <sup>-1</sup>	Grains spike <sup>-1</sup>	TGW	N <sup>o</sup> spikes m <sup>-2</sup>
<b>Normal planting</b>					
All	0.435**	-0.285 ns	0.130ns	-0.407*	0.276ns
Winter	-0.163 ns	0.260ns	-0.010ns	0.266ns	-0.203ns
Facultative	0.264ns	-0.592ns	-0.070ns	-0.605 ns	0.564ns
<b>Late planting</b>					
All	-0.430**	-	-	-	0.386*
Winter	-0.636**	-	-	-	0.429*
Facultative	0.076ns	-	-	-	0.472ns

Correlation values were calculated across the whole (All) set (38) of genotypes or within the winter (27) and facultative (11) subsets of genotypes. (each genotypic value being the mean of three plots). Level of significance: ns, non-significant; \*, p < 0.05; \*\*, p < 0.01.

**3.6. Performance of RGB and multispectral indices assessing GY within planting dates and genotypic attitude**

In the normal planting, during heading and using genotypic means (Table 7), all aerially assessed RGB vegetation indices together with the multispectral TCARIOSAVI.a correlated with GY across both subsets of genotypes, while the ground-assessed RGB indices and the rest of multispectral indices did not correlate. As per genotypic attitude, the RGB indices a\*.a, GA.a and GGA.a correlated within winter genotypes, while the Hue.a and multispectral indices EVI.a and TCARIOSAVI.a correlated with GY within facultative ones. In the late planting however, only the RGB parameters a\*.a and b\*.a correlated against GY; in this case across all genotypes as well as within winter genotypes.

During grain filling, for normal planting, all RGB and multispectral indices assessed at ground and aerially were significantly correlated against GY across both subsets of genotypes combined (Table 7). Regarding genotypic attitude however, only the RGB index a\*.a and the multispectral EVI.a correlated with GY within facultative genotypes, and no correlation existed within winter ones. In the late planting, only the RGB indices b\*.g and a\*.a, together with multispectral indices EVI.a and CCI.a correlated with GY across both categories of genotypes as well as (except for b\*.g) within winter genotypes only. No other vegetation index correlated with GY within the winter and facultative subsets of genotypes.

**3.7. Performance of canopy temperature, stable isotope signatures and N content assessing GY within planting dates and genotypes attitude**

In the normal planting (and except for ground-assessed CT at heading), CT correlated negatively with GY across the whole set of genotypes in the normal planting. In the late planting negative correlations were achieved only at heading and this index also correlated negatively with GY within the winter subset of genotypes. No other correlation between CT and GY within each of the two subsets of genotypes were recorded (Table 8).

$\delta^{13}\text{C}$  of grains correlated negatively with GY across the whole set of genotypes and replicates in both planting dates (Fig. 3). Significant correlations using genotypic means were also recorded across the whole set of genotypes as well as within the facultative subset of genotypes in the normal planting and within winter genotypes in the late planting (Table 8). In flag leaves however, the negative correlations of  $\delta^{13}\text{C}$  against GY were only reported in the late planting across all genotypes

**Table 7**  
Correlations of RGB and multispectral indices assessed during heading and grain filling against GY within each planting date (Normal vs Late), per genotypes attitude (Winter vs Facultative) and by placement of sensors (Aerial vs Ground).

Heading	RGB Indices										Multispectral Indices					
	Hue.g	a*.g	b*.g	GA.g	GGA.g	Hue.a	a*.a	b*.a	GA.a	GGA.a	NDVI.g	NDVI.a	EVI.a	PRIm.a	CCI.a	TCARIOSAVI.a
<i>Normal planting</i>																
All	0.058ns	0.222ns	-0.141ns	0.152ns	0.093ns	0.546**	0.495**	-0.538**	-0.537**	-0.517**	-0.100ns	0.235ns	0.281ns	0.125ns	-0.091ns	-0.489**
Winter	0.173ns	0.066ns	-0.109ns	0.160ns	0.100ns	0.363	0.392*	-0.357ns	-0.428*	-0.426*	-0.354ns	0.012ns	0.204ns	-0.119ns	-0.110ns	-0.184ns
Facultative	0.230ns	0.354ns	-0.556ns	0.191ns	0.173ns	0.658*	0.447ns	-0.562ns	-0.592ns	-0.565ns	0.256ns	0.206ns	0.819**	0.299ns	0.350ns	-0.246ns
<i>Late planting</i>																
All	-	-	-	-	-	0.159ns	0.590**	-0.486**	-0.147ns	0.170ns	-0.268ns	-	-	-	-	-
Winter	-	-	-	-	-	0.221ns	0.698**	-0.564**	-0.209ns	0.174ns	-0.329ns	-	-	-	-	-
Facultative	-	-	-	-	-	-0.080ns	-0.087ns	0.036ns	0.287ns	0.239ns	0.089ns	-	-	-	-	-
<i>Grain filling</i>																
<i>Normal planting</i>																
All	0.568**	-0.538**	-0.338*	0.580**	0.525**	0.531**	-0.456**	-0.340*	0.527**	0.464**	0.560**	0.585**	0.535**	0.457**	0.592**	-0.486**
Winter	0.141ns	0.078ns	-0.298ns	0.121ns	0.195ns	0.155ns	0.337ns	-0.235ns	-0.302ns	-0.034ns	0.057ns	0.158ns	0.190ns	0.112ns	0.194ns	-0.124ns
Facultative	0.529ns	-0.540ns	0.121ns	0.530ns	0.390ns	0.563ns	-0.807**	0.107ns	0.562ns	0.456ns	0.428ns	0.474ns	0.656*	0.106ns	0.593ns	-0.086ns
<i>Late planting</i>																
All	-0.077ns	0.294ns	-0.445**	-0.110ns	-0.109ns	-0.110ns	0.478**	-0.278ns	-0.160ns	-0.200ns	-0.222ns	-0.264ns	-0.384*	-0.250ns	-0.405*	0.065ns
Winter	0.089ns	0.462*	-0.551**	-0.119ns	0.023ns	-0.044ns	0.623**	-0.483*	-0.192ns	-0.202ns	-0.301ns	-0.260ns	-0.482*	-0.236ns	-0.481*	-0.182ns
Facultative	0.282ns	-0.246ns	-0.052ns	0.232ns	0.245ns	0.035ns	-0.381ns	0.270ns	0.101ns	0.143ns	0.220ns	-0.098ns	0.200ns	-0.004ns	0.054ns	0.188ns

Correlation values were calculated across the whole (All) set (38) of genotypes or within the winter (27) and facultative (11) subsets of genotypes (each genotypic value being the mean of three plots). Abbreviations for subscripts are a (aerial) and g (ground). Levels of significance: ns, non-significant; \*, P < 0.05; \*\*, P < 0.01. Sub-indices: g, ground; a, aerial.

**Table 8**

Correlations of ground-assessed (CT.g), and aerially assessed (CT.a) canopy temperature during heading and grain filling, carbon and nitrogen contents, carbon and nitrogen isotopic composition  $\delta^{13}\text{C}$  and  $\delta^{15}\text{N}$  in sampled flag leaves during grain filling and dry matter of mature grains, against GY within planting dates (Normal vs Late).

	Canopy temperature				Isotopic composition							
	Heading		Grain filling		Grain filling		Maturity		Maturity		Maturity	
	CT.g	CT.a	CT.g	CT.a	$\delta^{13}\text{C}_{\text{leaf}}$	$\delta^{15}\text{N}_{\text{leaf}}$	$\text{C}_{\text{leaf}}$	$\text{N}_{\text{leaf}}$	$\delta^{13}\text{C}_{\text{grain}}$	$\delta^{15}\text{N}_{\text{grain}}$	$\text{C}_{\text{grain}}$	$\text{N}_{\text{grain}}$
<i>Normal planting</i>												
All	-0.198ns	-0.505**	-0.475**	-0.452**	-0.128ns	0.273ns	-0.161ns	0.498**	-0.553**	0.106ns	-0.040ns	-0.624**
Winter	0.307ns	-0.222	-0.274ns	-0.250ns	0.083ns	0.078ns	-0.098ns	0.057ns	-0.188ns	-0.089ns	-0.106ns	-0.404*
Facultative	-0.523ns	-0.606	-0.520ns	-0.393ns	-0.242ns	0.017ns	-0.240ns	0.347ns	-0.755*	0.088ns	0.079ns	-0.536ns
<i>Late planting</i>												
All	-0.357*	-	0.150ns	-	-0.617**	-0.219ns	-0.053ns	-0.254ns	-0.591**	0.238ns	0.239ns	-0.575**
Winter	-0.583**	-	0.139ns	-	-0.692**	-0.160ns	-0.166ns	-0.330ns	-0.706**	0.357ns	0.215ns	-0.665**
Facultative	0.109ns	-	-0.161ns	-	-0.381ns	-0.152ns	0.382ns	0.370ns	0.037ns	-0.325ns	0.071ns	-0.287ns

Correlation values were calculated across the whole (All) set (38) of genotypes or within the winter (27) and facultative (11) subsets of genotypes (each genotypic value being the mean of three plots). Abbreviations for subscripts are a (aerial) and g (ground). Levels of significance: ns, non-significant; \*,  $P < 0.05$ ; \*\*,  $P < 0.01$ . Sub-indices: g, ground; a, aerial.

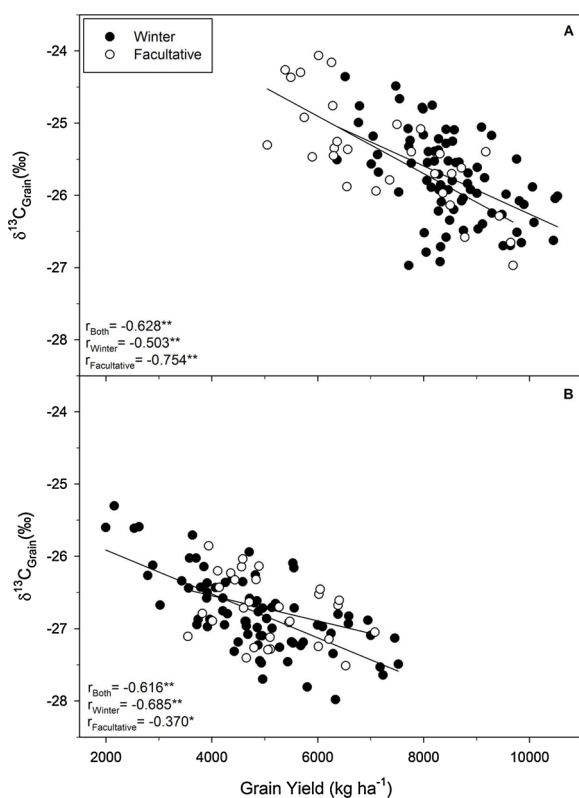


**Fig. 3.** Relationship between grain yield (GY) and carbon isotope composition ( $\delta^{13}\text{C}$ ) of mature grains, sorted by wheat genotype attitude (winter vs facultative), in both normal planting date (A) and late planting date (B). Each point represents a replication (i.e. plot value) for a given cultivar and growing condition.

as well as within winter genotypes. Nitrogen content of the flag leaf correlated positively with GY across the whole set of genotypes and replicates in both the normal and the late plantings (Fig. 4A), while nitrogen content in grains correlated negatively with GY (Fig. 4B). However phenotypic correlation (i.e. across the genotype means) between leaf N and GY was only significant at normal planting when both

subgroups of genotypes were considered together, while no correlations existed for late planting or within each of the subsets of genotypes (Table 8). N content of kernels correlated negatively with GY across the means of the whole set of genotypes at both the normal and late plantings as well as within the winter subset. Total carbon content and the  $\delta^{15}\text{N}$  of the flag leaf and grains did not correlate with GY in any case.

Correlations of CT against  $\delta^{13}\text{C}$  and nitrogen content of the flag leaf and the mature grains were also investigated in both planting dates (Supplemental Table 6). In normal planting and disregarding the placement of the sensor, CT measured at heading related negatively against N of the flag leaf and positively with N content of grains, as well as with the  $\delta^{13}\text{C}$  of flag leaf and grains. These correlations in the late planting were weaker, though.

Relationships between  $\delta^{15}\text{N}$  and nitrogen content of the flag leaf against ground and aerial remote sensing (RGB, thermal and multispectral) indices were also displayed (Supplemental Tables 7 and 8). For both  $\delta^{15}\text{N}$  and N content, correlations were stronger with remote sensing traits measured in normal rather than in late planting, particularly when measured during grain filling.

### 3.8. Performance of remote sensing techniques and stable isotopes on GY phenotyping

To evaluate the best GY predictors among all remote sensing (RGB, thermal and multispectral) indices and analytical (N content and isotopic parameters) values, multilinear stepwise regression models were tested for both planting dates, and using the genotypic means for GY as well as for all the phenotypic traits evaluated (Table 9). Three different categories of phenotyping models were tested: 1) only including remote sensing indices; 2) only including stable isotope signatures and N content and 3) combining the two previous categories. In general, and for each of these three categories of phenotyping characteristics, models explained better genotypic variability in GY in the normal compared with the late planting within each phenotyping category. Also, models using stable isotopes and nitrogen content alone predicted GY performance more efficiently than these using remote sensing indices alone; nevertheless, the best predictions were attained when both categories of traits were combined (Table 9).

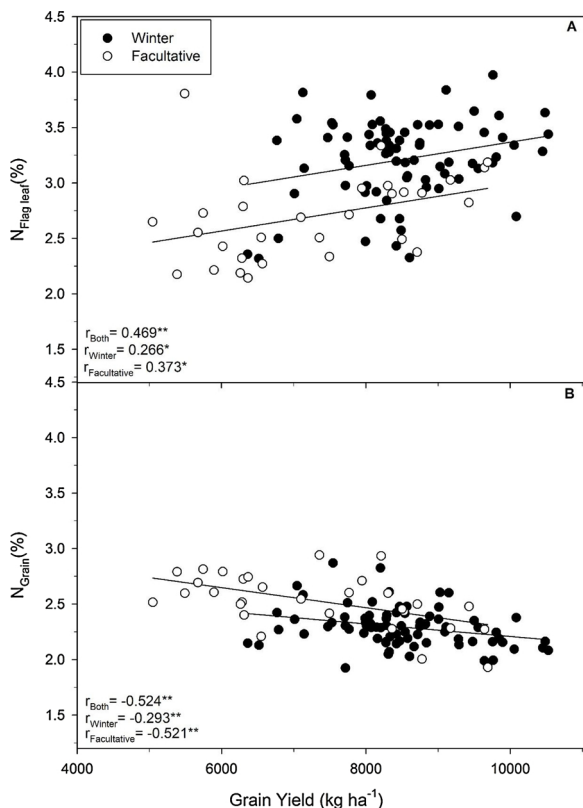


**Fig. 4.** Relationship between grain yield (GY) and nitrogen content (N) of flag leaves (A) and mature grains (B), sorted by genotypes attitude (winter vs facultative) in normal planting date. Each point represents a replication (i.e. plot value) for a given cultivar and growing condition.

**Table 9**

Multi-linear regression (stepwise) of grain yield (GY) as dependent variable, and the remote sensing traits (canopy RGB, multispectral vegetation indices and canopy temperature) measured from ground and aerial platforms and combined to carbon and nitrogen isotope composition ( $\delta^{13}C$  and  $\delta^{15}N$ ) as independent variables.  $R_{adjusted}^2$ , adjusted determination coefficient; RMSE, Root Mean Square Error; P-value, linear regression model significance.

Grain yield predictions		$R_{adjusted}^2$	RMSE	P-value	
Heading	<i>Normal planting</i>				
	All parameters	$Y = 597.5 - 2421.4 \%N_{grain} - 18738.6 TCARIOSAVI.a + 5764.7 EVI.a + 747.8 \delta^{13}C_{leaf} - 1218.7 \delta^{13}C_{grain}$	0.731	492.7	< 0.001
	Remote sensing	$Y = 1697.2 + 41.9 Hue.a + 262.2 b^*.g$	0.449	704.3	< 0.001
	<i>Late planting</i>				
	All parameters	$Y = -9614.1 - 559.1 \delta^{13}C_{leaf} - 1702.1 \%N_{grain} + 308.9 a^*.a + 7133.4 NDVI.g$	0.648	466.1	< 0.001
	Remote sensing	$Y = 8887.9 + 396.8 a^*.a$	0.329	643.7	< 0.001
Grain filling	<i>Normal planting</i>				
	All parameters	$Y = 2934.1 - 2942.2 \%N_{grain} + 29594.9 NDVI.a - 61017.9 PRIm.a - 673.9 \delta^{15}N_{grain}$	0.694	524.9	< 0.001
	Remote sensing	$Y = 4118.2 + 14465.4 CCL.a$	0.331	776.3	< 0.001
	<i>Late planting</i>				
	All parameters	$Y = -24815.4 - 617.7 \delta^{13}C_{leaf} - 1812.9 \%N_{grain} - 109.6 b^*.a + 417.2 \%C_{grain}$	0.654	462.4	< 0.001
	Remote sensing	$Y = 8154.9 + 333.6a^*.a$	0.205	700.7	< 0.001
Stable isotopes + nitrogen	<i>Normal planting</i>				
	Isotopes	$Y = -19.1 - 2389.2 \%N_{grain} + 961.1 \%N_{leaf} + 860.3 \delta^{13}C_{leaf} - 1309.8 \delta^{13}C_{grain}$	0.689	529.6	< 0.001
	<i>Late planting</i>				
	Isotopes	$Y = -9787.1 - 649.7 \delta^{13}C_{leaf} - 1770.1 \%N_{grain}$	0.529	539.4	< 0.001

## 4. Discussion

### 4.1. Effect of planting date and the genotype attitude on wheat performance

Sowing date is regarded as a key factor to adjust wheat growth cycle to the climate conditions prevailing in a site [1]. Late planting is an experimental approach frequently used to evaluate the effect of increased temperature in crop performance [44–46]. The interfering effects of factors other than temperature affecting the growth and development pattern of the crop may be excluded. In our experimental setup, differences in photoperiod were rather minor: one hour (corresponding to 10.39 h and 11.39 h, for the dates for normal and late planting, respectively), from a total annual variation of about 6 h at the latitude of Zamadueñas station). Moreover, both trials were exposed to a pattern of increasing daylength after seedling emergence (considering the days elapsed between sowing and emergence in the normal planting). The current study intended to evaluate the behavior of wheat cultivars planted in different dates in relation with the performance of phenotyping techniques, altogether with the interaction of planting temperature (i.e. planting date) with genotyping characteristics determining flowering induction by low temperature (i.e. winter versus facultative behavior).

Even after removing the effect of phenology (using heading time as a covariate), winter cultivars were still significantly different than facultative cultivars for GY, number of spikes  $m^{-2}$ ,  $\delta^{13}C_{leaf}$  and  $\delta^{13}C_{grain}$  and N content of the grain, as well as most of the RGB vegetation indices measured during grain filling. A decrease in GY is expected in the late planting as a result of higher temperatures which, not only shorten the duration of the crop cycle, but also increase respiration (dark respiration and photorespiration) rates and may eventually expose plants to heat stress during late growth stages [47,48]. Our results suggest that differences in yield between the two genotypic types were (at least in part) established prior grain filling. One factor involved may be the longer phenology (date of heading) of the winter phenotypes which has been reported before [10,49]. Moreover, it has been reported that

winter cultivars are more tolerant to low temperature than the facultative ones [7,8]. The negative effect of a late planting on GY was related with a shorter crop duration, which basically caused a decrease in spikes  $\text{m}^{-2}$ , particularly in the winter genotypes, given their poor flowering. By contrast, facultative cultivars, apart from not having the vernalization requirements to flowering [7,8,50], they express genes that confer heat tolerance [51–53]. The expected rise in temperature associated with climate change [4,5] will make on the long term winter genotypes more vulnerable than facultative ones, highlighting hence the potential adaptive ability of facultative genotypes that can secure better productivity under Mediterranean conditions. The increase in the atmospheric level of  $\text{CO}_2$  is not expected to play any differential effect between both categories of genotypes, besides to alleviate the negative effects of heat on the photosynthetic activity.

In the normal planting the  $\delta^{13}\text{C}$  of both the flag leaf and grains of the winter genotypes were slightly more negative than that of facultative genotypes, indicating better water status experienced by the winter genotypes in spite their somewhat larger crop cycle [54,55]. In agreement with that, days to heading was positively correlated with GY across the whole (winter plus facultative) set of genotypes. By contrast, in the late planting, facultative genotypes exhibited a more negative leaf  $\delta^{13}\text{C}$  than the winter genotypes, and days to heading were negatively correlated with GY across the whole set of genotypes as well as within winter genotypes. These results indicate that for a late planting, even if under well irrigated conditions shown by the very low  $\delta^{13}\text{C}$  values of both the flag leaf and the grains (even more negative than for the normal planting), escaping attitude, in terms of reaching fast the reproductive stage, is paramount under Mediterranean conditions as growing temperature increases [55,56].

#### 4.2. RGB and multispectral indices and wheat performance

Among RGB indices, GA, GGA,  $a^*$  and Hue, altogether with multispectral-derived indices NDVI, EVI, PRI<sub>m</sub> and TCARIOSAVI, are considered as efficient indicators of canopy growth and green vegetation [17]. In the present study, and regardless of data of measurement, these indices correlated in general better with GY in the normal planting compared with the late planting trial. In fact, late planting, by shortening crop cycle, is probably diminishing genotypic differences in canopy biomass and greenness, as well as in ground covering and thus yield. All these aspects may limit the performance of vegetation indices assessing genotypic differences in GY. Different explanations may be argued, as for instance the faster development and shorter crop duration in late planting, which moreover to limiting canopy growth may blur genotypic differences in canopy size as well as in stay green.

Generally, RGB and multispectral vegetation indices correlated better against GY during grain filling than at heading. Comparable results have been reported previously regarding durum wheat [27,41,57], the explanation being these indices, when assessed during grain filling, may catch differences across genotypes in terms of maintaining the photosynthetic capacity of the canopy for longer, which is known as stay green [58]. Besides that, grain filling is at a later stage than heading, and closer to maturity and harvest, therefore more representing the final GY.

Concerning stay green, in the case of CCI, this index reflects the chlorophyll/carotenoid ratio in the canopy, with senescence increasing this ratio. The negative correlation obtained in the late planting, not only across the whole set of genotypes, but also across the winter genotypes, can be explained by the fact the canopy of the winter genotypes remains greener for longer because reproductive stage is delayed (and irregular), and consequently the canopy senescence too. The more the senescence is delayed the poorer the reproductive stage is and consequently GY will be lower. On the contrary in the normal planting, stay green during grain filling is a positive trait in terms of increasing GY, particularly when water conditions are adequate such in our trials submitted to support irrigation.

Recent reports on barley [26] and maize [17,31] concluded for RGB indices that when assessed from ground they performed as well as assessed aerially. Nevertheless, different factors may explain the poor performance of ground images at heading. For each index differences across the whole set and the subsets of winter and facultative genotypes were similar regardless of being assessed at ground or from an UAV. Nevertheless, the absolute values varied between both ground and aerial acquired indices (Table 4). Ground and aerial measurements were held at the same time (though for ground measures the assessment period was considerably longer than these assessed aerially). Differences in environmental variables possibly affecting the images can be involved. Thus, while measurements during grain filling were performed on a sunny day, measurements during heading took place in a day of alternating sun and clouds. Therefore, sudden and/or transient changes in light conditions may affect the ground measurements. On the other hand, the potential effects of Bidirectional Reflectance Distribution Function (BRDF) were minimized by capturing ground and UAV images at approximately the same time of day and within 2 h of solar noon. Moreover, at least for the measurements during heading the conditions were partially cloudy which could minimize BRDF effects with diffuse light. The main advantage of ground assessment is that images resolution is higher compared to that of aerial images. In the case of the RGB images, the number of pixels per plot decreases drastically when images are acquired aerially. Nevertheless, aerial images provide full coverage of the entire plots at the same time, while ground assessed RGB images capture only approximately 35% plot area coverage based on ground sample distance calculations (data not shown). In the case of the NDVI measured with the hand spectroradiometer, again only a section of the plot is captured. Besides that, heading is not the optimal period to assess GY differences with RGB indices, particularly given the fact green biomass is larger at this stage than at grain filling. Thus, ground-acquired indices may be more saturated (excess of green because of very dense canopies) and then it is more complicated to assess differences among the genotypes.

#### 4.3. Canopy temperature and wheat performance

Water stress conditions can be detected through measuring CT, where stressed plants reveal higher CT compared to unstressed ones and in fact, negative correlations between CT and GY are expected [59,60]. In our study, even if trials were irrigated, significant negative correlations were found for the normal planting trial from both platforms. Similarly to the vegetation indices, at heading CT measured from the aerial platform correlated stronger against GY than those measured from ground level, whereas similar phenotypic correlations against GY were found during grain filling. In any case the potential advantage of an aerial platform relies in the fact that CT from the entire plots are measured simultaneously, which is not the case when temperature is assessed at ground level in individual plots. Soil but specially environmental conditions (air temperature, wind, sun brightness) may fluctuate from plot to plot throughout the sampling [12]. Moreover, whilst aerial images capture the entire plot canopy, the ground based ones cover only 40% to 50% of each plot's canopy [42].

In our study, a higher CT was coupled not only with a lower yield but also with lower leaf nitrogen content and higher  $\delta^{13}\text{C}$  values. Comparable relationships have been reported before in wheat under Mediterranean conditions, by combining different water and nitrogen fertilization regimes [27]. The positive correlation of CT with carbon isotopic composition is coherent with the fact a higher  $\delta^{13}\text{C}$  has been associated with a poorer water status [55]. In the same sense, a poorer water status assessed through high CT, may also negatively affect N accumulation in the plant [27,57,61].

However, CT may be affected by genotype attitude in a way it does not inform on the water status of the crop. The delay in the extrusion of the spikes, together with a larger leaf biomass of the winter genotypes is related with their lower CT during heading and grain filling compared



to the facultative ones in both plantings. In fact, leaves transpire more than the non-laminal parts (stems, ears) of the plant, and therefore the CT is strongly affected by phenology [62]. This should agree with the lower CT observed in the winter compared with facultative subset during grain filling at late planting. Interestingly, for the late planting  $\delta^{13}\text{C}$  of the flag leaf was higher (less negative) in the winter compared with the facultative group, suggesting poorer water status in the winter cultivars, and no differences in  $\delta^{13}\text{C}$  of mature grains were found between both groups (winter and facultative). These results in carbon isotope signature further support differences in CT between winter and facultative are not due to differential water status [55] but to phenology (ear emergence).

#### 4.4. Stable isotopes, N content and wheat performance

$\delta^{13}\text{C}$  is an efficient and accurate estimator of the effect of water status on stomatal conductance and thus photosynthesis and yield [43,63,64]. Correlations of GY with  $\delta^{13}\text{C}$  of mature grains were negative and significant in both planting dates, with correlation coefficients usually larger than for remote sensing data against GY. For the late planting  $\delta^{13}\text{C}$  flag leaf was also negatively correlated with GY. In fact, under Mediterranean field conditions and except for very severe stressed environments, the correlations between  $\delta^{13}\text{C}$  and GY are negative, which means that genotypes more productive are keeping stomata more open [33,55].

For both the normal and the late planting, the flag leaf of the winter genotypes exhibited higher  $\delta^{15}\text{N}$  values than the facultative genotypes. While the nitrogen chemical fertilizer used possesses  $\delta^{15}\text{N}$  values near 0‰, naturally available nitrogen in the soil exhibits values  $\delta^{15}\text{N}$  clearly higher [65,66]. Therefore, and regardless the planting date, the higher  $\delta^{15}\text{N}$  values of the winter genotypes may be related with their larger biomass compared with the facultative genotypes, which make the former more demanding of nitrogen sources other than that provided by the chemical fertilizer. In fact, leaf  $\delta^{15}\text{N}$  was positively related with the RGB (GA, GGA) and multispectral (NDVI, EVI) indices most suited as indicators of green biomass, while it correlated negatively with CT. However,  $\delta^{15}\text{N}$  did not correlate with GY in any case even if entered as a trait in most of the stepwise models explaining GY.

Nitrogen content of flag leaves in the normal planting was positively correlated with GY, while in mature grains, and for both planting dates, nitrogen content was negatively correlated to GY. In fact, we found a positive correlation between leaf nitrogen against canopy greenness measured as NDVI, GA or GGA measured during grain filling. This agrees with previous results [67] and suggests a higher N content in flag leaves is an indicator for stay-green and thereby for greater yield. Moreover, and for both planting dates, N content in leaves was higher in winter compared with facultative genotypes, which agrees with the delayed phenology of the former in terms of reproductive period. By contrast the negative correlation of nitrogen concentration in grains against GY is just a consequence of a concentration effect related with lower yield [68,69]. In this sense, for the normal planting nitrogen concentration of grains was lower in the winter compared with the facultative genotypes.

#### 4.5. Phenotyping approaches and grain yield prediction

Vegetation indices, both multispectral and RGB-derived, proved their efficiency in the normal planting at detecting genotypic variability in GY. Moreover, for late planting even if the stepwise models were less strong than for the normal planting, they still explained a relevant portion of genotypic variability in GY, and again with models using indices assessed at heading working better than those using indices measured at grain filling. These results illustrate the potential advantage of using a combination of selection indices to explain genotypic differences in GY rather than just a single index [17,31]. Furthermore, total nitrogen content and carbon isotopic composition of flag leaves

and mature grains proved to be appropriate phenotypical proxies for determining genotypic performance throughout the crop cycle and regardless of the planting date. These traits provide a time-integrated information of the crop performance in terms of water status in the case of  $\delta^{13}\text{C}$  [55], stay green in case of leaf nitrogen [70] or sink size as for the nitrogen content in grains [69]. Therefore, these analytical variables, contribute to a better understanding of the physiological differences existing between genotypes attitudes or and their adaptation to different growing conditions. Moreover, by adding these analytical variables the strength of the stepwise models based in remote sensing indices strongly improved regardless of the planting date and stage when remote sensing traits were acquired.

## 5. Conclusions

This study highlights the importance for wheat phenotyping performance of growing temperature, genotype attitude, trait category, phenological stage when evaluated, and even platform placement. In a normal planting the different remote sensing indices and regardless their nature (RGB or multispectral) performed quite similarly assessing yield. Later evaluation (i.e. at grain filling) performed clearly better than the earlier one (at heading) even if combined (e.g. stepwise) models may palliate such limitation. Concerning placement of the remote sensing sensors (at ground versus aerial) vegetation indices and CT evaluated aerially worked much better than from ground at heading but quite similarly at grain filling. At least on what concerns the RGB cameras potential minor differences between the images captured at the ground level and from the UAV may be due to differences in camera model and sensor (micro 4/3 size LiveMOS Panasonic GX7 vs CMOS Exmor size APS-C Sony QX1 in our study). However, camera comparisons made to the XRite ColorChecker Passport showed correlations  $r > 0.94$  for RGB values for both cameras under natural sunlight conditions (data not shown). Therefore, as indicated above other factors like sunlight conditions or the representativeness of the plot area assessed at ground may be involved in the poor performance of ground-acquired indices at heading.

With regard to genotype attitude, no clear pattern emerged; in some cases, remote sensing indices correlated better with GY within winter genotypes and in others the opposite. Late plating conditions strongly decreased the performance of remote sensing approaches for assessing yield. By contrast analytical traits such as  $\delta^{13}\text{C}$  as well as N content of mature kernels correlated quite similarly against GY regardless planting time and genotype attitude. Taken together these results indicate that for Mediterranean conditions while remote sensing techniques may lose efficiency as phenotyping traits due to miscellaneous factors, analytical traits, such as  $\delta^{13}\text{C}$  and %N, of kernels are less affected. Moreover, the performance of remote sensing approaches (RGB, multispectral and thermal) aiming to track genotypic differences in grain yield in wheat, can be clearly improved when combined with  $\delta^{13}\text{C}$  or N of mature kernels. However, the intrinsic limitation of these analytical traits is that they are assessed at maturity, which prevent their use to predict yield before the crop cycle ends. Using hyperspectral remote sensing to improve (in some cases) the ability of single indices to assess traits, or even to use the entire spectrum, in an empirical way, may represent other alternatives. The decreasing cost of hyperspectral imagers, together the improving capacity of data processing may pave the way for adopting these approaches [15].

## Author contributions

N.A.G., I.A., M.D.S. and J.L.A. conceived and designed the experiment. N.A. managed and directed the wheat trials at the experimental station of Zamadueñas (Valladolid, Spain). A.G.R., N.A.G. and J.L.A. conducted the field ground measurements. S.C.K., A.G.R. and F.Z.R. carried out the flights for the obtaining of the aerial measurements and processed and analyzed the images. F.Z.R. and M.D.S. run the

stable isotope analyses. F.Z.R. did the statistical analysis and wrote the draft paper under the supervision of J.L.A. and M.D.S.

## Acknowledgments

The study was developed within the context of the ERANET Project Concert Japan PCIN-2017-063 and the Project AGL2016-76527-R: from the MINECO, Spanish Government. FZR was a recipient of a master thesis grant sponsored by the International Center for Advanced Mediterranean Agronomic Studies (CIHEAM), in collaboration with the Mediterranean Agronomic Institute of Zaragoza (IAMZ) and Lleida University (UdL). JLA acknowledges the support from ICREA Academia, Autonomous Government of Catalonia, Spain.

## Appendix A. Supplementary data

Supplementary material related to this article can be found, in the online version, at doi:<https://doi.org/10.1016/j.plantsci.2019.110281>.

## References

- J. Hussain, T. Khaliq, A. Ahmad, J. Akhter, S. Asseng, Wheat responses to climate change and its adaptations: a focus on arid and semi-arid environment, *Int. J. Environ. Res.* 12 (2018) 117–126, <https://doi.org/10.1007/s41742-018-0074-2>.
- H. Kahiluoto, J. Kaseva, J. Balek, J.E. Olesen, M. Ruiz-Ramos, A. Gobin, K.C. Kersebaum, J. Takáč, F. Ruget, R. Ferrise, P. Bezak, G. Capellades, C. Dibari, H. Mäkinen, C. Nendel, D. Ventrella, A. Rodríguez, M. Bindi, M. Trnka, Decline in climate resilience of European wheat, *Proc. Natl. Acad. Sci. U. S. A.* (2018) 1–6, <https://doi.org/10.1073/pnas.1804387115>.
- F.X. Oury, C. Godin, A. Mailliar, A. Chassin, O. Gardet, A. Giraud, E. Heumez, J.Y. Morlais, B. Rolland, M. Rousset, M. Trotter, G. Charmet, A study of genetic progress due to selection reveals a negative effect of climate change on bread wheat yield in France, *Eur. J. Agron.* 40 (2012) 28–38, <https://doi.org/10.1016/j.eja.2012.02.007>.
- D.B. Lobell, S.M. Gourdj, The influence of climate change on global crop productivity, *Plant Physiol.* 160 (2012) 1686–1697, <https://doi.org/10.1104/pp.112.208298>.
- D.B. Lobell, W. Schlenker, J. Costa-Roberts, Climate trends and global crop production since 1980, *Science.* 333 (2011) 616–620, <https://doi.org/10.1126/science.1204531>.
- G.O. Ferrara, M.G. Mosaad, V. Mahalakshmi, S. Rajaram, Photoperiod and vernalisation response of Mediterranean wheats, and implications for adaptation, *Euphytica.* 100 (1998) 377–384, <https://doi.org/10.1023/A:1018375616915>.
- B. Trevaskis, D.J. Bagnall, M.H. Ellis, W.J. Peacock, E.S. Dennis, MADS box genes control vernalization-induced flowering in cereals, *Proc. Natl. Acad. Sci. U. S. A.* 100 (2003) 13099–13104, <https://doi.org/10.1073/pnas.1635053100>.
- U. Steinfort, B. Trevaskis, S. Fukai, K.L. Bell, M.F. Dreccer, Vernalisation and photoperiod sensitivity in wheat: impact on canopy development and yield components, *F. Crop. Res.* 201 (2017) 108–121, <https://doi.org/10.1016/j.fcr.2016.10.012>.
- K. Al-Khatib, G.M. Paulsen, Mode of high temperature injury to wheat during grain development, *Physiol. Plant.* 61 (1984) 363–368, <https://doi.org/10.1111/j.1399-3054.1984.tb06341>.
- B. Wang, D.L. Liu, S. Asseng, I. Macadam, Q. Yu, Impact of climate change on wheat flowering time in eastern Australia, *Agric. For. Meteorol.* 209–210 (2015) 11–21, <https://doi.org/10.1016/j.agrformet.2015.04.028>.
- M.P. Reynolds, M. Balota, M.I.B. Delgado, I. Amani, R.A. Fischer, Physiological and morphological traits associated with spring wheat yield under hot, irrigated conditions, *Aust. J. Plant Physiol.* 21 (1994) 717–730, <https://doi.org/10.1071/PP9940717>.
- J.L. Araus, J.E. Cairns, Field high-throughput phenotyping: the new crop breeding frontier, *Trends Plant Sci.* 19 (2014) 52–61, <https://doi.org/10.1016/j.tplants.2013.09.008>.
- S. Sankaran, L.R. Khot, C.Z. Espinoza, S. Jarolmasjed, V.R. Sathuvalli, G.J. Vandemark, P.N. Miklas, A.H. Carter, M.O. Pumphrey, N.R. Knowles, M.J. Pavek, Low-altitude, high-resolution aerial imaging systems for row and field crop phenotyping: a review, *Eur. J. Agron.* 70 (2015) 112–123, <https://doi.org/10.1016/j.eja.2015.07.004>.
- V.S. Weber, J.L. Araus, J.E. Cairns, C. Sanchez, A.E. Melchinger, E. Orsini, Prediction of grain yield using reflectance spectra of canopy and leaves in maize plants grown under different water regimes, *F. Crop. Res.* 128 (2012) 82–90, <https://doi.org/10.1016/j.fcr.2011.12.016>.
- J.L. Araus, S.C. Kefauver, M. Zaman-Allah, M.S. Olsen, J.E. Cairns, Translating high-throughput phenotyping into genetic gain, *Trends Plant Sci.* 23 (2018) 451–466, <https://doi.org/10.1016/j.tplants.2018.02.001>.
- A.S. Ray, Remote sensing in agriculture, *Int. J. Environ. Agric. Biotechnol.* 1 (2016) 2456, <https://doi.org/10.22161/ijeab/1.3.8-1878>.
- A. Gracia-Romero, O. Vergara-Díaz, C. Thierfelder, J.E. Cairns, S.C. Kefauver, J.L. Araus, Phenotyping conservation agriculture management effects on ground and aerial remote sensing assessments of maize hybrids performance in Zimbabwe, *Remote Sens. (Basel)* 10 (2018) 1–21, <https://doi.org/10.3390/rs10020349>.
- S.C. Kefauver, R. Vicente, O. Vergara-Díaz, J.A. Fernandez-Gallego, S. Kerfal, A. Lopez, J.P.E. Melichar, M.D. Serret Molins, J.L. Araus, Comparative UAV and field phenotyping to assess yield and nitrogen use efficiency in hybrid and conventional barley, *Front. Plant Sci.* 8 (2017) 1–15, <https://doi.org/10.3389/fpls.2017.01733>.
- G. Asrar, M. Fuchs, E.T. Kanemasu, J.L. Hatfield, Estimating absorbed photosynthetic radiation and leaf area index from spectral reflectance in wheat, *Agron. J.* 76 (1984) 300–306, <https://doi.org/10.2134/agronj1984.00021962007600020029x>.
- A.L. Nguy-Robertson, Y. Peng, A.A. Gitelson, T.J. Arkebauer, A. Pimstein, I. Herrmann, A. Karnieli, D.C. Rundquist, D.J. Bonfil, Agricultural and forest meteorology estimating green LAI in four crops: potential of determining optimal spectral bands for a universal algorithm, *Agric. For. Meteorol.* 192–193 (2014) 140–148, <https://doi.org/10.1016/j.agrformet.2014.03.004>.
- J.A. Gamon, K.F. Huemmrich, C.Y.S. Wong, I. Ensminger, S. Garrity, D.Y. Hollinger, A. Noormets, J. Peñuelas, A remotely sensed pigment index reveals photosynthetic phenology in evergreen conifers, *Proc. Natl. Acad. Sci. U. S. A.* 113 (2016) 13087–13092.
- A.A. Gitelson, A. Viña, V. Ciganda, D.C. Rundquist, T.J. Arkebauer, Remote estimation of canopy chlorophyll content in crops, *Geophys. Res. Lett.* 32 (2005) 1–4, <https://doi.org/10.1029/2005GL022688>.
- D. Haboudane, N. Tremblay, J.R. Miller, P. Vigneault, Remote estimation of crop chlorophyll content using spectral indices derived from hyperspectral data, *IEEE Trans. Geosci. Remote Sens.* 46 (2008) 423–436, <https://doi.org/10.1109/TGRS.2007.904836>.
- I. Herrmann, A. Karnieli, D.J. Bonfil, Y. Cohen, V. Alchanatis, SWIR-based spectral indices for assessing nitrogen content in potato fields, *Int. J. Re.* 31 (2010) 5127–5143, <https://doi.org/10.1080/01431160903283892>.
- W. Feng, X. Yao, Y. Zhu, Y.C. Tian, W.X. Cao, Monitoring leaf nitrogen status with hyperspectral reflectance in wheat, *Eur. J. Agron.* 28 (2008) 394–404, <https://doi.org/10.1016/j.eja.2007.11.005>.
- J.M. Costa, O.M. Grant, M.M. Chaves, Thermography to explore plant-environment interactions, *J. Exp. Bot.* 64 (2013) 3937–3949, <https://doi.org/10.1093/jxb/ert029>.
- S. Youfi, N. Kellas, L. Saidi, Z. Benlakehal, L. Chaou, D. Siad, F. Herda, M. Karrou, O. Vergara, A. Gracia, J.L. Araus, M.D. Serret, Comparative performance of remote sensing methods in assessing wheat performance under Mediterranean conditions, *Agric. Water Manag.* 164 (2016) 137–147, <https://doi.org/10.1016/j.agwat.2015.09.016>.
- M.S. Moran, T.R. Clarke, Y. Inoue, A. Vidal, Estimating crop water deficit using the relation between surface-air temperature and spectral vegetation index, *Remote Sens. Environ.* 49 (1994) 246–263, [https://doi.org/10.1016/0034-4257\(94\)90020-5](https://doi.org/10.1016/0034-4257(94)90020-5).
- R.D. Jackson, R.J. Reginato, S.B. Idso, Wheat canopy temperature: a practical tool for evaluating water requirements, *Water Resour. Res.* 13 (1988) 651–656, <https://doi.org/10.1029/WR013i003p0655>.
- J. Casadesús, D. Villegas, Conventional digital cameras as a tool for assessing leaf area index and biomass for cereal breeding, *J. Integr. Plant Biol.* 56 (2014) 7–14, <https://doi.org/10.1111/jipb.12117>.
- A. Gracia-Romero, S.C. Kefauver, O. Vergara-Díaz, M.A. Zaman-Allah, B.M. Prasanna, J.E. Cairns, J.L. Araus, Comparative performance of ground vs. Aerially assessed RGB and multispectral indices for early-growth evaluation of maize performance under phosphorus fertilization, *Front. Plant Sci.* 8 (2017) 1–13, <https://doi.org/10.3389/fpls.2017.02004>.
- J.L. Araus, L. Cabrera-Bosquet, M.D. Serret, J. Bort, M.T. Nieto-Taladriz, Combined use of  $\delta^{13}\text{C}$ ,  $\delta^{18}\text{O}$  and  $\delta^{15}\text{N}$  tracks nitrogen metabolism and genotypic adaptation of durum wheat to salinity and water deficit, *Funct. Plant Physiol.* 40 (2013) 595–608, <https://doi.org/10.1071/FP12254>.
- R. Sanchez-Bragado, G. Molero, M.P. Reynolds, J.L. Araus, Relative contribution of shoot and ear photosynthesis to grain filling in wheat under good agronomical conditions assessed by differential organ  $\delta^{13}\text{C}$ , *J. Exp. Bot.* 65 (2014) 5401–5413, <https://doi.org/10.1093/jxb/eru298>.
- R. Sanchez-Bragado, G. Molero, M.P. Reynolds, J.L. Araus, Photosynthetic contribution of the ear to grain filling in wheat: a comparison of different methodologies for evaluation, *J. Exp. Bot.* 67 (2016) 2787–2798, <https://doi.org/10.1093/jxb/erw116>.
- M.J. Santos, E.L. Hestir, S. Khanna, S.L. Ustin, Image spectroscopy and stable isotopes elucidate functional dissimilarity between native and nonnative plant species in the aquatic environment, *New Phytol.* 193 (2012) 683–695, <https://doi.org/10.1111/j.1469-8137.2011.03955.x>.
- A. Singh, S.P. Serbin, B.E. McNeil, C.C. Kingdon, P.A. Townsend, Imaging spectroscopy algorithms for mapping canopy foliar chemical and morphological traits and their uncertainties, *Ecol. Appl.* 25 (2015) 2180–2197, <https://doi.org/10.1890/14-2098.1>.
- J. Crain, I. Ortiz-Monasterio, B. Raun, Evaluation of a reduced cost active NDVI sensor for crop nutrient management, *J. Sensors.* 2012 (2012) 10, <https://doi.org/10.1155/2012/582028>.
- G. Barremer, U. Schmidhalter, High-throughput phenotyping of wheat and barley plants grown in single or few rows in small plots using active and passive spectral proximal sensing, *SENSORS.* 16 (2016) 1–14, <https://doi.org/10.3390/s16111860>.
- J. Bendig, A. Bolten, S. Bennertz, J. Broscheit, S. Eichfuss, G. Bareth, Estimating biomass of barley using crop surface models (CSMs) derived from UAV-based RGB imaging, *Remote Sens. (Basel)* 6 (2014) 10395–10412, <https://doi.org/10.3390/rs61110395>.



- [40] A. Gracia-Romero, S.C. Kefauver, J.A. Fernandez-Gallego, O. Vergara-Díaz, J.L. Araus, UAV and ground image-based phenotyping : a proof of concept with durum wheat, *Remote Sens. (Basel)* 11 (2019) 1–25, <https://doi.org/10.3390/rs11101244>.
- [41] J. Casadesús, Y. Kaya, J. Bort, M.M. Nachit, J.L. Araus, S. Amor, G. Ferrazzano, F. Maalouf, M. Maccaferri, V. Martos, H. Ouabbou, D. Villegas, Using vegetation indices derived from conventional digital cameras as selection criteria for wheat breeding in water-limited environments, *Ann. Appl. Biol.* 150 (2007) 227–236, <https://doi.org/10.1111/j.1744-7348.2007.00116.x>.
- [42] M.L. Buchailot, A. Gracia-Romero, O. Vergara-Díaz, M.A. Zaman-Allah, A. Tarekne, J.E. Cairns, B.M. Prasanna, J.L. Araus, S.C. Kefauver, Evaluating maize genotype performance under low nitrogen conditions using RGB UAV phenotyping techniques, *Sensors*. 19 (2019) 1–27, <https://doi.org/10.3390/s19081815>.
- [43] G.D. Farquhar, J.R. Ehleringer, K.T. Hubick, Carbon isotope discrimination and photosynthesis, *Annu. Rev. Plant Physiol.* 40 (1989) 503–537, <https://doi.org/10.1146/annurev.pp.40.060189.002443>.
- [44] R.K. Jat, P. Singh, M.L. Jat, M. Dia, H.S. Sidhu, S.L. Jat, D. Bijarniya, H.S. Jat, C.M. Parihar, U. Kumar, S.L. Ridaura, Heat stress and yield stability of wheat genotypes under different sowing dates across agro-ecosystems in India, *F. Crop. Res.* 218 (2018) 33–50, <https://doi.org/10.1016/j.fcr.2017.12.020>.
- [45] P. Paymard, M. Bannayan, R.S. Haghighi, Analysis of the climate change effect on wheat production systems and investigate the potential of management strategies, *Nat. Hazards Dordr. (Dordr)* 91 (2018) 1237–1255, <https://doi.org/10.1007/s11069-018-3180-8>.
- [46] W.J. Sacks, D. Deryng, J.A. Foley, N. Ramankutty, Crop planting dates: an analysis of global patterns, *Glob. Ecol. Biogeogr.* 19 (2010) 607–620, <https://doi.org/10.1111/j.1466-8238.2010.00551.x>.
- [47] I. Elbasyoni, Performance and stability of commercial wheat cultivars under terminal heat stress, *Agronomy*. 8 (2018) 1–20, <https://doi.org/10.3390/agronomy8040037>.
- [48] M.P. Reynolds, R.P. Singh, A. Ibrahim, O.A.A. Ageeb, A. Larque-Saavedra, J.S. Quick, Evaluating physiological traits to complement empirical selection for wheat in warm environments, *Euphytica*. 100 (1998) 85–94, <https://doi.org/10.1023/A:1018355906553>.
- [49] B.I. Cook, E.M. Wolkovich, C. Parmesan, Divergent responses to spring and winter warming drive community level flowering trends, *PNAS*. 109 (2012) 1–6, <https://doi.org/10.1073/pnas.1118364109>.
- [50] H.M. Rawson, M. Zajac, L.D.J. Penrose, Effect of seedling temperature and its duration on development of wheat cultivars differing in vernalization response, *F. Crop. Res.* 57 (1998) 289–300, [https://doi.org/10.1016/S0378-4290\(98\)00073-2](https://doi.org/10.1016/S0378-4290(98)00073-2).
- [51] B. Trevaskis, M.N. Hemming, E.S. Dennis, W.J. Peacock, The molecular basis of vernalization-induced flowering in cereals, *Trends Plant Sci.* 12 (2007) 352–357, <https://doi.org/10.1016/j.tplants.2007.06.010>.
- [52] A.A. Khan, M.R. Kabir, Evaluation of spring wheat genotypes (*Triticum aestivum* L.) for heat stress tolerance using different stress tolerance indices, *Cercet. Agron. Mold.* 47 (2015) 49–63, <https://doi.org/10.1515/cerce-2015-0004>.
- [53] M.S. Lopes, I. El-Basyoni, P.S. Baenziger, S. Singh, C. Royo, K. Ozbek, H. Aktas, E. Ozer, F. Ozdemir, A. Manickavelu, T. Ban, P. Vikram, Exploiting genetic diversity from landraces in wheat breeding for adaptation to climate change, *J. Exp. Bot.* 66 (2015) 3477–3486, <https://doi.org/10.1093/jxb/erv122>.
- [54] W.R. Whalley, C.W. Watts, A.S. Gregory, S.J. Mooney, L.J. Clark, A.P. Whitmore, The effect of soil strength on the yield of wheat, *Plant Soil* 306 (2008) 237–247, <https://doi.org/10.1007/s11104-008-9577-5>.
- [55] J.L. Araus, D. Villegas, N. Aparicio, L.F. Garcia del Moral, S. El-Hani, Y. Rharrabti, J.P. Ferrio, C. Royo, Environmental factors determining carbon isotope discrimination and yield in durum wheat under Mediterranean conditions, *Crop Sci.* 43 (2003) 170–180, <https://doi.org/10.2135/cropsci2003.0170>.
- [56] S.P. Loss, K.H.M. Siddique, Orphological and physiological traits associated with wheat yield increases in Mediterranean environments, *Adv. Agron.* 52 (1994) 229–276.
- [57] A. Elazab, J. Bort, B. Zhou, M.D. Serret, M.T. Nieto-Taladriz, J.L. Araus, The combined use of vegetation indices and stable isotopes to predict durum wheat grain yield under contrasting water conditions, *Agric. Water Manag.* 158 (2015) 196–208, <https://doi.org/10.1016/j.agwat.2015.05.003>.
- [58] G.J. Rebetzke, J.A. Jimenez-Berni, W.D. Bovill, D.M. Deery, R.A. James, High-throughput phenotyping technologies allow accurate selection of stay-green, *J. Exp. Bot.* 67 (2016) 4919–4924, <https://doi.org/10.1093/jxb/erw304>.
- [59] M.A. Joshi, S. Faridullah, A. Kumar, Effect of heat stress on crop phenology, yield and seed quality attributes of wheat (*triticum aestivum* L.), *J. Agrometeorol.* 18 (2016) 206–215 <https://search.proquest.com.sire.ub.edu/docview/1868569813?accountid=15293%0A>.
- [60] S. Thapa, K.E. Jessup, G.P. Pradhan, J.C. Rudd, S. Liu, J.R. Mahan, R.N. Devkota, J.A. Baker, Q. Xue, Canopy temperature depression at grain filling correlates to winter wheat yield in the U.S. Southern high plains, *F. Crop. Res.* 217 (2018) 11–19, <https://doi.org/10.1016/j.fcr.2017.12.005>.
- [61] S. Youfi, M.D. Serret, J.L. Araus, Shoot  $\delta^{15}\text{N}$  gives a better indication than ion concentration or  $\delta^{13}\text{C}$  of genotypic differences in the response of durum wheat to salinity, *Funct. Plant Biol.* 36 (2009) 144–155, <https://doi.org/10.1111/pce.12055>.
- [62] B. Zhou, A. Elazab, J. Bort, A. Sanz-Sáez, M.T. Nieto-Taladriz, M.D. Serret, J.L. Araus, Agronomic and physiological responses of Chinese facultative wheat genotypes to high-yielding Mediterranean conditions, *J. Agric. Sci.* 154 (2016) 870–889, <https://doi.org/10.1017/S0021859615000817>.
- [63] T. Ahmad Yasir, D. Min, X. Chen, A. Gerard, Y. Hu, The association of carbon isotope discrimination ( $\Delta$ ) with gas exchange parameters and yield traits in Chinese bread wheat cultivars under two water regimes, *Agric. Water Manag.* 119 (2013) 111–120, <https://doi.org/10.1016/j.agwat.2012.11.020>.
- [64] G.D. Farquhar, R.A. Richards, Isotopic composition of plant carbon correlates with water-use efficiency of wheat genotypes, *Aust. J. Plant Physiol.* 11 (1984) 539–552, <https://doi.org/10.1071/PP9840539>.
- [65] L.I. Wassenaar, Evaluation of the origin and fate of nitrate in the abbotsford aquifer using the isotopes of  $\delta^{15}\text{N}$  and  $\delta^{18}\text{O}$  in  $\text{NO}_3^-$ , *Appl. Geochem.* 10 (1995) 391–405, [https://doi.org/10.1016/0883-2927\(95\)00013-a](https://doi.org/10.1016/0883-2927(95)00013-a).
- [66] S.J. Kerley, S.C. Jarvis, Preliminary studies of the impact of excreted N on cycling and uptake of N in pasture systems using natural abundance stable isotopic discrimination, *Plant Soil* 178 (1996) 287–294, <https://doi.org/10.1007/BF00011595>.
- [67] J.L. Araus, T. Amaro, Y. Zuhair, M.M. Nachit, Effect of leaf structure and water status on carbon isotope discrimination in field-grown durum wheat, *Plant Cell Environ.* 20 (1997) 1484–1494, <https://doi.org/10.1046/j.1365-3040.1997.d01-43.x>.
- [68] Z. Chamekh, C. Karmous, S. Ayadi, A. Sahli, M. Belhaj Fraj, S. Youfi, S. Rezgui, N. Ben Aissa, M.D. Serret, I. McCann, Y. Trifa, H. Amara, J.L. Araus, Comparative performance of  $\delta^{13}\text{C}$ , ion accumulation and agronomic parameters for phenotyping durum wheat genotypes under various irrigation water salinities, *Ann. Appl. Biol.* 170 (2017) 229–239.
- [69] J.L. Araus, T. Amaro, J. Casadesús, A. Asbati, M.M. Nachit, Relationships between ash content, carbon isotope discrimination and yield in durum wheat, *Aust. J. Plant Physiol.* 25 (1998) 835–842, <https://doi.org/10.1071/PP98071>.
- [70] M.S. Lopes, M.P. Reynolds, Stay-green in spring wheat can be determined by spectral reflectance measurements (normalized difference vegetation index) independently from phenology, *J. Exp. Bot.* 63 (2012) 3789–3798, <https://doi.org/10.1093/jxb/ers071>.
- [71] A. Huete, K. Didan, H. Miura, E.P. Rodriguez, X. Gao, L.F. Ferreira, Overview of the radiometric and biophysical performance of the MODIS vegetation indices, *Remote Sens. Environ.* 83 (2002) 195–213, [https://doi.org/10.1016/S0034-4257\(02\)00096-2](https://doi.org/10.1016/S0034-4257(02)00096-2).
- [72] G. Rondeaux, M. Steven, F. Baret, Optimization of soil-adjusted vegetation indices, *Remote Sens. Environ.* 55 (1996) 95–107, [https://doi.org/10.1016/0034-4257\(95\)00186-7](https://doi.org/10.1016/0034-4257(95)00186-7).
- [73] J.A. Gamon, L. Serrano, J.S. Surfus, The photochemical reflectance index: an optical indicator of photosynthetic radiation use efficiency across species, functional types, and nutrient levels, *Oecologia*. 112 (1997) 492–501, <https://doi.org/10.1007/s004420050337>.
- [74] D. Haboudane, J.R. Miller, N. Tremblay, P.J. Zarco-Tejada, L. Dextraze, Integrated narrow-band vegetation indices for prediction of crop chlorophyll content for application to precision agriculture, *Remote Sens. Environ.* 81 (2002) 416–426, [https://doi.org/10.1016/S0034-4257\(02\)00018-4](https://doi.org/10.1016/S0034-4257(02)00018-4).
- [75] C. Zhang, I. Filella, D. Liu, R. Ogaya, J. Llusià, D. Asensio, J. Peñuelas, Photochemical reflectance index (PRI) for detecting responses of diurnal and seasonal photosynthetic activity to experimental drought and warming in a Mediterranean shrubland, *Remote Sens. (Basel)* 9 (2017) 1–21, <https://doi.org/10.3390/rs9111189>.
- [76] M.F. Garbulsky, J. Peñuelas, J. Gamon, Y. Inoue, I. Filella, The photochemical reflectance index (PRI) and the remote sensing of leaf, canopy and ecosystem radiation use efficiencies. A review and meta-analysis, *Remote Sens. Environ.* 115 (2011) 281–297, <https://doi.org/10.1016/j.rse.2010.08.023>.



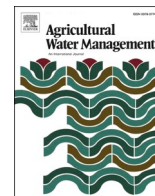
## CHAPTER III

# **Durum wheat ideotypes in Mediterranean environments differing in water and temperature conditions**

Fatima Zahra Rezzouk, Adrian Gracia-Romero, Shawn C. Kefauver, Maria Teresa Nieto-Taladriz, Maria Dolors Serret, José Luis Araus

Published in:  
Agricultural Water Management  
259 (2022): 107257





## Durum wheat ideotypes in Mediterranean environments differing in water and temperature conditions

Fatima Zahra Rezzouk<sup>a,b</sup>, Adrian Gracia-Romero<sup>a,b</sup>, Shawn C. Kefauver<sup>a,b</sup>,  
 Maria Teresa Nieto-Taladriz<sup>c</sup>, Maria Dolores Serret<sup>a,b</sup>, José Luis Araus<sup>a,b,\*</sup>

<sup>a</sup> Integrative Crop Ecophysiology Group, Plant Physiology Section, Faculty of Biology, University of Barcelona, 08028 Barcelona, Spain

<sup>b</sup> AGROTECNIO (Center for Research in Agrotechnology), Av. Rovira Roure 191, 25198 Lleida, Spain

<sup>c</sup> Instituto Nacional de Investigación y Tecnología Agraria y Alimentaria (INIA), Ctra. de La Coruña Km. 7,5, 28040 Madrid, Spain

### ARTICLE INFO

Handling Editor - Xiyang Zhang

#### Keywords:

Stable isotopes  
 Root traits  
 Leaf pigments  
 Canopy temperature

### ABSTRACT

Ideotypic characteristics of durum wheat associated with higher yield under different water and temperature regimes were studied under Mediterranean conditions. Six semi-dwarf cultivars with contrasting agronomic performance were grown during two consecutive years under winter-planted rainfed and winter-planted support-irrigation conditions and a late-planting trial under support irrigation, at the INIA station of Colmenar de Oreja (Madrid). Different traits were assessed to inform on: water status, root performance, phenology, photosynthetic capacity, crop growth, grain yield and agronomic yield components. Under support irrigation and normal planting, genotypes with higher grain yield exhibited better water status (lower  $\delta^{13}\text{C}$  and canopy temperature), assimilation of more superficial water (higher  $\delta^{18}\text{O}$ ), earlier heading and greater plant height and ear density. Under water-limited conditions (rainfed), the best genotypes also exhibited better water status (lower  $\delta^{13}\text{C}$ ) and earlier heading, but higher specific root length with extraction of water from deeper soil layers (lower  $\delta^{18}\text{O}$ ), more efficient N metabolism (higher  $\delta^{15}\text{N}$  and NBI) and consequently stronger growth (plant height and NDVI), and greater ear density and thousand grain weight. Under warmer conditions (late planting), the best genotypes also exhibited better water status (lower  $\delta^{13}\text{C}$ ) and greater plant height and photoprotective mechanisms (higher flavonoid content and lower chlorophyll content). However, the strong differences in drought between consecutive years determined other specific ideotypic traits within each of the three growing conditions and the particular year. Our study suggests specific ideotypes when breeding durum wheat under different agronomic scenarios, but also stresses that interannual variation in water conditions, typical of Mediterranean conditions, should be taken into account.

### 1. Introduction

Durum wheat is one of the major crops grown in the Mediterranean basin in terms of social importance and extent of cultivated area (Food and Agriculture Organization, 2019a). However, durum wheat production is usually conditioned by climate factors, particularly water availability and elevated temperatures (Araus et al., 2003; Loss and Siddique, 1994; Sabella et al., 2020; Xynias et al., 2020; Zampieri et al., 2020). To date, breeding programs have been mostly focused on

selecting genotypes based on grain yield, along with traits that include phenology and tolerance to local or regional pests and diseases. As a result, declining genetic advance has been reported in different regions of the Mediterranean basin (Chairi et al., 2018), and particularly when cultivars are confronted with weather variability (Kahiluoto et al., 2019). To deal with these circumstances, farmers are more and more directed towards tactical management, which relies on flexibility in sowing time and choice of cultivar (Hunt et al., 2019), monitoring of crops to adjust fertilizer application (basically nitrogen supply) and

*Abbreviations:* CT, canopy temperature; DTH, days to heading; HI, harvest index; INP, irrigated normal planting; ILP, irrigated late planting; NBI, nitrogen balance index; NDVI, normalized difference vegetation index; PH, plant height; RA, root angle; RNP, rainfed normal planting; SRL, specific root length; GNY, total grain nitrogen yield; TGW, thousand grain weight;  $\delta^{13}\text{C}$ , stable carbon isotope composition of mature grains;  $\delta^{15}\text{N}$ , stable nitrogen isotope composition of mature grains;  $\delta^{18}\text{O}$ , stable oxygen isotope composition of the water in the stem base.

\* Corresponding author at: Integrative Crop Ecophysiology Group, Plant Physiology Section, Faculty of Biology, University of Barcelona, 08028 Barcelona, Spain.

E-mail address: [jaraus@ub.edu](mailto:jaraus@ub.edu) (J.L. Araus).

<https://doi.org/10.1016/j.agwat.2021.107257>

Received 1 June 2021; Received in revised form 23 September 2021; Accepted 10 October 2021

Available online 26 October 2021

0378-3774/© 2021 The Authors. Published by Elsevier B.V. This is an open access article under the CC BY license (<http://creativecommons.org/licenses/by/4.0/>).

control the impact of biotic stresses, and wherever possible, providing support irrigation (Food and Agriculture Organization, 2019b; Mihailescu and Soares, 2020). The variability in growing conditions, together with the trends presented by ongoing climate change, call for the development and use of wheat cultivars that can adapt efficiently to the available water and withstand increased temperatures, while maintaining a relatively high yield. Therefore, there is a need for tailored breeding in terms of developing cultivars suitable to different growing conditions in the Mediterranean. Integrating phenotyping approaches within breeding strategies can pave the way to create more productive and resilient cultivars that are well adapted to specific agro-environments (Li et al., 2018).

Increasing emphasis has been given to field crop phenotyping where different remote sensing approaches are deployed, due to their high throughput and non-invasive nature, to assess crop growth, potential photosynthetic capacity or even water status (Araus and Cairns, 2014; Araus et al., 2018). Eventually the combination of remote sensing assessment with specific laboratory approaches such as stable carbon isotope signatures may improve the predictive capacity of the phenotyping process (Gracia-Romero et al., 2019; Kefauver et al., 2017; Rezzouk et al., 2020). Nevertheless, a critical hurdle for phenotyping approaches is the limited access to the belowground part of the plant under field conditions. Root phenotyping may be key when seeking to improve productivity and stability under conditions like those present in Mediterranean agro-environments where water availability limits, to a greater or lesser extent, yield and its stability (Li et al., 2019; Maccaferri et al., 2016). In fact, under elevated temperatures and water deficit, roots are reported to be more responsive in terms of growth than the aboveground parts of the plant, which may subsequently affect water uptake, plant growth and yield (Petr, 1991; Pinto and Reynolds, 2015).

Technologies developed for root phenotyping have been mainly applied to plants growing in containers under controlled conditions, making the subsequent translation of results to the real (i.e. field condition) often difficult (Atkinson et al., 2019). Under field conditions, the throughput of root phenotyping practices is still low to medium. Nevertheless, even if it is not feasible to screen the progeny of large breeding panels, these techniques may still serve to thoroughly characterize potential parents to inform strategic crosses and in general terms to define ideotypes for specific growing conditions (Maccaferri et al., 2011, 2016).

Root crown phenotyping, commonly known as “shovelomics” is a phenotyping technique to directly assess root properties. This technique was first developed for maize (Trachsel et al., 2011) and further applied to other crops, including wheat (Maccaferri et al., 2016; York et al., 2018b; York et al., 2018b). The approach consists of exploring the upper 15–30 cm of the rhizosphere via manual digging and root excavation to assess the properties of the roots (Wasson et al., 2020; York et al., 2018a). Root angle, among other root traits, was reported to be useful for improving plant productivity under drought conditions, and can contribute to breeding advances (Wasaya et al., 2018). In barley, for instance, wild genotypes exhibited a more vertical angular spread that allowed them to obtain water from deeper levels, therefore favouring survival (Bengough et al., 2004; Reynolds et al., 2007). A similar trend was observed in wheat genotypes grown under rainfed conditions, where deeper roots with higher root density at depth and lower root densities at the surface were related to higher grain yield (Passioura, 1982; Wasaya et al., 2018). Soil coring is another approach that aims to overcome some of the main limitations inherent to shovelomics, enabling exploration of the root system at deeper soil levels (Wasson et al., 2020; York et al., 2018b). However, this approach is substantially lower in throughput and much more costly than shovelomics. Other potential approaches to phenotype root architecture and/or functioning in the field were well documented, such as electrical resistance tomography (Srayeddin and Doussan, 2009), the use of electromagnetic inductance (Whalley et al., 2017) or ground penetrating radar (Liu et al., 2016, 2017) have been reported, but again the levels of throughput, cost

and/or precision are limitations.

Given the difficult nature of their direct assessment, root traits may be approached indirectly, using above-ground phenotyping as an alternative (Araus and Cairns, 2014; Wasaya et al., 2018; Tracy et al., 2020). For example, a widely considered parameter that reflects the roots' access to water resources is canopy temperature (CT). A study in wheat conducted under field conditions examined the phenotypic relationship between CT, soil moisture and the root dry weight in different soil profiles, and concluded that CT can serve as an indicator of a genotype's ability to maintain transpiration via the extraction of water from deeper soil profiles (Lopes and Reynolds, 2010). Further, in drought stressed environments and where water access is limited, transpiration and the subsequent canopy cooling effect can be supported by deeper roots (Li et al., 2019; Lopes and Reynolds, 2010). Enhanced photosynthesis due to an increase in stomatal conductance, provision of better access to water resources, and associated with genetic advance, are well documented in wheat (Roche, 2015; Li et al., 2019).

Stable isotope composition may also prove to be efficient for measuring root activities in an indirect manner. Under Mediterranean conditions (Araus et al., 2003, 2013), as well as in arid conditions under irrigation (Lopes and Reynolds, 2010), higher yielding wheat genotypes were associated with low carbon isotope composition ( $\delta^{13}\text{C}$ ) or high isotope discrimination from the surrounding  $\text{CO}_2$  atmosphere ( $\Delta^{13}\text{C}$ ) by the maturing grains. In fact, the  $\Delta^{13}\text{C}$  of plant tissues informs on the intercellular to atmospheric ratio of  $\text{CO}_2$  (Ci/Ca) within the plant (Farquhar et al., 1989), with stomatal conductance usually being the main factor determining Ci/Ca. Another approach for assessing root function is analysis of the stable water composition in plant water. Thus, oxygen isotope composition ( $\delta^{18}\text{O}$ ), when analysed in water from the base of the wheat stem (Kale Çelik et al., 2018; Millar et al., 2018; Sanchez-Bragado et al., 2019) as well as woody plants (West et al., 2006), has been proposed as a tracing method to assess the depth of soil from which the water has been extracted. In the case of plant nutrients like nitrogen, besides reflecting its source, the stable nitrogen isotope composition ( $\delta^{15}\text{N}$ ) in dry matter broadly informs about the effect of water status on nitrogen metabolism (Araus et al., 2013; Yousfi et al., 2009, 2012, 2013; Zhang et al., 2013).

Altogether, these approaches can contribute to a more efficient phenotyping, not only when supported by further simulation modelling (Condon, 2020), but even to empirically define the ideotype most suited for a particular growing condition. Therefore, the present study combines different phenotyping approaches (aboveground and belowground) to identify the ideotypic characteristics associated with a better genotypic performance in durum wheat under Mediterranean growing conditions in Spain, that vary in water availability and temperature. This range of conditions was achieved through winter planting under rainfed conditions and support irrigation and a late planting under support irrigation, and evaluating these conditions during two consecutive years.

## 2. Materials and methods

### 2.1. Plant material, field experiments and growth conditions

Field trials were located at the experimental station of Colmenar de Oreja-Aranjuez, Madrid (40°04 N. 3°31 W. 590 m a.s.l.), which belongs to the Spanish “Instituto Nacional de Investigación y Tecnología Agraria y Alimentaria” (INIA), and were undertaken during the 2017–2018 and 2018–2019 crop seasons. Trials were established in a complete block design with three replicates. Each plot consisted of seven rows planted 20 cm apart and a seed rate of 250 seeds  $\text{m}^{-2}$ , representing an area of  $7 \times 1.5 \text{ m}^2$ . For each of the two crop seasons, a normal (winter) planting under either rainfed conditions or support irrigation, and a late planting under support irrigation, were assessed. Hereafter, trials will be referred to as INP for irrigated normal planting, ILP for irrigated late planting, and RNP for rainfed normal planting.

In each trial, a set of 24 post green revolution commercial durum



wheat (*Triticum turgidum* L. subsp. *durum* (Desf) Husn.) cultivars were grown, from which six cultivars were selected with contrasting agronomic performance (i.e. high versus low yield). Selection of these cultivars was according to yield data from the previous crop season, together with the two crop seasons included in this study, which were evaluated at the INIA station stated above, as well as at a second INIA station located in Coria del Rio (Seville) under irrigated normal planting conditions (Data in brief Table 1). Information about the provenance of the six selected genotypes is presented in (Table 1), together with their comparative agronomic performance (grain yield) across twelve distinct environments, understood as the specific combination of crop season, growing condition and location. Grain yield in these environments ranged between slightly more than one Mg ha<sup>-1</sup> to seven Mg ha<sup>-1</sup>. Details about these twelve environments are included in the legend of Fig. 1, and their average grain yield is presented decreasingly in alphabetical order within the abscises of the same figure.

During the first season (2017–2018), INP and RNP trials were sown on November 28th (normal planting), and the ILP trial on February 26th (late planting). The normal planting season was characterized by an average temperature of 10.8 °C, and an accumulated precipitation of 326 mm for a total duration from planting to physiological maturity of 28 weeks. In contrast, the late planting season was shortened by about 13 weeks, recording an average temperature of 15.4 °C and accumulated rainfall of 228 mm. Fertilizers and phytosanitary treatments were supplied in all trials as recommended (Data in brief Table 2). Regarding the irrigation calendar, sprinklers were used on the INP trial with a total of 140 mm of water partitioned across three dates (60 mm on April 25th, 70 mm on May 7th and 10 mm on May 17th), and on the ILP trial with 220 mm of water was partitioned across four dates (60 mm on April 25th, 70 mm on May 7th, 60 mm on May 17th and 30 mm on June 19th) (Fig. 2A). The second crop season (2018–2019) was drier and relatively warmer compared to the previous one. Winter planting, for both the INP and RNP trials, took place on November 29th, 2018. The normal planting season recorded an average temperature of 11.4 °C and an accumulated precipitation of 110 mm, with the total duration from planting to physiological maturity being 26 weeks. In contrast, the late planting shortened the crop duration by 13 weeks, had an average temperature of 16.7 °C, and an accumulated precipitation of only 78 mm. Similar to the previous season, fertilizers and phytosanitary treatments were supplied as recommended (Data in brief Table 2). For irrigation, sprinklers were used for periodic watering of the INP trial (60 mm on February 7th and February 28th then 80 mm on March 22nd, April 1st, April 16th, May 9th and May 16th), totalling 520 mm; and on the ILP trial with 60 mm on February 28th, 30 mm on March 10th, 60 mm on March 22nd, April 1st and April 16th, 80 mm on May 9th, May 16th and May 24th, 90 mm on June 6th, and another 80 mm on June 17th, totalling 680 mm (Fig. 2B). As detailed below, different measurements were performed at anthesis, whereas samplings for further analyses were taken at anthesis and physiological maturity. For both seasons, trials were machine harvested during the first half of July.

### 2.2. Leaf pigments

The content of different leaf pigments per area basis was assessed at anthesis using a portable leaf-clip sensor (Dualox, Force-A, Orsay,

**Table 1**

List of the six durum wheat varieties compared for yield performance during the study, with year of release, country of origin and available information on provenance and/or pedigree.

Variety	Selection	Year of release	Country	Pedigree/Provenance
Vitron	High yield	1987	France	TURCHIA-77/3/JORI-69(SIB)/(SIB)ANHINGA/(SIB)FLAMINGO
Claudio	High yield	1999	Italy	(Sel. Cimmyt × Durango) × (IS193B × Grazia)
Core	High yield	2009	Spain	Eurogen, PROSEME seeds
Pedroso	Low yield	1992	Spain	Battle seeds
Solea	Low yield	2005	Spain	Monsanto Agriculture Spain.
Olivadur	Low yield	2013	Spain	RAGT 2 N SAS seeds

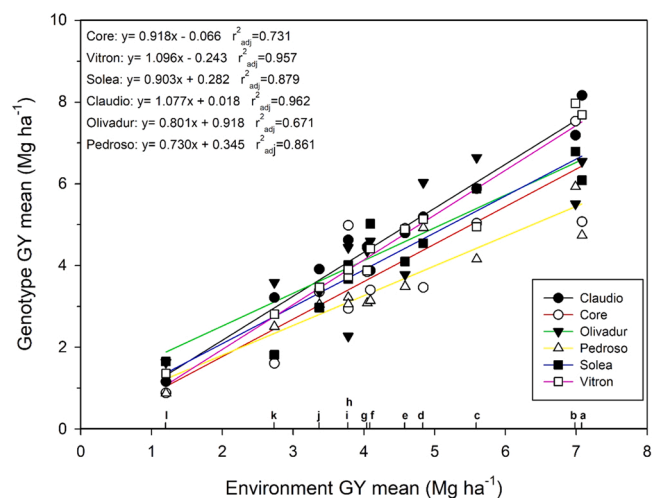


**Fig. 1.** Linear regressions of the relationship between the genotypic mean of grain yield (GY) of the six selected durum wheat genotypes in twelve environments (each one being a specific combination of year, site and growing conditions) and the mean grain yield across the whole set of genotypes tested in each environment. Letters in the horizontal axis of the figure refer to the values of the environmental means of the 24 durum wheat genotypes: a, support irrigation and normal planting in Colmenar de Oreja (Madrid) during the 2017–2018 crop season; b, rainfed and normal planting in Coria del Rio (Sevilla) during 2016–2017; c, rainfed and normal planting in Coria del Rio during 2017–2018; d, support irrigation and normal planting in Colmenar de Oreja during 2016–2017; e, support irrigation and normal planting in Colmenar de Oreja during 2018–2019; f, support irrigation and late planting in Colmenar de Oreja during 2018–2019; g, rainfed and normal planting in Coria del Rio during 2018–2019; h, support irrigation and late planting in Colmenar de Oreja during 2016–2017; i, support irrigation and late planting in Colmenar de Oreja during 2017–2018; j, rainfed and normal planting in Colmenar de Oreja during 2017–2018; k, rainfed and normal planting in Colmenar de Oreja during 2016–2017; l, rainfed and normal planting in Colmenar de Oreja during 2018–2019. Even when annual variation in rainfall and evapotranspirative demand significantly affected the pattern, the highest yields were recorded in the support irrigation and normal planting of Colmenar de Oreja, together with that of Coria del Rio, which in spite to be theoretically a rainfed site it gets water through the water table of Guadalquivir river, while the lowest yields were recorded in the rainfed normal planting of Colmenar de Oreja.

France), which operates with a red reference beam at 650 nm and a UV light at 375 nm (Cerovic et al., 2012). This sensor produces relative measures of chlorophyll (a + b), flavonoid and anthocyanin contents, and calculates the nitrogen balance index (NBI), which is the ratio of chlorophyll/flavonoids related to the nitrogen and carbon allocation. It is a nitrogen plant status indicator that is directly correlated with nitrogen mass content and therefore to the availability of N, and it is less sensitive to the variations in leaf age and leaf thickness than the chlorophylls (Cerovic et al., 2012). For each plot, measurements were carried out on the adaxial side of flag leaves of five random plants, selected from the central rows of each plot.

**Table 2**  
Effect of water supply, planting date, and genotype on grain yield (GY), harvest index (HI), thousand grain weight (TGW), number of grains per ear (GN ear<sup>-1</sup>), ear density (ears m<sup>-2</sup>), days to heading (DTH), total grain nitrogen yield (GNY), plant height (PH) and the normalized difference vegetation index (NDVI) at anthesis in the six wheat genotypes during two successive crop seasons (2017–2018) and (2018–2019).

		Agronomic traits									
		GY (Mg ha <sup>-1</sup> )	DTH (days)	HI	TGW (g)	GN ear <sup>-1</sup>	Ear density (ears m <sup>-2</sup> )	GNY (Mg ha <sup>-1</sup> )	PH (cm)	NDVI	
<b>2017–2018</b>	Irrigated (INP)	6.86 <sup>a</sup> ± 0.29	158.8 <sup>b</sup> ± 0.7	37.42 <sup>a</sup> ± 1.00	51.59 <sup>a</sup> ± 1.32	33.79 <sup>a</sup> ± 1.51	367.5 <sup>a</sup> ± 18.3	0.171 <sup>a</sup> ± 0.007	107.3 <sup>a</sup> ± 1.8	0.79 <sup>a</sup> ± 0.01	
	Late (ILP)	3.65 <sup>b</sup> ± 0.20	80.8 <sup>c</sup> ± 0.4	34.94 <sup>ab</sup> ± 1.14	37.81 <sup>c</sup> ± 0.98	25.35 <sup>c</sup> ± 1.00	348.5 <sup>b</sup> ± 16.3	0.102 <sup>b</sup> ± 0.005	90.8 <sup>b</sup> ± 1.6	0.77 <sup>a</sup> ± 0.01	
	Rainfed (RNP)	3.37 <sup>b</sup> ± 0.13	160.0 <sup>a</sup> ± 0.5	33.28 <sup>b</sup> ± 0.80	41.00 <sup>b</sup> ± 1.07	30.56 <sup>b</sup> ± 1.29	251.2 <sup>b</sup> ± 12.9	0.097 <sup>b</sup> ± 0.003	86.8 <sup>c</sup> ± 1.4	0.66 <sup>b</sup> ± 0.01	
	<b>ANOVA</b>										
	Environment	<0.001	<0.001	<0.010	<0.001	<0.001	<0.001	<0.001	<0.001	<0.001	
	Genotypes	<0.001	<0.001	<0.010	<0.001	<0.001	<0.001	<0.001	<0.001	<0.001	
	Interaction	ns	<0.001	<0.050	ns	<0.001	<0.001	<0.050	<0.001	ns	
<b>2018–2019</b>	Irrigated (INP)	4.33 <sup>a</sup> ± 0.17	–	29.09 <sup>b</sup> ± 1.03	41.17 <sup>b</sup> ± 1.24	29.66 <sup>a</sup> ± 1.62	337.5 <sup>a</sup> ± 19.4	0.110 <sup>a</sup> ± 0.004	108.7 <sup>a</sup> ± 1.4	0.76 <sup>a</sup> ± 0.01	
	Late (ILP)	4.08 <sup>a</sup> ± 0.19	–	36.17 <sup>a</sup> ± 1.45	50.39 <sup>a</sup> ± 0.92	32.39 <sup>a</sup> ± 2.10	235.2 <sup>b</sup> ± 9.7	0.097 <sup>b</sup> ± 0.004	92.8 <sup>b</sup> ± 1.2	0.74 <sup>a</sup> ± 0.01	
	Rainfed (RNP)	1.26 <sup>b</sup> ± 0.09	–	24.42 <sup>c</sup> ± 1.70	48.98 <sup>a</sup> ± 0.94	12.74 <sup>b</sup> ± 1.21	194.0 <sup>c</sup> ± 10.1	0.037 <sup>c</sup> ± 0.003	78.5 <sup>c</sup> ± 1.3	0.45 <sup>b</sup> ± 0.01	
	<b>ANOVA</b>										
	Environment	<0.001	–	<0.001	<0.001	<0.001	<0.001	<0.001	<0.001	<0.001	
	Genotypes	<0.001	–	<0.001	<0.001	<0.001	<0.050	<0.001	ns	ns	
	Interaction	<0.010	–	ns	<0.010	ns	ns	<0.010	ns	ns	

Values are means ± standard error of six genotypes with three replicates. Levels of significance for the ANOVA: P < 0.05, P < 0.01 and P < 0.001. Within each treatment, means exhibiting different letters a, b and c, are significantly different (P < 0.05) according the post-hoc test (Tukey-b) on independent samples.

### 2.3. Canopy temperature

Canopy temperature (CT) was assessed using a portable infrared (IR) thermometer (PhotoTemp™ MXSTM TD Raytek®, California; USA). The IR sensor was placed at a distance of 80 cm from the canopy, pointing the laser beam towards plant leaves with the sun towards the rear (Gracia-Romero et al., 2019).

### 2.4. Normalized difference vegetation index

The pattern of crop growth was estimated in real-time through a multispectral agronomic index known as the normalized difference vegetation index (NDVI). This index, based on the contrasting reflectance of the canopy within the visible and near infrared regions of the spectrum, is used to assess agronomic traits related to the density of green in the canopy, such as crop emergence/vigour, total biomass or the level of senescence/stay green during the last part of the crop cycle. NDVI measurements were performed using a GreenSeeker sensor (Trimble, Sunnyvale, CA, USA). This portable spectroradiometer operates through an active optical sensor in the red (660 ± 10 nm) and near infrared (NIR, 780 ± 15 nm) wavelengths (Crain et al., 2012). NDVI values were obtained by skimming the active sensor perpendicularly across the canopy of each selected plot at a constant height of 60 cm (Gracia-Romero et al., 2019). The acquired values are the average NDVI across all plants, defined as:

$$NDVI = (RNIR - Rred) / (RNIR + Rred) \tag{1}$$

### 2.5. Root image analysis

Five random plants were dug manually from the first 15 cm of soil of each selected plot, and the roots were washed carefully using a hose, then digitized in situ using a Sony ILCE-QX1 camera (Sony Europe Limited, Brooklands; United Kingdom). The digital camera has a 20.1 megapixel resolution, is equipped with a 23.2 mm × 15.4 mm sensor (type CMOS Exmor HD) and uses a 16 mm focal lens, and an exposure time of 1/60 s. The RGB images were captured zenithally at 60 cm above the roots alongside a scale reference, then saved in Tiff format for later analysis. Root angle (RA) was measured directly using a geometric protractor. Root RGB images were further analyzed using GiaRoots (General Image Analysis of Roots, Georgia Tech Research Corporation and Duke University; USA), which is an open-source software for the automated analysis of root architecture (Galkovskiy et al., 2012). Image processing was carried out using the adaptive image thresholding processing option, where around 200 images were computed per trial. The measured traits and the corresponding definition have been detailed previously in Galkovskiy et al. (2012). Briefly, GiaRoot detects pixels of the thresholded root image to estimate different root traits including: (i) crown root related parameters such as average root width (Width), number of connected components (CComp), and the maximum (MaxR) and median (MedR) number of roots; (ii) root system dimensions such as root network depth (Ndepth), root network length (Nlen), and root network width (Nwidth); (iii) root density through network area (NwA), network surface area (Nsurf), and network volume (Nvol); and (iv) root angle via network convex area (ConvA). In addition, relative traits presented as ratios were determined, such as: the ratio of network length to the network volume (specific root length (SRL)); the ratio of the maximum root number to the median root number (Network bushiness (Bush)); the total network area divided by the network convex area (Network solidity); the lower 2/3 of the root network depth (length distribution (Ldist)); and the ratio of the network width to the network depth (network width to depth ratio (NWDR)).

### 2.6. Agronomic traits

Days to heading (DTH) were determined for the first crop season

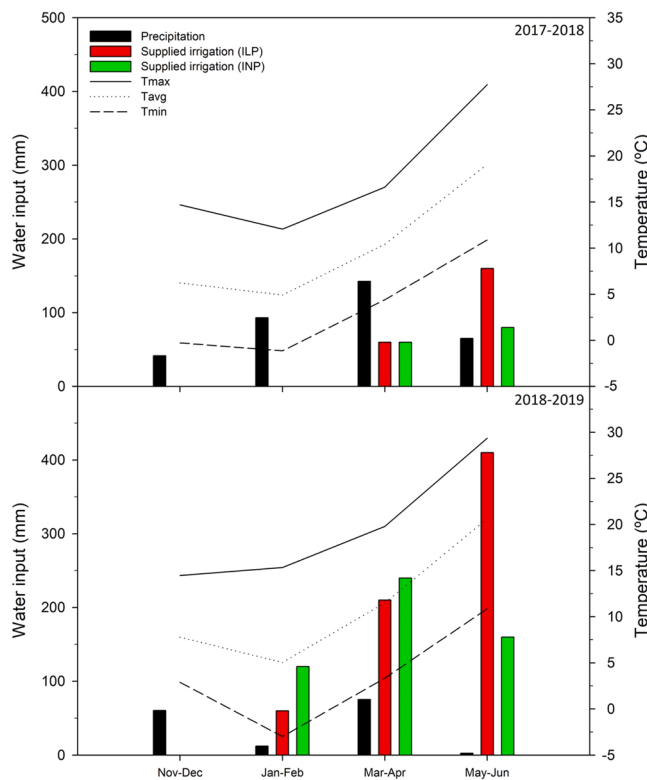


Fig. 2. Bimonthly accumulated precipitation, irrigation applied and average temperature recorded during the 2017–2018 and 2018–2019 seasons.

(2017–2018) only, for each plot, and when approximately 50% of ears had emerged. Plant height (PH) was determined at anthesis; a ruler was placed zenithally in the central rows of each selected plot, and values were taken by observing the whole canopy and averaging the distance from the ground to the overall tip of the ears, excluding the awns. At maturity, ear density (ears  $m^{-2}$ ) was determined by counting the ear density in a 1 m length of a central row. Grain number per ear (GN) and thousand grain weight (TGW) were assessed using a subset of ten representative plants from the central rows of each plot. Harvest index (HI), which is the ratio of grain weight to total aboveground biomass, was calculated from the same sampled plants.

### 2.7. Stable carbon and nitrogen isotope composition and total nitrogen content in dry matter

From each selected plot, samples of flag leaves taken at anthesis of the second crop season and mature grains collected at harvest from the two crop seasons were dried at 60 °C for a minimum of 48 h and pulverized to a fine powder, from which 1 mg was enclosed in tin capsules, and analyzed using an elemental analyser (Flash 1112 EA; ThermoFinnigan, Schwerte, Germany) coupled with an isotope ratio mass spectrometer (Delta C IRMS, ThermoFinnigan), operating in continuous flow mode at the Scientific and Technical facilities of the University of Barcelona. Different secondary standards were used for carbon (IAEA-CH7, IAEA-CH6 and IAEA-600, and USGS 40) and nitrogen (IAEA-600, N1, N2, NO3, urea and acetanilide) isotope analyses. Nitrogen content in leaves and grains were expressed in percentages (%), and the corresponding isotope compositions in parts per thousand (‰), with an analytical precision (standard deviation) of 0.1‰ for  $\delta^{13}C$  and 0.3‰ for  $\delta^{15}N$  and following the Eq. (2):

$$\delta^{13}C/\delta^{15}N(\text{‰}) = \left[ \left( R_{\text{sample}}/R_{\text{standard}} \right) - 1 \right] \times 1000 \quad (2)$$

where  $R_{\text{standard}}$  is the molar abundance ratio of the secondary standard

calibrated against the primary standard Pee Dee Belemnite in the case of carbon ( $\delta^{13}C$ ) and  $N_2$  from air in the case of nitrogen ( $\delta^{15}N$ ) (Farquhar et al., 1989).

### 2.8. Stable oxygen isotope composition of stem water

At anthesis, samples of the stem base (approximately 6–7 cm length) were harvested from five random plants (main stems) of each selected plot, sealed immediately in analytical tubes and frozen at  $-80$  °C until water distillation could be undertaken. Water analysis was performed at the Department of Crop and Forest Sciences, Universitat de Lleida (Spain), using a cryogenic vacuum distillation line (Dawson and Ehleringer, 1993). Sample tubes were placed in a heated silicone oil bath (120 °C), and connected with Ultra-Torr™ unions (Swagelok Company, Solon, OH, USA) to a vacuum system ( $\sim 10$ – $2$  mbar), in series, with U-shaped collector tubes cooled with liquid  $N_2$ . Ninety minutes after commencing extraction, the extracted xylem water was transferred into 2 ml vials and stored at 4 °C until analysis. Oxygen isotope composition ( $\delta^{18}O$ ) of water was determined by isotope-ratio infrared spectroscopy using a Picarro L2120-I isotopic water analyser coupled to an A0211 high-precision vaporizer (Picarro Inc., Sunnyvale, CA, USA). Analytical precision for  $\delta^{18}O$  was 0.10‰, and the occurrence of contaminants was tested using Picarro's ChemCorrect post-processing software and corrected, when necessary, following Martín-Gómez et al. (2015).

### 2.9. Statistical analysis

Analysis of variance (ANOVA) was performed using SPSS 25 (IBM SPSS Statistics 25, Inc., Chicago, IL; USA), to test the effects of year (crop season), trial, genotype and their interaction on all traits evaluated, and followed with Tukey-b tests to reveal differences within trials. A bivariate Pearson correlation was executed using the same statistical package to reveal relationships between grain yield and the assessed parameters. Principal component analyses were carried out with the open-source software, RStudio 1.2.5 (R Foundation for Statistical Computing, Vienna, Austria), to analyze all traits in a reduced bi-dimensional platform. Graphs were created using Sigma-plot 10.0 (Systat Software Inc, California; USA).

## 3. Results

### 3.1. Effects of planting date, water supply and season on grain yield, agronomic components, biomass and phenology

During the first season (2017–2018), GY was halved under irrigated late planting (ILP) and rainfed normal planting (RNP) compared to irrigated normal planting (INP). Under warmer conditions of ILP, harvest index (HI), thousand grain weight (TGW), grain number per ear (GN), ear density, total grain nitrogen yield (GNY) and plant height (PH) were decreased compared to the INP trial, with a significantly shortened days to heading (DTH) interval (Table 2). Similarly, under water-limited conditions (RNP), HI, TGW, GN, ear density, GNY and PH were lower compared to INP. In addition, NDVI was smaller under RNP than INP and even ILP. Genotypes exhibited significant differences in GY and all the other measured parameters included in the table (Table 2). Trial by genotype interaction was significant for all the traits except for GY, TGW and NDVI.

During the second season (2018–2019), GY and ear density in ILP were similar, but HI and TGW were higher, and ear density, GNY and PH were lower compared to INP. The rest of the traits were not significantly different. In contrast, under RNP, GY decreased threefold compared to the irrigated trials (INP, ILP). HI, GN, ear density, GNY, PH and NDVI were also lower in RNP than in the INP and ILP trials, while TGW increased in RNP compared to the other two trials. Genotypic differences were significant for GY, HI, TGW, GN, ear density and GNY (Table 2).



**Table 3**

Effect of planting date, water supply, and genotypes on nitrogen content (N) and stable isotope composition of carbon ( $\delta^{13}\text{C}$ ) and nitrogen ( $\delta^{15}\text{N}$ ) of the flag leaf and the mature grains, the oxygen isotope composition ( $\delta^{18}\text{O}$ ) of water in the shoot base, and the canopy temperature (CT) assessed at anthesis, in six wheat genotypes during two successive crop seasons (2017–2018) and (2018–2019).

		Stable isotope composition + Canopy temperature							
		$\delta^{18}\text{O}_{\text{shoot water}}$ (‰)	$\text{N}_{\text{leaf}}$ (%)	$\delta^{15}\text{N}_{\text{leaf}}$ (‰)	$\delta^{13}\text{C}_{\text{leaf}}$ (‰)	$\text{N}_{\text{grain}}$ (%)	$\delta^{15}\text{N}_{\text{grain}}$ (‰)	$\delta^{13}\text{C}_{\text{grain}}$ (‰)	$\text{CT}_{\text{anthesis}}$ (°C)
<b>2017–2018</b>	Irrigated (INP)	-4.25 <sup>b</sup> ± 0.07	–	–	–	2.51 <sup>b</sup> ± 0.06	3.26 <sup>a</sup> ± 0.15	-26.26 <sup>c</sup> ± 0.10	29.70 <sup>b</sup> ± 0.36
	Late (ILP)	-4.19 <sup>b</sup> ± 0.05	–	–	–	2.82 <sup>a</sup> ± 0.06	0.93 <sup>b</sup> ± 0.26	-25.69 <sup>b</sup> ± 0.11	–
	Rainfed (RNP)	-3.81 <sup>a</sup> ± 0.08	–	–	–	2.87 <sup>a</sup> ± 0.03	1.26 <sup>b</sup> ± 0.14	-24.45 <sup>a</sup> ± 0.07	33.89 <sup>a</sup> ± 0.39
	<b>ANOVA</b>								
	Environment	<0.001	–	–	–	<0.001	<0.001	<0.001	<0.001
	Genotypes	<0.001	–	–	–	<0.050	<0.050	<0.010	ns
	Interaction	<0.001	–	–	–	ns	ns	ns	ns
<b>2018–2019</b>	Irrigated (INP)	-5.11 <sup>c</sup> ± 0.06	3.90 <sup>a</sup> ± 0.15	3.10 <sup>a</sup> ± 0.16	-28.26 <sup>c</sup> ± 0.23	2.56 <sup>b</sup> ± 0.07	2.99 <sup>a</sup> ± 0.08	-25.81 <sup>b</sup> ± 0.07	28.83 <sup>b</sup> ± 0.41
	Late (ILP)	-4.55 <sup>b</sup> ± 0.09	4.09 <sup>a</sup> ± 0.06	2.45 <sup>b</sup> ± 0.18	-27.45 <sup>b</sup> ± 0.11	2.40 <sup>b</sup> ± 0.04	2.49 <sup>a</sup> ± 0.14	-25.98 <sup>b</sup> ± 0.08	25.36 <sup>c</sup> ± 0.27
	Rainfed (RNP)	-3.52 <sup>a</sup> ± 0.13	3.86 <sup>a</sup> ± 0.06	-0.09 <sup>c</sup> ± 0.16	-25.40 <sup>a</sup> ± 0.12	2.97 <sup>a</sup> ± 0.05	-0.05 <sup>b</sup> ± 0.12	-23.01 <sup>a</sup> ± 0.08	35.38 <sup>a</sup> ± 0.27
	<b>ANOVA</b>								
	Environment	<0.001	ns	<0.001	<0.001	<0.001	<0.001	<0.001	<0.001
	Genotypes	ns	ns	ns	ns	ns	ns	ns	ns
	Interaction	ns	<0.050	ns	ns	ns	ns	ns	ns

Values are means ± standard error of six genotypes with three replicates. Levels of significance for the ANOVA:  $P < 0.05$ ,  $P < 0.01$  and  $P < 0.001$ . Within each treatment, means exhibiting different letters a, b and c, are significantly different ( $P < 0.05$ ) by the post-hoc test (Tukey-b) on independent samples.

The genotype by trial interaction was only significant for GY, TGW and GNY.

Considering the trial, crop season and genotype effects, the three-way ANOVA revealed that all the traits (GY, HI, TGW, GN, ear density, GNY, PH and NDVI) included in Table 3 showed significant effects for the three factors (Data in brief Table 3). Interactions were also significant for most of the traits, except PH and NDVI. Moreover, values for all the traits, except for PH and NDVI, were higher in the first season than the second season (Table 2).

### 3.2. Effects of planting date, water supply and season on stable isotope compositions, nitrogen content and canopy temperature

During the first season (2017–2018), grain nitrogen content ( $\text{N}_{\text{grain}}$ ) and carbon isotope composition ( $\delta^{13}\text{C}_{\text{grain}}$ ) were higher, and grain nitrogen isotope composition ( $\delta^{15}\text{N}_{\text{grain}}$ ) was lower in ILP compared with INP. However, the oxygen isotope composition of the shoot water ( $\delta^{18}\text{O}_{\text{shoot water}}$ ) exhibited similar values in ILP to INP. Under RNP, canopy temperature (CT),  $\delta^{13}\text{C}_{\text{grain}}$ ,  $\delta^{18}\text{O}_{\text{shoot water}}$  and  $\text{N}_{\text{grain}}$  were higher, and  $\delta^{15}\text{N}_{\text{grain}}$  lower, compared to INP. Genotype differences were shown in all measured traits except for CT, where values were not

available for the ILP trial (Table 3). The genotype by trial interaction was only significant for  $\delta^{18}\text{O}_{\text{shoot water}}$ .

In the second season (2018–2019), CT and the nitrogen isotope composition of the leaf ( $\delta^{15}\text{N}_{\text{leaf}}$ ) were significantly lower in ILP than INP, while the  $\delta^{18}\text{O}_{\text{shoot water}}$  and the carbon isotope composition of the leaf ( $\delta^{13}\text{C}_{\text{leaf}}$ ) were significantly higher in ILP, compared with INP. In contrast, under RNP conditions, CT,  $\text{N}_{\text{grain}}$ ,  $\delta^{18}\text{O}_{\text{shoot water}}$ ,  $\delta^{13}\text{C}_{\text{leaf}}$  and  $\delta^{13}\text{C}_{\text{grain}}$  were greater, and the  $\delta^{15}\text{N}_{\text{leaf}}$  and  $\delta^{15}\text{N}_{\text{grain}}$  lower than in the INP trial. Genotypes were not significantly different across all measured traits (Table 3). The genotype by trial interaction was only significant for  $\delta^{15}\text{N}_{\text{leaf}}$ .

The three-way ANOVA (season, trial and genotype) showed a significant trial effect for all the traits included in Table 3 (Data in brief Table 4). A genotype effect was also significant for all the traits, except for CT, while season had a significant effect for all the traits except CT and the  $\delta^{15}\text{N}_{\text{grain}}$  (Data in brief Table 4). The interaction between season and trial was significant for all the traits, while almost all the other interactions were absent. Except for the ILP trials, the  $\delta^{13}\text{C}_{\text{grain}}$  was lower (i.e. more negative) in the first season than the second season. In the case of  $\delta^{18}\text{O}$ , and except for RNP, values were higher (less negative) in the first season.

**Table 4**

Effect of planting date, water supply and genotype on leaf chlorophyll, flavonoid and anthocyanin, and the nitrogen balance index (NBI) in six wheat genotypes during two successive crop seasons (2017–2018) and (2018–2019).

		Leaf pigments (arbitrary units)			
		Chlorophyll	Flavonoid	Anthocyanin	NBI
<b>2017–2018</b>	Irrigated (INP)	49.90 <sup>b</sup> ± 0.81	1.32 <sup>b</sup> ± 0.02	0.135 <sup>b</sup> ± 0.002	38.28 <sup>a</sup> ± 0.73
	Late (ILP)	51.82 <sup>a</sup> ± 0.51	1.34 <sup>ab</sup> ± 0.02	0.125 <sup>c</sup> ± 0.001	38.94 <sup>a</sup> ± 0.80
	Rainfed (RNP)	45.94 <sup>c</sup> ± 0.81	1.39 <sup>a</sup> ± 0.02	0.149 <sup>a</sup> ± 0.004	33.49 <sup>b</sup> ± 0.76
	<b>ANOVA</b>				
	Trials	<0.001	<0.050	<0.001	<0.010
	Genotypes	<0.001	<0.001	ns	<0.010
	Interaction	ns	ns	ns	ns
<b>2018–2019</b>	Irrigated (INP)	41.26 <sup>a</sup> ± 0.66	1.500 <sup>b</sup> ± 0.023	0.035 <sup>a</sup> ± 0.002	27.76 <sup>a</sup> ± 0.56
	Late (ILP)	43.24 <sup>a</sup> ± 0.78	1.481 <sup>b</sup> ± 0.034	0.037 <sup>a</sup> ± 0.004	29.63 <sup>a</sup> ± 0.94
	Rainfed (RNP)	45.43 <sup>a</sup> ± 1.03	1.662 <sup>a</sup> ± 0.015	0.031 <sup>a</sup> ± 0.003	27.21 <sup>a</sup> ± 0.59
	<b>ANOVA</b>				
	Trials	ns	<0.001	ns	<0.050
	Genotypes	ns	<0.001	ns	<0.050
	Interaction	ns	<0.010	ns	ns

Values are means ± standard error of six genotypes with three replicates. Levels of significance for the ANOVA:  $P < 0.05$ ,  $P < 0.01$  and  $P < 0.001$ . Within each treatment, means exhibiting different letters a, b and c, are significantly different ( $P < 0.05$ ) according to the post-hoc test (Tukey-b) on independent samples.

### 3.3. Effects of planting date, water supply and season on leaf pigments

The effect of trial was significant during the first season (2017–2018) for all leaf pigments, whereas the genotypic effect was present for chlorophylls, flavonoids and NBI. The chlorophyll and flavonoid contents were higher in ILP than in INP, while the anthocyanin content was lower in ILP than in INP, and NBI was not significantly different. However, the flavonoid and anthocyanin values under RNP conditions were higher, and chlorophylls and NBI lower than in INP (Table 4). There was no genotype by trial interaction for any of the traits included in the table.

In the second season (2018–2019), however, significant effects of trials and genotypes were shown for flavonoids and NBI alone. In fact, no significant differences were shown between the ILP and INP trials for the measured traits, while under RNP, only the flavonoid content was higher than in the rest of trials (Table 4). No interaction between genotype and trial existed.

The three-way ANOVA (trial, genotype and season) for the pigment traits included in Table 4 exhibited significant year effects for all the traits (Data in brief Table 4). Trial and genotype effects were also significant for all the traits. Interactions were only significant for season by trial.

### 3.4. Effects of planting date, water supply and season on root traits

To investigate root characteristics, the genotypic and trial effect and their interaction were analyzed in traits derived from the RGB images from the shovelomics study (Table 5). In the first season (2017–2018), trial and genotype effects were only significant for the root network surface (Nsurf), root network volume (Nvol) and specific root length (SRL). In addition, the effect of trials was also observed for root width, root connected components (CComp), maximum roots (MaxR) and root network length (Nlen), while a genotypic effect was shown for root network area (NwA). Root CComp, MaxR, Nlen, NwA and Nsurf traits were lower in the ILP than in the INP trial; in contrast, root width, Nvol and SRL did not exhibit any differences between ILP and INP. Root width, CComp, Nlen, NwA and Nsurf were lower under RNP than in INP conditions; oppositely, MaxR and SRL were higher in the RNP than in the INP trial (Table 6). There was no interaction between trial and genotypes for any of the traits.

During the second season (2018–2019), the effect of trial was significant across all root traits, except for root angle (RA) and the NWDR ratio, while genotypic effects were significant for width, CComp, MedR, Ndepth, SRL and NWDR. The interaction exhibited significant differences only for CComp, Ndepth, ConvA and SRL. CComp, Ndepth, NwA, Nsurf, Nvol, Network solidity and Ldist were lower, and MaxR, MedR, Nwidth, ConvA, Bush and SRL were higher in the ILP than in the INP trial. However, all traits were lower in RNP than in the INP trial, except for CComp, Bush, Network solidity, SRL and Ldist, which showed no differences (Table 5).

The three-way ANOVA (trial, genotype and season) for root traits exhibited significant year and trial effects for almost all the traits (Data in brief Table 5), while genotype effects were significant for less than half of the traits (width, CComp, Ndepth, Nvol, SRL and NWDR). The interaction between year and trial was significant for most traits, except for MedR, NwA, Nsurf, Nvol and NWDR. However, the two-way interaction between year and genotype was significant for Nlen, NwA, Nsurf, Nvol, ConvA and Ldist only, and between trial and genotype was significant for Ndepth and NWDR only, whereas the three-way interaction (year, trial and genotype) was only significant for CComp, Ndepth and RA.

### 3.5. Relationships between grain yield, and agronomic, physiological and root traits

Relationships between GY and yield components, stable isotopes, CT and leaf pigments in the three growing conditions combined and separated, are presented in Table 6. Most traits exhibited significant correlations against GY when combining all trials within each crop season.

During the first season, ear density, GNY and PH were positively

correlated with GY within each growing condition (INP, ILP and RNP). Under irrigated conditions (INP and ILP), higher HI, TGW and lower  $\delta^{13}\text{C}_{\text{grain}}$  and DTH were correlated with an increased GY. Higher  $\delta^{18}\text{O}_{\text{shoot water}}$  values correlated positively with GY under INP. The NDVI and NBI correlated negatively and flavonoids positively with GY under ILP, whereas under RNP the NDVI correlated positively with GY.

During the second crop season, HI and GNY correlated positively with GY within each of the three growing conditions. In addition, TGW, ear density, PH,  $\delta^{18}\text{O}_{\text{shoot water}}$  and flavonoid correlated positively, and  $\text{N}_{\text{grain}}$  negatively with GY under INP. GN correlated positively, and nitrogen content ( $\text{N}_{\text{leaf}}$  and  $\text{N}_{\text{grain}}$ ) negatively with GY under ILP. However, under RNP the GN, PH, and NDVI correlated positively and the carbon isotope compositions ( $\delta^{13}\text{C}_{\text{leaf}}$  and  $\delta^{13}\text{C}_{\text{grain}}$ ) negatively with GY.

The correlations of root traits with GY were studied for each crop season and the three different growing conditions (Data in brief Table 6). During the first season (2017–2018), positive correlations were exhibited only for a few traits (CComp, Nvol and network solidity) and when combining all growing conditions. Therefore, no correlations were found within any of the growing conditions. In the second season (2018–2019), most root traits (except MedR, Nwidth, RA and NWDR) were correlated significantly with GY when combining all three growing conditions. Within each growing condition, no correlations existed, except for a positive correlation of CComp with GY in the INP trial, and a negative correlation of Ndepth with GY under ILP (Data in brief Table 6).

Principal Component Analysis (PCA) was performed for each growing condition and season individually (Fig. 3). For the six different environments tested (the three growing conditions and the two seasons), GY was placed opposite to  $\delta^{13}\text{C}$  and the  $\delta^{15}\text{N}$  of grains and more or less close to TGW and ear density. DTH, which was only measured in the first season, was also placed more or less opposite to GY in the three growing conditions. Except for the INP in the first season, where RA was placed opposite to GY and very close to  $\delta^{13}\text{C}$  of grains, in the other five trials it was placed rather perpendicular to GY. SLR was placed on the same side as GY in the INP and RNP trials of both seasons and in ILP of the second season. Regarding the ILP of the first season, SLR was placed opposite to GY but the eigenvector for SLR was very short. The  $\delta^{18}\text{O}_{\text{shoot water}}$  was placed close to GY in the INP trials of both seasons, whereas in the ILP trial it was placed clearly opposite to the GY in the first season and rather perpendicular to the GY in the second season. In the case of the RNP trial,  $\delta^{18}\text{O}_{\text{shoot water}}$  was placed rather perpendicular to GY in the first season and opposite to GY in the second season. PH was placed close to GY in the four normal planting trials (INP and RNP of both seasons), but it was perpendicular to the two late planting trials. Other traits such as flavonoids, or the  $\delta^{15}\text{N}$  of the grains were placed either on the same side as, opposite to or perpendicular to GY, depending on the specific environmental conditions. The set of traits used in the PCA clearly separated the two categories of genotypes for the three growing conditions in the first year as well as for the INP in the second year, while for ILP and RNP in the second year, the separation was somewhat less evident.

PCA was also undertaken per agronomic condition (RNP, INP and ILP), which meant combining the two consecutive years for each agronomic condition, and only considering the traits in common measured during the two years (Data in brief Fig. 1). Under INP conditions, higher GY was related to a higher  $\delta^{18}\text{O}_{\text{shoot water}}$ , together with a higher HI and TGW and more open (i.e. higher) RA, as well as lower (more negative)  $\delta^{13}\text{C}_{\text{grains}}$ , PH and flavonoid content, whereas the other traits were less important or not associated. Under RNP conditions, GY was positively related with  $\delta^{18}\text{O}_{\text{shoot water}}$ , NBI,  $\delta^{15}\text{N}_{\text{grains}}$ , SRL and somehow HI and RA, whereas  $\delta^{18}\text{O}_{\text{shoot water}}$ ,  $\delta^{13}\text{C}_{\text{grains}}$ , CT and flavonoids, where the other traits were weakly or not related. In the case of ILP, GY was closely (and positively) associated with HI, and negatively associated with  $\delta^{13}\text{C}_{\text{grains}}$ , and to a lesser extent with  $\text{N}_{\text{grain}}$  and the biomass (NDVI) at anthesis.

**Table 5**  
Effect of crop season (2017–2018 vs 218–2019), trials (INP, ILP, RNP) and genotypes on root characteristics.

		Width (cm)	CComp	MaxR	MedR	Ndepth (cm)	Nlen (cm)	Nwidth (cm)	NwA	Nsurf (cm <sup>2</sup> )	Nvol (cm <sup>3</sup> )	ConvA (cm <sup>2</sup> )	RA <sub>protractor</sub>	Bush	Ldist	Network Solidity	NWDR	SRL (cm <sup>-2</sup> )	
2017–2018	INP	0.061 <sup>a</sup> ± 0.001	2.55 <sup>a</sup> ± 0.16	16.7 <sup>ab</sup> ± 1.0	9.5 <sup>a</sup> ± 0.8	6.1 <sup>a</sup> ± 0.3	114.3 <sup>a</sup> ± 10.3	6.22 <sup>a</sup> ± 0.37	5.77 <sup>a</sup> ± 0.55	21.78 <sup>a</sup> ± 2.09	0.40 <sup>a</sup> ± 0.04	31.37 <sup>a</sup> ± 2.62	92.28 <sup>a</sup> ± 5.34	2.00 <sup>a</sup> ± 0.11	0.88 <sup>a</sup> ± 0.09	0.18 <sup>a</sup> ± 0.01	1.08 <sup>a</sup> ± 0.07	297.1 <sup>b</sup> ± 10.4	
		0.064 <sup>a</sup> ± 0.001	1.32 <sup>b</sup> ± 0.07	13.8 <sup>b</sup> ± 0.9	7.8 <sup>a</sup> ± 0.6	5.4 <sup>a</sup> ± 0.3	82.6 <sup>b</sup> ± 6.8	5.86 <sup>a</sup> ± 0.29	4.36 <sup>ab</sup> ± 0.32	16.27 <sup>b</sup> ± 1.21	0.31 <sup>a</sup> ± 0.02	24.55 <sup>a</sup> ± 1.65	84.94 <sup>a</sup> ± 4.31	1.98 <sup>a</sup> ± 0.12	0.84 <sup>a</sup> ± 0.10	0.18 <sup>a</sup> ± 0.01	1.14 <sup>a</sup> ± 0.06	267.7 <sup>b</sup> ± 10.2	
		0.053 <sup>b</sup> ± 0.001	1.77 <sup>b</sup> ± 0.11	17.6 <sup>a</sup> ± 0.9	8.5 <sup>a</sup> ± 0.5	6.2 <sup>a</sup> ± 0.3	109.4 <sup>ab</sup> ± 9.8	6.51 <sup>a</sup> ± 0.25	4.91 <sup>b</sup> ± 0.42	18.23 <sup>ab</sup> ± 1.60	0.29 <sup>a</sup> ± 0.03	30.92 <sup>a</sup> ± 2.41	87.75 <sup>a</sup> ± 3.42	2.29 <sup>a</sup> ± 0.08	0.72 <sup>a</sup> ± 0.06	0.16 <sup>a</sup> ± 0.00	1.09 <sup>a</sup> ± 0.03	389.9 <sup>a</sup> ± 17.42	
	<b>ANOVA</b>																		
	Environment	<0.001	<0.001	<0.050	ns	ns	<0.050	ns	ns	<0.050	<0.050	ns	ns	ns	ns	ns	ns	ns	<0.001
	Genotypes	ns	ns	ns	ns	ns	ns	ns	<0.050	<0.050	<0.050	ns	ns	ns	ns	ns	ns	ns	<0.050
	Interaction	ns	ns	ns	ns	ns	ns	ns	ns	ns	ns	ns	ns	ns	ns	ns	ns	ns	ns
	2018–2019	INP	0.061 <sup>a</sup> ± 0.001	1.99 <sup>b</sup> ± 0.14	16.3 <sup>a</sup> ± 0.8	8.9 <sup>a</sup> ± 0.4	6.4 <sup>b</sup> ± 0.2	105.3 <sup>a</sup> ± 7.0	6.35 <sup>b</sup> ± 0.31	5.30 <sup>a</sup> ± 0.35	19.74 <sup>a</sup> ± 1.3	0.35 <sup>a</sup> ± 0.03	31.72 <sup>b</sup> ± 2.25	85.81 <sup>a</sup> ± 4.85	1.89 <sup>b</sup> ± 0.06	0.71 <sup>a</sup> ± 0.04	0.17 <sup>a</sup> ± 0.01	1.03 <sup>a</sup> ± 0.04	301.5 <sup>b</sup> ± 0.1
			0.046 <sup>b</sup> ± 0.001	5.95 <sup>a</sup> ± 0.37	12.8 <sup>b</sup> ± 0.5	6.1 <sup>b</sup> ± 0.3	9.0 <sup>a</sup> ± 0.3	113.8 <sup>a</sup> ± 6.9	7.96 <sup>a</sup> ± 0.35	4.48 <sup>b</sup> ± 0.26	26.42 <sup>b</sup> ± 0.97	0.23 <sup>b</sup> ± 0.01	51.22 <sup>a</sup> ± 3.73	83.69 <sup>a</sup> ± 4.74	2.30 <sup>a</sup> ± 0.10	0.13 <sup>b</sup> ± 0.01	0.09 <sup>b</sup> ± 0.00	0.93 <sup>a</sup> ± 0.04	504.8 <sup>a</sup> ± 13.7
			0.063 <sup>a</sup> ± 0.001	2.24 <sup>b</sup> ± 0.10	12.6 <sup>b</sup> ± 0.5	6.8 <sup>b</sup> ± 0.2	5.4 <sup>c</sup> ± 0.2	68.3 <sup>b</sup> ± 3.5	4.97 <sup>c</sup> ± 0.17	3.60 <sup>c</sup> ± 0.15	13.23 <sup>c</sup> ± 0.58	0.24 <sup>b</sup> ± 0.01	20.93 <sup>c</sup> ± 0.99	73.31 <sup>a</sup> ± 3.85	1.95 <sup>b</sup> ± 0.06	0.66 <sup>a</sup> ± 0.04	0.18 <sup>a</sup> ± 0.01	0.96 <sup>a</sup> ± 0.04	288.6 <sup>b</sup> ± 9.9
<b>ANOVA</b>																			
Environment		<0.001	<0.001	<0.001	<0.001	<0.001	<0.001	<0.001	<0.001	<0.001	<0.001	<0.001	ns	<0.001	<0.001	<0.001	ns	ns	<0.001
Genotypes		<0.010	<0.050	ns	<0.050	<0.050	ns	ns	ns	ns	ns	ns	ns	ns	ns	ns	ns	<0.050	<0.001
Interaction		ns	<0.001	ns	ns	<0.001	ns	ns	ns	ns	ns	<0.050	ns	ns	ns	ns	ns	ns	<0.050

Values are means ± standard error of six genotypes with 3 replicates. Levels of significance for the ANOVA: P < 0.05, P < 0.01 and P < 0.001. Within each crop season (2017–2018 vs 2018–2019), means exhibiting different letters a, b and c, are significantly different (P < 0.05) according to the Student *t*-test on independent samples. Width, average root width. CComp, number of connected components. MaxR, maximum number of roots. MedR, median number of roots. Ndepth, network depth. Nlen, network length. Nwidth, network width. NwA, network area. Nsurf, network surface area. Nvol, network volume. ConvA, convex area. Bush, bushiness. SRL, specific root length. Ldist, network length distribution. NWDR, network width to depth ratio. RA<sub>protractor</sub>, root angle measured with a protractor. INP, Irrigated normal planting. ILP, Irrigated late planting. RNP, Rainfed normal planting. For each year, and within each treatment, means exhibiting different letters are significantly different (P < 0.05) according to the post-hoc test (Tukey-b) on independent samples.

**Table 6**

Correlation coefficients of the significant linear regressions between grain yield (GY) and days to heading (DTH), harvest index (HI), thousand grain weight (TGW), ear density, grain number per ear (GN), total grain nitrogen yield (GNY), plant height (PH), the normalized difference vegetation index (NDVI) at anthesis, root angle (RA), oxygen isotope composition in shoot water ( $\delta^{18}\text{O}_{\text{shoot water}}$ ), nitrogen content in the flag leaf ( $\text{N}_{\text{leaf}}$ ) and grain ( $\text{N}_{\text{grain}}$ ), carbon and nitrogen stable isotope compositions in the flag leaf ( $\delta^{15}\text{N}_{\text{leaf}}$  and  $\delta^{13}\text{C}_{\text{leaf}}$ ) and grain ( $\delta^{15}\text{N}_{\text{grain}}$  and  $\delta^{13}\text{C}_{\text{grain}}$ ), canopy temperature (CT) at anthesis, and leaf pigments (chlorophyll, flavonoids, anthocyanins, and NBI). Assessed traits were evaluated under three growing conditions, combined (All growing conditions) and separated (INP, RNP, ILP), during two consecutive crop seasons (2017–2018 and 2018–2019) and using individual plot values.

		Crop season (2017–2018)				Crop season (2018–2019)			
		All growing conditions	INP	ILP	RNP	All growing conditions	INP	ILP	RNP
Yield components	DTH	0.354**	-0.534*	-0.475*	ns	–	–	–	–
	HI	0.543**	0.498*	0.679**	ns	0.639**	0.473*	0.754**	0.856**
	TGW	0.810**	0.519*	0.690**	ns	ns	0.686**	ns	ns
	GN	0.329*	ns	ns	ns	0.817**	ns	0.881**	0.863**
	Ear density	0.583**	0.589*	0.599**	0.544*	0.579**	0.582**	ns	ns
	GNY	0.966**	0.847**	0.923**	0.956**	0.979**	0.849**	0.948**	0.969**
	PH	0.865**	0.696**	0.533*	0.525*	0.784**	0.561*	ns	0.531*
	NDVI	0.478**	ns	-0.546*	0.491*	0.909**	ns	ns	0.691**
Nitrogen content & Stable isotope composition	$\delta^{18}\text{O}_{\text{shoot water}}$	-0.276*	0.614**	ns	ns	-0.661**	0.593*	ns	ns
	$\text{N}_{\text{leaf}}$	–	–	–	–	ns	ns	-0.510*	ns
	$\delta^{15}\text{N}_{\text{leaf}}$	–	–	–	–	0.801**	ns	ns	ns
	$\delta^{13}\text{C}_{\text{leaf}}$	–	–	–	–	-0.750**	ns	ns	-0.637**
	$\text{N}_{\text{grain}}$	-0.668**	ns	ns	ns	-0.768**	-0.516**	-0.659**	ns
	$\delta^{15}\text{N}_{\text{grain}}$	0.719**	ns	ns	ns	0.819**	ns	ns	ns
	$\delta^{13}\text{C}_{\text{grain}}$	-0.730**	-0.540*	-0.691**	ns	-0.882**	ns	ns	-0.493*
Canopy temperature	CT	-0.759**	ns	–	ns	-0.793**	ns	ns	ns
Leaf pigments	Chlorophyll	ns	ns	ns	ns	-0.355**	ns	ns	ns
	Flavonoid	ns	ns	0.512*	ns	-0.540**	0.558*	ns	ns
	Anthocyanin	ns	ns	ns	ns	ns	ns	ns	ns
	NBI	ns	ns	-0.569*	ns	ns	ns	ns	ns

INP, Irrigated Normal Planting; RNP, Rainfed Normal Planting; ILP, Irrigated Late planting. ns,  $P > 0.05$ ;

\*  $P < 0.05$

\*\*  $P < 0.001$ .

## 4. Discussion

### 4.1. Effect of growing conditions on grain yield, agronomic components and physiological traits

Grain yield is defined as the product of biomass and harvest index and is determined by the agronomic yield components of ear density, number of grains per ear and thousand grain weight (Donald and Hamblin, 1976). Depending on the severity and timing of stress during the crop cycle, all of the above agronomic traits may be affected to a greater or lesser degree (García del Moral et al., 2003; Giunta et al., 1993; Shpiler and Blum, 1990). In our study, the reduction in all agronomic traits, as in the case of rainfed versus irrigated conditions, was in agreement with these reports. Furthermore, interannual variability in environmental conditions was also evident, with the second crop season (2018–2019) being drier than the first one (2017–2018), as a consequence of much lower rainfall and higher temperatures (Fig. 2). As a result, grain yield was lower in the second (2018–2019) compared to the first season (2017–2018), particularly under rainfed conditions (RNP) but also under support irrigation (INP). Moreover, during the first season, the lower GY in the RNP compared with INP was associated with a major decrease in ear density as well as rather minor decreases in grain number per ear and TGW, which were the two agronomic yield components determined later in the crop cycle (Table 2). However, in the much drier conditions of the second season, ear density and GN in particular (which decreased by nearly 60%) were strongly affected under RNP compared with INP, while TGW was higher under RNP compared with INP, probably due to the strong decrease in sink capacity caused by the reduction in the number of grains per ear (Chairi et al., 2020; Slafer et al., 2005).

Increases in temperature also affected GY and its agronomic components negatively, through a shorter crop duration including grain

filling, accelerated leaf senescence and eventually a poorer grain set (García del Moral et al., 2003; Royo et al., 2000). In our study, late planting during the first season affected TGW and grains per ear negatively compared with the normal planting under support irrigation. However, under the drier conditions of the second season, the affected agronomic yield component was ear density, which is determined before TGW and grains per ear. Such results are in agreement with previous studies reporting the negative effect of late planting on GY and yield components in wheat grown under Mediterranean conditions (Joshi et al., 2016; Ma et al., 2018; Rezzouk et al., 2020). Moreover, exposure to high temperatures around anthesis induces pollen sterility, which reduces grain size and final yield in wheat (Wheeler et al., 1996). While this may have been the case in the RNP trials, late planting genotypes were grown under supplied irrigation and exhibited a canopy temperature below 30 °C (Table 3), which negates any relevance for heat decreasing the number of grains per ear.

Plant height reaches its maximum around anthesis. Provided that all genotypes have similar height in the absence of stress, this trait may be considered an indicator on how drought or shorter growth period associated with warmer temperatures may affect growth (Blum and Sullivan, 1997; De Vita et al., 2007). Thus, the late planting trials exhibited smaller plants than the normal planting trial under support irrigation, in accordance with a shorter crop duration. However, ILP produced taller plants than RNP, presumably as a consequence of the better water status in the former due to the support irrigation (Table 2). Here, PH was positively associated with high GY across the normal planting trials of the two seasons, regardless of whether they were under support irrigation or rainfed conditions (Table 6), but in the case of late planting, PH only correlated during the first season.

Canopy temperature and carbon isotope composition are physiological traits that are proposed as instantaneous (CT) and integrative ( $\delta^{13}\text{C}$ ) indicators for assessing crop water status (Araus et al., 2003;

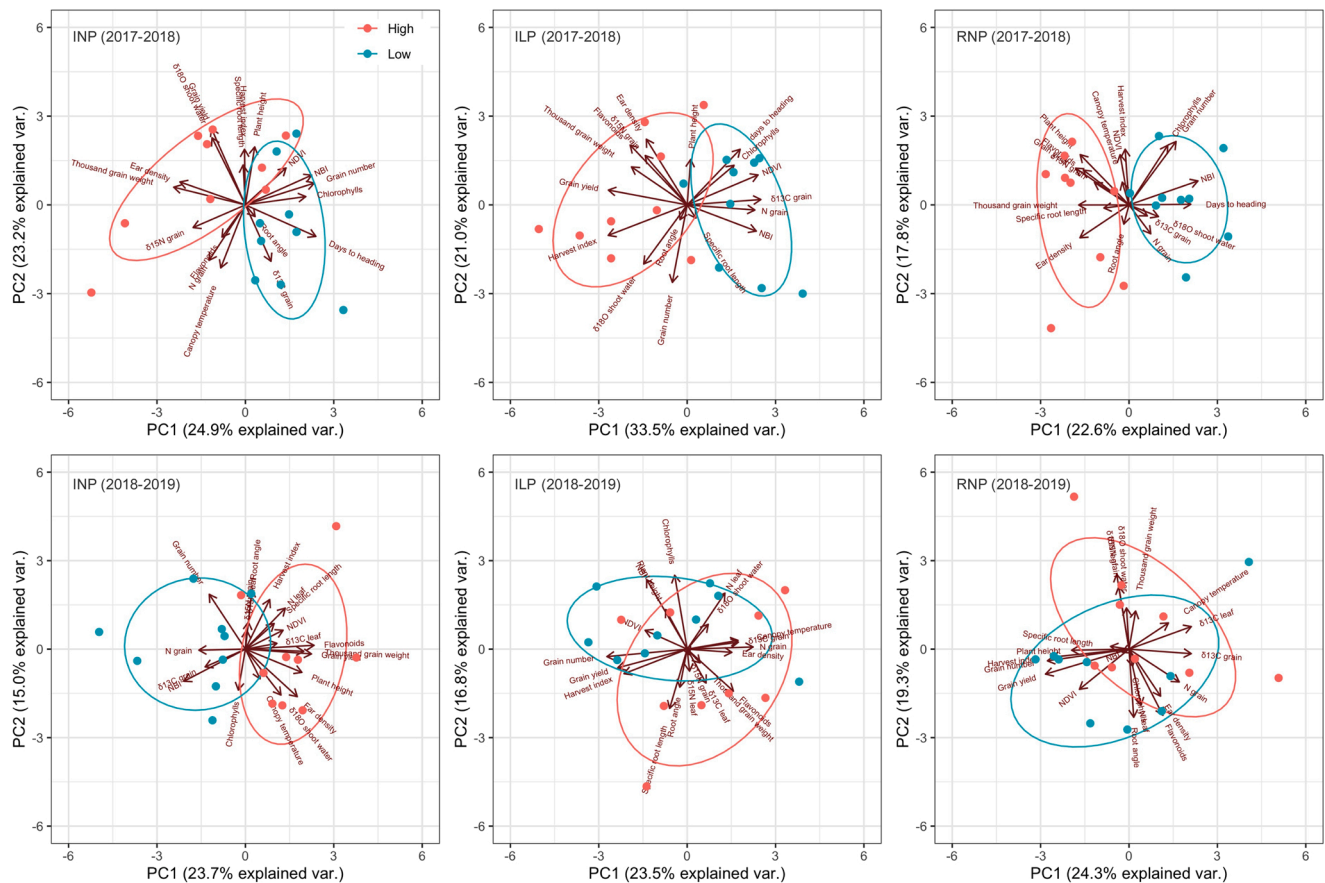


**Fig. 3.** Principal component analysis (PCA) of 6 genotypes of durum wheat grown during two consecutive crop seasons (2017–2018 and 2018–2019), and different water regimes and planting dates: A normal (winter) planting under support irrigation conditions during the first (INP (2017–2018) and second (INP (2018–2019)) season; a late planting under support irrigation conditions in the first (ILP (2017–2018)) and second (ILP (2018–2019)) seasons; a normal (winter) planting under rainfed conditions in the first (RNP (2017–2018)) and second (RNP (2018–2019)) crop season. The variables included in the analysis are grain yield (GY), days to heading (DTH), grain number (GN), ear density (ears), plant height (PH), the normalized difference vegetation index (NDVI) at anthesis, nitrogen content in flag leaves and mature grains ( $N_{\text{leaf}}$  and  $N_{\text{grain}}$ ), nitrogen isotope composition in flag leaves and mature grains ( $\delta^{15}\text{N}_{\text{leaf}}$  and  $\delta^{15}\text{N}_{\text{grain}}$ ), carbon isotope composition in flag leaves and mature grains ( $\delta^{13}\text{C}_{\text{leaf}}$  and  $\delta^{13}\text{C}_{\text{grain}}$ ), oxygen isotope composition in stem water ( $\delta^{18}\text{O}_{\text{shoot water}}$ ), canopy temperature (CT) at anthesis, chlorophyll content (Chl), flavonoids (Flav) and the nitrogen balance index (NBI) of the flag leaf, root angle (RA) and specific root length (SRL).

Araus and Cairns, 2014; Blum, 2009; Lopes and Reynolds, 2010). The negative relationships of GY with CT (Rezzouk et al., 2020; Thapa et al., 2018; Yousfi et al., 2016; Zhou et al., 2016), and  $\delta^{13}\text{C}$  (Araus et al., 2003; Rezzouk et al., 2020; Whalley et al., 2008) across trials (Table 6), support these traits as indicators of water regime during crucial phenological stages (e.g. CT measured at anthesis) and during the complete growth cycle (e.g.  $\delta^{13}\text{C}$  in mature grains). In fact, a lower CT has been associated with higher transpiration (Blum, 2009), while a more negative  $\delta^{13}\text{C}$ , particularly in mature grains, indicates that the water input received by the crop is greater (Araus et al., 2003), and in fact it is usually the consequence of a higher stomatal conductance (Condon, 2020; Roche, 2015) associated with a better water status. In agreement with this, the  $\delta^{13}\text{C}$  of grains was clearly more negative under support irrigation than under rainfed conditions in both seasons (Table 2). In addition, under the drier conditions of the second season,  $\delta^{13}\text{C}$  values of both INP and RNP were higher (less negative), and differences in the  $\delta^{13}\text{C}$  of grains between the support irrigation and the rainfed trials were also higher compared to the first season. The CT at anthesis was also clearly higher under rainfed than support irrigation conditions, particularly during the second season. Late planting trials, even when exposed to warmer temperatures and therefore to higher water demand than the normal planting, exhibited values of grain  $\delta^{13}\text{C}$  and CT much closer to INP than RNP, due to the irrigation regime. Crop water status not only depends on the water inputs (amount of irrigation and/or precipitation) and outputs (evapotranspirative demand). Water uptake from the soil

may also be involved in the differences in water status across trials. In our study, when the data from all trials were combined,  $\delta^{18}\text{O}_{\text{shoot water}}$  correlated positively with  $\delta^{13}\text{C}$  ( $r = 0.588$ ,  $p < 0.01$ ) and CT ( $r = 0.639$ ,  $p < 0.01$ ).  $\delta^{18}\text{O}_{\text{shoot water}}$  has been proposed as indicator of how deep in the soil the roots extract water, with lower  $\delta^{18}\text{O}_{\text{shoot water}}$  values indicating greater depth of water extraction (Kale Çelik et al., 2018; Millar et al., 2018; Sanchez-Bragado et al., 2019). Therefore, the above correlations suggest that the greater the depth of water extraction from the soil (lower  $\delta^{18}\text{O}_{\text{shoot water}}$ ), the better the water status (lower  $\delta^{13}\text{C}$  and CT) of the plant.

On the other hand, the negative relationships between GY and  $\delta^{13}\text{C}$  in mature grains within at least half of the six trials assayed (the combination of the three growing conditions and the two seasons) (Table 6), as well as the opposite placement of GY and  $\delta^{13}\text{C}$  in all six PCAs (Fig. 3), suggest that the best genotypes in all tested environments were these exhibiting better water status and thus higher stomatal conductance. These results also support the fact that even when trials were conducted under good agronomic conditions (provided through supplemental irrigation and a good rainy season), and consequently rather high yields, water may still limit productivity. This was the case in the support irrigation normal planting during the first season, which attained yields close to  $7 \text{ Mg ha}^{-1}$  (Araus et al., 2008; Roche, 2015), but even in the rainfed normal planting of the second season, which was the driest of the six trials (an average yield of  $1.3 \text{ Mg ha}^{-1}$ ), there was a significant negative correlation between GY and  $\delta^{13}\text{C}$ . These results are in line with the fact that



the effective use of water (Blum, 2009) makes the difference in terms of productivity under drought conditions (Araus et al., 2008; Roche, 2015).

Root architecture is another criterion that has been widely emphasized in the literature regarding the crucial role that roots play in water and nutrient uptake (Loss and Siddique, 1994; Rogers and Benfey, 2015). Although information on a direct relationship between grain yield and root growth angle is scarce, several studies have proven the contribution of deeper root growth in providing better water status, and thus higher grain yield in wheat genotypes grown in water-limited and/or elevated temperature environments (Bai et al., 2019; Condon, 2020; Pinto and Reynolds, 2015; Rogers and Benfey, 2015). In our study, but only for the second season (which was much drier), root angle spread (assessed through the ConvA parameter) was higher in the two trials under support irrigation than in the rainfed trial (Table 5). A similar pattern (but without reaching statistical significance) was observed for the RA measured with a protractor (Fig. 3). Higher RA indicates a shallower root system, probably associated with the irrigation regime imposed, while in the case of rainfed conditions, plants were more dependent on roots that explored deeper in the soil profile. However, in the case of the first season there was no clear pattern related to the different growing conditions.

Concerning the late planting under support irrigation, these conditions produced quite a different root system pattern compared to the normal planting, depending on the crop season. During the dry conditions of the second year, plants of the ILP trial exhibited more superficial roots (higher CComp), resulting in a wider root convex hull (higher ConvA), a wider root network width (higher Nwidth), and thinner roots (lower root width and higher SRL), when compared to the INP and the RNP trials (Table 5). However, during the first season all these root traits exhibited an opposite pattern under ILP compared to the two normal planting trials. In fact, during the first season, roots were thinner (lower width and higher SRL), and root number (CComp) was reduced in the rainfed trial (RNP) compared to the two trials under support irrigation. The trend of thinner roots in response to water deficit agrees with reports for durum wheat under controlled (lysimetric) conditions (Elazab et al., 2012, 2016) and for bread wheat under field conditions (Peng et al., 2019). However, unlike the findings of these studies, the SRL during the second season of our study was higher and root width lower under ILP in comparison to both the severe water conditions of the RNP trial and also INP conditions (Table 5). These root traits may contribute to a more efficient uptake of water and nutrients under the high irrigation regime of the ILP during the second season, where water and nutrients are already accessible in the upper soil layer. It is worth mentioning that the ILP of the second season received a huge amount of irrigation (Fig. 2) and exhibited a yield comparable to that of the irrigated trial in the normal planting. These different patterns of response across seasons, and irrespective of the agronomic growing conditions (irrigation and planting time), illustrate the strong plasticity of the root system in response to the water regime.

#### 4.2. Phenology: a keystone of Mediterranean ideotypes

Phenology, and particularly heading and anthesis dates, plays a major role in the adaptation of cereals to Mediterranean environments. Phenology has been progressively shortened through breeding for adaptation to Mediterranean conditions (Loss and Siddique, 1994; De Vita et al., 2007). In addition, an earlier anthesis usually contributes indirectly to an extended grain filling period (Van Oosterom and Acevedo, 1992; Araus et al., 2002). In our study, shorter DTH measured during the first crop season (2017–2018) was correlated with increased GY in genotypes grown in the support irrigation trials (INP and ILP) of the two growing conditions (Table 5) and was further supported by the different placement of the two sets of genotypes in the PCA biplots corresponding to the 2017–2018 season (Fig. 3).

However, the future ability to exploit such phenotypic adjustment using varieties with shorter crop durations has limits (Araus et al., 2002;

Chairi et al., 2018; Prieto et al., 2020). Therefore other ideotypic traits need to be identified. In that sense, the direct role of phenology was subsequently removed by assessing the PCA within each agronomic condition with only the traits that were common across the two years, thus excluding DTH (Data in brief Fig. 1). In this case and for the three conditions, a low  $\delta^{13}\text{C}_{\text{grain}}$  was a positive trait, meaning that plants that maintained more open stomata were the most productive. A better nitrogen assimilation capacity (higher NBI under INP and RNP, together with higher  $\delta^{15}\text{N}_{\text{grain}}$  under RNP) and a lower accumulation of photo-protective pigments (Flavonoids) in both the INP and RNP seem to be good ideotype indicators. The importance of other traits changed depending on the agronomic conditions (e.g. root traits), or even shifted from positive to negative when compared between INP and RNP, such as for  $\delta^{18}\text{O}_{\text{shoot water}}$ . In that particular case, the results suggested that the capacity for water capture in the upper soil layers under irrigation conditions, or deeper soil layers under rainfed, are positive traits. The specific traits associated with a better genotypic performance within each of the six growing conditions tested are discussed below.

#### 4.3. Genotypic ideotypes under support irrigation and normal planting date

Under the relatively good growing conditions provided by normal planting under support irrigation (INP), the most productive genotypes exhibited better water status (lower  $\delta^{13}\text{C}_{\text{grain}}$ ), more superficial water extracted (higher  $\delta^{18}\text{O}_{\text{shoot water}}$ ), enhanced growth (higher NDVI and PH at anthesis), and higher values in the agronomic yield components (ear density and TGW) and HI, in addition to phenological adjustment (through shorter days to heading) (Fig. 3). However, compared to the first crop season (2017–2018), drought conditions were more evident during the second season (2018–2019), resulting in an increase in protective pigments (flavonoids) being associated with a better genotypic performance. Increases in protective pigments such as flavonoids and anthocyanins in response to drought stress are well documented in wheat (Ma et al., 2014; Naderi et al., 2020). Meanwhile, RA was positioned opposite from GY during the first season (Fig. 3), meaning that the best genotypes were those that maintained shallow roots, while in the much drier conditions of the second season the trend changed, with GY and RA placed perpendicular to each other. While this suggests a lack of a clear role concerning RA during the second season, these results may be also understood as the root system being shaped to not only extract shallow water, but to also capturing water that percolates from the upper part of the soil profile via development of deeper roots. Elazab et al. (2016) reported in a study with durum wheat grown under lysimetric conditions and a rain shelter that better genotypic performance under water deficit conditions was associated with an increase in SRL (assessed as the ratio of root length to dry biomass). Thus SRL was positively correlated with shoot biomass across genotypes under moderate water stress, but absent under full irrigation (provided by maintaining container water capacity at 100%). In our study, even the support irrigation (INP and ILP) trials were exposed to some degree of water stress under field conditions, which agrees with the fact that in five of the six PCAs (Fig. 3) the relationship between SRL and GY was linear and negative, meaning that thinner roots is a rather positive genotypic trait regardless of the growing conditions.

#### 4.4. Genotypic performance under rainfed conditions

Under the moderate water-limited conditions of the rainfed trial during the first crop season, greater GY was achieved in genotypes exhibiting a better capacity for nitrogen assimilation (higher NBI and  $\delta^{15}\text{N}_{\text{grain}}$ ), deeper water extraction (lower  $\delta^{18}\text{O}_{\text{shoot water}}$ ), better water status (lower  $\delta^{13}\text{C}$  and CT), thinner roots (high SRL), deeper root growth (lower RA), phenotypical adjustment (lower DTH) and higher flavonoid content (Fig. 3). However, during the severe water stress experienced during the second season, the best genotypes, besides exhibiting again a

better water status (lower  $\delta^{13}\text{C}$ ), showed no clear pattern in terms of root angle or the soil profile location of extracted water ( $\delta^{18}\text{O}_{\text{shoot water}}$ ), the nitrogen status (NBI and  $\delta^{15}\text{N}_{\text{grain}}$ ), or the accumulation of flavonoids. In any case, for both years the best genotypes exhibited greater growth (higher PH) and biomass (higher NDVI) at anthesis, together with higher yield components, particularly higher TGW in the first crop season and higher grain number per ear in the second crop season. Our results agree with previous studies emphasizing the pivotal role of deep root development (Condon, 2020; Lopes and Reynolds, 2010; Rogers and Benfey, 2015; Wasaya et al., 2018), but particularly under the moderate water stress conditions of the rainfed crop during the first season. Thus, when grown under water-limited conditions, the most productive genotypes adjusted their root development into narrow root angle spreads (low RA and ConVA) for better access to water resources in deeper soil sections.

#### 4.5. Genotype performance under elevated temperatures

The most productive genotypes under ILP conditions were associated with better water status (lower  $\delta^{13}\text{C}$ ). Nevertheless, the relative importance of agronomic yield components, root characteristics and protection pigments varied depending on the crop season, as did other factors such as green biomass (Fig. 3). During the first season, the best genotypes exhibited lower green biomass (lower NDVI) and higher flavonoid content at anthesis, probably associated with a lower leaf biomass. However, they also demonstrated higher ear density and TGW, along with extraction of more superficial water due to the higher  $\delta^{18}\text{O}_{\text{shoot water}}$ , while RA played no clear role. During the second season, the best genotypes exhibited more biomass at anthesis, lower flavonoid content and larger grain number per ear, but had lower ear density. RA was positioned somewhat perpendicular to GY, particularly in the first season (Fig. 3), which did not support root angle (at least measured with the shovelomics approach) as a trait conferring genotypic adaptation. However, despite the fact that rRA had no clear involvement, the apparent extraction of deeper water (lower, more

negative,  $\delta^{18}\text{O}_{\text{shoot water}}$ ) was placed on the same side as GY (Fig. 3). In a study performed under conditions comparable to our late planting trial, genotypes with cooler canopies were reported as having deep root development, which was inferred from the higher root density in the 30–60 cm soil layer, and resulted in better agronomic performance (Pinto and Reynolds, 2015). Moreover, it is possible that plants invest their resources into simultaneous development of shallow roots and deep roots to catch superficial moisture and moisture retained deep in the soil profile, respectively, as it has been proposed in a recent study on root traits contributing to higher yields in wheat (Bai et al., 2019).

#### 4.6. Conclusions

Increased water deficit and temperature remain major challenges for sustainable production of wheat under Mediterranean conditions. Here we have studied the agronomic, phenological and physiological characteristics associated with ideotypic performance of durum wheat genotypes under different Mediterranean environment conditions. A trait that was clearly associated with genotypic performance was phenological adaptation, with genotypes that reached heading earlier being the best performers, regardless of the growing conditions considered. This was the case for all of the six different scenarios studied, across which occurred a nearly seven-fold difference in grain yield. In addition, physiological traits such as the carbon isotope composition ( $\delta^{13}\text{C}$ ) of mature grains, and to a lesser extent the oxygen isotope composition ( $\delta^{18}\text{O}$ ) of the shoot water and the canopy temperature at anthesis, were key traits for characterizing water status and crop adaptation to the different growing conditions, including assessment of genotypic performance. Root angle and specific root length, as assessed through the shovelomics approach, may give some further insights, particularly when characterizing the specific water regime imposed on the trials (rainfall alone or combined with irrigation). In any case, our study proves that beyond some traits (earlier reproductive stage, lower grain

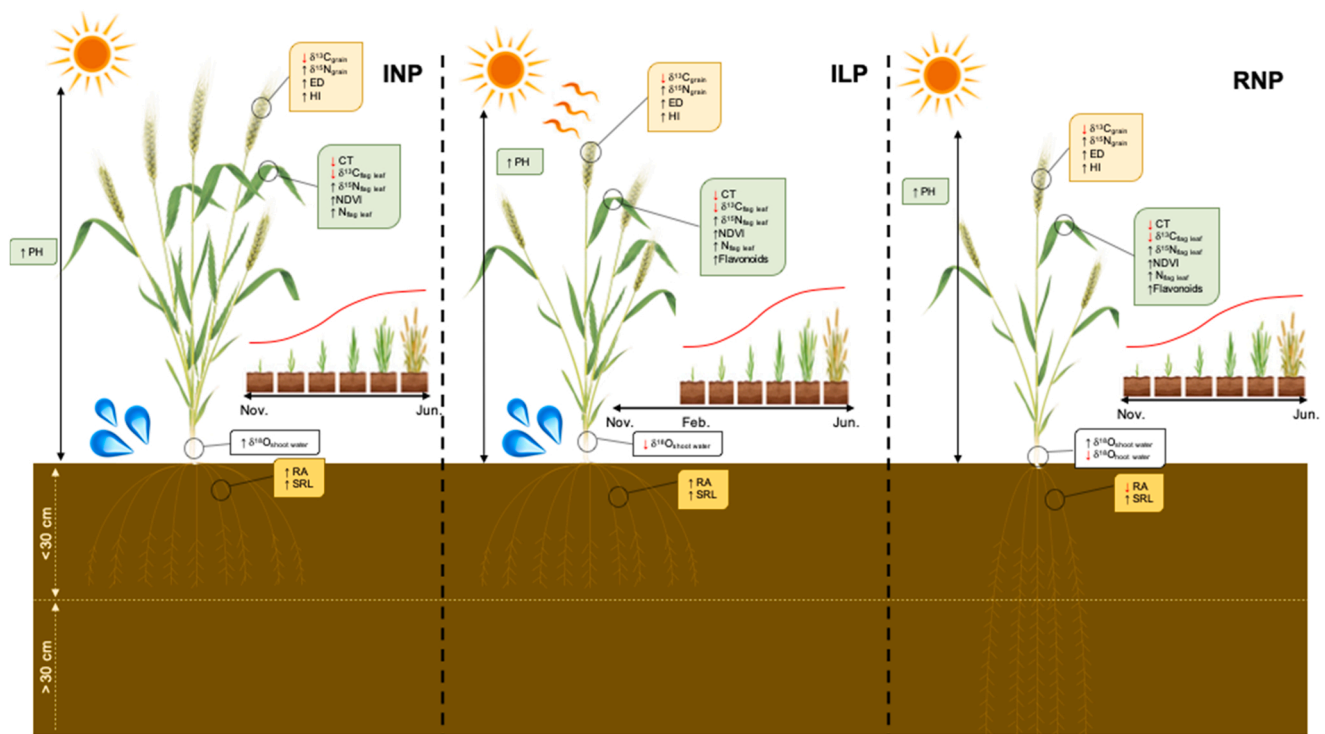


Fig. 4. A summary of potential traits contributing to the development of wheat ideotypes under different growing conditions: INP, Normal planting under irrigated conditions. RNP, Normal planting under rainfed conditions. ILP, Late planting under support irrigation conditions. ED, ear density; HI, harvest index; PH, plant height; RA, root angle; SRL, specific root length.

$\delta^{13}\text{C}$ ) associated with better genotypic performance under a wide range of Mediterranean conditions, other shoot and root traits are correlated with specific genotypic performance under a given growing condition (Fig. 4) and specific season. In this sense, rainfed and even standard support irrigation conditions are strongly affected by annual variability in precipitation and temperature, which makes it necessary to tailor the ideotype concept to the specific conditions of each environment (referred to as the particular combination of agronomic conditions and season). For this reason, introducing versatile and efficient root phenotyping techniques may contribute towards a deeper understanding of ideotype requirements within each particular environment. Nevertheless, further work is needed to improve high-throughput field phenotyping protocols to assess root performance.

#### CRediT authorship contribution statement

FZR wrote the first draft, collected samples, conducted the root studies and the stable isotope and statistical analyses, drew the tables and implemented the edits; JLA participated in the field evaluation, conceived the study and implemented the edits in the consecutive drafts; MDS collaborated on the stable isotope analyses and revised the drafts; AGR and SCK ran the remote sensing measurements and collaborated in the shovelomics; MTNT conducted the field trials and collected the grain yield, the agronomic yield components and the phenological data.

#### Declaration of Competing Interest

The authors declare that they have no known competing financial interests or personal relationships that could have appeared to influence the work reported in this paper.

#### Acknowledgments

This study was supported by the Spanish Projects PID2019-106650RB-C21 and PCIN-2017-063, Ministerio de Ciencia e Innovación, Spain. FZR is a recipient of a research grant (FI-AGAUR) sponsored by the Agency for Management of University and Research Grants (AGAUR), in collaboration with the University of Barcelona. SCK is supported by the Ramon y Cajal RYC-2019-027818-I research fellowship from the Ministerio de Ciencia e Innovación, Spain. JLA acknowledges support from the Catalan Institution for Research and Advanced Studies, Generalitat de Catalunya, Sains, through its program ICREA Academia. We thank the personnel from the experimental station of INIA at Colmenar de Oreja (Aranjuez) for their continued support of our research. We thank the members of the Integrative Crop Ecophysiology Group for their assistance during the data assessment of the study. We extend our thanks to The Water Research Institute (IdRA) for their financial support to cover laboratory analyses. We thank Dr. J. Voltas from the University of Lleida, Spain, for his support with the  $\delta^{18}\text{O}$  water analyses.

#### References

- Araus, J.L., Cairns, J.E., 2014. Field high-throughput phenotyping: the new crop breeding frontier. *Trends Plant Sci.* 19, 52–61. <https://doi.org/10.1016/j.tplants.2013.09.008>.
- Araus, J.L., Slafer, G.A., Reynolds, M.P., Royo, C., 2002. Plant breeding and drought in C3 cereals: what should we breed for? *Ann. Bot.* 89, 925–940. <https://doi.org/10.1093/aob/mcf049>.
- Araus, J.L., Slafer, G.A., Royo, C., Serret, M.D., 2008. Breeding for yield potential and stress adaptation in cereals. *Crit. Rev. Plant Sci.* 27, 377–412. <https://doi.org/10.1080/07352680802467736>.
- Araus, J.L., Villegas, D., Aparicio, N., García del Moral, L.F., El-Hani, S., Rharrabti, Y., Ferrio, J.P., Royo, C., 2003. Environmental factors determining carbon isotope discrimination and yield in durum wheat under mediterranean conditions. *Crop Sci.* 43, 170–180. <https://doi.org/10.2135/cropsci2003.0170>.
- Araus, J.L., Cabrera-Bosquet, L., Serret, M.D., Bort, J., Nieto-Taladriz, M.T., 2013. Comparative performance of  $\delta^{13}\text{C}$ ,  $\delta^{18}\text{O}$  and  $\delta^{15}\text{N}$  for phenotyping durum wheat adaptation to a dryland environment. *Funct. Plant Biol.* 40, 595–608. <https://doi.org/10.1071/FP12254>.
- Araus, J.L., Kefauver, S.C., Zaman-Allah, M., Olsen, M.S., Cairns, J.E., 2018. Translating high-throughput phenotyping into genetic gain. *Trends Plant Sci.* 23, 451–466. <https://doi.org/10.1016/j.tplants.2018.02.001>.
- Atkinson, J.A., Pound, M.P., Bennett, M.J., Wells, D.M., 2019. Uncovering the hidden half of plants using new advances in root phenotyping. *Curr. Opin. Biotechnol.* 55, 1–8. <https://doi.org/10.1016/j.copbio.2018.06.002>.
- Bai, C., Ge, Y., Ashton, R.W., Evans, J., Milne, A., Hawkesford, M.J., Whalley, W.R., Parry, M.A.J., Melichar, J., Feuerhelm, D., Basler, P.B., Bartsch, M., 2019. The relationships between seedling root screens, root growth in the field and grain yield for wheat. *Plant Soil* 440, 311–326. <https://doi.org/10.1007/s11104-019-04088-9>.
- Bengough, A.G., Gordon, D.C., Al-Menaie, H., Ellis, R.P., Allan, D., Keith, R., Thomas, W. T.B., Forster, B.P., 2004. Gel observation chamber for rapid screening of root traits in cereal seedlings. *Plant Soil* 262, 63–70. <https://doi.org/10.1023/B:PLSO.0000037029.82618.27>.
- Blum, A., 2009. Effective use of water (EUW) and not water-use efficiency (WUE) is the target of crop yield improvement under drought stress. *F. Crop. Res.* 112, 119–123. <https://doi.org/10.1016/j.fcr.2009.03.009>.
- Blum, A., Sullivan, C.Y., 1997. The effect of plant size on wheat response to agents of drought stress. I. root drying. *Aust. J. Plant Physiol.* 24, 35–41. <https://doi.org/10.1071/PP96022>.
- Cerovic, Z.G., Masdoumier, G., Ghozlen, N., Ben, Latouche, G., 2012. A new optical leaf-clip meter for simultaneous non-destructive assessment of leaf chlorophyll and epidermal flavonoids. *Physiol. Plant.* 146, 251–260. <https://doi.org/10.1111/j.1399-3054.2012.01639.x>.
- Chairi, F., Aparicio, N., Serret, M.D., Araus, J.L., 2020. Breeding effects on the genotype  $\times$  environment interaction for yield of durum wheat grown after the green revolution: the case of Spain. *Crop J.* 8, 623–634. <https://doi.org/10.1016/j.cj.2020.01.005>.
- Chairi, F., Vergara-Díaz, O., Vatter, T., Aparicio, N., Nieto-Taladriz, M.T., Kefauver, S.C., Bort, J., Serret, M.D., Araus, J.L., 2018. Post-green revolution genetic advance in durum wheat: the case of Spain. *F. Crop. Res.* 228, 158–169. <https://doi.org/10.1016/j.fcr.2018.09.003>.
- Condon, A.G., 2020. Drying times: plant traits to improve crop water use efficiency and yield. *J. Exp. Bot.* 71, 2239–2252. <https://doi.org/10.1093/jxb/eraa002>.
- Crain, J., Ortiz-Monasterio, I., Raun, B., 2012. Evaluation of a reduced cost active NDVI sensor for crop nutrient management. *J. Sens.* 2012, 1–10. <https://doi.org/10.1155/2012/582028>.
- Dawson, T.E., Ehleringer, J.R., 1993. Isotopic enrichment of water in the “woody” tissues of plants: implications for plant water source, water uptake, and other studies which use the stable isotopic composition of cellulose. *Geochim. Cosmochim. Acta* 57, 3487–3492. [https://doi.org/10.1016/0016-7037\(93\)90554-A](https://doi.org/10.1016/0016-7037(93)90554-A).
- De Vita, P., Nicosia, O.L.D., Nigro, F., Platani, C., Riefole, C., Di Fonzo, N., Cattivelli, L., 2007. Breeding progress in morpho-physiological, agronomic and qualitative traits of durum wheat cultivars released in Italy during the 20th century. *Eur. J. Agron.* 26, 39–53. <https://doi.org/10.1016/j.eja.2006.08.009>.
- Donald, C.M., Hamblin, J., 1976. The biological yield and harvest index of cereals as agronomic and plant breeding criteria. *Adv. Agron.* 28, 361–403. <https://doi.org/10.2135/cropsci2018.10.0645>.
- Elazab, A., Molero, G., Serret, M.D., Araus, J.L., 2012. Root traits and  $\delta^{13}\text{C}$  and  $\delta^{18}\text{O}$  of durum wheat under different water regimes. *Funct. Plant Biol.* 39, 379–393. <https://doi.org/10.1071/FP11237>.
- Elazab, A., Serret, M.D., Araus, J.L., 2016. Interactive effect of water and nitrogen regimes on plant growth, root traits and water status of old and modern durum wheat genotypes. *Planta* 244, 125–144. <https://doi.org/10.1007/s00425-016-2500-z>.
- Farquhar, G.D., Ehleringer, J.R., Hubick, K.T., 1989. Carbon isotope discrimination and photosynthesis. *Annu. Rev. Plant Physiol.* 40, 503–537. <https://doi.org/10.1146/annurev.pp.40.060189.002443>.
- Food and Agriculture Organization, 2019a. <http://www.fao.org/faostat/en/#compare> (Accessed 7 January 2021).
- Food and Agriculture Organization, 2019b. Handbook on climate information for farming communities – what Farmers Need and What Is Available. Rome: Food and Agriculture Organization. <http://www.fao.org/3/ca4059en/CA4059EN.pdf> (Accessed 7 January 2021).
- Galkovskiy, T., Milekyo, Y., Bucksch, A., Moore, B., Symonova, O., Price, C.A., Topp, C. N., Iyer-pascuzzi, A.S., Zurek, P.R., Fang, S., Harer, J., Benfey, P.N., Weitz, J.S., 2012. GiA Roots software for the high throughput analysis of plant root system. *BMC Plant Biol.* 12, 1–12. <https://doi.org/10.1186/1471-2229-12-116>.
- García del Moral, L.F., Rharrabti, Y., Villegas, D., Royo, C., 2003. Evaluation of grain yield and its components in durum wheat under mediterranean conditions: an ontogenic approach. *Agron. J.* 95, 266–274. <https://doi.org/10.2134/agnonj2003.2660>.
- Giunta, F., Motzo, R., Deidda, M., 1993. Effect of drought on yield and yield components of durum wheat and triticale in a Mediterranean environment. *F. Crop. Res.* 33, 399–409. [https://doi.org/10.1016/0378-4290\(93\)90161-F](https://doi.org/10.1016/0378-4290(93)90161-F).
- Gracia-Romero, A., Kefauver, S.C., Fernandez-Gallego, J.A., Vergara-Díaz, O., Araus, J.L., 2019. UAV and ground image-based phenotyping: a proof of concept with durum wheat. *Remote Sens.* 11, 1–25. <https://doi.org/10.3390/rs11101244>.
- Hunt, J.R., Lilley, J.M., Trevaskis, B., Flohr, B.M., Peake, A., Fletcher, A., Zwart, A.B., Gobbet, D., Kirkegaard, J.A., 2019. Early sowing systems can boost Australian wheat yields despite recent climate change. *Nat. Clim. Chang.* 9, 244–247. <https://doi.org/10.1038/s41558-019-0417-9>.
- Joshi, M.A., Faridullah, S., Kumar, A., 2016. Effect of heat stress on crop phenology, yield and seed quality attributes of wheat (*Triticum aestivum* L.). *J. Agrometeorol.* 18, 206–215.



- Kahiluoto, H., Kaseva, J., Balek, J., Olesen, J.E., Ruiz-Ramos, M., Gobin, A., Kersebaum, K.C., Takáč, J., Ruget, F., Ferrise, R., Bezak, P., Capellades, G., Dibari, C., Mäkinen, H., Nendel, C., Ventrella, D., Rodríguez, A., Bindl, M., Trnka, M., 2019. Decline in climate resilience of European wheat. *Proc. Natl. Acad. Sci. U.S.A.* 116, 123–128. <https://doi.org/10.1073/pnas.1804387115>.
- Kale Çelik, S., Madenoğlu, S., Sönmez, B., Avağ, K., Türker, U., Çaycı, G., Küttük, A.C., Heng, L.K., 2018. Oxygen isotope discrimination of wheat and its relationship with yield and stomatal conductance under irrigated conditions. *Turk. J. Agric.* 42, 22–28. <https://doi.org/10.3906/tar-1709-31>.
- Kefauver, S.C., Vicente, R., Vergara-Díaz, O., Fernandez-Gallego, J.A., Kerfal, S., Lopez, A., Melichar, J.P.E., Serret Molins, M.D., Araus, J.L., 2017. Comparative UAV and field phenotyping to assess yield and nitrogen use efficiency in hybrid and conventional barley. *Front. Plant Sci.* 8, 1–15. <https://doi.org/10.3389/fpls.2017.01733>.
- Li, H., Rasheed, A., Hickey, L.T., He, Z., 2018. Fast-forwarding genetic gain. *Trends Plant Sci.* 23, 184–186. <https://doi.org/10.1016/j.tplants.2018.01.007>.
- Li, X., Ingvordsen, C.H., Weiss, M., Rebetzke, G.J., Condon, A.G., James, R.A., Richards, R.A., 2019. Deeper roots associated with cooler canopies, higher normalized difference vegetation index, and greater yield in three wheat populations grown on stored soil water. *J. Exp. Bot.* 70, 4963–4974. <https://doi.org/10.1093/jxb/erz232>.
- Liu, X., Dong, X., Leskovar, D.I., 2016. Ground penetrating radar for underground sensing in agriculture: a review. *Int. Agrophys.* 30, 533–543. <https://doi.org/10.1515/intag-2016-0010>.
- Liu, X., Dong, X., Xue, Q., Leskovar, D.I., Jifon, J., Butnor, J.R., Marek, T., 2017. Ground penetrating radar (GPR) detects fine roots of agricultural crops in the field. *Plant Soil* 423, 517–531. <https://doi.org/10.1007/s11104-017-3531-3>.
- Lopes, M.S., Reynolds, M.P., 2010. Partitioning of assimilates to deeper roots is associated with cooler canopies and increased yield under drought in wheat. *Funct. Plant Biol.* 37, 147–156. <https://doi.org/10.1071/FP09121>.
- Loss, S.P., Siddique, K.H.M., 1994. Morphological and physiological traits associated with Wheat yield increases in Mediterranean environments. *Adv. Agron.* 52, 229–276. [https://doi.org/10.1016/S0065-2113\(08\)60625-2](https://doi.org/10.1016/S0065-2113(08)60625-2).
- Ma, D., Sun, D., Wang, C., Li, Y., Guo, T., 2014. Expression of flavonoid biosynthesis genes and accumulation of flavonoid in wheat leaves in response to drought stress. *Plant Physiol. Biochem.* 80, 60–66. <https://doi.org/10.1016/j.plaphy.2014.03.024>.
- Ma, S.C., Wang, T.C., Guan, X.K., Zhang, X., 2018. Effect of sowing time and seeding rate on yield components and water use efficiency of winter wheat by regulating the growth redundancy and physiological traits of root and shoot. *F. Crop. Res.* 221, 166–174. <https://doi.org/10.1016/j.fcr.2018.02.028>.
- Maccaferri, M., Sanguineti, M.C., Demontis, A., El-Ahmed, A., Garcia Del Moral, L., Maalouf, F., Nacht, M., Nserallah, N., Ouabou, H., Rhouma, S., Royo, C., Villegas, D., Tuberosa, R., 2011. Association mapping in durum wheat grown across a broad range of water regimes. *J. Exp. Bot.* 62, 409–438. <https://doi.org/10.1093/jxb/erq287>.
- Maccaferri, M., El-Feki, W., Nazemi, G., Salvi, S., Canè, M.A., Colalongo, M.C., Stefanelli, S., Tuberosa, R., 2016. Prioritizing quantitative trait loci for root system architecture in tetraploid wheat. *J. Exp. Bot.* 67, 1161–1178. <https://doi.org/10.1093/jxb/erw039>.
- Martín-Gómez, P., Barbeta, A., Voltas, J., Peñuelas, J., Dennis, K., Palacio, S., Dawson, T. E., Ferrio, J.P., 2015. Isotope-ratio infrared spectroscopy: A reliable tool for the investigation of plant-water sources? *New Phytol.* 207, 914–927. <https://doi.org/10.1111/nph.13376>.
- Mihailescu, E., Soares, M.B., 2020. The Influence of climate on agricultural decisions for three European crops: a systematic review. *Front. Sustain. Food Syst.* 4, 1–10. <https://doi.org/10.3389/fsufs.2020.00064>.
- Millar, C., Pratt, D., Schneider, D.J., McDonnell, J.J., 2018. A comparison of extraction systems for plant water stable isotope analysis. *Rapid Commun. Mass Spectrom.* 32, 1031–1044. <https://doi.org/10.1002/rcm.8136>.
- Naderi, S., Fakheri, B.A., Maali-Amiri, R., Mahdinezhad, N., 2020. Tolerance responses in wheat landrace Bolani are related to enhanced metabolic adjustments under drought stress. *Plant Physiol. Biochem.* 150, 244–253. <https://doi.org/10.1016/j.plaphy.2020.03.002>.
- Passioura, J.B., 1982. The role of root system characteristics in the drought resistance of crop plants. *Drought Resistance in Crops with Emphasis on Rice*. International Rice Research Institute, Los Banos, Philippines, pp. 71–82.
- Peng, B., Liu, X., Dong, X., Xue, Q., Neely, C.B., Marek, T., Ibrahim, A.M.H., Zhang, G., Leskovar, D.I., Rudd, J.C., 2019. Root morphological traits of winter wheat under contrasting environments. *J. Agron. Crop. Sci.* 205, 571–585. <https://doi.org/10.1111/jac.12360>.
- Petr, J., 1991. In: *Weather and yield*. Elsevier, Amsterdam, p. 289.
- Pinto, R.S., Reynolds, M.P., 2015. Common genetic basis for canopy temperature depression under heat and drought stress associated with optimized root distribution in bread wheat. *Theor. Appl. Genet.* 128, 575–585. <https://doi.org/10.1007/s00122-015-2453-9>.
- Prieto, P., Ochagavía, H., Griffiths, S., Slafer, G.A., 2020. Earliness per se × temperature interaction: consequences on leaf, spikelet, and floret development in wheat. *J. Exp. Bot.* 71, 1956–1968. <https://doi.org/10.1093/jxb/erz568>.
- Reynolds, M., Dreccer, F., Trethowan, R., 2007. Drought-adaptive traits derived from wheat wild relatives and landraces. *J. Exp. Bot.* 58, 177–186. <https://doi.org/10.1093/jxb/erl250>.
- Rezzouk, F.Z., Gracia-Romero, A., Kefauver, S.C., Gutiérrez, N.A., Aranjuelo, I., Serret, M.D., Araus, J.L., 2020. Remote sensing techniques and stable isotopes as phenotyping tools to assess wheat yield performance: effects of growing temperature and vernalization. *Plant Sci.* 295, 1–16. <https://doi.org/10.1016/j.plantsci.2019.110281>.
- Roche, D., 2015. Stomatal conductance is essential for higher yield potential of C3 crops. *Crit. Rev. Plant Sci.* 34, 429–453. <https://doi.org/10.1080/07352689.2015.1023677>.
- Rogers, E.D., Benfey, P.N., 2015. Regulation of plant root system architecture: implications for crop advancement. *Curr. Opin. Biotechnol.* 32, 93–98. <https://doi.org/10.1016/j.copbio.2014.11.015>.
- Royo, C., Abaza, M., Blanco, R., García del Moral, L.F., 2000. Triticale grain growth and morphology as affected by drought stress, late sowing and simulated drought stress. *Aust. J. Plant Physiol.* 27, 1051–1059. <https://doi.org/10.1071/pp99113>.
- Sabella, E., Aprile, A., Negro, C., Nicoli, F., Nutricati, E., Vergine, M., Luvisi, A., De Bellis, L., 2020. Impact of climate change on durum wheat yield. *Agronomy* 10, 1–13. <https://doi.org/10.3390/agronomy10060793>.
- Sanchez-Bragado, Rut, Serret, M.D., Marimon, R.M., Bort, J., Araus, J.L., 2019. The hydrogen isotope composition  $\delta^2\text{H}$  reflects plant performance. *Plant Physiol.* 180, 793–812. <https://doi.org/10.1104/pp.19.00238>.
- Shpiler, L., Blum, A., 1990. Heat tolerance for yield and its components in different wheat cultivars. *Euphytica* 51, 257–263. <https://doi.org/10.1007/BF00039727>.
- Slafer, G.A., Araus, J.L., Royo, C., García Del Moral, L.F., 2005. Promising eco-physiological traits for genetic improvement of cereal yields in Mediterranean environments. *Ann. Appl. Biol.* 146, 61–70. <https://doi.org/10.1111/j.1744-7348.2005.04048.x>.
- Srayeddin, I., Doussan, C., 2009. Estimation of the spatial variability of root water uptake of maize and sorghum at the field scale by electrical resistivity tomography. *Plant Soil* 319, 185–207. <https://doi.org/10.1007/s11104-008-9860-5>.
- Thapa, S., Jessup, K.E., Pradhan, G.P., Rudd, J.C., Liu, S., Mahan, J.R., Devkota, R.N., Baker, J.A., Xue, Q., 2018. Canopy temperature depression at grain filling correlates to winter wheat yield in the U.S. southern high plains. *Field Crop. Res.* 217, 11–19. <https://doi.org/10.1016/j.fcr.2017.12.005>.
- Trachsel, S., Kaeppeler, S.M., Brown, K.M., Lynch, J.P., 2011. Shovelomics: high throughput phenotyping of maize (*Zea mays* L.) root architecture in the field. *Plant Soil* 341, 75–87. <https://doi.org/10.1007/s11104-010-0623-8>.
- Tracy, S.R., Nagel, K.A., Postma, J.A., Fassbender, H., Wasson, A., Watt, M., 2020. Crop improvement from phenotyping roots: highlights reveal expanding opportunities. *Trends Plant Sci.* 25, 105–118. <https://doi.org/10.1016/j.tplants.2019.10.015>.
- Van Oosterom, E.J., Acevedo, E., 1992. Adaptation of barley (*Hordeum vulgare* L.) to harsh Mediterranean environments. *Euphytica* 62, 1–14. <https://doi.org/10.1007/BF00036082>.
- Wasaya, A., Zhang, X., Fang, Q., Yan, Z., 2018. Root phenotyping for drought tolerance: a review. *Agronomy* 8, 1–19. <https://doi.org/10.3390/agronomy8110241>.
- Wasson, A.P., Nagel, K.A., Tracy, S., Watt, M., 2020. Beyond digging: noninvasive root and rhizosphere phenotyping. *Trends Plant Sci.* 25, 119–120. <https://doi.org/10.1016/j.tplants.2019.10.011>.
- West, A.G., Patrickson, S.J., Ehleringer, J.R., 2006. Water extraction times for plant and soil materials used in stable isotope analysis. *Rapid Commun. Mass Spectrom.* 20, 1317–1321. <https://doi.org/10.1002/rcm.2456>.
- Whalley, W.R., Watts, C.W., Gregory, A.S., Mooney, S.J., Clark, L.J., Whitmore, A.P., 2008. The effect of soil strength on the yield of wheat. *Plant Soil* 306, 237–247. <https://doi.org/10.1007/s11104-008-9577-5>.
- Whalley, W.R., Binley, A., Watts, C.W., Shanahan, P., Dodd, I.C., Ober, E.S., Ashton, R. W., Webster, C.P., White, R.P., Hawkesford, M.J., 2017. Methods to estimate changes in soil water for phenotyping root activity in the field. *Plant Soil* 415, 407–422. <https://doi.org/10.1007/s11104-016-3161-1>.
- Wheeler, T.R., Batts, G.R., Ellis, R.H., Hadley, P., Morison, J.I.L., 1996. Growth and yield of winter wheat (*Triticum aestivum*) crops in response to CO<sub>2</sub> and temperature. *J. Agric. Sci.* 127, 37–48. <https://doi.org/10.1017/s0021859600077352>.
- Xynias, I.N., Mylonas, I., Korpetis, E.G., Ninou, E., Tsalaba, A., Avdikos, I.D., Mavromatis, A.G., 2020. Durum wheat breeding in the Mediterranean region: current status and future prospects. *Agronomy* 10, 1–28. <https://doi.org/10.3390/agronomy10030432>.
- York, L.M., Slack, S., Bennett, M.J., Foulkes, J., 2018a. Wheat shovelomics: phenotyping roots in tillering species. *BioRxiv* 1–17. <https://doi.org/10.1101/280875>.
- York, L.M., Slack, S., Bennett, M.J., Foulkes, J., 2018b. Wheat shovelomics II: revealing relationships between root crown traits and crop growth. *BioRxiv* 1–22. <https://doi.org/10.1101/280917>.
- Yousfi, S., Serret, M.D., Araus, J.L., 2009. Shoot  $\delta^{15}\text{N}$  gives a better indication than ion concentration or  $\delta^{13}\text{C}$  of genotypic differences in the response of durum wheat to salinity. *Funct. Plant Biol.* 36, 144–155. <https://doi.org/10.1111/pce.12055>.
- Yousfi, S., Serret, M.D., Márquez, A.J., Voltas, J., Araus, J.L., 2012. Combined use of  $\delta^{13}\text{C}$ ,  $\delta^{18}\text{O}$  and  $\delta^{15}\text{N}$  tracks nitrogen metabolism and genotypic adaptation of durum wheat to salinity and water deficit. *New Phytol.* 194, 230–244. <https://doi.org/10.1111/j.1469-8137.2011.04036.x>.
- Yousfi, S., Serret, M.D., Araus, J.L., 2013. Comparative response of  $\delta^{13}\text{C}$ ,  $\delta^{18}\text{O}$  and  $\delta^{15}\text{N}$  in durum wheat exposed to salinity at the vegetative and reproductive stages. *Plant, Cell Environ.* 36, 1214–1227. <https://doi.org/10.1111/pce.12055>.
- Yousfi, S., Kellas, N., Saidi, L., Benlakehal, Z., Chouli, L., Siad, D., Herda, F., Karrou, M., Vergara, O., Gracia, A., Araus, J.L., Serret, M.D., 2016. Comparative performance of remote sensing methods in assessing wheat performance under Mediterranean

- conditions. *Agric. Water Manag.* 164, 137–147. <https://doi.org/10.1016/j.agwat.2015.09.016>.
- Zampieri, M., Toreti, A., Ceglar, A., Naumann, G., Turco, M., Tebaldi, C., 2020. Climate resilience of the top ten wheat producers in the Mediterranean and the Middle East. *Reg. Environ. Chang.* 20, 1–9. <https://doi.org/10.1007/s10113-020-01622-9>.
- Zhang, X., Wang, Y., Sun, H., Chen, S., Shao, L., 2013. Optimizing the yield of winter wheat by regulating water consumption during vegetative and reproductive stages under limited water supply. *Irrig. Sci.* 31, 1103–1112. <https://doi.org/10.1007/s00271-012-0391-8>.
- Zhou, B., Elazab, A., Bort, J., Sanz-Sáez, A., Nieto-Taladriz, M.T., Serret, M.D., Araus, J. L., 2016. Agronomic and physiological responses of chinese facultative wheat genotypes to high-yielding Mediterranean conditions. *J. Agric. Sci.* 154, 870–889. <https://doi.org/10.1017/S0021859615000817>.





## CHAPTER IV

# **Root traits determining durum wheat performance under Mediterranean conditions**

Fatima Zahra Rezzouk, Adrian Gracia-Romero, Joel Segarra, Shawn C, Kefauver, Nieves Aparicio, Maria Dolors Serret, José Luis Araus

Submitted to:  
Science of The Total Environment



## Root traits determining durum wheat performance under Mediterranean conditions

Fatima Zahra Rezzouk<sup>1,2</sup>, Adrian Gracia-Romero<sup>1,2</sup>, Joel Segarra<sup>1,2</sup>, Shawn C. Kefauver<sup>1,2</sup>, Nieves Aparicio<sup>3</sup>, Maria Dolores Serret<sup>1,2</sup>, José Luis Araus<sup>1,2\*</sup>

<sup>1</sup>*Integrative Crop Ecophysiology Group, Plant Physiology Section, Faculty of Biology, University of Barcelona, Spain*

<sup>2</sup>*AGROTECNIO (Center for Research in Agrotechnology), Lleida, Spain*

<sup>3</sup>*Agro-technological Institute of Castilla y León (ITACyL), Valladolid, Spain*

### Highlights

- Water availability is the main environmental factor limiting durum wheat yield
- Durum wheat root architecture shows high plasticity under Mediterranean conditions
- Under rainfed conditions, higher yields are associated with deeper roots
- Under irrigation, higher yielding crops combined shallow and deep roots
- $\delta^{18}\text{O}$  of stem water is a promising phenotypic trait informing about soil water uptake

### Abstract

Crop performance is very dependent on roots because they determine the capture of water and nutrients, and the crop's subsequent growth and productivity. Durum wheat is a major crop in the Mediterranean region, where water and nitrogen availability limit its productivity. Determining the combination of root characteristics related to an efficient acquisition of resources, alongside canopy traits that illustrate the effective use of these resources, may allow improvements in the adaptation of durum wheat to different Mediterranean conditions. This study evaluated crop performance in a set of modern durum wheat cultivars grown during four consecutive seasons and under contrasting water regimes, temperatures and nitrogen supplies, totalling 12 different growing conditions. Grain yield, biomass, other crop-growth traits (plant height, the Normalised Difference Vegetation Index), together with physiological indicators of water (carbon isotope composition,  $\delta^{13}\text{C}$ , and canopy temperature depression, CTD) and nitrogen (nitrogen isotope composition,  $\delta^{15}\text{N}$ , and grain nitrogen yield, GNY) status were assessed. In addition, root architecture and distribution were measured using shovelomics and soil coring, and the provenance of the water captured by roots was

determined by comparing the oxygen ( $\delta^{18}\text{O}$ ) and hydrogen ( $\delta^2\text{H}$ ) isotope compositions of water at the base of the stem with water in different soil sections. Water and nitrogen status indicators combined with shovelomic traits allowed development of yield-prediction models. While higher yields were associated in most cases with better water status, root architecture was very responsive to different growing conditions. Overall, genotypes better adapted to rainfed conditions exhibited roots favouring deeper water extraction, whereas under support irrigation, the root system enabled water extraction from the topsoil as well as from deeper soil sections. Our study highlights the limitation of shovelomics and soil coring as phenotyping approaches and proposes the  $\delta^{18}\text{O}$  and  $\delta^2\text{H}$  of stem water as a promising functional phenotypic approach.

Keywords: Soil coring, shovelomics, stable isotopes, canopy temperature.

Abbreviations:

$\delta^2\text{H}$ , hydrogen isotope composition.  $\delta^{13}\text{C}$ , carbon isotope composition.  $\delta^{15}\text{N}$ , nitrogen isotope composition.  $\delta^{18}\text{O}$ , oxygen isotope composition. Bush, root network bushiness. ConvA, root network convex area. CTD, canopy temperature depression. GNY, grain nitrogen yield. GY, grain yield. NDVI, normalised difference vegetation index. HI, harvest index. ILP, irrigated late planting. INP, irrigated normal planting. Ldist, root length distribution. MaxR, maximum root number. MedR, median root number. Ndepth, root network length. Nlen, root network length. N<sub>grain</sub>, nitrogen content in grains. N<sub>leaf</sub>, nitrogen content in leaf. Nsurf, root network surface area. Nvol, root network volume. NwA, root network area. NWDR, root network width to depth ratio. Nwidth, root network width. RA, root angle. Rcomp, root number of connected components. RDW, root dry weight. RF, random forest. RNP, rainfed normal planting. RLN, rainfed normal planting and low nitrogen. Rwidth, root width. PH, plant height. SRL, specific root length. TKW, thousand kernel weight.

## 1. Introduction

Durum wheat is a major crop in the Mediterranean basin, encompassing more than 50% of the total wheat growing area (Guzman et al., 2016). It is grown mainly under rainfed conditions and used in the production of various staple food in the Mediterranean region (Dainelli et al., 2022; Xinias et al., 2020). Mediterranean climatic conditions are known for

their high annual variability with fluctuating precipitation and temperatures (Hoffmann et al., 2018). Moreover, climatic projections forecast that a warmer and drier climate across the Mediterranean will increase the risk of yield loss in durum wheat (Celgar et al., 2011; Ferrise et al., 2011). In addition, nitrogen availability is also a major factor limiting yield in many Mediterranean areas (Cossani et al., 2010; Savin et al., 2019). With food demands continuing to grow amid population increase, wheat breeders and producers are thus challenged by and expected to overcome these climatic limitations and secure higher production with fewer resources.

Crop growth and its subsequent yield depend on the effective acquisition of resources from the soil, namely water and nutrients. While the crucial role of the root system in determining crop performance is evident, studying roots under field conditions has been limited by the lack of precise high-throughput phenotypic approaches (Vadez, 2014; Wasson et al., 2014). Nevertheless, the root system may provide further understanding about plant coping mechanisms during growth under the drought, high temperature and/or low fertility conditions encountered by Mediterranean agriculture. Therefore, deepening our understanding of how root architecture and function respond to a wide range of growing conditions is necessary to provide insights into root characteristics suitable for tailoring higher yielding cultivars with better adaptation to Mediterranean conditions, and to design more efficient crop management practices. Despite the evident limitations of the current methods for root phenotyping in the field, combining even low throughput methodologies may still provide comprehensive information on root traits when aiming to characterise ideotypes and the effect of crop management conditions.

The wheat root system is characterised by seminal roots that stem from the seed, and nodal or adventitious roots that initiate after germination (Chochois et al., 2015; Maccaferri et al., 2016). Seminal roots are the first to penetrate soil layers to provide anchorage and stability, establish root system architecture and remain functional for the entire crop growth cycle (Pinto and Reynolds, 2015). Nodal roots are known for harvesting late season precipitation and acquiring nutrients from the topsoil (Chochois et al., 2015; Wasaya et al., 2018). Throughout the crop growth cycle, both seminal and nodal roots spread in the soil in horizontal and vertical directions, giving rise to a fibrous system that reaches its optimum growth by anthesis (Barraclough and Weir, 1988; Fageria and Moreira, 2011; Foulkes et al.,



2009). Although phenotyping for root traits remains a real challenge given its laborious, destructive and costly nature, several techniques that seek to unveil root characteristics in the field have been developed and are in use, such as shovelomics and soil coring (Araus et al., 2022; Bucksch et al., 2014; Lynch, 1995, 2013; Ober et al., 2021; Trachsel et al., 2013; Wasson et al., 2014; York et al., 2018a, 2018b). The former is an approach that studies roots in the upper soil layer (ca. 0-20 cm) and defines root crown architecture characteristics (Bucksch et al., 2014; Fradgley et al., 2020; Rezzouk et al., 2022; Wasson et al., 2016). The latter targets root distribution throughout the soil profile, and changes in root traits focussed on length and density (Box Jnr and Ramseur, 1993; Hodgkinson et al., 2017; Kätterer et al., 1993; Kirkegaard and Lilley, 2007; Wasson et al., 2014). These techniques inform about the architecture and structure of root systems and are usually coupled with imagery for quicker and more efficient root trait assessment (Araus et al., 2022; Bai et al., 2019; Chen et al., 2017; Wasson et al., 2016). Thus, root characteristics such as root depth, angle, density, diameter and specific length have been studied to explain the mechanisms that facilitate drought stress tolerance, and that allow the capture of nutrients and water from the soil and contribute to higher grain yield (Foulkes et al., 2009; He et al., 2022; Narayanan et al., 2014; Rezzouk et al., 2022; York et al., 2018a;2018b).

While assessing root architecture and its growth through the soil profile is relevant in terms of phenotyping, adding information such as root functionality at the soil depth from which water is extracted, may provide a more comprehensive view on how roots contribute to crop adaptation. In this sense,  $\delta^2\text{H}$  and  $\delta^{18}\text{O}$  in stem water have been proposed as tracers to determine the movement of soil moisture and evapotranspiration in plants (Zimmermann et al., 1966). Previous studies in other crops have shown that  $\delta^{18}\text{O}$  and  $\delta^2\text{H}$  from the stem water reflect the isotopic signature of the water source (e.g. precipitation and/or irrigation) together with the depth in the soil profile from which the water is captured by the roots (Berry et al., 2019; Dawson and Goldsmith, 2018; de Deurwaerder et al., 2020; Schreel and Steppe, 2020; Treydte et al., 2014; Wang et al., 2010; Zhao et al., 2016). More recent studies on durum wheat also support the use of  $\delta^{18}\text{O}$  and  $\delta^2\text{H}$  from stem water as a tracer for root water uptake (Kale Çelik et al., 2018; Sanchez-Bragado et al., 2019; Rezzouk et al., 2022).

As the functioning of the roots determines the overall performance of the crop (Lopes and Reynolds, 2020; Pinto and Reynolds, 2015), assessing traits that inform about the water and nutrient status of the crop may further improve our mechanistic understanding of key root traits while facilitating more efficient phenotyping. In terms of nitrogen status, a crop capable of assimilating more nitrogen should translate to a higher grain nitrogen yield, while also affecting the nitrogen content of the leaves and grains (Chairi et al., 2020; Haberle et al., 2008; Rezzouk et al., 2020; 2022; Slafer et al., 1990), as well as the stable nitrogen isotope composition ( $\delta^{15}\text{N}$ ) of the plant tissues (Choi et al., 2003; Wassenaar, 1995). Thus, the  $\delta^{15}\text{N}$  of plant tissues not only works as a tracer of the nitrogen source used by the crop, but also of the water conditions experienced by the crop. Whereas chemical nitrogen fertilisers are characterised by low  $\delta^{15}\text{N}$  values, nitrogen derived from nitrification of organic matter present in the soil exhibits far higher  $\delta^{15}\text{N}$  (Araus et al. 2013; Serret et al. 2009). On the other hand,  $\delta^{15}\text{N}$  use increases as growing conditions improve and productivity increases (Rezzouk et al., 2022; Sanchez-Bragado et al., 2017; Yousfi et al., 2009).

Regarding water status, canopy temperature depression (CTD) is a relevant parameter that is used to quantify crop water status, which is related to root performance under field conditions (Lopes and Reynolds, 2010). CTD has been reported to be positively correlated with photosynthetic traits such as stomatal conductance and leaf water potential (Wasaya et al., 2018), as well as grain yield (Fischer et al. 1998; Chairi et al., 2020; Wasaya et al., 2018). On the other hand, the stable isotope composition ( $\delta^{13}\text{C}$ ) (Farquhar and Richards, 1984; Farquhar et al., 1989) when analysed in plant tissues such as mature grains, it has been frequently used in wheat as a time-integrative indicator of the water used by plants (Araus et al., 2003; 2008), which is also known as the effective use of water (Blum, 2009). In fact, for wheat, the lower the  $\delta^{13}\text{C}$  values of plant tissues, the better the water status of the crop and the higher the grain yield achieved (Araus et al. 2003, 2013).

Finally, a better water and nutrient status will translate to a higher crop growth and stay green (Christopher et al., 2016; Fischer, 2011; Padovan et al., 2020; Rezzouk et al., 2020; Spano et al., 2003). Canopy height at anthesis/grain filling (Blum and Sullivan, 1997; de Vita et al., 2010), together with the green canopy biomass inferred through remote sensing vegetation indices

such as the Normalised Difference Vegetation Index (NDVI) may also be useful as indicators (Christopher et al., 2014; Fischer et al., 1998; Kipp et al., 2014; Lopes and Reynolds, 2012).

Combining traits that inform about the growth and water and nitrogen status of the crop, together with a wide range of root traits, may prove a solid approach to define ideotypes adapted to Mediterranean conditions and to develop prediction-models amenable for crop management and breeding. Therefore, the objective of this study is to uncover the response of root traits in durum wheat to different Mediterranean growing conditions and how they relate to better yield performance. To achieve this, different methodologies examining root architecture in the topsoil (shovelomics) as well as at depth (soil coring) were deployed alongside a functional approach (isotope signature of the stem water) under field conditions. Twelve trials, with contrasting water (rainfed vs irrigated), temperature (normal vs late planting) and nitrogen (low versus recommended N fertilisation) conditions, were carried out through four consecutive crop seasons under the continental Mediterranean conditions of Valladolid, Spain. A set of modern durum wheat cultivars with contrasting yield performance were evaluated. In conjunction with grain yield and the above-mentioned indicators of crop growth and water and nitrogen status, shovelomics was carried out for all genotypes and trials, and soil coring as well as measurements of the stable isotopic signature of the stem and soil water were undertaken in a subset of seasons.

## **2. Materials and Methods**

### **2.1 Plant material, field experiment and growth conditions**

Field trials were carried out over four consecutive crop seasons (2017-2018, 2018-2019, 2019-2020 and 2020-2021) at the experimental station of Zamadueñas of the Agro-technological Institute of Castilla y León (ITACyL), Valladolid, Spain (41° 39' 8" N and 4° 43' 24" W, 690 m.a.s.l.). For each season, six to eight semi-dwarf durum wheat (*Triticum turgidum* L. subsp. *durum* (Desf) Husn.) post green revolution cultivars were selected according to grain yield data from a panel of 24 modern durum wheat cultivars grown in Spain during the last five decades. Genotype selection was based on the grain yields achieved during different seasons at the ITACyL station stated above, and at the Spanish stations of INIA "Instituto Nacional de Investigación y Tecnología Agraria y Alimentaria" located in Colmenar de Oreja-Aranjuez

(Madrid) and Coria del Rio (Seville), under different growing conditions: irrigated normal planting (INIA, Coria del Rio); irrigated normal planting, irrigated late planting and rainfed normal planting conditions (INIA, Aranjuez); and irrigated normal planting, rainfed normal planting and rainfed normal planting and low nitrogen trials (ITACyL, Valladolid). Briefly, for the first two seasons of this study (2017-2018 and 2018-2019), six genotypes out of twenty-four were selected from yield data obtained at the INIA stations (Aranjuez and Coria del Rio) during the seasons 2016-2017, 2017-2018 and 2018-2019, totalling twelve growth conditions (i.e. environments). During the third season of this study (2019-2020), eight genotypes were selected from yield data collected at the INIA stations (Aranjuez and Coria del Rio) and ITACyL station (Valladolid) from the season 2018-2019, totalling eight environments. In the fourth season (2020-2021), six genotypes were selected from yield data obtained at the INIA station (Aranjuez) from the seasons 2017-2018 and 2018-2019, and the ITACyL station (Valladolid) from the seasons 2017-2018, 2018-2019 and 2019-2020, totalling sixteen environments. Information of the chosen genotypes in each season and their provenances is provided in Supplemental Table 1, as well as elsewhere (Chairi et al., 2018; Rezzouk et al., 2022). In fact, for each of the trials of this study, the tested cultivars were grown within the panel of 24 genotypes, designed in a complete block design with three replicates. In all seasons and for each trial, cultivars were sown in six rows, 0.25 m apart plots, and planting density consisted of 250 seeds per m<sup>2</sup>. Plot size was 1.5 m x 7 m during 2017-2018, 1.5 m x 9 m during 2018-2019, and 1.5 m x 10 m during 2019-2020 and 2020-2021. The following growing conditions were tested: support irrigation normal planting (INP), support irrigation late planting (ILP), rainfed normal planting and low nitrogen (RLN), and rainfed normal planting (RNP) (Table 1). Each season consisted of three different growing conditions: INP, RNP and RLN during the seasons 2017-2018 and 2018-2019; INP, ILP and RLN during 2019-2020; and INP, ILP and RNP during 2020-2021; totalling twelve tested environments. During the first two seasons (2017-2018 and 2018-2019), all trials (INP, RLN and RNP) received 300 kg ha<sup>-1</sup> of 8-15-15 as basic-dressing, and afterwards the INP and RNP trials received 150 kg ha<sup>-1</sup> of calcium ammonium nitrate (NAC 27%) as a first top-dressing during tillering, and another 150 kg ha<sup>-1</sup> of nitrosyl sulfuric acid (NSA 26%) as a second top-dressing during jointing. During the second two seasons (2019-2020 and 2020-2021), the INP, ILP and RNP trials were supplied with 300 kg ha<sup>-1</sup> of 8-15-15 as basic dressing, and afterwards the INP and RNP trials received 150 kg ha<sup>-1</sup> of calcium ammonium nitrate (NAC 27%) during tillering as top-dressing, and ILP received the

same top-dressing fertilisation during the 2019-2020 season (Table 1). In terms of phytosanitary treatment, pests, diseases and weeds were treated as recommended by the farmers of the region. Soil was xerofluent with a sandy loam texture and alkaline pH. Regarding the water regimen, the irrigated trials (INP and ILP) received a total of 109.8 mm, fractionated eight times during 2017-2018, 152.7 mm, fractionated thirteen times during 2018-2019, 66.0 mm fractionated four times during 2019-2020, and 71.0 mm fractionated nine times during 2020-2021. The accumulated precipitation for normal planting trials (INP, RLN and RNP) totalled 443.8 mm, 124.7 mm, 348,5 mm and 186-5 mm during the four consecutive seasons, respectively. For the ILP, accumulated precipitation was 217.9 mm and 94.2 mm during 2019-2020 and 2020-2021, respectively. Further information on the fertilisation calendar, water input, sowing and harvest dates are detailed in Table 1 while climate conditions for each crop season are presented in Figure 1.

**Table 1.** Nitrogen fertilization and water inputs as occurred throughout the four crop seasons (2017-2018; 2018-2019; 2019-2020; 2020-2021) in different trials (INP, ILP, RLN, RNP). Nitrogen was supplied as a basic dressing using N-P-K, and a top dressing supplied as calcium ammonium nitrate (CAN) as a first amendment, and nitrosyl sulfuric acid (NSA) as a second amendment. Accumulated precipitation and accumulated effective precipitation were obtained from the Spanish meteorological platform SIAR (Servicio de Informacion Agroclimática para el Regadio, www.siar.es), and presented as the accumulated precipitation from sowing to physiological maturity. INP, irrigated normal planting; ILP, irrigated late planting; RLN, rainfed normal planting and low nitrogen; RNP, rainfed normal planting.

		Crop season												
		2017-2018			2018-2019			2019-2020			2020-2021			
		Date	kg ha <sup>-1</sup>	UN	Date	kg ha <sup>-1</sup>	UN	Date	kg ha <sup>-1</sup>	UN	Date	kg ha <sup>-1</sup>	UN	
Basic dressing	INP	8-15-15	11/12/17	300	24	11/16/18	300	24	11/06/19	300	24	10/29/20	300	24
	ILP		-	-	-	-	-	-	02/12/20	300	24	02/15/21	300	24
	RLN		11/22/17	300	24	11/16/18	300	24	-	-	-	-	-	-
	RNP		11/22/17	300	24	11/16/18	300	24	11/06/19	300	24	10/29/20	300	24
1 <sup>st</sup> top dressing	INP	NAC 27%	02/20/18	150	40.5	02/28/19	150	40.5	02/12/20	150	40.5	02/16/21	150	40.5
	ILP		04/17/18	150	40.5	04/22/19	150	40.5	04/22/20	150	40.5	-	-	-
	RLN		-	-	-	-	-	-	-	-	-	-	-	-
	RNP		02/20/18	150	40.5	02/28/19	150	40.5	02/12/20	150	40.5	02/16/21	150	40.5
2 <sup>nd</sup> top dressing	INP	NSA 26%	04/17/18	150	39	04/12/19	150	39	-	-	-	-	-	-
	ILP		05/07/18	150	39	05/16/19	150	39	-	-	-	-	-	-
	RLN		-	-	-	-	-	-	-	-	-	-	-	-
	RNP		04/17/18	150	39	04/12/19	150	39	-	-	-	-	-	-
Total N	INP				103.5			103.5			64.5			64.5
	ILP				103.5			103.5			64.5			64.5
	RLN				24			24			0			0
	RNP				103.5			103.5			64.5			64.5
Water input	Irrigation		109.8 mm			152.7 mm			66.0 mm			71.0 mm		
	Fractionation		8-fold			13-fold			4-fold			9-fold		
	Accumulated precipitation	INP	443.8 mm			124.7 mm			348.5 mm			186.5 mm		
		ILP	-			-			217.9 mm			94.2 mm		
Acc. Effective Precipitation	INP	210.1 mm			44.6 mm			153.8 mm			52.2 mm			
	ILP	-			-			99.8 mm			28.2 mm			
Previous crop	Normal planting		Fallow			Barley			Peas			Fallow		
	Late planting		-			-			Vetch					
Sowing	Normal planting		11/23/2017 (INP, RLN) 11/13/2017 (RNP)			12/03/2018			11/18/2019			11/19/2020		
	Late planting		-			-			02/13/2020			02/18/2021		
Harvest	Normal planting		07/20/2018			07/03/2019			07/16/2020			07/16/2023 (RNP) 07/21/2021 (INP)		
	Late planting		-			-			07/23/2020			07/23/2021		

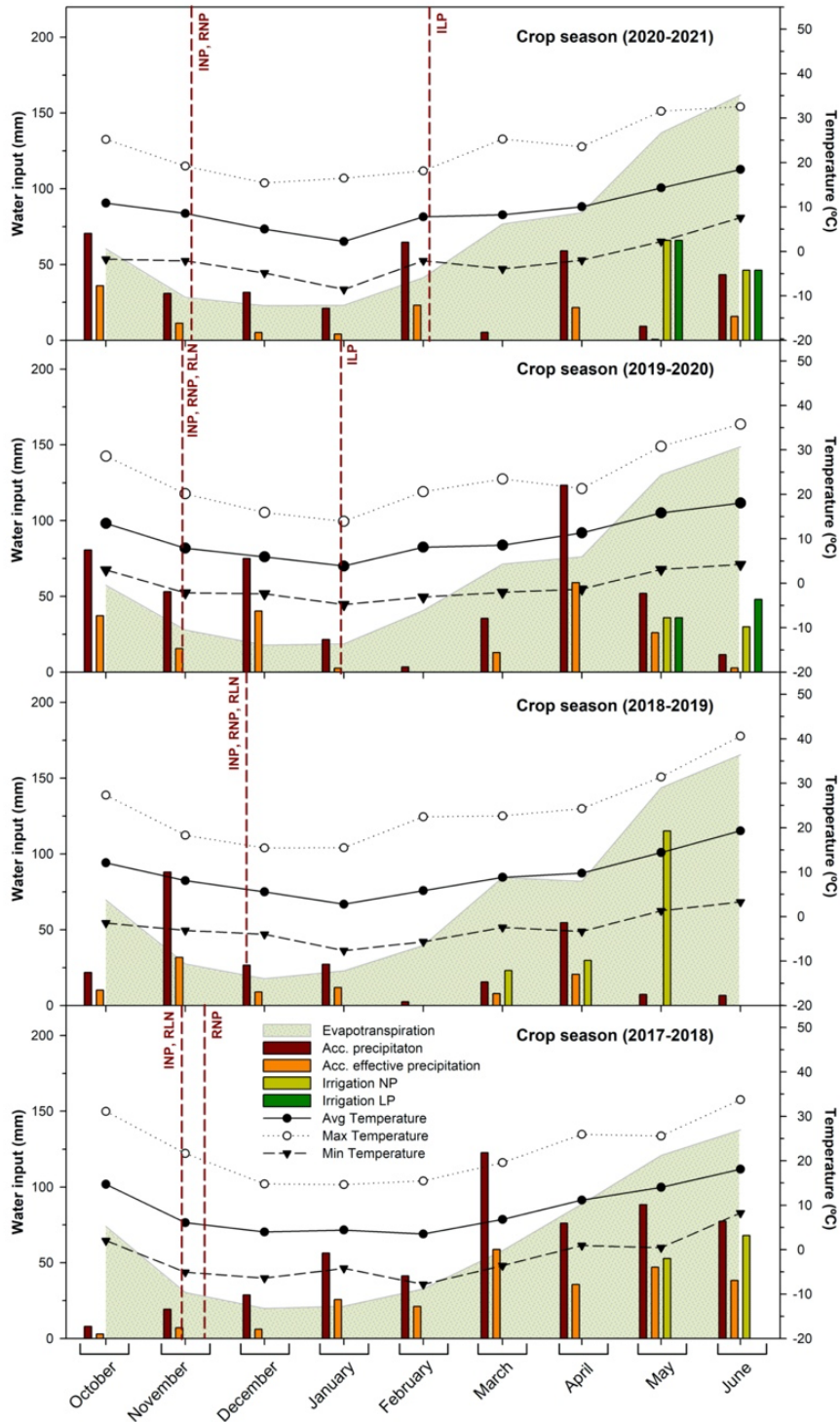


**Figure 1.** Distribution of monthly water input (accumulated precipitation, accumulated effective precipitation and irrigation and evapotranspiration), and mean temperature (average, minimum and maximum) during the growing period covering the crop seasons (2017-2018), (2018-2019) and (2019-2020). Climatic conditions were obtained from the Agro-climatic Information System for Irrigation (Sistema de Información Agroclimática para el Regadío, SIAR) (<http://portal.magrama.gob.es/websiar/>); Ministry of Agriculture, Food and Environment, Government of Spain and the European Agricultural Fund for Rural Development.

## 2.2 Agronomic and crop growth traits

At anthesis, plant height (PH) was determined across the whole plot using a ruler, and the NDVI was measured using a portable ground sensor (GreenSeeker, Trimble, Sunnyvale, CA, USA), following the protocol described previously in Rezzouk et al. (2020). At maturity, plant density (plants m<sup>-2</sup>) and ear density (ears m<sup>-2</sup>) were determined by counting the number of plants and ears in a 1 m length of a central row. Afterwards, each plot was machine harvested and grain yield (GY) was determined after an adjustment to a 10% moisture level. Total biomass was measured for each plot in a subset of 10 plants. Then, thousand kernel weight (TKW) and harvest index (HI) were calculated.

## 2.3 Canopy temperature depression

Measurements of canopy temperature (CT) were assessed during the seasons 2017-2018, 2018-2019 and 2020-2021 from an aerial platform using a thermal camera (FLIR Tau2 640, FLIR Systems, Nashua, NH, USA) with a VOx uncooled microbolometer equipped with a TeAx Thermal Capture 2.0 (TeAx Technology, Wilnsdorf, Germany), and mounted on an unmanned aerial vehicle (6S12 XL oktokofter, HiSystems GmbH, Moomerland, Germany). During 2019-2020, CT was assessed at ground level using a portable infrared thermometer (PhotoTemp™ MXSTM TD Raytek®, California; USA). In all cases, measurements took place between solar noon and early afternoon. Initially, the thermal frames were stacked to raw 16-bit TIFF format images (temperature values expressed in Kelvin x 10000) using ThermoViewer software (v1.3.13) by TEAX (TeAx Technology, Wilnsdorf, Germany). Secondly, images were 3D-reconstructed using Agisoft Photoscan Pro (Agisoft LLC, St. Petersburg, Russia, [www.agisoft.com](http://www.agisoft.com)) and processed to produce ortho-mosaic images (Bendig et al., 2014). Thirdly, plots were cropped and aerial CT analysed using the MosaicTool software integrated as a plugin for the open source image analysis platform FIJI (Fiji is Just ImageJ; <http://fiji.sc/Fiji>), then converted to 32-bit temperatures in Celsius using a custom batch processing macro function in FIJI (Kefauver et al., 2017) to determine aerial CT. Afterwards, canopy temperature depression (CTD) for each plot, trial and crop season was calculated as the difference between the maximum air temperature of the day and the canopy temperature CT measured during the same day as follows:

$$\text{CTD} = T_{\text{air}} - \text{CT} \quad (1)$$



## 2.4 Shovelomics, soil coring and image processing

For all trials and crop seasons, five random plants were dug manually from the upper 20 cm of soil layer in each plot between anthesis and mid-grain filling. Afterwards, roots of individual plants were washed carefully using a hose, digitised in situ using a Sony ILCE-QX1 camera (Sony Europe Limited, Brooklands; United Kingdom), and the resulting RGB images were processed using GiaRoots software (General Image Analysis of Roots, Georgia Tech Research Corporation and Duke University; USA) as described in Galkovskyi et al. (2012). Assessed traits were crown root-related parameters as follows: the number of connected components (Rccomp); the maximum (MaxR) and median (MedR) number of roots; root system dimensions such as average root width (Rwidth), root network depth (Ndepth), root network length (Nlen) and root network width (Nwidth); the root density by measuring the network area (NwA), the network surface area (Nsurf) and network volume (Nvol); and the root angle via the network convex area (ConvA). In addition, relative traits presented as ratios such as the ratio of network length to the network volume (specific root length (SRL)), the ratio of the maximum root number to the median root number (Network bushiness (Bush)), the total network area divided by the network convex area (Network solidity), the lower 2/3 of the root network depth (length distribution (Ldist)), and the ratio of the network width to the network depth (network width to depth ratio (NWDR)) were also calculated. Root angle (RA) was measured manually using a protractor. Root samples were oven dried afterwards at 60 °C for 72 h, and root dry weight (RDW<sub>0-20</sub>) was determined.

Soil coring was carried out at around mid-grain filling in the INP trial during 2018-2019, 2019-2020 and 2020-2021, in the ILP trial during 2019-2020 and 2020-2021, and in the RLN and RNP trials during 2019-2020 and 2020-2021, respectively. Cores of 100 cm depth were extracted from the centre of each plot using a hydraulic soil corer, then divided into four soil sections (0-25 cm; 20-50 cm; 50-75 cm and 75-100 cm). Approximately 800 g of soil cores were weighed, and from these roots were manually isolated by washing away the soil using tweezers and sieves of different diameters. Once isolated, the roots were saved in a 50% ethanol. The isolation process took a few months and therefore the sampled cores and roots were kept at low temperatures (-8 °C) temperature at all times. To scan the roots, a 0.1% methyl violet solution was prepared to dye them for greater contrast. Initially, a 1 g of methyl violet powder was diluted in 100 ml of 100% ethanol, and then a 1 ml of the concentrated

solution was diluted a second time in 9 ml of 100% ethanol, with the resulting 10 ml solution being further diluted by adding 90 ml of distilled water to give a 0.1 % methyl violet solution. Roots were placed in petri dishes, submerged in the methyl violet solution and kept under dark conditions overnight (Pask et al., 2012). The next day, the dyed roots were carefully dried, scanned (EPSON Perfection 1260, EPSON America Inc., Chicago, USA), and then oven dried at 60 °C for 48 hours to determine the root dry weight of each soil section (RDW<sub>0-25cm</sub>, RDW<sub>25-50cm</sub>, RDW<sub>50-75cm</sub> and RDW<sub>75-100cm</sub>). The scanned root images of different soil sections were analysed using the open-source image analysis platform FIJI (Fiji is Just ImageJ; <http://fiji.sc/Fiji>), to determine root area (Area<sub>Roots</sub>) and the coefficient Area/RDW.

## 2.5 Carbon and nitrogen stable isotope composition and nitrogen content

Analyses were performed in mature grains from all the plots, trials and seasons of the study, and in flag leaves sampled at anthesis during the 2018-2019, 2019-2020 and 2020-2021 seasons. Leaves and grains were dried at 60 °C for a minimum of 48 h and reduced to a fine powder, from which approximately 1 mg was enclosed in tin capsules and analysed using an elemental analyser (Flash 1112 EA; Thermo- Finnigan, Schwerte, Germany) coupled with an isotope ratio mass spectrometer (Delta C IRMS, ThermoFinnigan) operating in continuous flow mode, at the Scientific and Technical facilities of the University of Barcelona. Different secondary standards were used for carbon (IAEA-CH7, IAEA-CH6 and IAEA-600, and USGS 40) and nitrogen (IAEA-600, N1, N2, NO<sub>3</sub>, urea and acetanilide) isotope analyses. The nitrogen concentrations (N) in leaves and grains were expressed in percentages (%), and carbon ( $\delta^{13}\text{C}$ ) and nitrogen ( $\delta^{15}\text{N}$ ) isotope compositions in parts per thousand (‰). The  $\delta^{13}\text{C}$  and  $\delta^{15}\text{N}$  results permitted an analytical precision (standard deviation) of 0.1‰ and 0.3‰, respectively, and were determined following Eq. (2):

$$\delta^{13}\text{C} \text{ or } \delta^{15}\text{N} (\text{‰}) = [R_{\text{sample}}/R_{\text{standard}} - 1] \times 1000 \quad (2)$$

Where  $R_{\text{standard}}$  is the molar abundance ratio of the secondary standard calibrated against the primary standard Pee Dee Belemnite in the case of carbon ( $\delta^{13}\text{C}$ ) and N<sub>2</sub> from air in the case of nitrogen ( $\delta^{15}\text{N}$ ) (Farquhar et al., 1989).

Grain nitrogen yield (GNY) was then calculated as:

$$\text{GNY (Mg ha}^{-1}\text{)} = (\text{N concentration in grains} \times \text{GY})/100 \quad (3)$$

## 2.6 Oxygen and hydrogen stable isotope composition

Post anthesis, samples of the stem base (approximately 6–7 cm length) were harvested from five random plants (main stems) of each selected plot, sealed immediately in analytical tubes and frozen at  $-80\text{ }^{\circ}\text{C}$ . Similarly, samples from different soil sections of the cores collected during grain filling (see Section 2.4) were sealed immediately in analytical tubes and kept at  $-80\text{ }^{\circ}\text{C}$ . The frozen stems and soil samples were sent for water extraction at the Department of Crop and Forest Sciences, University of Lleida (Spain). Briefly, the first phase (water extraction) was performed using a cryogenic vacuum distillation line (Dawson and Ehleringer, 1993). Sample tubes were placed in a heated silicone oil bath ( $120\text{ }^{\circ}\text{C}$ ), and connected with Ultra-Torr™ unions (Swagelok Company, Solon, OH, USA) to a vacuum system ( $\sim 10^{-2}$  mbar), in series, with U-shaped collector tubes cooled with liquid  $\text{N}_2$ . Ninety minutes after commencing extraction, the extracted soil water and xylem water in stems was transferred into 2 ml vials and stored at  $4\text{ }^{\circ}\text{C}$  until analysis. Afterwards, the oxygen ( $\delta^{18}\text{O}$ ) and hydrogen ( $\delta^2\text{H}$ ) stable isotope compositions of stem water were determined at the Scientific Facilities of University of Lleida (Spain), and the  $\delta^{18}\text{O}$  and  $\delta^2\text{H}$  of the water soil sections were measured at the Scientific Facilities of the University of Barcelona (Spain). Analyses in both facilities were carried out by isotope-ratio infrared spectroscopy using a Picarro L2120-I isotopic water analyser coupled to an A0211 high-precision vaporiser (Picarro Inc., Sunnyvale, CA, USA). The analytical precision for  $\delta^{18}\text{O}$  and  $\delta^2\text{H}$  was 0.10‰, and the occurrence of contaminants was tested using Picarro's ChemCorrect post-processing software and corrected, when necessary, following Martín-Gómez et al. (2015).

The values for  $\delta^{18}\text{O}$  and  $\delta^2\text{H}$  of the precipitation water throughout the successive seasons (Supplemental Figure 2) were derived from the monthly values of Valladolid city (a few km from the Zamadueñas station) as provided by the “Centro de Estudios y Experimentación de Obras Públicas (CEDEX)” (CEDEX, 2022), in collaboration with the Spanish “Agencia Estatal de Meteorología” (<https://www.cedex.es/centros-laboratorios/centro-estudios-tecnicas-aplicadas-ceta/lineas-actividad/disenio-metodologia-muestreo-analisis>). In addition, the  $\delta^{18}\text{O}$  and  $\delta^2\text{H}$  of the precipitation and irrigation water at Zamadueñas Station were collected during anthesis/grain filling for the 2018-2019 (only precipitation) and 2020-2021 (precipitation and irrigation) seasons, and analysed as above at the facilities of the University of Barcelona.

## 2.7 Statistical analyses

Analyses of variance (ANOVA) were performed to test the effect of crop seasons, trials, genotypes and soil sections on the studied traits using SPSS software (IBM SPSS Statistics 25, Inc., Chicago, IL; USA). The same software was used (i) to reveal differences within trials and soil sections following the post-hoc Tukey-b test, (ii) to determine Pearson correlations between GY and the rest of the studied traits, and (iii) to perform a stepwise multi-regression analysis with GY as the dependent trait. In addition, Random Forest multi-regression analysis was performed to predict GY under different trials, and to measure the importance of variables introduced by each fitted model using RStudio 1.2.5 (R Foundation for Statistical Computing, Vienna, Austria). For this, the database was randomly split into a training set (80%) and a test set (20%). For each trial, the model was trained using a resampling in the form of 10 times repeated 10-fold cross-validation, with the final selected models exhibiting the optimum determination coefficient ( $R^2_{\text{train}}$ ) with the lowest root mean square error ( $\text{RMSE}_{\text{train}}$ ). To evaluate the models' predictive ability on the test set, the  $R^2_{\text{test}}$  and  $\text{RMSE}_{\text{test}}$  were shown as the Pearson correlation between the tested and the predicted values and the corresponding root mean square error, respectively. Principal component analyses (PCA) were carried out to analyse all the trait categories (including crop growth) in a reduced bi-dimensional platform for each trial using RStudio 1.2.5. Graphs were created using Sigma-plot 10.0 (Systat Software Inc, California; USA).

## 3. Results

### 3.1 Season, growth conditions and genotypic effects on crop growth and yield

When the four crop seasons of the study were combined, the effects of season and trial were highly significant on GY, yield components (plant and ear densities, TKW and HI) and crop growth (PH, NDVI and biomass) traits. However, the genotypic effect was only significant for GY and PH (Table 2). The interaction season x trial was significant for all traits except for TKW and plant density, whereas the interaction year x genotype was significant for GY and ear density alone, and the interaction trial x genotype was only significant for GY. The effect of the triple interaction season x trial x genotype was absent on the studied traits. Genotypes across seasons performed best under INP conditions, exhibiting the highest GY, biomass, HI,

ear density and PH, as opposed to the RLN conditions where GY overall decreased on average by 35%. In addition, RLN generally exhibited lower biomass and HI, lower plant and ear densities, and reduced PH and NDVI compared to INP. Under ILP and RNP, genotypes showed similar performance in combined seasons (29% GY decrease compared to INP), with similar ear density and PH, albeit higher NDVI under ILP compared to RNP.

In separate seasons, the trial effect was significant on all traits in each season. However, the genotypic effect was significant only for HI, TKW, plant and ear densities and PH during 2017-2018; for HI and ear number during 2018-2019; for GY, PH and NDVI during 2019-2020; and for GY, TKW, and PH during 2020-2021. The interaction trial x genotype was absent for any of the traits studied during 2017-2018, significant only for biomass during 2018-2019, significant for GY, PH and NDVI during 2019-2020, and significant for GY and PH during 2020-2021 (Table 2). GY, yield components and crop growth traits showed a similar trend in separate seasons as the four seasons combined, with GY performing the best under INP, and the worst under RLN with decreases of 20%, 65% and 28% compared to INP during the 2017-2018, 2018-2019 and 2019-2020 seasons, respectively. The second worst condition was RNP, where, compared to INP, GY decreased 5%, 62% and 28% during 2017-2018, 2018-2019 and 2020-2021, respectively. In the case of ILP, GY decreased 35% and 24% during 2019-2020 and 2020-2021, respectively. Differences between irrigation and rainfed trials in grain yield and most of the other traits were maximal during the driest (2018-2019) of the four seasons.

**Table 2.** Effects of crop season (2018; 2019; 2020; 2021), trial (INP, ILP, RNP, RLN), and durum wheat genotypes on yield components. ANOVA was tested for trials and genotypes in each crop season and across combined crop seasons.

Crop season	Trial	GY (Mg ha <sup>-1</sup> )	Biomass (Mg ha <sup>-1</sup> )	HI	TKW (g)	Plants (m <sup>-2</sup> )	Ears (m <sup>-2</sup> )	PH (cm)	NDVI
2017-2018	INP	6.16a±0.26	13.94a±0.62	0.441a±0.011	48.15a±1.44	170.4a±7.0	351.1a±15.1	100.4a±1.3	0.73a±0.01
	RNP	5.85ab±0.17	12.89a±0.33	0.455a±0.010	47.63a±1.13	178.9a±9.9	328.4a±11.7	99.4a±1.2	0.67a±0.01
	RLN	4.93b±0.38	10.88b±0.75	0.451a±0.014	49.36a±1.26	142.0b±7.4	325.3a±17.4	90.3b±1.9	0.61b±0.02
	Trial (T)	<0.050	<0.010	ns	ns	<0.010	ns	<0.001	<0.001
	Genotype (G)	ns	ns	<0.001	<0.001	<0.050	<0.010	<0.001	ns
T*G	ns	ns	ns	ns	ns	ns	ns	ns	
2018-2019	INP	7.88a±0.24	15.41a±0.70	0.403a±0.010	46.11a±1.85	208.9a±12.9	417.6a±19.5	86.88a±1.24	0.49a±0.02
	RNP	2.96b±0.14	7.15b±0.35	0.294b±0.015	40.93a±10.13	182.2a±7.2	305.6b±15.9	68.99b±1.38	0.43b±0.02
	RLN	2.76b±0.17	7.04b±0.52	0.297b±0.014	31.38a±1.65	188.7a±14.3	397.3b±23.0	67.06b±2.13	-
	Trial (T)	<0.001	<0.001	<0.001	ns	ns	<0.001	<0.001	<0.050
	Genotype (G)	ns	ns	<0.010	ns	ns	<0.010	ns	ns
T*G	ns	<0.010	ns	ns	ns	ns	ns	ns	
2019-2020	INP	8.36a±0.18	-	-	-	-	-	104.8a±1.3	0.75a±0.01
	ILP	5.43c±0.16	-	-	-	-	-	100.2b±1.5	0.67b±0.01
	RLN	6.04b±0.30	-	-	-	-	-	100.3b±0.9	0.58c±0.02
	Trial (T)	<0.001	-	-	-	-	-	<0.001	<0.001
	Genotype (G)	<0.001	-	-	-	-	-	<0.001	<0.001
T*G	<0.010	-	-	-	-	-	<0.001	<0.001	
2020-2021	INP	6.31a±0.14	-	-	52.02a±0.90	171.1a±7.8	321.2a±13.4	92.28a±1.12	0.68b±0.02
	ILP	4.82b±0.11	-	-	48.98b±1.14	185.7a±5.1	309.4a±7.6	77.03c±0.90	0.74a±0.01
	RNP	4.52b±0.17	-	-	42.39c±0.95	171.8a±4.5	308.5a±7.5	87.94b±0.98	0.61c±0.01
	Trial (T)	<0.001	-	-	<0.001	ns	ns	<0.001	<0.001
	Genotype (G)	<0.001	-	-	<0.001	ns	ns	<0.050	ns
T*G	<0.001	-	-	ns	ns	ns	<0.010	ns	
All seasons	INP	7.26a±0.15	14.17a±0.48	0.42a±0.01	48.76a±0.90	183.5a±6.1	364.0a±10.9	96.77a±0.10	0.67b±0.01
	ILP	5.17b±0.11	-	-	48.98a±1.14	185.7a±5.1	309.4b±7.6	90.60b±2.03	0.70a±0.01
	RLN	4.75c±0.25	9.02b±0.57	0.38b±0.02	40.63a±1.84	164.7a±8.8	315.8b±12.3	87.65c±2.01	0.59c±0.01
	RNP	5.19b±0.19	10.02b±0.54	0.37b±0.02	43.65a±3.43	177.6a±4.4	320.1b±7.2	90.68b±1.59	0.60c±0.01
	Season (S)	<0.001	<0.001	<0.001	ns	ns	ns	<0.001	<0.001
	Trial (T)	<0.001	<0.001	<0.050	ns	ns	<0.010	<0.001	<0.001
	Genotype (G)	<0.010	ns	ns	ns	ns	ns	<0.010	ns
	S*T	<0.001	<0.001	<0.001	ns	ns	<0.050	<0.001	<0.050
	S*G	<0.010	ns	ns	ns	ns	<0.050	ns	ns
	T*G	<0.050	ns	ns	ns	ns	ns	ns	ns
S*T*G	ns	ns	ns	ns	ns	ns	ns	ns	

Values are means of the selected genotypes in each season with 3 replicates. Levels of significance for the ANOVA:  $P < 0.05$ ,  $P < 0.01$  and  $P < 0.001$ . Means exhibiting different letters a, b Values are means of the selected genotypes in each season with three replicates. Levels of significance for the ANOVA:  $P < 0.05$ ,  $P < 0.01$  and  $P < 0.001$ . Means exhibiting different letters a, b and c, are significantly different ( $P < 0.05$ ) according to Student's *t*-test on independent samples, within each crop season and across combined seasons. GY, grain yield; HI, harvest index; TKW, thousand kernel weight; PH, plant height; NDVI, nitrogen difference vegetation index; CTD, canopy temperature depression; INP, irrigated normal planting. ILP, irrigated late planting. RNP, rainfed normal planting. RLN, rainfed low nitrogen. S, crop season. T, trial. G, genotype.

### 3.2 Season, growth conditions and genotypic effects on crop nitrogen status

To assess crop nitrogen status, the grain nitrogen yield (GNY), nitrogen concentration (N) and nitrogen isotope composition ( $\delta^{15}\text{N}$ ) in leaves and grains were evaluated across seasons and trials (Table 3). When combining seasons, the effects of season and trial were significant on all traits, whereas the effect of genotype was significant on GNY alone. The interaction year x trial was significant for GNY,  $N_{\text{grain}}$  and  $\delta^{15}\text{N}_{\text{grain}}$ , while the triple interaction year x trial x genotype was only significant for GNY. Overall, GNY was the highest under INP and lower under ILP, RNP and RLN.  $N_{\text{grain}}$  was the highest under RNP and similar (albeit lower) under INP, ILP and RLN.  $\delta^{15}\text{N}_{\text{leaf}}$  and  $\delta^{15}\text{N}_{\text{grain}}$  were higher under irrigated trials (INP and ILP), and lower under rainfed trials (RNP and RLN).

In separate seasons, the trial effect was significant on GNY and  $\delta^{15}\text{N}_{\text{grain}}$  during the four seasons, on  $N_{\text{grain}}$  during 2017-2018, 2018-2019 and 2019-2020, on  $N_{\text{leaf}}$  during 2018-2019, on  $\delta^{15}\text{N}_{\text{grain}}$  during 2017-2018 and on  $\delta^{15}\text{N}_{\text{leaf}}$  during 2018-2019 and 2020-2021. The genotypic effect was significant on GNY during 2018-2019, and on GNY and  $N_{\text{grain}}$  during 2020-2021. The trial x genotype interaction was significant for GNY during 2020-2021 alone (Table 3). Except for the first season (2017-2018), GNY was higher under INP than in the other treatments, with differences being again maximal during the driest season (2018-2019). Moreover, during 2017-2018,  $\delta^{15}\text{N}_{\text{grain}}$  was higher under RNP and lower under INP and RLN, while  $N_{\text{grain}}$  was higher under RLN, intermediate under RNP and lower under INP. During 2018-2019,  $N_{\text{leaf}}$ ,  $\delta^{15}\text{N}_{\text{leaf}}$  and  $\delta^{15}\text{N}_{\text{grain}}$  were the highest and  $N_{\text{grain}}$  the lowest under irrigated conditions (INP). During the third season (2019-2020),  $\delta^{15}\text{N}_{\text{grain}}$  was the highest under INP, and lower under ILP and RLN, whereas  $N_{\text{grain}}$  was the highest under irrigated conditions (INP followed by ILP), and lower under RLN. During 2020-2021,  $\delta^{15}\text{N}_{\text{grain}}$  was higher under INP and RNP than under ILP, whereas the opposite occurred for  $\delta^{15}\text{N}_{\text{leaf}}$ .

**Table 3.** Effects of crop season (2018; 2019; 2020; 2021), trial (INP, ILP, RNP, RLN), and durum wheat genotypes on nitrogen status traits (grain nitrogen yield (GNY), leaf and grain nitrogen concentrations ( $N_{\text{leaf}}$  and  $N_{\text{grain}}$ ), nitrogen isotope compositions ( $\delta^{15}N_{\text{leaf}}$  and  $\delta^{15}N_{\text{grain}}$ ), and water status parameters (canopy temperature depression (CTD), carbon isotope compositions ( $\delta^{13}C_{\text{leaf}}$  and  $\delta^{13}C_{\text{grain}}$ )) measured in the dry matter of leaves at anthesis and grains at maturity, and oxygen ( $\delta^{18}O$ ) and hydrogen ( $\delta^2H$ ) isotope compositions in the water of the stem base at anthesis. ANOVA was tested for trials and genotypes in each crop season and across combined crop seasons.

Season	Trial	Nitrogen status					Water status				
		GNY (Mg ha <sup>-1</sup> )	$N_{\text{leaf}}$ (%)	$N_{\text{grain}}$ (%)	$\delta^{15}N_{\text{leaf}}$ (‰)	$\delta^{15}N_{\text{grain}}$ (‰)	CTD (°C)	$\delta^{13}C_{\text{leaf}}$ (‰)	$\delta^{13}C_{\text{grain}}$ (‰)	$\delta^{18}O_{\text{stem}}$ (‰)	$\delta^2H_{\text{stem}}$ (‰)
2017-2018	INP	0.123ab±0.007	-	1.9b±0.0	-	2.2b±0.1	0.51a±0.37	-	-26.6a±0.1	-6.1±0.2	-57.3±1.0
	RNP	0.130a±0.006	-	2.2a±0.1	-	3.5a±0.3	1.19a±0.51	-	-26.5a±0.1	-5.4±0.4	-58.5±2.0
	RLN	0.101b±0.010	-	2.0ab±0.1	-	2.3b±0.2	-1.25b±0.41	-	-26.5a±0.1	-4.2±0.7	-53.5±2.5
	Trial (T)	<0.050	-	<0.050	-	<0.001	<0.010	-	ns	-	-
	Genotype (G)	ns	-	ns	-	ns	ns	-	<0.010	-	-
T*G	ns	-	ns	-	ns	ns	-	ns	-	-	
2018-2019	INP	0.173a±0.007	4.1a±0.1	2.2b±0.1	3.0a±0.1	2.5a±0.1	-2.71a±0.71	-28.3b±0.1	-25.4c±0.2	-6.5c±0.2	-55.2b±0.8
	RNP	0.086b±0.004	4.1a±0.3	3.0a±0.1	0.6c±0.1	1.2b±0.1	-13.40b±1.02	-26.3a±0.2	-22.6b±0.3	-5.2b±0.2	-57.1b±1.1
	RLN	0.071c±0.002	3.5b±0.1	2.7a±0.1	1.7b±0.2	2.3a±0.2	-14.36b±0.92	-26.0a±0.2	-22.4a±0.2	-3.7a±0.3	-51.9a±1.0
	Trial (T)	<0.001	<0.050	<0.001	<0.001	<0.001	<0.001	<0.001	<0.001	<0.001	<0.001
	Genotype (G)	<0.010	ns	ns	ns	ns	ns	<0.010	<0.050	ns	ns
T*G	ns	ns	ns	ns	ns	ns	ns	ns	ns	ns	
2019-2020	INP	0.196a±0.006	-	2.3a±0.0	1.7a±0.2	2.5a±0.1	-2.05b±0.25	-29.0b±0.2	-26.6b±0.1	-	-
	ILP	0.122b±0.005	-	2.2ab±0.1	-	2.0b±0.1	0.05a±0.28	-	-26.4ab±0.1	-	-
	RLN	0.127b±0.007	-	2.1b±0.1	2.1a±0.3	2.0b±0.1	-1.68b±0.31	-28.4a±0.2	-26.3a±0.1	-	-
	Trial (T)	<0.001	-	<0.050	ns	<0.001	<0.001	<0.001	<0.050	-	-
	Genotype (G)	ns	-	<0.010	<0.050	ns	<0.010	<0.001	<0.050	-	-
T*G	ns	-	ns	ns	ns	ns	ns	<0.010	-	-	
2020-2021	INP	0.124a±0.003	-	2.0a±0.1	3.4b±0.2	3.5a±0.1	-0.88b±0.62	-28.3a±0.4	-26.5b±0.1	-5.8a±0.2	-52.5a±0.9
	ILP	0.100b±0.005	-	2.1a±0.1	4.9a±0.2	3.0b±0.1	2.33ab±0.66	-28.0a±0.2	-26.2b±0.2	-5.8a±0.2	-53.0a±1.1
	RNP	0.097b±0.004	-	2.2a±0.1	2.7c±0.1	3.4a±0.1	2.87a±1.61	-27.4a±0.1	-25.0a±0.1	-6.7a±0.1	-60.0b±0.7
	Trial (T)	<0.001	-	ns	<0.001	<0.001	<0.050	ns	<0.001	ns	<0.050
	Gen (G)	<0.010	-	<0.001	ns	ns	ns	ns	<0.010	ns	ns
T*G	<0.050	-	ns	ns	ns	ns	ns	ns	ns	ns	
All seasons	INP	0.157a±0.005	-	2.1b±0.1	2.6b±0.1	2.7a±0.1	-1.34b±0.28	-28.6b±0.2	-26.3b±0.1	-6.2b±0.1	-54.3a±0.6
	ILP	0.112b±0.004	-	2.2b±0.0	4.9a±0.2	2.4ab±0.1	1.03a±0.37	-28.0b±0.2	-26.3b±0.1	-5.8b±0.2	-53.0a±1.1
	RNP	0.105b±0.004	-	2.4a±0.1	1.7c±0.2	2.2b±0.2	-5.36d±0.83	-26.9a±0.1	-25.2a±0.2	-5.9b±0.2	-58.6b±0.7
	RLN	0.102b±0.005	-	2.2b±0.1	1.9c±0.2	2.2b±0.1	-3.08c±1.08	-27.2a±0.2	-25.2a±0.2	-3.9a±0.3	-52.3a±1.0
	Season (S)	<0.001	-	<0.001	-	<0.001	<0.001	-	<0.001	ns	ns
	Trial (T)	<0.001	-	<0.001	-	<0.010	<0.001	-	<0.001	<0.001	<0.001
	Genotype (G)	<0.050	-	ns	-	ns	ns	-	ns	ns	ns
	S*T	<0.001	-	<0.050	-	<0.001	<0.001	-	<0.001	ns	ns
	S*G	ns	-	ns	-	ns	ns	-	<0.010	ns	ns
	T*G	ns	-	ns	-	ns	ns	-	ns	ns	ns
S*T*G	<0.050	-	ns	-	ns	ns	-	ns	ns	ns	

Values are means of the selected genotypes in each season with the replicates. Levels of significance for the ANOVA:  $P < 0.05$ ,  $P < 0.01$  and  $P < 0.001$ . Means exhibiting different letters a, b and c, are significantly different ( $P < 0.05$ ) according to Student's t-test on independent samples, within each crop season and across combined seasons. INP, irrigated normal planting. ILP, irrigated late planting. RNP, rainfed normal planting. RLN, rainfed low nitrogen. S, crop season. T, trial. G, genotype. Values of  $\delta^{18}O_{\text{stem}}$  and  $\delta^2H_{\text{stem}}$  during 2017-2018 are given for one replicate only.



### 3.3 Season, growth conditions and genotypic effects on crop water status

Crop water status was evaluated through carbon isotope composition ( $\delta^{13}\text{C}$ ) in leaves and grains, and canopy temperature depression (CTD) (Table 3). When combining all seasons, the effects of season and trial and the interaction season x trial were significant on CTD and  $\delta^{13}\text{C}_{\text{grain}}$ . The genotypic effect was not significant for  $\delta^{13}\text{C}_{\text{grain}}$  and CTD, whereas only the season x genotype interaction was significant for  $\delta^{13}\text{C}_{\text{grain}}$ . The effect of the triple interaction was not significant on the assessed traits. Overall, CTD was the highest and  $\delta^{13}\text{C}_{\text{grain}}$  the lowest under irrigated conditions (INP and ILP), as opposed to rainfed conditions (RNP and RLN), where CTD was the lowest and  $\delta^{13}\text{C}_{\text{grain}}$  the highest.

In separate seasons, the trial effect was significant on CTD,  $\delta^{13}\text{C}_{\text{leaf}}$  and  $\delta^{13}\text{C}_{\text{grain}}$  in all seasons, except for  $\delta^{13}\text{C}_{\text{grain}}$  during 2017-2018, and  $\delta^{13}\text{C}_{\text{leaf}}$  during 2020-2021. The genotypic effect was significant for  $\delta^{13}\text{C}_{\text{grain}}$  during all seasons,  $\delta^{13}\text{C}_{\text{leaf}}$  during 2018-2019 and 2019-2020, and CTD during 2019-2020, while the trial x genotype interaction effect was absent, except for  $\delta^{13}\text{C}_{\text{grain}}$  during 2019-2020. CTD was higher under INP and RNP and lower under RLN during 2017-2018; during 2018-2019, CTD was higher, and  $\delta^{13}\text{C}_{\text{leaf}}$  and  $\delta^{13}\text{C}_{\text{grain}}$  lower under irrigated (INP) compared with rainfed conditions. During 2019-2020, CTD was higher under ILP than under INP and RLN, whereas  $\delta^{13}\text{C}_{\text{leaf}}$  and  $\delta^{13}\text{C}_{\text{grain}}$  were the lowest under irrigated conditions (INP and ILP), and the highest under RLN. During 2020-2021, both CTD and  $\delta^{13}\text{C}_{\text{grain}}$  were lower under irrigated conditions (INP and ILP) compared with RNP.

### 3.4 Season, growth conditions and genotype and soil section effects on root characteristics

The structure of the upper part of the root system was assessed through shovelomics. When all seasons were considered together, the effects of season, trial, genotype and the interaction season x trial were significant for most shovelomics-derived traits (Table 4). Under irrigated conditions (INP and ILP),  $\text{RDW}_{0-20}$  and root ratios (Bush, Ldist, NWDR and SRL) were lower, and root crown traits (Rccomp, MaxR and MedR), root dimension traits (Rwidth, Ndepth and Nwidth), root density traits (NwA, Nsurf, Nvol) and root angle (ConvA) were higher than under rainfed conditions (RNP and RLN). Concerning the root ratios, their values were the highest under RLN conditions.

In separate seasons, trial and genotypic effects were significant on most root traits during all seasons, except for 2019-2020, where significance was associated mostly with trial effect. The trial x genotype interaction was significant mostly during the first two seasons (2017-2018 and 2018-2019). During 2017-2018, Rcomp and SRL were higher, and root density (RDW<sub>0-20</sub>, Nwidth, NwA, Nsurf and Nvol) and dimensions (Rwidth, Ndepth and Nlen), root angle (RA and ConvA) and NWDR were lower under irrigated conditions (INP) compared with rainfed conditions (RNP). As for RLN, RDW<sub>0-20</sub> and Nwidth, root angle spread (RA) and NWDR were higher, with a generally reduced root density, dimension and SRL. During 2018-2019, most root traits were higher under irrigated conditions (INP), except for Rcomp, which was the lowest under INP compared to rainfed trials (RNP and RLN). Comparing rainfed conditions, root density and dimension were higher under RNP than RLN, whereas Rcomp was higher under RLN than under RNP. During 2019-2020, root number, density, dimension and root angle traits were the highest under ILP conditions, and lower under INP and RLN, except for RDW<sub>0-20</sub>, which was the second highest under RNP and low under INP. During the fourth season (2020-2021), root number, root density and dimension, root angle (mainly ConvA) and all root ratios were higher under irrigated conditions (ILP and INP) compared with rainfed conditions (RNP).

**Table 4.** Effects of crop season (2018; 2019; 2020; 2021), trial (INP, ILP, RNP, RLN), and durum wheat genotypes on root characteristics. ANOVA was tested for trials and genotypes in each crop season and across combined crop seasons.

Season	Trial	RDW <sub>0-20</sub> (g .plant <sup>-1</sup> )	Root crown			Root dimensions			Root density				Root angle		Ratios					
			Rccomp	MaxR	MedR	Rwidth (cm)	Ndepth (cm)	Nlen (cm)	Nwidth (cm)	NwA	Nsurf (cm <sup>2</sup> )	Nvol (cm <sup>3</sup> )	ConvA (cm <sup>2</sup> )	RA (°)	Bush	Ldist	Network Solidity	NWDR	SRL (cm <sup>-2</sup> )	
2017-2018	INP	1.02b	2.77a	21.86a	10.91a	0.03b	6.44ab	135.8b	5.71b	3.96b	14.62b	0.15b	28.22b	66.71b	2.27a	1.15a	0.14a	0.96b	949.2a	
	RNP	2.42a	1.13b	21.75a	10.32a	0.05a	7.01a	161.5a	7.51a	5.80a	22.00a	0.30a	40.54a	90.91a	2.30a	1.17a	0.15a	1.12ab	577.4c	
	RLN	2.03a	1.12b	20.26a	9.40a	0.04c	6.22b	124.1ab	6.76a	4.04b	15.03b	0.17b	31.50b	84.07a	2.48a	1.37a	0.13a	1.15a	744.0b	
	Trial (T)	<0.001	<0.001	ns	ns	<0.001	<0.050	<0.050	<0.001	<0.001	<0.001	<0.001	<0.001	<0.001	<0.001	ns	ns	ns	<0.050	<0.001
2018-2019	INP	0.67a	1.21c	22.78a	11.63a	0.05a	9.18a	197.9a	7.95a	8.31a	31.09a	0.47a	55.13a	71.65a	2.13a	0.70a	0.16a	0.90a	437.4a	
	RNP	0.72a	2.90b	17.64b	8.66b	0.05a	7.63b	126.9b	6.63b	5.39b	19.86b	0.30b	37.44b	71.07a	2.14a	0.46b	0.15a	0.91a	441.1a	
	RLN	0.60a	4.13a	13.56c	6.56c	0.05a	7.26b	90.9c	6.33b	3.89c	14.15c	0.21c	33.66b	71.34a	2.27a	0.66a	0.12b	0.90a	467.5a	
	Trial (T)	<0.001	<0.001	<0.001	<0.001	<0.001	<0.001	<0.001	<0.001	<0.001	<0.001	<0.001	<0.001	ns	ns	<0.001	<0.001	ns	ns	<0.001
2019-2020	INP	0.43c	3.84a	19.43b	9.81b	0.03a	7.41b	131.3b	6.99b	3.82b	13.94b	0.13a	40.87b	75.86ab	2.15a	0.81a	0.10a	0.98a	1019.6a	
	ILP	0.67a	3.88a	25.81a	13.08a	0.03a	8.80a	209.7a	8.60a	6.01a	21.99a	0.21a	60.04a	81.01a	2.03a	0.79a	0.10a	1.00a	1022.7a	
	RLN	0.55b	3.14a	18.80b	10.19b	0.03a	7.54b	135.8b	6.86b	4.04b	14.42b	0.25a	41.67b	70.61b	2.01a	0.87a	0.14a	0.97a	1024.0a	
	Trial (T)	<0.001	<0.050	<0.001	<0.001	ns	<0.001	<0.001	<0.010	<0.001	<0.001	ns	<0.001	<0.010	ns	ns	ns	ns	ns	ns
2020-2021	INP	1.07a	7.20a	16.73a	8.42a	0.06a	9.97a	174.4a	9.10a	8.73a	34.14a	0.73a	69.78a	71.58b	2.09a	0.69a	0.13b	0.96a	256.9a	
	ILP	1.06a	6.03ab	15.90a	8.75a	0.07a	10.72a	177.6a	7.13b	9.38a	36.80a	0.84a	57.73b	65.91c	1.95a	0.61a	0.17a	0.72a	229.6a	
	RNP	0.69b	3.78b	4.88b	2.88b	0.01b	1.87b	35.9b	2.12c	1.63b	6.26b	0.13b	12.11c	79.08a	0.64b	0.33b	0.04c	0.35b	94.4b	
	Trial (T)	<0.001	<0.050	<0.001	<0.001	<0.001	<0.001	<0.001	<0.001	<0.001	<0.001	<0.001	<0.001	<0.001	<0.001	<0.001	<0.001	<0.001	<0.001	<0.001
All seasons	INP	0.77c	3.76b	20.14a	10.16b	0.04a	8.19b	157.7b	7.40a	6.02b	22.72b	0.35b	47.91b	71.85b	2.16ab	0.83ab	0.13a	0.95ab	693.0b	
	ILP	0.92bc	4.79a	20.28a	10.37a	0.05a	9.77a	186.7a	8.23a	7.09a	26.70a	0.43a	60.49a	73.93b	2.09b	0.53c	0.12a	0.88b	640.9b	
	RNP	1.28a	2.60c	14.49c	7.17d	0.04c	5.44d	106.0c	5.34c	4.21c	15.81c	0.24c	29.67d	79.95a	1.67c	0.63bc	0.11a	0.78c	363.0c	
	RLN	1.01b	2.83c	17.67b	8.87c	0.04b	7.06c	118.9c	6.67b	4.00c	14.52c	0.22c	36.25c	74.87b	2.23a	0.96a	0.13a	1.00a	773.0a	
	Season (S)	<0.001	<0.001	<0.001	<0.001	<0.001	<0.001	ns	ns	<0.001	<0.001	<0.001	<0.001	<0.001	<0.001	<0.001	<0.001	<0.001	<0.001	<0.001
	Trial (T)	<0.001	<0.001	<0.001	<0.001	<0.001	<0.001	<0.001	<0.001	<0.001	<0.001	<0.001	<0.001	<0.001	<0.001	<0.001	<0.001	<0.010	<0.001	<0.001
	Genotype (G)	ns	<0.001	<0.050	<0.050	<0.050	<0.001	<0.001	<0.001	<0.001	<0.001	<0.050	<0.001	ns	ns	ns	ns	<0.001	ns	
	S*T	<0.001	<0.001	<0.001	<0.001	<0.001	<0.001	<0.001	<0.001	<0.001	<0.001	<0.001	<0.001	<0.001	<0.001	ns	ns	<0.010	<0.010	<0.001
	S*G	ns	ns	ns	ns	ns	ns	ns	ns	ns	ns	ns	ns	ns	ns	ns	ns	<0.050	ns	ns
T*G	ns	ns	ns	ns	ns	ns	ns	ns	ns	ns	ns	ns	ns	ns	ns	ns	ns	ns	ns	
S*T*G	ns	ns	ns	ns	ns	ns	ns	ns	ns	ns	ns	ns	ns	ns	ns	ns	ns	ns	ns	

Values are means of the selected genotypes in each season with three replicates. Levels of significance for the ANOVA:  $P < 0.05$ ,  $P < 0.01$  and  $P < 0.001$ . Means exhibiting different letters a, b and c, are significantly different ( $P < 0.05$ ) according to Student's t-test on independent samples, within each crop season and across combined seasons. Rwidth, average root width. Rccomp, number of connected components. MaxR, maximum number of roots. MedR, median number of roots. Ndepth, network depth. Nlen, network length. Nwidth, network width. NwA, network area. Nsurf, network surface area. Nvol, network volume. ConvA, convex area. Bush, bushiness. SRL, specific root length. Ldist, network length distribution. NWDR, network width to depth ratio. RA, root angle measured with a protractor. INP, irrigated normal planting. ILP, irrigated late planting. RNP, rainfed normal planting. RLN, rainfed low nitrogen. S, crop season. T, trial. G, genotype.

Distribution of the root system across the soil profile was assessed through soil coring during the last three seasons and under different growing conditions (Table 5; Figure 2). The genotypic effect was absent when combining all seasons and in separate seasons, therefore, the effects of season, trial, soil section and their interactions were evaluated alternatively on soil cores and water traits. When combining all seasons and treatments, the effects of season, soil section and the season x soil section interaction were significant on the three traits (RDW, Area<sub>roots</sub> and Area/RDW) assessed (Table 5). However, the effects of trial and the interactions season x trial, season x soil section and season x trial x soil section were significant on RDW only (Table 5). RDW was higher under normal planting (INP, RNP and RLN) than at ILP (Figure 2). Across seasons, the first soil section (0-25 cm) exhibited the highest RDW and Area<sub>Roots</sub> and the lowest Area/RDW, followed by the third soil section (50-75 cm), then the second soil section (20-50 cm) with average RDW, an Area<sub>Roots</sub> similar to the third section, but a lower Area/RDW (Table 5). The fourth soil section (70-100 cm) exhibited the lowest RDW and Area<sub>Roots</sub>, and the highest Area/RDW.

RDW, Area<sub>roots</sub> and Area/RDW in separate seasons varied across soil sections in a rather similar manner as they did when combining seasons. Thus, in separate seasons, the effect of soil section was significant on RDW, Area<sub>roots</sub> and Area/RDW during 2018-2019 and 2019-2020, and on RDW and Area/RDW during 2020-2021 (Figure 2; Table 5), whereas the effect of trial was significant on RDW during 2019-2020 (Table 5).

**Table 5.** Effects of crop season (2018-2019; 2019-2020; 2020-2021), trial (INP, ILP, RNP, RLN), genotypes and soil section (0-25cm; 20-50cm; 50-75cm; 75-100cm) on root dry weight (RDW), root area (Area<sub>Roots</sub>) the Area/RDW ratio; and on soil water oxygen ( $\delta^{18}\text{O}_{\text{soil}}$ ) and hydrogen ( $\delta^2\text{H}_{\text{soil}}$ ) stable isotope compositions.

		Genotype effect					Soil section effect							
		Cores			Soil water					Cores			Soil water	
Season		RDW	Area <sub>Roots</sub>	Area/RDW	$\delta^{18}\text{O}_{\text{soil}}$	$\delta^2\text{H}_{\text{soil}}$		RDW	Area <sub>Roots</sub>	Area/RDW	$\delta^{18}\text{O}_{\text{soil}}$	$\delta^2\text{H}_{\text{soil}}$		
2018-2019	Genotype (G)	ns	ns	ns	-	-	Section (Sect)	<0.001	<0.001	<0.001	-	-		
2019-2020	Trial (T)	ns	ns	ns	<0.001	<0.001	Trial (T)	<0.010	ns	ns	<0.001	<0.001		
	Genotype (G)	ns	ns	ns	ns	ns	Section (Sect)	<0.001	<0.001	<0.010	<0.001	<0.001		
	T*G	ns	ns	ns	ns	ns	T*Sect	<0.010	ns	ns	ns	ns		
2020-2021	Trial (T)	ns	ns	ns	ns	<0.050	Trial (T)	ns	ns	ns	ns	<0.050		
	Genotype (G)	ns	ns	ns	ns	ns	Section (Sect)	<0.001	ns	<0.001	<0.001	<0.010		
	T*G	ns	ns	ns	ns	ns	T*Sect	ns	ns	ns	<0.001	<0.050		
All seasons	INP	95.4	484.2	45.5a	-6.4a	-54.4bc	0-25	210.4a	559.9a	20.6c	-5.5a	-48.7a		
	ILP	98.2	577.4	72.2a	-6.2b	-52.0b	25-50	67.3c	545.0b	55.6b	-6.1b	-53.7b		
	RNP	118.9	625.2	107.1	-6.4b	-56.6c	50-75	92.9b	535.2b	31.9bc	-6.3b	-54.3b		
	RLN	126.6	512.9	27.8	-4.6a	-43.4a	75-100	36.3d	494.8c	151.7a	-6.5b	-54.6b		
	Season (S)	<0.050	<0.001	<0.010	ns	ns	Season (S)	<0.001	<0.001	<0.001	ns	<0.001		
	Trial (T)	ns	ns	ns	<0.001	<0.001	Trial (T)	<0.010	ns	ns	<0.001	<0.001		
	Genotype (G)	ns	ns	ns	ns	ns	Section (Sect)	<0.001	<0.001	<0.001	<0.001	<0.001		
	S*T	ns	ns	ns	ns	ns	S*T	<0.050	ns	ns	ns	ns		
	S*G	ns	<0.010	ns	ns	ns	S*Sect	<0.001	<0.001	<0.001	ns	<0.001		
	T*G	ns	ns	ns	ns	ns	T*Sect	<0.001	ns	ns	<0.001	<0.010		
S*T*G	ns	ns	ns	ns	ns	S*T*Sect	<0.010	ns	ns	ns	ns			

Values are means of the selected genotypes in each season with three replicates. Levels of significance for the ANOVA:  $P < 0.05$ ,  $P < 0.01$  and  $P < 0.001$ . Means exhibiting different letters a, b and c, are significantly different ( $P < 0.05$ ) according to Student's t-test on independent samples, within each crop season and across combined seasons. INP, irrigated normal planting. ILP, irrigated late planting. RNP, rainfed normal planting. RLN, rainfed low nitrogen. S, crop season. T, trial. G, genotype. Sect, soil section. Trials tested were INP during 2018-2019; INP, ILP and RLN during 2019-2020; and INP, ILP and RNP during 2020-2021.

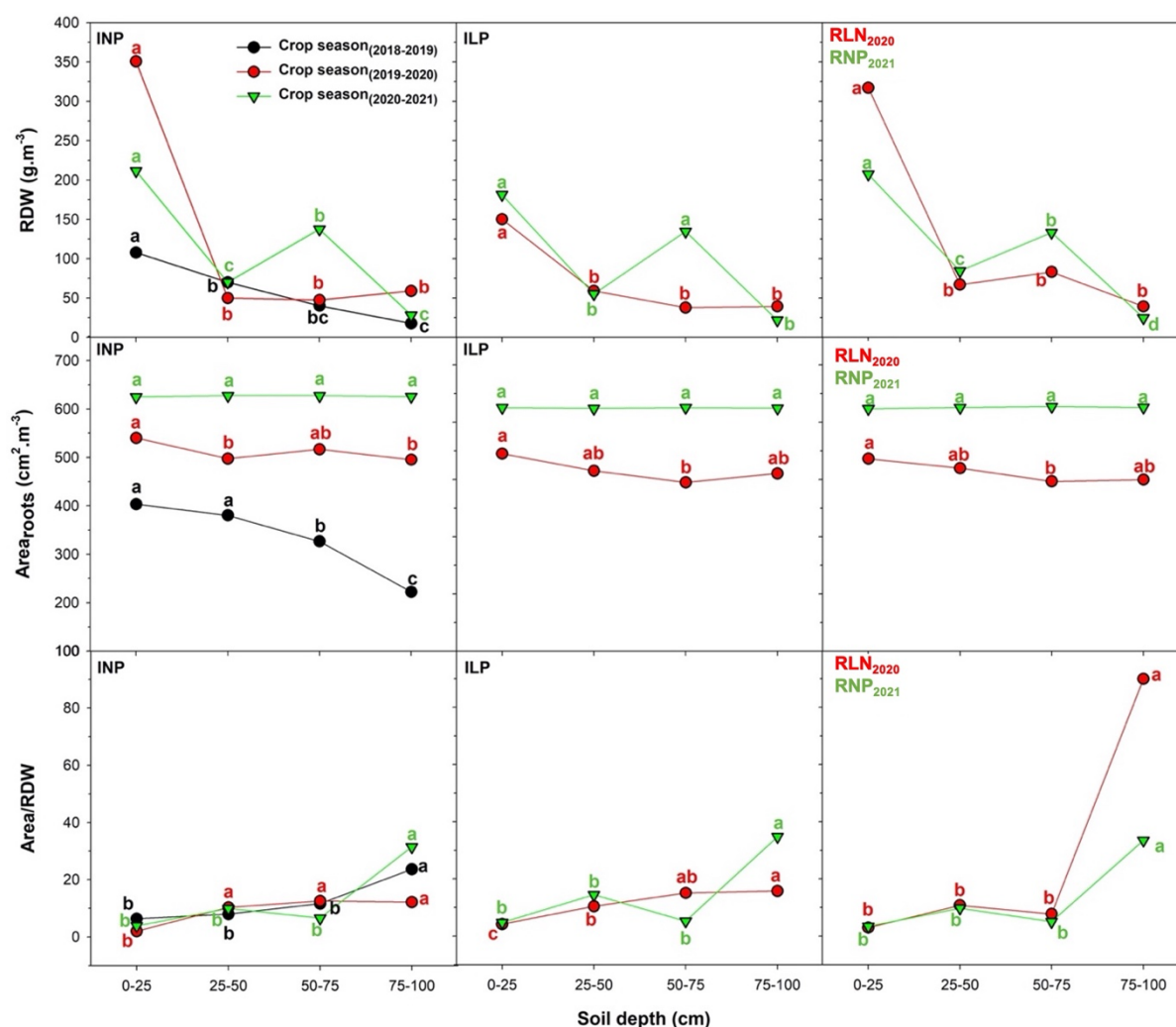


**Figure 2.** Average root dry weight (RDW), root area ( $Area_{Roots}$ ) and the Area/RDW ratio of selected wheat genotypes grown during different crop seasons (2018-2019; 2019-2020 and 2020-2021) and in trials (INP; ILP; RLN; RNP). Means exhibiting different letters are significantly different ( $P < 0.05$ ) (Tukey-b test) on independent samples for each crop season and within each treatment.

### 3.5 Oxygen and hydrogen isotope composition of the soil, plant-stem water and water inputs

To understand from which soil depth the plants extracted water, the oxygen ( $\delta^{18}O$ ) and hydrogen ( $\delta^2H$ ) isotope compositions were evaluated in stem water during 2018-2019 and 2020-2021 (Table 3). In addition, the oxygen ( $\delta^{18}O_{soil}$ ) and hydrogen ( $\delta^2H_{soil}$ ) isotope compositions were assessed in different soil sections for the last two seasons (Table 5, Figure 3), in the water inputs (precipitation and irrigation) (Supplemental Figure 2).

The  $\delta^{18}O$  and  $\delta^2H$  of precipitation ( $\delta^{18}O_{precipitation}$  and  $\delta^2H_{precipitation}$ ) increased from January throughout the crop seasons. Predicted values of  $\delta^{18}O_{precipitation}$  and  $\delta^2H_{precipitation}$  during May, the month when the isotopic signatures in the stem base were analysed, were around -4.7 ‰

and -28.8 ‰ for  $\delta^{18}\text{O}$  and  $\delta^2\text{H}$ , respectively (Supplemental Figure 2). The isotopic values of the irrigation water during 2020-2021 for late May were -4.5 ‰ and -35 ‰ for  $\delta^{18}\text{O}$ , respectively.

The effect of season was only significant on water  $\delta^2\text{H}_{\text{soil}}$ , whereas the effects of soil section and trials were significant on both  $\delta^{18}\text{O}_{\text{soil}}$  and  $\delta^2\text{H}_{\text{soil}}$  (Table 5). Also, the season x soil section interaction was significant on  $\delta^2\text{H}_{\text{soil}}$ , and the trial x soil section interaction was significant on  $\delta^{18}\text{O}_{\text{soil}}$  and  $\delta^2\text{H}_{\text{soil}}$ . Across both seasons,  $\delta^{18}\text{O}_{\text{soil}}$  and  $\delta^2\text{H}_{\text{soil}}$  were the highest in the first soil section (0-25 cm), and similar in the rest of the soil sections (25-50 cm; 50-75 cm; 75-100 cm). In separate seasons, the effects of trial and soil section were significant on  $\delta^{18}\text{O}_{\text{soil}}$  and  $\delta^2\text{H}_{\text{soil}}$  during 2019-2020, whereas during 2020-2021, the trial effect was only significant on  $\delta^2\text{H}_{\text{soil}}$ , and the effect of soil section was significant on  $\delta^{18}\text{O}_{\text{soil}}$  and  $\delta^2\text{H}_{\text{soil}}$  (Table 5). Although the  $\delta^{18}\text{O}_{\text{soil}}$  and  $\delta^2\text{H}_{\text{soil}}$  values in both irrigation trials (INP and ILP) were rather similar and steady across the soil sections, with just a decrease in the  $\delta^2\text{H}_{\text{soil}}$  values in the upper soil section (which was less evident in the ILP), decreases in both  $\delta^{18}\text{O}_{\text{soil}}$  and  $\delta^2\text{H}_{\text{soil}}$  across the upper soil sections were steeper under rainfed conditions (RNP and RLP), in addition,  $\delta^{18}\text{O}_{\text{soil}}$  and  $\delta^2\text{H}_{\text{soil}}$  further decreased through the deeper sections in the case of RNP (Figure 3). On the other hand, the  $\delta^{18}\text{O}_{\text{soil}}$  and  $\delta^2\text{H}_{\text{soil}}$  values of RLN (2019-2020) were higher than those of RNP and both irrigation trials (INP, ILP).

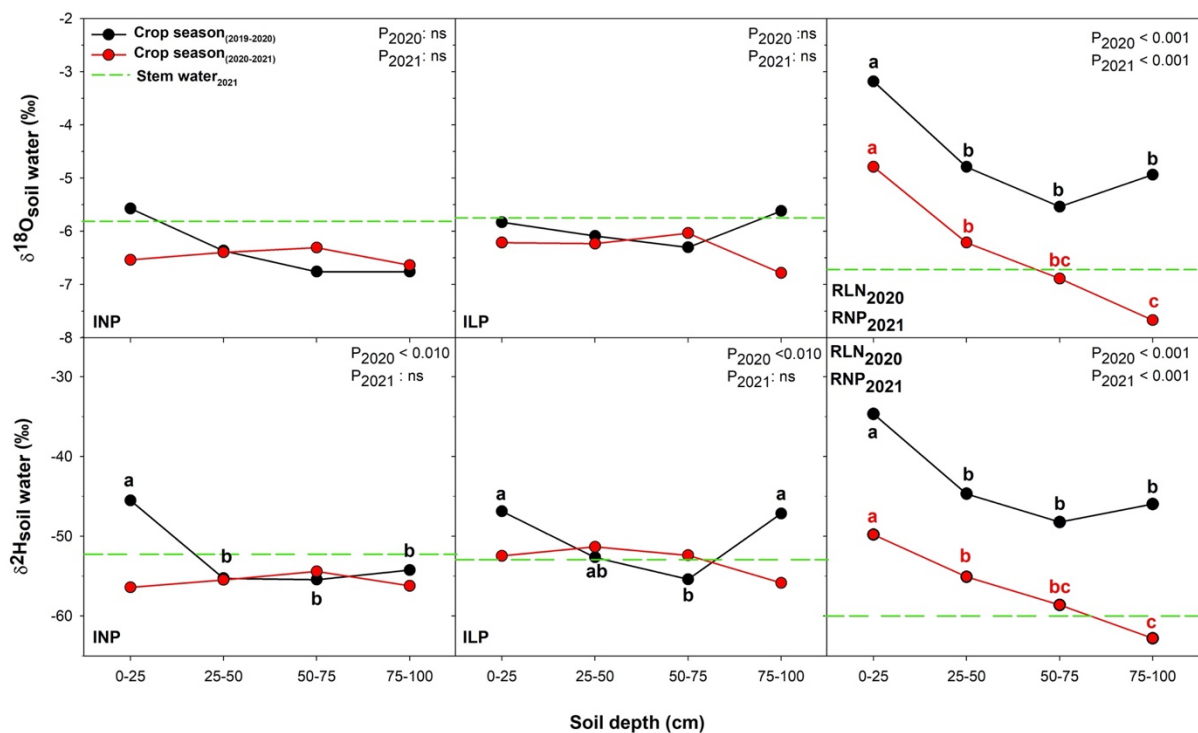


**Figure 3.** Average values of soil water oxygen ( $\delta^{18}O$ ) and hydrogen ( $\delta^2H$ ) stable isotope compositions sampled in different soil sections (0-25 cm; 20-50 cm; 50-75 cm and 75-100 cm), during the crop seasons 2019-2020 and 2020-2021. Means exhibiting different letters are significantly different ( $P < 0.05$ ) (Tukey-b test) on independent samples for each crop season and within each treatment. The baselines represent the mean values of oxygen ( $\delta^{18}O$ ) and hydrogen ( $\delta^2H$ ) stable isotope compositions sampled in irrigation water and precipitation during soil sampling.

In stem water, when combining both seasons, only the effect of trial was significant on  $\delta^{18}O_{\text{stem}}$  and  $\delta^2H_{\text{stem}}$  (Table 3). Thus, the treatment with the lowest (i.e. most negative) values was INP, followed by both ILP and RNP, while rainfed conditions under low nitrogen (RLN) exhibited the highest values. Likewise, in separate seasons, only the trial effect was significant on  $\delta^{18}O_{\text{stem}}$  and  $\delta^2H_{\text{stem}}$  during 2018-2019, and on  $\delta^2H_{\text{stem}}$  during 2020-2021.

### 3.6 Relationships between grain yield and the studied traits

Pearson correlations of GY against agronomic and crop growth traits, and nitrogen and water status indicators were determined under combined and separated seasons and trials (Supplemental Tables 2 and 3). When combining all cases (seasons and trials), GY was positively correlated with all agronomic yield components and crop growth traits, together with CTD, and  $\delta^{15}N_{\text{grain}}$ , and negatively correlated with  $N_{\text{grain}}$  and most of the of stable isotopes ( $\delta^{15}N_{\text{leaf}}$ ,  $\delta^{13}C_{\text{leaf}}$  and  $\delta^{13}C_{\text{grain}}$ , and  $\delta^{18}O_{\text{stem}}$ ). Across all seasons and for irrigated trials, biomass, plant and ear densities and PH, and  $N_{\text{grain}}$  were positively correlated with GY, whereas  $\delta^{15}N_{\text{leaf}}$ ,



$\delta^{18}\text{O}_{\text{stem}}$  and  $\delta^2\text{H}_{\text{stem}}$  were correlated negatively with GY under INP, and only PH was positively correlated with GY under ILP. For the rainfed trials across all seasons, GY was correlated positively with most agronomic traits (except for plant density) and CTD, and negatively with  $N_{\text{grain}}$ ,  $\delta^{15}\text{N}_{\text{leaf}}$ ,  $^{15}\text{N}_{\text{grain}}$ ,  $\delta^{13}\text{C}_{\text{leaf}}$  and  $\delta^{13}\text{C}_{\text{grain}}$  under RLN. Likewise, GY correlated positively with biomass, HI, PH and NDVI, CTD and  $^{15}\text{N}_{\text{leaf}}$ , and negatively with  $N_{\text{grain}}$ ,  $\delta^{13}\text{C}_{\text{leaf}}$ ,  $\delta^{13}\text{C}_{\text{grain}}$ ,  $^{18}\text{O}_{\text{stem}}$  and  $\delta^2\text{H}_{\text{stem}}$  under RNP (Supplemental table 3). In separate seasons, similar correlation trends were observed of GY crop growth traits and water status in each season, for the trials combined and separated, during 2017-2018 and 2018-2019. In addition, GY correlated with nitrogen status traits mainly under 2018-2019 for the combined trials, as well as within RNP (Supplemental Table 3).

Further, Pearson correlations of GY against root traits were evaluated combining all seasons and trials (Supplemental Tables 4 and 5). Thus, most shovelomic traits correlated positively with GY, whereas in soil coring-derived traits,  $\text{RDW}_{50-75\text{cm}}$  correlated negatively, and  $\text{RDW}_{75-100\text{cm}}$  positively with GY. The  $\text{Area}_{\text{Roots}}$  of all soil sections correlated negatively with GY, while the ratio  $\text{Area}/\text{RDW}$  correlated negatively with GY in three soil sections (0-25 cm, 25-50 cm and 75-100 cm), and positively in the 50-75 cm soil section. In separate trials and combined seasons (Supplemental Table 4), GY correlations were negative with  $\text{RDW}_{0-20}$ ,  $\text{Rwidth}$  and network solidity under INP; positive with  $\text{MaxR}$ ,  $\text{MedR}$ ,  $\text{Nwidth}$ ,  $\text{RA}$ ,  $\text{NWDR}$  and  $\text{SRL}$ , and negative with  $\text{Rwidth}$  and  $\text{Ldist}$  under ILP; positive under  $\text{MaxR}$ ,  $\text{MedR}$ ,  $\text{Nlen}$ ,  $\text{Nwidth}$ ,  $\text{ConvA}$  and  $\text{SRL}$ , and negative with  $\text{Rwidth}$  under RLN; and positive with  $\text{RDW}_{0-20}$ ,  $\text{RA}$  and  $\text{Ldist}$ , and negative with  $\text{Rcomp}$  under RNP. Soil coring-derived traits were correlated under irrigated conditions only; under INP, GY correlated negatively with  $\text{RDW}_{50-75\text{cm}}$ ,  $\text{Area}_{\text{Roots}}$  of all soil sections and  $\text{Area}/\text{RDW}$  in all soil sections but 50-75 cm, and negatively with  $\text{Area}_{\text{Roots}}$  at 70-100 cm under ILP.

In separate seasons and combined trials (Supplemental Table 5), GY correlations were mostly shown with shovelomics-derived traits during 2018-2019 and 2020-2021. In separate seasons and separate trials, positive correlations of GY were shown with root crown, density, dimension, root angle and  $\text{Ldist}$  under INP during 2018-2019; and with density and dimensions under RLN and RNP during the same season. During 2019-2020, GY correlated positively with root crown, density, dimension and root angle under RLN; and with  $\text{RA}$  and  $\text{NWDR}$  under ILP.

### 3.7 Relationships of $\delta^{18}\text{O}_{\text{stem}}$ and $\delta^2\text{H}_{\text{stem}}$ with water and nitrogen status and root traits

Besides the correlation of  $\delta^{18}\text{O}_{\text{stem}}$  with GY (and to a lesser extent  $\delta^2\text{H}_{\text{stem}}$  with GY) of both rainfed and support irrigation normal planting trials (Figure 4),  $\delta^{18}\text{O}_{\text{stem}}$  was also negatively correlated with the CTD of the rainfed trials, as well as with both categories (normal planting rainfed and irrigation) of the combined trials. Moreover,  $\delta^{18}\text{O}_{\text{stem}}$  was positively correlated with  $\delta^{13}\text{C}$  of mature grains from the rainfed trials, and also negatively correlated with the  $\delta^{15}\text{N}$  of mature grains from the rainfed trials, as well as combining both categories (rainfed and support irrigation) (Figure 4). Furthermore, in the case of the two support-irrigation categories of trials (INP and ILP),  $\delta^{18}\text{O}_{\text{stem}}$  was positively correlated with the total digital (i.e. pixel) root area of the two deeper (50-100 cm) core sections, and negatively correlated with the  $\text{Area}/\text{RDW}_{50-75\text{cm}}$ .  $\delta^2\text{H}_{\text{stem}}$  followed the same pattern but in general the relationships were weaker.  $\delta^{18}\text{O}_{\text{stem}}$  and  $\delta^{12}\text{H}_{\text{stem}}$  were also correlated with some shovelomic traits, but in this case only in the INP trial. Thus, the root-dimensional trait  $R_{\text{width}}$  together with the RA correlated positively with  $\delta^{18}\text{O}_{\text{stem}}$  and  $\delta^{12}\text{H}_{\text{stem}}$ , while the ratios  $L_{\text{dist}}$  and  $\text{SRL}_{0-20\text{cm}}$  correlated negatively. Under rainfed conditions the relationships between root characteristics and  $\delta^{18}\text{O}_{\text{stem}}$  and  $\delta^2\text{H}_{\text{stem}}$  were scarcer, the shovelomics  $L_{\text{dist}}$  ratio correlated negatively with  $\delta^{12}\text{H}_{\text{stem}}$ . However, unlike the support irrigation trials,  $\text{Area}_{\text{Roots } 50-75\text{cm}}$  was negatively correlated with  $\delta^{18}\text{O}_{\text{stem}}$  (Supplemental Table 6).

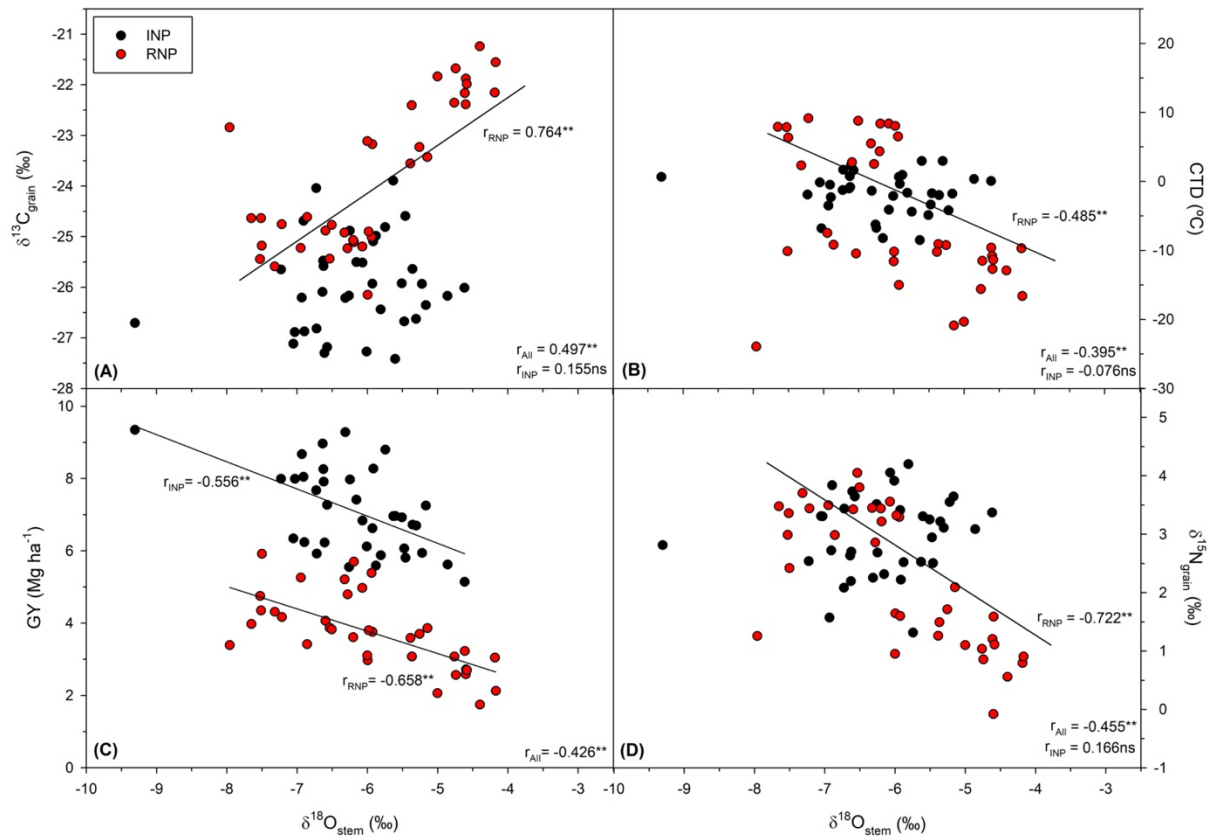


**Figure 4.** Relationship between the oxygen isotope composition of the water in the base of the stem ( $\delta^{18}O_{stem}$ ) and the carbon isotope composition ( $\delta^{13}C$ ) of mature grains (A), the canopy temperature depression (CTD) measured during grain filling (B), grain yield (GY) (C) and the nitrogen isotope composition ( $\delta^{15}N$ ) of mature grains (D). Each symbol represents an individual plot value of a rainfed (open symbols) or a support irrigation (filled symbols) trial, under normal planting (INP and RNP, respectively) from the 2018-2019 and 2020-2021 growing seasons.

### 3.8 GY-prediction models

Multilinear regression analyses were carried out to evaluate the contribution of nitrogen and water status traits, together with root traits to explain GY performance across seasons and under combined and separated trials (Table 6), and under separated seasons and trials (Supplemental Table 7). Given their direct relation with GY, all the agronomic yield components and growth traits were excluded from the prediction models. When combining all seasons and trials, regression models explained 47.6 % of GY variability with  $\delta^{13}C_{grain}$  and  $RDW_{0-20}$  as negative explicative variables, and  $MaxR$  and  $\delta^{15}N_{grain}$  as positive explicative variables. Across seasons and under INP, 44.6 % of GY variability was explained using  $RDW_{0-20}$ ,  $RA_{0-20}$  and network solidity as negative traits, and  $Nlen$  as a positive trait; under ILP, 39.7 %

of GY was explained with  $RA_{0-20}$  and CTD as positive traits; under RLN, 66.3 % of GY variability was explained using  $\delta^{13}C_{\text{grain}}$  as a negative trait, and Rcomp and  $\delta^{15}N_{\text{grain}}$  as positive traits; and finally under RNP, 77.4 % of GY variability was explained using  $\delta^{13}C_{\text{grain}}$  as a negative trait and Ldist as a positive trait (Table 6). Similar results were achieved when performing analysis using Random Forest (RF) models (also excluding all agronomic yield components and growth traits), with  $R^2_{\text{train}}$  being 47.8 % when combining all seasons and trials, 22.5 % under INP, 52.2 % under RLN, and 69.6 % under RNP, but only 0.2 % under ILP (Table 8). Furthermore, similar explanatory traits were given by the RF regression model to the stepwise model when combining all seasons and trials, and in combined seasons and separate trials (Table 7). When separating seasons and combining trials, GY performance was explained as the best during 2018-2019 ( $R^2_{\text{stepwise}} = 90.8 \%$ ;  $R^2_{\text{RF}} = 82.9 \%$ ), by introducing  $\delta^{13}C_{\text{grain}}$ ,  $\delta^{18}O_{\text{stem}}$  and Nwidth as negative explanatory variables, and Nlen, Ldist and  $\delta^2H_{\text{stem}}$  as positive explanatory variables in the stepwise model (Supplemental Table 8). Similar traits were introduced in the RF model as well (Supplemental Table 8).

**Table 6.** Multi-linear regression (stepwise) of grain yield (GY) as the dependent variable, and canopy temperature depression (CTD), stable carbon and nitrogen isotope compositions ( $\delta^{13}\text{C}$  and  $\delta^{15}\text{N}$ ) and nitrogen concentration (N) of mature grains, and shovelomic root traits as independent variables. For each stepwise equation, the fitted model was significant ( $P < 0.001$ ) with ( $1.2 < \text{Durbin-Watson} < 2$ ) and collinearity was within the acceptable range ( $\text{VIF} < 10$ ).  $R^2$  displays the reliability of the fitted regression line to the data used in the stepwise regression ( $R^2_{\text{stepwise}}$ ), and random forest regression ( $R^2_{\text{Train}}$  and  $R^2_{\text{Test}}$ ). Standard error of the dependent variable was given for the stepwise regression as (SE), and for random forest regression as RMSE of the training set ( $\text{RMSE}_{\text{Train}}$ ) and the test set ( $\text{RMSE}_{\text{Test}}$ ).

Model	Equation	Stepwise		Random Forest			
		$R^2$	SE	$R^2_{\text{Train}}$	$\text{RMSE}_{\text{Train}}$	$R^2_{\text{Test}}$	$\text{RMSE}_{\text{Test}}$
All	$\text{GY} = -13.065 - 0.57 * \delta^{13}\text{C}_{\text{grain}} - 0.29 * \text{RDW}_{0-20} + 0.25 * \text{MaxR} + 0.16 * \delta^{15}\text{N}_{\text{grain}}$	0.476	1.3	0.478	1.8	0.590	1.3
INP	$\text{GY} = 11.85 - 0.69 * \text{RDW}_{0-20} + 0.34 * \text{Nlen} - 0.26 * \text{RA} - 0.23 * \text{Network solidity}$	0.446	1.0	0.225	1.3	0.344	1.3
ILP	$\text{GY} = 2.03 + 0.69 * \text{RA} + 0.26 * \text{CTD}$	0.397	0.6	0.020	0.6	0.340	0.6
RLN	$\text{GY} = -23.78 - 1.02 * \delta^{13}\text{C}_{\text{grain}} + 0.48 * \text{Rccomp} + 0.21 * \delta^{15}\text{N}_{\text{grain}}$	0.663	1.1	0.522	1.7	0.820	1.0
RNP	$\text{GY} = -10.63 - 0.76 * \delta^{13}\text{C}_{\text{grain}} + 0.22 * \text{Ldist}$	0.774	0.7	0.696	0.5	0.727	0.9

*Regressions were generated using individual plots of the selected genotypes across all crop seasons. To generate stepwise and random forest regression models, 234 plots were used for All, 78 plots for INP, 42 plots for ILP, 60 plots for RLN and 54 plots for RNP.*

**Table 7.** List of the top 20 explanatory variables for grain yield (GY) ranked by importance in each Random Forest model. Ranking is expressed as a percentage (%). Orange coloured cells show the variables that were introduced by the stepwise regression models as explanatory variables, and the green coloured cells highlight CTD ranking as the main explicit parameter to temperature.

Random Forest ranking (%)									
Trait	All	Trait	INP	Trait	ILP	Trait	RLN	Trait	RNP
$\delta^{13}\text{C}_{\text{grain}}$	100.0	RDW <sub>0-20</sub>	100.0	RA	100	$\delta^{13}\text{C}_{\text{grain}}$	100.0	$\delta^{13}\text{C}_{\text{grain}}$	100.0
CTD	49.1	Ldist	16.3	NWDR	88.3	CTD	89.1	CTD	98.2
N <sub>grain</sub>	18.9	N <sub>grain</sub>	13.2	Nwidth	87.0	SRL	43.4	Rccomp	69.4
SRL	9.4	SRL	9.9	Rwidth	85.1	Rwidth	37.2	$\delta^{15}\text{N}_{\text{grain}}$	35.7
RDW <sub>0-20</sub>	6.3	CTD	9.0	MaxR	72.3	MedR	25.2	Ldist	12.8
Nlen	5.6	Network solidity	8.8	SRL	60.7	Rccomp	18.2	N <sub>grain</sub>	7.4
MedR	5.2	$\delta^{15}\text{N}_{\text{grain}}$	8.2	Nvol	54.4	MaxR	13.8	SRL	6.1
MaxR	5.1	RA	8.0	N <sub>grain</sub>	52.9	RA	13.7	RA	5.5
Ldist	4.3	Nlen	7.7	MedR	49.0	Nlen	13.0	RDW <sub>0-20</sub>	4.7
Bush	4.2	MedR	6.7	Network solidity	35.2	N <sub>grain</sub>	11.6	NWDR	4.1
Rccomp	4.1	Rwidth	6.4	ConvA	34.4	RDW <sub>0-20</sub>	11.5	MaxR	3.8
NWDR	4.0	NWDR	6.1	RDW <sub>0-20</sub>	31.5	Ndepth	10.2	Nwidth	3.4
ConvA	3.4	MaxR	5.4	Nlen	30.5	$\delta^{15}\text{N}_{\text{grain}}$	8.8	Nlen	3.3
Rwidth	3.4	Nvol	4.4	Ndepth	30.3	NwA	8.3	Rwidth	3.0
$\delta^{15}\text{N}_{\text{grain}}$	3.1	NwA	4.0	Ldist	26.7	NWDR	7.6	MedR	2.7
Ndepth	1.9	Nwidth	3.9	$\delta^{15}\text{N}_{\text{grain}}$	25.4	Nsurf	5.5	Ndepth	2.4
Nwidth	1.8	ConvA	3.6	NwA	19.6	Nvol	3.3	NwA	2.3
NwA	1.8	Ndepth	3.4	Bush	14.9	Ldist	2.2	ConvA	2.2
Nsurf	1.3	Nsurf	2.8	$\delta^{13}\text{C}_{\text{grain}}$	11.7	ConvA	2.1	Nsurf	1.8
Nvol	1.0	$\delta^{13}\text{C}_{\text{grain}}$	1.8	CTD	4.70	Network solidity	1.7	Network solidity	1.1

Introduced variables were: GY, grain yield. CTD, canopy temperature depression. N<sub>grain</sub>, nitrogen concentration in grains.  $\delta^{13}\text{C}_{\text{grain}}$ , carbon isotope composition in grains.  $\delta^{15}\text{N}_{\text{grain}}$ , nitrogen isotope composition in grains. RDW<sub>0-20</sub>, root dry weight in the first 0-20 cm soil layer. Rwidth, average root width. Rccomp, number of connected components. MaxR, maximum number of roots. MedR, median number of roots. Ndepth, network depth. Nlen, network length. Nwidth, network width. NwA, network area. Nsurf, network surface area. Nvol, network volume. ConvA, convex area. Bush, bushiness. SRL, specific root length. Ldist, network length distribution. NWDR, network width to depth ratio. RA, root angle. Models were generated by combining all trials and seasons (All), and across seasons for INP (irrigated normal planting). ILP (irrigated late planting), RNP (rainfed normal planting) and RLN (rainfed low nitrogen).

Additionally, principal components analyses were carried out to assess further relationships between all studied traits (GY, growth parameters, together with nitrogen status, water status and selected root traits), in a bi-dimensional platform for each growing condition across seasons (Figure 5) and in separate seasons (Supplemental Figure 1). Across seasons, the two principal components explained 53.5 % of the variability under INP, with  $N_{\text{grain}}$ , RA, Rcomp and SRL traits positioned in the same direction as GY, and RDW,  $\delta^{15}N_{\text{grain}}$  and Rwidth in the opposite direction from GY. In a similar manner, 60.8 % of the variability was explained under ILP, with  $N_{\text{grain}}$ , PH, Rcomp, RA and SRL positioned in the same direction as GY, and  $\delta^{13}C_{\text{grain}}$ ,  $\delta^{15}N_{\text{grain}}$  and Rwidth in the opposite direction. Regarding the two rainfed conditions, the results were very similar. Thus, under RLN, 69.4 % of the variability was explained, with PH, CTD, SRL and Rcomp traits placed in the same direction as GY, and  $N_{\text{grain}}$ ,  $\delta^{13}C_{\text{grain}}$ ,  $\delta^{15}N_{\text{grain}}$  and Rwidth in the opposite direction. Under RNP, 69.3% of the variability was explained, with PH, NDVI,  $\delta^{15}N_{\text{grain}}$ , CTD, RA and RDW placed in the same direction with GY, and  $\delta^{13}C_{\text{grain}}$ , Rcomp,  $N_{\text{grain}}$  and Rwidth in the opposite direction to GY (Figure 5).

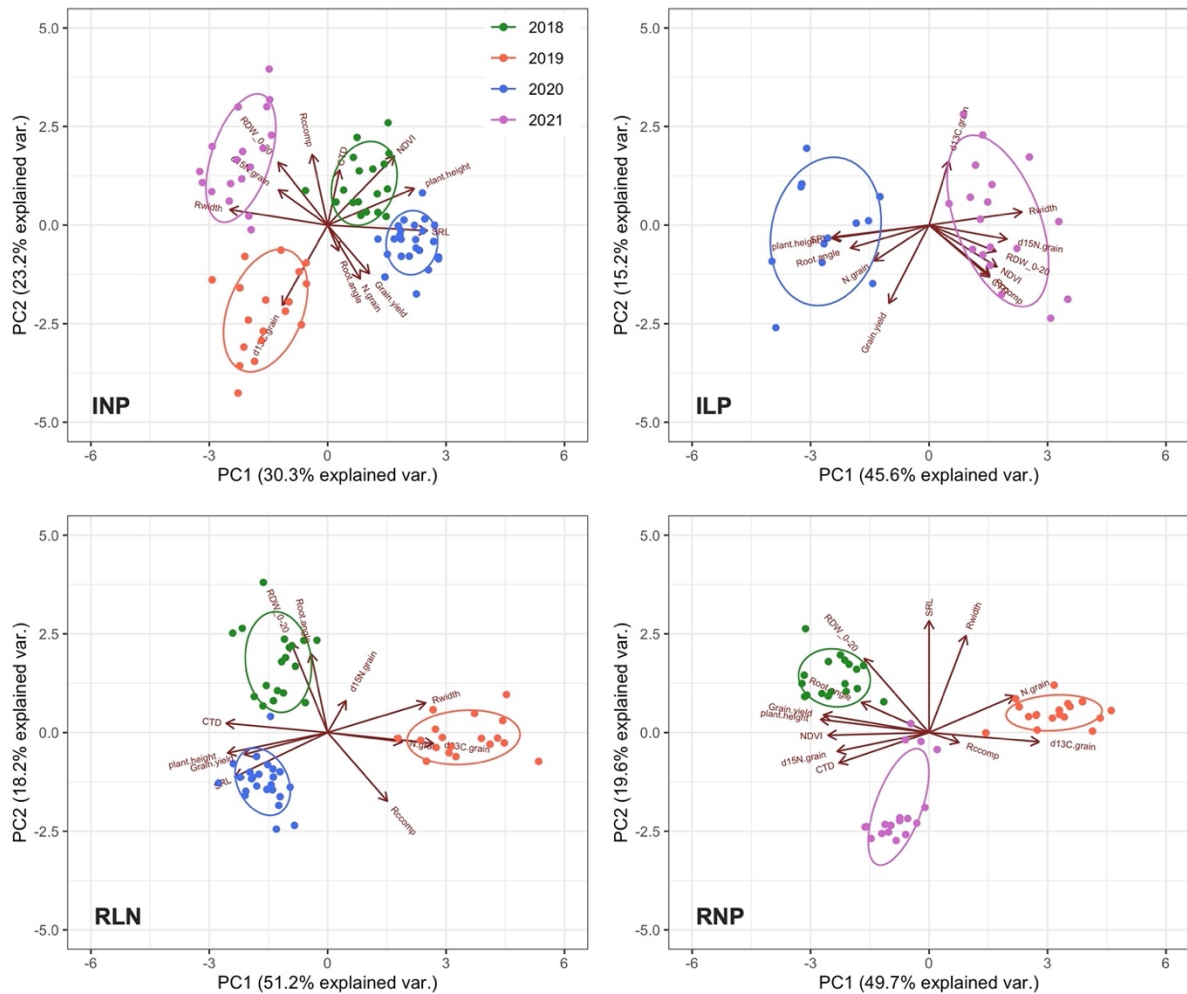


**Figure 5.** Principal component analysis (PCA) of the selected wheat cultivars grown during four consecutive crop seasons (2017-2018; 2018-2019; 2019-2020 and 2020-2021) combined, and under different treatments (INP, ILP, RLN and RNP). The variables included in the analysis are grain yield, plant height, NDVI, canopy temperature depression (CTD), nitrogen concentration ( $N_{\text{grain}}$ ) of grain dry matter, stable carbon ( $\delta^{13}\text{C}_{\text{grain}}$ ) and nitrogen ( $\delta^{15}\text{N}_{\text{grain}}$ ) compositions of grain dry matter, oxygen ( $\delta^{18}\text{O}_{\text{stem}}$ ) and hydrogen ( $\delta^2\text{H}_{\text{stem}}$ ) isotope compositions of the stem water, and selected root traits: root dry weight in the 0-20 cm soil layer ( $\text{RDW}_{0-20}$ ), average root width (Rwidth), number of connected components in the root crown (Rcomp), specific root length ( $\text{SRL}_{0-20}$ ), and root angle measured with a protractor (Root angle).

In separate seasons, the variability explained under INP trials ranged from 39.1% (2019-2020) to 52.8% (2017-2018), with CTD and  $\text{RDW}_{0-20}$  being positive traits with GY during the three consecutive seasons (2017-2018; 2018-2019 and 2019-2020),  $\delta^{18}\text{O}_{\text{stem}}$  and  $\delta^2\text{H}_{\text{stem}}$  being negative traits during 2018-2019 and 2020-2021, and  $\delta^{13}\text{C}_{\text{grain}}$  being a negative trait in all seasons. RA however, was placed positively relative to GY during the humid season (2017-2018), and negatively relative to GY in the rest of the seasons (2018-2019; 2019-2020 and 2020-2021). Under ILP, the explained variabilities were 45.5% during 2019-2020 and 48.8% during 2020-2021, with  $\text{RDW}_{0-20}$ , Rcomp and  $\delta^{15}\text{N}_{\text{grain}}$  being positive traits, and  $\delta^{13}\text{C}_{\text{grain}}$  being a negative trait relative to GY during both seasons, RA being a positive trait relative to GY



under 2019-2020, and  $\delta^{18}\text{O}_{\text{stem}}$  and  $\delta^2\text{H}_{\text{stem}}$  being negative traits relative to GY during 2020-2021. Under RLN, the explained variabilities were 55.3 %, 49.9% and 51.3% during 2017-2018, 2018-2019 and 2020-2021, respectively. For the three seasons, CTD,  $\text{RDW}_{0-20}$ ,  $\delta^{15}\text{N}_{\text{grain}}$  were positive traits relative to GY, and  $\delta^{13}\text{C}_{\text{grain}}$  was a negative trait to GY. Moreover, RA was placed in the same direction as GY during 2017-2018 and 2020-2021, and opposite to GY with  $\delta^{18}\text{O}_{\text{stem}}$  and  $\delta^2\text{H}_{\text{stem}}$  during 2018-2019. Under RNP, variabilities of 50.3%, 48.5% and 41.3% were explained during 2017-2018, 2018-2019 and 2019-2020, respectively. For each of the three seasons, Rwidth, PH and NDVI were positive traits relative to GY, and  $\text{RDW}_{0-20}$ , RA and  $\delta^{13}\text{C}_{\text{grain}}$  were negative traits to GY.  $\delta^{18}\text{O}_{\text{stem}}$  and  $\delta^2\text{H}_{\text{stem}}$  were negative traits during 2018-2019, as were RA and SRL during 2018-17-2018 and 2018-2019 (Supplemental Figure 1).

## 4. Discussion

### 4.1 Environmental and genotypic effects on crop growth and yield performance

The field experiments included in this study covered a broad environmental range of effects on durum wheat growth and yield performance. The comparative effect of season, trial and genotypes were assessed through the percentage of the sum of squares (SS) on GY. Season ( $\text{SS}_{\text{season}} = 13.70\%$  of  $\text{SS}_{\text{model}}$ ) and crop management ( $\text{SS}_{\text{trial}} = 48.7\%$  of  $\text{SS}_{\text{model}}$ ) were major factors in the study and accounted for a wide range of grain yield under different Mediterranean scenarios. By contrast, the genotypic effect, even if significant, was minor on GY ( $\text{SS}_{\text{genotype}} = 2.97\%$  of  $\text{SS}_{\text{model}}$ ), which agrees with previous studies highlighting the reduced genotypic variation in durum wheat compared with bread wheat (Asins and Carbonell, 1989; Martínez-Moreno et al., 2020). Similarly, the genotypic effect was significant, albeit minor, on water and nitrogen status and most shovelomics-derived traits, and was absent from soil-coring root traits. The lack of genotypic differences for the soil coring root traits in our study was likely due to different factors, which may offset minor differences related to genotypic variability (Hodgkinson et al., 2017; Wasson et al., 2014). Among these factors was the low accuracy or the relatively high error inherent in the methodology for root assessment, but also because of the strong plasticity of roots in response to specific growing conditions (Bai et al., 2019; Paez-Garcia et al., 2015; Wasaya et al., 2018). Furthermore, the season and trial effects were highly significant, not only for the growth, water and nitrogen physiological parameters, but also for most of the root traits studied, which make them amenable for

characterisation during yield-performance studies under different crop management conditions or for given growth conditions across seasons. Moreover, since most of the root characteristics studied have shown genotypic differences, they were amenable for defining wheat ideotypes under specific management practices and seasons.

#### 4.2 GY-prediction models and root traits

The importance of traits that inform about root architecture mostly relies on the interplay between root distribution and root function and their effects on crop productivity, as well as the availability of water and nutrients in the soil (Chen et al., 2017). Root architecture is also characterised by a wide phenotypic plasticity (Clark et al., 2011; Hodge, 2009; Malamy, 2005). In this sense, root architecture associated with good agronomic performance often depends on the target environment and agronomic conditions (Wasaya et al., 2018). Therefore, it is advisable to study the contribution of root traits under different settings, including different environmental growing conditions such as combinations of management methods across seasons (i) and within a season (ii), as well as in a given crop management condition across seasons (iii) and within a season (iv). We addressed these factors through GY-prediction models that included water and nitrogen status traits and shovelomics derived root traits (Boudiar et al., 2021; Manschadi et al., 2010; Nehe et al., 2021; Thoday-Kennedy et al., 2022).

For the first three scenarios we ran stepwise and random forest (RF) models, complemented with principal component analysis, while for the fourth setup, given the limited size of the data set, RF was not run. Some season-specific models also included stable oxygen and hydrogen signatures of the stem water. Similarly, the PCA analyses included crop growth traits, while these traits were omitted in the multilinear stepwise and RF analyses.

The strength of the predicting models was good overall. When combining all seasons and agronomic conditions, stepwise and RF models explained nearly 50% of the variability in GY. Within each season, prediction models that combined all the growing conditions were highly variable in their performance, explaining from around 20% variability in GY in the wettest season (2017-2018) to 90% in the driest season (2018-2019). The rather variable performance of the prediction models was related to the GY variability, which was the highest in the driest season (where GY was about three-fold different in trials' average values) and the lowest

(around 20% difference) in the wet season. This illustrates the need for a wide range of values in the data set to develop strong GY prediction models, particularly when combining very diverse agronomic conditions, including different irrigation, fertilisation and planting date designs (Barraclough et al., 1989; Chapman et al., 2012; Hernandez-Ochoa et al., 2019). By contrast, models for each growing condition alone, across seasons, were more stable, explaining between 40-80% of the variability in GY, particularly when using stepwise models.

#### 4.3 Crop performance and root traits across agronomic conditions

When combining all seasons and growth conditions, GY prediction provided by stepwise and RF models integrated water status traits (CTD and/or  $\delta^{13}\text{C}_{\text{grain}}$ ) as primary explicative variables, which indicates that water status was the main driver of GY variability when considering the overall effect of season x growth conditions. CTD and  $\delta^{13}\text{C}$  have been used as time instantaneous (CTD) and integrative ( $\delta^{13}\text{C}$ ) indicators of the effect of water stress on yield (Araus and Cairns, 2014). Cooler canopies, as shown by higher CTD values, have been linked to deeper roots (Lopes and Reynolds, 2010; Reynolds et al., 2007; Wasaya et al., 2018), and higher CTD and lower  $\delta^{13}\text{C}$  values are often related to higher grain yield performance in wheat genotypes (Araus et al., 2003; 2008; Blum, 2009; Chairi et al., 2020; Farquhar et al., 1989; Rezzouk et al., 2020, 2022). Crown root traits informing on root density ( $\text{RDW}_{0-20}$ ) and number (MaxR) in the upper part of the soil (Fradgley et al., 2020; He et al., 2022; York et al., 2018a) were the second most relevant variables to integrate into the GY prediction model.

When considering seasons separately but combining all the growing conditions assayed in a season, the main trait introduced by the model also informed about better water status (lower  $\delta^{13}\text{C}$  or higher CTD). This agrees with water conditions being the main factor affecting wheat productivity across Mediterranean environments (Araus et al. 2014; Rezzouk et al. 2022). In addition, for the most robust model, which corresponded to the driest season (2018-2019), root traits informing about deep rooting tendencies such as greater root length in the upper soil (Nlen and Ldist) (Armengaud, 2009; Clark et al., 2011; He et al., 2022; Iyer-Pascuzzi et al., 2010) and root system spread such as a lower Nwidth (Clark et al., 2011; Iyer-Pascuzzi et al., 2010) were also involved. Moreover, the oxygen ( $\delta^{18}\text{O}$ ) and hydrogen ( $\delta^2\text{H}$ ) isotopic compositions of the stem water, which in principle inform about the depth that water is

extracted from the soil (Kale Çelik et al., 2018; Sanchez-Bragado et al., 2019; Rezzouk et al., 2022) were also included.

#### 4.4 Crop performance within agronomic conditions

Except for support irrigation and normal planting conditions, the specific models for each growing condition throughout the four seasons also included better water status (lower  $\delta^{13}\text{C}$  or higher CTD) as the first chosen trait in the models for rainfed conditions. In the case of rainfed low nitrogen fertilisation conditions, better nitrogen status (higher  $\delta^{15}\text{N}$ ) was also included in the model. These results again stress that the variability in precipitation/evapotranspiration is an important factor affecting wheat productivity under Mediterranean conditions, particularly (but not only) under rainfed conditions (Araus and Slafer, 2011; Rezzouk et al., 2022). Besides that, all four growth condition-specific models included shovelomic-assessed root traits. In the case of support irrigation conditions, root angle spread had a clear role, with steeper roots (lower RA) being fundamental during INP, while shallower roots (higher RA) were involved in the ILP conditions. Moreover, lower root mass dry weight (lower  $\text{RDW}_{0-20}$  and Network solidity) but a greater root length (greater Nlen) in the topsoil were introduced into the INP model. The shallow root system of ILP is coherent with the fact that Mediterranean conditions are characterised by a progressive decrease in precipitation together with an increase in evapotranspiration during late spring, which makes irrigation the main source of water. In the case of INP, a root system that is more evenly distributed (keeping greater root length in the topsoil alongside steeper roots) across the soil profile represents a more efficient alternative. Such a dichotomy in the root system associated with planting date has been reported before (Bai et al., 2019; Rezzouk et al., 2022).

The rainfed conditions included a denser root system in the topsoil as a positive trait; specifically, a greater root ramification (higher Rccomp) in the case of RLN, and a higher network length distribution (higher Ldist) under RNP. This root architecture may contribute to a more efficient capture of effective water by the crop, particularly under low and erratic precipitation conditions. A developed root system in the topsoil has been reported to be an adaptation strategy to tackle Mediterranean conditions (Condon, 2020; Passioura, 1983; Rezzouk et al., 2022). Nevertheless, this conclusion does not preclude the presence of a well-developed root architecture down the soil profile (Barraclough et al., 1989).

The PCA added further information on the traits involved in crop performance within given agronomic conditions across seasons. Under RNP conditions, the best yielding genotypes were associated with stronger aerial growth (higher PH and NDVI), better water (higher CTD and lower  $\delta^{13}\text{C}$ ) and nitrogen status (higher  $\delta^{15}\text{N}$ ), together with shallower root angle (higher RA), and related to this a somewhat greater root density (higher  $\text{RDW}_{0-20}$  but lower  $\text{Rcomp}$ ) in the topsoil. Under RLN, crops with higher GY were associated again with stronger aerial growth (higher PH) together with a better water status (higher CTD and lower  $\delta^{13}\text{C}$ ), while the root system was characterised by thinner roots (higher SRL and lower  $\text{Rwidth}$ ) in the topsoil. However, root angle and root density were not involved, suggesting that the lack of nitrogen prevented roots from properly exploring the soil profile. Higher root density together with thinner roots are considered positive root traits contributing to water and nutrient uptake (Kong et al., 2014; Paez-Garcia et al., 2015; Robbins and Dinneney, 2015; Sun et al., 2015; Tian et al., 2014). Under INP, GY was not clearly associated with higher growth or better water or nitrogen status, but with root characteristics such as shallower root angle (higher RA but close to the centroid of the PCA), lower root density (lower  $\text{RDW}_{0-20}$  and  $\text{Rcomp}$ ) and thinner roots (higher SRL and lower  $\text{Rwidth}$ ) in the topsoil. Under ILP, highly productive crops were again not clearly associated with greater growth, but exhibited better water status (lower  $\delta^{13}\text{C}$ ), shallower root angle (higher RA) and thinner roots (higher SRL and lower  $\text{Rwidth}$ ). The lack of a clear association of grain yield with growth and green biomass under irrigation conditions may be due to the saturation of NDVI above values of 0.5 (Aparicio et al., 2000; Cabrera-Bosquet et al., 2011) and a minor effect of moderate/mild heat stress on plant height. However, rainfed conditions, and to a lesser extent the lack of N fertilisation, placed NDVI values in a linear relationship with green biomass and grain yield (Marti et al. 2007; Cabrera-Bosquet et al. 2011). Moreover, plant height has proven to be a good indicator of the effect of severe water stress on crop growth and yield (Khaliq et al. 2004; Akram et al., 2008).

#### 4.5 Genotypic performance within a given agronomic condition and season

In order to explore genotypic performance, PCA and multilinear stepwise analyses were run for each of the trials and seasons. This included for some seasons the isotope signatures of the stem water as additional traits. Concerning PCA, when evaluating INP in separate seasons, high yielding genotypes exhibited higher growth in general (higher PH and/or NDVI) and better water status (lower  $\delta^{13}\text{C}$  and/or higher CTD), together with steeper root angle (lower

RA). The association between deep rooting and a greater seminal root that grown vertically in wheat was reported previously in high yielding cultivars (Bai et al., 2019; Wasaya et al., 2018). In addition, in the two seasons where stem water was analysed, both  $\delta^{18}\text{O}$  and  $\delta^2\text{H}$  were positioned opposite to GY, suggesting the most productive genotypes extracted water deeper from the soil profile (Martín-Gómez et al., 2015; Rezzouk et al., 2022; Wang et al., 2010). These results support the concept that deeper root systems may confer genotypic adaptation under the mild to moderate water stress conditions experienced under support irrigation (Hodge, 2009; Li et al., 2019; Malamy, 2005; Vadez, 2014). Moreover, the stepwise analysis for 2018-2019 also supports a higher root density (higher Nsurf, Rcomp and Ldist) in the topsoil for the driest season. Overall, these results evidence a dual (shallow and at depth) soil system.

Under ILP, the best yielding genotypes again exhibited stronger plant growth (higher PH) and better water status (lower  $\delta^{13}\text{C}$  and/or higher CTD), but also better nitrogen status (higher  $\delta^{15}\text{N}$ ), together with more superficial rooting, as shown by wider angle spread (higher RA), but also access at depth of water as shown by thinner roots (higher SRL and lower Rwidth) and deeper water uptake (lower  $\delta^{18}\text{O}$  and  $\delta^2\text{H}$  of stem water). These results suggest that even if shallow, deep rooting is an obvious adaptation to late planting under irrigation conditions, ensuring that access to water at deeper soil profiles may be of value. Promoting canopy cooling mechanisms such as deep rooting and superficial root growth, is a common response of wheat plants as a coping mechanism to elevated temperatures when under irrigation conditions (Pinto and Reynolds, 2015; Rezzouk et al., 2022). In addition, a better nitrogen status can reflect a greater stay green status in genotypes, which maintain greener canopies through an active photosynthesis rate (Joshi et al., 2007; York et al., 2018), and it promotes the development of deeper roots in wheat genotypes under drought stress (Christopher et al., 2008).

Under RNP, high yielding genotypes were correlated positively with higher levels of growth (higher NDVI and/or PH) and better water status (lower  $\delta^{13}\text{C}$  and higher CTD). Moreover, the best yielding genotypes also exhibited less superficial root growth with lower root density (lower RDW<sub>0-20</sub>), together with steeper root angle growth (lower RA) and lower  $\delta^{18}\text{O}$  and  $\delta^2\text{H}$  of the stem water. In addition, the stepwise analysis also supported more vertical growth

(greater Ndepth), at least for the driest season (2018-2019). A root system prioritising deeper roots may be able to take advantage of strong but scarce rainfall and optimise the capture of water at depth (Wasson et al., 2012).

Likewise, genotypes with the highest yield under RLN conditions were also associated with higher crop growth and better water (lower  $\delta^{13}\text{C}$  and/or higher CTD) and better nitrogen status (higher  $\delta^{15}\text{N}_{\text{grain}}$ ). The higher  $\delta^{15}\text{N}$  associated with high yielding genotypes may be due to a direct physiological effect on nitrogen metabolism associated with better water status (Yousfi et al. 2009, 2012) or because of a higher soil nitrogen uptake by the plant (Rezzouk et al., 2022; Sanchez-Bragado et al., 2017; Serret et al., 2008; Yousfi et al., 2009) or both. In the last case, the crop not only uses nitrogen derived from chemical fertilisers (with a  $\delta^{15}\text{N}$  close to 0 ‰) but also derives nitrogen from nitrification of the organic matter already present in the soil (which has markedly higher  $\delta^{15}\text{N}$ ). Moreover, the best yielding genotypes under RLN exhibited somewhat higher crown root density (higher  $\text{RDW}_{0-20}$  and/or higher  $\text{Rccomp}$ ) together with steeper root angle (lower RA). A higher root density (higher  $\text{MedR}$ ) and weight (higher  $\text{RDW}$ ) in topsoil was also evidenced through stepwise analysis, at least during the 2019-2020 season. A dual root system comprising shallow roots and others at depth may allow the plant to take advantage of low precipitation as well as a lack of nitrogen, optimising the capture of resources (water and nitrogen) at different depths in the soil (Wasson et al., 2012) and therefore increasing the effective use of water (Blum 2009) and mineral resources. In that sense, Trachsel et al. (2013) reported for maize that genotypes form shallow roots when grown under well fertilised environments (ample nitrogen), and steeper roots that grow at depth when under low nitrogen fertilisation conditions.

#### 4.6 Exploring root architecture at depth: soil coring traits and $\delta^{18}\text{O}$ and $\delta^2\text{H}$ of stem water as phenotyping traits

The high plasticity of the root system may explain why the pattern of root traits conferring adaptation may differ among growing conditions and seasons. The shovelomics approach has proven its value in our study in formulating GY-prediction models. However, an implicit limitation of shovelomics is that, besides crown root informing traits, this methodological approach does not allow a clear inference of the root architecture throughout the soil profile. This is why soil core-derived traits have been used as an extension to root studies at given soil

depths, with root length density (total root length per unit soil volume) as the main determined trait (Chen et al., 2017; Elazab et al., 2012; Foulkes et al., 2009; York et al., 2018b). A higher root length density at soil depth have been reported to improve the capture of belowground resources under drought stress in wheat (Foulkes et al., 2009; Manschadi et al., 2006; Reynolds et al., 2007). However, a larger root system is not necessarily related to higher aerial biomass and yield. Thus, our study showed that core traits such as RDW,  $Area_{\text{roots}}$  and  $Area/RDW$  for the different soil sections were negatively correlated with GY across seasons, under INP, as well as combining all the agronomic conditions together. In this sense, Elazab et al. (2016) working with durum wheat in lysimeters concluded that under water stress, aerial biomass was negatively correlated with root dry biomass, root length and root weight density and positively correlated with the specific root length.

Except for the severe dry season of 2018-2019, our results suggest that regardless of the observed effects of growing conditions (water regimen and planting date) and seasons affecting total RDW across soil sections, and that root biomass decreases at depth, the  $Area_{\text{roots}}$  as an indicator of root functionality remained rather constant across the one metre depth soil profile studied. This was achieved by roots becoming progressively thinner (lower  $Area/RDW$ ) as they moved down through the soil profile. In fact, thinner roots or roots with higher specific root length have been reported as possessing positive traits in terms of wheat performance, not only under lysimeter setups (Elazab et al. 2012, 2016) but also under field conditions (Barraclough et al., 1989; Corneo et al., 2016; Peng et al., 2019; Rezzouk et al., 2022). In addition, the constancy in  $Area_{\text{roots}}$  across soil sections supports the possible existence of a dual root system for all the growing conditions, with the presence of a shallow and deep rooting system (Bai et al., 2019; Rezzouk et al., 2022). However, soil coring, particularly under field conditions, is by no means a high throughput methodology, and is prone to errors associated with separating the fine roots from the soil. Moreover, root architecture does not necessarily directly inform about root functioning. This is why our study also evaluated the  $\delta^{18}\text{O}$  and  $\delta^2\text{H}$  of the stem base water as a phenotyping alternative to assess root function.

The negative correlations of  $\delta^{18}\text{O}_{\text{stem}}$  and  $\delta^2\text{H}_{\text{stem}}$  with the GY of both rainfed and support irrigation normal planting trials (INP and RNP) suggest that the most productive genotypes are those that are capable of exploring water and related resources (e.g. nitrogen) deeper in



soil profiles. This was further supported by the correlations of  $\delta^{18}\text{O}_{\text{stem}}$  with CTD (negative),  $\delta^{13}\text{C}$  (positive) and  $\delta^{15}\text{N}$  (negative), particularly under RNP conditions. In fact, the isotope signatures of  $\delta^{18}\text{O}$  and  $\delta^2\text{H}$  in stem water have been proposed (particularly, but not exclusively, in ecology studies with woody plants) as indicators of the soil depth from which water is extracted by roots (Barbour, 2007; Lin and Sternberg, 1993; Sanchez-Bragado et al. 2019; Wang et al., 2010). The rationality of the approach is simple overall, with the  $\delta^{18}\text{O}$  and  $\delta^2\text{H}$  of the soil water increasing in response to the effect of evaporation, while the deeper the water in the soil the less exposed it is to evaporation (Barbour, 2007; DeNiro and Epstein, 1979; Mateo et al., 2004). On the other hand, the approach assumes that no evaporation (thus isotopic fractionation) occurs once the water is captured and further transported by the root xylem (Cernusak et al., 2016; Dawson and Ehleringer, 1993). The poorer performance of  $\delta^2\text{H}_{\text{stem}}$  compared with  $\delta^{18}\text{O}_{\text{stem}}$  (weaker correlations with GY and related traits) may be due to the fact that the former is much more affected than the latter by fractionation processes and exchanges with atoms of the plant tissue (Sanchez-Bragado et al. 2019). On the other hand, despite the  $\delta^{18}\text{O}$  and  $\delta^2\text{H}$  of the source water (precipitation and irrigation) possibly differing substantially due to climatic factors such as temperature, this was not the case for the precipitation and irrigation water during May, which was the month when stem water was sampled.

Under INP, the negative relationship of the Area/RDW ratio at 50-70 cm with the  $\delta^{18}\text{O}$  and  $\delta^2\text{H}$  of the stem water supports the idea that thinner roots in deeper soil sections are the most functional at extracting water. In the same way, the shovelomic trait informing about root thickness (Rwidth) was also negatively correlated with  $\delta^{18}\text{O}$  and  $\delta^2\text{H}$ . In addition, RA was also positively correlated with  $\delta^{18}\text{O}$  and  $\delta^2\text{H}$ , which supports the concept that the steeper the roots, the greater the depth of water extraction. Under RNP conditions,  $\text{Area}_{\text{Roots } 50-75\text{cm}}$  was negatively correlated with  $\delta^{18}\text{O}_{\text{stem}}$ , suggesting that roots captured water from deeper soil sections. In addition, the shovelomic indicator of tendency to higher root density at depth (Ldist) was negatively correlated with the isotope composition of stem water, which also suggests deeper water extraction under rainfed conditions. In fact, within rainfed conditions, the isotope composition of the soil water clearly decreased with soil depth. The contrasting pattern of relationships between  $\delta^2\text{H}_{\text{stem}}$  and  $\delta^{18}\text{O}_{\text{stem}}$ , with shovelomic and core root traits may be due to the fact that the  $\delta^{18}\text{O}_{\text{soil}}$  and  $\delta^2\text{H}_{\text{soil}}$  followed a different pattern. In the support

irrigation trials,  $\delta^{18}\text{O}_{\text{soil}}$  and  $\delta^2\text{H}_{\text{soil}}$  remained rather stable across the soil profile, while under rainfed conditions a clear gradient towards lower values was found. The pattern of  $\delta^{18}\text{O}_{\text{soil}}$  and  $\delta^2\text{H}_{\text{soil}}$  throughout the soil profile further supports the dual pattern of the root system under support irrigation conditions, while under rainfed conditions, root architecture optimises water extraction at depth.

## 5. Conclusion

The four crop management settings combined with the four consecutive seasons included in this study covered a wide range of grain yields scenarios within the Mediterranean region. However, in all cases higher GY was associated with higher levels of growth (higher PH) and larger green biomass that was maintained longer during grain filling (higher NDVI). Moreover, in almost all cases, greater crop growth was positively associated with a more effective use of resources, particularly water, as inferred from the higher transpiration (higher CTD) and stomatal conductance (lower  $\delta^{13}\text{C}$ ), and to a lesser extent the better nitrogen status, as concluded from the higher nitrogen accumulation (higher GNY and  $\text{N}_{\text{leaf}}$  concentration) associated with a greater demand for nitrogen from the soil (higher  $\delta^{15}\text{N}$ ). This study highlights the highly plastic nature of wheat root architecture when adapting to different Mediterranean conditions. Thus, for given crop management conditions such as rainfed and normal planting, root architecture traits (e.g. root angle) chosen by the models varied between the individual-season models and the model integrating the four seasons. Nevertheless, a broader view was achieved through the shovelomic studies, with RNP conditions inducing deeper root systems, INP presenting a more dual root system (superficial as well as deeper), while ILP and even RLN exhibited more superficial root systems. Nevertheless, our study also highlights the limitation of shovelomics. Thus, soil coring suggests that a constancy in root area is achieved by crops throughout the agricultural soil profile, except for severe drought conditions. However, soil coring is not high throughput enough as a phenotyping approach, and similar to shovelomics, the information derived on root architecture is not necessarily linked to root functioning. On the other hand, the  $\delta^{18}\text{O}$  and  $\delta^2\text{H}$  of the stem water appears as a potential functional phenotyping approach to select crops that are better adapted to Mediterranean conditions, and even though this approach may be affected by the dynamic pattern (i.e. timing) of precipitation/irrigation and sampling time points, the negative relationship of  $\delta^{18}\text{O}$ ,  $\delta^2\text{H}$  to GY suggests that the most productive

crops take water up from deeper soil sections, which makes this approach relatively high throughput for selecting more efficient root systems. This is particularly evident for the rainfed trials, where a clear gradient from a less to a more negative stable isotope composition of soil water was established across soil depths. In the case of support irrigation trials, the gradient was less obvious, which implies that extracting water from deeper soil sections is not necessarily the issue.

### **Credit authorship contribution statement**

FZR wrote the first draft, collected samples, assessed the shovelomics and soil coring root traits, analysed thermal and root images, conducted stable isotope and statistical analyses, drew the tables and figures, and implemented edits under the supervision of JLA and MDS; JLA, MDS and NA conceived and designed the experiment. JLA and MDS revised the draft and implemented edits in the consecutive drafts; NA conducted the field trials and coordinated the agronomic and soil coring data collection. AGR and SCK conducted the flights for thermal imaging. SCK developed the FIJI codes for analysis of the thermal and scanned root images. JS, JLA and NA collaborated to isolate root cores. All authors collaborated in field data assessment.

### **Declaration of Competing Interest**

The authors declare that they have no known competing financial interests or personal relationships that could have appeared to influence the work reported in this paper.

### **Acknowledgments**

This study was supported by the Spanish Project PID2019-106650RB-C21 from the Ministerio de Ciencia e Innovación. JLA acknowledges support from the Catalan Institution for Research and Advanced Studies, Generalitat de Catalunya, Spain, through its ICREA Academia program. FZR is a recipient of a research grant (FI-AGAUR) sponsored by the Agency for Management of University and Research Grants (AGAUR), in collaboration with the University of Barcelona. SCK is supported by the Ramon y Cajal RYC-2019-027818-I research fellowship from the Ministerio de Ciencia e Innovación, Spain. AGR was funded by a Margarita Salas post-doctoral contract from the Spanish Ministry of Universities affiliated with the Research Vice-Rector of

the University of Barcelona. We thank members of the Integrative Crop Ecophysiology Group of the University of Barcelona and the personnel from the experimental station of ITACYL at Zamadueñas (Valladolid) for their assistance during the study's data assessments. We extend our thanks to The Water Research Institute (IdRA) for their financial support to cover laboratory analyses. We thank Dr. J. Voltas from the University of Lleida, Spain, for his support with the  $\delta^{18}\text{O}$  water analyses.

## References

Akram, Z., Ajmal, S. U., Munir, M. (2008). Estimation of correlation coefficient among some yield parameters of wheat under rainfed conditions. *Pak. J. Bot*, 40, 1777-1781.

Amani, I., Fischer, R. A., Reynolds, M. P. (1996). Canopy temperature depression association with yield of irrigated spring wheat cultivars in a hot climate. *J. Agron. Crop Sci.*, 176, 119–129. <https://doi.org/10.1111/j.1439-037X.1996.tb00454.x>

Aparicio, N., Villegas, D., Casadesus, J., Araus, J. L., Royo, C. (2000). Spectral vegetation indices as nondestructive tools for determining durum wheat yield. *Agron. J.*, 92, 83–91. <https://doi.org/10.2134/agronj2000.92183x>

Armengaud, P. (2009). EZ-Rhizo software: The gateway to root architecture analysis. *Plant Signal. Behav.*, 4, 139–141. <https://doi.org/10.4161/psb.4.2.7763>

Araus, J. L., Cairns, J. E. (2014). Field high-throughput phenotyping: the new crop breeding frontier. *Trends Plant Sci.*, 19, 52-61. <https://doi.org/10.1016/j.tplants.2013.09.008>

Araus, J. L., Slafer, G. A. (2011). Crop stress management and global climate change. In *Crop Stress Management and Global Climate Change*. Vol 2. CABI. (pp 1-210). <https://doi.org/10.1079/9781845936808.0000>

Araus, J.L., Villegas, D., Aparicio, N., Garcia del Moral, L. F., El-Hani, S., Rharrabti, Y., Ferrio, J. P., Royo, C. (2003). Environmental factors determining carbon isotope discrimination and yield in durum wheat under Mediterranean conditions. *Crop Sci.*, 43, 170–180. <https://doi.org/10.2135/cropsci2003.0170>

Araus, Jose Luis, Kefauver, S. C., Vergara-Díaz, O., Gracia-Romero, A., Rezzouk, F. Z., Segarra, J., Buchaillet, M. L., Chang-Espino, M., Vatter, T., Sanchez-Bragado, R., Fernandez-Gallego, J. A., Serret, M. D., Bort, J. (2022). Crop phenotyping in a context of global change: what to measure and how to do it. *J. Integr. Plant Biol.*, 64, 592–618. <https://doi.org/10.1111/jipb.13191>

Araus, J. L., Slafer, G. A., Royo, C., Serret, M. D. (2008). Breeding for yield potential and stress adaptation in cereals. *CRC. Crit. Rev. Plant Sci.*, 27, 377–412. <https://doi.org/10.1080/07352680802467736>

Asins, M. J., Carbonell, E. A. (1989). Distribution of genetic variability in a durum wheat world collection. *Theor. Appl. Genet.*, 77, 287–294. <https://doi.org/10.1007/BF00266199>

Aziz, M. M., Palta, J. A., Siddique, K. H. M., Sadras, V. O. (2017). Five decades of selection for yield reduced root length density and increased nitrogen uptake per unit root length in Australian wheat varieties. *Plant Soil*, 413, 181–192. <https://doi.org/10.1007/s11104-016-3059-y>

Bai, C., Ge, Y., Ashton, R. W., Evans, J., Milne, A., Hawkesford, M. J., Whalley, W. R., Parry, M. A. J., Melichar, J., Feuerhelm, D., Basler, P. B., Bartsch, M. (2019). The relationships between seedling root screens, root growth in the field and grain yield for wheat. *Plant Soil*, 440, 311–326. <https://doi.org/10.1007/s11104-019-04088-9>

Barbour, M. M. (2007). Stable oxygen isotope composition of plant tissue: a review. *Funct. Plant Biol.*, 34, 83–94. <https://doi.org/10.1071/FP06228>

Barraclough, P. B., Kuhlmann, H., Weir, A. H. (1989). The effects of prolonged drought and nitrogen fertilizer on root and shoot growth and water uptake by winter wheat. *J. Agron. Crop Sci.*, 163, 352–360. <https://doi.org/10.1111/j.1439-037X.1989.tb00778.x>

Barraclough, P. B., Weir, A. H. (1988). Effects of a compacted subsoil layer on root and shoot growth, water use and nutrient uptake of winter wheat. *J. Agric. Sci.*, 110, 207–216. <https://doi.org/10.1017/S0021859600081235>

Bindi, M., Olesen, J. E. (2011). The responses of agriculture in Europe to climate change. *Reg. Environ. Change*, 11, 151–158. <https://doi.org/10.1007/s10113-010-0173-x>

Bendig, J., Bolten, A., Bennertz, S., Broscheit, J., Eichfuss, S., Bareth, G. (2014). Estimating biomass of barley using crop surface models (CSMs) derived from UAV-based RGB imaging. *Remote Sens.*, 6, 10395–10412. <https://doi.org/10.3390/rs61110395>

Berntson, G. M. (1994). Modelling root architecture: are there tradeoffs between efficiency and potential of resource acquisition? *New Phytol.*, 127, 483–493. <https://doi.org/10.1111/j.1469-8137.1994.tb03966.x>

Berry, Z. C., Emery, N. C., Gotsch, S. G., Goldsmith, G. R. (2019). Foliar water uptake: processes, pathways, and integration into plant water budgets. *Plant Cell Environ.*, 42, 410–423. <https://doi.org/10.1111/pce.13439>

Blum, A. (2009). Effective use of water (EUW) and not water-use efficiency (WUE) is the target of crop yield improvement under drought stress. *F. Crop. Res.*, 112, 119–123. <https://doi.org/10.1016/j.fcr.2009.03.009>

Blum, A., Sullivan, C. Y. (1997). The effect of plant size on wheat response to agents of drought stress. I. root drying. *J. Plant Physiol.*, 24, 35–41. <https://doi.org/https://doi.org/10.1071/PP96022>

Boudiar, R., Cabeza, A., Fernández-Calleja, M., Pérez-Torres, A., Casas, A. M., González, J. M., Mekhlouf, A., Igartua, E. (2021). Root trait diversity in field grown durum wheat and comparison with seedlings. *Agronomy*, 11, 1–18. <https://doi.org/10.3390/agronomy11122545>

Box Jnr, J. E., Ramseur, E. L. (1993). Minirhizotron wheat root data: Comparisons to soil core root data. *Agron. J.*, 85, 1058–1060. <https://doi.org/10.2134/agronj1993.00021962008500050019x>

Bucksch, A., Burrridge, J., York, L. M., Das, A., Nord, E., Weitz, J. S., Lynch, J. P. (2014). Image-based high-throughput field phenotyping of crop roots. *Plant Physiol.*, 166, 470–486. <https://doi.org/10.1104/pp.114.243519>

Cabrera-Bosquet, L., Molero, G., Stellacci, A., Bort, J., Nogués, S., Araus, J. (2011). NDVI as a potential tool for predicting biomass, plant nitrogen content and growth in wheat genotypes subjected to different water and nitrogen conditions. *Cereal Res. Commun.*, 39, 147-159. <https://doi.org/10.1556/crc.39.2011.1.15>

Casper, B. B., Jackson, R. B. (1997). Plant competition belowground. *Annu. Rev. Ecol. and Syst.*, 28, 545–570. <https://doi.org/10.1146/annurev.ecolsys.28.1.545>

Cernusak, L. A., Barbour, M. M., Arndt, S. K., Cheesman, A. W., English, N. B., Feild, T. S., Helliker, B. R., Holloway-Phillips, M. M., Holtum, J. A. M., Kahmen, A., Mcinerney, F. A., Munksgaard, N. C., Simonin, K. A., Song, X., Stuart-Williams, H., West, J. B., Farquhar, G. D. (2016). Stable isotopes in leaf water of terrestrial plants. *Plant Cell Environ.*, 39, 1087–1102. <https://doi.org/10.1111/pce.12703>

Chairi, F., Aparicio, N., Serret, M. D., Araus, J. L. (2020). Breeding effects on the genotype × environment interaction for yield of durum wheat grown after the green revolution: the case of Spain. *Crop J.*, 8, 623–634. <https://doi.org/10.1016/j.cj.2020.01.005>

Chairi, F., Vergara-Diaz, O., Vatter, T., Aparicio, N., Nieto-Taladriz, M. T., Kefauver, S. C., Bort, J., Serret, M. D., Araus, J. L. (2018). Post-green revolution genetic advance in durum wheat: The case of Spain. *F. Crop. Res.*, 228, 158–169. <https://doi.org/10.1016/j.fcr.2018.09.003>

Chapman, S. C., Chakraborty, S., Dreccer, M. F., Howden, S. M. (2012). Plant adaptation to climate change-opportunities and priorities in breeding. *Crop Pasture Sci.*, 63, 251–268. <https://doi.org/10.1071/CP11303>

Ceglar, A., Toreti, A., Zampieri, M., Royo, C. (2021). Global loss of climatically suitable areas for durum wheat growth in the future. *Environ. Res. Lett.*, 16, 1–12. <https://doi.org/10.1088/1748-9326/ac2d68>

Centro de Estudios y Experimentación de Obras Públicas (CEDEX), 2022. <https://www.cedex.es/centros-laboratorios/centro-estudios-tecnicas-aplicadas-ceta/lineas-actividad/disenio-metodologia-muestreo-analisis> (Accessed April 11<sup>th</sup>, 2023).

Chen, X., Ding, Q., Błaszkiwicz, Z., Sun, J., Sun, Q., He, R., Li, Y. (2017). Phenotyping for the dynamics of field wheat root system architecture. *Sci. Rep.*, 7, 1–11. <https://doi.org/10.1038/srep37649>

Chochois, V., Voge, J. P., Rebetzke, G. J., Watt, M. (2015). Variation in adult plant phenotypes and partitioning among seed and stem-borne roots across *Brachypodium distachyon* accessions to exploit in breeding cereals for well-watered and drought environments. *Plant Physiol.*, 168, 953–967. <https://doi.org/10.1104/pp.15.00095>

Choi, W., Ro, H., Lee, S. (2003). Natural <sup>15</sup>N abundances of inorganic nitrogen in soil treated with fertilizer and compost under changing soil moisture regimes. *Soil Biol. Chem.*, 35, 1289–1298. [https://doi.org/10.1016/S0038-0717\(03\)00199-8](https://doi.org/10.1016/S0038-0717(03)00199-8)

Christopher, J. T., Christopher, M. J., Borrell, A. K., Fletcher, S., Chenu, K. (2016). Stay-green traits to improve wheat adaptation in well-watered and water-limited environments. *J. Exp. Bot.*, 67, 5159–5172. <https://doi.org/10.1093/jxb/erw276>

Christopher, J. T., Manschadi, A. M., Hammer, G. L., Borrell, A. K. (2008). Developmental and physiological traits associated with high yield and stay-green phenotype in wheat. *Aust. J. Agric. Res.*, 59, 354–364. <https://doi.org/10.1071/AR07193>

Christopher, J. T., Veyradier, M., Borrell, A. K., Harvey, G., Fletcher, S., Chenu, K. (2014). Phenotyping novel stay-green traits to capture genetic variation in senescence dynamics. *Funct. Plant Biol.*, 41, 1035–1048. <https://doi.org/10.1071/FP14052>

Clark, R. T., MacCurdy, R. B., Jung, J. K., Shaff, J. E., McCouch, S. R., Aneshansley, D. J., Kochian, L. V. (2011). Three-dimensional root phenotyping with a novel imaging and software platform. *Plant Physiol.*, 156, 455–465. <https://doi.org/10.1104/pp.110.169102>

Condon, A. G. (2020). Drying times: plant traits to improve crop water use efficiency and yield. *J. Exp. Bot.*, 71, 2239–2252. <https://doi.org/10.1093/jxb/eraa002>

Corneo, P. E., Suenaga, H., Kertesz, M. A., Dijkstra, F. A. (2016). Effect of twenty four wheat genotypes on soil biochemical and microbial properties. *Plant Soil*, 404, 141–155. <https://doi.org/10.1007/s11104-016-2833-1>



Cossani, C. M., Slafer, G. A., Savin, R. (2010). Co-limitation of nitrogen and water, and yield and resource-use efficiencies of wheat and barley. *Crop Pasture Sci.*, 61, 844–851. <https://doi.org/10.1071/CP10018>

Dainelli, R., Calmanti, S., Pasqui, M., Rocchi, L., Di Giuseppe, E., Monotti, C., Quaresima, S., Matese, A., Di Gennaro, S. F., Toscano, P. (2022). Moving climate seasonal forecasts information from useful to usable for early within-season predictions of durum wheat yield. *Clim. Serv.*, 28, 100324. <https://doi.org/10.1016/j.cliser.2022.100324>

Dawson, T. E., Ehleringer, J. R. (1993). Isotopic enrichment of water in the “woody” tissues of plants: Implications for plant water source, water uptake, and other studies which use the stable isotopic composition of cellulose. *Geochim. Cosmochim. Acta*, 57, 3487–3492. [https://doi.org/10.1016/0016-7037\(93\)90554-A](https://doi.org/10.1016/0016-7037(93)90554-A)

Dawson, T. E., Goldsmith, G. R. (2018). The value of wet leaves. *New Phytol.*, 219, 1156–1169. <https://doi.org/10.1111/nph.15307>

de Deurwaerder, H., Visser, M., Detto, M., Boeckx, P., Meunier, F., Zhao, L., Wang, L., Verbeeck, H. (2020). Diurnal variation in the isotope composition of plant xylem water biases the depth of root-water uptake estimates. *Biogeosciences Discuss.*, Preprint, 1–48.

de Dorlodot, S., Forster, B., Pagès, L., Price, A., Tuberosa, R., Draye, X. (2007). Root system architecture: opportunities and constraints for genetic improvement of crops. *Trends Plant Sci.*, 12, 474–481. <https://doi.org/10.1016/j.tplants.2007.08.012>

DeNiro, M. J., Epstein, S. (1979). Relationship between the oxygen isotope ratios of terrestrial. *Science*, 204, 51–53. <https://doi.org/10.1126/science.204.4388.51>

de Oliveira Silva, A., Ciampitti, I. A., Slafer, G. A., and Lollato, R. P. (2020). Nitrogen utilization efficiency in wheat: A global perspective. *Eur. J. Agron.*, 114, 1–13. <https://doi.org/10.1016/j.eja.2020.126008>

de Vita, P., Mastrangelo, A. M., Matteu, L., Mazzucotelli, E., Virzì, N., Palumbo, M., Storto, M. Lo, Rizza, F., Cattivelli, L. (2010). Genetic improvement effects on yield stability in durum

wheat genotypes grown in Italy. *F. Crop. Res.*, 119, 68–77.  
<https://doi.org/10.1016/j.fcr.2010.06.016>

Eissenstat, D. M. (1991). On the relationship between specific root length and the rate of root proliferation: a field study using citrus rootstocks. *New Phytol.*, 118, 63–68.  
<https://doi.org/10.1111/j.1469-8137.1991.tb00565.x>

Elazab, A., Molero, G., Serret, M. D., Araus, J. L. (2012). Root traits and  $\delta^{13}\text{C}$  and  $\delta^{18}\text{O}$  of durum wheat under different water regimes. *Funct. Plant Biol.*, 39, 379–393.  
<https://doi.org/http://dx.doi.org/10.1071/FP11237>

Elazab, A., Serret, M. D., Araus, J. L. (2016). Interactive effect of water and nitrogen regimes on plant growth, root traits and water status of old and modern durum wheat genotypes. *Planta*, 244, 125–144. <https://doi.org/http://dx.doi.org/10.1007/s00425-016-2500-z>

Fageria, N. K., Moreira, A. (2011). The role of mineral nutrition on root growth of crop plants. In *Adv. Agron.* (1st ed.). Elsevier Inc. <https://doi.org/10.1016/B978-0-12-385531-2.00004-9>

Farquhar, G. D., Ehleringer, J. R., Hubick, K. T. (1989). Carbon isotope discrimination and photosynthesis. *Annu. Rev. Plant Physiol.*, 40, 503–537.  
<https://doi.org/10.1146/annurev.pp.40.060189.002443>

Ferrise, R., Moriondo, M., Bindi, M. (2011). Probabilistic assessments of climate change impacts on durum wheat in the Mediterranean region. *Nat. Hazards Earth System Sci.*, 11, 1293–1302. <https://doi.org/10.5194/nhess-11-1293-2011>

Fischer, R. A. (2011). Wheat physiology: a review of recent developments. *Crop Pasture Sci.*, 62, 95–114. <https://doi.org/10.1071/CP10344>

Fischer, R. A., Rees, D., Sayre, K. D., Lu, Z. M., Condon, A. G., and Larque Saavedra, A. (1998). Wheat yield progress associated with higher stomatal conductance and photosynthetic rate, and cooler canopies. *Crop Sci.*, 38, 1467–1475.  
<https://doi.org/10.2135/cropsci1998.0011183X003800060011x>

Foulkes, M. J., Hawkesford, M. J., Barraclough, P. B., Holdsworth, M. J., Kerr, S., Kightley, S., Shewry, P. R. (2009). Identifying traits to improve the nitrogen economy of wheat: recent advances and future prospects. *F. Crop. Res.*, 114, 329–342. <https://doi.org/10.1016/j.fcr.2009.09.005>

Fradgley, N., Evans, G., Biernaskie, J. M., Cockram, J., Marr, E. C., Oliver, A. G., Ober, E., Jones, H. (2020). Effects of breeding history and crop management on the root architecture of wheat. *Plant Soil*, 452, 587–600. <https://doi.org/10.1007/s11104-020-04585-2>

Galkovskyi, T., Mileyko, Y., Bucksch, A., Moore, B., Symonova, O., Price, C. A., Topp, C. N., Iyer-Pascuzzi, A. S., Zurek, P., Fang, S., Harer, J., Benfey, P. N., Weitz, J. S. (2012). GiA Roots: software for the high throughput analysis of plant root system architecture. *BMC Plant Biol.*, 12, 1-54. <https://doi.org/10.1186/1471-2229-12-116>

Guzmán, C., Autrique, J. E., Mondal, S., Singh, R. P., Govindan, V., Morales-Dorantes, A., Posadas-Romano, G., Crossa, J., Ammar, K., Peña, R. J. (2016). Response to drought and heat stress on wheat quality, with special emphasis on bread-making quality, in durum wheat. *F. Crop. Res.*, 186, 157–165. <https://doi.org/10.1016/j.fcr.2015.12.002>

Haberle, J., Svoboda, P., Raimanová, I. (2008). The effect of post-anthesis water supply on grain nitrogen concentration and grain nitrogen yield of winter wheat. *Plant Soil Environ.*, 54, 304–312. <https://doi.org/10.17221/422-pse>

He, M., Jiang, Y., Liu, L., Zhong, X., Zhao, Y., Ma, W., Tang, G. (2022). Benefits of high nitrogen fertilizer on nitrogen metabolism, nitrogen transfer rate, root system architecture and grain yield of wheat (*Triticum aestivum* L.) under water deficit at heading stage. *Act. Physiol. Plant.*, 44, 1–10. <https://doi.org/10.1007/s11738-022-03460-0>

Ho, M. D., McCannon, B. C., Lynch, J. P. (2004). Optimization modeling of plant root architecture for water and phosphorus acquisition. *J. Theor. Biol.*, 226, 331–340. <https://doi.org/10.1016/j.jtbi.2003.09.011>

Hernandez-Ochoa, I. M., Luz Pequeno, D. N., Reynolds, M., Babar, M. A., Sonder, K., Milan, A. M., Hoogenboom, G., Robertson, R., Gerber, S., Rowland, D. L., Fraise, C. W., Asseng, S. (2019). Adapting irrigated and rainfed wheat to climate change in semi-arid environments:

management, breeding options and land use change. *Eur. J. Agron.*, 109, 1–11. <https://doi.org/10.1016/j.eja.2019.125915>

Hochholdinger, F., Tuberosa, R. (2009). Genetic and genomic dissection of maize root development and architecture. *Curr. Opin. Plant Biol.*, 12, 172–177. <https://doi.org/10.1016/j.pbi.2008.12.002>

Hodge, A. (2004). The plastic plant: root responses to heterogeneous supplies of nutrients. *New Phytol.*, 162, 9–24. <https://doi.org/10.1111/j.1469-8137.2004.01015.x>

Hodge, A. (2009). Root decisions. *Plant Cell Environ.*, 32, 628–640. <https://doi.org/10.1111/j.1365-3040.2008.01891.x>

Hodgkinson, L., Dodd, I. C., Binley, A., Ashton, R. W., White, R. P., Watts, C. W., Whalley, W. R. (2017). Root growth in field-grown winter wheat: Some effects of soil conditions, season and genotype. *Eur. J. Agron.*, 91, 74–83. <https://doi.org/10.1016/j.eja.2017.09.014>

Hoffmann, M. P., Haakana, M., Asseng, S., Höhn, J. G., Palosuo, T., Ruiz-Ramos, M., Fronzek, S., Ewert, F., Gaiser, T., Kassie, B. T., Paff, K., Rezaei, E. E., Rodríguez, A., Semenov, M., Srivastava, A. K., Stratonovitch, P., Tao, F., Chen, Y., Rötter, R. P. (2018). How does inter-annual variability of attainable yield affect the magnitude of yield gaps for wheat and maize? An analysis at ten sites. *Agric. Syst.*, 159, 199–208. <https://doi.org/10.1016/j.agsy.2017.03.012>

Iyer-Pascuzzi, A. S., Symonova, O., Mileyko, Y., Hao, Y., Belcher, H., Harer, J., Weitz, J. S., Benfey, P. N. (2010). Imaging and analysis platform for automatic phenotyping and trait ranking of plant root systems. *Plant Physiol.*, 152, 1148–1157. <https://doi.org/10.1104/pp.109.150748>

Joshi, A. K., Kumari, M., Singh, V. P., Reddy, C. M., Kumar, S., Rane, J., Chand, R. (2007). Stay green trait: variation, inheritance and its association with spot blotch resistance in spring wheat (*Triticum aestivum* L.). *Euphytica*, 153, 59–71. <https://doi.org/10.1007/s10681-006-9235-z>

Kale Çelik, S., Madenoğlu, S., Sönmez, B., Avağ, K., Türker, U., Çaycı, G., Kütük, A. C., Heng, L. K. (2018). Oxygen isotope discrimination of wheat and its relationship with yield and stomatal conductance under irrigated conditions. *Turkish J. Agric. For.*, 42, 22–28. <https://doi.org/10.3906/tar-1709-31>

Kätterer, T., Hansson, A. C., Andrén, O. (1993). Wheat root biomass and nitrogen dynamics-effects of daily irrigation and fertilization. *Plant Soil*, 151, 21–30. <https://doi.org/10.1007/BF00010782>

Kefauver, S.C.; Vicente, R.; Vergara-Díaz, O.; Fernandez-Gallego, J.A.; Kerfal, S.; Lopez, A.; Melichar, J.P.E.; Serret Molins, M.D.; Araus, J.L. (2017). Comparative UAV and field phenotyping to assess yield and nitrogen use efficiency in hybrid and conventional barley. *Front. Plant Sci.* 8, 1-15. <https://doi:10.3389/fpls.2017.01733>

Kembel, S. W., De Kroon, H., Cahill, J. F., Mommer, L. (2008). Improving the scale and precision of hypotheses to explain root foraging ability. *Ann. Bot.*, 101, 1295–1301. <https://doi.org/10.1093/aob/mcn044>

Khaliq, I., Parveen, N., Chowdhry, M. A. (2004). Correlation and path coefficient analyses in bread wheat. *Int. J. Agric. Biol*, 6, 633-635.

Kipp, S., Mistele, B., Schmidhalter, U. (2014). Identification of stay-green and early senescence phenotypes in high-yielding winter wheat, and their relationship to grain yield and grain protein concentration using high-throughput phenotyping techniques. *Funct. Plant Biol.*, 41, 227–235. <https://doi.org/10.1071/FP13221>

Kirkegaard, J. A., Lilley, J. M. (2007). Root penetration rate - a benchmark to identify soil and plant limitations to rooting depth in wheat. *Aust. J. Exp. Agric.*, 47, 590–602. <https://doi.org/10.1071/EA06071>

Kong, X., Zhang, M., De Smet, I., Ding, Z. (2014). Designer crops: optimal root system architecture for nutrient acquisition. *Trends Biotechnol.*, 32, 597–598. <https://doi.org/10.1016/j.tibtech.2014.09.008>

Li, X., Ingvordsen, C. H., Weiss, M., Rebetzke, G. J., Condon, A. G., James, R. A., Richards, R. A. (2019). Deeper roots associated with cooler canopies, higher normalized difference vegetation index, and greater yield in three wheat populations grown on stored soil water. *J. Exp. Bot.*, 70, 4963–4974. <https://doi.org/10.1093/jxb/erz232>

Lin, G., Sternberg, L. D. S. L. (1993). Hydrogen isotopic fractionation by plant roots during water uptake in coastal wetland plants. In J. R. Ehleringer, A. E. Hall, G. D. Farquhar (Eds.), *Stable isotopes and plant carbon-water relations* (pp. 497–510). Academic Press, Inc. <https://doi.org/10.1016/b978-0-08-091801-3.50041-6>

Lopes, M. S., Reynolds, M. P. (2012). In *Posidonia oceanica* cadmium induces changes in DNA methylation and chromatin patterning index independently from phenology. *J. Exp. Bot.*, 63, 695–709. <https://doi.org/10.1093/jxb/err313>

López-Bellido, L., López-Bellido, R. J., Redondo, R. (2005). Nitrogen efficiency in wheat under rainfed Mediterranean conditions as affected by split nitrogen application. *F. Crop. Res.*, 94, 86–97. <https://doi.org/10.1016/j.fcr.2004.11.004>

Lynch, J. (1995). Root architecture and plant productivity. *Plant Physiol.*, 109, 7–13. <https://doi.org/10.1104/pp.109.1.7>

Lynch, J. P. (2013). Steep, cheap and deep: An ideotype to optimize water and N acquisition by maize root systems. *Ann. Bot.*, 112, 347–357. <https://doi.org/10.1093/aob/mcs293>

Maccaferri, M., El-Feki, W., Nazemi, G., Salvi, S., Canè, M. A., Colalongo, M. C., Stefanelli, S., Tuberosa, R. (2016). Prioritizing quantitative trait loci for root system architecture in tetraploid wheat. *J. Exp. Bot.*, 67, 1161–1178. <https://doi.org/10.1093/jxb/erw039>

Malamy, J. E. (2005). Intrinsic and environmental response pathways that regulate root system architecture. *Plant Cell Environ.*, 1, 67–77. <https://doi.org/10.1111/j.1365-3040.2005.01306.x>

Manschadi, A. M., Christopher, J., Devoil, P., Hammer, G. L. (2006). The role of root architectural traits in adaptation of wheat to water-limited environments. *Funct. Plant Biol.*, 33, 823–837. <https://doi.org/10.1071/FP06055>

Manschadi, A. M., Christopher, J. T., Hammer, G. L., Devoil, P. (2010). Experimental and modelling studies of drought-adaptive root architectural traits in wheat (*Triticum aestivum* L.). *Plant Biosyst.*, 144, 458–462. <https://doi.org/10.1080/11263501003731805>

Marti, J., Bort, J., Slafer, G. A., Araus, J. L. (2007). Can wheat yield be assessed by early measurements of normalized difference vegetation index? *Ann. Appl. Biol.*, 150, 253–257. <https://doi.org/10.1111/j.1744-7348.2007.00126.x>

Martín-Gómez, P., Barbeta, A., Voltas, J., Peñuelas, J., Dennis, K., Palacio, S., Dawson, T. E., Ferrio, J. P. (2015). Isotope-ratio infrared spectroscopy: a reliable tool for the investigation of plant-water sources? *New Phytol.*, 207, 914–927. <https://doi.org/10.1111/nph.13376>

Martínez-Moreno, F., Solís, I., Noguero, D., Blanco, A., Özberk, İ., Nsarellah, N., Elias, E., Mylonas, I., Soriano, J. M. (2020). Durum wheat in the Mediterranean Rim: historical evolution and genetic resources. *Genet. Resour. Crop Evol.*, 67, 1415–1436. <https://doi.org/10.1007/s10722-020-00913-8>

Mateo, M. A., Ferrio, P., Araus, J. L. (2004). Isótopos estables en fisiología vegetal. In M. J. Reigosa, N. Pedrol, A. Sánchez (Eds.), *La ecofisiología vegetal, una ciencia de síntesis* (pp. 1–38). Paranimfo, S.A.

Narayanan, S., Mohan, A., Gill, K. S., Vara Prasad, P. V. (2014). Variability of root traits in spring wheat germplasm. *PLoS One*, 9, 1–15. <https://doi.org/10.1371/journal.pone.0100317>

Nehe, A. S., Foulkes, M. J., Ozturk, I., Rasheed, A., York, L., Kefauver, S. C., Ozdemir, F., Morgounov, A. (2021). Root and canopy traits and adaptability genes explain drought tolerance responses in winter wheat. *PLoS ONE*, 16, 1–25. <https://doi.org/10.1371/journal.pone.0242472>

Ober, E. S., Alahmad, S., Cockram, J., Forestan, C., Hickey, L. T., Kant, J., Maccaferri, M., Marr, E., Milner, M., Pinto, F., Rambla, C., Reynolds, M., Salvi, S., Sciara, G., Snowdon, R. J., Thomelin,

P., Tuberosa, R., Uauy, C., Voss-Fels, K. P., Wallington, E., Watt, M. (2021). Wheat root systems as a breeding target for climate resilience. *Theor. Appl. Genet.*, 134, 1645–1662. <https://doi.org/10.1007/s00122-021-03819-w>

Padovan, G., Martre, P., Semenov, M. A., Masoni, A., Bregaglio, S., Ventrella, D., Lorite, I. J., Santos, C., Bindi, M., Ferrise, R., Dibari, C. (2020). Understanding effects of genotype × environment × sowing window interactions for durum wheat in the Mediterranean basin. *F. Crop. Res.*, 259, 1–15. <https://doi.org/10.1016/j.fcr.2020.107969>

Paez-Garcia, A., Motes, C. M., Scheible, W. R., Chen, R., Blancaflor, E. B., Monteros, M. J. (2015). Root traits and phenotyping strategies for plant improvement. *Plants*, 4, 334–355. <https://doi.org/10.3390/plants4020334>

Pask, A.J.D., Pietragalla, J., Mullan, D.M. Reynolds, M.P. (Eds.) (2012) *Physiological breeding II: A field guide to wheat phenotyping*. Mexico, D.F.: CIMMYT. [http://onlinelibrary.wiley.com/doi/10.1002/cbdv.200490137/abstract%0Ahttps://www.cambridge.org/core/product/identifier/CBO9781107415324A009/type/book\\_part](http://onlinelibrary.wiley.com/doi/10.1002/cbdv.200490137/abstract%0Ahttps://www.cambridge.org/core/product/identifier/CBO9781107415324A009/type/book_part)

Passioura, J. B. (1983). Roots and Drought Resistance. *Agric. Water Manag.*, 12, 265–280. <https://doi.org/10.1016/b978-0-444-42214-9.50025-9>

Peng, B., Liu, X., Dong, X., Xue, Q., Neely, C. B., Marek, T., Ibrahim, A. M. H., Zhang, G., Leskovar, D. I., Rudd, J. C. (2019). Root morphological traits of winter wheat under contrasting environments. *J. Agron. Crop Sci.*, 205, 571–585. <https://doi.org/10.1111/jac.12360>

Pinto, R. S., Reynolds, M. P. (2015). Common genetic basis for canopy temperature depression under heat and drought stress associated with optimized root distribution in bread wheat. *Theor. Appl. Genet.*, 128, 575–585. <https://doi.org/10.1007/s00122-015-2453-9>

Price, A. H., Steele, K. A., Moore, B. J., Jones, R. G. W. (2002). Upland rice grown in soil-filled chambers and exposed to contrasting water-deficit regimes. II. Mapping quantitative trait loci for root morphology and distribution. *F. Crop. Res.*, 76, 25–43. [https://doi.org/10.1016/S0378-4290\(02\)00010-2](https://doi.org/10.1016/S0378-4290(02)00010-2)



Rezzouk, F. Z., Gracia-Romero, A., Kefauver, S. C., Gutiérrez, N. A., Aranjuelo, I., Serret, M. D., Araus, J. L. (2020). Remote sensing techniques and stable isotopes as phenotyping tools to assess wheat yield performance: effects of growing temperature and vernalization. *Plant Sci.*, 295, 1–16. <https://doi.org/10.1016/j.plantsci.2019.110281>

Rezzouk, F. Z., Gracia-Romero, A., Kefauver, S. C., Nieto-Taladriz, M. T., Serret, M. D., Araus, J. L. (2022). Durum wheat ideotypes in Mediterranean environments differing in water and temperature conditions. *Agric. Water Manag.*, 259, 1–15. <https://doi.org/10.1016/j.agwat.2021.107257>

Reynolds, M., Dreccer, F., Trethowan, R. (2007). Drought-adaptive traits derived from wheat wild relatives and landraces. *J. Exp. Bot.*, 58, 177–186. <https://doi.org/10.1093/jxb/erl250>

Robbins, N. E., Dinneny, J. R. (2015). The divining root: moisture-driven responses of roots at the micro- and macro-scale. *J. Exp. Bot.*, 66, 2145–2154. <https://doi.org/10.1093/jxb/eru496>

Sanchez-Bragado, R., Serret, M. D., Araus, J. L. (2017). The nitrogen contribution of different plant parts to wheat grains: exploring genotype, water, and nitrogen effects. *Frontiers in Plant Science*, 7, 1–14.

Sanchez-Bragado, R., Serret, M. D., Marimon, R. M., Bort, J., Araus, J. L. (2019). The hydrogen isotope composition  $\delta^2\text{H}$  reflects plant performance. *Plant Physiol.*, 180, 793–812. <https://doi.org/10.1104/pp.19.00238>

Savin, R., Sadras, V. O., Slafer, G. A. (2019). Benchmarking nitrogen utilisation efficiency in wheat for Mediterranean and non-Mediterranean European regions. *F. Crop. Res.*, 241, 1–7. <https://doi.org/10.1016/j.fcr.2019.107573>

Schreel, J. D. M., Steppe, K. (2020). Foliar Water Uptake in Trees: Negligible or Necessary? *Trends in Plant Sci.*, 25(6), 590–603. <https://doi.org/10.1016/j.tplants.2020.01.003>

Serret, M. D., Ortiz-Monasterio, I., Pardo, A., Araus, J. L. (2008). The effects of urea fertilisation and genotype on yield, nitrogen use efficiency,  $\delta^{15}\text{N}$  and  $\delta^{13}\text{C}$  in wheat. *Ann. Appl. Biol.*, 153, 243–257. <https://doi.org/10.1111/j.1744-7348.2008.00259.x>

- Slafer, G. A., Andrade, F. H., Feingold, S. E. (1990). Genetic improvement of bread wheat (*Triticum aestivum* L.) in Argentina: relationships between nitrogen and dry matter. *Euphytica*, 50, 63–71. <https://doi.org/10.1007/BF00023162>
- Spano, G., Di Fonzo, N., Perrotta, C., Platani, C., Ronga, G., Lawlor, D. W., Napier, J. A., Shewry, P. R. (2003). Physiological characterization of “stay green” mutants in durum wheat. *J. Exp. Bot.*, 54, 1415–1420. <https://doi.org/10.1093/jxb/erg150>
- Steele, K. A., Price, A. H., Shashidhar, H. E., Witcombe, J. R. (2006). Marker-assisted selection to introgress rice QTLs controlling root traits into an Indian upland rice variety. *Theor. Appl. Genet.*, 112, 208–221. <https://doi.org/10.1007/s00122-005-0110-4>
- Sun, H., Li, J., Song, W., Tao, J., Huang, S., Chen, S., Hou, M., Xu, G., Zhang, Y. (2015). Nitric oxide generated by nitrate reductase increases nitrogen uptake capacity by inducing lateral root formation and inorganic nitrogen uptake under partial nitrate nutrition in rice. *J. Exp. Bot.*, 66, 2449–2459. <https://doi.org/10.1093/jxb/erv030>
- Thoday-Kennedy, E., Good, N., Kant, S. (2022). Accelerated Breeding of Cereal Crops. In A. Bilichak J. D. Laurie (Eds.), *Accelerated breeding of cereal crops* (pp. 305–331). Springer Science+Business Media, LLC. <https://doi.org/10.1007/978-1-0716-1526-3>
- Tian, H., De Smet, I., Ding, Z. (2014). Shaping a root system: regulating lateral versus primary root growth. *Trends Plant Sci.*, 19, 426–431. <https://doi.org/10.1016/j.tplants.2014.01.007>
- Trachsel, S., Kaeppler, S. M., Brown, K. M., Lynch, J. P. (2013). Maize root growth angles become steeper under low N conditions. *Fi. Crop. Rese.*, 140, 18–31. <https://doi.org/10.1016/j.fcr.2012.09.010>
- Trachsel, Samuel, Kaeppler, S. M., Brown, K. M., Lynch, J. P. (2011). Shovelomics: high throughput phenotyping of maize (*Zea mays* L.) root architecture in the field. *Plant Soil*, 341, 75–87. <https://doi.org/10.1007/s11104-010-0623-8>
- Treydte, K., Boda, S., Graf Pannatier, E., Fonti, P., Frank, D., Ullrich, B., Saurer, M., Siegwolf, R., Battipaglia, G., Werner, W., Gessler, A. (2014). Seasonal transfer of oxygen isotopes from precipitation and soil to the tree ring: source water versus needle water enrichment. *New Phytol.*, 202, 772–783. <https://doi.org/10.1111/nph.12741>

Tuberosa, R., Salvi, S., Sanguineti, M. C., Landi, P., Maccaferri, M., Conti, S. (2002). Mapping QTLs regulating morpho-physiological traits and yield: case studies, shortcomings and perspectives in drought-stressed maize. *Ann. Bot.*, 89, 941–963. <https://doi.org/10.1093/aob/mcf134>

Vadez, V. (2014). Root hydraulics: the forgotten side of roots in drought adaptation. *F. Crop. Res.*, 165, 15–24. <https://doi.org/10.1016/j.fcr.2014.03.017>

Verma, V., Foulkes, M. J., Worland, A. J., Sylvester-Bradley, R., Caligari, P. D. S., and Snape, J. W. (2004). Mapping quantitative trait loci for flag leaf senescence as a yield determinant in winter wheat under optimal and drought-stressed environments. *Euphytica*, 135, 255–263. <https://doi.org/10.1023/B:EUPH.0000013255.31618.14>

Wang, P., Song, X., Han, D., Zhang, Y., Liu, X. (2010). A study of root water uptake of crops indicated by hydrogen and oxygen stable isotopes: A case in Shanxi Province, China. *Agric. Water Manag.*, 97, 475–482. <https://doi.org/10.1016/j.agwat.2009.11.008>

Wasaya, A., Zhang, X., Fang, Q., Yan, Z. (2018). Root phenotyping for drought tolerance: a review. *Agronomy*, 8, 1–19. <https://doi.org/10.3390/agronomy8110241>

Wassenaar, L. I. (1995). Evaluation of the origin and fate of nitrate in the Abbotsford Aquifer using the isotopes of  $\delta^{15}\text{N}$  and  $\delta^{18}\text{O}$  in  $\text{NO}_3^-$ . *Appl. Geochemistry*, 10, 391–405. [https://doi.org/10.1016/0883-2927\(95\)00013-a](https://doi.org/10.1016/0883-2927(95)00013-a)

Wasson, A., Bischof, L., Zwart, A., Watt, M. (2016). A portable fluorescence spectroscopy imaging system for automated root phenotyping in soil cores in the field. *J. Exp. Bot.*, 67, 1033–1043. <https://doi.org/10.1093/jxb/erv570>

Wasson, A. P., Rebetzke, G. J., Kirkegaard, J. A., Christopher, J., Richards, R. A., Watt, M. (2014). Soil coring at multiple field environments can directly quantify variation in deep root traits to select wheat genotypes for breeding. *J. Exp. Bot.*, 65, 6231–6249. <https://doi.org/10.1093/jxb/eru250>

Wasson, A. P., Richards, R. A., Chatrath, R., Misra, S. C., Prasad, S. V.Sai, Rebetzke, G. J., Kirkegaard, J. A., Christopher, J., Watt, M. (2012). Traits and selection strategies to improve

root systems and water uptake in water-limited wheat crops. *J. Exp. Bot.*, 63, 3485-3498. <https://doi.org/10.1093/jxb/ers111>

Xynias, I. N., Mylonas, I., Korpetis, E. G., Ninou, E. (2020). Durum wheat breeding in the Mediterranean region: current status and future prospects. *Agronomy*, 10, 1–27. <https://doi.org/10.3390/agronomy10030432>

York, L. M., Slack, S., Bennett, M. J., Foulkes, J. (2018a). Wheat shovelomics: phenotyping roots in tillering species. *BioRxiv*, 1–17. <https://doi.org/https://doi.org/10.1101/280875>

York, L. M., Slack, S., Bennett, M. J., Foulkes, J. (2018b). Wheat shovelomics II: revealing relationships between root crown traits and crop growth. *BioRxiv*, 1–22. <https://doi.org/10.1101/280917>

Yousfi, S., Serret, M. D., Araus, J. L. (2009). Shoot  $\delta^{15}\text{N}$  gives a better indication than ion concentration or  $\delta^{13}\text{C}$  of genotypic differences in the response of durum wheat to salinity. *Funct. Plant Biol.*, 36, 144–155. <https://doi.org/10.1111/pce.12055>

Yousfi, S., Serret, M. D., Márquez, A. J., Voltas, J., Araus, J. L. (2012). Combined use of  $\delta^{13}\text{C}$ ,  $\delta^{18}\text{O}$  and  $\delta^{15}\text{N}$  tracks nitrogen metabolism and genotypic adaptation of durum wheat to salinity and water deficit. *New Phytologist*, 194(1), 230-244. <https://doi.org/10.1111/j.1469-8137.2011.04036.x>

Zimmermann, U., Münnich, K. O., Roether, W., Kreutz, W., Schubach, K., Siegel, O. (1966). Tracers determine movement of soil moisture and evapotranspiration. *Science*, 152, 346–347. <https://doi.org/10.1126/science.152.3720.346>

Zhao, L., Wang, L., Cernusak, L. A., Liu, X., Xiao, H., Zhou, M., Zhang, S. (2016). Significant difference in hydrogen isotope composition between xylem and tissue Water in *Populus Euphratica*. *Plant Cell Environ.*, 39, 1848–1857. <https://doi.org/10.1111/pce.12753>

## Supplemental Tables and Figures

**Supplemental Table 1.** List of the twelve selected durum wheat varieties with contrasting yield performance (high vs low) during the study, with year of release, country of origin and available information on provenance and/or pedigree.

Variety	Yield performance	Crop season				Year of release	Country	Pedigree/Provenance
		2017-2018	2018-2019	2019-2020	2020-2021			
<i>Athorix</i>	High yield	-	-	-	X	2011	-	<i>Limagrain Europe</i>
<i>Avispa</i>	High yield	-	-	-	X	2003	Spain	Limagrain-CIMMYT
<i>Claudio</i>	High yield	X	X	X	-	1999	Italy	(Sel. Cimmyt × Durango) × (IS193B × Grazia)
<i>Core</i>	High yield	X	X	X	-	2009	Spain	Eurogen. PROSEME seeds
<i>Haristide</i>	Low yield	-	-	X	X	-	-	-
<i>Olivadur</i>	Low yield	X	X	X	-	2013	Spain	RAGT 2N SAS seeds
<i>Pedroso</i>	Low yield	X	X	X	X	1992	Spain	Batlle seeds
<i>Regallo</i>	High yield	-	-	-	X	1990	Italy	Diputación General de Aragón CIMMYT
<i>Sculpture</i>	Low yield	-	-	X	-	2011	-	-
<i>Simeto</i>	Low yield	-	-	-	X	1988	Spain	RUFF/FLAMINGO//MEXICALI-75/3/SHEARWATER
<i>Solea</i>	Low yield	X	X	X	-	2005	Spain	Monsanto Agriculture Spain.
<i>Vitron</i>	High yield	X	X	X	-	1983	France	TURCHIA-77/3/JORI-69(SIB)/(SIB)ANHINGA//(SIB)FLAMINGO

*A subset of six varieties was used during 2017-2018, 2018-2019 and 2020-2021; and a subset of eight varieties were used during 2019-2020.*

**Supplemental Table 2.** Pearson correlations of grain yield (GY) with agronomic traits (Biomass; HI; TKW; Plants m<sup>-2</sup>; Ears<sup>-2</sup>; PH and NDVI), canopy temperature depression (CTD), nitrogen concentration in the flag leaf (N<sub>leaf</sub>) and grain (N<sub>grain</sub>), carbon and nitrogen stable isotopes measured in the dry matter of the flag leaf ( $\delta^{15}\text{N}_{\text{leaf DM}}$  and  $\delta^{13}\text{C}_{\text{leaf DM}}$ ) and grains ( $\delta^{15}\text{N}_{\text{grain DM}}$  and  $\delta^{13}\text{C}_{\text{grain DM}}$ ), and oxygen and hydrogen stable isotopes measured in stem water ( $\delta^{18}\text{O}_{\text{stem water}}$  and  $\delta^2\text{H}_{\text{stem water}}$ ). Correlations were given when combining all seasons and trials, and across seasons per trial.

		Combined seasons and trials	INP	Across seasons		
				ILP	RLN	RNP
Agronomical traits	Biomass	0.901**	0.552**	-	0.929**	0.950**
	HI	0.598**	ns	-	0.724**	0.780**
	TKW	0.209**	ns	ns	0.645**	ns
	Plants m <sup>-2</sup>	0.166*	0.446**	ns	ns	ns
	Ears <sup>-2</sup>	0.499**	0.523**	ns	0.585**	ns
	PH	0.648**	0.231*	0.435**	0.735**	0.860**
	NDVI	0.403**	ns	ns	0.626**	0.845**
Canopy temperature	CTD	0.434**	ns	ns	0.690**	0.663**
Nitrogen concentration	N <sub>leaf</sub>	ns	ns	ns	ns	ns
	N <sub>grain</sub>	-0.299**	0.355**	ns	-0.426**	-0.600**
Stable isotopes	$\delta^{15}\text{N}_{\text{leaf}}$	-0.418**	-0.478**	ns	-0.792**	0.700**
	$\delta^{15}\text{N}_{\text{grain}}$	0.210**	ns	ns	0.099	0.635**
	$\delta^{13}\text{C}_{\text{leaf}}$	-0.622**	ns	ns	-0.844**	-0.734**
	$\delta^{13}\text{C}_{\text{grain}}$	-0.631**	ns	ns	-0.726**	-0.863**
	$\delta^{18}\text{O}_{\text{stem}}$	-0.544**	-0.556**	ns	ns	-0.658**
	$\delta^2\text{H}_{\text{stem}}$	ns	-0.419*	ns	ns	-0.356*

Level of significance: ns, not significant; \*,  $P < 0.05$ ; \*\*,  $P < 0.01$

**Supplemental Table 3.** Pearson correlations between grain yield (GY) against agronomic traits (Biomass; HI; TKW; N<sup>o</sup> plants; N<sup>o</sup> ears; PH and NDVI), canopy temperature depression (CTD), nitrogen content in the flag leaf (N<sub>leaf</sub>) and grain (N<sub>grain</sub>), carbon and nitrogen stable isotopes measured in the dry matter of the flag leaf ( $\delta^{15}\text{N}_{\text{leaf DM}}$  and  $\delta^{13}\text{C}_{\text{leaf DM}}$ ) and grain ( $\delta^{15}\text{N}_{\text{grain DM}}$  and  $\delta^{13}\text{C}_{\text{grain DM}}$ ), and oxygen and hydrogen stable isotopes measured in stem water ( $\delta^{18}\text{O}_{\text{stem water}}$  and  $\delta^2\text{H}_{\text{stem water}}$ ). Correlations were given for each season separated (2017-2018; 2018-2019; 2019-2020; 2020-2021), for trials combined and separated.

		Combined trials				2017-2018			2018-2019			2019-2020			2020-2021		
		2017-2018	2018-2019	2019-2020	2020-2021	INP	RLN	RNP	INP	RLN	RNP	ILP	INP	RLN	ILP	INP	RNP
Agronomical traits	Biomass	0.902**	0.895**	-	-	0.852**	0.943**	0.701**	ns	0.784**	0.784**	-	-	-	-	-	-
	HI	0.326*	0.694**	-	-	ns	ns	ns	ns	0.620**	ns	-	-	-	-	-	-
	TKW	ns	ns	-	ns	ns	ns	ns	0.581*	0.663**	ns	-	-	-	ns	-0.542*	-0.566*
	Plant density	0.492**	ns	-	ns	0.488*	0.547*	ns	ns	ns	ns	-	-	-	ns	ns	-0.475*
	Ear density	0.737**	0.561**	-	ns	0.734**	0.826**	0.630**	ns	ns	ns	-	-	-	ns	ns	ns
	PH	0.574**	0.870**	0.273*	0.405**	0.511*	ns	0.696**	0.516*	0.820**	0.557*	ns	ns	ns	ns	ns	ns
	NDVI	0.686**	0.392*	0.650**	0.307*	0.558*	0.630**	0.741**	ns	-	ns	ns	ns	0.800**	ns	ns	0.532*
Canopy temperature	CTD	0.502**	0.783**	ns	ns	ns	0.595**	ns	ns	ns	ns	ns	ns	0.528**	ns	ns	ns
Nitrogen content	N <sub>leaf DM</sub>	-	ns	-	-	-	-	-	ns	ns	ns	-	-	-	-	-	-
	N <sub>grain DM</sub>	ns	-0.641**	ns	ns	ns	ns	ns	ns	-0.891**	-0.476*	ns	ns	ns	ns	-0.596**	ns
Stable isotopes	$\delta^{15}\text{N}_{\text{leaf DM}}$	-	0.704**	-0.500**	ns	-	-	-	ns	ns	0.607**	-	ns	-0.478*	ns	ns	ns
	$\delta^{15}\text{N}_{\text{grain DM}}$	ns	0.391**	0.407**	ns	ns	0.530*	ns	ns	ns	0.630**	ns	ns	ns	ns	ns	ns
	$\delta^{13}\text{C}_{\text{leaf DM}}$	-	-0.870**	-	ns	ns	-	-	ns	-0.844**	-0.868**	-	-	-	ns	0.551*	ns
	$\delta^{13}\text{C}_{\text{grain DM}}$	-0.332*	-0.877**	-0.364**	-0.585**	ns	-0.549*	ns	-0.531*	-0.799**	-0.554*	ns	ns	-0.537**	ns	ns	ns
	$\delta^{18}\text{O}_{\text{stem water}}$	ns	-0.684**	-	ns	ns	ns	ns	-0.557*	ns	-0.480*	-	-	-	ns	ns	ns
	$\delta^2\text{H}_{\text{stem water}}$	ns	ns	-	0.333*	ns	ns	ns	ns	ns	ns	-	-	-	ns	ns	ns

Level of significance: ns, not significant; \*,  $P < 0.05$ ; \*\*,  $P < 0.01$

**Supplemental Table 4.** Pearson correlations between grain yield (GY) and shovelomics traits measured in the 0-20cm soil depth, and core traits measured in different soil sections (0-25cm; 20-50cm; 50-75cm; 75-100cm). Correlations were given when combining all seasons and trials, and across seasons per trial.

		Combined seasons and trials		Across seasons				
			INP	ILP	RLN	RNP		
Shovelomics traits	Root crown	RDW <sub>0-20cm</sub>	ns	-0.562**	ns	ns	0.552**	
		Rccomp	ns	ns	ns	ns	-0.279*	
		MaxR	0.320**	ns	0.448**	0.504**	ns	
		MedR	0.305**	ns	0.408**	0.536**	ns	
	Root dimensions	Rwidth	ns	-0.254*	-0.378*	-0.634**	ns	
		Ndepth	0.185**	ns	ns	ns	ns	
		Nlen	0.302**	ns	ns	0.512**	ns	
	Root density	Nwidth	0.249**	ns	0.418**	0.274*	ns	
		NwA	0.167*	ns	ns	ns	ns	
		Nsurf	0.162*	ns	ns	ns	ns	
		Nvol	ns	ns	ns	ns	ns	
	Root angle	ConvA	0.257**	ns	ns	0.337**	ns	
		RA	ns	ns	0.604**	ns	0.508**	
	Ratios	Bush	ns	ns	ns	ns	ns	
		Ldist	0.147*	ns	ns	ns	0.587**	
		Network Solidity	ns	-0.279*	-0.397*	ns	ns	
		NWDR	0.144*	ns	0.451**	ns	ns	
		SRL	0.325**	ns	0.397*	0.625**	ns	
	Cores traits	RDW	RDW <sub>0-25cm</sub>	ns	ns	ns	ns	ns
			RDW <sub>25-50cm</sub>	ns	ns	ns	ns	ns
RDW <sub>50-75cm</sub>			-0.420**	-0.509**	ns	ns	ns	
RDW <sub>75-100cm</sub>			0.268*	ns	ns	ns	ns	
Area <sub>Root</sub>		Area <sub>Roots 0-25cm</sub>	-0.509**	-0.449**	ns	ns	ns	
		Area <sub>Roots 25-50cm</sub>	-0.560**	-0.543**	ns	ns	ns	
		Area <sub>Roots 50-75cm</sub>	-0.517**	-0.428**	ns	ns	ns	
		Area <sub>Roots 75-100cm</sub>	-0.566**	-0.369**	-0.410*	ns	ns	
Area/RDW		Area/RDW <sub>0-25cm</sub>	-0.449**	-0.555**	ns	ns	ns	
		Area/RDW <sub>25-50cm</sub>	-0.349**	-0.630**	ns	ns	ns	
	Area/RDW <sub>50-75cm</sub>	0.246*	ns	ns	ns	ns		
	Area/RDW <sub>75-100cm</sub>	-0.350**	-0.417**	ns	ns	ns		

Level of significance: ns, not significant; \*,  $P < 0.05$ ; \*\*,  $P < 0.01$ . Root traits were Area<sub>Roots 0-25cm</sub>, Area<sub>Roots 25-50cm</sub>, Area<sub>Roots 50-75cm</sub>, Area<sub>Roots 75-100cm</sub> representing root area from soil cores in the 0-25 cm, 25-50 cm, 50-75 cm and 75-100 cm soil layers, respectively. MaxR, maximum number of roots. Bush, bushiness. ConvA, convex area. Ldist, network length distribution. MedR, median number of roots. Ndepth, network depth. Nlen, network length. Nsurf, network surface area. Nvol, network volume. Nwidth, network width. NwA, network area. NWDR, network width to depth ratio. SRL, specific root length. RA, root angle. RDW<sub>0-20</sub>, RDW<sub>0-25</sub>, RDW<sub>25-50</sub>, RDW<sub>50-75</sub> and RDW<sub>75-100</sub> are root dry weight in 0-20 cm, 0-25 cm, 25-50 cm, 50-75 cm and 75-100 cm soil layers, respectively. Rwidth, average root width. Rccomp, number of connected components.



**Supplemental Table 5.** Pearson correlations between grain yield (GY) and shovelomic traits measured in the 0-20cm soil depth, and core traits measured in different soil sections (0-25cm; 20-50cm; 50-75cm; 75-100cm). Correlations were given for each season separated (2017-2018; 2018-2019; 2019-2020; 2020-2021), for trials combined and separated.

		Combined trials				2017-2018			2018-2019			2019-2020			2020-2021			
		2017-2018	2018-2019	2019-2020	2020-2021	INP	RLN	RNP	INP	RLN	RNP	ILP	INP	RLN	ILP	INP	RNP	
Shovelomics traits	Root Crown	RDW <sub>0-20</sub>	ns	ns	ns	ns	ns	ns	ns	ns	ns	ns	ns	0.755**	ns	ns	ns	
		Rccomp	0.326*	-0.760**	ns	ns	ns	ns	ns	0.563*	ns	ns	ns	ns	0.417*	ns	ns	ns
		MaxR	ns	0.713**	ns	0.431**	ns	ns	ns	ns	ns	ns	ns	ns	0.642**	ns	ns	ns
		MedR	ns	0.615**	ns	0.367**	ns	ns	ns	ns	ns	ns	ns	ns	0.677**	ns	ns	ns
	Root dimensions	Rwidth	ns	0.125	ns	0.378**	ns	ns	ns	0.114	ns	0.287	ns	ns	ns	ns	ns	ns
		Ndepth	ns	0.618**	ns	0.422**	ns	ns	ns	0.532*	ns	0.496*	ns	ns	ns	ns	ns	ns
		Nlen	ns	0.771**	ns	0.441**	ns	ns	ns	ns	0.557*	ns	ns	ns	0.546**	ns	ns	ns
	Root density	Nwidth	ns	0.609**	ns	0.555**	ns	ns	ns	ns	ns	ns	ns	ns	0.576**	ns	ns	ns
		NwA	ns	0.756**	ns	0.417**	ns	ns	ns	ns	0.560*	0.475*	ns	ns	0.496*	ns	ns	ns
		Nsurf	ns	0.762**	ns	0.412**	ns	ns	ns	ns	0.575*	ns	ns	ns	0.539**	ns	ns	ns
		Nvol	ns	0.734**	ns	0.358**	ns	ns	ns	ns	0.562*	0.506*	ns	ns	ns	ns	ns	ns
	Root angle	ConvA	ns	0.706**	ns	0.540**	ns	ns	ns	0.566*	ns	ns	ns	ns	0.486*	ns	ns	ns
		RA	-0.332*	ns	ns	ns	-0.501*	ns	ns	ns	ns	ns	0.560**	ns	ns	ns	ns	ns
	Ratios	Bush	ns	ns	ns	0.415**	ns	ns	ns	ns	ns	ns	ns	ns	ns	ns	ns	ns
		Ldist	ns	0.363**	ns	0.376**	ns	ns	ns	0.642**	ns	ns	ns	ns	ns	ns	ns	ns
		Network Solidity	ns	0.399**	ns	ns	ns	ns	ns	-0.514*	ns	ns	ns	ns	ns	ns	ns	ns
NWDR		ns	ns	ns	0.459**	ns	ns	ns	ns	ns	ns	0.428*	ns	ns	ns	ns	ns	
SRL		ns	ns	ns	0.384**	ns	ns	ns	ns	ns	ns	ns	ns	ns	ns	ns	ns	
Cores traits	RDW	RDW <sub>0-25cm</sub>	-	ns	ns	ns	-	-	-	ns	-	-	ns	ns	ns	ns	ns	ns
		RDW <sub>25-50cm</sub>	-	ns	ns	ns	-	-	-	ns	-	-	ns	ns	ns	ns	ns	ns
		RDW <sub>50-75cm</sub>	-	ns	ns	ns	-	-	-	ns	-	-	ns	ns	ns	ns	ns	ns
		RDW <sub>75-100cm</sub>	-	ns	ns	ns	-	-	-	ns	-	-	ns	ns	ns	ns	0.492*	ns
	Area <sub>Root</sub>	Area <sub>Roots 0-25cm</sub>	-	ns	ns	ns	-	-	-	ns	-	-	ns	ns	ns	ns	ns	ns
		Area <sub>Roots 25-50cm</sub>	-	ns	ns	ns	-	-	-	ns	-	-	ns	ns	ns	ns	ns	ns
		Area <sub>Roots 50-75cm</sub>	-	ns	ns	ns	-	-	-	ns	-	-	ns	ns	ns	ns	ns	ns
		Area <sub>Roots 75-100cm</sub>	-	ns	ns	ns	-	-	-	ns	-	-	-0.649*	ns	ns	ns	ns	ns
	Area/RDW	Area <sub>Roots</sub> /RDW <sub>0-25cm</sub>	-	ns	-0.440**	ns	-	-	-	ns	-	-	ns	ns	ns	ns	ns	ns
		Area <sub>Roots</sub> /RDW <sub>25-50cm</sub>	-	ns	ns	ns	-	-	-	ns	-	-	ns	ns	ns	ns	ns	ns
Area <sub>Roots</sub> /RDW <sub>50-75cm</sub>		-	ns	ns	ns	-	-	-	ns	-	-	ns	ns	ns	ns	ns	ns	
Area <sub>Roots</sub> /RDW <sub>75-100cm</sub>		-	ns	ns	ns	-	-	-	ns	-	-	ns	ns	ns	ns	ns	ns	

Level of significance: ns, not significant; \*,  $P < 0.05$ ; \*\*,  $P < 0.01$

**Supplemental Table 6.** Pearson correlations between oxygen ( $\delta^{18}\text{O}_{\text{stem}}$ ) and hydrogen ( $\delta^2\text{H}_{\text{stem}}$ ) isotope compositions in stem water, and shovelomic traits measured in the first 20 cm of the upper soil layer, and soil cores measured in different soil sections (0-25cm, 20-50cm, 50-75 cm and 75-100 cm). Correlations were given across the seasons (2018-2019 and 2020-2021) for INP, and during 2020-2021 for ILP and RNP.

		INP		ILP		RNP		
		$\delta^{18}\text{O}_{\text{stem}}$	$\delta^2\text{H}_{\text{stem}}$	$\delta^{18}\text{O}_{\text{stem}}$	$\delta^2\text{H}_{\text{stem}}$	$\delta^{18}\text{O}_{\text{stem}}$	$\delta^2\text{H}_{\text{stem}}$	
Shovelomics traits	Root Crown	RDW <sub>0-20cm</sub>	0.271	0.185	-0.316	-0.358	-0.252	-0.251
		Rccomp	0.220	0.108	-0.492*	-0.480	-0.082	-0.285
		MaxR	-0.203	-0.150	-0.167	-0.187	-0.227	-0.396
		MedR	-0.139	-0.131	-0.301	-0.348	-0.237	-0.417
	Root dimension	Rwidth	0.365*	0.330*	-0.136	-0.182	-0.167	-0.318
		Ndepth	-0.155	-0.172	-0.341	-0.273	-0.209	-0.363
		Nlen	-0.157	-0.154	-0.342	-0.316	-0.251	-0.413
	Root density	Nwidth	0.035	-0.078	0.006	-0.038	-0.241	-0.396
		NwA	0.006	-0.015	-0.414	-0.407	-0.265	-0.400
		Nsurf	0.050	0.030	-0.396	-0.388	-0.267	-0.401
		Nvol	0.267	0.232	-0.367	-0.378	-0.273	-0.368
	Root angle	ConvA	-0.010	-0.067	-0.407	-0.393	-0.288	-0.415
		RA	0.467**	0.431**	0.034	0.112	0.124	0.264
	Ratios	Bush	-0.070	0.043	0.319	0.320	-0.247	-0.399
		Ldist	-0.367*	-0.277	0.240	0.331	-0.409	-0.485*
		Network Solidity	0.137	0.216	-0.074	-0.102	-0.172	-0.340
NWDR		0.136	0.063	0.277	0.197	-0.207	-0.371	
SRL <sub>0-20cm</sub>		-0.401*	-0.373*	0.219	0.230	-0.134	-0.335	
Cores traits	RDW	RDW <sub>0-25cm</sub>	0.281	0.127	-0.053	-0.066	0.296	0.290
		RDW <sub>25-50cm</sub>	0.003	-0.041	-0.273	-0.340	0.378	0.261
		RDW <sub>50-75cm</sub>	0.486**	0.454**	0.348	0.364	-0.055	-0.217
		RDW <sub>75-100cm</sub>	-0.186	-0.082	0.137	0.116	-0.261	-0.160
	Area <sub>Root</sub>	Area <sub>Roots 0-25cm</sub>	0.274	0.249	0.077	0.180	-0.180	-0.254
		Area <sub>Roots 25-50cm</sub>	0.299	0.268	0.185	0.092	-0.194	0.018
		Area <sub>Roots 50-75cm</sub>	0.336*	0.317	0.508*	0.432	-0.562*	-0.247
		Area <sub>Roots 75-100cm</sub>	0.406*	0.351*	0.542*	0.420	0.076	0.196
	Area/RDW	Area/RDW <sub>0-25cm</sub>	0.216	0.192	0.096	0.132	-0.168	-0.211
		Area/RDW <sub>25-50cm</sub>	0.309	0.307	0.193	0.247	-0.396	-0.286
		Area/RDW <sub>50-75cm</sub>	-0.499**	-0.505**	-0.336	-0.356	0.006	0.169
		Area/RDW <sub>75-100cm</sub>	0.051	0.028	-0.386	-0.633	0.244	0.262

Level of significance: ns, not significant; \*,  $P < 0.05$ ; \*\*,  $P < 0.01$ .

**Supplemental Table 7.** Multi-linear regression (stepwise) of grain yield (GY) as the dependent variable, and canopy temperature depression (CTD), stable carbon and nitrogen isotope compositions ( $\delta^{13}\text{C}$  and  $\delta^{15}\text{N}$ ) and nitrogen concentration (N) of mature grains, and shovelomic root traits as independent variables. For each stepwise equation, the fitted model was significant ( $P < 0.001$ ) with ( $1.2 < \text{Durbin-Watson} < 2$ ) and collinearity was within the acceptable range ( $\text{VIF} < 10$ ).  $R^2_{\text{adjusted}}$  displays the reliability of the fitted regression line to the data in use in the stepwise regression, and SE the standard error of the dependent variable (GY).

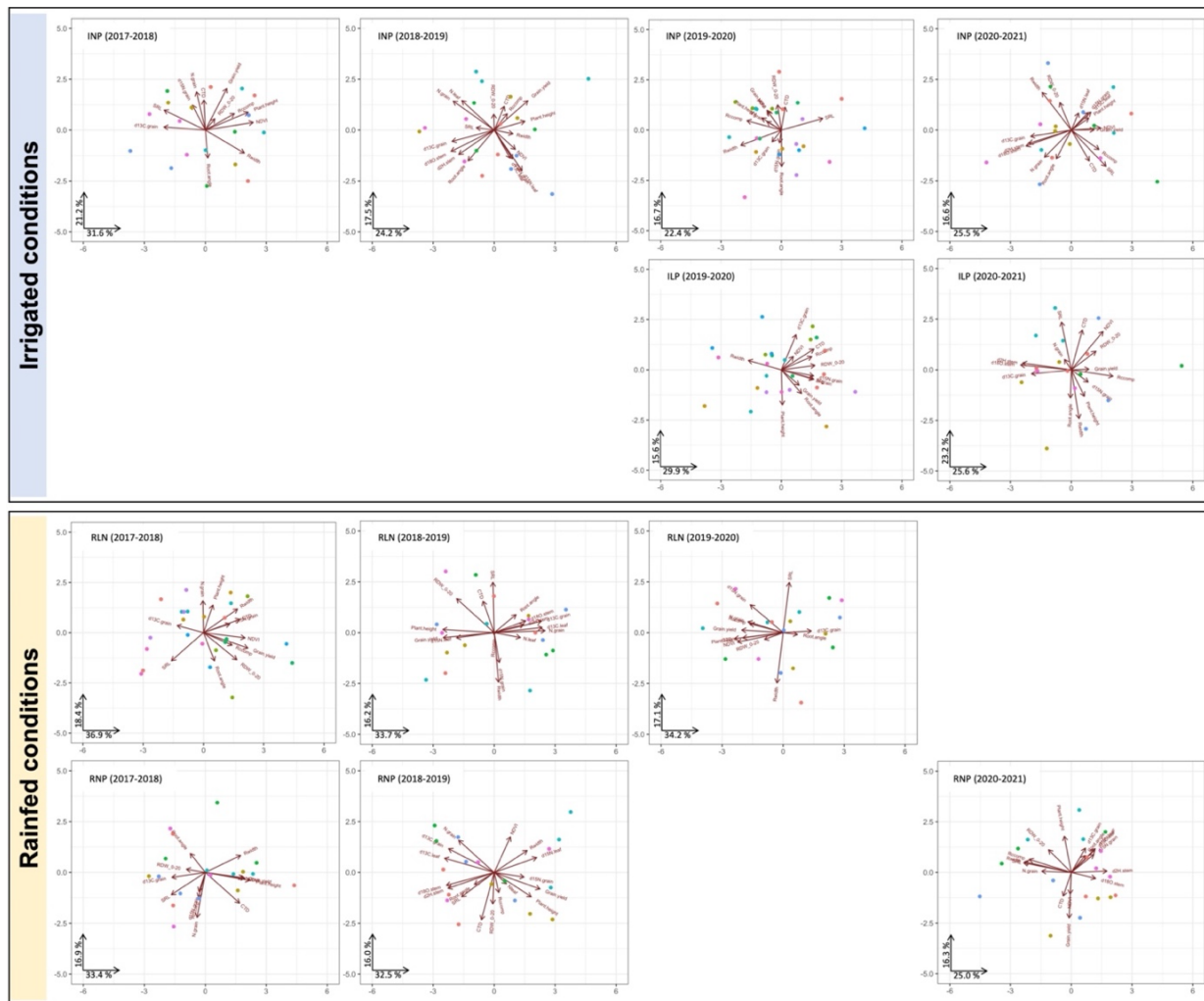
		Stepwise			Random Forest			
	Model	Equation	$R^2_{\text{adjusted}}$	SE	$R^2_{\text{Train}}$	RMSE <sub>Train</sub>	$R^2_{\text{Test}}$	RMSE <sub>Test</sub>
2017-2018	All	$\text{GY} = -14.08 + 0.46 \cdot \text{CTD} - 0.26 \cdot \delta^{13}\text{C}_{\text{grain}}$	29.0 %	1.1	26.7%	1.4	1.4%	1.0
	INP	$\text{GY} = -0.56 + 0.54 \cdot \text{N}_{\text{grain}}$	24.5 %	1.0				
	RLN	$\text{GY} = 5.61 + 0.60 \cdot \text{CTD}$	31.4 %	1.4				
	RNP	-	-	-				
2018-2019	All	$\text{GY} = -2.90 - 0.47 \cdot \delta^{13}\text{C}_{\text{grain}} + 0.37 \cdot \text{N}_{\text{len}} + 0.10 \cdot \text{Ldist} + 0.48 \cdot \delta^2\text{H}_{\text{stem}} - 0.54 \cdot \delta^{18}\text{O}_{\text{stem}} - 0.17 \cdot \text{Nwidth}$	90.8 %	0.8	82.9%	1.1	89.7%	0.8
	INP	$\text{GY} = 2.09 + 0.68 \cdot \text{Ldist} + 0.46 \cdot \text{Rccomp} + 0.35 \cdot \text{Nsurf}$	76.3 %	0.5				
	RLN	$\text{GY} = 6.11 - 0.89 \cdot \text{N}_{\text{grain}}$	77.9 %	0.3				
	RNP	$\text{GY} = 0.53 + 0.58 \cdot \delta^{15}\text{N}_{\text{grain}} + 0.42 \cdot \text{Ndepth}$	51.5 %	0.4				
2019-2020	All	$\text{GY} = -26.38 + 0.36 \cdot \delta^{15}\text{N}_{\text{grain}} - 0.30 \cdot \delta^{13}\text{C}_{\text{grain}}$	23.3 %	1.5	19.8%	2.1	33.7%	1.7
	INP	-	-	-				
	ILP	$\text{GY} = 2.47 + 0.56 \cdot \text{RA}$	28.2 %	0.7				
	RLN	$\text{GY} = -30.88 + 0.48 \cdot \text{RDW}_{0-20} - 0.37 \cdot \delta^{13}\text{C}_{\text{grain}} + 0.30 \cdot \text{MedR}$	73.1 %	0.8				
2020-2021	All	$\text{GY} = -12.87 - 0.59 \cdot \delta^{13}\text{C}_{\text{grain}}$	33.0 %	0.8	33.4%	0.6	36.4%	1.0
	INP	$\text{GY} = 8.54 - 0.60 \cdot \text{N}_{\text{grain}}$	31.5 %	0.5				
	ILP	-	-	-				
	RNP	-	-	-				

*Regressions were generated using individual plots of the selected genotypes for each trial in separated crop seasons. 18 (2018; 2019 and 2021) to 24 (2020) plots per trial were used. The dash marks show that no variables were introduced to predict GY using the stepwise regression method.*

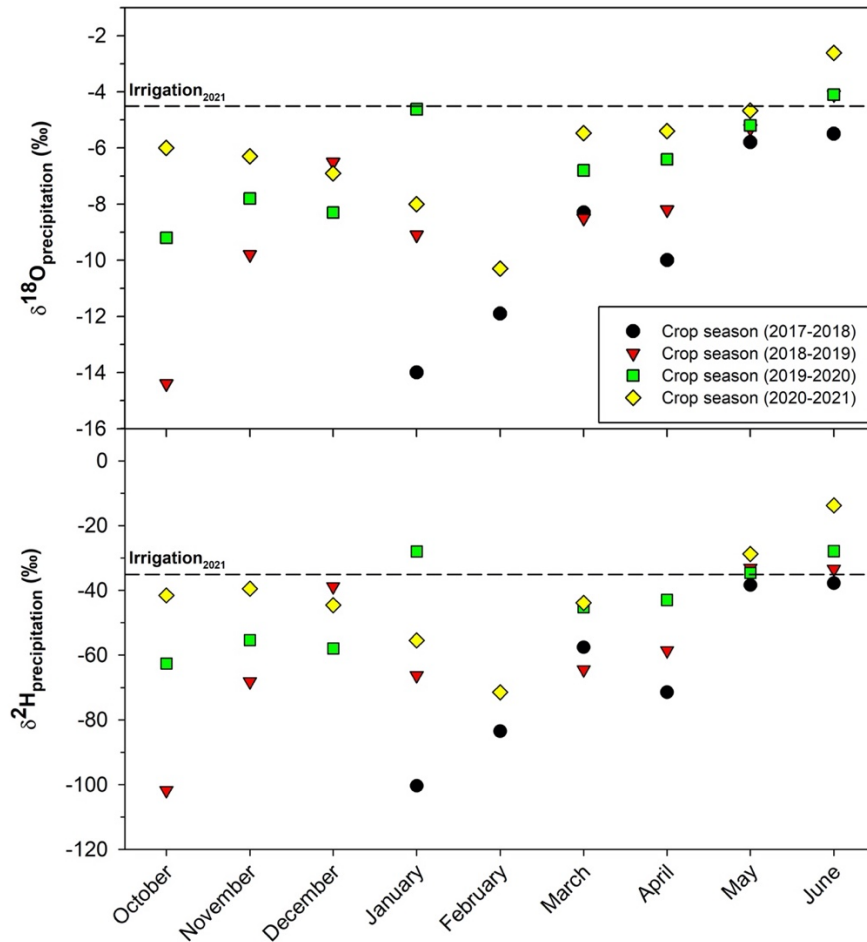
**Supplemental Table 8.** List of the top 20 explanatory variables for grain yield (GY) ranked by importance in each Random Forest model. Ranking is expressed as a percentage (%). Orange coloured cells show the variables that were introduced by the stepwise regression models as explanatory variables, and the green coloured cells highlight CTD ranking as the main explicit parameter to temperature.

Random Forest ranking (%)							
Trait	2017-2018	Trait	2018-2019	Trait	2019-2020	Trait	2020-2021
N <sub>grain</sub>	100.0	Rccomp	100.0	Rccomp	100.0	Nwidth	100.0
CTD	86.2	$\delta^{13}\text{C}_{\text{leaf}}$	99.4	RA	57.6	$\delta^{13}\text{C}_{\text{grain}}$	36.4
RA	70.8	CTD	69.0	$\delta^{13}\text{C}_{\text{grain}}$	48.9	ConvA	29.2
$\delta^{13}\text{C}_{\text{grain}}$	64.3	$\delta^{18}\text{O}_{\text{stem}}$	50.0	$\delta^{15}\text{N}_{\text{grain}}$	48.2	NWDR	27.6
$\delta^{15}\text{N}_{\text{grain}}$	60.8	$\delta^{13}\text{C}_{\text{grain}}$	46.1	Ldist	35.3	Network solidity	20.9
NWDR	38.0	$\delta^{15}\text{N}_{\text{grain}}$	36.7	RDW <sub>0-20</sub>	32.3	Nlen	18.9
Rccomp	37.9	MaxR	29.1	Nvol	25.6	CTD	15.5
RDW <sub>0-20</sub>	32.9	Nlen	28.2	CTD	24.4	N <sub>grain</sub>	14.6
Nvol	32.2	ConvA	25.8	Nlen	23.6	MaxR	13.7
Network solidity	31.5	Nsurf	19.0	Ndepth	22.1	SRL	13.5
Nsurf	27.6	NwA	15.3	NwA	20.5	Ldist	13.2
Rwidth	26.6	Ndepth	9.9	Rwidth	18.7	Bush	13.0
SRL	26.2	Nvol	7.5	N <sub>grain</sub>	18.6	NwA	12.7
Bush	25.6	N <sub>grain</sub>	5.9	NWDR	17.5	Nsurf	12.2
ConvA	25.5	MedR	5.5	Network solidity	17.1	Ndepth	12.2
Ndepth	24.7	Nwidth	4.6	SRL	16.7	Nvol	12.0
NwA	24.5	Ldist	4.5	Nsurf	14.7	RDW <sub>0-20</sub>	11.3
Nwidth	23.4	$\delta^2\text{H}_{\text{stem}}$	2.3	ConvA	11.9	Rccomp	10.9
Ldist	20.4	Network solidity	2.1	MedR	10.4	$\delta^{15}\text{N}_{\text{grain}}$	9.3
MaxR	10.6	Bush	1.7	MaxR	4.6	MedR	7.8

Introduced variables were GY, grain yield. CTD, canopy temperature depression.  $N_{\text{grain}}$ , nitrogen concentration in grains.  $\delta^{13}\text{C}_{\text{leaf}}$ , carbon isotope composition in leaves.  $\delta^{13}\text{C}_{\text{grain}}$ , carbon isotope composition in grains.  $\delta^{15}\text{N}_{\text{grain}}$ , nitrogen isotope composition in grains. RDW<sub>0-20</sub>, root dry weight in the first 0-20 cm soil layer. Rwidth, average root width. Rccomp, number of connected components. MaxR, maximum number of roots. MedR, median number of roots. Ndepth, network depth. Nlen, network length. Nwidth, network width. NwA, network area. Nsurf, network surface area. Nvol, network volume. ConvA, convex area. Bush, bushiness. SRL, specific root length. Ldist, network length distribution. NWDR, network width to depth ratio. RA, root angle. Models were generated by combining all trials in each season.

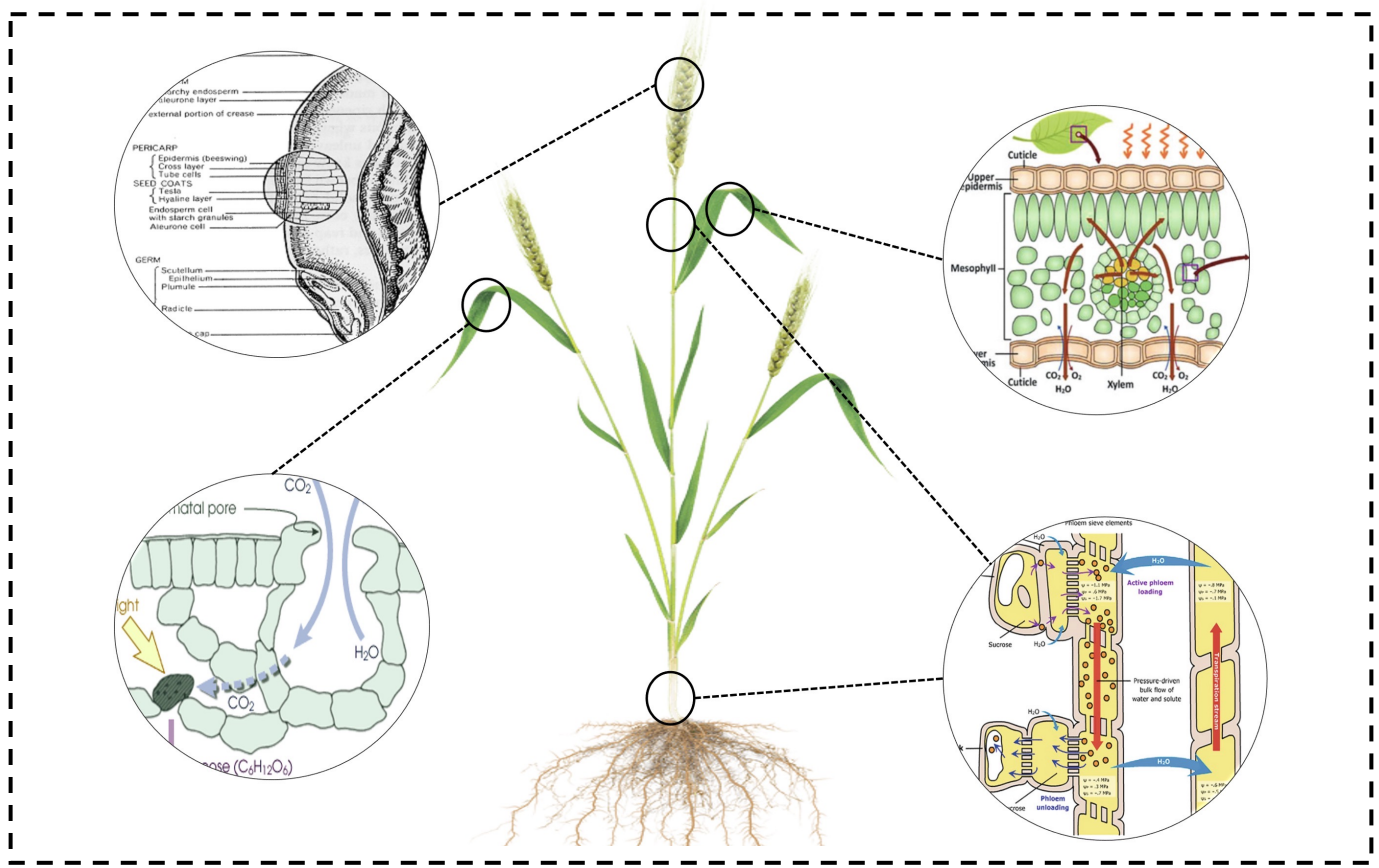


**Supplemental Figure 1.** Principal component analysis (PCA) of the selected wheat cultivars grown during four consecutive crop seasons (2017-2018; 2018-2019; 2019-2020 and 2020-2021) separated, and under different treatments (INP, ILP, RLN and RNP). The variables included in the analysis are grain yield, plant height, NDVI, canopy temperature depression (CTD), nitrogen concentration of leaf ( $N_{leaf}$ ) and grain dry matter ( $N_{grain}$ ), stable carbon ( $\delta^{13}C_{leaf}$ ,  $\delta^{13}C_{grain}$ ) and nitrogen ( $\delta^{15}N_{grain}$ ) compositions of leaf and grain dry matter, oxygen ( $\delta^{18}O_{stem}$ ) and hydrogen ( $\delta^2H_{stem}$ ) isotope compositions of the stem water, and selected root traits: root dry weight in 0-20 cm soil layer ( $RDW_{0-20}$ ), average root width ( $Rwidth$ ), number of connected components in the root crown ( $Rcomp$ ), specific root length ( $SRL$ ), and root angle measured with a protractor ( $Root\ angle$ ).



**Supplemental Figure 2.** Monthly distribution of average predicted oxygen and hydrogen isotope compositions ( $\delta^{18}\text{O}$  and  $\delta^2\text{H}$ ) throughout the four studied crop seasons. The predicted precipitation water isotopes were obtained from “la Red de Vigilancia de Isótopos en Precipitación (REVIP), managed by the “Centro de Estudios y Experimentación de Obras Públicas (CEDEX)” in collaboration with “la Agencia Estatal de Meteorología (AEMET)”.  $\delta^{18}\text{O}$  and  $\delta^2\text{H}$  values in precipitation during May of 2019, and  $\delta^{18}\text{O}$  and  $\delta^2\text{H}$  values in irrigation during May 2021 were analysed at the Scientific Facilities of the University of Barcelona.





## CHAPTER V

# $\delta^2\text{H}$ and $\delta^{18}\text{O}$ assessment of transpirative and photosynthetic performance in wheat under different humidity conditions

Fatima Zahra Rezzouk, Rut Sanchez-Bragado, José Luis Araus

In preparation





## **$\delta^{18}\text{O}$ and $\delta^2\text{H}$ assessment of transpirative and photosynthetic performance in wheat under different humidity conditions.**

Fatima Zahra Rezzouk<sup>1,2</sup>, José Luis Araus<sup>1,2</sup>, Rut Sanchez Bragado<sup>1,2\*</sup>

<sup>1</sup>*Integrative Crop Ecophysiology Group, Plant Physiology Section, Faculty of Biology, University of Barcelona, 08028 Barcelona, Spain.*

<sup>2</sup>*AGROTECNIO (Center for Research in Agrotechnology), Av. Rovira Roure 191, 25198 Lleida, Spain.*

### Abstract

It is well known that hydrogen isotope composition ( $\delta^2\text{H}$ ) is strongly affected by the trophic nature of the plant part considered. In addition,  $\delta^2\text{H}$  has been observed to provide simultaneous time-integrated records of the photosynthetic and evaporative performance of the plant during crop development, through its tight association with carbon ( $\delta^{13}\text{C}$ ) and oxygen ( $\delta^{18}\text{O}$ ) isotope compositions. To estimate isotopic fractionation during transport and assimilates load and unload from source to sink tissues, an experiment was held under controlled growing conditions. Ninety-six plants of durum wheat (*Triticum aestivum var durum*) genotype cv. Sula were planted in growth chambers with two levels of humidity conditions (40% and 80%). For both growing conditions, half number of plants was submitted to irrigation since anthesis using water enriched with hydrogen isotope labeling ( $\delta^2\text{H}$ ), and by mid grain filling, to irrigation using water enriched with oxygen isotope labeling ( $\delta^{18}\text{O}$ ). Four days later, gas exchange measurements were assessed and wheat stems, flag leaves, peduncles, awns, glumes and grains were collected, and isotope compositions of  $\delta^{18}\text{O}$ ,  $\delta^2\text{H}$ ,  $\delta^{13}\text{C}$  and  $\delta^{15}\text{N}$  were analysed in dry matter (DM), water soluble fraction (WSF) and plant water (WT) from different tissues. For each tissue, high and positive correlations between  $\delta^2\text{H}$  and  $\delta^{18}\text{O}$  in all WT samples indicated a similar source of variation related to evaporation. However, in the case of DM and WSF correlations between  $\delta^{18}\text{O}$  and  $\delta^2\text{H}$  were poorer, suggesting that an additional source of variation might be affecting either  $\delta^{18}\text{O}$  or  $\delta^2\text{H}$ . In that sense,  $\delta^2\text{H}$  has been associated with not only changes in transpiration, but also with trophism in plant tissues.  $\delta^2\text{H}$  was depleted in the leaves and glumes, whereas the  $\delta^2\text{H}$  in awns and grains were enriched. The depletion of  $\delta^2\text{H}$  suggested a possible effect of autotrophic metabolism in leaves and

glumes, whereas enriched  $\delta^2\text{H}$  values indicated a heterotrophic metabolism in awns and grains. The present study highlighted the effect of relative humidity on wheat transpiration and isotopic signature performance in different plant tissues.

Keywords: Oxygen and hydrogen exchange, isotope fractionation, relative humidity, wheat tissues.

## 1. Introduction

Analysis of stable isotopes have been widely used to study the integrated plant performance during last decades for ecological, climatological or physiological or biochemical purposes (Barbour et al., 2007; Sternberg 1989; Sternberg et al., 1989). Carbon stable isotope composition ( $\delta^{13}\text{C}$ ) has been widely used not only as time integrated indicator of water use efficiency (WUE), understood as the ratio between photosynthesis and transpiration (Farquhar and Richards, 1994; Farquhar et al., 1989), but also of the plant water status (Araus et al., 2003; Condon et al. 2004), and therefore, when comparing growing water conditions or even genotypes, plants exhibiting a lower (more negative)  $\delta^{13}\text{C}$  are those performing better in terms of water conditions, keeping a higher stomatal conductance ( $g_s$ ) which translates to a better photosynthesis and productivity, no matter how much WUE decreases.

Similarly to  $\delta^{13}\text{C}$ , the stable isotope compositions oxygen ( $\delta^{18}\text{O}$ ) and hydrogen ( $\delta^2\text{H}$ ) have been observed to provide simultaneous time-integrated records of transpirative and photosynthetic performance of the plant during crop development (Sanchez-Bragado et al., 2019). Both  $\delta^{18}\text{O}$  and  $\delta^2\text{H}$  enrichment in leaf plant water is driven by evaporation as a result of environment's influence on transpiration and/or by changes in stomatal conductance ( $g_s$ ) (Smith and Freeman, 2006; Feakins and Sessions, 2010; Kahmen et al., 2013; Cernusak et al., 2016). Leaf temperature and  $g_s$  together with air humidity can have an effect on  $\delta^{18}\text{O}$  and  $\delta^2\text{H}$  leaf water enrichment model, either directly or indirectly (Flanagan et al., 1991;1993). The model links the enrichment of  $\delta^{18}\text{O}$  and  $\delta^2\text{H}$  in leaf water above the source of water during evaporation to (1) the kinetic fractionation occurring during diffusion via the stomata (Farquhar et al., 2007), (2) the Péclet number by its effect on transpiration; (Cuntz et al., 2007), (3) the leaf border layer,  $\epsilon_k$  (kinetic fractionation that happens during diffusion and through the pores of the stomata in the leaf layer), and (4)  $\epsilon_+$  (the heavier  $\text{H}_2^{18}\text{O}$  molecule reduces

water vapor pressure proportionally), which is temperature dependent. Moreover,  $\delta^2\text{H}$  has its own characteristics informing on the photosynthetic metabolism. Thus, the  $\delta^2\text{H}$  in organic matter can be strongly affected by the plant trophism (photoautotrophic versus heterotrophic) of the plant tissues where  $\delta^2\text{H}$  is analysed (Yakir, 1992; Farquhar and Lloyd, 1993; Pande et al., 1994; Sessions et al., 1999; Hayes, 2001; Cernusak et al., 2016; Cormier et al., 2018). However, up to now, mechanisms of photosynthetic metabolism that affect  $^2\text{H}$  fractionation and thus  $\delta^2\text{H}$  isotope composition in different organic matter pools are poorly understood. On photoautotrophic tissues such as the leaves, the  $\delta^2\text{H}$  of the leaf plant water may be imprinted in sugars and metabolites and thus reflected in the  $\delta^2\text{H}$  of the organic compounds (Cernusak et al., 2016). The  $^2\text{H}$  used for reduction of  $\text{NADP}^+$  to  $\text{NADPH}$  have been observed to have a major impact on the  $\delta^2\text{H}$  of organic matter in photosynthetic tissues (Hayes, 2001; Yakir and De Niro, 1990). Consequently, the  $\delta^2\text{H}$  in plant organic compounds may be influenced by the photosynthetic  $^2\text{H}$  fractionation processes that take place during  $\text{NADPH}$  synthesis in the photosynthetic light reactions (Roden et al., 2000). As a consequence,  $\delta^2\text{H}$  isotopic signal has been demonstrated to be depleted in autotrophic tissues and enriched in heterotrophic tissues (Estep and Hoering, 1981; Yakir and DeNiro, 1990). Depletion occurs as a consequence of photosynthesis activities during carbohydrate metabolism in autotrophic sites (e.g. leaves), whereas enrichment in heterotrophic tissues (e.g. the growing grains in the case of cereals) is the result of different fractionation processes associated with the biosynthetic pathway occurring in the Calvin cycle, during which a large proportion of hydrogen atoms are transferred from ribulose-1,5-bisphosphate to triose phosphates, the  $\text{NADPH}$  produced via the oxidative pentose phosphate pathway during sugar metabolism, and the cellular water (Siegwolf et al., 2022). Therefore, and similarly to  $\delta^{13}\text{C}$ , photosynthesis has a significant impact on the  $\delta^2\text{H}$  of plant organic matter (Ziegler et al., 1976; Luo et al., 1991; Yakir, 1992; Schmidt et al., 2003; Sachse et al., 2012). However, the processes behind the impact of photosynthetic metabolism on plant  $\delta^2\text{H}$  remain unclear (Sachse et al., 2012) even if and these mechanisms appear to be distinct from those that determine  $\delta^{13}\text{C}$ .

Moreover, similarly to  $\delta^{18}\text{O}$ , the  $\delta^2\text{H}$  in plant water is strongly affected by the isotopic signature of the (i) water source in the topsoil, which varies in its turn depending on precipitation and/or irrigation water and the temporal evaporation that occurs from the soil surface before root water uptake and (ii) environmental effects such as the influence of

relative humidity on plant evaporation processes (Roden and Ehleringer, 1999). Nevertheless, no fractionation of  $\delta^{18}\text{O}$  and  $\delta^2\text{H}$  has been observed between roots or shoot tissues and the water transported in the xylem (Cernusak et al., 2016; Dawson and Ehleringer, 1993). In transpiring tissues such as leaves, evaporative processes associated with leaf biochemical reactions are involved in organic matter synthesis and transport, and water diffusion through the stomata and even the cuticle, as well as other factors such as the length of the pathway through the plant exposed to evaporation (e.g. plant height and leaf blade length) which may also affect  $\delta^{18}\text{O}$  and  $\delta^2\text{H}$  in plant water and in turn the imprint of  $\delta^{18}\text{O}$  and  $\delta^2\text{H}$  in plant organic matter (Helliker and Ehleringer, 2002). In organic matter however,  $\delta^{18}\text{O}$  and  $\delta^2\text{H}$  demonstrated rather different fractioning patterns during biosynthesis reactions (Sternberg 1989; Yakir and DeNiro, 1990). The imprinted  $\delta^{18}\text{O}$  in organic compounds is mainly influenced by  $\delta^{18}\text{O}$  of the plant water, therefore the isotope effects associated with evaporation and water transport to the leaf explain the enrichment in  $\delta^{18}\text{O}$  isotopic signal in organic matter above water source isotopic signature (DeNiro and Epstein, 1979; Yakir, 1992). In  $\delta^2\text{H}$  of organic matter however, fractionation of  $^2\text{H}$  is not only affected by evaporative effects but also as mentioned above by the nature of organ trophism as a consequence of biochemical processes between organic compounds and cellular water causing (Ziegler et al., 1976; Sternberg et al., 1984; Ziegler, 1989; Yakir and Deniro, 1990; Luo and Sternberg, 1991; Yakir, 1992).

Differences between the atmospheric vapor pressure deficit (VPD) and the stomatal cavities VPD are the main drivers to changes in intrinsic water movements in plants. Enrichment tendencies in  $\delta^{18}\text{O}$  and  $\delta^2\text{H}$  signatures was previously reported in leaf water of wheat (Liu et al., 2017), and in  $\delta^{18}\text{O}$  of the organic matter in rice (Kaushal and Ghosh, 2018a, 2018b), maize (Cabrera-Bosquet et al., 2009) and other C3 plants (Helliker and Ehleringer, 2002) when grown under higher VPD conditions. The aim of this study is to assess the potential effect of two contrasting growing conditions (40% vs 80% relative humidity levels) on photosynthesis and transpiration and how these circumstances affect the  $\delta^2\text{H}$  on autotrophic (leaves and glumes), mixotrophic (awns) and heterophic (grains) tissues compared with  $\delta^{13}\text{C}$  and  $\delta^{18}\text{O}$ . To this end,  $\delta^2\text{H}$  and  $\delta^{18}\text{O}$  were labeled in order to zoom in the fractionation effects caused by the different growing conditions. The association of the different isotopic signatures with physiological parameters such as transpiration and photosynthetic mechanisms may help to

explain such effects. We hypothesized that under higher VPD (40% relative humidity), the photosynthesis and associated parameters such as ETR (Electron transport rate) might decrease, resulting in enriched plant organic  $\delta^2\text{H}$  compared plants grown under lower VPD (80% relative humidity). This effect should be zoomed under labeling using heavy  $\delta^{18}\text{O}$  and  $\delta^2\text{H}$  enriched water to label root uptake water in plants. To the best of our knowledge, there have been no studies in crop species that have reported on the variation in  $\delta^2\text{H}$  within different detailed tissues of durum wheat grown under contrasting conditions (with different VPD) and therefore, comparison among these three stable lights ( $\delta^{13}\text{C}$ ,  $\delta^2\text{H}$  and  $\delta^{18}\text{O}$ ) as an eco-physiological tool.

## 2. Materials and methods

### 2.1. Experimental setup

The experiment was conducted under controlled conditions on the Spanish durum wheat cultivar “*Sula*” (*Triticum durum* Desf. cv. *Sula*). “*Sula*” is a modern semi-dwarf post green revolution cultivar, commonly cultivated in the Mediterranean region for its drought tolerance and higher grain yield (Erice et al., 2019). Ninety-six individual plants from the genotype “*Sula*” were evaluated in two different growth chambers with contrasting and constant relative humidity conditions (40% and 80%). Plants were grown in 3-L pots filled with sand (one plant per pot). Plants were watered three times a week with Hoagland nutrient solution and were grown under controlled conditions in a growth chamber (Conviron E15, Controlled Environments Ltd., Winnipeg, Canada). Plants were supplied with illumination reaching a photosynthetic photon flux density PPFD of about  $400 \mu\text{M m}^{-2}\text{s}^{-1}$  at plant level during the light period (14 h). Plants were grown in a constant RH of 40% or 80% within two different growth chambers, with a temperature of  $23^\circ\text{C} / 17^\circ\text{C}$  during the light and dark periods, respectively. Plants were subjected to a VPD of 1.03 KPa (considering an average temperature of  $20^\circ\text{C}$ ), day/night in the 40% RH growth chamber, and 0.09 KPa (considering an average temperature of  $20^\circ\text{C}$ ), day/night in the 80% RH growth chamber. To trace  $\text{d}^{18}\text{O}$  fractionation patterns within the plant from source to sink tissues, oxygen isotope composition was labeled with normalized water  $^{18}\text{O}$  97% ( $\text{H}_2^{18}\text{O}$ , EURISO-TOP, France and) and was applied together with Hoagland solution two weeks after anthesis. Hydrogen isotope composition was labeled with Deuterium Oxide 99% ( $^2\text{H}_2\text{O}$ , EURISO-TOP, France and) and was

applied together with Hoagland every irrigation after anthesis. The tracer solutions were created to achieve a  $\text{H}_2^{18}\text{O}$  enrichment of 36‰ for  $^{18}\text{O}$  and 816‰ for  $^2\text{H}$ . In each growth chamber and RH condition, half plants were supplied with heavy  $\text{d}^{18}\text{O}$  and  $\text{d}^2\text{H}$  water (labeled), whereas the other half kept receiving irrigation using tap water (control). Two weeks after anthesis 48 h after finishing the labeling in the case of  $\text{d}^{18}\text{O}$ ), stem basis, flag leaves, peduncle, glumes, awns and developing grains were collected and prepared for further  $\text{d}^{18}\text{O}$  and  $\text{d}^2\text{H}$  isotope composition analyses.

## 2.2. Agronomic traits

Shoot fresh matter was sampled during mid grain filling were oven-dried for 72 h at 60 °C to determine shoot dry weight ( $\text{DW}_{\text{shoot}}$ ). At maturity, biomass, and grain number per ears were sampled in individual plants, oven-dried for 72 h at 60 °C, and grain number per ear ( $\text{GN}_{\text{ear}}$ ) was determined together with the dry weight of biomass ( $\text{DW}_{\text{biomass}}$ ), ear dry weight ( $\text{DW}_{\text{ear}}$ ) and grain dry weight per ear ( $\text{DW}_{\text{grain}}$ ).

## 2.3. Photosynthesis and gas exchange

During mid grain filling, photosynthesis and gas exchange measurements were assessed in flag leaves using a LI-6400XT portable gas exchange photosynthesis system (Li-COR, Lincoln, NE). Under saturating conditions of PPFD of 1500  $\mu\text{mol m}^{-2} \text{s}^{-1}$  and 20°C, the photosynthetic rate ( $A_{\text{max}}$ ), stomatal conductance ( $g_s$ ), sub-stomatal  $\text{CO}_2$  ( $C_i$ ), intrinsic efficiency of photosystem II ( $F_v'/F_m'$ ), quantum efficiencies of photosynthetic electron transport through photosystem II ( $\Phi_{\text{PS2}}$ ), photosynthetic electron transport rate (ETR), and transpiration (Tr) were determined.

## 2.4. Chlorophyll content

Chlorophyll content was assessed by mid grain filling in individual plants using the leaf clip sensor SPAD (Minolta SPAD-502, Spectrum Technologies Inc., Plainfield, IL, USA). For each measurement, five replicates were taken and averaged to determine chlorophyll content.

## 2.5. Carbon isotope composition analysis

Under each growing condition (relative humidity level and isotope labeling), sampled plant tissues were oven-dried at 60 °C for a minimum of 48h, pulverized to a fine powder from which approximately 1mg was enclosed in tin capsules. Afterwards, carbon isotope composition ( $\delta^{13}\text{C}_{\text{DM}}$ ) was performed using an elemental analyzer operating in a continuous flow mode with a mass spectrometer (Delta C IRMS; ThermoFinnigan, Bremen; Germany), at the Scientific and Technical facilities of the University of Barcelona following the Eq. (1):

$$\delta^{13}\text{C}_{\text{DM}} (\text{‰}) = [\text{R}_{\text{sample}} / \text{R}_{\text{standard}} - 1] \times 1000 \quad (1)$$

Where  $\delta^{13}\text{C}_{\text{DM}}$  values are expressed per mil (‰), sample refers to plant material and standard to Pee Dee Belemnite (PDB) calcium carbonate (Farquhar et al., 1989). International isotope secondary standards of known  $^{13}\text{C}/^{12}\text{C}$  ratios (IAEA-CH7, IAEA-CH6 and IAEA-600, and USGS 40) were used with an analytical precision of 0.1‰.

## 2.6. Hydrogen isotope composition analyses in dry matter

Hydrogen isotope composition ( $\text{d}^2\text{H}_{\text{DM}}$ ) was determined in the plant tissue samples (flag leaves, peduncle, awn, glume and developing grains) by mid grain filling. Samples were oven dried for 72 h under 60 °C, then reduced to a fine powder. Afterwards, approximately 1 mg (oxygen) and 0.15 mg (hydrogen) were weighed in silver capsules, enclosed and kept under moisture free conditions using silica-gel in a desiccator, until stable isotope analysis.  $\text{d}^2\text{H}$  was determined by an online pyrolysis technique using a Thermo-Chemical Elemental Analyzer (TC/EA; Thermo Fisher Scientific) coupled with an IRMS (Delta C Finnigan MAT). Results were expressed in (‰) using the standards (IAEA CH7 polyethylene foil, 5 $\alpha$ - androstane, coumarin, and eicosanoic acid methyl ester), in addition to the internal standard (IAEA 601), calibrated against Vienna Standard Mean Oceanic Water (VSMOW), with an analytical precision of 0.5‰.  $\text{d}^2\text{H}$  values were expressed per mil (‰) and determined following Eq. (2):

$$\delta^2\text{H}_{\text{DM}} (\text{‰}) = [\text{R}_{\text{sample}} / \text{R}_{\text{standard}} - 1] \times 1000 \quad (2)$$

Where  $\delta^2\text{H}_{\text{DM}}$  values are the stable isotope composition of hydrogen.  $\text{R}_{\text{sample}}$  and  $\text{R}_{\text{standard}}$  are the isotope ratios of the organic matter of the plant material and the VSMOW standard, respectively. In addition, a dual-water equilibration method was performed in order to



quantify the fraction of exchangeable H and to determine the  $\delta^2\text{H}$  in the nonexchangeable H fraction (Schimmelmann et al., 2001; Sauer et al., 2009; Qi and Coplen, 2011). Dry leaf, glumes, awns and grains material of the same sample and tissues used in the experiment, plus standards, were used for the dual-water equilibration method as explained in Sanchez-Bragado et al 2019. Then the true  $\delta^2\text{H}_n$  values of DM were calculated and the  $\delta^2\text{H}$  of DM in the flag leaves, awns, glumes and the grains were corrected using the fraction of total hydrogen that is exchangeable, obtained within the different equilibration conditions. Thus the  $\delta^2\text{H}$  of the DM presented in the results is the  $\delta^2\text{H}$  of nonexchangeable H of the organics.

## 2.7. Oxygen and hydrogen composition in plant water

To determine water source and movements in plant tissues, samples of the stem base were harvested by mid grain filling together with flag leaves, peduncle samples and developing grains, and sealed immediately in analytical tubes and frozen at  $-80\text{ }^\circ\text{C}$ . Afterwards, water was extracted from the sampled plant tissues using a cryogenic vacuum distillation line (Dawson and Ehleringer, 1993). Sample tubes were placed in a heated silicone oil bath ( $120\text{ }^\circ\text{C}$ ), and connected with Ultra-Torr<sup>TM</sup> unions (Swagelok Company, Solon, OH, USA) to a vacuum system ( $\sim 10^{-2}$  mbar), in series, with U-shaped collector tubes cooled with liquid  $\text{N}_2$ . Ninety minutes after commencing extraction, the extracted water in each plant tissue was transferred into 2 ml vials and stored at  $4\text{ }^\circ\text{C}$  until analysis. Water tissues oxygen ( $\delta^{18}\text{O}_{\text{WT}}$ ) and hydrogen ( $\delta^2\text{H}_{\text{WT}}$ ) stable isotope compositions were determined by isotope-ratio infrared spectroscopy, using a Picarro L2120-I isotopic water analyser, coupled to an A0211 high-precision vaporizer (Picarro Inc., Sunnyvale, CA, USA) at the scientific facilities of University of Lleida. Isotopes were expressed in delta (d) notation (‰) relative to VSMOW (i.e. isotopic composition of oxygen,  $\text{d}^{18}\text{O}$ , and hydrogen,  $\text{d}^2\text{H}$ ). Raw values were calibrated against three internal laboratory references [calibrated against IAEA standards VSMOW2, Standard Light Antarctic Precipitation2 (SLAP2), and Greenland Ice Sheet Precipitation]. Analytical precisions for  $\delta^{18}\text{O}$  and  $\delta^2\text{H}$  was  $0.05\text{‰}$  and  $0.17\text{‰}$ , respectively, and the occurrence of contaminants was tested using Picarro's ChemCorrect post-processing software and corrected, when necessary, following (Martín-Gómez et al., 2015).

## 2.8. Carbon and oxygen water soluble fraction analyses

For each pulverized sample, a 50 mg was suspended with 1 mL of Milli-Q water in an Eppendorf tube (Eppendorf Scientific, Hamburg, Germany) for 20 min under 5 °C; the sample was then centrifuged at 12 000 rpm for 5 min under 5 °C. Afterwards, the supernatant containing the water-water soluble fraction was pipetted into a new Eppendorf and heated at 100 °C for 3 min for proteins denaturation. Samples were centrifuged a second time (12 000 rpm for 5 min under 5 °C), then around 100 µL of the resulting aliquot was placed in tin ( $\delta^{13}\text{C}$ ) and silver ( $\delta^{18}\text{O}$ ) capsules and dried at 70 °C for 2 h. The water soluble fraction of carbon ( $\delta^{13}\text{C}_{\text{WSF}}$ ) and oxygen ( $\delta^{18}\text{O}_{\text{WSF}}$ ) isotope compositions was then determined at the Scientific Facilities of the University of Barcelona as described in the previous paragraph.

## 2.9. Statistical analysis

Variance analysis (ANOVA) was performed using SPSS 25 (IBM SPSS Statistics 25, Inc., Chicago, IL; USA), to assess the effects of relative humidity levels (40% vs 80%) on the assessed physiological traits, stable isotopes and yield components, under different isotope labeling conditions (control and labeled); Followed with Tukey-b post-hoc tests to reveal differences within plant tissues. A bivariate Pearson correlation was carried using the same statistical package to assess relationships between stable isotopes and physiological traits, as well as the relationships between stable isotopes within the same plant tissues. Graphs were created using Sigma-plot 10.0 (Systat Software Inc, California; USA) and the open-source software, RStudio 1.2.5 (R Foundation for Statistical Computing, Vienna, Austria).

## 3. Results

### 3.1 The effect of relative humidity (VPD) on physiological and agronomical parameters

#### *Physiological traits and agronomic components*

Relative humidity of 40% (high VPD) significantly decreased all photosynthetic traits and shoot biomass measured during grain filling, compared with a relative humidity of 80% (low VPD) (Table 1). Likewise, by maturity, a decreasing trend was observed in grain number (GN), grain dry weight ( $\text{DW}_{\text{Grain}}$ ), biomass dry weight ( $\text{DW}_{\text{Biomass}}$ ) and ear dry weight ( $\text{DW}_{\text{Ear}}$ ) under high VPD, compared with low VPD.

**Table 1.** Effect of relative humidity (40% vs 80%) on chlorophyll content, sub-stomatal CO<sub>2</sub> (Ci), photosynthetic rate (Amax), stomatal conductance (g<sub>s</sub>), intrinsic efficiency of photosystem II (Fv'/Fm'), quantum efficiencies of photosynthetic electron transport through photosystem II (PhiPS2), photosynthetic electron transport rate (ETR), transpiration (Tr) and shoot dry weight (DW<sub>Shoot</sub>) during mid grain filling, and dry matter of biomass (DW<sub>Biomass</sub>), ear per plant (DW<sub>Ear</sub>) and grain per ear (DW<sub>Grain</sub>), and grain number per ear (GN) at maturity.

Mid grain filling										Maturity			
Chlorophyll	Ci	Amax ( $\mu\text{mol}\cdot\text{CO}_2\cdot\text{m}^{-2}\cdot\text{s}^{-1}$ )	g <sub>s</sub> ( $\text{mmol}\cdot\text{H}_2\text{O}\cdot\text{m}^{-2}\cdot\text{s}^{-1}$ )	Fv'/Fm'	PhiPS2	ETR	Tr (mmol)	DW <sub>Shoot</sub> (g)	GN (ear <sup>-1</sup> )	DW <sub>ear</sub> (g)	DW <sub>grain</sub> (g.ear <sup>-1</sup> )	DW <sub>biomass</sub> (g)	
40%	50.26±1.73	175.8±11.5	15.61±0.77	0.12±0.01	0.42±0.02	0.26±0.01	133.5±7.2	2.31±0.13	1.83±0.23	46.00±6.60	3.38±0.39	2.36±0.38	17.16±2.11
80%	57.00±1.98	203.4±5.3	17.95±0.49	0.17±0.01	0.53±0.01	0.34±0.01	170.7±3.0	3.30±0.17	3.40±0.36	60.00±3.20	4.06±0.27	2.65±0.29	21.50±1.99
ANOVA	<0.001	<0.050	<0.050	<0.010	<0.010	<0.010	<0.010	<0.010	<0.001	ns	ns	ns	ns

Values shown are the mean ± SE for twenty-four replicates under 40% and 80% of relative humidity, under control and labeled conditions. Level of significance for the ANOVA: P<0.001, P<0.010 and P<0.050.

### 3.2. Effect of VPD (relative humidity) under stable isotope composition

#### *Carbon isotope composition in plant organic matter*

Carbon isotope composition ( $\delta^{13}\text{C}$ ) was assessed in the dry matter (DM) and water soluble fraction (WSF) of different plant tissues (flag leaf, peduncle, glume, awn, grains), and under different relative humidity levels (Table 2; Supplemental Table 1). When combining control and labeled treatments,  $\delta^{13}\text{C}$  was significantly enriched (higher  $\delta^{13}\text{C}$  values) in all tissues under high VPD (Table 2). Nevertheless, considering only the controlled conditions,  $\delta^{13}\text{C}$  in WSF was significantly enriched across all plant tissues, whereas under labeled conditions, only the peduncle was enriched in  $\delta^{13}\text{C}$  under higher VPD conditions (Supplemental Table 1).

**Table 2.** Effect of relative humidity (40% vs 80%) on carbon stable isotope composition ( $\delta^{13}\text{C}$ ) of the water soluble fraction of flag leaves, peduncles, glumes and awn, and the dry matter of flag leaves and grains. Flag leaves, peduncles, glumes and awns were sampled during mid grain filling, and grains at maturity.

	Water soluble fraction				Dry matter	
	$\delta^{13}\text{C}_{\text{flag leaf}}$ (‰)	$\delta^{13}\text{C}_{\text{peduncle}}$ (‰)	$\delta^{13}\text{C}_{\text{glume}}$ (‰)	$\delta^{13}\text{C}_{\text{awn}}$ (‰)	$\delta^{13}\text{C}_{\text{flag leaf}}$ (‰)	$\delta^{13}\text{C}_{\text{grain}}$ (‰)
40%	-27.1±0.6	-23.9±0.5	-25.9±0.5	-25.8±0.5	-27.8±0.7	-24.3±0.6
80%	-30.1±0.3	-27.6±0.3	-27.8±0.3	-28.2±0.3	-30.2±0.4	-28.7±0.5
<b>ANOVA</b>	<b>&lt;0.010</b>	<b>&lt;0.001</b>	<b>&lt;0.010</b>	<b>&lt;0.001</b>	<b>&lt;0.050</b>	<b>&lt;0.001</b>

*Values shown are the mean  $\pm$  SE under 40% and 80% of relative humidity. In water soluble fraction, twelve replicates were used under control and labeled conditions combined. In dry matter, six replicates were used under control conditions only. Level of significance for the ANOVA:  $P < 0.001$ ,  $P < 0.010$  and  $P < 0.050$*

#### *Oxygen and hydrogen isotope compositions in plant organic matter*

$\delta^{18}\text{O}_{\text{WSF}}$  (WSF of plant tissues) was enriched in the flag leaf, peduncle, glumes, awns and grains under higher VPD and for control conditions (Table 3). Under labeled conditions, a similar trend was observed, although only the flag leaf and awns were enriched. Regarding the differences among tissues,  $\delta^{18}\text{O}_{\text{WSF}}$  was mostly enriched in the flag leaf and the grains, and depleted in the glumes, under both VPDs studied under control conditions. For the labeling conditions,  $\delta^{18}\text{O}_{\text{WSF}}$  was enriched in the peduncle and depleted the rest of tissues (Table 3).

Hydrogen isotope composition in the dry matter of plant tissues ( $\delta^2\text{H}_{\text{DM}}$ ) has shown a similar enrichment pattern to  $\delta^{18}\text{O}_{\text{WSF}}$  and  $\delta^{13}\text{C}_{\text{WSF}}$  (Table 3), although  $\delta^2\text{H}_{\text{DM}}$  enrichment was found under high VPD conditions in awns and grains only for control, and in the flag leaf and grains for labeled conditions (Table 3). Concerning differences among tissues,  $\delta^2\text{H}_{\text{DM}}$  was enriched in awns and grains and depleted in the flag leaf, glumes and the peduncle, under both VPD conditions for the control. For the labelling conditions however,  $\delta^2\text{H}_{\text{DM}}$  was enriched in the peduncle and grains, and depleted in the flag leaf, glumes and awns under high VPD conditions, and enriched in the peduncle and depleted in the rest of tissues under low VPD conditions (Table 3).

**Table 3.** Effect of relative humidity (40% vs 80%) on oxygen stable isotope composition ( $\delta^{18}\text{O}$ ) of water soluble fraction, and hydrogen stable isotope compositions ( $\delta^2\text{H}$ ) of dry matter, analyzed in flag leaves, peduncles, glumes, awns during mid grain filling, and grains at maturity.

		Water soluble fraction					Dry matter				
		$\delta^{18}\text{O}_{\text{flag leaf}}$	$\delta^{18}\text{O}_{\text{peduncle}}$	$\delta^{18}\text{O}_{\text{glume}}$	$\delta^{18}\text{O}_{\text{awn}}$	$\delta^{18}\text{O}_{\text{grain}}$	$\delta^{12}\text{H}_{\text{flag leaf}}$	$\delta^{12}\text{H}_{\text{peduncle}}$	$\delta^{12}\text{H}_{\text{glume}}$	$\delta^{12}\text{H}_{\text{awn}}$	$\delta^{12}\text{H}_{\text{grain}}$
		(‰)	(‰)	(‰)	(‰)	(‰)	(‰)	(‰)	(‰)	(‰)	(‰)
Control	40%	32.7 $\mathbf{a}$ $\pm$ 0.5	28.4 $\mathbf{c}$ $\pm$ 0.2	27.0 $\mathbf{c}$ $\pm$ 0.4	28.3 $\mathbf{c}$ $\pm$ 0.2	30.3 $\mathbf{b}$ $\pm$ 0.4	-95.1 $\mathbf{c}$ $\pm$ 3.9	-95.2 $\mathbf{c}$ $\pm$ 2.2	-116.2 $\mathbf{d}$ $\pm$ 3.1	-62.4 $\mathbf{b}$ $\pm$ 3.3	-13.1 $\mathbf{a}$ $\pm$ 3.5
	80%	27.4 $\mathbf{a}$ $\pm$ 0.3	27.2 $\mathbf{a}$ $\pm$ 0.3	24.1 $\mathbf{b}$ $\pm$ 0.6	24.9 $\mathbf{b}$ $\pm$ 0.3	26.7 $\mathbf{a}$ $\pm$ 0.1	-113.6 $\mathbf{c}$ $\pm$ 8.2	-124.8 $\mathbf{c}$ $\pm$ 3.0	-128.5 $\mathbf{c}$ $\pm$ 4.2	-77.7 $\mathbf{b}$ $\pm$ 3.3	-29.0 $\mathbf{a}$ $\pm$ 2.4
	<b>ANOVA</b>	<b>&lt;0.001</b>	<b>&lt;0.050</b>	<b>&lt;0.010</b>	<b>&lt;0.001</b>	<b>&lt;0.001</b>	<b>ns</b>	<b>ns</b>	<b>ns</b>	<b>&lt;0.050</b>	<b>&lt;0.010</b>
Labeled	40%	37.5 $\mathbf{b}$ $\pm$ 1.3	42.2 $\mathbf{a}$ $\pm$ 1.0	33.6 $\mathbf{b}$ $\pm$ 1.0	34.8 $\mathbf{b}$ $\pm$ 0.7	36.0 $\mathbf{b}$ $\pm$ 1.3	-26.2 $\mathbf{b}$ $\pm$ 7.42	147.0 $\mathbf{a}$ $\pm$ 35.5	-14.5 $\mathbf{b}$ $\pm$ 7.8	7.9 $\mathbf{b}$ $\pm$ 4.8	166.7 $\mathbf{a}$ $\pm$ 22.7
	80%	30.6 $\mathbf{b}$ $\pm$ 0.6	41.1 $\mathbf{a}$ $\pm$ 0.6	30.5 $\mathbf{b}$ $\pm$ 0.9	29.9 $\mathbf{b}$ $\pm$ 0.1	32.9 $\mathbf{b}$ $\pm$ 0.5	-78.1 $\mathbf{d}$ $\pm$ 4.7	196.5 $\mathbf{a}$ $\pm$ 19.2	62.5 $\mathbf{b}$ $\pm$ 5.3	10.4 $\mathbf{c}$ $\pm$ 10.9	84.9 $\mathbf{b}$ $\pm$ 14.0
	<b>ANOVA</b>	<b>&lt;0.010</b>	<b>ns</b>	<b>ns</b>	<b>&lt;0.001</b>	<b>ns</b>	<b>&lt;0.001</b>	<b>ns</b>	<b>&lt;0.001</b>	<b>ns</b>	<b>&lt;0.050</b>

Values shown are the mean  $\pm$  SE for six replicates under 40% and 80% of relative humidity, under control and labeled conditions. Level of significance for the ANOVA:  $P < 0.001$ ,  $P < 0.010$  and  $P < 0.050$ . Means exhibiting different letters are significantly different ( $P < 0.05$ ) across plant tissues by the post-hoc test (Tukey-b) on independent samples

### 3.3. Relationships between physiological traits and yield components, with the $\delta^{13}\text{C}$ and $\delta^{18}\text{O}_{\text{WSF}}$ and $\delta^2\text{H}_{\text{DM}}$ in different plant fractions and tissues

Correlations of physiological traits assessed by mid grain filling against the organic matter of carbon isotope composition ( $\delta^{13}\text{C}_{\text{WSF}}$ ) were evaluated by combining water labeling conditions in (Table 4). Under combined VPD conditions,  $\delta^{13}\text{C}_{\text{WSF}}$  in the flag leaf and grains correlated negatively against  $A_{\text{max}}$  and  $g_s$  whereas the  $\delta^{13}\text{C}_{\text{WSF}}$  in the peduncle and glume correlated negatively against  $g_s$ . Under high VPD, not many correlations were observed, whereas under low VPD, negative correlations were observed between  $\delta^{13}\text{C}_{\text{WSF}}$  versus  $g_s$ , Tr and different photochemical (PhiPS2 and ETR) and different photosynthetic/photochemical parameters mainly in the flag leaf and in a lesser extent the peduncle and awns.

**Table 4.** Pearson correlations of carbon isotope composition ( $\delta^{13}\text{C}$ ) in the water soluble fraction during mid grain filling in different plant tissues (flag leaf, peduncle, glume, awn, grain), against chlorophyll content, sub-stomatal  $\text{CO}_2$  ( $\text{C}_i$ ), photosynthetic rate ( $A_{\text{max}}$ ), stomatal conductance ( $g_s$ ), intrinsic efficiency of photosystem two ( $F_v'/F_m'$ ), quantum efficiencies of photosynthetic electron transport through photosystem II ( $\text{PhiPS2}$ ), Photosynthetic electron transport rate (ETR) and transpiration (Tr) during mid grain filling, under different relative humidity levels (40% vs 80%), and combining control and labeled conditions.

	Combined RH				40%				80%			
	$\delta^{13}\text{C}_{\text{flag leaf}}$	$\delta^{13}\text{C}_{\text{Peduncle}}$	$\delta^{13}\text{C}_{\text{Glume}}$	$\delta^{13}\text{C}_{\text{Awn}}$	$\delta^{13}\text{C}_{\text{flag leaf}}$	$\delta^{13}\text{C}_{\text{Peduncle}}$	$\delta^{13}\text{C}_{\text{Glume}}$	$\delta^{13}\text{C}_{\text{Awn}}$	$\delta^{13}\text{C}_{\text{flag leaf}}$	$\delta^{13}\text{C}_{\text{Peduncle}}$	$\delta^{13}\text{C}_{\text{Glume}}$	$\delta^{13}\text{C}_{\text{Awn}}$
Chlorophyll	-0.058 <sup>ns</sup>	-0.201 <sup>ns</sup>	-0.004 <sup>ns</sup>	-0.283 <sup>ns</sup>	0.472 <sup>ns</sup>	0.509 <sup>ns</sup>	0.558 <sup>ns</sup>	0.191 <sup>ns</sup>	0.452 <sup>ns</sup>	0.233 <sup>ns</sup>	0.372 <sup>ns</sup>	0.456 <sup>ns</sup>
$\text{C}_i$	-0.749 <sup>**</sup>	-0.832 <sup>**</sup>	-0.708 <sup>**</sup>	-0.746 <sup>**</sup>	-0.357 <sup>ns</sup>	-0.407 <sup>ns</sup>	-0.463 <sup>ns</sup>	-0.262 <sup>ns</sup>	-0.769 <sup>**</sup>	-0.883 <sup>**</sup>	-0.361 <sup>ns</sup>	-0.663 <sup>ns</sup>
$A_{\text{max}}$	-0.477 <sup>*</sup>	-0.448 <sup>ns</sup>	-0.358 <sup>ns</sup>	-0.476 <sup>*</sup>	-0.347 <sup>ns</sup>	-0.262 <sup>ns</sup>	-0.255 <sup>ns</sup>	-0.339 <sup>ns</sup>	-0.261 <sup>ns</sup>	-0.138 <sup>ns</sup>	0.146 <sup>ns</sup>	-0.154 <sup>ns</sup>
$g_s$	-0.713 <sup>**</sup>	-0.748 <sup>**</sup>	-0.590 <sup>**</sup>	-0.652 <sup>**</sup>	-0.354 <sup>ns</sup>	-0.562 <sup>ns</sup>	-0.479 <sup>ns</sup>	-0.044 <sup>ns</sup>	-0.798 <sup>**</sup>	-0.734 <sup>*</sup>	-0.219 <sup>ns</sup>	-0.704 <sup>*</sup>
$F_v'/F_m'$	-0.304 <sup>ns</sup>	-0.413 <sup>ns</sup>	-0.290 <sup>ns</sup>	-0.432 <sup>ns</sup>	0.560 <sup>ns</sup>	0.660 <sup>ns</sup>	0.609 <sup>ns</sup>	0.316 <sup>ns</sup>	-0.597 <sup>ns</sup>	-0.438 <sup>ns</sup>	-0.125 <sup>ns</sup>	-0.582 <sup>ns</sup>
$\text{PhiPS2}$	-0.152 <sup>ns</sup>	-0.226 <sup>ns</sup>	-0.070 <sup>ns</sup>	-0.282 <sup>ns</sup>	0.476 <sup>ns</sup>	0.583 <sup>ns</sup>	0.518 <sup>ns</sup>	0.245 <sup>ns</sup>	-0.699 <sup>*</sup>	-0.615 <sup>ns</sup>	0.065 <sup>ns</sup>	-0.509 <sup>ns</sup>
ETR	-0.147 <sup>ns</sup>	-0.223 <sup>ns</sup>	-0.067 <sup>ns</sup>	-0.278 <sup>ns</sup>	0.482 <sup>ns</sup>	0.586 <sup>ns</sup>	0.522 <sup>ns</sup>	0.252 <sup>ns</sup>	-0.695 <sup>*</sup>	-0.612 <sup>ns</sup>	0.069 <sup>ns</sup>	-0.506 <sup>ns</sup>
Tr	-0.498 <sup>*</sup>	-0.459 <sup>ns</sup>	-0.353 <sup>ns</sup>	-0.414 <sup>ns</sup>	-0.378 <sup>ns</sup>	-0.486 <sup>ns</sup>	-0.564 <sup>ns</sup>	-0.135 <sup>ns</sup>	-0.807 <sup>**</sup>	-0.760 <sup>*</sup>	-0.205 <sup>ns</sup>	-0.721 <sup>*</sup>
$\text{DW}_{\text{shoot}}$	0.175 <sup>ns</sup>	0.020 <sup>ns</sup>	0.051 <sup>ns</sup>	0.088 <sup>ns</sup>	0.968 <sup>**</sup>	0.754 <sup>*</sup>	0.701 <sup>*</sup>	0.929 <sup>**</sup>	0.486 <sup>ns</sup>	0.459 <sup>ns</sup>	0.232 <sup>ns</sup>	0.812 <sup>**</sup>

For each relative humidity level (40% vs 80%), correlations were calculated using twelve replicates by combining control and labeled conditions. Level of significance: ns, not significant; \*\*,  $P < 0.01$ ; \*,  $P < 0.05$



By combining both VPD levels, and under each water labeling condition, correlations of  $\delta^{18}\text{O}_{\text{WSF}}$  and  $\delta^2\text{H}_{\text{DM}}$  were evaluated against physiological traits (Table 5) and yield components (Supplemental Table 3). Under control conditions, the flag leaf and particularly the grains were the tissues that showed most negative correlations of  $\delta^{18}\text{O}_{\text{WSF}}$  against photosynthetic/photochemical parameters. In addition, the  $\delta^{18}\text{O}$  of all organs showed a negative correlation against  $g_s$ . Under labelled conditions however, almost no correlations were observed. Similarly to the  $\delta^{18}\text{O}$ , the  $\delta^2\text{H}_{\text{DM}}$  in the grains grown under control conditions, were the organ which showed the most correlations with photosynthetic and photochemical parameters. In terms of agronomical traits (Supplemental Table 3), no correlations were found between the isotopes ( $\delta^{18}\text{O}_{\text{WSF}}$  and  $\delta^2\text{H}_{\text{DM}}$ ) and yield components, except for the negative correlation of  $\delta^{18}\text{O}_{\text{WSF}}$  in the flag leaf and DW and GN of the ear.

**Table 5.** Pearson correlations of oxygen ( $\delta^{18}\text{O}$ ) and hydrogen ( $\delta^2\text{H}$ ) stable isotope compositions in the organic matter ( $\delta^{12}\text{H}$  in dry matter,  $\delta^{18}\text{O}$  in water soluble fraction), during mid grain filling in different plant tissues (flag leaf, peduncle, glume, awn, grain), against chlorophyll content, sub-stomatal  $\text{CO}_2$  (Ci), photosynthetic rate (Amax), stomatal conductance ( $g_s$ ), intrinsic efficiency of photosystem two (Fv'/Fm'), quantum efficiencies of photosynthetic electron transport through photosystem II (PhiPS2), Photosynthetic electron transport rate (ETR), transpiration (Tr), and shoot dry weight ( $\text{DW}_{\text{shoot}}$ ) during mid grain filling and combining humidity levels (40% and 80%).

	Water soluble fraction					Dry matter					
	$\delta^{18}\text{O}_{\text{flag leaf}}$	$\delta^{18}\text{O}_{\text{Peduncle}}$	$\delta^{18}\text{O}_{\text{Glume}}$	$\delta^{18}\text{O}_{\text{Awn}}$	$\delta^{18}\text{O}_{\text{Grain}}$	$\delta^2\text{H}_{\text{flag leaf}}$	$\delta^2\text{H}_{\text{Peduncle}}$	$\delta^2\text{H}_{\text{Glume}}$	$\delta^2\text{H}_{\text{Awn}}$	$\delta^2\text{H}_{\text{Grain}}$	
Control	Chlorophyll	-0.366 <sup>ns</sup>	-0.493 <sup>ns</sup>	-0.383 <sup>ns</sup>	-0.515 <sup>ns</sup>	-0.926**	-0.666*	0.078 <sup>ns</sup>	-0.639*	-0.865**	-0.694*
	Ci	-0.876**	-0.800**	-0.881**	-0.889**	0.082 <sup>ns</sup>	-0.469 <sup>ns</sup>	-0.345 <sup>ns</sup>	-0.317 <sup>ns</sup>	-0.536 <sup>ns</sup>	0.404 <sup>ns</sup>
	Amax	-0.695*	-0.143 <sup>ns</sup>	-0.278 <sup>ns</sup>	-0.606 <sup>ns</sup>	-0.687*	-0.290 <sup>ns</sup>	-0.246 <sup>ns</sup>	-0.625 <sup>ns</sup>	-0.508 <sup>ns</sup>	-0.768**
	$g_s$	-0.913**	-0.694*	-0.837**	-0.830**	-0.753**	-0.475 <sup>ns</sup>	-0.423 <sup>ns</sup>	-0.479 <sup>ns</sup>	-0.548 <sup>ns</sup>	-0.737**
	Fv'/Fm'	-0.816**	-0.433 <sup>ns</sup>	-0.534 <sup>ns</sup>	-0.696*	-0.724**	-0.073 <sup>ns</sup>	-0.356 <sup>ns</sup>	-0.558 <sup>ns</sup>	-0.513 <sup>ns</sup>	-0.730**
	PhiPS2	-0.390 <sup>ns</sup>	-0.112 <sup>ns</sup>	-0.209 <sup>ns</sup>	-0.090 <sup>ns</sup>	-0.714**	-0.024 <sup>ns</sup>	-0.042 <sup>ns</sup>	-0.711*	-0.252 <sup>ns</sup>	-0.731**
	ETR	-0.386 <sup>ns</sup>	-0.112 <sup>ns</sup>	-0.206 <sup>ns</sup>	-0.089 <sup>ns</sup>	-0.714**	-0.024 <sup>ns</sup>	-0.033 <sup>ns</sup>	-0.713*	-0.257 <sup>ns</sup>	-0.731**
	Tr	-0.812**	-0.571 <sup>ns</sup>	-0.783**	-0.651*	-0.695*	-0.487 <sup>ns</sup>	-0.413 <sup>ns</sup>	-0.503 <sup>ns</sup>	-0.425 <sup>ns</sup>	-0.679*
	$\text{DW}_{\text{shoot}}$	-0.263 <sup>ns</sup>	-0.153 <sup>ns</sup>	-0.272 <sup>ns</sup>	-0.461 <sup>ns</sup>	-0.464 <sup>ns</sup>	-0.543 <sup>ns</sup>	-0.290 <sup>ns</sup>	-0.150 <sup>ns</sup>	-0.655*	-0.414 <sup>ns</sup>
Labeled	Chlorophyll	-0.208 <sup>ns</sup>	-0.367 <sup>ns</sup>	-0.326 <sup>ns</sup>	-0.739*	0.075 <sup>ns</sup>	-0.503 <sup>ns</sup>	0.095 <sup>ns</sup>	0.461 <sup>ns</sup>	-0.356 <sup>ns</sup>	-0.153 <sup>ns</sup>
	Ci	-0.845**	0.072 <sup>ns</sup>	-0.321 <sup>ns</sup>	-0.516 <sup>ns</sup>	-0.499 <sup>ns</sup>	-0.370 <sup>ns</sup>	0.345 <sup>ns</sup>	0.032 <sup>ns</sup>	-0.229 <sup>ns</sup>	-0.365 <sup>ns</sup>
	Amax	-0.029 <sup>ns</sup>	0.434 <sup>ns</sup>	0.171 <sup>ns</sup>	0.184 <sup>ns</sup>	-0.311 <sup>ns</sup>	-0.084 <sup>ns</sup>	0.044 <sup>ns</sup>	0.228 <sup>ns</sup>	0.144 <sup>ns</sup>	-0.543 <sup>ns</sup>
	$g_s$	-0.274 <sup>ns</sup>	0.363 <sup>ns</sup>	0.245 <sup>ns</sup>	0.214 <sup>ns</sup>	-0.527 <sup>ns</sup>	-0.010 <sup>ns</sup>	0.308 <sup>ns</sup>	0.546 <sup>ns</sup>	0.409 <sup>ns</sup>	-0.527 <sup>ns</sup>
	Fv'/Fm'	-0.291 <sup>ns</sup>	0.110 <sup>ns</sup>	-0.564 <sup>ns</sup>	-0.303 <sup>ns</sup>	-0.321 <sup>ns</sup>	-0.685*	0.402 <sup>ns</sup>	0.666 <sup>ns</sup>	-0.268 <sup>ns</sup>	-0.253 <sup>ns</sup>
	PhiPS2	-0.069 <sup>ns</sup>	0.199 <sup>ns</sup>	-0.463 <sup>ns</sup>	-0.179 <sup>ns</sup>	-0.307 <sup>ns</sup>	-0.560 <sup>ns</sup>	0.313 <sup>ns</sup>	0.498 <sup>ns</sup>	-0.244 <sup>ns</sup>	-0.209 <sup>ns</sup>
	ETR	-0.067 <sup>ns</sup>	0.201 <sup>ns</sup>	-0.463 <sup>ns</sup>	-0.176 <sup>ns</sup>	-0.305 <sup>ns</sup>	-0.557 <sup>ns</sup>	0.317 <sup>ns</sup>	0.502 <sup>ns</sup>	-0.240 <sup>ns</sup>	-0.203 <sup>ns</sup>
	Tr	0.185 <sup>ns</sup>	0.633 <sup>ns</sup>	0.438 <sup>ns</sup>	0.512 <sup>ns</sup>	-0.517 <sup>ns</sup>	0.522 <sup>ns</sup>	0.212 <sup>ns</sup>	-0.396 <sup>ns</sup>	0.528 <sup>ns</sup>	-0.530 <sup>ns</sup>
	$\text{DW}_{\text{shoot}}$	-0.086 <sup>ns</sup>	-0.254 <sup>ns</sup>	-0.405 <sup>ns</sup>	-0.417 <sup>ns</sup>	-0.263 <sup>ns</sup>	-0.519 <sup>ns</sup>	0.230 <sup>ns</sup>	0.632*	-0.342 <sup>ns</sup>	-0.283 <sup>ns</sup>

For each isotope labeling condition (control vs labeled), all correlations were calculated using twelve replicates by combining relative humidity levels (40% and 80%). Levels of significance: ns, not significant; \*\*,  $P < 0.01$ ; \*,  $P < 0.05$

### 3.4 The effect of relative humidity (VPD) on stable isotope composition of plant water tissues

#### *Oxygen and hydrogen isotope compositions*

The effect of relative humidity was analysed on oxygen ( $\delta^{18}\text{O}$ ) and hydrogen ( $\delta^2\text{H}$ ) isotope compositions in different plant water tissues (Table 6). No significant differences were observed in the  $\delta^{18}\text{O}$  of water analysed in the studied tissues under control conditions when different VPD were compared, except for the peduncle in which  $\delta^{18}\text{O}$  was enriched under higher VPD and depleted under low VPD. Under labelled conditions,  $\delta^{18}\text{O}$  was enriched in leaves and grains under high VPD conditions, compared with low VPD conditions. For  $\delta^2\text{H}$  of plant water,  $\delta^2\text{H}$  was enriched in the flag leaf and depleted in the peduncle when VPD was increased under control conditions. Under labelled conditions,  $\delta^2\text{H}$  was enriched mainly in the flag leaf and grains under high VPD conditions.

Across plant tissues,  $\delta^{18}\text{O}$  and  $\delta^2\text{H}$  exhibited similar fractionation patterns, being both depleted in water of the stem and peduncle, moderately enriched in grain water, and highly enriched in flag leaf water for each humidity studied (Table 6). On the contrary under labelling conditions the opposite trend was observed,  $\delta^{18}\text{O}$  and  $\delta^2\text{H}$  in the water of the peduncle and stem showed the most enriched values, followed by the grain water, being the flag leaf water with the most depleted value (Table 6).

**Table 6.** Effect of relative humidity (40% vs 80%) on oxygen and hydrogen stable isotope compositions ( $\delta^{18}\text{O}$  and  $\delta^2\text{H}$ ) in water extracted and analysed in stem base, peduncle, flag leaves and grains of wheat genotypes during mid grain filling.

		Water in plant tissues							
		$\delta^{18}\text{O}_{\text{Stem}}$	$\delta^{18}\text{O}_{\text{Flag leaf}}$	$\delta^{18}\text{O}_{\text{Peduncle}}$	$\delta^{18}\text{O}_{\text{Grain}}$	$\delta^2\text{H}_{\text{Stem}}$	$\delta^2\text{H}_{\text{Flag leaf}}$	$\delta^2\text{H}_{\text{Peduncle}}$	$\delta^2\text{H}_{\text{Grain}}$
		(‰)	(‰)	(‰)	(‰)	(‰)	(‰)	(‰)	(‰)
Control	40%	-5.06 <sub>c</sub> ±0.55	3.30 <sub>a</sub> ±0.78	-6.29 <sub>c</sub> ±0.27	-0.89 <sub>b</sub> ±0.58	-38.92 <sub>c</sub> ±0.77	22.72 <sub>a</sub> ±6.41	-40.12 <sub>c</sub> ±1.52	-2.21 <sub>b</sub> ±4.36
	80%	-4.66 <sub>c</sub> ±0.27	2.82 <sub>a</sub> ±0.53	-4.29 <sub>c</sub> ±0.32	-0.73 <sub>b</sub> ±0.37	-36.57 <sub>b</sub> ±1.05	-2.35 <sub>a</sub> ±3.37	-33.47 <sub>b</sub> ±1.52	-8.40 <sub>a</sub> ±2.03
	<b>ANOVA</b>	<b>ns</b>	<b>ns</b>	<b>&lt;0.001</b>	<b>ns</b>	<b>ns</b>	<b>&lt;0.010</b>	<b>&lt;0.010</b>	<b>ns</b>
Labeled	40%	34.15 <sub>a</sub> ±0.78	19.39 <sub>c</sub> ±1.39	32.42 <sub>a</sub> ±1.16	26.73 <sub>b</sub> ±0.39	796.2 <sub>a</sub> ±13.2	298.2 <sub>c</sub> ±28.9	773.1 <sub>a</sub> ±18.8	683.7 <sub>b</sub> ±10.9
	80%	32.87 <sub>a</sub> ±0.42	12.89 <sub>c</sub> ±0.72	31.02 <sub>a</sub> ±0.46	19.04 <sub>b</sub> ±0.79	750.0 <sub>a</sub> ±8.7	194.9 <sub>c</sub> ±13.0	729.5 <sub>a</sub> ±7.85	483.3 <sub>b</sub> ±22.4
	<b>ANOVA</b>	<b>ns</b>	<b>&lt;0.050</b>	<b>ns</b>	<b>&lt;0.001</b>	<b>&lt;0.050</b>	<b>&lt;0.010</b>	<b>ns</b>	<b>&lt;0.001</b>

Values shown are the mean  $\pm$  SE for twelve replicates under 40% and 80% of relative humidity, under control and labeled conditions. Level of significance for the ANOVA:  $P < 0.001$ ,  $P < 0.010$  and  $P < 0.050$ . Means exhibiting different letters are significantly different ( $P < 0.05$ ) across plant tissues by the post-hoc test (Tukey-b) on independent samples

### 3.5. Relationships between the isotopes $\delta^{13}\text{C}$ , $\delta^{18}\text{O}$ and $\delta^2\text{H}$ in plant tissues

#### *Dry matter and water soluble fraction*

To trace similarities between fractionation patterns of the different isotopes, correlations between  $\delta^{13}\text{C}_{\text{WSF}}$ ,  $\delta^{13}\text{C}_{\text{DM}}$ ,  $\delta^{18}\text{O}_{\text{WSF}}$  and  $\delta^2\text{H}_{\text{DM}}$  in organic matter of tissues were evaluated under control and labeled conditions combining humidity levels (Supplemental Table 4). Under control conditions,  $\delta^{13}\text{C}_{\text{WSF}}$  was significant and positively correlated with  $\delta^{18}\text{O}_{\text{WSF}}$  in most plant tissues; under labeled conditions however,  $\delta^{13}\text{C}_{\text{WSF}}$  of all tissues was mainly correlated with the  $\delta^{18}\text{O}_{\text{WSF}}$  in the flag leaf. In the case of  $\delta^2\text{H}_{\text{DM}}$ , the strongest correlation was observed between the  $\delta^2\text{H}$  in the grains and the  $\delta^{13}\text{C}_{\text{WSF}}$  of the grains. In addition,  $\delta^2\text{H}$  in the grains was strongly correlated with the  $\delta^{18}\text{O}$  of all tissues.  $\delta^2\text{H}$  in the awns also showed significant correlations against  $\delta^{18}\text{O}$  and  $\delta^{13}\text{C}$  of awns and grains. Correlations between the different isotopes under labeled conditions were still present between the  $\delta^{18}\text{O}$  flag leaf and  $\delta^{13}\text{C}$  of most plant tissues. With the rest of isotopes under labeled conditions correlations were more dispersed and without a clear trend (Supplemental Table 4). In summary, under control conditions,  $\delta^{18}\text{O}_{\text{WSF}}$  and  $\delta^{13}\text{C}_{\text{WSF}}$  were mainly correlated in the flag leaf, peduncle, and awn.  $\delta^2\text{H}_{\text{DM}}$  was only correlated against  $\delta^{18}\text{O}_{\text{WSF}}$  in awns (Figure 1). Similarly, under labeled conditions,  $\delta^{13}\text{C}_{\text{WSF}}$  and  $\delta^{18}\text{O}_{\text{WSF}}$  were positively related in the flag leaf alone. However, relationship between  $\delta^{18}\text{O}_{\text{WSF}}$  and  $\delta^2\text{H}_{\text{DM}}$  was present in almost all tissues with the exception of glumes.

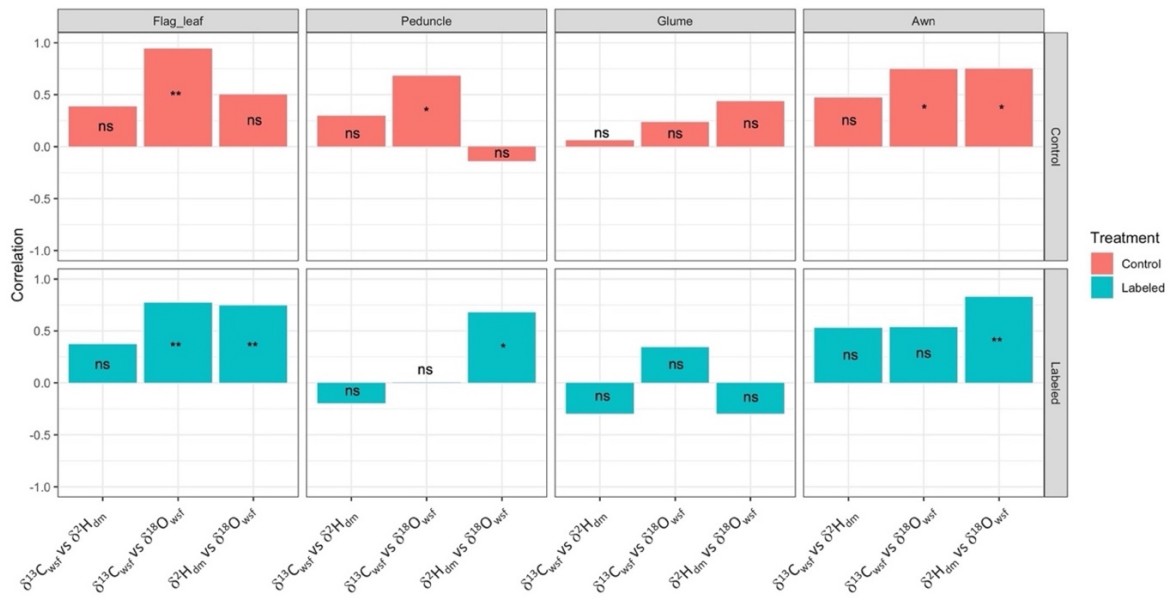


**Figure 1.** Linear regression relationships among carbon ( $\delta^{13}C$ ), oxygen ( $\delta^{18}O$ ), hydrogen ( $\delta^2H$ ) stable isotope compositions assessed during mid grain filling in the organic matter (water soluble fraction and dry matter) of different plant tissues (flag leaf, peduncle, glume, awn), when combining humidity levels (40% and 80%) and under separate isotope labeling (control vs labeled).  $\delta^{13}C_{wsf}$ , carbon isotope composition in the water soluble fraction;  $\delta^{13}C_{dm}$ , carbon isotope composition in the dry matter;  $\delta^2H_{dm}$ , hydrogen isotope composition of the dry matter;  $\delta^{18}O_{wsf}$ , oxygen isotope composition in the water soluble fraction.

### Water in the different tissues

Correlation between  $\delta^{18}O$  and  $\delta^2H$  in different water tissues were analysed under different humidity and water labeling conditions (Figure 2) in order to trace the physiological source of variation of this parameter. Under control conditions, positive linear correlations were shown between  $\delta^{18}O$  and  $\delta^2H$  in the water of the stem, flag leaf, peduncle and grain, under VPD conditions separated and combined. A similar trend was observed under labeled conditions.

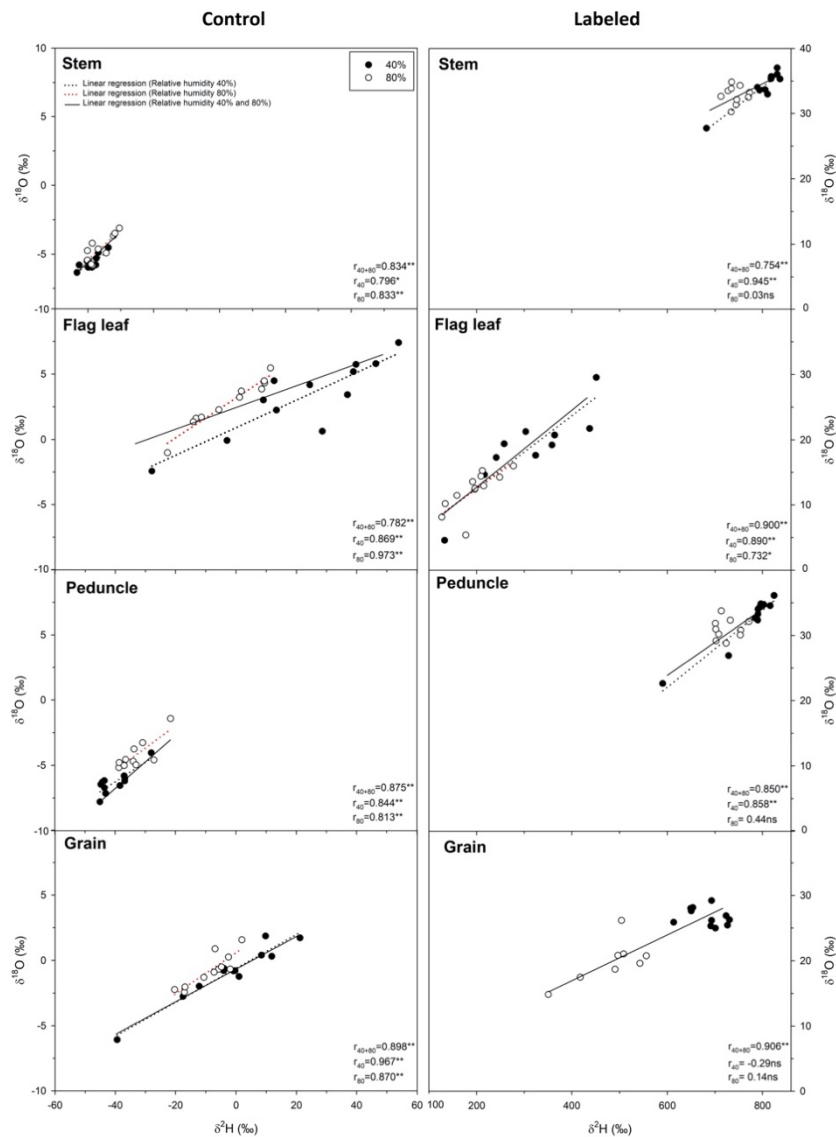


**Figure 2.** Linear regression relationships between oxygen and hydrogen isotope compositions assessed during mid grain filling in water in plant tissues (stem, flag leaf, peduncle, grain), under different humidity levels (40% vs 80%) and distinct isotope labeling (control vs labeled).

## 4. Discussion

### 4.1 Relative humidity effect on photosynthesis and agronomical traits

Exposure to elevated temperatures even under well-watered conditions leads to decreased atmospheric relative humidity, increase in air vapor pressure deficit (VPD) and a subsequent increase in evaporative demands and transpiration in wheat genotypes. Stomatal conductance and photosynthesis rates were often reported to decrease under low relative humidity conditions and impact carbon assimilation, affecting therefore crop growth and grain yield (Fakhret et al., 2021; Jauregui et al., 2018; Rashid et al., 2018; Xue et al., 2004). The

growth chamber experiment under 40% RH simulated higher VPD conditions, which triggered higher transpiration rates in plants compared with 80% RH conditions. Despite the constant irrigation supplying, water status was lower (higher  $\delta^{13}\text{C}$ ) in the assimilates and the dry matter of plant tissues under higher VPD conditions compared with lower VPD conditions, regardless of water labeling conditions (separated or combined). Likewise, strong correlations were shown between most photosynthesis traits ( $C_i$ ,  $g_s$  and  $Tr$ ) and the water status ( $\delta^{13}\text{C}_{\text{WSF}}$ ) of the flag leaf under low VPD and combined VPD conditions. The increase in evaporative demands in plants resulted in a reduction in all photosynthetic traits ( $A_{\text{max}}$ ,  $g_s$ ,  $C_i$ ,  $F_v'/F_m'$ ,  $\text{PhiPS2}$ ,  $Tr$ ,  $\text{ETR}$ ) and chlorophyll content during grain filling, and subsequently a decrease in biomass growth (low  $\text{DW}_{\text{shoot}}$  and  $\text{DW}_{\text{biomass}}$ ) and grain setting (lower  $\text{GN}$ ,  $\text{DW}_{\text{ear}}$  and  $\text{DW}_{\text{grain}}$ ) by maturity.

Furthermore, in our experiment, growth conditions applied in each growth chamber not only successfully depicted two contrasting environments with high vs low VPD conditions, but also provided a static water source that allowed a better understanding and interpretation to water movements and fractionation patterns across plants tissues. The use of heavy water labeling highlighted repeatedly significant differences in  $\delta^{18}\text{O}$  and  $\delta^2\text{H}$  isotopic signatures associated with VPD conditions, and which were subtle under normal irrigation (control). Those differences were mostly marked with  $\delta^2\text{H}$  in water (stem and grain) and the organic matter (flag leaf and glumes) of plant tissues, and with  $\delta^{18}\text{O}$  in water plant tissues (flag leaf and grain). Even though correlations under labeled treatment were not as efficient as under control. The use of isotopically heavy water as a tracing method to oxygen and hydrogen water movements in plant species was documented previously (Bachmann et al., 2015; Sternberg, 1989).

#### 4.2. hydrogen and oxygen isotopes in the organic matter across plant tissues

$\delta^{18}\text{O}$  and  $\delta^2\text{H}$  isotopic signatures in the organic matter of plant tissues have shown distinct variation patterns across plant tissues. Under control conditions,  $\delta^{18}\text{O}_{\text{WSF}}$  correlated with  $g_s$  in the peduncle, with the evapotranspiration related parameters ( $C_i$ ,  $A_{\text{max}}$ ,  $g_s$ ,  $F_v'/F_m'$  and  $Tr$ ) in sink the flag leaf, glume and awn; and all photosynthesis traits except for  $C_i$  in grains. These results indicate that  $\delta^{18}\text{O}$  fractionation patterns in the organic matter of plant tissues are somehow dictated by evapotranspiration processes related with gas exchange mechanisms.



In fact, in the case of oxygen, Helliker and Ehleringer in (2002) reported that during CO<sub>2</sub> fixation, most atmospheric oxygen gets exchanged with oxygen incorporated in water molecules that are transported through the xylem, which results in an enrichment in the isotopic signature of  $\delta^{18}\text{O}$  in newly formed sugars and metabolites (Helliker and Ehleringer, 2002). Which explains the consistent negative correlations of  $\delta^{18}\text{O}$  against stomatal conductance and transpiration, as well as the negative correlation of water  $\delta^{18}\text{O}_{\text{WT}}$  against water soluble fraction  $\delta^{18}\text{O}_{\text{WSF}}$  in peduncle.

In the case of hydrogen,  $\delta^2\text{H}_{\text{DM}}$  correlated with chlorophyll in flag leaf, glume, awn and grain, and most photosynthesis traits in glumes and grains, moreover,  $\delta^{18}\text{O}_{\text{WSF}}$  and  $\delta^2\text{H}_{\text{DM}}$  were mostly correlated in awns. suggesting thus that fractionation patterns in hydrogen involve a combination of evapotranspiration processes and photosynthesis mechanisms.

Furthermore, unlike  $\delta^{13}\text{C}$  and  $\delta^2\text{H}$ ,  $\delta^{18}\text{O}$  is not strongly affected by photosynthetic rate. Thereby assessing  $\delta^{13}\text{C}$  and  $\delta^{18}\text{O}$  in plant tissues separately enables a clearer understanding to fractionation patterns related to evaporative events in  $\delta^{18}\text{O}$  of plant tissues (Barbour 2007). In this sense, water status ( $\delta^{13}\text{C}_{\text{DM}}$  and  $\delta^{13}\text{C}_{\text{WSF}}$  in the flag leaf and grain, and  $\delta^{13}\text{C}_{\text{WSF}}$  in the peduncle) correlated positively against  $\delta^{18}\text{O}_{\text{WSF}}$  in all tissues, which indicates further that  $\delta^{18}\text{O}$  fractionation processes are driven primarily by evaporative processes.

On the other hand, no relationships were found between  $\delta^{13}\text{C}_{\text{WSF}}$  and  $\delta^2\text{H}_{\text{DM}}$  when assessed in the flag leaf, peduncle, glume and awn; likewise, correlations between  $\delta^{18}\text{O}_{\text{WSF}}$  and  $\delta^2\text{H}_{\text{DM}}$  were absent when assessed in the peduncle and the transpiring tissues such as the flag leaf and glumes. In the less transpiring tissues however,  $\delta^2\text{H}_{\text{DM}}$  in awns correlated positively against  $\delta^{18}\text{O}_{\text{WSF}}$  in the peduncle, awn and grain; and  $\delta^2\text{H}_{\text{DM}}$  in grains correlated positively against  $\delta^{18}\text{O}_{\text{WSF}}$  in all tissues (flag leaf, peduncle, glume, awn and grain). The variation in correlation significance between  $\delta^{18}\text{O}$  and  $\delta^2\text{H}$  in the organic matter of transpiring tissues with high evaporative sites and non-transpiring tissues suggests the presence of possible plant trophism defining  $\delta^2\text{H}$  isotopic signature in plant tissues.

#### 4.3. Hydrogen and oxygen isotopes in plant water tissues

$\delta^{18}\text{O}$  and  $\delta^2\text{H}$  have long been used as indicators to water source when assessed in stem water (DeNiro and Epstein, 1979; Mateo et al., 2004) and intrinsic water movement across water

plant tissues (Barbour, 2007). In this study oxygen and hydrogen in water tissues ( $\delta^{18}\text{O}$  and  $\delta^2\text{H}$ ) were strongly and positively correlated against each other, under combined and separated VPD conditions, and under control treatment better than under labeled treatment. The positive correlations demonstrate the presence of a similar source of variation in fractionation patterns shared between  $\delta^{18}\text{O}$  and  $\delta^2\text{H}$ , which is mainly related to evaporation processes.

Moreover, results under different VPD conditions and water labeling have shown that  $\delta^{18}\text{O}$  and  $\delta^2\text{H}$  isotopic signatures were similar in the water of the stem and peduncle. These results are expected in non-transpiring tissues since no water molecule exchange occurs. By contrast, in transpiring tissues, both  $\delta^{18}\text{O}$  and  $\delta^2\text{H}$  were enriched in the water of the flag leaf followed by the grain under the control treatment. In fact, transpiration leads to isotopic enrichment above the water source in evaporative sites within transpiring tissues (Gonfiatini et al., 1965).  $\delta^{18}\text{O}$  and  $\delta^2\text{H}$  become enriched on leaf surface during transpiration because of water molecules composed of heavy  $\delta^{18}\text{O}$  and  $\delta^2\text{H}$  ( $\text{H}_2^{18}\text{O}$ ) being slower to evaporate compared with  $\text{H}_2^{16}\text{O}$ . Afterwards, the isotopically enriched water in the leaf is transported through the phloem to the sink tissues (Cernusak et al., 2016).

#### 4.4. Hydrogen and oxygen isotope fractionation and plant trophism

$\delta^2\text{H}$  and  $\delta^{18}\text{O}$  isotopic signatures in stem water reflect depleted values since the assumption is that no fractionation occurs in water movement between roots and the stem basis. From the stem onwards, the depleted  $\delta^2\text{H}$  and  $\delta^{18}\text{O}$  undergo distinct processes (i.e. fractionation patterns) from source to sink tissues. In fact,  $\delta^{18}\text{O}$  fractionation patterns are defined by environmental evaporative events only, consequently, an enrichment gradient was observed in all sink tissues above the stem. Under higher VPD conditions,  $\delta^{18}\text{O}$  enrichment was the highest in the tissue with the most active evapotranspiration sites (flag leaf), followed by the grain, whereas glumes, awns and peduncles have shown similar  $\delta^{18}\text{O}$  enrichment levels. Likewise, under lower VPD,  $\delta^{18}\text{O}$  was mostly enriched in the flag leaf, peduncle and grains, and less enriched in glumes and awns.

In the case of  $\delta^2\text{H}$ , fractionation processes are dictated by two main mechanisms, evapotranspiration and photosynthetic chemical reactions. The former triggers an

enrichment in  $\delta^2\text{H}$  isotopic signature, while the latter causes depletion in  $\delta^2\text{H}$ . In this sense, evaluating the isotopic signature of  $\delta^2\text{H}$  in different plant tissues makes more sense since trophism enables a clearer understanding to the mechanisms behind hydrogen fractionation. In fact,  $\delta^2\text{H}$  in plant organic matter was depleted in the transpiring autotrophic tissues (glumes then the flag leaf) and enriched in heterotrophic tissues (i.e. grains) under control and labeled treatments and in each VPD condition. Moreover, positive correlations were shown between  $\delta^{18}\text{O}_{\text{WSF}}$  in all plant tissues and  $\delta^2\text{H}_{\text{DM}}$  in the heterotrophic tissue (grains) under control conditions, which indicates that  $\delta^2\text{H}$  fractionation processes in heterotrophic tissues are limited to environmental evapotranspiration only. In contrast, autotrophic tissues were more depleted in  $\delta^2\text{H}_{\text{DM}}$ . Furthermore,  $\delta^2\text{H}_{\text{DM}}$  depletion was more pronounced in glumes than in leaves, which is to be expected giving the xeromorphic anatomy and osmotic adjustment of ears which were reported to ensure better water status under drought conditions, and consequently, maintain higher photosynthetic activities and greater production, compared with the flag leaf (Araus et al., 1993; Tambussi et al., 2005). In the case of awns,  $\delta^2\text{H}_{\text{DM}}$  values were somewhat between hydrogen isotopic values observed in autotrophic and heterotrophic tissues, which suggests that  $\delta^2\text{H}$  isotopic signature in awns may be regulated by a mixotrophic metabolism.

## 5. Conclusion

The present study demonstrated the efficiency of  $\delta^{18}\text{O}$  and  $\delta^2\text{H}$  as phenotyping traits physiologically assess wheat performance under water limited conditions.  $\delta^{18}\text{O}$  and  $\delta^2\text{H}$  in stem water have shown a shared source of variation in fractionation patterns driven mainly by environmental evaporative processes, whereas in organic matter,  $\delta^{18}\text{O}$  and  $\delta^2\text{H}$  fractionation patterns not only were different, but also were related to plant trophism. This experiment was a proof of concept to oxygen enrichment process from source to sink tissues, and to hydrogen depletion in autotrophic (leaves and glumes) and mixotrophic (awns) tissues, enrichment in heterotrophic tissues (grains).

### Credit authorship contribution statement

FZR wrote the original draft and conducted a part of the stable isotope analyses, carried out statistical analyses, drew the tables and figures and implemented the edits; RC conducted the

greenhouse experiment, collected physiological and agronomic data and conducted a part of the stable isotope analysis. RC and JLA conceived the study and contributed to the revision of the consecutive drafts.

#### Declaration of Competing Interest

The authors declare that they have no known competing financial interests or personal relationships that could have appeared to influence the work reported in this paper.

#### Acknowledgments

FZR is a recipient of a research grant (FI-AGAUR) sponsored by the Agency for Management of University and Research Grants (AGAUR), in collaboration with the University of Barcelona. JLA acknowledges support from the Catalan Institution for Research and Advanced Studies, Generalitat de Catalunya, Spain, through its program ICREA Academia. We extend our thanks to The Water Research Institute (IdRA) for their financial support to cover laboratory analyses.

#### References

Araus, J. L., Brown, H. R., Febrero, A., Bort, J., Serret, M. D. (1993). Ear photosynthesis, carbon isotope discrimination and the contribution of respiratory CO<sub>2</sub> to differences in grain mass in durum wheat. *Plant, Cell Environ.*, 16, 383–392. <https://doi.org/10.1111/j.1365-3040.1993.tb00884.x>

Araus, J. L., Cabrera-Bosquet, L., Serret, M. D., Bort, J., Nieto-Taladriz, M. T. (2013). Combined use of  $\delta^{13}\text{C}$ ,  $\delta^{18}\text{O}$  and  $\delta^{15}\text{N}$  tracks nitrogen metabolism and genotypic adaptation of durum wheat to salinity and water deficit. *Funct. Plant Physiol.*, 40, 595–608. <https://doi.org/10.1071/FP12254>

Araus, J. L., Villegas, D., Aparicio, N., Garcia del Moral, L. F., El-Hani, S., Rharrabti, Y., Ferrio, J. P., Royo, C. (2003). Environmental factors determining carbon isotope discrimination and yield in durum wheat under mediterranean conditions. *Crop Sci.*, 43, 170–180. <https://doi.org/10.2135/cropsci2003.0170>

Bachmann, D., Gockele, A., Ravenek, J. M., Roscher, C., Strecker, T., Weigelt, A., Buchmann, N. (2015). No evidence of complementary water use along a plant species richness gradient

in temperate experimental grasslands. PLoS ONE, 10, 1–14.  
<https://doi.org/10.1371/journal.pone.0116367>

Barbour, M. M. (2007). Stable oxygen isotope composition of plant tissue: a review. *Funct. Plant Biol.*, 34, 83–94. <https://doi.org/10.1071/FP06228>

Blum, A. (2009). Effective use of water (EUW) and not water-use efficiency (WUE) is the target of crop yield improvement under drought stress. *F. Crop. Res.*, 112, 119–123.  
<https://doi.org/10.1016/j.fcr.2009.03.009>

Cabrera-Bosquet, L., Sánchez, C., Araus, J.L., 2009. How yield relates to ash content,  $\Delta^{13}\text{C}$  and  $\Delta^{18}\text{O}$  in maize grown under different water regimes. *Ann. Bot.* 104, 1207–1216.  
<https://doi.org/10.1093/aob/mcp229>

Cernusak, L. A., Barbour, M. M., Arndt, S. K., Cheesman, A. W., English, N. B., Feild, T. S., Helliker, B. R., Holloway-Phillips, M. M., Holtum, J. A. M., Kahmen, A., Mcinerney, F. A., Munksgaard, N. C., Simonin, K. A., Song, X., Stuart-Williams, H., West, J. B., Farquhar, G. D. (2016). Stable isotopes in leaf water of terrestrial plants. *Plant Cell Environ.*, 39, 1087–1102.  
<https://doi.org/10.1111/pce.12703>

Chairi, F., Vergara-Diaz, O., Vatter, T., Aparicio, N., Nieto-Taladriz, M. T., Kefauver, S. C., Bort, J., Serret, M. D., Araus, J. L. (2018). Post-green revolution genetic advance in durum wheat: the case of Spain. *F. Crop. Res.*, 228, 158–169. <https://doi.org/10.1016/j.fcr.2018.09.003>

Chaves, M. M., Flexas, J., Pinheiro, C. (2009). Photosynthesis under drought and salt stress: regulation mechanisms from whole plant to cell. *Ann. Bot.*, 103, 551–560.  
<https://doi.org/10.1093/AOB/MCN125>

Condon, A. G., Richards, R. A., Rebetzke, G. J., Farquhar, G. D. (2002). Improving Intrinsic Water-Use Efficiency and crop yield. *Crop Sci.*, 42(1), 122–131.  
<https://doi.org/10.2135/CROPSCI2002.1220>

Condon, A. G., Richards, R. A., Rebetzke, G. J., and Farquhar, G. D. (2004). Breeding for high water-use efficiency. *J. Exp. Bot.*, 55, 2447–2460. <https://doi.org/10.1093/JXB/ERH277>

Cormier, M. A., Werner, R. A., Sauer, P. E., Gröcke, D. R., Leuenberger, M. C., Wieloch, T., Schleucher, J., Kahmen, A. (2018).  $^2\text{H}$ -fractionations during the biosynthesis of carbohydrates and lipids imprint a metabolic signal on the  $\delta^2\text{H}$  values of plant organic compounds. *New Phytol.*, 218, 479–491. <https://doi.org/10.1111/NPH.15016>

Cuntz, M., Ogee, J., Farquhar, G. D., Peylin, P., and Cernusak, L. A. (2007). Modelling advection and diffusion of water isotopologues in leaves. *Plant, Cell Environ.*, 30, 892–909. <https://doi.org/10.1111/j.1365-3040.2007.01676.x>

Dawson, T. E., Ehleringer, J. R. (1993). Isotopic enrichment of water in the “woody” tissues of plants: implications for plant water source, water uptake, and other studies which use the stable isotopic composition of cellulose. *Geochim. Cosmochim. Acta*, 57, 3487–3492. [https://doi.org/10.1016/0016-7037\(93\)90554-A](https://doi.org/10.1016/0016-7037(93)90554-A)

DeNiro, M. J., Epstein, S. (1979). Relationship between the oxygen Isotope ratios of terrestrial. *Science*, 204, 51–53. <https://doi.org/10.1126/science.204.4388.51>

Drobinski, P., Da Silva, N., Bastin, S., Mailler, S., Muller, C., Ahrens, B., Christensen, O. B., Lionello, P. (2020). How warmer and drier will the Mediterranean region be at the end of the twenty-first century? *Reg. Environ. Chang.*, 20, 1–12. <https://doi.org/10.1007/s10113-020-01659-w>

Erice, G., Sanz-Sáez, Á., González-Torralba, J., Méndez-Espinoza, A. M., Urretavizcaya, I., Nieto, M. T., Serret, M. D., Araus, J. L., Irigoyen, J. J., Aranjuelo, I. (2019). Impact of elevated CO<sub>2</sub> and drought on yield and quality traits of a historical (Blanqueta) and a modern (Sula) durum wheat. *J. Cereal Sci.*, 87, 194–201. <https://doi.org/10.1016/j.jcs.2019.03.012>

Estep, M. F., Hoering, T. C. (1981). Stable hydrogen isotope fractionations during autotrophic and mixotrophic growth of microalgae. *Plant Physiol.*, 67, 474–477. <https://doi.org/10.1104/pp.67.3.474>

Fakhet, D., Morales, F., Jauregui, I., Erice, G., Aparicio-Tejo, P. M., González-Murua, C., Aroca, R., Irigoyen, J. J., Aranjuelo, I. (2021). Short-term exposure to high atmospheric vapor pressure deficit (VPD) severely impacts durum wheat carbon and nitrogen metabolism in the absence

of Eeaphic water stress. *Plants*, 120, 1–16. <https://doi.org/https://doi.org/10.3390/plants10010120>

Farquhar, G.D., Cernusak, L. A., Barnes, B. (2007). Heavy water fractionation during transpiration. *Plant Physiol.*, 143, 11–18. <https://doi.org/10.1104/PP.106.093278>

Farquhar, G.D., O’Leary, M. H., Berry, J. A. (1982). On the relationship between carbon isotope discrimination and the intercellular carbon dioxide concentration in leaves. *Aust. J. Plant Physiol.*, 9, 121–137. <https://doi.org/10.1071/PP9820121>

Farquhar, G.D., Ehleringer, J. R., Hubick, K. T. (1989). Carbon isotope discrimination and photosynthesis. *Annu. Rev. Plant Physiol.*, 40, 503–537. <https://doi.org/10.1146/annurev.pp.40.060189.002443>

Farquhar, G.D., Richards, R. A. (1984). Isotopic composition of plant carbon correlates with water-use efficiency of wheat genotypes. *Funct. Plant Biol.*, 11, 539–552. <https://doi.org/10.1071/PP9840539>

Farquhar, Graham D., Lloyd, J. (1993). Carbon and oxygen isotope effects in the exchange of carbon dioxide between terrestrial plants and the atmosphere. In J. R. Ehleringer, A. E. Hall, and G. D. Farquhar (Eds.), *Stable isotopes and plant carbon-water relations* (pp. 47–70). Academic Press, Inc. <https://doi.org/10.1016/C2009-0-03312-1>

Fischer, R. A., Rees, D., Sayre, K. D., Lu, Z. M., Condon, A. G., and Larque Saavedra, A. (1998). Wheat yield progress associated with higher stomatal conductance and photosynthetic rate, and cooler canopies. *Crop Sci.*, 38, 1467–1475. <https://doi.org/10.2135/cropsci1998.0011183X003800060011x>

Feakins, S. J., Sessions, A. L. (2010). Controls on the D/H ratios of plant leaf waxes in an arid ecosystem. *Geochim. Cosmochim. Acta*, 74, 2128–2141. <https://doi.org/10.1016/J.GCA.2010.01.016>

Flanagan L.B. (1993) Environmental and biological influences on the stable oxygen and hydrogen isotopic composition of leaf water. In *Stable Isotopes and Plant Carbon-Water*

Relations (eds J.R. Ehleringer, A.E. Hall, G.D. Farquhar) pp. 71–90. Academic Press, San Diego, CA, USA

Flanagan, L. B., Comstock, J. P., Ehleringer, J. R. (1991). Comparison of modeled and observed environmental influences on the stable oxygen and hydrogen isotope composition of leaf water in *Phaseolus vulgaris* L. *Plant Physiol.*, 96, 588–596. <https://doi.org/10.1104/PP.96.2.588>

Hayes, J. M. (2001). Fractionation of carbon and hydrogen isotopes in biosynthetic processes. *Rev. Mineral. Geochem.*, 43, 225–277. <https://doi.org/10.2138/GSRMG.43.1.225>

Helliker, B. R., Ehleringer, J. R. (2002). Differential  $^{18}\text{O}$  enrichment of leaf cellulose in  $\text{C}_3$  versus  $\text{C}_4$  grasses. *Funct. Plant Biol.*, 29, 435–442. <https://doi.org/10.1071/PP01122>

Jauregui, I., Rothwell, S. A., Taylor, S. H., Parry, M. A. J., Carmo-Silva, E., Dodd, I. C. (2018). Whole plant chamber to examine sensitivity of cereal gas exchange to changes in evaporative demand. *Plant Methods*, 14, 1–13. <https://doi.org/10.1186/s13007-018-0357-9>

Kahmen, A., Schefuß, E., Sachse, D. (2013). Leaf water deuterium enrichment shapes leaf wax n-alkane  $\delta\text{D}$  values of angiosperm plants I: Experimental evidence and mechanistic insights. *Geochim Cosmochim Acta*, 111, 39–49. <https://doi.org/10.1016/J.GCA.2012.09.003>

Kaushal, R., Ghosh, P., 2018a. Stable oxygen and carbon isotopic composition of rice (*Oryza sativa* L.) grains as recorder of relative humidity. *J. Geophys. Res. Biogeosciences* 123, 423–439. <https://doi.org/10.1002/2017JG004245>

Kaushal, R., Ghosh, P., 2018b. Oxygen isotope enrichment in rice (*Oryza sativa* L.) grain organic matter captures signature of relative humidity. *Plant Sci.* 274, 503–513. <https://doi.org/10.1016/j.plantsci.2018.05.022>

Liu, H.T., Schäufele, R., Gong, X.Y., Schnyder, H., 2017. The  $\delta^{18}\text{O}$  and  $\delta^2\text{H}$  of water in the leaf growth-and-differentiation zone of grasses is close to source water in both humid and dry atmospheres. *New Phytol.* 214, 1423–1431. <https://doi.org/10.1111/nph.14549>



- Luo, Y., Sternberg, L. (1991). Deuterium heterogeneity in starch and cellulose nitrate of cam and C3 plants. *Phytochemistry*, 30, 1095–1098. [https://doi.org/10.1016/S0031-9422\(00\)95179-3](https://doi.org/10.1016/S0031-9422(00)95179-3)
- Luo, Y. H., Steinberg, L., Suda, S., Kumazawa, S., Mitsui, A. (1991). Extremely low D/H ratios of photoproduced hydrogen by cyanobacteria. *Plant cell physiol.*, 32, 897-900.
- Martín-Gómez, P., Barbeta, A., Voltas, J., Peñuelas, J., Dennis, K., Palacio, S., Dawson, T. E., Ferrio, J. P. (2015). Isotope-ratio infrared spectroscopy: A reliable tool for the investigation of plant-water sources? *New Phytol.*, 207, 914–927. <https://doi.org/10.1111/nph.13376>
- Mateo, M. A., Ferrio, P., and Araus, J. L. (2004). Isótopos estables en fisiología vegetal. In M. J. Reigosa, N. Pedrol, A. Sánchez (Eds.), *La ecofisiología vegetal, una ciencia de síntesis* (pp. 1–38). Paranimfo, S.A.
- Pande, P.C., Datta, P.S., Bhattacharya, S.K. (1994). Biphasic enrichment of H<sub>2</sub><sup>18</sup>O in developing wheat grain water. *Indian J. Plant Physiol.*, 37, 30–31.
- Qi, H., Coplen, T.B. (2011) Investigation of preparation techniques for d<sup>2</sup>H analysis of keratin materials and a proposed analytical protocol. *Rapid Commun. Mass Spectrom.*, 25, 2209–2222. <https://doi.org/10.1002/rcm.5095>
- Rashid, M. A., Andersen, M. N., Wollenweber, B., Zhang, X., Olesen, J. E. (2018). Acclimation to higher VPD and temperature minimized negative effects on assimilation and grain yield of wheat. *Agric. For.Meteor.*, 248, 119–129. <https://doi.org/10.1016/j.agrformet.2017.09.018>
- Rezzouk, F. Z., Gracia-Romero, A., Kefauver, S. C., Gutiérrez, N. A., Aranjuelo, I., Serret, M. D., Araus, J. L. (2020). Remote sensing techniques and stable isotopes as phenotyping tools to assess wheat yield performance: effects of growing temperature and vernalization. *Plant Sci.*, 295, 1–16. <https://doi.org/10.1016/j.plantsci.2019.110281>
- Roden, J. S., Ehleringer, J. R. (1999). Hydrogen and oxygen isotope ratios of tree-ring cellulose for riparian trees grown long-term under hydroponically controlled environments. *Oecologia*, 121, 467–477. <https://doi.org/10.1007/s004420050953>

Roden, J. S., Lin, G., Ehleringer, J. R. (2000). A mechanistic model for interpretation of hydrogen and oxygen isotope ratios in tree-ring cellulose. *Geochim. Cosmochim. Acta*, 64, 21–35. [https://doi.org/10.1016/S0016-7037\(99\)00195-7](https://doi.org/10.1016/S0016-7037(99)00195-7)

Sachse, D., Billault, I., Bowen, G. J., Chikaraishi, Y., Dawson, T. E., Feakins, S. J., Freeman, K. H., Magill, C. R., McInerney, F. A., van der Meer, M. T. J., Polissar, P., Robins, R. J., Sachs, J. P., Schmidt, H. L., Sessions, A. L., White, J. W. C., West, J. B., Kahmen, A. (2012). Molecular paleohydrology: interpreting the hydrogen-isotopic composition of lipid biomarkers from photosynthesizing organisms. *Annu. Rev. Earth Planet. Sci.*, 40, 221–249. <https://doi.org/10.1146/ANNUREV-EARTH-042711-105535>

Sanchez-Bragado, R., Serret, M. D., Marimon, R. M., Bort, J., Araus, J. L. (2019). The hydrogen isotope composition  $\delta^2\text{H}$  reflects plant performance. *Plant Physiol.*, 180, 793–812. <https://doi.org/10.1104/pp.19.00238>

Sauer, P.E., Schimmelmann, A., Sessions, A.L., Topalov, K. (2009) Simplified batch equilibration for D/H determination of non-exchangeable hydrogen in solid organic material. *Rapid Commun. Mass Spectrom.*, 23, 949–956. <https://doi.org/10.1002/rcm.3954>

Schimmelmann, A., Lawrence, M., Michael, E. (2001) Stable isotopes ratios of organic H, C and N in the Miocene Monterey Formation, California. In CM Isaac, J Rullkötter, eds, *Monterey Formation: From Rocks to Molecules*, Columbia University Press, New York, pp 86–106

Schmidt, H. L., Werner, R. A., Eisenreich, W. (2003). Systematics of  $^2\text{H}$  patterns in natural compounds and its importance for the elucidation of biosynthetic pathways. *Phytochem. Rev.*, 1–2, 61–85. <https://doi.org/10.1023/B:PHYT.0000004185.92648.AE>

Sessions, A., Burgoyne, T., Schimmelmann, A., Hayes, J. (1999). Fractionation of hydrogen isotopes in lipid biosynthesis. *Org. Geochem.*, 30, 1193–1200. [https://doi.org/10.1016/S0146-6380\(99\)00094-7](https://doi.org/10.1016/S0146-6380(99)00094-7)

Siegwolf, R., Brooks, R., Roden, J., Saurer, M. (2022). Stable isotopes in tree rings (R. Siegwolf, R. Brooks, J. Roden, M. Saurer (eds.)). <https://doi.org/10.1007/978-3-030-92698-4>

Smith, F. A., Freeman, K. H. (2006). Influence of physiology and climate on  $\delta D$  of leaf wax n-alkanes from C3 and C4 grasses. *Geochim. Cosmochim. Acta*, 70, 1172–1187. <https://doi.org/10.1016/J.GCA.2005.11.006>

Sternberg, L. (1989). Oxygen and hydrogen isotope ratios in plant cellulose: mechanisms and applications. In P. W. Rundel, J. R. Ehleringer, K. A. Nagy (Eds.), *Stable Isotopes in Ecological Research* (pp. 124–141). Springer-Verlag New York Inc. [https://doi.org/10.1007/978-1-4612-3498-2\\_9](https://doi.org/10.1007/978-1-4612-3498-2_9)

Sternberg, L., DeNiro, M. J. (1983). Isotopic composition of cellulose from C3, C4, and CAM plants growing near one another. *Science*, 220, 947–949. <https://doi.org/10.1126/science.220.4600.947>

Sternberg, L., Mulkey, S. S., Wright, S. J. (1989). Ecological interpretation of leaf carbon isotope ratios: Influence of respired carbon dioxide. *Ecology*, 70, 1317–1324. <https://doi.org/10.2307/1938191>

Tambussi, E. A., Nogués, S., Araus, J. L. (2005). Ear of durum wheat under water stress: water relations and photosynthetic metabolism. *Planta*, 221, 446–458. <https://doi.org/10.1007/s00425-004-1455-7>

Voltas, J., Romagosa, I., Lafarga, A., Armesto, A. P., Sombrero, A., Araus, J. L. (1999). Genotype by environment interaction for grain yield and carbon isotope discrimination of barley in Mediterranean Spain. *Aust. J. Agric. Res.*, 50, 1263–1271. <https://doi.org/10.1071/AR98137>

Xue, Q., Weiss, A., Arkebauer, T. J., Baenziger, P. S. (2004). Influence of soil water status and atmospheric vapor pressure deficit on leaf gas exchange in field-grown winter wheat. *Environ. Exp. Bot.*, 51, 167–179. <https://doi.org/10.1016/j.envexpbot.2003.09.003>

Yakir, D. (1992). Variations in the natural abundance of oxygen-18 and deuterium in plant carbohydrates. *Plant, Cell Environ.*, 15, 1005–1020. <https://doi.org/10.1111/J.1365-3040.1992.TB01652.X>

Yakir, D., DeNiro, M. J. (1990). Oxygen and hydrogen isotope fractionation during cellulose metabolism in *Lemna gibba* L. *Plant Physiol.*, 93, 325–332. <https://doi.org/10.1104/pp.93.1.325>

Ziegler, H. (1989). Hydrogen isotope fractionation in plant tissues. In: Rundel, P.W., Ehleringer, J.R., Nagy, K.A. (Eds) *Stable isotopes in ecological research*. Ecological Studies, Vol 68. Springer, New York, 105–123. [https://doi.org/10.1007/978-1-4612-3498-2\\_8](https://doi.org/10.1007/978-1-4612-3498-2_8)

Ziegler, H., Osmond, C. B., Stichler, W., Trimborn, P. (1976). Hydrogen isotope discrimination in higher plants: Correlations with photosynthetic pathway and environment. *Planta*, 128(1), 85–92. <https://doi.org/10.1007/BF00397183>

Supplemental tables

**Supplemental Table 1.** Effect of relative humidity (40% vs 80%) on carbon stable isotope composition ( $\delta^{13}\text{C}$ ) of the water soluble fraction of flag leaves, peduncles, glumes and awn, and the dry matter of flag leaves and grains. Flag leaves, peduncles, glumes and awns were sampled during mid grain filling, and grains at maturity.

		Water soluble fraction				Dry matter	
		$\delta^{13}\text{C}_{\text{flag leaf}}$ (‰)	$\delta^{13}\text{C}_{\text{Peduncle}}$ (‰)	$\delta^{13}\text{C}_{\text{Glume}}$ (‰)	$\delta^{13}\text{C}_{\text{Awn}}$ (‰)	$\delta^{13}\text{C}_{\text{flag leaf}}$ (‰)	$\delta^{13}\text{C}_{\text{Grain}}$ (‰)
Control	40%	-26.6±0.8	-23.7±0.8	-25.6±0.8	-25.3±0.6	-27.8±0.7	-24.3±0.6
	80%	-30.7±0.4	-28.2±0.4	-28.1±0.5	-28.6±0.3	-30.2±0.4	-28.7±0.5
	<b>ANOVA</b>	<b>&lt;0.001</b>	<b>&lt;0.001</b>	<b>&lt;0.050</b>	<b>&lt;0.001</b>	<b>&lt;0.050</b>	<b>&lt;0.001</b>
Labeled	40%	-27.5±0.9	-24.6±0.7	-26.1±0.6	-26.1±0.5	-	-
	80%	-29.5±0.6	-26.7±0.5	-27.5±0.2	-27.5±0.3	-	-
	<b>ANOVA</b>	<b>ns</b>	<b>&lt;0.050</b>	<b>ns</b>	<b>ns</b>	-	-

Values shown are the mean  $\pm$  SE for six replicates under 40% and 80% of relative humidity, under control and labeled conditions. Level of significance for the ANOVA:  $P<0.001$ ,  $P<0.010$  and  $P<0.050$

**Supplemental Table 2.** Pearson correlations of carbon isotope composition ( $\delta^{13}\text{C}$ ) in the organic matter (water soluble fraction, dry matter), during mid grain filling in different plant tissues (flag leaf, peduncle, glume, awn, grain), against chlorophyll content, sub-stomatal  $\text{CO}_2$  (Ci), photosynthetic rate (Amax), stomatal conductance ( $g_s$ ), intrinsic efficiency of photosystem two ( $F_v'/F_m'$ ), quantum efficiencies of photosynthetic electron transport through photosystem II (PhiPS2), Photosynthetic electron transport rate (ETR), transpiration (Tr) during mid grain filling, under different relative humidity levels (40% vs 80%), and combining control and labeled conditions.

	40%						80%					
	Water soluble fraction				Dry matter		Water soluble fraction				Dry matter	
	$\delta^{13}\text{C}_{\text{flag}}$	$\delta^{13}\text{C}_{\text{Peduncle}}$	$\delta^{13}\text{C}_{\text{Glume}}$	$\delta^{13}\text{C}_{\text{Awn}}$	$\delta^{13}\text{C}_{\text{flag leaf}}$	$\delta^{13}\text{C}_{\text{Grain}}$	$\delta^{13}\text{C}_{\text{flag}}$	$\delta^{13}\text{C}_{\text{Peduncle}}$	$\delta^{13}\text{C}_{\text{Glume}}$	$\delta^{13}\text{C}_{\text{Awn}}$	$\delta^{13}\text{C}_{\text{flag}}$	$\delta^{13}\text{C}_{\text{Grain}}$
<b>Mid grain filling</b>												
Chlorophyll	0.472 <sup>ns</sup>	0.509 <sup>ns</sup>	0.558 <sup>ns</sup>	0.191 <sup>ns</sup>	0.398 <sup>ns</sup>	-0.133 <sup>ns</sup>	0.452 <sup>ns</sup>	0.233 <sup>ns</sup>	0.372 <sup>ns</sup>	0.456 <sup>ns</sup>	0.211 <sup>ns</sup>	-0.089 <sup>ns</sup>
Ci	-0.357 <sup>ns</sup>	-0.407 <sup>ns</sup>	-0.463 <sup>ns</sup>	-0.262 <sup>ns</sup>	0.642 <sup>ns</sup>	0.962**	-0.769**	-0.883**	-0.361 <sup>ns</sup>	-0.663 <sup>ns</sup>	-0.954**	-0.324 <sup>ns</sup>
Amax	-0.347 <sup>ns</sup>	-0.262 <sup>ns</sup>	-0.255 <sup>ns</sup>	-0.339 <sup>ns</sup>	0.037 <sup>ns</sup>	-0.305 <sup>ns</sup>	-0.261 <sup>ns</sup>	-0.138 <sup>ns</sup>	0.146 <sup>ns</sup>	-0.154 <sup>ns</sup>	0.574 <sup>ns</sup>	-0.096 <sup>ns</sup>
$g_s$	-0.354 <sup>ns</sup>	-0.562 <sup>ns</sup>	-0.479 <sup>ns</sup>	-0.044 <sup>ns</sup>	0.926 <sup>ns</sup>	0.020 <sup>ns</sup>	-0.798**	-0.734*	-0.219 <sup>ns</sup>	-0.704*	-0.887*	-0.506 <sup>ns</sup>
$F_v'/F_m'$	0.560 <sup>ns</sup>	0.660 <sup>ns</sup>	0.609 <sup>ns</sup>	0.316 <sup>ns</sup>	-0.587 <sup>ns</sup>	-0.607 <sup>ns</sup>	-0.597 <sup>ns</sup>	-0.438 <sup>ns</sup>	-0.125 <sup>ns</sup>	-0.582 <sup>ns</sup>	0.234 <sup>ns</sup>	0.080 <sup>ns</sup>
PhiPS2	0.476 <sup>ns</sup>	0.583 <sup>ns</sup>	0.518 <sup>ns</sup>	0.245 <sup>ns</sup>	-0.685 <sup>ns</sup>	-0.533 <sup>ns</sup>	-0.699*	-0.615 <sup>ns</sup>	0.065 <sup>ns</sup>	-0.509 <sup>ns</sup>	-0.405 <sup>ns</sup>	0.219 <sup>ns</sup>
ETR	0.482 <sup>ns</sup>	0.586 <sup>ns</sup>	0.522 <sup>ns</sup>	0.252 <sup>ns</sup>	-0.680 <sup>ns</sup>	-0.535 <sup>ns</sup>	-0.695*	-0.612 <sup>ns</sup>	0.069 <sup>ns</sup>	-0.506 <sup>ns</sup>	-0.390 <sup>ns</sup>	0.220 <sup>ns</sup>
Tr	-0.378 <sup>ns</sup>	-0.486 <sup>ns</sup>	-0.564 <sup>ns</sup>	-0.135 <sup>ns</sup>	0.032 <sup>ns</sup>	0.045 <sup>ns</sup>	-0.807**	-0.760*	-0.205 <sup>ns</sup>	-0.721*	-0.916*	-0.184 <sup>ns</sup>
DW <sub>shoot</sub>	0.968**	0.754*	0.701*	0.929**	0.274 <sup>ns</sup>	-0.235 <sup>ns</sup>	0.486 <sup>ns</sup>	0.459 <sup>ns</sup>	0.232 <sup>ns</sup>	0.812**	0.329 <sup>ns</sup>	-0.470 <sup>ns</sup>
<b>Maturity</b>												
DW <sub>Biomass</sub>	0.594 <sup>ns</sup>	0.644*	0.676*	0.618 <sup>ns</sup>	0.652 <sup>ns</sup>	-0.082 <sup>ns</sup>	0.071 <sup>ns</sup>	0.193 <sup>ns</sup>	0.118 <sup>ns</sup>	0.382 <sup>ns</sup>	0.498 <sup>ns</sup>	-0.339 <sup>s</sup>
DW <sub>Ear</sub>	0.322 <sup>ns</sup>	0.063 <sup>ns</sup>	-0.006 <sup>ns</sup>	0.597 <sup>ns</sup>	-0.163 <sup>ns</sup>	-0.727 <sup>ns</sup>	0.212 <sup>ns</sup>	0.201 <sup>ns</sup>	-0.023 <sup>ns</sup>	0.210 <sup>ns</sup>	0.909*	0.581 <sup>ns</sup>
GN <sub>ear</sub>	0.072 <sup>ns</sup>	-0.130 <sup>ns</sup>	-0.167 <sup>ns</sup>	0.458 <sup>ns</sup>	-0.272 <sup>ns</sup>	-0.868*	0.048 <sup>ns</sup>	-0.032 <sup>ns</sup>	0.113 <sup>ns</sup>	-0.166 <sup>ns</sup>	0.769 <sup>ns</sup>	0.744 <sup>ns</sup>
DW <sub>grain ear</sub>	0.346 <sup>ns</sup>	0.098 <sup>ns</sup>	0.012 <sup>ns</sup>	0.633*	-0.157 <sup>ns</sup>	-0.763 <sup>ns</sup>	0.285 <sup>ns</sup>	0.177 <sup>ns</sup>	0.357 <sup>ns</sup>	0.196 <sup>ns</sup>	0.706 <sup>ns</sup>	0.257 <sup>ns</sup>

For each relative humidity level (40% vs 80%), correlations of traits measured during mid grain filling against  $\delta^{13}\text{C}$  in water soluble fraction were calculated using twelve replicates by combining control and labeled conditions, and against  $\delta^{13}\text{C}$  in dry matter using six replicates under control conditions only. Correlations of yield components at maturity against  $\delta^{13}\text{C}$  in the water soluble fraction and the dry matter were calculated using six replicates only, when combining control and labeled conditions and for each relative humidity level. Level of significance: ns, not significant; \*\*,  $P < 0.01$ ; \*,  $P < 0.05$ .

**Supplemental Table 3.** Pearson correlations of oxygen ( $\delta^{18}\text{O}$ ) and hydrogen ( $\delta^2\text{H}$ ) stable isotope compositions in the organic matter ( $\delta^{12}\text{H}$  in dry matter,  $\delta^{18}\text{O}$  in water soluble fraction), during mid grain filling in different plant tissues (flag leaf, peduncle, glume, awn, grain), against chlorophyll content, sub-stomatal  $\text{CO}_2$  (Ci), photosynthetic rate (Amax), stomatal conductance (Gs), intrinsic efficiency of photosystem two (Fv'/Fm'), quantum efficiencies of photosynthetic electron transport through photosystem II (PhiPS2), Photosynthetic electron transport rate (ETR), transpiration (Tr) and shoot dry weight ( $\text{DW}_{\text{shoot}}$ ) during mid grain filling, and dry matter of biomass ( $\text{DW}_{\text{Biomass}}$ ), ear per plant ( $\text{DW}_{\text{Ear}}$ ) and grain per ear ( $\text{DW}_{\text{Grain}}$ ), and grain number per ear (GN) at maturity, under different isotope labeling (control and labeled), and combining humidity levels (40% and 80%).

	Water soluble fraction					Dry matter					
	$\delta^{18}\text{O}_{\text{flag leaf}}$	$\delta^{18}\text{O}_{\text{peduncle}}$	$\delta^{18}\text{O}_{\text{glume}}$	$\delta^{18}\text{O}_{\text{awn}}$	$\delta^{18}\text{O}_{\text{grain}}$	$\delta^2\text{H}_{\text{flag leaf}}$	$\delta^2\text{H}_{\text{peduncle}}$	$\delta^2\text{H}_{\text{glume}}$	$\delta^2\text{H}_{\text{awn}}$	$\delta^2\text{H}_{\text{grain}}$	
Control	Chlorophyll	-0.366 <sup>ns</sup>	-0.493 <sup>ns</sup>	-0.383 <sup>ns</sup>	-0.515 <sup>ns</sup>	-0.926**	-0.666*	0.078 <sup>ns</sup>	-0.639*	-0.865**	-0.694*
	Ci	-0.876**	-0.800**	-0.881**	-0.889**	0.082 <sup>ns</sup>	-0.469 <sup>ns</sup>	-0.345 <sup>ns</sup>	-0.317 <sup>ns</sup>	-0.536 <sup>ns</sup>	0.404 <sup>ns</sup>
	Amax	-0.695*	-0.143 <sup>ns</sup>	-0.278 <sup>ns</sup>	-0.606 <sup>ns</sup>	-0.687*	-0.290 <sup>ns</sup>	-0.246 <sup>ns</sup>	-0.625 <sup>ns</sup>	-0.508 <sup>ns</sup>	-0.768**
	gs	-0.913**	-0.694*	-0.837**	-0.830**	-0.753**	-0.475 <sup>ns</sup>	-0.423 <sup>ns</sup>	-0.479 <sup>ns</sup>	-0.548 <sup>ns</sup>	-0.737**
	Fv'/Fm'	-0.816**	-0.433 <sup>ns</sup>	-0.534 <sup>ns</sup>	-0.696*	-0.724**	-0.073 <sup>ns</sup>	-0.356 <sup>ns</sup>	-0.558 <sup>ns</sup>	-0.513 <sup>ns</sup>	-0.730**
	PhiPS2	-0.390 <sup>ns</sup>	-0.112 <sup>ns</sup>	-0.209 <sup>ns</sup>	-0.090 <sup>ns</sup>	-0.714**	-0.024 <sup>ns</sup>	-0.042 <sup>ns</sup>	-0.711*	-0.252 <sup>ns</sup>	-0.731**
	ETR	-0.386 <sup>ns</sup>	-0.112 <sup>ns</sup>	-0.206 <sup>ns</sup>	-0.089 <sup>ns</sup>	-0.714**	-0.024 <sup>ns</sup>	-0.033 <sup>ns</sup>	-0.713*	-0.257 <sup>ns</sup>	-0.731**
	Tr	-0.812**	-0.571 <sup>ns</sup>	-0.783**	-0.651*	-0.695*	-0.487 <sup>ns</sup>	-0.413 <sup>ns</sup>	-0.503 <sup>ns</sup>	-0.425 <sup>ns</sup>	-0.679*
	$\text{DW}_{\text{shoot}}$	-0.263 <sup>ns</sup>	-0.153 <sup>ns</sup>	-0.272 <sup>ns</sup>	-0.461 <sup>ns</sup>	-0.464 <sup>ns</sup>	-0.543 <sup>ns</sup>	-0.290 <sup>ns</sup>	-0.150 <sup>ns</sup>	-0.655*	-0.414 <sup>ns</sup>
	$\text{DW}_{\text{Biomass}}$	-0.297 <sup>ns</sup>	-0.002 <sup>ns</sup>	-0.366 <sup>ns</sup>	-0.346 <sup>ns</sup>	-0.523 <sup>ns</sup>	-0.196 <sup>ns</sup>	-0.439 <sup>ns</sup>	0.070 <sup>ns</sup>	-0.199 <sup>ns</sup>	-0.462 <sup>ns</sup>
	$\text{DW}_{\text{Ear}}$	-0.046 <sup>ns</sup>	0.146 <sup>ns</sup>	0.125 <sup>ns</sup>	-0.231 <sup>ns</sup>	-0.114 <sup>ns</sup>	0.196 <sup>ns</sup>	0.020 <sup>ns</sup>	0.111 <sup>ns</sup>	-0.161 <sup>ns</sup>	-0.265 <sup>ns</sup>
	$\text{GN}_{\text{ear}}$	-0.242 <sup>ns</sup>	0.048 <sup>ns</sup>	-0.028 <sup>ns</sup>	-0.291 <sup>ns</sup>	-0.149 <sup>ns</sup>	0.166 <sup>ns</sup>	0.109 <sup>ns</sup>	0.063 <sup>ns</sup>	-0.079 <sup>ns</sup>	-0.365 <sup>ns</sup>
	$\text{DW}_{\text{grain ear}}$	0.133 <sup>ns</sup>	0.212 <sup>ns</sup>	0.107 <sup>ns</sup>	0.005 <sup>ns</sup>	0.061 <sup>ns</sup>	0.383 <sup>ns</sup>	0.308 <sup>ns</sup>	0.391 <sup>ns</sup>	0.189 <sup>ns</sup>	-0.195 <sup>ns</sup>
Labeled	Chlorophyll	-0.208 <sup>ns</sup>	-0.367 <sup>ns</sup>	-0.326 <sup>ns</sup>	-0.739*	0.075 <sup>ns</sup>	-0.503 <sup>ns</sup>	0.095 <sup>ns</sup>	0.461 <sup>ns</sup>	-0.356 <sup>ns</sup>	-0.153 <sup>ns</sup>
	Ci	-0.845**	0.072 <sup>ns</sup>	-0.321 <sup>ns</sup>	-0.516 <sup>ns</sup>	-0.499 <sup>ns</sup>	-0.370 <sup>ns</sup>	0.345 <sup>ns</sup>	0.032 <sup>ns</sup>	-0.229 <sup>ns</sup>	-0.365 <sup>ns</sup>
	Amax	-0.029 <sup>ns</sup>	0.434 <sup>ns</sup>	0.171 <sup>ns</sup>	0.184 <sup>ns</sup>	-0.311 <sup>ns</sup>	-0.084 <sup>ns</sup>	0.044 <sup>ns</sup>	0.228 <sup>ns</sup>	0.144 <sup>ns</sup>	-0.543 <sup>ns</sup>
	Gs	-0.274 <sup>ns</sup>	0.363 <sup>ns</sup>	0.245 <sup>ns</sup>	0.214 <sup>ns</sup>	-0.527 <sup>ns</sup>	-0.010 <sup>ns</sup>	0.308 <sup>ns</sup>	0.546 <sup>ns</sup>	0.409 <sup>ns</sup>	-0.527 <sup>ns</sup>
	Fv'/Fm'	-0.291 <sup>ns</sup>	0.110 <sup>ns</sup>	-0.564 <sup>ns</sup>	-0.303 <sup>ns</sup>	-0.321 <sup>ns</sup>	-0.685*	0.402 <sup>ns</sup>	0.666 <sup>ns</sup>	-0.268 <sup>ns</sup>	-0.253 <sup>ns</sup>
	PhiPS2	-0.069 <sup>ns</sup>	0.199 <sup>ns</sup>	-0.463 <sup>ns</sup>	-0.179 <sup>ns</sup>	-0.307 <sup>ns</sup>	-0.560 <sup>ns</sup>	0.313 <sup>ns</sup>	0.498 <sup>ns</sup>	-0.244 <sup>ns</sup>	-0.209 <sup>ns</sup>
	ETR	-0.067 <sup>ns</sup>	0.201 <sup>ns</sup>	-0.463 <sup>ns</sup>	-0.176 <sup>ns</sup>	-0.305 <sup>ns</sup>	-0.557 <sup>ns</sup>	0.317 <sup>ns</sup>	0.502 <sup>ns</sup>	-0.240 <sup>ns</sup>	-0.203 <sup>ns</sup>
	Tr	0.185 <sup>ns</sup>	0.633 <sup>ns</sup>	0.438 <sup>ns</sup>	0.512 <sup>ns</sup>	-0.517 <sup>ns</sup>	0.522 <sup>ns</sup>	0.212 <sup>ns</sup>	-0.396 <sup>ns</sup>	0.528 <sup>ns</sup>	-0.530 <sup>ns</sup>
	$\text{DW}_{\text{shoot}}$	-0.086 <sup>ns</sup>	-0.254 <sup>ns</sup>	-0.405 <sup>ns</sup>	-0.417 <sup>ns</sup>	-0.263 <sup>ns</sup>	-0.519 <sup>ns</sup>	0.230 <sup>ns</sup>	0.632*	-0.342 <sup>ns</sup>	-0.283 <sup>ns</sup>
	$\text{DW}_{\text{Biomass}}$	0.419 <sup>ns</sup>	0.058 <sup>ns</sup>	-0.225 <sup>ns</sup>	-0.066 <sup>ns</sup>	-0.145 <sup>ns</sup>	0.296 <sup>ns</sup>	0.002 <sup>ns</sup>	0.153 <sup>ns</sup>	-0.082 <sup>ns</sup>	0.070 <sup>ns</sup>

DW <sub>Ear</sub>	-0.635*	-0.398 <sup>ns</sup>	-0.369 <sup>ns</sup>	-0.567 <sup>ns</sup>	-0.120 <sup>ns</sup>	-0.539 <sup>ns</sup>	0.110 <sup>ns</sup>	0.454 <sup>ns</sup>	-0.390 <sup>ns</sup>	-0.360 <sup>ns</sup>
GN <sub>ear</sub>	-0.790**	-0.185 <sup>ns</sup>	-0.366 <sup>ns</sup>	-0.552 <sup>ns</sup>	-0.409 <sup>ns</sup>	-0.481 <sup>ns</sup>	0.397 <sup>ns</sup>	0.546 <sup>ns</sup>	-0.189 <sup>ns</sup>	-0.533 <sup>ns</sup>
DW <sub>grain ear</sub>	-0.598 <sup>ns</sup>	-0.305 <sup>ns</sup>	-0.379 <sup>ns</sup>	-0.492 <sup>ns</sup>	0.030 <sup>ns</sup>	-0.448 <sup>ns</sup>	0.212 <sup>ns</sup>	0.517 <sup>ns</sup>	-0.196 <sup>ns</sup>	-0.390 <sup>ns</sup>

For each isotope labeling condition (control vs labeled), correlations of traits measured during mid grain filling against  $\delta^{18}\text{O}$  in water soluble fraction and  $\delta^2\text{H}$  in dry matter were calculated using twelve replicates by combining relative humidity levels (40% and 80%); and correlations of yield components at maturity against  $\delta^{18}\text{O}$  in water soluble fraction and  $\delta^2\text{H}$  in dry matter were calculated using six replicates only when combining relative humidity levels (40% and 80%). Levels of significance: ns, not significant; \*\*,  $P < 0.01$ ; \*,  $P < 0.05$ .



**Supplemental Table 4.** Pearson correlations between carbon ( $\delta^{13}\text{C}$ ), oxygen ( $\delta^{18}\text{O}$ ) and hydrogen ( $\delta^2\text{H}$ ) isotope compositions in the organic matter ( $\delta^{13}\text{C}$  and  $\delta^2\text{H}$  in dry matter,  $\delta^{13}\text{C}$  and  $\delta^{18}\text{O}$  in water soluble fraction), in different plant tissues (flag leaf, peduncle, glume, awn, grain). Isotopes were assessed during mid grain filling by combining both humidity levels (40% and 80%) and under different isotope labeling (control and labeled).

	Water soluble fraction					Dry matter					
	$\delta^{18}\text{O}_{\text{flag leaf}}$	$\delta^{18}\text{O}_{\text{peduncle}}$	$\delta^{18}\text{O}_{\text{glume}}$	$\delta^{18}\text{O}_{\text{awn}}$	$\delta^{18}\text{O}_{\text{grain}}$	$\delta^{12}\text{H}_{\text{flag leaf}}$	$\delta^{12}\text{H}_{\text{peduncle}}$	$\delta^{12}\text{H}_{\text{glume}}$	$\delta^{12}\text{H}_{\text{awn}}$	$\delta^{12}\text{H}_{\text{grain}}$	
$\delta^{13}\text{C}_{\text{WSF,flag leaf}}$	0.945**	0.592 <sup>ns</sup>	0.673*	0.764*	0.658*	0.385 <sup>ns</sup>	0.344 <sup>ns</sup>	0.462 <sup>ns</sup>	0.453 <sup>ns</sup>	0.559 <sup>ns</sup>	
$\delta^{13}\text{C}_{\text{WSF,peduncle}}$	0.948**	0.684*	0.683*	0.830**	0.705*	0.338 <sup>ns</sup>	0.297 <sup>ns</sup>	0.453 <sup>ns</sup>	0.598 <sup>ns</sup>	0.624*	
$\delta^{13}\text{C}_{\text{WSF,glume}}$	0.711*	0.369 <sup>ns</sup>	0.235 <sup>ns</sup>	0.781**	0.401 <sup>ns</sup>	0.118 <sup>ns</sup>	0.334 <sup>ns</sup>	0.060 <sup>ns</sup>	0.470 <sup>ns</sup>	0.247 <sup>ns</sup>	
$\delta^{13}\text{C}_{\text{WSF,awn}}$	0.883**	0.670*	0.626 <sup>ns</sup>	0.746*	0.790**	0.210 <sup>ns</sup>	0.201 <sup>ns</sup>	0.473 <sup>ns</sup>	0.473 <sup>ns</sup>	0.494 <sup>ns</sup>	
$\delta^{13}\text{C}_{\text{DM,flag leaf}}$	0.896**	0.714**	0.628*	0.783**	0.601*	0.252 <sup>ns</sup>	0.226 <sup>ns</sup>	0.354 <sup>ns</sup>	0.646*	0.577*	
$\delta^{13}\text{C}_{\text{DM,grain}}$	0.910**	0.685*	0.830**	0.923**	0.846**	0.521 <sup>ns</sup>	0.339 <sup>ns</sup>	0.321 <sup>ns</sup>	0.670*	0.877**	
Control	$\delta^{18}\text{O}_{\text{WSF,flag leaf}}$	1	0.641*	0.771**	0.892**	0.829**	0.502 <sup>ns</sup>	0.391 <sup>ns</sup>	0.482 <sup>ns</sup>	0.595 <sup>ns</sup>	0.727*
	$\delta^{18}\text{O}_{\text{WSF,peduncle}}$	-	1	0.823**	0.691*	0.696*	0.457 <sup>ns</sup>	-0.138 <sup>ns</sup>	0.434 <sup>ns</sup>	0.610*	0.770**
	$\delta^{18}\text{O}_{\text{WSF,glume}}$	-	-	1	0.711*	0.822**	0.538 <sup>ns</sup>	0.169 <sup>ns</sup>	0.438 <sup>ns</sup>	0.447 <sup>ns</sup>	0.909**
	$\delta^{18}\text{O}_{\text{WSF,awn}}$	-	-	-	1	0.909**	0.621 <sup>ns</sup>	0.291 <sup>ns</sup>	0.266 <sup>ns</sup>	0.751*	0.767**
	$\delta^{18}\text{O}_{\text{WSF,grain}}$	-	-	-	-	1	0.451 <sup>ns</sup>	0.306 <sup>ns</sup>	0.557 <sup>ns</sup>	0.684*	0.792**
	$\delta^{12}\text{H}_{\text{DM,flag leaf}}$	0.502 <sup>ns</sup>	0.457 <sup>ns</sup>	0.538 <sup>ns</sup>	0.621 <sup>ns</sup>	0.451 <sup>ns</sup>	1	0.235 <sup>ns</sup>	0.595 <sup>ns</sup>	0.717*	0.473 <sup>ns</sup>
	$\delta^{12}\text{H}_{\text{DM,peduncle}}$	0.391 <sup>ns</sup>	-0.138 <sup>ns</sup>	0.169 <sup>ns</sup>	0.291 <sup>ns</sup>	0.306 <sup>ns</sup>	-	1	0.098 <sup>ns</sup>	0.184 <sup>ns</sup>	0.141 <sup>ns</sup>
	$\delta^{12}\text{H}_{\text{DM,glume}}$	0.482 <sup>ns</sup>	0.434 <sup>ns</sup>	0.438 <sup>ns</sup>	0.266 <sup>ns</sup>	0.557 <sup>ns</sup>	-	-	1	0.600 <sup>ns</sup>	0.305 <sup>ns</sup>
	$\delta^{12}\text{H}_{\text{DM,awn}}$	0.595 <sup>ns</sup>	0.610*	0.447 <sup>ns</sup>	0.751*	0.684*	-	-	-	1	0.480 <sup>ns</sup>
	$\delta^{12}\text{H}_{\text{DM,grain}}$	0.727*	0.770**	0.909**	0.767**	0.792**	-	-	-	-	1
	$\delta^{13}\text{C}_{\text{WSF,flag leaf}}$	0.771**	-0.004 <sup>ns</sup>	0.117 <sup>ns</sup>	0.547 <sup>ns</sup>	0.505 <sup>ns</sup>	0.375 <sup>ns</sup>	0.016 <sup>ns</sup>	-0.383 <sup>ns</sup>	0.340 <sup>ns</sup>	0.417 <sup>ns</sup>
	$\delta^{13}\text{C}_{\text{WSF,peduncle}}$	0.887**	0.005 <sup>ns</sup>	0.428 <sup>ns</sup>	0.732 <sup>ns</sup>	0.590 <sup>ns</sup>	0.572 <sup>ns</sup>	-0.198 <sup>ns</sup>	-0.553 <sup>ns</sup>	0.562 <sup>ns</sup>	0.665 <sup>ns</sup>
	$\delta^{13}\text{C}_{\text{WSF,glume}}$	0.743**	-0.286 <sup>ns</sup>	0.347 <sup>ns</sup>	0.611 <sup>ns</sup>	0.618*	0.337 <sup>ns</sup>	-0.365 <sup>ns</sup>	-0.296 <sup>ns</sup>	0.520 <sup>ns</sup>	0.676*
	$\delta^{13}\text{C}_{\text{WSF,awn}}$	0.759*	0.103 <sup>ns</sup>	0.144 <sup>ns</sup>	0.538 <sup>ns</sup>	0.356 <sup>ns</sup>	0.621 <sup>ns</sup>	0.141 <sup>ns</sup>	-0.349 <sup>ns</sup>	0.531 <sup>ns</sup>	0.295 <sup>ns</sup>
	$\delta^{13}\text{C}_{\text{DM,flag leaf}}$	-	-	-	-	-	-	-	-	-	-
Labeled	$\delta^{18}\text{O}_{\text{WSF,flag leaf}}$	1	0.361 <sup>ns</sup>	0.381 <sup>ns</sup>	0.864**	0.439 <sup>ns</sup>	0.747**	-0.128 <sup>ns</sup>	-0.713*	0.375 <sup>ns</sup>	0.456 <sup>ns</sup>
	$\delta^{18}\text{O}_{\text{WSF,peduncle}}$	-	1	-0.305 <sup>ns</sup>	0.160 <sup>ns</sup>	-0.308 <sup>ns</sup>	0.587 <sup>ns</sup>	0.681*	-0.340 <sup>ns</sup>	-0.234 <sup>ns</sup>	-0.444 <sup>ns</sup>
	$\delta^{18}\text{O}_{\text{WSF,glume}}$	-	-	1	0.669*	0.411 <sup>ns</sup>	0.358 <sup>ns</sup>	-0.592 <sup>ns</sup>	-0.294 <sup>ns</sup>	0.610*	0.352 <sup>ns</sup>
	$\delta^{18}\text{O}_{\text{WSF,awn}}$	-	-	-	1	0.249 <sup>ns</sup>	0.721*	-0.172 <sup>ns</sup>	-0.562 <sup>ns</sup>	0.829**	0.297 <sup>ns</sup>
	$\delta^{18}\text{O}_{\text{WSF,grain}}$	-	-	-	-	1	0.274 <sup>ns</sup>	-0.588 <sup>ns</sup>	-0.350 <sup>ns</sup>	0.279 <sup>ns</sup>	0.824**

$\delta^{12}\text{H}_{\text{DM,flag leaf}}$	0.747**	0.587 <sup>ns</sup>	0.358 <sup>ns</sup>	0.721*	0.274 <sup>ns</sup>	1	0.115 <sup>ns</sup>	-0.714*	0.500 <sup>ns</sup>	0.397 <sup>ns</sup>
$\delta^{12}\text{H}_{\text{DM,peduncle}}$	-0.128 <sup>ns</sup>	0.681*	-0.592 <sup>ns</sup>	-0.172 <sup>ns</sup>	-0.588 <sup>ns</sup>	-	1	0.249 <sup>ns</sup>	-0.046 <sup>ns</sup>	-0.697*
$\delta^{12}\text{H}_{\text{DM,glume}}$	-0.713*	-0.340 <sup>ns</sup>	-0.294 <sup>ns</sup>	-0.562 <sup>ns</sup>	-0.350 <sup>ns</sup>	-	-	1	0.100 <sup>ns</sup>	-0.613 <sup>ns</sup>
$\delta^{12}\text{H}_{\text{DM,awn}}$	0.375 <sup>ns</sup>	-0.234 <sup>ns</sup>	0.610*	0.829**	0.279 <sup>ns</sup>	-	-	-	1	0.313 <sup>ns</sup>
$\delta^{12}\text{H}_{\text{DM,grain}}$	0.456 <sup>ns</sup>	-0.444 <sup>ns</sup>	0.352 <sup>ns</sup>	0.297 <sup>ns</sup>	0.824**	-	-	-	-	1

For each isotope labeling condition (control vs labeled), correlations were calculated using twelve replicates by combining relative humidity levels (40% and 80%); Level of significance: ns, not significant; \*\*,  $P < 0.01$ ; \*,  $P < 0.05$ .

**Supplemental Table 5.** Pearson correlations between oxygen ( $\delta^{18}\text{O}$ ) and hydrogen ( $\delta^2\text{H}$ ) isotope compositions in the organic matter ( $\delta^{12}\text{H}$  in dry matter,  $\delta^{18}\text{O}$  in water soluble fraction), against oxygen ( $\delta^{18}\text{O}$ ) and hydrogen ( $\delta^2\text{H}$ ) stable isotope compositions in the water in plant tissues. Isotopes were assessed during mid grain filling in different plant tissues (flag leaf, peduncle, glume, awn, grain), combining humidity levels (40% and 80%) and under different isotope labeling (control and labeled).

	Water soluble fraction					Dry matter					
	$\delta^{18}\text{O}_{\text{flag leaf}}$	$\delta^{18}\text{O}_{\text{peduncle}}$	$\delta^{18}\text{O}_{\text{glume}}$	$\delta^{18}\text{O}_{\text{awn}}$	$\delta^{18}\text{O}_{\text{grain}}$	$\delta^2\text{H}_{\text{flag leaf}}$	$\delta^2\text{H}_{\text{peduncle}}$	$\delta^2\text{H}_{\text{glume}}$	$\delta^2\text{H}_{\text{awn}}$	$\delta^2\text{H}_{\text{grain}}$	
Control	$\delta^{18}\text{O}_{\text{WT-Stem H}_2\text{O}}$	-0.333	-0.342	-0.203	-0.567	-0.040	-0.086	0.335	0.085	-0.102	-0.217
	$\delta^{18}\text{O}_{\text{WT-Flag leaf H}_2\text{O}}$	0.438	0.027	0.218	0.055	0.079	0.020	-0.023	0.135	-0.146	0.036
	$\delta^{18}\text{O}_{\text{WT-Peduncle H}_2\text{O}}$	-0.950**	-0.610*	-0.478	-0.916**	-0.597	-0.097	-0.234	-0.299	-0.778**	-0.579
	$\delta^{18}\text{O}_{\text{WT-Grain H}_2\text{O}}$	0.021	0.042	-0.057	-0.075	0.006	-0.422	-0.358	-0.256	0.065	0.132
	$\delta^2\text{H}_{\text{WT-Stem H}_2\text{O}}$	-0.359	-0.239	-0.166	-0.364	0.096	-0.018	0.045	0.018	0.100	-0.023
	$\delta^2\text{H}_{\text{WT-Flag leaf H}_2\text{O}}$	0.980**	0.597*	0.739**	0.820**	0.825**	0.448	0.315	0.575	0.552	0.642*
	$\delta^2\text{H}_{\text{WT-Peduncle H}_2\text{O}}$	-0.754*	-0.398	-0.214	-0.728*	-0.124	0.113	-0.155	0.122	-0.334	-0.209
	$\delta^2\text{H}_{\text{WT-Grain H}_2\text{O}}$	0.315	0.221	0.121	0.336	0.238	-0.231	-0.312	-0.087	0.389	0.347
Labeled	$\delta^{18}\text{O}_{\text{WT-Stem H}_2\text{O}}$	0.327	0.261	-0.383	0.198	-0.250	-0.105	0.193	0.138	-0.175	-0.248
	$\delta^{18}\text{O}_{\text{WT-Flag leaf H}_2\text{O}}$	0.433	-0.355	0.415	0.155	0.850**	0.005	-0.664*	-0.130	0.041	0.664*
	$\delta^{18}\text{O}_{\text{WT-Peduncle H}_2\text{O}}$	0.330	-0.220	0.288	0.080	0.786**	0.055	-0.643*	-0.253	-0.072	0.643*
	$\delta^{18}\text{O}_{\text{WT-Grain H}_2\text{O}}$	0.794**	0.463	0.405	0.660	0.440	0.771**	-0.184	-0.903**	0.059	0.475
	$\delta^2\text{H}_{\text{WT-Stem H}_2\text{O}}$	0.657*	0.006	0.164	0.358	0.672*	0.205	-0.393	-0.264	0.043	0.438
	$\delta^2\text{H}_{\text{WT-Flag leaf H}_2\text{O}}$	0.565	-0.216	0.484	0.324	0.659*	0.057	-0.446	-0.069	0.143	0.358
	$\delta^2\text{H}_{\text{WT-Peduncle H}_2\text{O}}$	0.252	-0.258	0.214	-0.046	0.756**	-0.086	-0.607	-0.152	-0.183	0.589
	$\delta^2\text{H}_{\text{WT-Grain H}_2\text{O}}$	0.745**	0.113	0.512	0.612	0.595	0.577	-0.465	-0.844**	0.033	0.598

For each isotope labeling condition (control vs labeled), correlations were calculated using twelve replicates by combining relative humidity levels (40% and 80%); Level of significance: ns, not significant; \*\*,  $P < 0.01$ ; \*,  $P < 0.05$ .

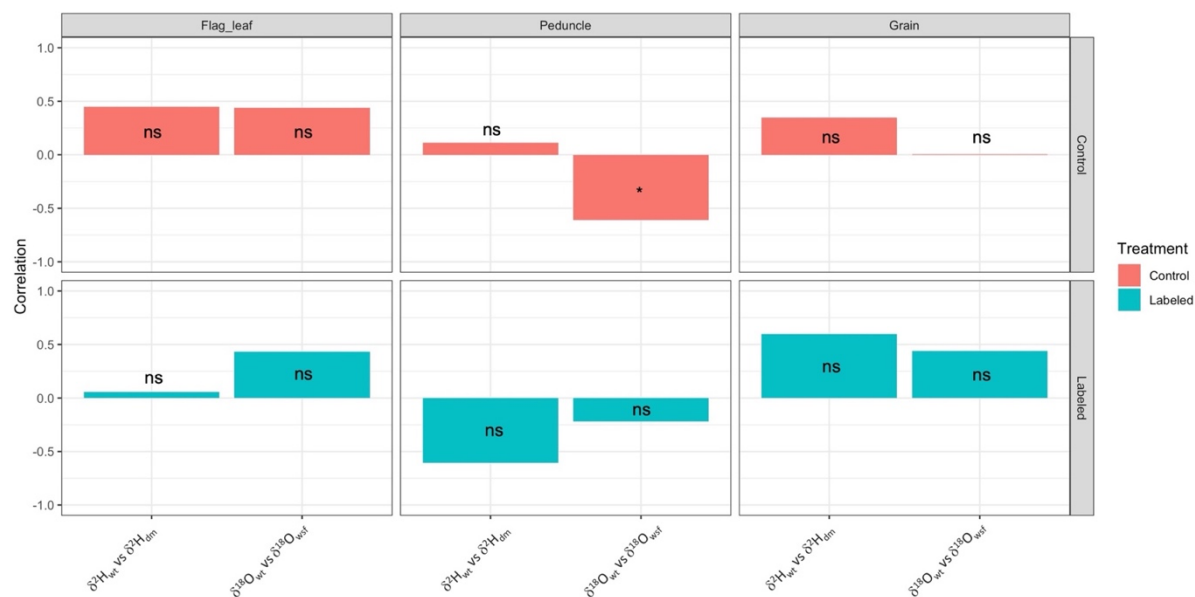


**Figure 3.** Linear regression relationships among hydrogen ( $\delta^2H$ ) and oxygen ( $\delta^{18}O$ ), stable isotope compositions assessed during mid grain filling in the organic matter (water soluble fraction and dry matter), and water in plant tissues for the flag leaf, peduncle and grain, when combining humidity levels (40% and 80%) and under separate isotope labeling (control vs labeled).  $\delta^2H_{dm}$ , hydrogen isotope composition of the dry matter;  $\delta^2H_{wt}$ , hydrogen isotope composition in water in plant tissue;  $\delta^{18}O_{wsf}$ , oxygen isotope composition in the water soluble fraction;  $\delta^{18}O_{wt}$ , oxygen isotope composition in the water in plant tissue.



## **GENERAL DISCUSSION**



## GENERAL DISCUSSION

Interannual variability in the Mediterranean region and the accompanied fluctuations in climatic events, mainly increased temperatures and reduced rainfall, are expected to increase evapotranspiration demands, accentuate the occurrence and the severity of drought episodes and restrict final grain yield in field grown wheat (Araus and Slafer, 2011; Feng et al., 2013). Although the need to achieve higher production to maintain the food balance is indisputable, the prospects for achieving such objective are less certain. Therefore, releasing new climate-resilient and high yielding cultivars tailored with traits for improved adaptation to drought stress and heat is of primary importance (Feng et al., 2013). The present work has demonstrated through its chapters the effect of environment (season and management practices) and genotypic on different traits associated with growth, phenology, water and nitrogen status, root traits and yield performance in wheat under Mediterranean conditions. To this end, a set of high yielding bread wheat cultivars (*Triticum aestivum* L.) selected from across Europe were evaluated under normal planting and rainfed conditions, different nitrogen fertilization levels and for three consecutive seasons (Chapter 1), and under normal and late planting conditions during one season (Chapter 2). Another set, this time of modern durum wheat cultivars (*Triticum turgidum* L. *subsp. durum* (Desf) Husn.) cultivated in Spain during the last five decades and with contrasting yield performance (high vs low) was evaluated under different planting dates (normal vs late), water regimes (irrigated vs rainfed) and nitrogen fertilizations (low vs recommended N fertilization) across different consecutive seasons (Chapters 3 and 4). Moreover, the uptake of water resources captured by roots, and its further release to sink tissues, was studied in the drought tolerant cultivar “*Sula*” grown under controlled vapor deficit pressure (VPD) conditions (high vs low), through assessing hydrogen and oxygen fractionation patterns in different plant tissues, with an overview on the trophism nature of some plant tissues (Chapter 5).

### ***Yield potential under Mediterranean conditions***

The recent decades have shown important increases in wheat yields as a response to the green revolution. However, the tradeoffs of such remarkable success were the dependence on the use of fertilization, pesticides and supplied irrigation (Lobell et al., 2009). Achieving yield potential in wheat cultivars requires unconstrained crop growth conditions facilitated by

optimum crop management practices (irrigation and N fertilization among others), that deals with abiotic (e.g. water stress and higher temperatures) and biotic stresses (e.g. weed, pests and diseases). Therefore, a balanced interplay between interannual variability, crop management and genotypic effects are paramount to achieve optimal yield potential (Schils et al., 2018). Water availability was shown throughout the Chapters 1, 3 and 4 to play a determinant role in grain yield (GY) performance. In fact, in elite high yielding bread wheat cultivars, the average rainfed-grown GY was reduced three-folds under the dry crop season (2018-2019) compared with the humid crop season (2017-2018), exhibiting thus an important yield gap of 5.9 Mg ha<sup>-1</sup> (Chapter 1). Likewise, when crop management practices and crop season were involved, the difference between the highest average GY achieved in durum wheat cultivars under irrigated normal planting trial (INP) during the humid season (2017-2018) and the rainfed normal planting trial (RNP) for the driest season (2018-2019), accounted for 5.7 Mg ha<sup>-1</sup> (Chapter 3), and under INP for the mild season (2019-2020) and the rainfed normal planting and low N fertilization conditions (RLN) for 5.6 Mg ha<sup>-1</sup> (Chapter 4). These consistent yield gap values that were reported repeatedly across this work's chapters are clear evidence of the necessity to optimize crop management to approach yield potential in wheat, particularly when crop growth is constrained by the expected, albeit unpredictable, interannual variability. Similar results were reported by different researchers on yield gaps in cereals including wheat, ranging from 1 Mg ha<sup>-1</sup> to 5 Mg ha<sup>-1</sup> as a response to crop management practices when grown under environments with optimal climatic conditions, and that crop management can narrow down up to 70% of the yield difference and optimize the final grain yield, when applied efficiently (Boogaard et al., 2013; Gobbett et al., 2017; Hochman et al., 2013; Lobell et al., 2009; Schils et al., 2018; Senapati and Semenov, 2019; Van Ittersum et al., 2013).

### ***Interannual variability, management practices and genotypic effects on yield performance***

The recent years have known constant fluctuations in climatic events as a response to climate change. These events, seen as the interannual variability in rainfalls and temperatures, were previously reported to explain around 31-51% of yield variability in Western Europe, Spain included (Ray et al., 2015). In this work, the crop season not only was significant on GY and most assessed traits (Chapters 1, 3 and 4), but also, water status was the main factor explaining GY performance. In fact, the seasonal water status assessed mainly through the

carbon isotope composition of mature grains ( $\delta^{13}\text{C}_{\text{grain}}$ ) was the primary explicative variable in the predictive models of GY in bread wheat genotypes grown under combined seasons (2017-2018; 2018-2019 and 2019-2020), and European regions (north, central and south) combined and separated (Chapter 1), and in durum wheat in genotypes grown under combined seasons (2017-2018; 2018-2019; 2019-2020 and 2020-2021), and growing conditions (INP, ILP, RNP and RLN) combined and separated (Chapter 4).

As stated above, crop management can optimize yield production significantly when practiced adequately. Irrigation and, to a lesser extent, N fertilization were proven to be efficient practices, among others, that are commonly used by farmers in the Mediterranean region. When addressing wheat production in the Mediterranean climate, water availability is usually the main limiting factor to grain yield (Jacobsen et al., 2012). In each crop season of this present work, GY was consistently reduced under RNP compared with INP conditions, as a consequence of poorer water status, shown by  $\delta^{13}\text{C}_{\text{grain}}$ . Moreover, under severe drought conditions as experienced during the season (2018-2019), GY reduction was threefold lesser under RNP conditions, compared with INP conditions (Chapter 3 and 4). The determinant role of water status in explaining the variability in GY performance was further demonstrated in stepwise and random forest predictive models in the four separate crop seasons (2017-2018; 2018-2019; 2019-2020 and 2020-2021) (Chapter 4), as well as reviewed by different authors in similar studies (Araus et al., 2003; Blum, 2009; Jacobsen et al., 2012; Lopes and Reynolds, 2010).

Similar to water status, planting date is another crop management strategy that is used to optimize root development (Incerti and O'Leary, 1990; Kirkegaard and Lilley, 2007) and yield production (Fischer, 2011; Hunt et al., 2019; Sacks et al., 2010) under field conditions. Late planting has long been considered as a key methodological approach to assess how crop duration and yield adjust to future temperature increases expected in the Mediterranean region (Jat et al., 2018; Paymard et al., 2018; Sacks et al., 2010). In terms of yield production, GY and number of spikes per square meter were decreased under late planting and support irrigation (ILP) conditions compared with INP as a consequence of a shortening in crop duration, increased respiration losses and transpiration rates and possible terminal heat stress during grain filling in bread wheat genotypes (Chapter 2). The same decreases were observed



for durum wheat genotypes in GY, yield components (harvest index, thousand grain weight, grain number and grain nitrogen yield) and crop phenological and growth traits (days to heading and plant height) during the different seasons investigated (Chapters 3 and 4).

On the other hand, when addressing crop fertilization, despite the major role of N fertilization in achieving higher yields in wheat in the recent decades, further increases in the already established recommendations of N fertilization input in Spanish fields (Fertiberia, 2022; Sativum, 2022) has shown a saturation pattern in N input in the rainfed regions of central and northern Spain (Chapter 1). In fact, when assessing the effect of three different N top dressing doses (50% of the recommended N dose “N1”, recommended N dose “N2” and 30% above the recommended N dose “N3”) on yield performance of different high yielding bread wheat genotypes grown under three consecutive crop seasons (2017-2018, 2018-2019 and 2019-2020), GY exhibited a minor increase (3 %) under N3 compared with N2, during the humid crop season (2017-2018), whereas in the following crop seasons (2018-2019 and 2019-2020), there was no effect of N fertilization on GY (Chapter 1). These results suggested that the already recommended N fertilization doses in Spanish fields fully cover the crop needs under humid and dry seasons (Chapter 1).

The genotypic effect is another major factor to assess wheat genotypes responses to their environment especially when restricted by water and nutrients deficits of the Mediterranean climate. Indeed, in European high yielding winter wheat genotypes (*Triticum aestivum* L.), the effect of genotypic effect on GY was the second most prevalent factor after the crop season, albeit strongly affected by seasonal conditions (Chapter 1). It appears that under wet (i.e humid) crop seasons (2017-2018 and 2019-2020), northern Europe cultivars yielded the highest, whereas central and southern Europe cultivars yielded 5-10% less (Chapter 1). These results were in accordance with Senapati and Semenov (2020) in their study on the large genetic yield potential estimated for bread wheat in Europe, in which they ranked yield potential as the highest in northern west Europe, followed by central Europe then southern Europe (Senapati and Semenov, 2020), with the optimal yield potential of bread wheat under the rainfed continental Mediterranean conditions of Spain being around 8 Mg ha<sup>-1</sup> (Chapter 2). In contrast, under drier seasons, southern Europe cultivars yielded the highest, followed by northern and central Europe cultivars which GY decreased by around 5% when evaluated during the dry season (2018-2019). Moreover, the range of variability was larger in genotypes

from the same provenance than these from different European regions, which suggest the presence of a large pool of winter wheat germplasm in northern and central Europe that holds potential adaptation traits to the Mediterranean growing conditions (Chapter 1). It is noteworthy to mention that under future climatic conditions, as simulated by late planting experiments, winter bread wheat cultivars which require vernalization are much more vulnerable under elevated temperatures than facultative wheats in which vernalization needs are optional (Kamran et al., 2014; Steinfort et al., 2017; Trevaskis et al., 2003), which infers another potential adjustment abilities against increased temperatures that facultative wheat genotypes may uphold (Chapter 2). Ullah and coworkers (2019) reported that targeting physiological traits that are associated with drought tolerance in a broad range of genetic variability might increase grain yield by 20-30% above the current high yielding cultivars (Reynolds and Trethowan, 2007).

Differently than winter bread wheat genotypes, the genotypic variability of durum wheat in terms of GY was mediated through phenology (Chapter 3). Albeit genotypic variability of durum wheat in terms of GY, water and nitrogen status and shovelomics derived traits were minor (Chapter 4). In fact, the narrow genotypic variability in grain yield of durum wheat compared with bread wheat cultivars was previously discussed (Asins and Carbonell, 1989; Martínez-Moreno et al., 2020; Ullah et al., 2019). Explanations on the lack of genotypic variability in physiological and root traits in durum wheat cultivars could be the low accuracy of the methodology applied in Chapter 4, particularly in root traits assessment, or the strong plasticity in roots in a targeted environment (Canè et al., 2014; Malamy, 2005; Sadras and Lawson, 2011).

### ***Phenotyping approaches to select for ideotypic traits***

Tailoring wheat ideotypes that are climate resilient under the Mediterranean field conditions require the implementation of efficient phenotyping techniques that can assess traits with potential ideotypic characteristics in a targeted environment. Phenology, leaf canopy, photosynthesis, root water uptake and drought tolerant traits such as stay green, have been for long targeted as candidate traits to design wheat ideotypes in the Mediterranean region (Rybka and Nita, 2015; Semenov et al., 2014; Senapati and Semenov, 2019; Stratonovitch and Semenov, 2015).

- Phenology

When addressing wheat growth, understanding phenology is key for proper management practices. Whereas the duration extending from emergence till flowering time defines ear density and grain size, grain filling affects the thousand kernel weight (Sadras and Slafer, 2012; Slafer et al., 2014). In Mediterranean region, an extended grain filling period achieved through an early anthesis is often desirable to achieve higher grain yields under dry conditions (Araus et al., 2002; van Oosterom and Acevedo, 1992). Under rainfed conditions, phenology duration can be season-specific: during wet seasons, an extended duration from stem elongation to anthesis was associated with high yielding in northern and central European bread wheat genotypes; In contrast, during dry seasons, an early anthesis combined with a longer grain filling stage, as shown by the southern Europe cultivars, was the trait best adapted to the growing conditions and secured an optimized final yield (Chapter 1). Under irrigated conditions, and regardless of the planting date (normal or late planting), a shorter days to heading was associated with higher yielding in post green revolution durum wheat cultivars (Chapter 3). In fact, shortening phenology to escape drought under Mediterranean conditions has been a common trait selected in breeding programs to achieve higher yields (De Vita et al., 2007; Loss and Siddique, 1994).

- Vegetation indices

In the recent decades, researchers have shifted their focus concerning phenotyping, from controlled conditions and biochemical traits frequently related with susceptibility to stress, towards optimizing phenotyping techniques for ideotypic traits in crops grown under field conditions (Araus et al., 2022; Araus and Cairns, 2014; Chen et al., 2017; Pieruschka and Schurr, 2019). Currently, a wide range of phenotyping approaches are available for crop ecophysiology purposes, mostly of remote sensing nature. For instance, high throughput phenotyping platforms (HTPPs), either proximate (e.g. at ground level) or remote (from aerial platforms placed in UAV to drones), with different categories or sensors and imagers, are often deployed for their non-invasive, rapid and efficient implementation. The usefulness of these devices (particularly thermal, multispectral and RGB cameras has been evidenced in many studies aiming to assess crop growth and biomass (Christopher et al., 2016; Padovan et al., 2020; Spano et al., 2003), photosynthesis (Gitelson and Merzlyak, 1998; Goulas et al., 2004;

Haboudane et al., 2002; Hunt et al., 2011; Sims and Gamon, 2003) and water status (Amani et al., 1996; Fischer et al., 1998; Jones et al., 2009; Pinto et al., 2017; Rezzouk et al., 2022; Thapa et al., 2018), as well as their contribution of these traits to higher grain yield. In agreement with these findings, in our study the canopy greenness vegetation indices, derived from RGB (mainly GA, GGA and a\*) and multispectral images (NDVI, EVI, PRI<sub>m</sub> and TCARIOSAVI) have shown overall strong correlations with GY, under INP better than under ILP, and during grain filling better than during heading, probably because the range of variability is larger under normal phenology (INP) compared with the accelerated phenology of a late planting (ILP), as well as because of the stay green characteristics which are expressed later during the crop cycle (i.e. grain filling rather than heading). The same indices detected the genotypic variability in yield and contributed to GY prediction models (Chapter 2). In fact, grain filling is a critical phenological stage in terms of grain setting and determining the final grain yield. Correlations between vegetation indices against GY during grain filling can be associated with the stay green status of genotypes, where greater stay green maintains photosynthetic activities longer. Similar results on the role of stay green in promoting higher yields were found in previous studies on durum wheat (Casadesùs et al., 2007; Elazab et al., 2015; Yousfi et al., 2016).

Canopy temperature depression (CTD) is another potentially useful trait that's often used as an indicator to transpiration (Blum, 2009), stomatal conductance (Condon, 2020; Roche, 2015) and therefore on crop water status (Fischer et al., 1998), eventually root depth (Li et al., 2019; Lopes and Reynolds, 2010), and therefore and grain yield (Chairi et al., 2020a, 2020b; Fischer et al., 1998; Lopes and Reynolds, 2010; Wasaya et al., 2018). In this work, ground and aerial CTD correlated positively with GY under combined seasons (2017-2018, 2018-2019, 2019-2020 and 2020-2021) and trials (INP, ILP, RNP, RLN), and separated rainfed trials (RNP and RLN) (Chapter 4).

- Photosynthesis derived indices

It is well established that increased photosynthesis translates into higher grain production under optimum growth conditions. For decades, breeding programs targeted photosynthesis related parameters as ideotypic traits for grain yield increase, traits such as the photosynthetic rate and stomatal conductance, but also stay green status were viewed as valuable drought

tolerant traits (Rybka and Nita, 2015; Semenov et al., 2014; Senapati and Semenov, 2019). In this work, higher air vapor pressure deficit (VPD) conditions clearly decreased the photosynthetic performance in the drought tolerant wheat cultivar “*Sula*” when grown under the controlled conditions of higher VPD conditions, compared with lower VPD conditions (Chapter 5). Comparable results were reported in other studies on wheat under VPD controlled conditions (Fakhet et al., 2021; Jauregui et al., 2018; Rashid et al., 2018; Xue et al., 2004). On the other hand, stay green status, approached often through biomass, and the multispectral index NDVI and chlorophyll content indices (Christopher et al., 2008), allowed differentiating between winter and facultative wheat genotypes under late planting conditions, with GY in facultative genotypes outperforming that of winter genotypes as a consequence of more extended reproductive stage (Chapter 2). Overall, a greener canopy (higher stay green status) was consistently associated with higher yielding wheat genotypes when grown under different Mediterranean field scenarios (Chapters 1, 2, 3 and 4).

- Root phenotyping derived indices

Root system architecture upholds valuable characteristics that can potentially confer better crop adaptation to drought. In fact, root growth is often influenced by environmental events and therefore exhibits a broad plasticity as response to the growing condition (Malamy, 2005). Unveiling root structure, distribution and functionality across soil depths in a target environment may pave the way towards designing a high yielding and climate resilient cultivars under Mediterranean conditions. In this work, roots plasticity was evidenced through root angle (RA) in the topsoil mainly, where in separate seasons, steeper root angle (lower RA) was associated with higher GY under irrigated and rainfed trials, separately; by contrast, when combining seasons, a shallower root angle spread (higher RA) is rather a positive trait to GY, under irrigated and rainfed trials, separately (Chapter 4).

Regardless, and despite the tedious and low throughput nature of phenotyping techniques often used to assess root characteristics, the derived root traits can still inform on root ability to access and acquire water and nutrients through root angle and depth (Rezzouk et al., 2022; York et al., 2018a, 2018b), soil exploration potential through total root length (Armengaud, 2009; He et al., 2022) and roots spatial distribution by assessing roots diameter and ramification (Eissenstat, 1991; Price et al., 2002). In agreement with this, for the more yielding

conditions the crown root system assessed through shovelomics exhibited overall an enhanced superficial root development with shallower root angle spread (higher RA) across seasons and under irrigated conditions (INP and ILP), but also thinner roots (higher SRL and lower Rwidth), which may allow roots to explore the soil on deeper levels (Chapters 3 and 4). The dual root development (superficially and in depth) under irrigated conditions was reported previously in high yielding wheat cultivars (Bai et al., 2019; Rezzouk et al., 2022). Under rainfed conditions, root system exhibited a tendency for deeper rooting, as shown by the steeper root angle (lower RA) (Chapter 3), the thinner roots (higher SRL and lower Rwidth) and the decreased root ramification (lower Rcomp) despite the high root density (higher RDW) under RNP conditions (Chapter 4). A higher root density combined with thinner roots were reported as positive traits to water and nutrients capture (Kong et al., 2014; Paez-Garcia et al., 2015; Robbins and Dinneny, 2015).

Concerning soil coring derived traits, root dry weight (RDW) and root area and area/RDW were negatively associated with GY under INP conditions as well as across all growing conditions (Chapter 4). Comparable results were previously reported in wheat grown under controlled lysimeter conditions, where correlations between the aerial biomass against root biomass (root length and density) were negative, and against specific root length were positive (Elazab et al., 2016). Furthermore, in all growing conditions, root area remained rather constant across the studied soil profile, whereas Area/RDW was progressively lower down to one meter soil depth, which supports the presence of thinner roots across soil sections and suggests their functional role at capturing water from deeper levels (Chapter 4). Thinner roots in depth have been previously reported as positive traits to wheat performance under controlled conditions (Elazab et al., 2012; 2016) as well as under field conditions (Barraclough et al., 1989; Corneo et al., 2016; Peng et al., 2019; Rezzouk et al., 2022).

- Phenotyping platforms limitations

While root traits and shoot phenotyping indices often offer valuable overview on plant physiological traits, it is still important to consider the limitations of the implemented techniques. The performance of the HTPPs-derived vegetation can be mainly affected by reaching saturation level, particularly when dealing with dense canopies and/or reproductive stages, when green biomass is maximal (Chapter 2). Comparable results reported that

enhanced senescence, assessed through chlorophyll and NDVI indices, caused losses in grain yield in bread wheat genotypes under high temperatures conditions (Cao et al., 2015). Compared with techniques dealing with phenotyping crop aerial part, when considering root phenotyping, the margin of error increases while to the throughput of the implemented techniques decreases. These factors, together with the high plasticity of root system under the Mediterranean field conditions, may present a lesser inference to root architecture traits (Chapters 3 and 4). Nevertheless, combining the information derived from root phenotyping techniques and stable isotopes of the water source, even if it's less cost effective, can still provide valuable information to the functioning and therefore roots distribution across soil profiles (Chapter 4).

- Stable isotopes as potential ideotypic traits

Besides vegetation and root indices, assessing analytical traits through the stable isotope approach provides accurate information on water status, and to a lesser extent, nitrogen status, and contribute to a greater grain yield prediction. For instance, the use of carbon isotope composition ( $\delta^{13}\text{C}$ ) as an indicator to water status (Araus et al., 2003; Whalley et al., 2008) and the effective use of water (Blum, 2009) in wheat under the Mediterranean region was often reported. Comparable results integrating  $\delta^{13}\text{C}$  as a primary explicative variable to GY variability in wheat grown under Mediterranean conditions was evidenced in (Chapters 1, 2 and 4), as well as a trait negatively associated with GY in principle components analyses (PCAs) across the different evaluated growing conditions in (Chapter 1, 3 and 4).

Likewise, nitrogen (N) status can be assessed through the analyses of nitrogen concentration in different plant tissues, mainly in leaves and grains (Feng et al., 2008; Sanchez-Bragado et al., 2014; Yousfi et al., 2012), and to a lesser extent through nitrogen isotope composition ( $\delta^{15}\text{N}$ ) (Yousfi et al., 2012). Higher nitrogen concentration in leaves ( $N_{\text{leaf}}$ ) was positively correlated against canopy greenness traits (NDVI, GA and GGA) during grain filling, which support the role of  $N_{\text{leaf}}$  as a physiological stay green indicator (Chapter 2). In mature grains however, nitrogen concentration ( $N_{\text{grain}}$ ) is usually the result of the concentration effect of nitrogen in grains. Therefore, the lower the  $N_{\text{grain}}$ , the better the N partitioning during grain filling and the greater the grain yield (Chapters 1, 2, 3 and 4).

Oxygen ( $\delta^{18}\text{O}$ ) and hydrogen ( $\delta^2\text{H}$ ) isotope compositions are other phenotypical traits. In that case they inform on the source of water extracted by roots and therefore roots functioning (Barbour, 2007; Lin and Sternberg, 1993; Sanchez-Bragado et al., 2019; Wang et al., 2010), but also on water movements ( $\delta^{18}\text{O}$  and  $\delta^2\text{H}$ ) and photosynthesis metabolism ( $\delta^2\text{H}$ ) across plant tissues (Cernusak et al., 2016; Hayes, 2019; Roden et al., 2000; Sanchez-Bragado et al., 2019). In chapter 5, GY correlated negatively against  $\delta^{18}\text{O}$  and  $\delta^2\text{H}$  of the stem water under irrigated and rainfed normal planting conditions (INP and RNP), separated. Similarly, correlations between  $\delta^{18}\text{O}_{\text{stem water}}$  against CTD were negative, and against  $\delta^{13}\text{C}_{\text{grain}}$  and  $\delta^{15}\text{N}_{\text{grain}}$  positive, particularly under RNP. Moreover, lower  $\delta^{18}\text{O}_{\text{stem water}}$  and  $\delta^2\text{H}_{\text{stem water}}$  were associated with steeper root angle (lower RA) and thinner roots in the topsoil (lower Rwidth) as well as across soil sections (Area/RDW) under INP conditions; likewise, lower  $\delta^{18}\text{O}_{\text{stem water}}$  was associated with higher root length (Ldist) in the topsoil and root area at 50-75 cm soil depth under RNP conditions (Chapter 4), suggesting therefore the presence of deeper root development promoting water and nutrients capturing from deeper soil sections under both growing conditions. These results also support the potential use of stem water  $\delta^{18}\text{O}$  and  $\delta^2\text{H}$  isotope compositions as a phenotyping approach to select for ideotypic traits associated with root water uptake in breeding programs, particularly under rainfed conditions. This conclusion was further supported by the positioning of  $\delta^{18}\text{O}_{\text{stem water}}$  in opposite direction from GY in PCA analysis under RNP conditions (Chapter 3) as well as under the different season-specific growing conditions (Chapter 4), and in agreement with previous studies highlighting the usefulness of  $\delta^{18}\text{O}$  and  $\delta^2\text{H}$  at inferring the source of water extracted by roots under field conditions (Wang et al., 2010).

Besides the water source, understanding the physiological processes through which the water extracted by roots undergoes from source to sink organs is of a paramount importance. To this end,  $\delta^{18}\text{O}$  and  $\delta^2\text{H}$  have been used in dual-isotope labeling method as artificially enriched tracers (Bachmann et al., 2015; Kagawa, 2020; Sternberg et al., 1989) under different VPD conditions to approach photosynthetic and transpirative gas exchange and the level of photosynthetic autotrophy (Cernusak et al., 2016; Roden et al., 2000). Therefore,  $\delta^{18}\text{O}$  and  $\delta^2\text{H}$  in water tissues were both enriched with the heavier isotopes (positive values) when transported from the stem to the transpiring tissues (flag leaf and ears). Furthermore, the positive relationship shown between  $\delta^{18}\text{O}$  and  $\delta^2\text{H}$  in the flag leaf and the grain, under



combined and separated VPD conditions, and under control treatment better than under labeled treatment, indicates the presence of a shared fractionation pattern in these isotopes triggered by evaporation processes (Chapter 5). Similar findings were documented previously on the similar isotopic fractionation of  $\delta^{18}\text{O}$  and  $\delta^2\text{H}$  in water of leaves and grains (Cernusak et al., 2016). In non-transpiring tissues (stem and peduncle),  $\delta^{18}\text{O}$  and  $\delta^2\text{H}$  have shown similar values and strong positive correlations when assessed in the water of the stem and the peduncle (Chapter 5). The similar isotopic signal between the stem and the peduncle further supports that fractionation in water tissues is caused mainly by environmental effects: evaporation in transpiring organs. In plants organic matter however, oxygen ( $\delta^{18}\text{O}_{\text{WSF}}$ ) and hydrogen ( $\delta^2\text{H}_{\text{DM}}$ ) measured in water soluble fraction and dry matter, respectively, have shown rather distinct fractionation patterns when assessed in the flag leaf, peduncle, glumes, awns and grains. A depleted gradient (less positive values) was observed in  $\delta^{18}\text{O}_{\text{WSF}}$  of sink organs (glumes, awns and grains) compared with the flag leaf, particularly under high VPD conditions. The sink tissues, being less transpiring than the flag leaf, were less subject to evapotranspiration factors, which explains the depleted gradient observed (Chapter 5). In the case of hydrogen,  $\delta^2\text{H}_{\text{DM}}$  was strongly depleted in the flag leaf and glumes, and somehow more enriched in grains, followed by awns (Chapter 5). These findings suggest that plant trophism is involved in the fractionation processes of  $\delta^2\text{H}$  in the organic matter. In fact, the knowledge that  $\delta^2\text{H}$  fractionation in the dry matter is associated mainly with photosynthetic processes such as electron transport within the chloroplast (Luo and Sternberg, 1991; Roden et al., 2000), and post-photosynthetic processes in biosynthesis processes involving NADP reactions, isomerases, reductases, kinases and carboxylases activities (Luo and Sternberg, 1991; Roden et al., 2000; Sanchez-Bragado et al., 2019; Yakir, 1992) has been widely documented. Furthermore, our study suggests that in addition to the flag leaf, glumes can be viewed as autotrophic tissues of the same importance as leaves. The even more depleted values in  $\delta^2\text{H}_{\text{DM}}$  signal observed in glumes under both high and low VPD conditions, compared with leaves, can be explained by the xeromorphic anatomy and osmotic adjustment of ears to ensure better water status under drought conditions, and consequently, maintain higher photosynthetic activities and greater production, compared with the flag leaf (Araus et al., 1993; Tambussi et al., 2005). As for awns and grains, and only by observing the  $\delta^2\text{H}_{\text{DM}}$  values under different VPD conditions which were enriched, awns appear to have a mixotrophic to a

heterotrophic metabolism which interferes with  $\delta^2\text{H}_{\text{DM}}$  isotopic signature, while grains show a heterotrophic metabolism (Chapter 5).

### ***Combining ideotypic characteristics in wheat genotypes under Mediterranean conditions***

The variation observed for traits in genotypes as a response to the different environmental cues presented as the combinations of season x crop management practices, offers an opportunity to improve further grain yield, particularly under optimal conditions in the Mediterranean region (Ullah et al., 2019). Traits associated with optimal phenology, greener status and improved root system that allows water and nutrients capturing under Mediterranean environments are often desirable to design high yielding Mediterranean-resilient cultivars (Devasirvatham et al., 2016; Rybka and Nita, 2015). Identifying how these traits respond to different scenarios within the Mediterranean region would facilitate selection in target environments in breeding programs.

- Under optimized conditions

Irrigation and nitrogen supply are often characteristics of an optimized environment under the Mediterranean region. Under these optimal management practices, an extended anthesis and maturity periods, together with greener leaves at grain filling, taller plants, higher thousand grain weight and optimal grain size were proposed before as potential traits to achieve high grain weight and subsequently high grain yield in wheat (Reynolds et al., 2007; Reynolds and Trethowan, 2007; Semenov and Stratonovitch, 2013; Ullah et al., 2019). In accordance with these studies, a higher growth (taller plants and/or higher NDVI) was achieved under INP conditions together with higher water status as shown by higher CTD and lower  $\delta^{13}\text{C}_{\text{grain}}$  in combined (Chapter 3) and separated seasons (Chapter 4). In addition, the high yielding genotypes exhibited shorter days to heading (DTH) and higher ear density (ED), thousand grain weight (TGW) and harvest index (HI) (Chapter 3). As for the belowground part, the best yielding genotypes exhibited a shallow root angle (higher RA) in the topsoil with more superficial water extracted (higher  $\delta^{18}\text{O}_{\text{stem}}$ ) (Chapter 3). However and in Chapter 4, the high yielding genotypes have shown shallower root angle (higher RA), with lesser root density (lower RDW and Rcomp), albeit thinner roots (higher SRL and lower Rwidth) when evaluating INP across combined seasons. By contrast, when evaluating genotypic performance per

season, higher yielding genotypes exhibited steeper root angle (lower RA) in the topsoil with deeper water extracted (lower  $\delta^{18}\text{O}_{\text{stem}}$ ), exhibiting therefore a dual root growth (superficially and deeper) across the soil profile. In fact, a root system characterized with few axial roots of varied angles, with long and dense root hair and responsive lateral roots within the topsoil was previously reported as a root ideotype under irrigated systems in arid soils (Schmidt and Gaudin, 2017), while the root growth duality (horizontally and vertically) has been reported under irrigated normal planting conditions (Bai et al., 2019).

- Under high temperatures

When addressing high growing temperatures conditions, phenology becomes the primary key for a better adaptation to drought conditions. Escaping drought through shorter days to flowering is a common strategy adopted by wheat to secure high yields (Devasirvatham et al., 2016; Shavrukov et al., 2017). In addition to phenology, maintaining longer stay green status through grain filling allows an extended photosynthesis activities, which contributes into achieving higher harvest index and higher productivity (Semenov et al., 2014; Stratonovitch and Semenov, 2015; Ullah et al., 2019). Herein, during the dry season (2018-2019), the highest yielding genotypes exhibited shorter days to heading, limited growth (lower NDVI) and higher protective pigment content (higher flavonoids), together with higher ear density and TGW. In terms of roots, root architecture was somehow shallow, roots were thinner (higher SRL) and the water extracted was more superficial (higher  $\delta^{18}\text{O}_{\text{stem}}$ ) indicating that roots were active superficially (Chapter 3). During milder seasons, high yielding was associated with higher growth (higher PH and NDVI) and better water (higher CTD and lower  $\delta^{13}\text{C}_{\text{grain}}$ ) and nitrogen status (somehow higher NBI and  $\delta^{15}\text{N}_{\text{grain}}$ ) (Chapters 3 and 4), which contributed to higher ED and harvest index, and ultimately higher GY. Furthermore, roots in high yielding genotypes exhibited a rather dual root development. root growth was shallow (higher RA), roots were thinner (higher SRL and Rwidth) and water extracted was deeper (lower  $\delta^{18}\text{O}_{\text{stem}}$  and  $\delta^2\text{H}_{\text{stem}}$ ) (Chapters 3 and 4). Pinto and Reynolds (2015) have reported before the association between deep rooting and cooling canopies under heat stress (Pinto and Reynolds, 2015). Presumably, the higher nitrogen status observed under the mild seasons was the consequence of a higher stay green status (Joshi et al., 2007; York et al., 2018b), which allowed promoting deep rooting growth to ensure higher water status under elevated temperatures (Christopher et al., 2008).

- Under rainfed conditions

The best yielding genotypes under RNP conditions exhibited greater nitrogen assimilation (higher NBI and  $\delta^{15}\text{N}_{\text{grain}}$ ) and higher flavonoid content (Chapter 3), higher aerial growth (taller plants and higher NDVI) and higher water status (higher CTD and lower  $\delta^{13}\text{C}_{\text{grain}}$ ) (Chapter 2 and 3). In terms of phenology, a longer crop duration was associated with higher yields under humid conditions (2017-2018) (Chapter 1). In contrast, under severe drought conditions as presented by the season (2018-2019), the best yielding genotypes exhibited shorter phenological durations, mainly days until flowering time (Chapters 1 and 3). Regarding the root system, roots were overall thinner (higher SRL) (Chapter 3) with a shallower development (higher RDW and RA) albeit lower root number (lower Rcomp) when evaluating the crop across combined seasons (Chapter 4). In fact, higher density combined with thinner roots were reported before as positive traits to water and nutrients capturing (Kong et al., 2014). Moreover, deep rooting is often a valuable trait to improve crops accessibility to water and nutrient resources. An ideotypic root system would be a combination of a steeper root angle and deeper root growth, with thick primary and seminal roots and few lateral roots (Lynch, 2013; Schmidt and Gaudin, 2017). In agreement with this, in separate seasons, root system exhibited consistently lower root biomass (lower RDW), steeper root angle lower (RA), a tendency to higher root depth (higher Ndepth) (Chapter 4) together with deeper water extracted (lower  $\delta^{18}\text{O}_{\text{stem}}$  and  $\delta^2\text{H}_{\text{stem}}$ ) (Chapters 3 and 4), which supports the deep rooting strategy under rainfed conditions.

- Under rainfed and low N conditions

When grown under rainfed conditions and limited nitrogen supply, the highest yielding genotypes exhibited overall a higher growth (taller plants), better water status (higher CTD and lower  $\delta^{13}\text{C}_{\text{grain}}$ ) but also higher nitrogen status (higher  $\delta^{15}\text{N}_{\text{grain}}$ ). Moreover, the root system associated with these best yielding genotypes exhibited somewhat higher root biomass (higher RDW and MedR) with deeper water extracted (lower  $\delta^{18}\text{O}_{\text{stem}}$  and  $\delta^2\text{H}_{\text{stem}}$ ), suggesting therefore a somewhat dual root system which involves shallow and deeper roots, even though the rooting system is less developed than when under irrigated conditions (Chapter 4). Furthermore, the observed optimized nitrogen status in our study can be the consequence of a higher nitrogen assimilation, supported by the deeper roots, capturing water and nutrients,

together with an increased uptake of organic nitrogen as an alternative to cover an increased plants needs in nitrogen (Sanchez-Bragado et al., 2017; Serret et al., 2008; Yousfi et al., 2012, 2009).



## **GENERAL CONCLUSIONS**



## GENERAL CONCLUSIONS

The interplay between interannual variability, management practices and genotypic effects in determining grain yield when dealing with wheat grown under the Mediterranean climate is evident. Identifying ideotypic traits that hold the potential for better adaptation to the environmental cues of the Mediterranean is of a paramount importance in order to tailor high yielding and climate resilient wheat cultivars. To achieve this, implementing phenotyping techniques that are amenable to assess these traits and potentially predict grain yield is necessary.

### *The Mediterranean region: challenges and potentiality*

- Nitrogen fertilization is key management practice to maximize grain yield and grain quality. However, its application for field crops, such as wheat, under Mediterranean conditions must be rationalized in the context of the environmental conditions and most importantly water availability.
- Northern and southern European genotypes have shown to possess candidate traits that give further insights into the strategies that crop breeders use to adapt wheat to drought through manipulating the relative duration of the different phenological stages.
- The yield gap among the top winter wheat cultivars originating from different regions was minor when grown under Mediterranean conditions, which suggests that selection for the high-yielding conditions of central and northern Europe may deliver genetic increases under Mediterranean water stress conditions.
- Regarding genotypes attitude, while winter genotypes were shown vulnerable to increased temperatures (i.e., late planting) due to their vernalization needs, facultative genotypes have shown comparable performance regardless of the planting date. The study stresses the potential adaptive ability of facultative genotypes that can contribute to more stable yields under Mediterranean condition.

### *Ideotypic traits for better adaptation to the Mediterranean climate*

- Water status in crops is crucial for optimizing grain yield production under Mediterranean conditions. The use of stable isotopes (mainly grain carbon " $\delta^{13}\text{C}_{\text{grain}}$ ")



and stem water oxygen “ $\delta^{18}\text{O}_{\text{stem}}$ ” isotope compositions) as a phenotyping approach to assess water status, together with the assessment of canopy temperature and root performance, proved to be efficient to identify the source of water extracted ( $\delta^{18}\text{O}_{\text{stem}}$  and root traits) and assess yield performance ( $\delta^{13}\text{C}_{\text{grain}}$  and to a lesser extend CTD).

- Phenology is a trait directly associated with genotypic performance. Determining an optimal phenological adaptation is key to achieve high yielding under Mediterranean conditions. Depending on the prevalence of wet or dry seasons, a longer stem elongation to anthesis stage may be an approach to adapt to wet seasons. On the other hand, a drought escape strategy (early anthesis), combined with a longer reproductive phase, may be the alternative for an efficient response to dry seasons.
- Vegetation indices (VIs) are non-invasive, rapid and cost-effective phenotyping tools to assess differences in wheat genotypes performance. These VIs allow the assessment of different crucial growth traits mainly the stay green status, which plays a clear role in plant productivity, stress tolerance and delayed senescence. Overall, VIs performed better in assessing yield differences under normal planting than late planting, and during grain filling than heading.
- Root phenotyping techniques under field conditions are considered laborious, invasive and cost-ineffective. Nevertheless, the implementation of such techniques in the topsoil (shovelomics) and across the soil profile (soil coring) allows the extraction of valuable information on roots morphology, distribution and functionality belowground. Overall, genotypes under irrigated conditions exhibited dual root growth, with steeper angle and deeper and thinner root development regardless of the planting date. Whereas under rainfed conditions, genotypes exhibited deeper albeit less developed root growth, with tendencies to grow superficially under low nitrogen conditions.
- The use of  $\delta^2\text{H}$  and  $\delta^{18}\text{O}$  stable isotopes under contrasting VPD conditions revealed valuable information on the oxygen and hydrogen fractionation patterns across plant tissues. In plant water, both  $\delta^2\text{H}$  and  $\delta^{18}\text{O}$  shared the same source of variation (evaporation processes) and were more enriched in autotrophic than heterotrophic tissues. In organic matter,  $\delta^2\text{H}$  fractionation patterns appear to be affected by plant trophism. Autotrophic tissues (leaves and glumes) get depleted in  $\delta^2\text{H}$ , whereas mixotrophic (awns) and heterotrophic (grains) tissues get enriched in  $\delta^2\text{H}$ .

*Phenotyping techniques: limitations and recommendations*

- Whereas vegetation indices rely on the assessment of spectral reflectance in plants, miscellaneous factors can limit the performance of these indices particularly around flowering time, for instance, the sunlight conditions, the saturation level of the sensor or the representativeness of the plot area assessed at ground. Combining VIs with analytical traits such as  $\delta^{13}\text{C}$  or N concentration of mature kernels can improve significantly yield assessment, but their implicit limitation is that these traits are evaluated in mature grains.
- The intrinsic limitation of physiological traits such as carbon isotope composition and  $N_{\text{grain}}$  is that they are assessed at maturity, which prevent their use predict yield before the crop cycle ends.
- Root phenotyping can be challenging due to the tedious process in extracting roots and the high margin of error that comes with, but also because of the inevitable broad plasticity of roots to the environment. Combining  $\delta^{18}\text{O}$  and  $\delta^2\text{H}$  of stem water as a promising functional phenotypic approach to root traits may provide better understanding to roots responsiveness to their environment and propose candidate traits that can contribute to tailoring climate resilient and high yielding cultivars under Mediterranean conditions.





## **RESUMEN GENERAL DE LA TESIS**



## RESUMEN GENERAL DE LA TESIS

El trigo es un cultivo dominante en el mundo. Su importancia cultural y económica se destaca principalmente en la región Mediterránea, particularmente por lo que se refiere al trigo duro. Sin embargo, la producción del trigo está sujeta con frecuencia a diferentes factores ambientales tal como la variabilidad interanual de las precipitaciones y las temperaturas, lo que se traduce en una escasez de agua. Además, diversos modelos climáticos pronostican que estos eventos ambientales van a empeorar más en el futuro cercano, por lo tanto, desarrollar nuevos cultivares de trigo que muestran una adaptación a la sequía y elevadas temperaturas y que mantengan rendimientos altos en condiciones de cultivo Mediterráneas, permanece en el foco principal de atención de los mejoradores y fisiólogos vegetales. Con este fin, el objetivo principal de la presente tesis ha sido identificar las características ideotípicas de los cultivares de trigo harinero y duro crecidos en diferentes condiciones Mediterráneas. Para tal fin, se implementó un conjunto de plataformas de fenotipado con el objetivo de evaluar las características de biomasa aérea mediante técnicas de teledetección remota y próxima, y las características de raíces empleando técnicas de fenotipado para su extracción de raíces. Además, se midieron los isotopos estables en diferentes partes de la planta para evaluar tanto el estado hídrico (composición isotópica de carbono) y de nitrógeno (composición isotópica de nitrógeno) del cultivo, como el funcionamiento de las raíces para extraer el agua (composiciones isotópicas de oxígeno e hidrogeno). Los parámetros que se deducen de estas técnicas de fenotipados se combinaron con aquellos de crecimiento (fenología, biomasa y altura de planta) y de los componentes del rendimiento para identificar unas características ideotípicas con alta capacidad de adaptarse a los escenarios Mediterráneos que contribuyan a desarrollar cultivares con alto rendimiento y que estén mejor adaptados a los retos climáticos futuros. En general, la fenología tuvo un papel evidente frente a la adaptación ambiental, además, dependiendo de la temporada de cultivo, los genotipos que rindieron mejor mostraron duraciones de fenología más extendidos durante temporadas húmedas, en cambio, durante temporadas secas, los genotipos con el rendimiento más alto mostraron unas duraciones de días a floración más cortas, seguidas por una duración de llenado de grano más extendida. Además, los modelos de predicción integraron el estado hídrico (a través de la composición isotópica de carbono ( $\delta^{13}\text{C}$ ) y la temperatura del dosel vegetal (CTD)) como el factor principal afectando al rendimiento final, seguido por las características de las raíces y el

estado de nitrógeno. Los mejores genotipos mostraron menos días entre la siembra al espigado, con un periodo de llenado de granos más largo, y se asociaron a mejores estados hídrico (menor  $\delta^{13}\text{C}$  y mayor CTD) y nitrogenado (mayor altura de plantas y biomasa), asociados a raíces más profundas (menor  $\delta^{18}\text{O}$  y  $\delta^2\text{H}$ ), lo que ha contribuido en un mejor desarrollo de la parte aérea a través de proporcionar mejor extracción de recursos hídricos y de nutrientes. Como consecuencia, estos genotipos mostraron una senescencia retrasada (mejor estado stay green), mayor biomasa aérea y crecimiento y por lo tanto mejores componentes de rendimiento y productividad de granos. Además, las características de las raíces en la capa superficial del suelo han sido afectadas por el manejo de cultivos y variabilidad estacional, debido a la alta plasticidad de este órgano, tal como se ha mostrado con el ángulo de la raíz. Aún así, se puede concluir que, bajo condiciones de riego, los genotipos con mejor rendimiento mostraron un desarrollo de raíz a la vez superficial y más profundo, con raíces más finas para explorar mayor espacio de suelo y extraer agua y nutrientes de forma más eficiente. Sin embargo, bajo condiciones de sequía, los genotipos con mejor rendimiento mostraron ángulos radiculares más cerrados, con raíces más finas lo que sugiere una tendencia a extraer el agua de secciones de suelo más profundas. Además, el análisis de las composiciones isotópicas de oxígeno ( $\delta^{18}\text{O}$ ) e hidrógeno ( $\delta^2\text{H}$ ) en diferentes tejidos de la planta mostraron unos procesos de fraccionamiento parecidos en el agua de tejidos, debido a efectos evaporativos. En cambio, en la materia orgánica de tejidos, estos isótopos se comportaron de forma distinta. Las variaciones en la firma isotópica del oxígeno ( $\delta^{18}\text{O}$ ) quedaron afectadas por la evaporación, mientras que en la del hidrógeno ( $\delta^2\text{H}$ ), el fraccionamiento se asoció al trofismo de la planta. Finalmente, indicar que los diferentes capítulos que se exponen en esta Tesis han destacado las capacidades y las limitaciones de las técnicas de fenotipado aéreo y de raíces, a la vez que apoyan el empleo de los isótopos estables en los programas de mejora de cultivos en condiciones mediterráneas.



## **REFERENCES**





## REFERENCES

- Amani, I., Fischer, R.A., Reynolds, M.P., 1996. Canopy temperature depression association with yield of irrigated spring wheat cultivars in a hot climate. *J. Agron. Crop Sci.* 176, 119–129. <https://doi.org/10.1111/j.1439-037X.1996.tb00454.x>
- Araus, J.L., Brown, H.R., Febrero, A., Bort, J., Serret, M.D., 1993. Ear photosynthesis, carbon isotope discrimination and the contribution of respiratory CO<sub>2</sub> to differences in grain mass in durum wheat. *Plant. Cell Environ.* 16, 383–392. <https://doi.org/10.1111/j.1365-3040.1993.tb00884.x>
- Araus, J.L., Cabrera-Bosquet, L., Serret, M.D., Bort, J., Nieto-Taladriz, M.T., 2013. Combined use of  $\delta^{13}\text{C}$ ,  $\delta^{18}\text{O}$  and  $\delta^{15}\text{N}$  tracks nitrogen metabolism and genotypic adaptation of durum wheat to salinity and water deficit. *Funct. Plant Physiol.* 40, 595–608. <https://doi.org/10.1071/FP12254>
- Araus, J.L., Cairns, J.E., 2014. Field high-throughput phenotyping: the new crop breeding frontier. *Trends Plant Sci.* 19, 52–61. <https://doi.org/10.1016/j.tplants.2013.09.008>
- Araus, J.L., Kefauver, S.C., Vergara-Díaz, O., Gracia-Romero, A., Rezzouk, F.Z., Segarra, J., Buchailot, M.L., Chang-Espino, M., Vatter, T., Sanchez-Bragado, R., Fernandez-Gallego, J.A., Serret, M.D., Bort, J., 2022. Crop phenotyping in a context of global change: What to measure and how to do it. *J. Integr. Plant Biol.* 64, 592–618. <https://doi.org/10.1111/jipb.13191>
- Araus, J.L., Santiveri, P., Bosch-Serra, D., Royo, C., Romagosa, I., 1992. Carbon isotope ratios in ear parts of triticale: Influence of grain filling. *Plant Physiol.* 100, 1033–1035. <https://doi.org/10.1104/pp.100.2.1033>
- Araus, J.L., Slafer, G.A., 2011. Crop stress management and global climate change, *Crop Stress Management and Global Climate Change*. CABI. <https://doi.org/10.1079/9781845936808.0000>
- Araus, J.L., Slafer, G.A., Reynolds, M.P., Royo, C., 2002. Plant breeding and drought in C3 cereals: what should we breed for? *Ann. Bot.* 89, 925–940. <https://doi.org/10.1093/aob/mcf049>

- Araus, J.L., Villegas, D., Aparicio, N., García del Moral, L.F., El-Hani, S., Rharrabti, Y., Ferrio, J.P., Royo, C., 2003. Environmental factors determining carbon isotope discrimination and yield in durum wheat under Mediterranean conditions. *Crop Sci.* 43, 170–180. <https://doi.org/10.2135/cropsci2003.0170>
- Armengaud, P., 2009. EZ-Rhizo software: The gateway to root architecture analysis. *Plant Signal. Behav.* 4, 139–141. <https://doi.org/10.4161/psb.4.2.7763>
- Asins, M.J., Carbonell, E.A., 1989. Distribution of genetic variability in a durum wheat world collection. *Theor. Appl. Genet.* 77, 287–294. <https://doi.org/10.1007/BF00266199>
- Atkinson, J.A., Pound, M.P., Bennett, M.J., Wells, D.M., 2019. Uncovering the hidden half of plants using new advances in root phenotyping. *Curr. Opin. Biotechnol.* 55, 1–8. <https://doi.org/10.1016/j.copbio.2018.06.002>
- Bachmann, D., Gockele, A., Ravenek, J.M., Roscher, C., Strecker, T., Weigelt, A., Buchmann, N., 2015. No evidence of complementary water use along a plant species richness gradient in temperate experimental grasslands. *PLoS One* 10, 1–14. <https://doi.org/10.1371/journal.pone.0116367>
- Bai, C., Ge, Y., Ashton, R.W., Evans, J., Milne, A., Hawkesford, M.J., Whalley, W.R., Parry, M.A.J., Melichar, J., Feuerhelm, D., Basler, P.B., Bartsch, M., 2019. The relationships between seedling root screens, root growth in the field and grain yield for wheat. *Plant Soil* 440, 311–326. <https://doi.org/10.1007/s11104-019-04088-9>
- Barbour, M.M., 2007. Stable oxygen isotope composition of plant tissue: a review. *Funct. Plant Biol.* 34, 83–94. <https://doi.org/10.1071/FP06228>
- Barbour, M.M., Roden, J.S., Farquhar, G.D., Ehleringer, J.R., 2004. Expressing leaf water and cellulose oxygen isotope ratios as enrichment above source water reveals evidence of a Péclet effect. *Oecologia* 138, 426–435. <https://doi.org/10.1007/s00442-003-1449-3>
- Barraclough, P.B., Kuhlmann, H., Weir, A.H., 1989. The Effects of prolonged drought and nitrogen fertilizer on root and Shoot growth and water uptake by winter wheat. *J. Agron. Crop Sci.* 163, 352–360. <https://doi.org/10.1111/j.1439-037X.1989.tb00778.x>

- Barracough, P., Leigh, R., 1984. The growth and activity of winter wheat roots in the field: The effect of sowing date and soil type on root growth of high-yielding crops. *J. Agric. Sci.* 103, 59–74. <https://doi.org/10.1017/S002185960004332X>
- Beerling, D.J., Woodward, F.I., 1995. Leaf stable carbon isotope composition records increased water-use efficiency of C3 plants in response to atmospheric CO2 enrichment. *Funct. Ecol.* 9, 394. <https://doi.org/10.2307/2390002>
- Belgiu, M., Marshall, M., Boschetti, M., Pepe, M., Stein, A., Nelson, A., 2023. PRISMA and Sentinel-2 spectral response to the nutrient composition of grains. *Remote Sens. Environ.* 292, 113567. <https://doi.org/10.1016/j.rse.2023.113567>
- Bindi, M., Olesen, J.E., 2011. The responses of agriculture in Europe to climate change. *Reg. Environ. Chang.* 11, 151–158. <https://doi.org/10.1007/s10113-010-0173-x>
- Blum, A., 2009. Effective use of water (EUW) and not water-use efficiency (WUE) is the target of crop yield improvement under drought stress. *F. Crop. Res.* 112, 119–123. <https://doi.org/10.1016/j.fcr.2009.03.009>
- Blum, A., Mayer, J., Gozlan, G., 1982. Infrared thermal sensing of plant canopies as a screening technique for dehydration avoidance in wheat. *F. Crop. Res.* 5, 137–146. [https://doi.org/10.1016/0378-4290\(82\)90014-4](https://doi.org/10.1016/0378-4290(82)90014-4)
- Boogaard, H., Wolf, J., Supit, I., Niemeyer, S., van Ittersum, M., 2013. A regional implementation of WOFOST for calculating yield gaps of autumn-sown wheat across the European Union. *F. Crop. Res.* 143, 130–142. <https://doi.org/10.1016/j.fcr.2012.11.005>
- Bremner, J.M., 1965. Isotope-ratio analysis of nitrogen in nitrogen-15 tracer investigations. *Methods Soil Anal. Part 2 Chem. Microbiol. Prop.* 9, 1256–1286. <https://doi.org/10.2134/agronmonogr9.2.c35>
- Bucksch, A., Burrridge, J., York, L.M., Das, A., Nord, E., Weitz, J.S., Lynch, J.P., 2014. Image-based high-throughput field phenotyping of crop roots. *Plant Physiol.* 166, 470–486. <https://doi.org/10.1104/pp.114.243519>

- Canè, M.A., Maccaferri, M., Nazemi, G., Salvi, S., Francia, R., Colalongo, C., Tuberosa, R., 2014. Association mapping for root architectural traits in durum wheat seedlings as related to agronomic performance. *Mol. Breed.* 34, 1629–1645. <https://doi.org/10.1007/s11032-014-0177-1>
- Cao, X., Mondal, S., Cheng, D., Wang, C., Liu, A., Song, J., Li, H., Zhao, Z., Liu, J., 2015. Evaluation of agronomic and physiological traits associated with high temperature stress tolerance in the winter wheat cultivars. *Acta Physiol. Plant.* 37, 1–10. <https://doi.org/10.1007/s11738-015-1835-6>
- Casadesùs, J., Kaya, Y., Bort, J., Nachit, M.M., Araus, J.L., Amor, S., Ferrazzano, G., Maalouf, F., Maccaferri, M., Martos, V., Ouabbou, H., Villegas, D., 2007. Using vegetation indices derived from conventional digital cameras as selection criteria for wheat breeding in water-limited environments. *Ann. Appl. Biol.* 150, 227–236. <https://doi.org/10.1111/j.1744-7348.2007.00116.x>
- Cernusak, L.A., Barbour, M.M., Arndt, S.K., Cheesman, A.W., English, N.B., Feild, T.S., Helliker, B.R., Holloway-Phillips, M.M., Holtum, J.A.M., Kahmen, A., Mcinerney, F.A., Munksgaard, N.C., Simonin, K.A., Song, X., Stuart-Williams, H., West, J.B., Farquhar, G.D., 2016. Stable isotopes in leaf water of terrestrial plants. *Plant Cell Environ.* 39, 1087–1102. <https://doi.org/10.1111/pce.12703>
- Cerovic, Z.G., Masdoumier, G., Ghazlen, N. Ben, Latouche, G., 2012. A new optical leaf-clip meter for simultaneous non-destructive assessment of leaf chlorophyll and epidermal flavonoids. *Physiol. Plant.* 146, 251–260. <https://doi.org/10.1111/j.1399-3054.2012.01639.x>
- Chairi, F., Aparicio, N., Serret, M.D., Araus, J.L., 2020a. Breeding effects on the genotype × environment interaction for yield of durum wheat grown after the green revolution: the case of Spain. *Crop J.* 8, 623–634. <https://doi.org/10.1016/j.cj.2020.01.005>
- Chairi, F., Sanchez-Bragado, R., Serret, M.D., Aparicio, N., Nieto-Taladriz, M.T., Luis Araus, J., 2020b. Agronomic and physiological traits related to the genetic advance of semi-dwarf durum wheat: the case of Spain. *Plant Sci.* 295, 1–14. <https://doi.org/10.1016/j.plantsci.2019.110210>

- Chairi, F., Vergara-Diaz, O., Vatter, T., Aparicio, N., Nieto-Taladriz, M.T., Kefauver, S.C., Bort, J., Serret, M.D., Araus, J.L., 2018. Post-green revolution genetic advance in durum wheat: The case of Spain. *F. Crop. Res.* 228, 158–169. <https://doi.org/10.1016/j.fcr.2018.09.003>
- Chen, X., Ding, Q., Błaszkiwicz, Z., Sun, J., Sun, Q., He, R., Li, Y., 2017. Phenotyping for the dynamics of field wheat root system architecture. *Sci. Rep.* 7, 1–11. <https://doi.org/10.1038/srep37649>
- Christopher, J.T., Christopher, M.J., Borrell, A.K., Fletcher, S., Chenu, K., 2016. Stay-green traits to improve wheat adaptation in well-watered and water-limited environments. *J. Exp. Bot.* 67, 5159–5172. <https://doi.org/10.1093/jxb/erw276>
- Christopher, J.T., Manschadi, A.M., Hammer, G.L., Borrell, A.K., 2008. Developmental and physiological traits associated with high yield and stay-green phenotype in wheat. *Aust. J. Agric. Res.* 59, 354–364. <https://doi.org/10.1071/AR07193>
- Christopher, J.T., Veyradier, M., Borrell, A.K., Harvey, G., Fletcher, S., Chenu, K., 2014. Phenotyping novel stay-green traits to capture genetic variation in senescence dynamics. *Funct. Plant Biol.* 41, 1035–1048. <https://doi.org/10.1071/FP14052>
- Clark, R.T., MacCurdy, R.B., Jung, J.K., Shaff, J.E., McCouch, S.R., Aneshansley, D.J., Kochian, L. V., 2011. Three-dimensional root phenotyping with a novel imaging and software platform. *Plant Physiol.* 156, 455–465. <https://doi.org/10.1104/pp.110.169102>
- Condon, A.G., 2020. Drying times: Plant traits to improve crop water use efficiency and yield. *J. Exp. Bot.* 71, 2239–2252. <https://doi.org/10.1093/jxb/eraa002>
- Condon, A.G., Richards, R.A., Farquhar, G.D., 1992. The effect of variation in soil water availability, vapour pressure deficit and nitrogen nutrition on carbon isotope discrimination in wheat. *Aust. J. Agric. Res.* 43, 935–947. <https://doi.org/10.1071/AR9920935>
- Corneo, P.E., Suenaga, H., Kertesz, M.A., Dijkstra, F.A., 2016. Effect of twenty four wheat genotypes on soil biochemical and microbial properties. *Plant Soil* 404, 141–155. <https://doi.org/10.1007/s11104-016-2833-1>

- Craig, H., 1954. Carbon-13 variations in sequoia rings and the atmosphere. *Science*. 119, 141–143. <https://doi.org/10.1126/science.119.3083.141>
- Dansgaard, W., 1964. Stable isotopes in precipitation. *Tellus* 16, 436–468. <https://doi.org/10.3402/tellusa.v16i4.8993>
- DeNiro, M.J., Epstein, S., 1979. Relationship between the oxygen Isotope ratios of terrestrial. *Science*. 204, 51–53. <https://doi.org/10.1126/science.204.4388.51>
- De Vita, P., Nicosia, O.L.D., Nigro, F., Platani, C., Riefolo, C., Di Fonzo, N., Cattivelli, L., 2007. Breeding progress in morpho-physiological, agronomical and qualitative traits of durum wheat cultivars released in Italy during the 20th century. *Eur. J. Agron.* 26, 39–53. <https://doi.org/10.1016/j.eja.2006.08.009>
- Devasirvatham, V., Tan, D.K.Y., Trethowan, R.T., 2016. Breeding strategies for enhanced plant tolerance to heat stress, in: Al-Khayri, J.M., Jain, S.M., Johnson, D. V. (Eds.), *Advances in Plant Breeding Strategies: Agronomic, Abiotic and Biotic Stress Traits*. Springer International Publishing, pp. 477–513. [https://doi.org/10.1007/978-3-319-22518-0\\_15](https://doi.org/10.1007/978-3-319-22518-0_15)
- Eissenstat, D.M., 1991. On the relationship between specific root length and the rate of root proliferation: a field study using citrus rootstocks. *New Phytol.* 118, 63–68. <https://doi.org/10.1111/j.1469-8137.1991.tb00565.x>
- Elazab, A., Bort, J., Zhou, B., Serret, M.D., Nieto-Taladriz, M.T., Araus, J.L., 2015. The combined use of vegetation indices and stable isotopes to predict durum wheat grain yield under contrasting water conditions. *Agric. Water Manag.* 158, 196–208. <https://doi.org/10.1016/j.agwat.2015.05.003>
- Elazab, A., Molero, G., Serret, M.D., Araus, J.L., 2012. Root traits and  $\delta^{13}\text{C}$  and  $\delta^{18}\text{O}$  of durum wheat under different water regimes. *Funct. Plant Biol.* 39, 379–393. <https://doi.org/http://dx.doi.org/10.1071/FP11237>
- Elazab, A., Ordóñez, R.A., Savin, R., Slafer, G.A., Araus, J.L., 2016. Detecting interactive effects of N fertilization and heat stress on maize productivity by remote sensing techniques. *Eur. J. Agron.* 73, 11–24. <https://doi.org/10.1016/j.eja.2015.11.010>

- Elazab, Abdelhalim, Serret, M.D., Araus, J.L., 2016. Interactive effect of water and nitrogen regimes on plant growth, root traits and water status of old and modern durum wheat genotypes. *Planta* 244, 125–144. <https://doi.org/10.1007/s00425-016-2500-z>
- Epstein, S., Thompson, P., Yapp, C., 1977. Oxygen and hydrogen isotopic ratios in plant cellulose. *Science*. 198, 1209–1215. <https://doi.org/10.1126/science.198.4323.1209>
- Estep, M.F., Hoering, T.C., 1981. Stable hydrogen isotope fractionations during autotrophic and mixotrophic growth of microalgae. *Plant Physiol.* 67, 474–477. <https://doi.org/10.1104/pp.67.3.474>
- Fakhet, D., Morales, F., Jauregui, I., Erice, G., Aparicio-Tejo, P.M., González-Murua, C., Aroca, R., Irigoyen, J.J., Aranjuelo, I., 2021. Short-term exposure to high atmospheric vapor pressure deficit (VPD) severely impacts durum wheat carbon and nitrogen metabolism in the absence of Eeaphic water stress. *Plants* 1–16. <https://doi.org/https://doi.org/10.3390/plants10010120>
- Farquhar, G.D., O’Leary, M.H., Berry, J.A., 1982. On the relationship between carbon isotope discrimination and the intercellular carbon dioxide concentration in leaves. *Aust. J. Plant Physiol.* 9, 121–137. <https://doi.org/10.1071/PP9820121>
- Farquhar, Graham D., Lloyd, J., 1993. Carbon and oxygen isotope effects in the exchange of carbon dioxide between terrestrial plants and the atmosphere, in: Ehrlinger, J.R., Hall, A.E., Farquhar, G.D. (Eds.), *Stable isotopes and plant carbon-water relations*. Academic Press, Inc., pp. 47–70. <https://doi.org/10.1016/C2009-0-03312-1>
- Feng, W., Yao, X., Zhu, Y., Tian, Y.C., Cao, W.X., 2008. Monitoring leaf nitrogen status with hyperspectral reflectance in wheat. *Eur. J. Agron.* 28, 394–404. <https://doi.org/10.1016/j.eja.2007.11.005>
- Feng, X., Porporato, A., Rodriguez-Iturbe, I., 2013. Changes in rainfall seasonality in the tropics. *Nat. Clim. Chang.* 3, 811–815. <https://doi.org/10.1038/nclimate1907>
- Fertiberia, 2022. <https://www.fertiberia.com/es/agricultura/servicios-al-agricultor/guia-delabonado/trigo> (Accessed on April 12th, 2022)



- Fischer, R.A., 2011. Wheat physiology: a review of recent developments. *Crop Pasture Sci.* 62, 95–114. <https://doi.org/10.1071/CP10344>
- Fischer, R.A., Rees, D., Sayre, K.D., Lu, Z.M., Condon, A.G., Larque Saavedra, A., 1998. Wheat yield progress associated with higher stomatal conductance and photosynthetic rate, and cooler canopies. *Crop Sci.* 38, 1467–1475. <https://doi.org/10.2135/cropsci1998.0011183X003800060011x>
- Food and agriculture organization (FAOSTAT), 2021. <https://www.fao.org/faostat/en/#data/QCL/visualize> (visited on May 17<sup>th</sup>, 2023)
- Fradgley, N., Evans, G., Biernaskie, J.M., Cockram, J., Marr, E.C., Oliver, A.G., Ober, E., Jones, H., 2020. Effects of breeding history and crop management on the root architecture of wheat. *Plant Soil* 452, 587–600. <https://doi.org/10.1007/s11104-020-04585-2>
- Gitelson, A.A., Merzlyak, M.N., 1998. Remote sensing of chlorophyll concentration in higher plant leaves. *Adv. Sp. Res.* 22, 689–692. [https://doi.org/10.1016/S0273-1177\(97\)01133-2](https://doi.org/10.1016/S0273-1177(97)01133-2)
- Gobbett, D.L., Hochman, Z., Horan, H., Navarro Garcia, J., Grassini, P., Cassman, K.G., 2017. Yield gap analysis of rainfed wheat demonstrates local to global relevance. *J. Agric. Sci.* 155, 282–299. <https://doi.org/10.1017/S0021859616000381>
- Gonfiantini, R., Gratziu, S., Tongiorgi, E., 1965. Oxygen isotopic composition of water in leaves, in: *Isotopes and Radiation in Soil-Plant Nutrition Studies*. IAEA, Vienna, pp. 405–410.
- Goulas, Y., Cerovic, Z.G., Cartelat, A., Moya, I., 2004. Dualex: a new instrument for field measurements of epidermal ultraviolet absorbance by chlorophyll fluorescence. *Appl. Opt.* 43, 4488–4496.
- Gracia-Romero, A., Kefauver, S.C., Fernandez-Gallego, J.A., Vergara-Díaz, O., Araus, J.L., 2019. UAV and ground image-based phenotyping: a proof of concept with durum wheat. *Remote Sens.* 11, 1–25. <https://doi.org/10.3390/rs11101244>
- Haboudane, D., Miller, J.R., Tremblay, N., Zarco-Tejada, P.J., Dextraze, L., 2002. Integrated narrow-band vegetation indices for prediction of crop chlorophyll content for application to

precision agriculture. *Remote Sens. Environ.* 81, 416–426. [https://doi.org/10.1016/S0034-4257\(02\)00018-4](https://doi.org/10.1016/S0034-4257(02)00018-4)

Hayes, J.M., 2019. Fractionation of carbon and hydrogen isotopes in biosynthetic processes. *Stable Isot. Geochemistry* 43, 225–277. <https://doi.org/10.1515/9781501508745-006>

He, M., Jiang, Y., Liu, L., Zhong, X., Zhao, Y., Ma, W., Tang, G., 2022. Benefits of high nitrogen fertilizer on nitrogen metabolism, nitrogen transfer rate, root system architecture and grain yield of wheat (*Triticum aestivum* L.) under water deficit at heading stage. *Acta Physiol. Plant.* 44, 1–10. <https://doi.org/10.1007/s11738-022-03460-0>

Helliker, B.R., Ehleringer, J.R., 2002. Differential  $^{18}\text{O}$  enrichment of leaf cellulose in C3 versus C4 grasses. *Funct. Plant Biol.* 29, 435–442. <https://doi.org/10.1071/PP01122>

Henderson, C.W.L., 1991. Sensitivity of eight cereal and legume species to the compaction status of deep sandy soils. *Aust. J. Exp. Agric.* 31, 347–355. <https://doi.org/10.1071/EA9910347>

Hochman, Z., Gobbett, D., Holzworth, D., McClelland, T., van Rees, H., Marinoni, O., Garcia, J.N., Horan, H., 2013. Reprint of “quantifying yield gaps in rainfed cropping systems: A case study of wheat in Australia.” *F. Crop. Res.* 143, 65–75. <https://doi.org/10.1016/j.fcr.2013.02.001>

Hoering, T., 1955. Variations of nitrogen-15 abundance in naturally occurring substances. *Science.* 122, 1233–1234. <https://doi.org/10.1126/science.122.3182.1233>

Hunt, J.R., Lilley, J.M., Trevaskis, B., Flohr, B.M., Peake, A., Fletcher, A., Zwart, A.B., Gobbett, D., Kirkegaard, J.A., 2019. Early sowing systems can boost Australian wheat yields despite recent climate change. *Nat. Clim. Chang.* 9, 244–247. <https://doi.org/10.1038/s41558-019-0417-9>

Hunt, R.E., Daughtry, C.S.T., Eitel, U H, Long, D.S., 2011. Remote sensing leaf chlorophyll content using a visible band index. *Agron. J.* 103, 1090–1099. <https://doi.org/10.2134/agronj2010.0395>

Incerti, M., O’Leary, G.J., 1990. Rooting depth of wheat in the Victorian Mallee. *Aust. J. Exp. Agric. Anim. Husb.* 30, 817–824. <https://doi.org/10.1071/EA9900817>

- Innes, P.J., Tan, D.K.Y., Van Ogtrop, F., Amthor, J.S., 2015. Effects of high-temperature episodes on wheat yields in New South Wales, Australia. *Agric. For. Meteorol.* 208, 95–107. <https://doi.org/10.1016/j.agrformet.2015.03.018>
- Iyer-Pascuzzi, A.S., Symonova, O., Mileyko, Y., Hao, Y., Belcher, H., Harer, J., Weitz, J.S., Benfey, P.N., 2010. Imaging and analysis platform for automatic phenotyping and trait ranking of plant root systems. *Plant Physiol.* 152, 1148–1157. <https://doi.org/10.1104/pp.109.150748>
- Jacobsen, S.E., Jensen, C.R., Liu, F., 2012. Improving crop production in the arid mediterranean climate. *F. Crop. Res.* 128, 34–47. <https://doi.org/10.1002/9781118517994.ch12>
- Jat, R.K., Singh, P., Jat, M.L., Dia, M., Sidhu, H.S., Jat, S.L., Bijarniya, D., Jat, H.S., Parihar, C.M., Kumar, U., Ridaura, S.L., 2018. Heat stress and yield stability of wheat genotypes under different sowing dates across agro-ecosystems in India. *F. Crop. Res.* 218, 33–50. <https://doi.org/10.1016/j.fcr.2017.12.020>
- Jauregui, I., Rothwell, S.A., Taylor, S.H., Parry, M.A.J., Carmo-Silva, E., Dodd, I.C., 2018. Whole plant chamber to examine sensitivity of cereal gas exchange to changes in evaporative demand. *Plant Methods* 14, 1–13. <https://doi.org/10.1186/s13007-018-0357-9>
- Jones, H.G., Serraj, R., Loveys, B.R., Xiong, L., Wheaton, A., Price, A.H., 2009. Thermal infrared imaging of crop canopies for the remote diagnosis and quantification of plant responses to water stress in the field. *Funct. Plant Biol.* 36, 978–989. <https://doi.org/10.1071/FP09123>
- Joshi, A.K., Kumari, M., Singh, V.P., Reddy, C.M., Kumar, S., Rane, J., Chand, R., 2007. Stay green trait: variation, inheritance and its association with spot blotch resistance in spring wheat (*Triticum aestivum* L.). *Euphytica* 153, 59–71. <https://doi.org/10.1007/s10681-006-9235-z>
- Kagawa, A., 2020. Foliar water uptake as a source of hydrogen and oxygen in plant biomass. *bioRxiv* 1–53. <https://doi.org/10.1093/treephys/tpac055>
- Kamran, A., Iqbal, M., Spaner, D., 2014. Flowering time in wheat (*Triticum aestivum* L.): A key factor for global adaptability. *Euphytica* 197, 1–26. <https://doi.org/10.1007/s10681-014-1075-7>

- Kefauver, S.C., El-Haddad, G., Vergara-Díaz, O., Araus, J.L., 2015. RGB picture vegetation indexes for high-throughput phenotyping platforms (HTPPs). *Remote Sens. Agric. Ecosyst. Hydrol.* XVII 9637, 1–9.
- Kefauver, S.C., Vicente, R., Vergara-Díaz, O., Fernandez-Gallego, J.A., Kerfal, S., Lopez, A., Melichar, J.P.E., Serret Molins, M.D., Araus, J.L., 2017. Comparative UAV and field phenotyping to assess yield and nitrogen use efficiency in hybrid and conventional barley. *Front. Plant Sci.* 8, 1–15. <https://doi.org/10.3389/fpls.2017.01733>
- Kipp, S., Mistele, B., Schmidhalter, U., 2014. Identification of stay-green and early senescence phenotypes in high-yielding winter wheat, and their relationship to grain yield and grain protein concentration using high-throughput phenotyping techniques. *Funct. Plant Biol.* 41, 227–235. <https://doi.org/10.1071/FP13221>
- Kirkegaard, J.A., Lilley, J.M., 2007. Root penetration rate - a benchmark to identify soil and plant limitations to rooting depth in wheat. *Aust. J. Exp. Agric.* 47, 590–602. <https://doi.org/10.1071/EA06071>
- Kohl, D.H., Shearer, G., 1980. Isotopic fractionation associated with symbiotic N<sub>2</sub> fixation and uptake of NO<sub>3</sub><sup>-</sup> by plants. *Plant Physiol.* 66, 51–56. <https://doi.org/10.1104/pp.66.1.51>
- Kohl, D.H., Shearer, G.B., Commoner, B., 1973. Variation of <sup>15</sup>N in corn and soil following application of fertilizer nitrogen. *soil Sci. Soc. Am. J.* 37, 1–5. <https://doi.org/10.2136/sssaj1973.03615995003700060028x>
- Kong, X., Zhang, M., De Smet, I., Ding, Z., 2014. Designer crops: optimal root system architecture for nutrient acquisition. *Trends Biotechnol.* 32, 597–598. <https://doi.org/10.1016/j.tibtech.2014.09.008>
- Li, X., Ingvordsen, C.H., Weiss, M., Rebetzke, G.J., Condon, A.G., James, R.A., Richards, R.A., 2019. Deeper roots associated with cooler canopies, higher normalized difference vegetation index, and greater yield in three wheat populations grown on stored soil water. *J. Exp. Bot.* 70, 4963–4974. <https://doi.org/10.1093/jxb/erz232>

- Lin, C., Popescu, S.C., Huang, S.C., Chang, P.T., Wen, H.L., 2015. A novel reflectance-based model for evaluating chlorophyll concentrations of fresh and water-stressed leaves. *Biogeosciences* 12, 49–66. <https://doi.org/10.5194/bg-12-49-2015>
- Lin, G., Sternberg, L.D.S.L., 1993. Hydrogen isotopic fractionation by plant roots during water uptake in coastal wetland plants, in: Ehrlinger, J.R., Hall, A.E., Farquhar, G.D. (Eds.), *Stable Isotopes and Plant Carbon-Water Relations*. Academic Press, Inc., pp. 497–510. <https://doi.org/10.1016/b978-0-08-091801-3.50041-6>
- Lobell, D.B., Burke, M.B., Tebaldi, C., Mastrandrea, M.D., Falcon, W.P., Naylor, R.L., 2008. Prioritizing climate change adaptation needs for food security in 2030. *Science*. 319, 607–610. <https://doi.org/10.1126/science.1152339>
- Lobell, D.B., Cassman, K.G., Field, C.B., 2009. Crop yield gaps: their importance, magnitudes, and causes. *Annu. Rev. Environ. Resour.* 34, 179–204. <https://doi.org/10.1146/annurev.environ.041008.093740>
- Lopes, M.S., Reynolds, M.P., 2010. Partitioning of assimilates to deeper roots is associated with cooler canopies and increased yield under drought in wheat. *Funct. Plant Biol.* 37, 147–156. <https://doi.org/https://doi.org/10.1071/FP09121>
- Lopes, M.S., Reynolds, M.P., 2012. In *Posidonia oceanica* cadmium induces changes in DNA stay-green in spring wheat can be determined by spectral reflectance measurements (normalized difference vegetation methylation and chromatin patterning index) independently from phenology. *J. Exp. Bot.* 63, 695–709. <https://doi.org/10.1093/jxb/err313>
- Loss, S.P., Siddique, K.H.M., 1994. Morphological and Physiological Traits Associated with Wheat Yield Increases in Mediterranean Environments. *Adv. Agron.* 52, 229–276. [https://doi.org/10.1016/S0065-2113\(08\)60625-2](https://doi.org/10.1016/S0065-2113(08)60625-2)
- Luo, Y., Sternberg, L., 1991. Deuterium heterogeneity in starch and cellulose nitrate of cam and C<sub>3</sub> plants. *Phytochemistry* 30, 1095–1098. [https://doi.org/10.1016/S0031-9422\(00\)95179-3](https://doi.org/10.1016/S0031-9422(00)95179-3)

- Lynch, J., 1995. Root architecture and plant productivity. *Plant Physiol.* 109, 7–13. <https://doi.org/10.1104/pp.109.1.7>
- Lynch, J.P., 2013. Steep, cheap and deep: An ideotype to optimize water and N acquisition by maize root systems. *Ann. Bot.* 112, 347–357. <https://doi.org/10.1093/aob/mcs293>
- Malamy, J.E., 2005. Intrinsic and environmental response pathways that regulate root system architecture. *Plant Cell Environ.* 67–77. <https://doi.org/10.1111/j.1365-3040.2005.01306.x>
- Martínez-Moreno, F., Solís, I., Noguero, D., Blanco, A., Özberk, İ., Nsarellah, N., Elias, E., Mylonas, I., Soriano, J.M., 2020. Durum wheat in the Mediterranean Rim: historical evolution and genetic resources. *Genet. Resour. Crop Evol.* 67, 1415–1436. <https://doi.org/10.1007/s10722-020-00913-8>
- Mateo, M.A., Ferrio, P., Araus, J.L., 2004. Isótopos estables en fisiología vegetal, in: Reigosa, M.J., Pedrol, N., Sánchez, A. (Eds.), *La Ecofisiología Vegetal, Una Ciencia de Síntesis*. Paraninfo, S.A., pp. 1–38.
- Mondal, S., Singh, R.P., Crossa, J., Huerta-Espino, J., Sharma, I., Chatrath, R., Singh, G.P., Sohu, V.S., Mavi, G.S., Sukaru, V.S.P., Kalappanavarg, I.K., Mishra, V.K., Hussain, M., Gautam, N.R., Uddin, J., Barma, N.C.D., Hakim, A., Joshi, A.K., 2013. Earliness in wheat: A key to adaptation under terminal and continual high temperature stress in South Asia. *F. Crop. Res.* 151, 19–26. <https://doi.org/10.1016/j.fcr.2013.06.015>
- Nielsen, D.C., Halvorson, A.D., 1991. Nitrogen fertility influence on water stress and yield of winter wheat. *Agron. J.* 83, 1065–1070. <https://doi.org/10.2134/agronj1991.00021962008300060025x>
- O’Leary, M.H., 1981. Carbon isotope fractionation in plants. *Phytochemistry* 20, 553–567. [https://doi.org/10.1016/0031-9422\(81\)85134-5](https://doi.org/10.1016/0031-9422(81)85134-5)
- Ober, E.S., Alahmad, S., Cockram, J., Forestan, C., Hickey, L.T., Kant, J., Maccaferri, M., Marr, E., Milner, M., Pinto, F., Rambla, C., Reynolds, M., Salvi, S., Sciara, G., Snowdon, R.J., Thomelin, P., Tuberosa, R., Uauy, C., Voss-Fels, K.P., Wallington, E., Watt, M., 2021. Wheat root systems as a

breeding target for climate resilience. *Theor. Appl. Genet.* 134, 1645–1662. <https://doi.org/10.1007/s00122-021-03819-w>

Ogée, J., Cuntz, M., Peylin, P., Bariac, T., 2007. Non-steady-state, non-uniform transpiration rate and leaf anatomy effects on the progressive stable isotope enrichment of leaf water along monocot leaves. *Plant, Cell Environ.* 30, 367–387. <https://doi.org/10.1111/j.1365-3040.2006.01621.x>

Padovan, G., Martre, P., Semenov, M.A., Masoni, A., Bregaglio, S., Ventrella, D., Lorite, I.J., Santos, C., Bindi, M., Ferrise, R., Dibari, C., 2020. Understanding effects of genotype × environment × sowing window interactions for durum wheat in the Mediterranean basin. *F. Crop. Res.* 259, 1–15. <https://doi.org/10.1016/j.fcr.2020.107969>

Paez-Garcia, A., Motes, C.M., Scheible, W.R., Chen, R., Blancaflor, E.B., Monteros, M.J., 2015. Root traits and phenotyping strategies for plant improvement. *Plants* 4, 334–355. <https://doi.org/10.3390/plants4020334>

Park, R., Epstein, S., 1960. Carbon isotope fractionation during photosynthesis. *Geochim. Cosmochim. Acta* 21, 110–120. [https://doi.org/10.1016/S0016-7037\(60\)80006-3](https://doi.org/10.1016/S0016-7037(60)80006-3)

Pask, A., Pietragalla, J., Mullan, D., 2012. Physiological breeding II: a field guide to wheat phenotyping, *Climate Change 2013 - The Physical Science Basis*.

Paymard, P., Bannayan, M., Haghighi, R.S., 2018. Analysis of the climate change effect on wheat production systems and investigate the potential of management strategies. *Nat. Hazards* 91, 1237–1255. <https://doi.org/10.1007/s11069-018-3180-8>

Peng, B., Liu, X., Dong, X., Xue, Q., Neely, C.B., Marek, T., Ibrahim, A.M.H., Zhang, G., Leskovar, D.I., Rudd, J.C., 2019. Root morphological traits of winter wheat under contrasting environments. *J. Agron. Crop Sci.* 205, 571–585. <https://doi.org/10.1111/jac.12360>

Pieruschka, R., Schurr, U., 2019. Plant Phenotyping: Past, Present, and Future. *Plant Phenomics* 2019, 1–6. <https://doi.org/10.34133/2019/7507131>

- Pinto, R.S., Molero, G., Reynolds, M.P., 2017. Identification of heat tolerant wheat lines showing genetic variation in leaf respiration and other physiological traits. *Euphytica* 213, 1–15. <https://doi.org/10.1007/s10681-017-1858-8>
- Pinto, R.S., Reynolds, M.P., 2015. Common genetic basis for canopy temperature depression under heat and drought stress associated with optimized root distribution in bread wheat. *Theor. Appl. Genet.* 128, 575–585. <https://doi.org/10.1007/s00122-015-2453-9>
- Polley, H.W., Johnson, H.B., Marinot, B.D., Mayeux, H.S., 1993. Increase in C3 plant water-use efficiency and biomass over Glacial to present CO<sub>2</sub> concentrations. *Nature* 361, 61–64. <https://doi.org/10.1038/361061a0>
- Price, A.H., Steele, K.A., Moore, B.J., Jones, R.G.W., 2002. Upland rice grown in soil-filled chambers and exposed to contrasting water-deficit regimes. II. Mapping quantitative trait loci for root morphology and distribution. *F. Crop. Res.* 76, 25–43. [https://doi.org/10.1016/S0378-4290\(02\)00010-2](https://doi.org/10.1016/S0378-4290(02)00010-2)
- Rashid, M.A., Andersen, M.N., Wollenweber, B., Zhang, X., Olesen, J.E., 2018. Acclimation to higher VPD and temperature minimized negative effects on assimilation and grain yield of wheat. *Agric. For. Meteorol.* 248, 119–129. <https://doi.org/10.1016/j.agrformet.2017.09.018>
- Ray, D.K., Gerber, J.S., Macdonald, G.K., West, P.C., 2015. Climate variation explains a third of global crop yield variability. *Nat. Commun.* 6, 1–9. <https://doi.org/10.1038/ncomms6989>
- Reynolds, M., Dreccer, F., Trethowan, R., 2007. Drought-adaptive traits derived from wheat wild relatives and landraces. *J. Exp. Bot.* 58, 177–186. <https://doi.org/10.1093/jxb/erl250>
- Reynolds, M., Pask, A., Mullan, D., 2012. *Physiological breeding I: Interdisciplinary Approaches to Improve Crop Adaptation*. Mexico.
- Reynolds, M.P., Trethowan, R.M., 2007. Physiological interventions in breeding for adaptation to abiotic stress, in: Spiertz, J.H.J., Struik, P.C., van Laar, H.H. (Eds.), *Scale and Complexity in Plant Systems Research*. pp. 129–146. [https://doi.org/10.1007/1-4020-5906-x\\_11](https://doi.org/10.1007/1-4020-5906-x_11)
- Rezzouk, F.Z., Gracia-Romero, A., Kefauver, S.C., Gutiérrez, N.A., Aranjuelo, I., Serret, M.D., Araus, J.L., 2020. Remote sensing techniques and stable isotopes as phenotyping tools to



- assess wheat yield performance: effects of growing temperature and vernalization. *Plant Sci.* 295, 1–16. <https://doi.org/10.1016/j.plantsci.2019.110281>
- Rezzouk, F.Z., Gracia-Romero, A., Kefauver, S.C., Nieto-Taladriz, M.T., Serret, M.D., Araus, J.L., 2022. Durum wheat ideotypes in Mediterranean environments differing in water and temperature conditions. *Agric. Water Manag.* 259, 1–15. <https://doi.org/10.1016/j.agwat.2021.107257>
- Robbins, N.E., Dinneny, J.R., 2015. The divining root: Moisture-driven responses of roots at the micro- and macro-scale. *J. Exp. Bot.* 66, 2145–2154. <https://doi.org/10.1093/jxb/eru496>
- Roche, D., 2015. Stomatal Conductance Is Essential for Higher Yield Potential of C3 Crops. *CRC. Crit. Rev. Plant Sci.* 34, 429–453. <https://doi.org/10.1080/07352689.2015.1023677>
- Roden, J.S., Lin, G., Ehleringer, J.R., 2000. A mechanistic model for interpretation of hydrogen and oxygen isotope ratios in tree-ring cellulose. *Geochim. Cosmochim. Acta* 64, 21–35. [https://doi.org/10.1016/S0016-7037\(99\)00195-7](https://doi.org/10.1016/S0016-7037(99)00195-7)
- Royo, C., 2005. Durum wheat breeding: Current approaches and future strategies, Volume 1. Haworth press, NewYork.
- Rybka, K., Nita, Z., 2015. Physiological requirements for wheat ideotypes in response to drought threat. *Acta Physiol. Plant.* 37, 1–13. <https://doi.org/10.1007/s11738-015-1844-5>
- Sacks, W.J., Deryng, D., Foley, J.A., Ramankutty, N., 2010. Crop planting dates: an analysis of global patterns. *Glob. Ecol. Biogeogr.* 19, 607–620. <https://doi.org/10.1111/j.1466-8238.2010.00551.x>
- Sadras, V.O., Lawson, C., 2011. Genetic gain in yield and associated changes in phenotype, trait plasticity and competitive ability of South Australian wheat varieties released between 1958 and 2007. *Crop Pasture Sci.* 62, 533–549. <https://doi.org/10.1071/CP11060>
- Sadras, V.O., Slafer, G.A., 2012. Environmental modulation of yield components in cereals: heritabilities reveal a hierarchy of phenotypic plasticities. *F. Crop. Res.* 127, 215–224. <https://doi.org/10.1016/j.fcr.2011.11.014>

- Sanchez-Bragado, R., Elazab, A., Zhou, B., Serret, M.D., Bort, J., Nieto-Taladriz, M.T., Araus, J.L., 2014. Contribution of the ear and the flag leaf to grain filling in durum wheat inferred from the carbon isotope signature: Genotypic and growing conditions effects. *J. Integr. Plant Biol.* 56, 444–454. <https://doi.org/10.1111/jipb.12106>
- Sanchez-Bragado, R., Serret, M.D., Araus, J.L., 2017. The nitrogen contribution of different plant parts to wheat grains: exploring genotype, water, and nitrogen effects. *Front. Plant Sci.* 7, 1–14.
- Sanchez-Bragado, R., Serret, M.D., Marimon, R.M., Bort, J., Araus, J.L., 2019. The hydrogen isotope composition  $\delta^2\text{H}$  reflects plant performance. *Plant Physiol.* 180, 793–812. <https://doi.org/10.1104/pp.19.00238>
- Sativum, 2022. <https://www.sativum.es/web/sativum/home#queEsSativum> (Accessed on April 12th, 2022)
- Schils, R., Olesen, J.E., Kersebaum, K.C., Rijk, B., Oberforster, M., Kalyada, V., Khitrykau, M., Gobin, A., Kirchev, H., Manolova, V., Manolov, I., Trnka, M., Hlavinka, P., Paluoso, T., Peltonen-Sainio, P., Jauhiainen, L., Lorgeou, J., Marrou, H., Danalatos, N., Archontoulis, S., Fodor, N., Spink, J., Roggero, P.P., Bassu, S., Pulina, A., Seehusen, T., Uhlen, A.K., Żyłowska, K., Nieróbca, A., Kozyra, J., Silva, J.V., Maçãs, B.M., Coutinho, J., Ion, V., Takáč, J., Mínguez, M.I., Eckersten, H., Levy, L., Herrera, J.M., Hiltbrunner, J., Kryvobok, O., Kryvoshein, O., Sylvester-Bradley, R., Kindred, D., Topp, C.F.E., Boogaard, H., de Groot, H., Lesschen, J.P., van Bussel, L., Wolf, J., Zijlstra, M., van Loon, M.P., van Ittersum, M.K., 2018. Cereal yield gaps across Europe. *Eur. J. Agron.* 101, 109–120. <https://doi.org/10.1016/j.eja.2018.09.003>
- Schmidt, J.E., Gaudin, A.C.M., 2017. Toward an Integrated Root Ideotype for Irrigated Systems. *Trends Plant Sci.* 22, 433–443. <https://doi.org/10.1016/j.tplants.2017.02.001>
- Segarra, J., Buchailot, M.L., Araus, J.L., Kefauver, S.C., 2020. Remote sensing for precision agriculture: Sentinel-2 improved features and applications. *Agronomy* 10, 1–18. <https://doi.org/10.3390/agronomy10050641>

- Shearer, G., Kohl, D.H., 1978.  $^{15}\text{N}$  abundance in N-fixing and non-N-fixing plants, in: Frigerio, A. (Ed.), *Recent Developments in Mass Spectrometry in Biochemistry and Medicine*. Springer, Boston, MA., pp. 605–622. [https://doi.org/10.1007/978-1-4613-3991-5\\_51](https://doi.org/10.1007/978-1-4613-3991-5_51)
- Skendži, S., Zovko, M., Leši, V., Pajac Živkovic, I., Lemic, D., 2023. Detection and evaluation of environmental Stress in winter wheat using remote and proximal sensing methods and vegetation indices—a review. *Diversity* 15, 1–30. <https://doi.org/10.3390/d15040481>
- Semenov, M.A., Stratonovitch, P., 2013. Designing high-yielding wheat ideotypes for a changing climate. *Food Energy Secur.* 2, 185–196. <https://doi.org/10.1002/fes3.34>
- Semenov, M.A., Stratonovitch, P., Alghabari, F., Gooding, M.J., 2014. Adapting wheat in Europe for climate change. *J. Cereal Sci.* 59, 245–256. <https://doi.org/10.1016/j.jcs.2014.01.006>
- Senapati, N., Semenov, M.A., 2020. Large genetic yield potential and genetic yield gap estimated for wheat in Europe. *Glob. Food Sec.* 24, 1–9. <https://doi.org/10.1016/j.gfs.2019.100340>
- Senapati, N., Semenov, M.A., 2019. Assessing yield gap in high productive countries by designing wheat ideotypes. *Sci. Rep.* 9, 1–12. <https://doi.org/10.1038/s41598-019-40981-0>
- Serret, M.D., Ortiz-Monasterio, I., Pardo, A., Araus, J.L., 2008. The effects of urea fertilisation and genotype on yield, nitrogen use efficiency,  $\delta^{15}\text{N}$  and  $\delta^{13}\text{C}$  in wheat. *Ann. Appl. Biol.* 153, 243–257. <https://doi.org/10.1111/j.1744-7348.2008.00259.x>
- Shavrukov, Y., Kurishbayev, A., Jatayev, S., Shvidchenko, V., Zotova, L., Koekemoer, F., de Groot, S., Soole, K., Langridge, P., 2017. Early flowering as a drought escape mechanism in plants: how can it aid wheat production? *Front. Plant Sci.* 8, 1–8. <https://doi.org/10.3389/fpls.2017.01950>
- Sims, D.A., Gamon, J.A., 2003. Estimation of vegetation water content and photosynthetic tissue area from spectral reflectance: A comparison of indices based on liquid water and chlorophyll absorption features. *Remote Sens. Environ.* 84, 526–537. [https://doi.org/10.1016/S0034-4257\(02\)00151-7](https://doi.org/10.1016/S0034-4257(02)00151-7)

- Slafer, G.A., Savin, R., Sadras, V.O., 2014. Coarse and fine regulation of wheat yield components in response to genotype and environment. *F. Crop. Res.* 157, 71–83. <https://doi.org/10.1016/j.fcr.2013.12.004>
- Spano, G., Di Fonzo, N., Perrotta, C., Platani, C., Ronga, G., Lawlor, D.W., Napier, J.A., Shewry, P.R., 2003. Physiological characterization of “stay green” mutants in durum wheat. *J. Exp. Bot.* 54, 1415–1420. <https://doi.org/10.1093/jxb/erg150>
- Steinfart, U., Trevaskis, B., Fukai, S., Bell, K.L., Dreccer, M.F., 2017. Vernalisation and photoperiod sensitivity in wheat: impact on canopy development and yield components. *F. Crop. Res.* 201, 108–121. <https://doi.org/10.1016/j.fcr.2016.10.012>
- Sternberg, L., Mulkey, S.S., Wright, S.J., 1989. Ecological interpretation of leaf carbon isotope ratios: Influence of respired carbon dioxide. *Ecology* 70, 1317–1324. <https://doi.org/10.2307/1938191>
- Stratonovitch, P., Semenov, M.A., 2015. Heat tolerance around flowering in wheat identified as a key trait for increased yield potential in Europe under climate change. *J. Exp. Bot.* 66, 3599–3609. <https://doi.org/10.1093/jxb/erv070>
- Tambussi, E.A., Nogués, S., Araus, J.L., 2005. Ear of durum wheat under water stress: Water relations and photosynthetic metabolism. *Planta* 221, 446–458. <https://doi.org/10.1007/s00425-004-1455-7>
- Thapa, S., Jessup, K.E., Pradhan, G.P., Rudd, J.C., Liu, S., Mahan, J.R., Devkota, R.N., Baker, J.A., Xue, Q., 2018. Canopy temperature depression at grain filling correlates to winter wheat yield in the U.S. southern high plains. *F. Crop. Res.* 217, 11–19. <https://doi.org/10.1016/j.fcr.2017.12.005>
- Telfer, P., Edwards, J., Bennett, D., Ganesalingam, D., Able, J., Kuchel, H., 2018. A field and controlled environment evaluation of wheat (*Triticum aestivum*) adaptation to heat stress. *F. Crop. Res.* 229, 55–65. <https://doi.org/10.1016/j.fcr.2018.09.013>
- Tennant, D., 1976. Wheat root penetration and total available water on a range of soil types. *Aust. J. Exp. Agric. Anim. Husb.* 16, 570–577. <https://doi.org/10.1071/EA9760570>

- Tennant, D., Hall, D., 2001. Improving water use of annual crops and pastures—limitations and opportunities in Western Australia. *Crop pasture Sci.* 52, 171–182. <https://doi.org/10.1071/AR00005>
- The Intergovernmental panel of climate change (IPCC). 2023. <https://www.ipcc.ch/report/ar6/syr/> (visited on May 17<sup>th</sup>, 2023)
- Trevaskis, B., Bagnall, D.J., Ellis, M.H., Peacock, W.J., Dennis, E.S., 2003. MADS box genes control vernalization-induced flowering in cereals. *Proc. Natl. Acad. Sci.* 100, 13099–13104. <https://doi.org/10.1073/pnas.1635053100>
- Ullah, S., Bramley, H., Mahmood, T., Trethowan, R., 2019. A strategy of ideotype development for heat-tolerant wheat. *J. Agron. Crop Sci.* 206, 229–241. <https://doi.org/10.1111/jac.12378>
- Van Ittersum, M.K., Cassman, K.G., Grassini, P., Wolf, J., Tittone, P., Hochman, Z., 2013. Yield gap analysis with local to global relevance—a review. *F. Crop. Res.* 143, 4–17. <https://doi.org/10.1016/j.fcr.2012.09.009>
- van Oosterom, E.J., Acevedo, E., 1992. Adaptation of barley (*Hordeum vulgare* L.) to harsh Mediterranean environments - I. Morphological traits. *Euphytica* 62, 1–14. <https://doi.org/10.1007/BF00036082>
- Wada, E., Hattori, A., 1978. Nitrogen isotope effects in the assimilation of inorganic nitrogenous compounds by marine diatoms. *Geomicrobiol. J.* 1, 85–101. <https://doi.org/10.1080/01490457809377725>
- Wang, P., Song, X., Han, D., Zhang, Y., Liu, X., 2010. A study of root water uptake of crops indicated by hydrogen and oxygen stable isotopes: A case in Shanxi Province, China. *Agric. Water Manag.* 97, 475–482. <https://doi.org/10.1016/j.agwat.2009.11.008>
- Wasaya, A., Zhang, X., Fang, Q., Yan, Z., 2018. Root phenotyping for drought tolerance: A review. *Agronomy* 8, 1–19. <https://doi.org/10.3390/agronomy8110241>
- Whalley, W.R., Watts, C.W., Gregory, A.S., Mooney, S.J., Clark, L.J., Whitmore, A.P., 2008. The effect of soil strength on the yield of wheat. *Plant Soil* 306, 237–247. <https://doi.org/10.1007/s11104-008-9577-5>

- Wasson, A., Bischof, L., Zwart, A., Watt, M., 2016. A portable fluorescence spectroscopy imaging system for automated root phenotyping in soil cores in the field. *J. Exp. Bot.* 67, 1033–1043. <https://doi.org/10.1093/jxb/erv570>
- Xue, Q., Weiss, A., Arkebauer, T.J., Baenziger, P.S., 2004. Influence of soil water status and atmospheric vapor pressure deficit on leaf gas exchange in field-grown winter wheat. *Environ. Exp. Bot.* 51, 167–179. <https://doi.org/10.1016/j.envexpbot.2003.09.003>
- Yakir, D., 1992. Variations in the natural abundance of oxygen-18 and deuterium in plant carbohydrates. *Plant. Cell Environ.* 15, 1005–1020. <https://doi.org/10.1111/j.1365-3040.1992.tb01652.x>
- Yakir, D., DeNiro, M.J., 1990. Oxygen and hydrogen isotope fractionation during cellulose metabolism in *Lemna gibba* L. *Plant Physiol.* 93, 325–332. <https://doi.org/10.1104/pp.93.1.325>
- York, L.M., Slack, S., Bennett, M.J., Foulkes, J., 2018a. Wheat shovelomics II: revealing relationships between root crown traits and crop growth. *bioRxiv* 1–22. <https://doi.org/10.1101/280917>
- York, L.M., Slack, S., Bennett, M.J., Foulkes, J., 2018b. Wheat shovelomics: phenotyping roots in tillering species. *bioRxiv* 1–17. <https://doi.org/https://doi.org/10.1101/280875>
- Yousfi, S., Kellas, N., Saidi, L., Benlakehal, Z., Chaou, L., Siad, D., Herda, F., Karrou, M., Vergara, O., Gracia, A., Araus, J.L., Serret, M.D., 2016. Comparative performance of remote sensing methods in assessing wheat performance under mediterranean conditions. *Agric. Water Manag.* 164, 137–147. <https://doi.org/10.1016/j.agwat.2015.09.016>
- Yousfi, S., Serret, M.D., Araus, J.L., 2009. Shoot  $\delta^{15}\text{N}$  gives a better indication than ion concentration or  $\delta^{13}\text{C}$  of genotypic differences in the response of durum wheat to salinity. *Funct. Plant Biol.* 36, 144–155. <https://doi.org/10.1111/pce.12055>
- Yousfi, S., Serret, M.D., Márquez, A.J., Voltas, J., Araus, J.L., 2012. Combined use of  $\delta^{13}\text{C}$ ,  $\delta^{18}\text{O}$  and  $\delta^{15}\text{N}$  tracks nitrogen metabolism and genotypic adaptation of durum wheat to salinity and water deficit. *New Phytol.* 194, 230–244. <https://doi.org/10.1111/j.1469-8137.2011.04036.x>

Wasaya, A., Zhang, X., Fang, Q., Yan, Z. (2018). Root phenotyping for drought tolerance: a review. *Agronomy*, 8, 1–19. <https://doi.org/10.3390/agronomy8110241>

Zampieri, M., Toreti, A., Ceglar, A., Naumann, G., Turco, M., Tebaldi, C., 2020. Climate resilience of the top ten wheat producers in the Mediterranean and the Middle East. *Reg. Environ. Chang.* 20, 1–9. <https://doi.org/10.1007/s10113-020-01622-9>







June 2023